

**Synthesis and properties of hydrolysable  
polyesters catalysed by hemilabile aluminium  
pendant arm macrocycle complexes**

**Mark James Sullivan**



**A thesis submitted to Cardiff University in  
accordance with the requirements for the degree of  
Doctor of Philosophy**

**School of Chemistry, Cardiff University  
United Kingdom**

**November 2020**

## **Acknowledgments**

Firstly, I would like to thank my PhD supervisor Dr. Ben Ward for his help and guidance throughout my studies. Working with you over the last few years has been a pleasure, your passion and enthusiasm is infectious.

I would like to thank the members of the Ward group both past and present for making my time in laboratory so enjoyable and rewarding. I would also like to thank all my friends and colleagues within the Inorganic Department and in the School of Chemistry at Cardiff University for so many good times over the past years: Roddy Stark, Owaen Guppy, Sion Edwards, Bria Thomas, Rob Amesbury, Adam Day, Jamie Carden, Darren Ould, Kurt Polidano, Matt Shaw, Mohammed Bahili, Luke Kidwell, Ben Woods, Mauro Monti, Andy Woods and Sam Adams.

I would like to thank the support staff at Cardiff University for their assistance throughout my studies. Thanks also go to Susana Guadix Montero and Prof. Matthew Jones and his research group for carrying out GPC measurements. Also I would like to thank Dr Mark Eaton and Kyriaki Gkaliou for DMA measurements and Prof. Baljinder Kandola and Chen Zhou for fire testing.

Finally, I must thank all my family for their love and support throughout my PhD studies. To Mum, Dad, Matt, Natalie, Grandma and Grandpa thank you so much for all you have done for me; your unwavering encouragement and support has made this thesis possible.

## Abstract

Hydrolysable polyesters were synthesised via the ring-opening copolymerisation of epoxides and cyclic anhydrides, and the ring-opening polymerisation of  $\epsilon$ -caprolactone. These reactions were catalysed by aluminium complexes bearing a phenoxy pendant arm triazacyclononane ligand. The properties of the polymers produced were investigated.

**Chapter 1** provides an overview into the chemistry of polymers and introduces the environmental issues caused by the use of unsustainable plastics. The ring-opening polymerisation of cyclic monomers is discussed as potential routes to hydrolysable polyesters. The chemistry of complexes based on triazacyclononane ligands is reviewed and the influence of hemilability in homogeneous catalysis is introduced.

**Chapter 2** provides an introduction to the ring-opening copolymerisation of epoxides and cyclic anhydrides. An aluminium chloride complex bearing a phenoxy pendant arm triazacyclononane ligand was evaluated as catalyst for this copolymerisation under various conditions. The molecular weight, dispersity and ester selectivity of the copolymers produced was measured. The mechanism for this copolymerisation, catalysed by the aluminium pendant arm macrocycle complex, was investigated using density functional calculations and influence of hemilability on the mechanism is described. Efforts to reduce the bimodality of the polymers produced are also presented.

**Chapter 3** investigates how the thermal and flame retardant properties of the copolymers described in Chapter 2, can be altered and tuned by varying the monomers used in the copolymerisation. The flame retardancy of the copolymers was primarily measured by pyrolysis combustion flow calorimetry. Thermal degradation was investigated by thermogravimetric analysis and glass transition temperatures were obtained by dynamic mechanical analysis.

**Chapter 4** evaluates the potential to undertake post-polymerisation modification on the copolymers formed from the ring-opening copolymerisation of epoxides and cyclic anhydrides. The thiol-ene click reaction between a copolymer containing pendant vinyl groups and a variety of thiols was investigated. Crosslinking of this copolymer using

1,6-hexanedithiol was also explored. The effect on the glass transition temperature of crosslinking or appendage of the thiols to the copolymer was measured.

**Chapter 5** investigates the efficacy of aluminium pendant arm macrocycle complexes as catalysts for the ring-opening polymerisation of  $\epsilon$ -caprolactone. The molecular weight and dispersity of the polymers produced was measured. The mechanism of this polymerisation, catalysed by an aluminium pendant arm macrocycle complex, was investigated using density functional calculations and the influence of hemilability on the mechanism is described.

**Chapter 6** summarises and concludes the thesis.

**Chapter 7** contains full experimental details and characterising data for the catalysts and polymers described within the thesis.



## Abbreviations

### General

Å	Angstrom
ASAP	Atmospheric Solids Analysis Probe
AIBN	Azobisisobutyronitrile
Bn	Benzyl
PPNCl	Bis(triphenylphosphoranylidene)ammonium chloride
<i>cf.</i>	Compared with
°C	Degrees Celsius
DCM	Dichloromethane
DMAP	4-Dimethylaminopyridine
DMF	Dimethylformamide
DMSO	Dimethyl sulfoxide
E.I.	Electron Impact
Et	Ethyl
h	Hour
iPr	<i>iso</i> -Propyl
kJ	Kilojoules
MS	Mass Spectrometry
MALDI-TOF	Matrix-Assisted Laser Desorption/Ionisation-Time Of Flight
Me	Methyl
min	Minute
ppm	Parts per million
Ph	Phenyl

P	Polymer chain
rt	Room temperature
<sup>t</sup> Bu	<i>tert</i> -Butyl
THF	Tetrahydrofuran
TACN	1,4,7-Triazacyclononane
vdW	van der Waals

### **Nuclear Magnetic Resonance spectroscopic data**

br	Broad
δ	Chemical shift in ppm
COSY	Correlation Spectroscopy
J	Coupling constant
DEPT	Distortionless Enhancement by Polarisation Transfer
d	Doublet
Hz	Hertz
HMBC	Heteronuclear Multiple Bond Connectivity
HSQC	Heteronuclear Single Quantum Coherence
MHz	Megahertz
m	Multiplet
NMR	Nuclear Magnetic Resonance
<sup>13</sup> C-{ <sup>1</sup> H}	Proton-decoupled <sup>13</sup> C
q	Quartet
sept	Septet
s	Singlet

t	Triplet
VT	Variable temperature

### **Theoretical calculations**

QTAIM	Bader's quantum theory of atoms in molecules
BCP	Bond Critical Point
DFT	Density Functional Theory
$\rho$	Electron density maxima
INT	Intermediate
NBO	Natural Bonding Orbital
TS	Transition State

### **Polymerisation**

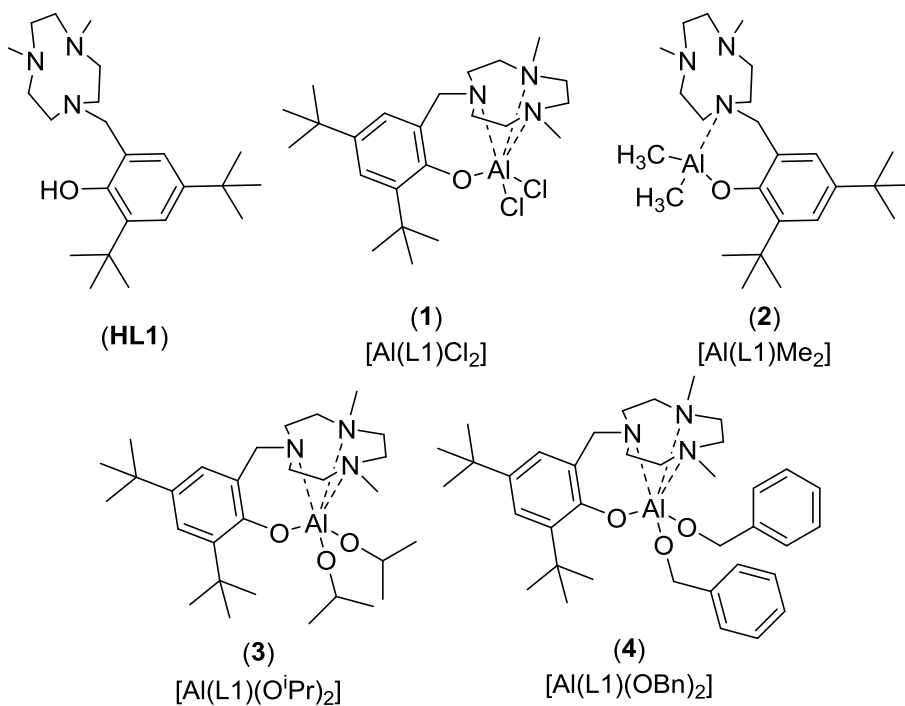
CTA	Chain Transfer Agent
$\bar{D}$	Dispersity
DMA	Dynamic Mechanical Analysis
GPC	Gel Permeation Chromatography
$T_g$	Glass transition temperature
$M_n$	Number-average molecular weight
PCL	Polycaprolactone
PLA	Poly(lactic acid)
$T_m$	Polymer melting point
PPM	Post-Polymerisation Modification
ROCOP	Ring-Opening Copolymerisation

ROP	Ring-Opening Polymerisation
Mw	Weight-average molecular weight

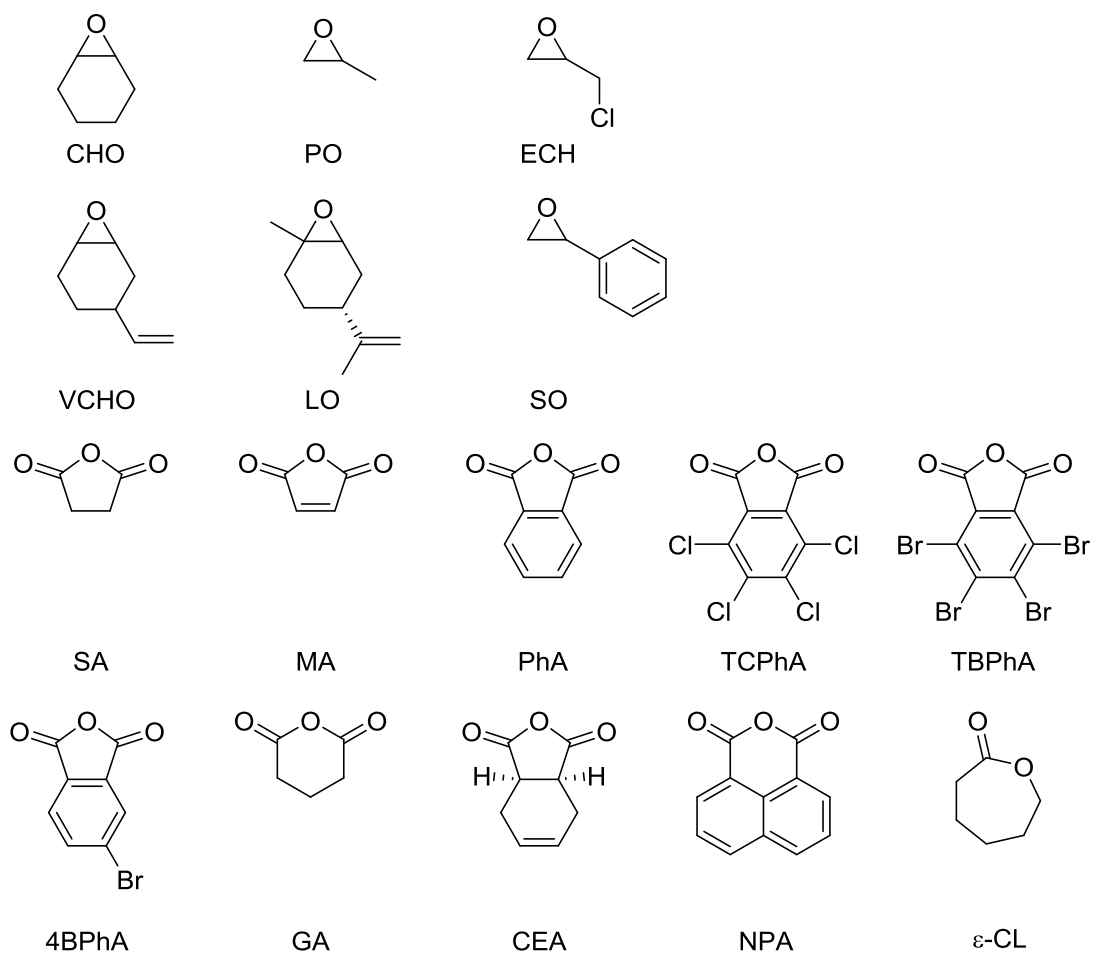
### **Fire retardancy**

HRC	Heat Release Capacity
LOI	Limiting Oxygen Index
PHRR	Peak of Heat Release Rate
P <sub>b</sub>	Probability of a fire spreading in a material
PCFC	Pyrolysis Combustion Flow Calorimetry
T <sub>10%</sub>	Temperature at 10% mass loss
T <sub>50%</sub>	Temperature at 50% mass loss
T <sub>max</sub>	Temperature at peak release rate
TGA	Thermogravimetric Analysis
THR	Total Heat Release

## Pro-ligand and catalysts



## Monomers



### **Note on copolymer nomenclature**

Specific copolymers will be referred to as Epoxide–Anhydride, where *epoxide* and *anhydride* correspond to abbreviations of the monomers used in its synthesis. For example, the product of the ROCOP of cyclohexene oxide (CHO) and phthalic anhydride (PhA) is poly(cyclohexylene phthalate), which will be referred to as CHO–PhA.

## Contents

<b>Chapter 1 - An Introduction</b>	<b>1</b>
1.1 Introduction to polymers	2
1.2 Polymer synthesis	9
1.2.1 Ring-opening polymerisation	12
1.3 Environmental issues caused by plastics	19
1.4 Alternatives to unsustainable plastics	23
1.5 Introduction to macrocyclic ligands and complexes	29
1.6 Hemilabile ligands	35
1.7 References for Chapter 1	39
 <b>Chapter 2 - Formation of polyesters via the ring-opening copolymerisation of epoxides and cyclic anhydrides</b>	 <b>46</b>
2.1 Ring-opening copolymerisation (ROCOP) of epoxides and cyclic anhydrides	47
2.2 Synthesis and characterisation of $[Al(L1)Cl_2]$ (1)	61
2.3 Ring-opening copolymerisation (ROCOP) of epoxides and cyclic anhydrides catalysed by $[Al(L1)Cl_2]$ (1)	66
2.3.1 Choice of monomers	66
2.3.2 Initial polymerisation studies	68
2.3.3 Ring-opening copolymerisation (ROCOP) in solvent	73
2.3.4 Ring-opening copolymerisation (ROCOP) in bulk epoxide	77
2.4 Mechanistic studies	86
2.5 Detailed polymer analysis using MALDI-TOF mass spectrometry	101
2.6 Reducing the bimodality of polymer molecular weight distributions	108
2.7 Summary	119
2.8 References for Chapter 2	120
 <b>Chapter 3 - Thermal and flame retardant properties of the copolymers</b>	 <b>126</b>
3.1 Flame retardancy and thermal properties of copolymers	127
3.2 Introduction to flame retardancy in plastics	128

3.3	Thermal properties of polyesters synthesised from the ring-opening copolymerisation (ROCOP) of epoxides and cyclic anhydrides.....	138
3.4	Flame retardancy analysis of epoxide and anhydride copolymers.....	148
3.4.1	Pyrolysis combustion flow calorimetry (PCFC) analysis.....	152
3.4.2	Thermogravimetric analysis (TGA) of the copolymers.....	160
3.5	Thermal properties of the copolymers.....	169
3.6	Summary.....	175
3.7	References for Chapter 3.....	176
<b>Chapter 4 - Post-polymerisation modification of copolymers.....</b>		<b>181</b>
4.1	Introduction.....	182
4.1.1	Post-polymerisation modification of polymers.....	182
4.1.2	Post-polymerisation modification (PPM) reactions.....	183
4.1.2.1	Modification of copolymers synthesised from the ring-opening copolymerisation (ROCOP) of epoxides and cyclic anhydrides.....	192
4.1.3	Introduction to the crosslinking of polymers.....	195
4.2	Post-polymerisation modification of vinyl-containing copolymers using thiol-ene click chemistry.....	198
4.3	Crosslinking of copolymers with dithiols.....	207
4.4	Summary.....	212
4.5	References for Chapter 4.....	213
<b>Chapter 5 - Ring-opening polymerisation of <math>\epsilon</math>-caprolactone.....</b>		<b>218</b>
5.1	Introduction.....	219
5.1.1	Poly( $\epsilon$ -caprolactone).....	219
5.1.2	Ring-opening polymerisation (ROP) mechanisms for the formation of polycaprolactone (PCL) from $\epsilon$ -caprolactone ( $\epsilon$ -CL).....	221
5.1.3	Catalysts for the ring-opening polymerisation (ROP) of $\epsilon$ -caprolactone ( $\epsilon$ -CL).....	223
5.2	Synthesis and characterisation of $[\text{Al}(\text{L1})(\text{O}^i\text{Pr})_2]$ (3).....	236
5.3	ROP of $\epsilon$ -CL catalysed by $[\text{Al}(\text{L1})(\text{O}^i\text{Pr})_2]$ (3) and $[\text{Al}(\text{L1})(\text{Me})_2]$ (2).....	238
5.4	Mechanistic investigation.....	242



5.5	Summary.....	249
5.6	References for Chapter 5.....	251
<b>Chapter 6 - Overall summary and conclusion.....</b>		<b>256</b>
6.1	Overall summary and conclusion.....	257
6.2	References for Chapter 6.....	261
<b>Chapter 7 - Experimental.....</b>		<b>262</b>
7.1	General methods and instrumentation.....	263
7.2	Ring-opening copolymerisation (ROCOP) with solvent.....	264
7.3	Ring-opening copolymerisation (ROCOP) in bulk epoxide.....	265
7.4	Post-polymerisation modification (PPM) of VCHO–PhA.....	265
7.5	Cross-linking of VCHO–PhA.....	266
7.6	Ring-opening polymerisation (ROP) of $\epsilon$ -caprolactone ( $\epsilon$ -CL).....	266
7.7	Density functional calculations.....	266
7.8	L1 pro-ligand synthesis.....	267
7.9	Synthesis of $[\text{Al}(\text{L1})\text{Cl}_2]$ (1).....	267
7.10	Synthesis of $[\text{Al}(\text{L1})(\text{O}^i\text{Pr})_2]$ (3).....	268
7.11	Synthesis of $[\text{Al}(\text{L1})(\text{Me})_2]$ (2).....	269
7.12	Synthesis of $[\text{Al}(\text{L1})(\text{OBn})_2]$ (4).....	270
7.13	Synthesis of $\text{PPN}_2\text{ADC}$ and $\text{PPN}_2\text{TPA}$ .....	271
7.14	Preparation of polymer plates for flame-retardant testing.....	272
7.15	Representative $^1\text{H}$ NMR spectra of polymers.....	272
7.16	TGA curves of copolymers.....	283
7.17	DMA curves for copolymers.....	287
7.18	References for Chapter 7.....	295
<b>Appendix.....</b>		<b>297</b>

# **Chapter 1**

## **An Introduction**

### 1.1 Introduction to polymers

Plastics are extremely versatile materials that find widespread use in a range of applications, and therefore play a pivotal role in facilitating our modern lives. A plethora of different plastics have been developed which show hugely diverse and varied properties such as high mechanical strength, chemical resistance, elasticity, low weight and high durability.<sup>1–3</sup>

The production of plastics has increased substantially ever since the development of the first commercial example in the 1950's. Global demand, driven by the developing world is increasing rapidly. In 2018, 360 million tonnes of plastic was produced world-wide. In Europe, the amount of plastic generated decreased slightly in 2018 (61.8 million tonnes) compared to the previous year (64.4 million tonnes) in favour of greater production outside Europe. The only dip in the global production of plastic was following the 2008 financial crisis (Figure 1).<sup>4</sup>

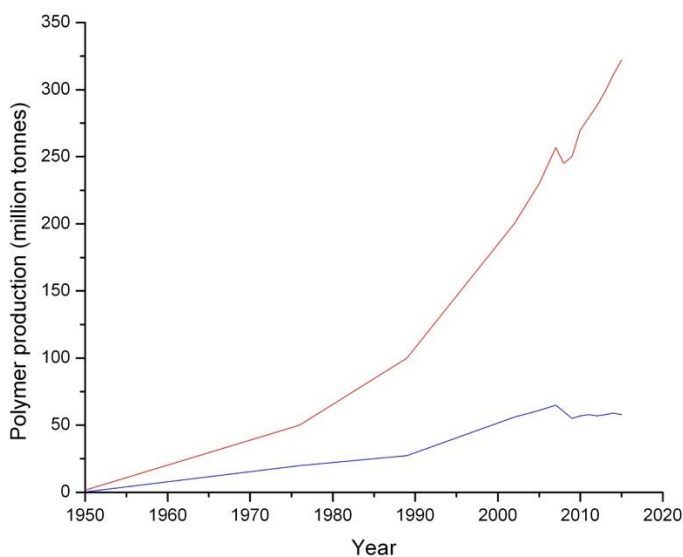


**Figure 1** Polymer production 1950 – 2015 (global: red; Europe: blue)<sup>4</sup>

Plastics are comprised of polymers (along with plasticisers to modify their properties) which are macromolecules formed from the serial addition of small (normally organic) compounds or monomers. These monomers react with each other forming covalent linkages and yielding molecular chains. Polymer chains can be long, containing thousands of monomer units, or can be very

## **Chapter 1 - An Introduction**

short (oligomers), comprising of only a few units. Polymers can be composed of linear chains or a branched network.<sup>2</sup>

Many of the useful properties of plastics are a result of their long polymer chain lengths or molecular weight. Monomers show very different physical properties to polymers and are therefore not suitable for the myriad of applications that plastics are used for. For example, the oligomer *n*-hexatriacontane, which has a molecular weight of  $437 \text{ g mol}^{-1}$ , is chemically identical to polyethylene ( $M_n > 20,000 \text{ g mol}^{-1}$ ) but shows distinctly different properties. The former yields weak, brittle crystals whereas polyethylene is a strong durable plastic used for drink bottles or cable jackets and numerous other applications. The large polymer chains interact very strongly with each other due to the high overall van der Waals forces forming a polymer matrix where chains are intertwined and cannot easily move past each other.<sup>5</sup>

Plastics can be characterised as either thermoplastics or thermosets. A thermoplastic softens and flows at high temperatures and can therefore be moulded easily into useful shapes. When cooled, these plastics regain their hardness and retain the shape imposed on them during moulding. A thermoset plastic does not soften or change shape upon heating; the material will decompose before the material reaches a temperature high enough to induce these changes.<sup>5</sup>

Examples of thermoplastics include the linear polymers: polystyrene (PS), polyethylene (PE), poly(vinylchloride) (PVC) and poly(ethyl terephthalate) (PET). Examples of thermoset plastics are polyurethanes or cured phenolic resins. They are comprised of highly interconnected networks which offer hard and rigid materials. A thermosetting polymer undergoes crosslinking reactions to become a thermoset. An example of this is an epoxy resin. The crosslinking may be initiated by a change of reaction conditions such as heat, or by addition of a catalyst or combination of reactants.<sup>5</sup>

Polymers can be characterised as either crystalline or amorphous. A crystalline or semi-crystalline polymer contains highly ordered regions where chains are arranged in lamellae.<sup>5</sup> In semi-crystalline polymers, the crystalline regions are surrounded by areas of amorphous polymer, where chains are

## Chapter 1 - An Introduction

arrayed in a disordered, irregular manner. Amorphous plastics do not contain any ordered, crystalline regions. Highly crystalline polymers are often rigid materials with high melting points, whereas amorphous polymers tend to be softer and lose their mechanical strength at lower temperatures compared to crystalline polymers.<sup>6,7</sup>

The degree of crystallinity in a plastic can significantly influence the thermal properties of the material. At low temperature, amorphous regions of polymer chains exhibit a glassy state with similar properties to crystalline polymers, however as the temperature is increased, the amorphous polymer chains begin to move around one another more easily giving plastic rubbery properties. The temperature at which this occurs is the glass transition temperature ( $T_g$ ). Crystalline regions of a polymer do not exhibit this transformation and the chains remain ordered until the temperature reaches the melting point of the plastic ( $T_m$ ), where the plastic changes to a low viscosity liquid. Semi-crystalline polymers exhibit both a  $T_g$  and a  $T_m$  whereas amorphous plastics only show a  $T_g$ .<sup>7</sup> Polystyrene (PS) and poly(methyl methacrylate) (PMMA) are examples of amorphous polymers and PE and PET are crystalline plastics (Figure 2).<sup>5,6</sup>

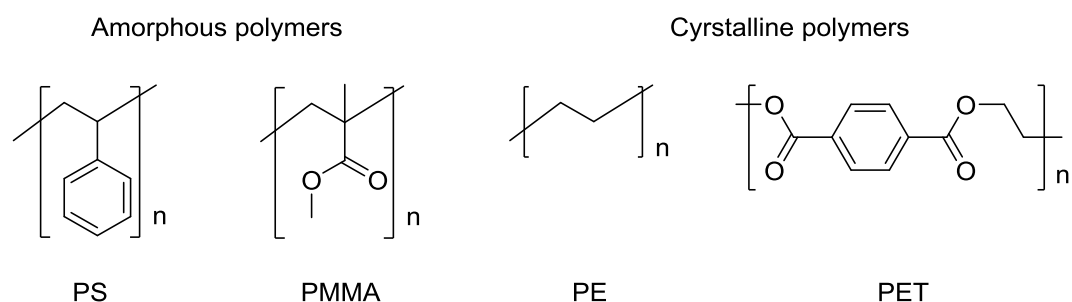
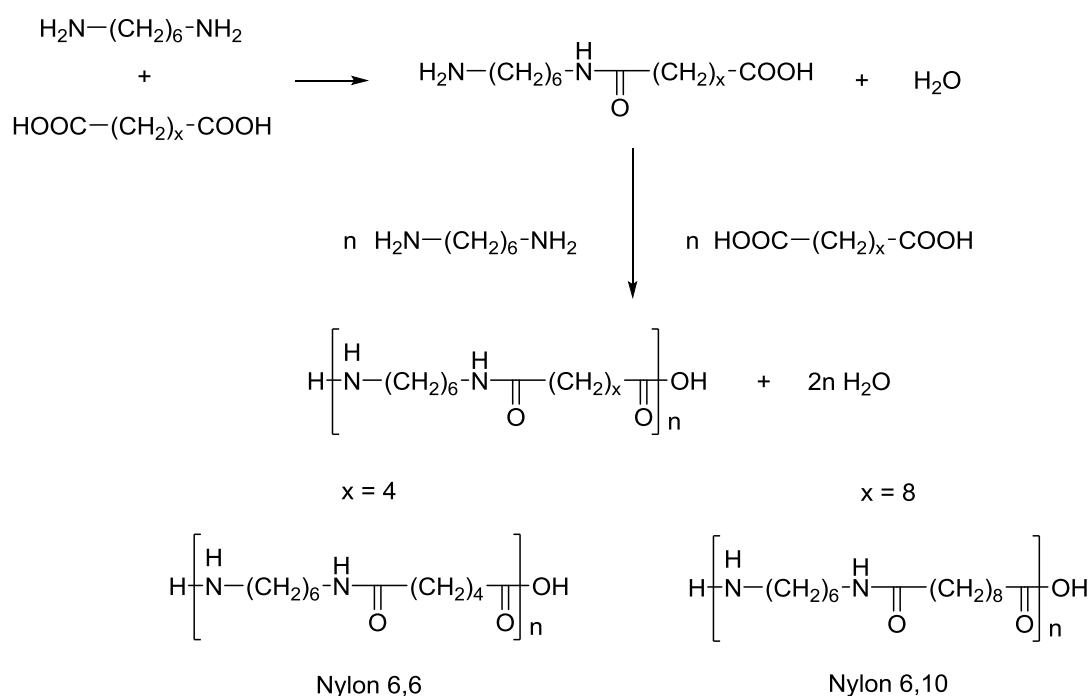


**Figure 2** The amorphous polymers, polystyrene (PS) and poly(methyl methacrylate) (PMMA) and the crystalline polymers, polyethylene (PE) and polyethylene terephthalate (PET)<sup>6</sup>

The thermal properties of a plastic depend on the flexibility of the polymer chains and how easily they can move past each other. The more mobile the polymer chains the lower the  $T_g$  or  $T_m$ , while restricting this mobility can increase these values. The  $T_g$  of a polymer depends on the rate of heating or cooling and the measurement method.<sup>6,7</sup>

## Chapter 1 - An Introduction

Polymers with more polar groups, such as polyesters or polyamides show stronger interactions between chains, due to intermolecular forces such as hydrogen bonding. Polymers with hydrogen bonding exhibit greater mechanical strength at lower molecular weights than hydrocarbon based plastics such as PE.<sup>2,7</sup> Simply increasing the number of polar bonds in a polymer chain can alter the polymer properties. For example, two nylon polymers synthesised from diamines and dicarboxylic acid monomers have different properties depending on the size of the monomer unit. Nylon 6,10 was synthesised from  $\text{H}_2\text{N}-(\text{CH}_2)_6-\text{NH}_2$  and  $\text{HOOC}-(\text{CH}_2)_8-\text{COOH}$ , while nylon 6,6 was formed from the reaction of the same diamine with adipic acid,  $\text{HOOC}-(\text{CH}_2)_4-\text{COOH}$ , (Scheme 1). For polymers of equal molecular weights, nylon 6,6 would contain more polar amide bonds and therefore exhibit greater hydrogen bonding, this results in a higher melting point (265 °C) than nylon 6,10 (225 °C). The length of the alkyl linkers between the amide bonds in the polymer also affects hydrophobicity, flexibility and other mechanical properties. Nylon 6,6 has a tensile strength of 80 MPa and percentage water absorption at saturation of 8% compared to 60 MPa and 2.5% respectively for Nylon 6,10.<sup>5,8</sup>



**Scheme 1** Synthesis of Nylon 6,6 and 6,10<sup>5,8</sup>

## Chapter 1 - An Introduction

The flexibility of a polymer chain can be reduced by including functional groups such as amides or carbonyl moieties and alkene or aromatic groups in the polymer backbone. For example, the  $T_g$  of PET is far higher (69 °C) than PE (-120 °C) due to the benzene ring present in the backbone of the former.<sup>6,7</sup>

The presence of pendant chemical groups along the polymer chains can influence the thermal properties of the polymer. In a crystalline polymer, branching results in a reduction in  $T_m$  due to the disruption and defects caused to the tightly packed crystalline regions. The presence of bulky chemical groups can increase the  $T_g$  of a polymer as it can restrict rotational movement of chains limiting their mobility. For example, PS has a much higher  $T_g$  (100 °C) compared to polypropylene (PP) (-18 °C) (Figure 3). The presence of flexible groups appended to a polymer backbone gives rise to a reduction in  $T_g$  as it limits the packing efficiency of polymer chains increasing their rotational freedom and mobility. PMMA has a  $T_g$  of 105 °C, whereas poly(butyl methacrylate) (PBMA) containing n-butyl groups as opposed to methyl has a lower value of 20 °C (Figure 3).<sup>6</sup>

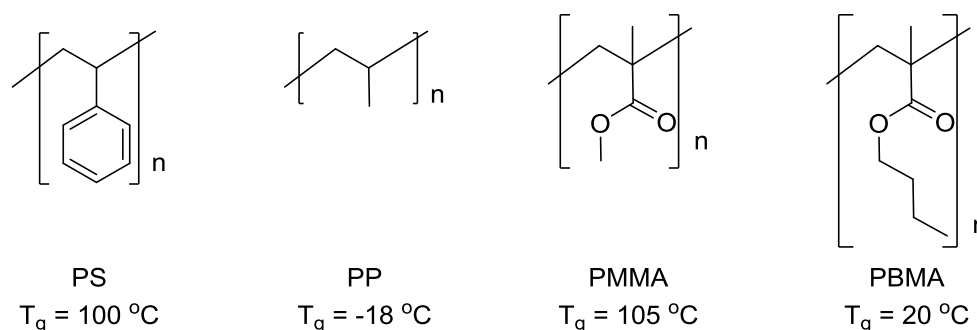


**Figure 3** The glass transition temperatures ( $T_g$ ) of polystyrene (PS), polypropylene (PP), poly(methyl methacrylate) (PMMA) and poly(butyl methacrylate) (PBMA)<sup>6</sup>

The  $T_g$  of a polymer is increased following the crosslinking of polymer chains.  $T_g$  rises with the degree of crosslinking in a material which corresponds to decreasing mobility and rotational motion.<sup>9</sup> Crosslinking of amine terminated poly(ether sulfone) caused the  $T_g$  to increase from 209 °C to 220 °C.<sup>10</sup>

$T_g$  is affected by the molecular weight of the polymer and rises as polymer chain length increases. Molecular weight can be related to  $T_g$  by the Fox-Flory

## Chapter 1 - An Introduction

equation (Equation 1). Where  $M_n$  is the number average molecular weight,  $K$  is the Fox-Flory parameter (related to polymer free volume) and  $T_{g\infty}$  is the  $T_g$  at infinite molecular weight.<sup>6</sup>

$$T_g = T_{g\infty} - \frac{K}{M_n}$$

### Equation 1 Fox-Flory equation<sup>6</sup>

Macromolecules produced via polymerisation have a distribution of polymer chain lengths or molecular weights. There are several averages that define the length of polymer chains, however the most commonly used are the number average molecular weight ( $M_n$ ) and the weight average molecular weight ( $M_w$ ), whilst the distribution of molecular weights is defined by the polymer dispersity ( $\mathfrak{D}$ ). These characterising properties can be determined by various techniques, the most commonly used are gel permeation chromatography (GPC) and MALDI mass spectrometry.<sup>11</sup>

The  $M_n$  is defined as the sum of the number of molecules ( $N_i$ ) with a specific molecular weight ( $M_i$ ), divided by the total number of molecules.<sup>12</sup>

$$M_n = \frac{\sum N_i M_i}{\sum N_i}$$

### Equation 2 Definition of the number average molecular weight ( $M_n$ )<sup>12</sup>

$M_w$  is defined as the sum of the weight fraction of a polymer ( $W_i$ ) multiplied by the mass of the polymers in the weight fraction ( $M_i$ ).  $W_i$  is the total weight of all polymers with a specific mass divided by the total weight of the sample.<sup>12</sup>

$$M_w = \sum W_i M_i$$

### Equation 3 Definition of the weight average molecular weight ( $M_w$ )<sup>12</sup>

The distribution of polymer molecular weights in a sample can vary significantly, the dispersity ( $\mathfrak{D}$ ) of a polymer sample gives a mathematical description of this distribution.  $\mathfrak{D}$  is calculated by dividing  $M_w$  by  $M_n$ . The more selective the polymerisation the lower the  $\mathfrak{D}$ . For a perfectly selective polymerisation where all molecules are the same mass, the  $\mathfrak{D}$  is equal to 1.<sup>12</sup>



$$\mathcal{D} = \frac{M_w}{M_n}$$

**Equation 4** Definition of polymer dispersity ( $\mathcal{D}$ )<sup>12</sup>

Gel Permeation Chromatography (GPC) is a powerful technique for determining the molecular weight distribution of a polymer sample and is considered the standard technique for polymer molecular weight determination. In a GPC experiment, the polymer chains in a sample are separated by their molecular weight. This is achieved by using a size exclusion column. GPC is also known as Size Exclusion Chromatography (SEC). The stationary phase or gel, is made of a column consisting of porous, polymeric spheres often made of PS crosslinked with divinylbenzene. The mobile phase, the solvent in which the polymer is dissolved, is passed over the stationary phase. The dissolved polymer is separated by molecular size or more specifically hydrodynamic volume. The smaller size or lower molecular weight polymers can more easily enter the pores of stationary phase than larger molecules, therefore the residence time in the column of the smaller molecules is higher and they elute more slowly than the larger polymers. Once a polymer molecule has passed through the size exclusion column it can be detected by a range of techniques, most commonly a refractive index detector is used, but viscosity or light scattering detectors are also utilised.<sup>11</sup>

In a standard GPC experiment, a calibration of polymer samples with known molecular weights is carried out. The calibration must be undertaken using the same method, solvent and at the same temperature. This means that the molecular weights calculated are relative to a polymer standard. The most commonly used standards are polystyrene for organic solvents and polyethylene glycol for aqueous media. A relative molecular weight may be converted to a real value using the Mark-Houwink-Sakurada relationship. This equation describes the relationship between the intrinsic viscosity of a polymer ( $\eta_1$ ) and its molecular weight ( $M_1$ ).  $K$  and  $a$  are the Mark-Houwink parameters and their values depend on the temperature and nature of the polymer and solvent.

$$[\eta] = KM^a$$

**Equation 5** The Mark-Houwink-Sakurada relationship<sup>11</sup>

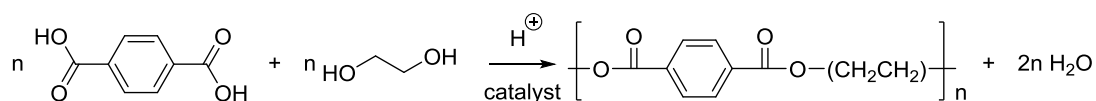
The molecular weights of two different polymers can be related using the Mark-Houwink equation when the two polymers have the same intrinsic viscosity in a particular solvent.

$$K_1M_1^{1+a_1} = K_2M_2^{1+a_2}$$

**Equation 6** Two polymers related by the Mark-Houwink equation<sup>11</sup>

If the Mark-Houwink parameters of the two polymers and molecular weight of one polymer is known, the molecular weight of the second polymer can be calculated from the equation above.<sup>11</sup>

## **1.2 Polymer synthesis**



**Scheme 2** Synthesis of polyethylene terephthalate (PET)<sup>2,13</sup>

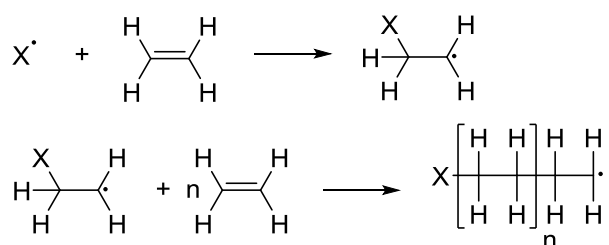
There are two main routes for the synthesis of polymers: step-growth polymerisation and chain-growth polymerisation. In a step-growth polymerisation, monomers containing two (or more) functional groups react and combine to form a dimer. This process continues as polymers or oligomers react further via the same reaction to yield longer chains. In a step-growth polymerisation, the average molecular weight increases very slowly and only at very high conversions >95% are high molecular weight polymers formed. Many of the polymerisations which proceed via a step-growth mechanism are copolymerisations between two different monomers. For example, the polyester PET can be synthesised by the reaction of ethylene glycol and phthalic acid (Scheme 2). Homopolymerisation via a step-growth mechanism is less common, but examples of monomers which undergo this type of reaction exist, such as the formation of Nylon 6 from the aminocarboxylic acid,  $\text{H}_2\text{N}-(\text{CH}_2)_5\text{-COOH}$ . Most of the polymerisations that proceed through a step-

## Chapter 1 - An Introduction

growth mechanism are considered to be condensation reactions. The reaction between monomers or polymers of this type yields a by-product, usually a small organic molecule. For the PET example above, the reaction of the carboxylic acid and the alcohol produces an ester functionality, linking the two reactants and a molecule of water as a side product (Scheme 2).<sup>2,13</sup>

Not all step-growth polymerisations are condensation reactions. For example, in the formation of polyurethanes from isocyanates and alcohols there are no byproducts produced. This is advantageous as the reaction is 100% atom economic and removal of side products is not required. For condensation reactions, byproduct removal can be difficult and if overlooked can prevent the attainment of high conversions, resulting in the formation of low polymer molecular weights. In the production of PET discussed above, water is removed from the reaction to shift the equilibrium towards ester formation.<sup>13</sup>

The other main type of mechanism is a chain-growth polymerisation. Chain-growth polymerisations begin with the initiation of a monomer by a reactive species, the activated monomer then reacts sequentially with further monomers growing a polymer chain in a process known as propagation. Generally these polymerisations are addition polymerisations and do not produce side products in the reaction; chain-growth polymerisations are also often carried out at lower temperatures than step-growth polymerisations. The molecular weight of the polymers increases very quickly, even at low conversions and far greater control over molecular weight is possible with this type of polymerisation compared to the step-growth mechanism.<sup>2,13</sup>



**Scheme 3** Free-radical polymerisation of ethene<sup>14</sup>

A chain-growth polymerisation may proceed through a free-radical mechanism, an approach often utilised for the polymerisation of alkenes. The reaction is initiated by a radical species, which causes the homolytic bond

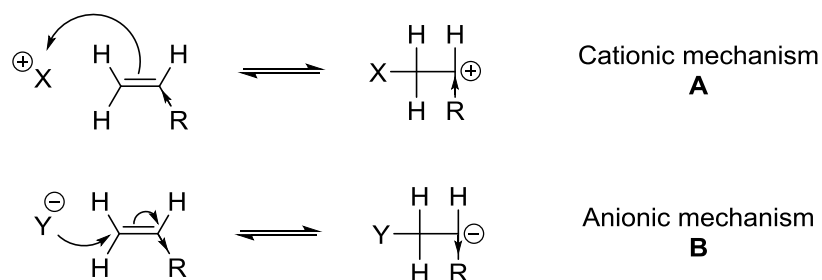
## Chapter 1 - An Introduction

cleavage of an alkene  $\pi$  bond, thereby forming an activated radical monomer which can react with further monomers to grow the polymer chain (Scheme 3). In a free-radical polymerisation, termination reactions are common. In a termination step, two radical species combine producing a non-reactive product which halts polymerisation.<sup>14</sup>

Ionic chain polymerisation is another polymerisation route. The active species in this type of reaction can be either positively charged (cationic) or negatively charged (anionic). A major advantage of this type of polymerisation compared to a free-radical mechanism is that termination through recombination is unlikely due to repulsion between like charges.<sup>15</sup>

Unlike the free-radical polymerisation, which is effective for the vast majority of alkene double bonds, the type of ionic polymerisation depends on the substituents of the alkene. Electron-donating substituents such as alkoxy, alkyl or phenyl groups increase the electron density in the alkene double bond and therefore favour a cationic mechanism (Scheme 4A). Catalytic amounts of HCl can initiate a cationic polymerisation of an alkene, however, reaction of the carbocation with  $\text{Cl}^-$  can terminate the polymerisation. Initiators with less nucleophilic anions such as  $\text{HClO}_4$  or  $\text{CF}_3\text{COOH}$  are more effective than HCl. Lewis acids can also be used to polymerise electron rich double bonds and are particularly useful for reactions in organic solvents. They must be used in conjunction with either water or an alcohol which acts as a source of  $\text{H}^+$ .<sup>15</sup>

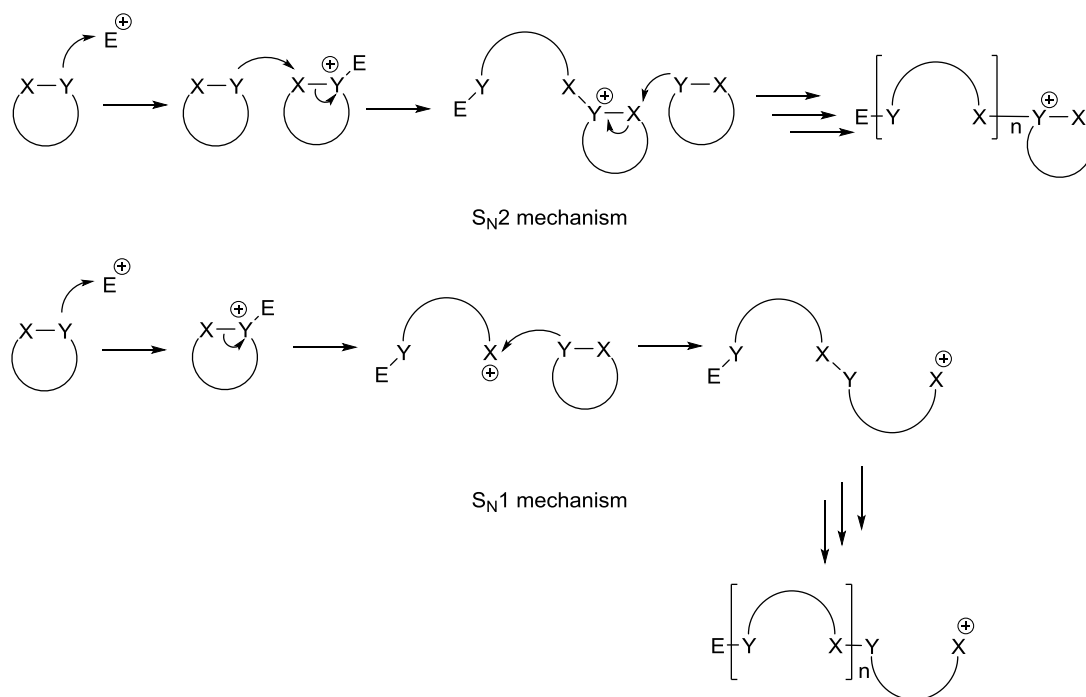
Conversely electron-withdrawing substituents such as carbonyl or nitrile groups stabilise an incipient anion (Scheme 4B) formed in an anionic polymerisation. Initiation can be achieved by using highly reactive, air/moisture sensitive organometallic compounds such as butyl lithium.<sup>15</sup>



**Scheme 4** **A** Cationic mechanism, **B** Anionic mechanism<sup>15</sup>

### 1.2.1 Ring-opening polymerisation

An effective route to linear polymers is the ring-opening polymerisation (ROP) of cyclic monomers. There are many examples of cyclic monomers which are capable of undergoing ROP (or the related ring-opening copolymerisation, ROCOP) to yield useful polymers. Most of the reactive cyclic monomers contain heteroatoms which act as a reactive site for the ROP. ROP can be well controlled and produce polymers with high molecular weights and low Đ. Well-known examples of this type of polymerisation is the curing of epoxy resins, the formation of polyesters from lactones or lactide and the formation of polyamides from cyclic amides. Cyclic monomers are generally polymerised by either a cationic, anionic or coordination-insertion mechanism.<sup>16</sup>

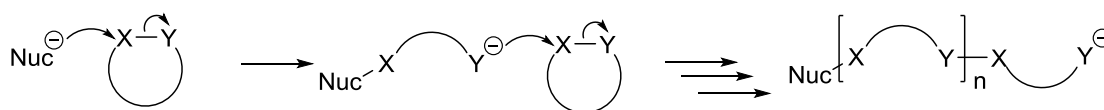


**Scheme 5** Cationic ring-opening polymerisation (ROP) mechanisms<sup>17</sup>

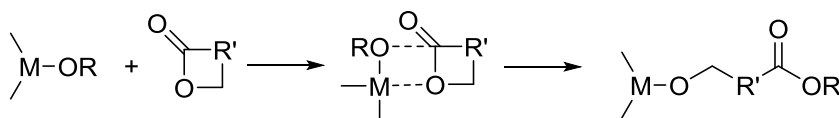
The ROP of heterocycles may take place via a cationic mechanism (Scheme 5) where the reaction is initiated by an electrophile causing ring-opening of the monomer to form a new cationic centre, which can subsequently react with further monomers. Commonly used electrophiles are Brønsted acids, Lewis acids or alkyl esters. In a heterocycle with a polarized bond such as an ester (represented by X-Y in Scheme 5), the electron rich centre (Y) acts as a Lewis base and reacts with the electrophilic initiator. Following this step, a cationic

heterocycle is formed which can react (by an  $S_N2$  mechanism) with another monomer causing ring-opening; alternatively, the cationic heterocycle can undergo a unimolecular ring-opening ( $S_N1$  reaction) forming a linear cationic species which can propagate by reaction with further monomers. The reaction pathway depends on the stability of the carbocation ( $X^+$ ) formed. Cationic ROP is often unreliable, producing low molecular weight polymers.<sup>17</sup>

The anionic ring-opening of cyclic monomers is initiated by nucleophilic reagents such as alkyl lithium, alkyl aluminium, metal amides or alkoxides. Cyclic esters, carbonates, amides and phosphates will undergo anionic ROP. For monomers with less electronegative functionalities such as an ether, only examples with a three-membered ring system will react as a result of the high ring strain. Scheme 6 illustrates a typical anionic ROP; X-Y equates to a polarized functional group where Y is an electronegative atom such as oxygen or nitrogen and X is typically an electron deficient carbon. Attack of the nucleophile causes the monomer to ring-open, forming a new nucleophile ( $Y^-$ ) which can attack further monomers resulting in polymerisation.<sup>17</sup>



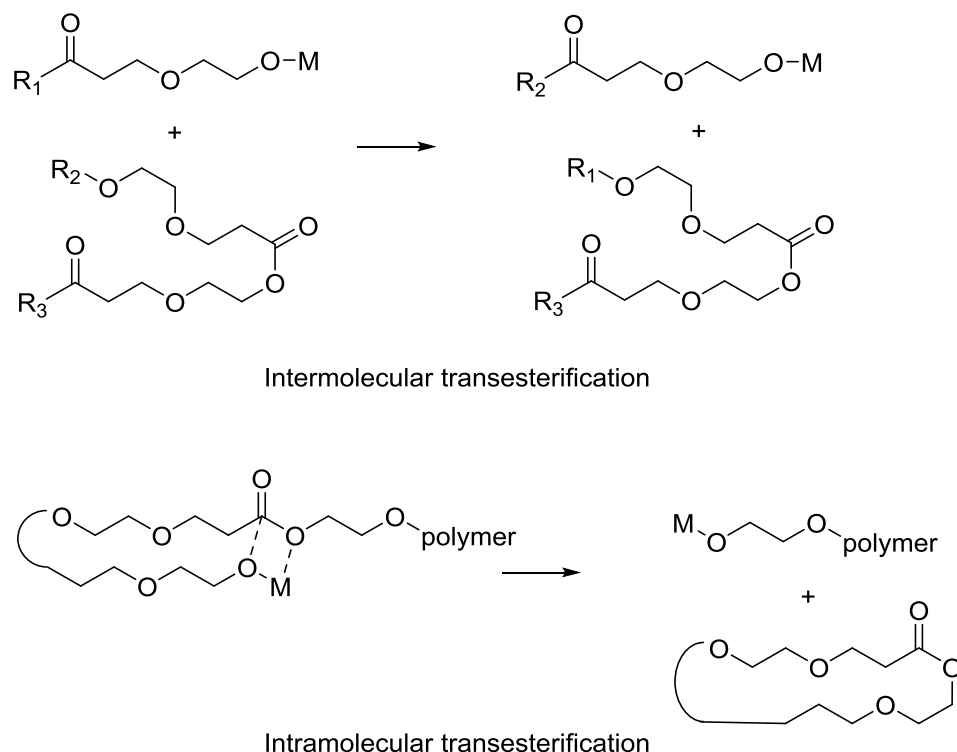
**Scheme 6** Typical anionic ring-opening polymerisation (ROP) mechanism<sup>17</sup>



**Scheme 7** General coordination-insertion mechanism for the ring-opening polymerisation (ROP) of cyclic esters<sup>17</sup>

ROP of heterocyclic monomers may be carried out by a coordination-insertion mechanism. In this mechanism, a monomer is activated by coordination to a metal centre, this activated monomer is then attacked by a nucleophile causing ring-opening. This type of polymerisation has been studied extensively for the polymerisation and copolymerisation of epoxides, lactones, lactide, cyclic anhydrides and episulfides.<sup>16</sup> Using this method of polymerisation, polymers with high molecular weights and narrow dispersities can be produced.<sup>17</sup> This

type of polymerisation has been utilised in industry to produce polyether elastomers from epichlorohydrin, ethylene oxide, propylene oxide and allyl glycidyl ether.<sup>18</sup> The ROP of cyclic esters via a coordination-insertion mechanism is shown in Scheme 7.<sup>19</sup> The cyclic monomer coordinates to a metal centre and subsequently, insertion of a metal-alkoxide ligand into the carbonyl group of the ester takes place. Ring-opening of the monomer is achieved via acyl-oxygen cleavage.<sup>20,21</sup>



**Scheme 8** Inter- and intramolecular transesterification<sup>17</sup>

A major side reaction in the ROP of cyclic esters is transesterification. This process often occurs in reactions with long reaction times or high temperatures and causes lower molecular weights and higher dispersities.<sup>22</sup> Two variations of transesterification exist, either intramolecular or intermolecular (Scheme 8). Intramolecular transesterification, or back-biting, causes degradation of the polymer chain and the formation of macrocyclic polymers. Intermolecular transesterification can prevent the formation of block copolymers as it blends polymer chains randomising polymer sequences.<sup>23</sup> Greater flexibility in the polymer chains can lead to more side reactions such as transesterification. For example, more side reactions were present in the polymerisation of D,L-

## Chapter 1 - An Introduction

lactide (which yielded a more flexible polymer) than the polymerisation of L,L-lactide.<sup>24</sup>

The reactivity of cyclic monomers depends on both thermodynamic and kinetic factors. A polymerisation is thermodynamically favourable if a linear polymer is more stable than the cyclic monomer, for example by reducing ring-strain. Figure 4 shows the key steps in a polymerisation reaction: initiation, propagation/depropagation and termination reactions, which are defined by the rate constants  $k_i$ ,  $k_p$ ,  $k_d$  and  $k_t$ . The initiation reaction of a monomer must yield a new active species ( $M^*$ ), capable of reacting with further monomers and thereby creating or growing a polymer chain whether linear or branched (Figure 4a). In a ROP of a cyclic monomer, an equilibrium exists between the monomer and polymer. The forward reaction is propagation and the backward is depropagation, which are defined by the relative rate constants  $k_p$  and  $k_d$  respectively (Figure 4b). For a polymer to form  $k_p > k_d$ . For a successful polymerisation, this equilibrium must be shifted towards the polymer product. Depending on the monomer and type of polymerisation, it is not unusual to observe relatively high concentrations of monomer remaining when equilibrium is reached ( $[M]_{eq}$ ). In order for a polymerisation to take place at all, the initial monomer concentration ( $[M]_0$ ) must be  $[M]_0 > [M]_{eq}$ . The rate of propagation must also be greater than the rate of termination,  $k_p > k_t$  (Figure 4c).<sup>16</sup>

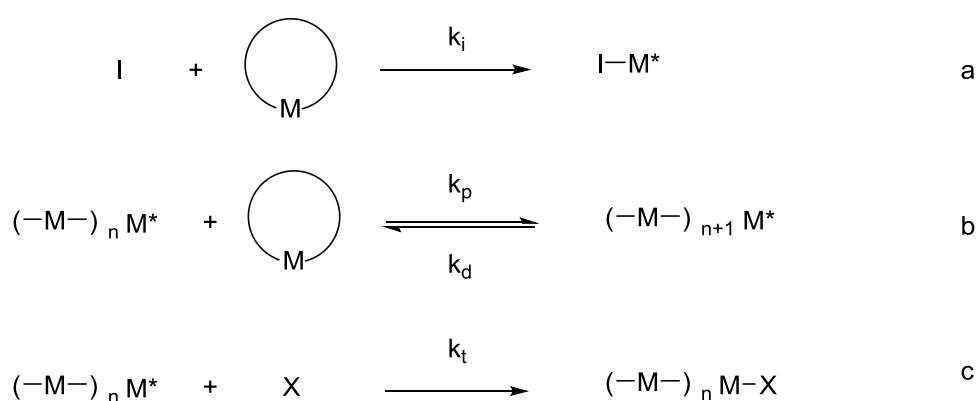


**Figure 4** Key reaction steps in ring-opening polymerisation (ROP) <sup>16</sup>



$$\Delta G_p = \Delta H_p^0 - T(\Delta S_p^0 + R \ln[M])$$

**Equation 7** Relationship of Gibbs energy, enthalpy of polymerisation, entropy of polymerisation and monomer concentration<sup>16</sup>

As is the case with any chemical reaction, polymerisation is thermodynamically feasible if the Gibbs energy is negative ( $\Delta G_p < 0$ ). Equation 7 shows how  $\Delta G_p$  is related to the enthalpy of polymerisation ( $\Delta H_p^0$ ), entropy of polymerisation  $\Delta S_p^0$  and monomer concentration  $[M]$ . This equation only applies to systems which agree with Flory's assumption that a polymer is sufficiently long that the reactivity of the active centre does not depend on the degree of polymerisation. A monomer can be polymerised at any temperature when  $\Delta H_p^0 < 0$  and  $\Delta S_p^0 > 0$ , while no reaction is possible if  $\Delta H_p^0 > 0$  and  $\Delta S_p^0 < 0$ . The thermodynamic feasibility of a ROP is in most cases reliant on the enthalpy of the reaction. As a polymerisation forms large macromolecules from small monomers the vast majority of these reactions have  $\Delta S < 0$ . This is due in the most part to a loss of translational freedom. For the polymerisations where  $\Delta H_p^0 < 0$  and  $\Delta S_p^0 < 0$ , increasing the temperature causes an increase in the  $[M]_{eq}$ . A maximum temperature exists where  $[M]_0 = [M]_{eq}$  and polymerisation will not take place. For example, THF cannot be polymerised at temperatures over 84 °C.<sup>25</sup> For the majority of monomers however, this maximum temperature is well above the temperatures commonly utilised for reaction.<sup>16</sup>

The stability of the cyclic monomer therefore has a significant influence on the feasibility of a polymerisation reaction. Ring strain in cyclic monomers often dictates its reactivity. The degree of ring strain varies for different size rings. For 3- and 4- membered rings the strain is very high, whereas for 5-, 6- and 7- membered rings it is considerably lower. The instability of smaller rings is due to high bond angle strain caused by conformations in which bond angles are far removed from the optimum 109.5° for  $sp^3$  carbons. As the ring size increases, the bond angles become closer to the optimal tetrahedral angle and bond angle strain is reduced. Torsional strain also contributes to ring strain and is a result of the repulsion of different substituents when they are arranged in an eclipsed manner. As the rings become larger, they have greater flexibility

## Chapter 1 - An Introduction

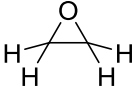
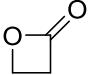
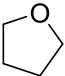
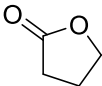
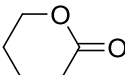
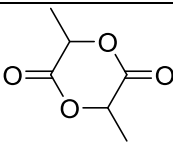
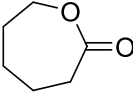
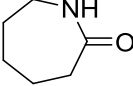
and adopt non-planar conformations which reduces torsional strain. Transannular strain caused by repulsive interactions of substituents in the interior of the ring structure also contributes towards rings strain in rings between 8- and 13-members. For rings with >13 members the transannular strain is removed because the interior of these rings is sufficiently large to accommodate all substituents. For polymerisations where the effects of solvent-monomer-polymer interactions are negligible,  $\Delta H_p^0$  can be considered as a measure of ring strain. The higher the ring strain or the more negative the  $\Delta H_p^0$ , the lower the  $[M]_{eq}$ .<sup>16,26</sup>

**Table 1** Ring-opening polymerisation (ROP) of cycloalkanes at 25 °C<sup>27,28</sup>

$(CH_2)_n$	$\Delta H_p^0$ (KJ/mol)	$\Delta S_p^0$ (J/Kmol)	$[M]_{eq}$ (mol/dm <sup>3</sup> )
3	-113.0	-69.1	$1.7 \times 10^{-15}$
4	-105.1	-55.3	$3 \times 10^{-15}$
5	-21.2	-42.7	$3.4 \times 10^{-1}$
6	2.9	-10.5	$1.36 \times 10^2$
7	-21.8	-15.9	$1.4 \times 10^{-2}$

## Chapter 1 - An Introduction

**Table 2** Thermodynamic parameters of polymerisation of selected monomers<sup>16</sup>

Monomer	$\Delta H_p^0$ (KJ/mol)	$\Delta S_p^0$ (J/Kmol)	$[M]_{eq}$ (mol/dm <sup>3</sup> )
	-140	-174	$7.9 \times 10^{-15}$
	-82.3	-74	$3 \times 10^{-11}$
	-19.1	-74	3.3
	5.1	-29.9	$3.3 \times 10^3$
	-27.4	-65	$3.9 \times 10^{-1}$
	-22.9	-41.1	$1.2 \times 10^{-2}$
	-28.8	-53.9	$5.1 \times 10^{-2}$
	-13.8	4.6	$2 \times 10^{-2}$

Cyclic monomers containing heteroatoms such as epoxides, ethers, esters or amides show a similar trend of decreasing ring strain or  $\Delta H_p^0$  with increasing ring size. The thermodynamic polymerisation parameters of selected monomers are shown in Table 2. Additional functionality in the cyclic monomers can enable reactivity where a simple cycloalkane is inert. For example, cyclohexane will not polymerise under any conditions whereas lactide and  $\delta$ -valerolactone will readily polymerise. The introduction of the ester group into the six membered ring increases the planarity and therefore the ring strain compared to cyclohexane.

Although all of the cycloalkanes except cyclohexane have  $\Delta G < 0$ , in reality only the most unstable, cyclopropane shows any activity for ROP (only forming

oligomers). This illustrates the effect of kinetics. These cycloalkanes are inert as they are only comprised of C-C bonds, meaning there are no reactive sites.<sup>26</sup> For a polymerisation to occur, the reaction requires a viable kinetic pathway. For cyclic monomers, the inclusion of heteroatoms in the ring makes reactivity more likely, providing a site for nucleophilic or electrophilic attack of an initiator or a propagating polymer chain.<sup>26</sup>

In a chain growth mechanism, the reaction may be deemed as a living polymerisation when chain termination is not possible. Living polymerisations give rise to polymers with controlled molecular weights and low Đ and are effective routes to block copolymers. In a reversible-deactivation mechanism, otherwise known as an immortal polymerisation, polymer chains cycle between an active and a dormant state by proton transfer. The presence chain transfer agents (CTA) enables the immortal polymerisation. CTA's initiate polymer chains and act as source of protons which facilitate the reversible deactivation mechanism. The use of CTA's gives rise to multiple polymer chains per metal centre which offers another approach to control molecular weight while retaining the control of a living polymerisation.<sup>29</sup>

### **1.3 Environmental issues caused by plastics**

Conventional plastics have brought many benefits to society, and for many applications there are no non-plastic alternatives that can compete with the exceptional properties exhibited by the plastic materials employed. However, the demand and reliance on synthetic plastics poses important challenges. Firstly, many of the most commonly used plastics are synthesised from non-renewable fossil fuel sources; currently 8% of the crude oil produced globally is used in the synthesis of plastics,<sup>30</sup> this dependence on fossil fuels is unsustainable as it is a finite resource. Secondly, many commonly used polymers are extremely environmentally persistent, meaning that they can take hundreds of years to degrade.<sup>31</sup>

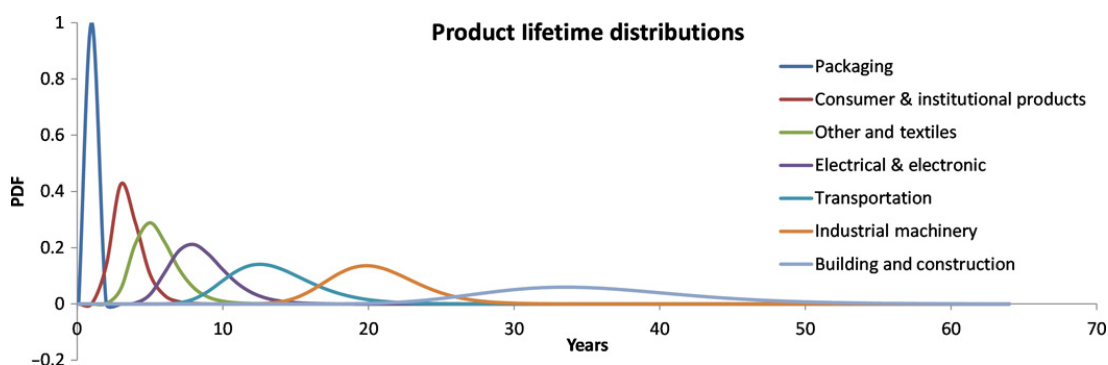


**Figure 5** Lifetime distributions of plastics used in eight industrial sectors plotted as log-normal probability distribution functions (PDF)<sup>4</sup>

Due to the vast amounts of plastic produced and the ever increasing global demand, plastic pollution has become an important societal issue. 8,300 million metric tonnes (Mt) of plastic has been produced to date which has led to the generation of 6,300 Mt of plastic waste. In 2015, 407 Mt of new plastic entered use, while 302 Mt was discarded meaning that 105 Mt of additional plastic could be considered as in-use. The lifetime of a plastic varies greatly depending on its application. Figure 5 shows the average lifetime of plastics in eight key industries. One of the major contributors to plastic pollution is single-use plastic packaging, with an average lifetime of less than a year. Conversely, the plastic materials used in the building and construction industry often have a lifetime of decades.<sup>4</sup>

Currently there are typically three possible fates for waste plastics. A plastic may either be recycled, incinerated or discarded into the environment. Recycling and incineration with energy recovery are more sustainable approaches to plastic waste management than depositing plastic waste into landfill.

Recycling of plastics can reduce environmental impact and resource depletion. Recycling recovers waste material and converts it to new useful products, thereby reducing the need for newly synthesised plastic and the amount going to landfill or discarded into the environment.<sup>30</sup> Of the 8,300 Mt of plastic produced, 600 Mt has been recycled.<sup>32</sup> Recycling of PET bottles contributes to a net reduction of 1.5 tonnes of CO<sub>2</sub> per tonne of PET recycled.<sup>30</sup> While recycling has many benefits it only delays rather than avoids final

disposal. Recycling is not always possible or can lead to poor quality material due to contamination with additives and blending of different polymer types. Reprocessing of certain plastics can lead to thermal degradation making the material useless. Of the plastic recycled only 10% has been recycled more than once.<sup>4</sup>

Incineration is another form of plastic waste management and reduces the amount of material sent to landfill. There are however concerns about the production of hazardous degradation products which can be damaging to the environment if released.<sup>30,33</sup> The risk of releasing toxic substances can be mitigated by emission control technology, this however causes additional cost and design complications. The combination of plastic waste incineration with energy recovery is an effective way of harnessing the energy content of the material.<sup>30</sup> This approach can reduce the quantity of fossil fuels used directly for electricity production. The pyrolysis of plastic waste is another form of thermal degradation but in this case the process converts the high molecular weight polymer chains into combustible oil and gas which can be utilised as fuel. Pyrolysis is the thermal degradation of a material in the absence of air producing smaller fragments which can be separated into useful products by the same processes used in petrochemical separation.<sup>34</sup>

Plastic waste can be discarded into either a managed landfill site, an open refuse dump or into the natural environment. 60% of all the plastic produced globally is discarded in this way.<sup>4</sup> A well-managed landfill site can prevent substantial environmental damage, but there are concerns over the long-term impact of these sites. These landfill sites are unsustainable, as the material cannot be converted into other useful products, chemical feedstocks or utilised for energy recovery. As plastic degrades over time harmful chemicals may be produced, which can contaminate the site. Leaching of degradation products or toxic additives into groundwater can lead to the contamination of the wider environment with persistent organic pollutants. Open refuse dumps exhibit even greater contamination of the surrounding ecosystem with environmentally persistent plastics, fragments, microplastics and harmful organic pollutants from polymer degradation or plastic additives. Pollution by

## ***Chapter 1 - An Introduction***

directly discarding waste into the natural environment or by contamination from landfill causes immense damage.<sup>35,36</sup>

Plastic pollution can have a devastating impact on wildlife. Due to the durability of many of the most common plastics, very little degradation occurs in the natural environment. For example, photodegradation and hydrolysis is almost non-existent in plastics underwater.<sup>37</sup> Plastic debris can cause species of all kinds to become entangled, causing serious injury and restricted movement which can prevent animals from feeding and can cause asphyxiation in mammals. It is especially dangerous for juvenile animals where they can become entangled, subjected to serious injury and health problems as they grow larger.<sup>38</sup> Larger plastic items may appear to degrade in the environment due to processes such as weathering, however they in fact break down only to smaller plastic fragments or microplastics;<sup>30</sup> this is physical degradation, as opposed to chemical degradation which involves polymer chain scission. Plastic may also be ingested by wildlife where it can accumulate in the digestive system leading to decreased feeding stimuli, blockages, reproductive problems and decreased levels of important enzymes and steroids. Wildlife may mistake plastics for food, or consume them as a result of indiscriminate feeding strategies such as filter feeding. Predators may consume plastic indirectly by trophic transfer.<sup>39</sup> Some of the worst affected species are marine birds, sea turtles, cetaceans, fur seals, sharks and filter feeders.<sup>37</sup>

While plastics themselves can cause immense damage to ecosystems and wildlife, small organic chemicals utilised as monomers or additives to improve polymer properties can pollute the environment and poison organisms.<sup>37</sup> For example, the monomer bisphenol A exerts oestrogenic effects, and phthalate plasticisers have been shown to reduce testosterone production affecting reproduction in humans and other organisms.<sup>35,40</sup> Polychlorinated biphenols are a persistent organic pollutant with wide ranging toxic and environmentally damaging effects. Organotin compounds which are added as plastic stabilisers are extremely toxic causing endocrine disruption and impairment of the immune system. The water solubility of the additives and the ease at which

the chemical can migrate in the polymer matrix determines how quickly leaching takes place.<sup>36</sup>

In addition to toxic chemicals leaching into the environment from plastics, the opposite process may also occur where contaminants are absorbed. This has the effect of concentrating toxic pollutants which poses elevated risks to animals which may ingest the plastic. In the low pH environment of the digestive system the toxic organic pollutants can desorb and poison an animal.<sup>36</sup> Ryan *et al.* showed a positive correlation between the concentration of polychlorinated biphenols in the fat tissue of birds and the quantity of ingested plastic.<sup>41</sup>

### **1.4 Alternatives to unsustainable plastics**

Due to the detrimental environmental impact of many conventional plastics there is a need for sustainable alternatives. A polymer may be bio-derived if it is formed from renewable chemical feedstocks. A polymer is degradable if under suitable conditions the polymer matrix breaks down. Degradation here refers to chemical degradation where the polymer chains are broken down by chain scission reactions. A polymer is biodegradable if this degradation occurs under natural environmental conditions. A polymer which is both bio-derived and biodegradable is ideal in terms of sustainability as it is not produced from a finite resource such as crude oil and following completion of its purpose, it will degrade into non-toxic products which will not pollute the environment. An example of a polymer which meets these criteria is the polyester, poly(lactic acid) (PLA). There are polymers which are bio-derived but non-degradable. For example, bio-derived polyethylene (bio-PE) or poly(ethyl terephthalate) (bio-PET) and conversely polymers which are petrochemical based can be biodegradable, such as poly(caprolactone) (PCL). A polymer may also be compostable, where degradation occurs under specific conditions which are not found naturally in the environment.<sup>32</sup>

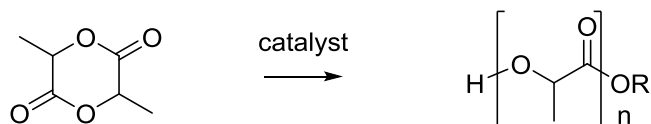
If current levels of plastic consumption continue or, as is more likely, increases then sustainable alternatives are required if the negative impacts of current plastic technologies are to be reduced. For a sustainable plastic to be a viable



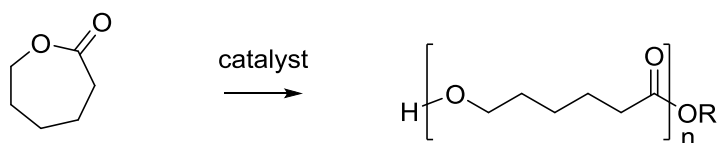
alternative it must be cost effective and exhibit competitive properties to the non-sustainable materials that are currently employed.<sup>42</sup>

Polyesters have the potential to provide alternative sustainable plastics for a variety of applications, from rigid thermosets to flexible elastomers. The inherent hydrolysability of the polyester bonds in these plastics enables facile degradation under suitable conditions.<sup>43</sup> Polyesters can be synthesised through either a step-growth or a chain growth polymerisation. The ROP of cyclic monomers is an efficient route to polyesters and allows for excellent control over molecular weight and polymer dispersity.<sup>17</sup>

ROP of lactide



ROP of  $\epsilon$ -caprolactone



**Scheme 9** Ring-opening polymerisation (ROP) of lactide and  $\epsilon$ -caprolactone

The ROP of lactide and  $\epsilon$ -caprolactone are two well-established routes to hydrolysable polyesters (Scheme 9). These plastics are biodegradable, bio-compatible and exhibit good mechanical properties. They have been utilised as packaging and as biomedical implants. Hundreds of thousands of tonnes of PLA are produced every year globally.<sup>44</sup>

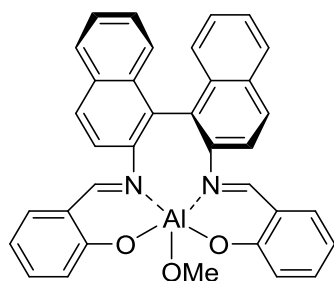
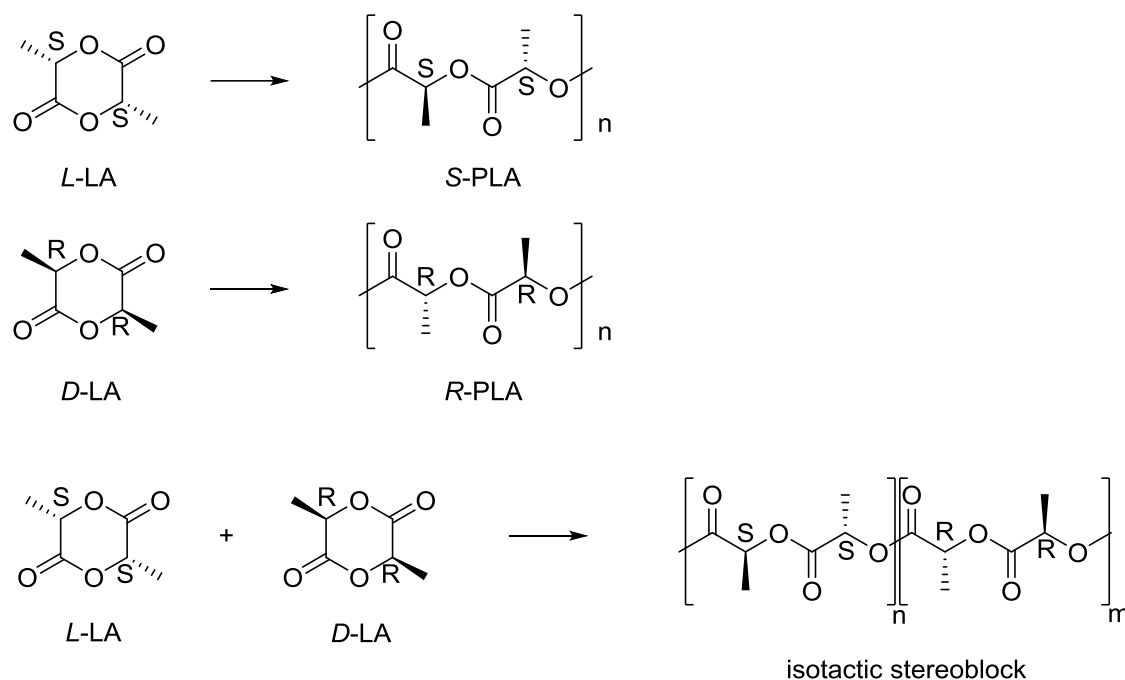


**Figure 6** Enantiomerically pure Schiff base aluminium complex (**1.1**)<sup>45</sup>

PLA is formed from the ring-opening polymerisation of lactide, which itself is formed from lactic acid. Lactide contains two stereocentres and exists in three configurations; D-lactide (*RR*-LA), L-lactide (*SS*-LA) and meso-lactide (*RS*-LA);<sup>46</sup> the arrangement of *R* and *S* stereogenic centres along the polymer chain affects the mechanical and physical properties of the polymer. Polymers with high stereoregularity form highly crystalline plastics which can yield improved properties. Stereoregular PLA can be produced from a racemic mixture of lactide (*rac*-LA) when a stereoselective catalyst is utilised. Spassky and colleagues reported that in the polymerisation of *rac*-LA catalysed by an enantiomerically pure Schiff base aluminium complex (**1.1**) (Figure 6), the rate of reaction of *RR*-LA was 19 times faster than that of *SS*-LA. At 50% conversion the polymer synthesised was predominantly isotactic *R*-PLA. At 100% conversion the PLA produced had a tapered stereoblock microstructure where the stereochemistry of the polymer chain changed gradually from *R*-PLA to *S*-PLA. The stereoblock PLA had a melting point ( $T_m$ ) of 187 °C which is higher than the  $T_m$  of the pure isotactic *R*-PLA and *S*-PLA which have values between 170 – 180 °C.<sup>45</sup> The stereocomplex between *R*-PLA and *S*-PLA has an elevated  $T_m$  (230 °C) resulting from the high crystallinity in the material (Scheme 10).<sup>47,48</sup> The stereoselectivity can be achieved either through enantiomorphic site control or chain-end control. Under enantiomorphic site control, the relative rates of reaction of *RR*-LA and *SS*-LA at the active site of a catalyst are significantly different, leading to a kinetic preference for the ROP of one monomer over the other. This selectivity is a result of a chiral environment at the catalyst produced by supporting ligands. Conversely chain-end control operates when the stereochemistry of the previous ring-opened monomer unit influences which monomer is incorporated next; any chirality of the catalyst is incidental and has no bearing on the tacticity of the resulting polymer and catalysts are often achiral. This means that the initiation reaction occurs without any preference to a particular monomer.<sup>49–51</sup>

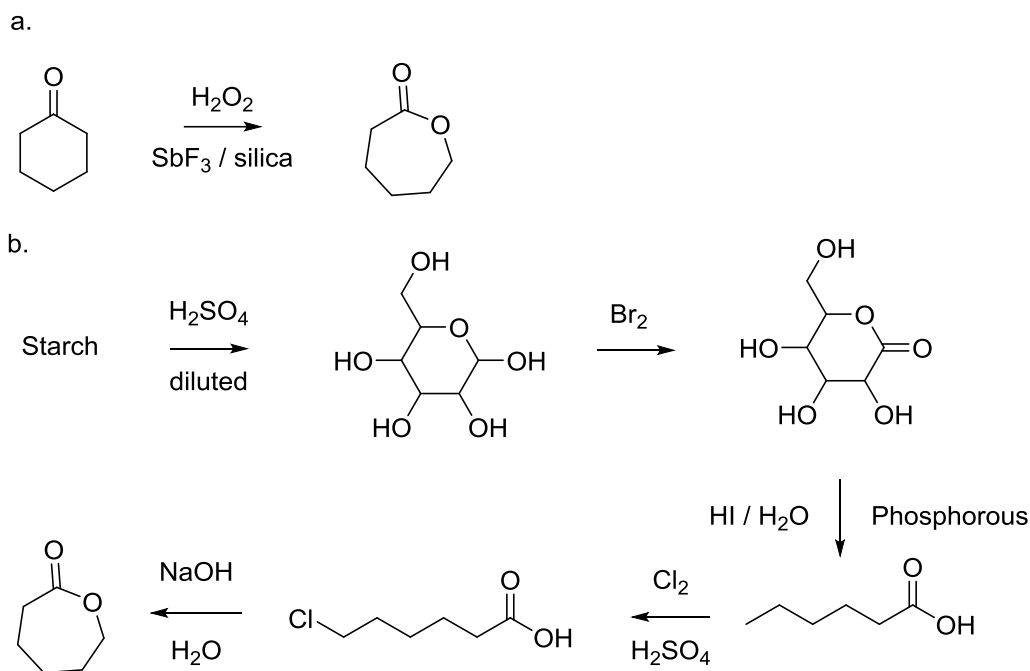
## Chapter 1 - An Introduction



**Scheme 10** Production of isotactic PLA and an isotactic stereoblock PLA<sup>47,48</sup>

The ROP of lactones is an effective route to degradable polyesters.<sup>52</sup> PCL can be produced from the monomer  $\epsilon$ -caprolactone. PCL is highly biocompatible and is therefore ideal for use in biomedical and pharmaceutical applications. The material shows negligible toxicity with the oral LD<sub>50</sub> for rats expected to be over 2,000 mg/kg. Whilst the majority of  $\epsilon$ -caprolactone is produced through the Bayer Villiger oxidation of cyclohexanone (a non-renewable feedstock), it is possible to form the monomer from biorenewable starch (Scheme 11).<sup>53</sup> PCL can be produced by polycondensation,<sup>54</sup> enzymatic polymerisation,<sup>55</sup> cationic polymerisation,<sup>56</sup> anionic polymerisation<sup>57</sup> or a coordination-insertion mechanism.<sup>23,58</sup> A wide variety of catalysts have been utilised with a wide range of ligands and metals including alkali and alkali earth metals, lanthanides, Group IV metals and a variety of transition metals.<sup>53</sup>

## Chapter 1 - An Introduction



**Scheme 11** a. Bayer Villiger oxidation of cyclohexanone b. Production of  $\epsilon$ -caprolactone from starch<sup>53</sup>

Whilst PCL and PLA have proven to be extremely useful for some specific applications they have limited applications. There is limited capacity to vary the properties of PCL and PLA due to the lack of potential monomer variations and lack of opportunities for post-polymerisation modification.<sup>59,60</sup> It is possible to alter the properties of a plastic by using additives or polymer blends, however these approaches can have a detrimental effect on the biodegradability and recyclability of the plastics. Stabilisers are added to a plastic in order to extend the lifespan of the material, however this also has the effect of increasing the resistance to degradation following the end of a products life-cycle. For example, starch based plastics are no longer considered biodegradable if additives are used or if the starch is blended with another plastic.<sup>32</sup>

Whilst these polymers have many advantageous properties, a major challenge is to produce sustainable plastics which can maintain mechanical strength at elevated temperatures. The temperature at which a polymer changes from a hard solid material to a soft and rubbery one is defined as the glass-transition temperature ( $T_g$ ). Sustainable polyesters with a  $T_g > 100$  °C are particularly sought after as these materials will not deform in the presence of boiling

## ***Chapter 1 - An Introduction***

water.<sup>59</sup> Amorphous PLA starts to soften at relatively modest temperatures due to a low  $T_g$  (50 – 60 °C). The  $T_g$  of PCL and PLA is far lower than what is routinely achieved with traditional plastics.<sup>61</sup>

Due to the limitations of the established biodegradable polyesters such as PLA and PCL, there is a need for a new type of hydrolysable polymer which can exhibit a wide range of properties. The alternating ROCOP of epoxides and cyclic anhydrides has the potential to produce polyesters with tunable properties thanks to the plethora of possible monomer combinations, some of which also offer the potential for post-polymerisation modification.<sup>44,59</sup>

### 1.5 Introduction to macrocyclic ligands and complexes

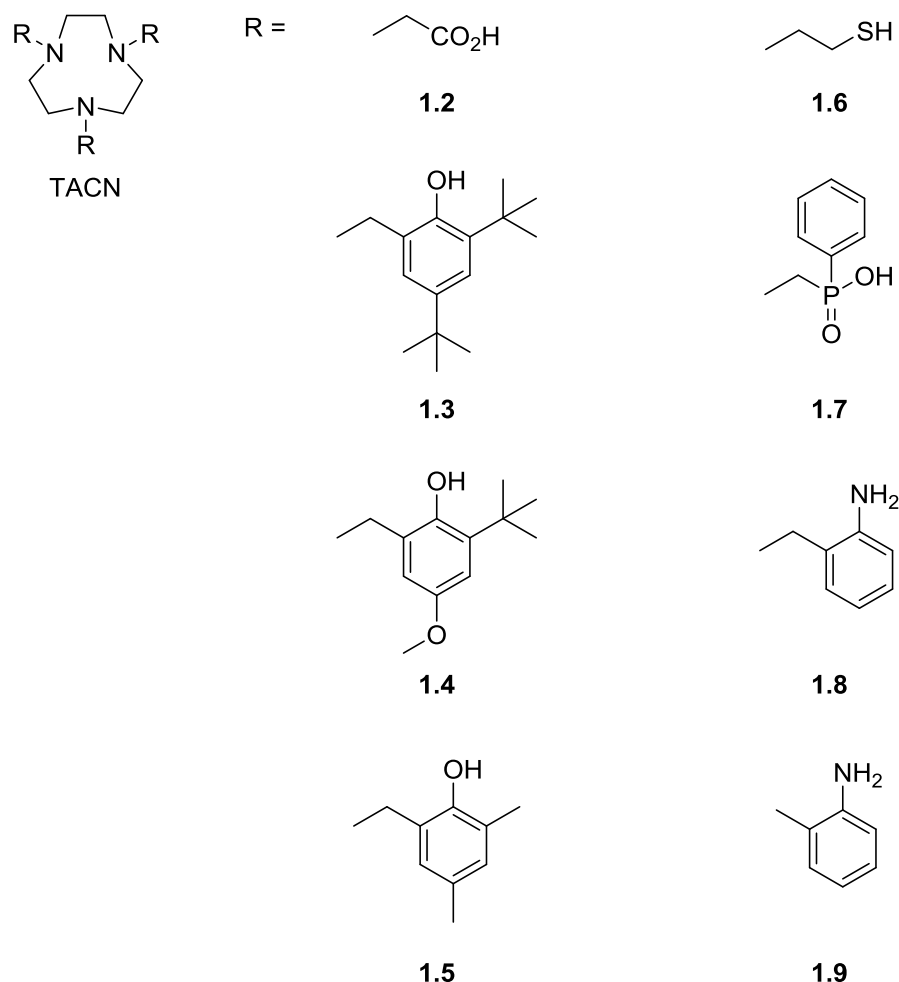


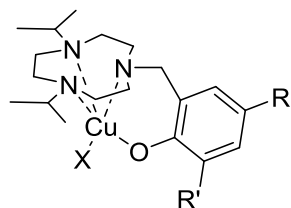
**Figure 7** Trisubstituted 1,4,7-triazacyclononane (TACN) rings<sup>62</sup>

Macrocycles have been explored as ligands for a large number of metals. They often form extremely stable metal complexes resulting from strong ligand field stabilisation, especially for the aza macrocycles containing nitrogen donors.<sup>62</sup> The chelate effect gives rise to stable complexes due to the entropic benefit of polydentate ligands. Macrocyclic ligands exhibit additional benefits due to the macrocyclic effect which is a result of the constrained cyclic ligands “pre-organised” for coordination to a metal centre.<sup>63</sup> Triaza, tetraaza and pentaaza macrocycles are commonly utilised in coordination chemistry.<sup>64</sup> The tridentate 1,4,7-triazacyclononane (TACN) macrocycle has been used extensively with many metals, particularly d-block elements. In order to increase the coordination number of these ligands, additional donors can be added to the ring. Trisubstitution of the TACN macrocycle with appropriate donor-containing

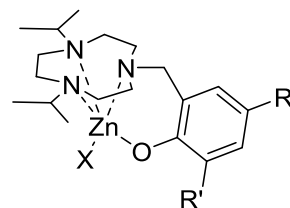
pendant arms increases the number of donor atoms to six, potentially affording coordinatively saturated complexes. Pendant arms with alcohol, amine, thiol, phosphine, and carboxylate functionalities have been reported (Figure 7).<sup>62</sup>

The ligand 1,4,7-triacetate-TACN (**1.2**) has been complexed with indium and gallium to give very stable complexes. <sup>111</sup>In, <sup>67</sup>Ga and <sup>68</sup>Ga are possible radioisotopes for tumour imaging and good stability is crucial for the development of effective radiopharmaceuticals.<sup>65</sup> TACN trisubstituted with 3,5-di-*tert*-butylphenol (**1.3**), 3-*tert*-butyl-5-methoxyphenol (**1.4**) and 3,5-dimethylphenol (**1.5**) were coordinated to Ga<sup>III</sup>, Sc<sup>III</sup> and Fe<sup>III</sup>. These complexes can be reversibly oxidised electrochemically to give ligand-centred phenoxyl radicals.<sup>66</sup> Al<sup>III</sup> and In<sup>III</sup> complexes with **1.2** and 1,4,7-tris(2-mercaptoethyl)-TACN (**1.6**) have been reported.<sup>67</sup> 1,4,7-trimethylenetrakis(phenylphosphinate)-TACN (**1.7**) was ligated to Co<sup>II</sup>, Ni<sup>II</sup>, Cu<sup>II</sup>, Zn<sup>II</sup>, Fe<sup>III</sup>, Co<sup>III</sup>, Ga<sup>III</sup> and In<sup>III</sup>. The *in vivo* biodistribution of radiolabelled <sup>67</sup>Ga and <sup>111</sup>In complexes were investigated.<sup>68</sup> Wieghardt and colleagues have extensively studied the ligand 1,4,7-tris(*o*-aminobenzyl)-TACN (**1.8**) with a variety of metals, Fe<sup>II</sup>, Fe<sup>III</sup>, Co<sup>II</sup>, Co<sup>III</sup>, Mn<sup>II</sup>, Mn<sup>IV</sup>, Ni<sup>II</sup>, Cu<sup>II</sup>, Pd<sup>II</sup>, Zn<sup>II</sup>, Cd<sup>II</sup>, Hg<sup>II</sup>.<sup>69–71</sup> Fallis *et al.* reported the complexation of the more rigid 1,4,7-tris(2-aminophenyl)-TACN (**1.9**) ligand with divalent first-row transition metal perchlorate salts to yield compounds of the type [M<sup>II</sup>(L)][ClO<sub>4</sub>]<sub>2</sub> where L = **1.9** and M = Fe<sup>II</sup>, Ni<sup>II</sup>, Cu<sup>II</sup> and Zn<sup>II</sup>.<sup>72</sup> The use of trisubstituted TACN ligands has proved to be an effective route to very stable metal complexes. Evidence of this can be seen by comparison of stability constants (log K) of Mn<sup>II</sup> complexes bearing the unsubstituted TACN ligand and **1.2** for which values of 5.8 and 14.3 were recorded respectively.<sup>62</sup>

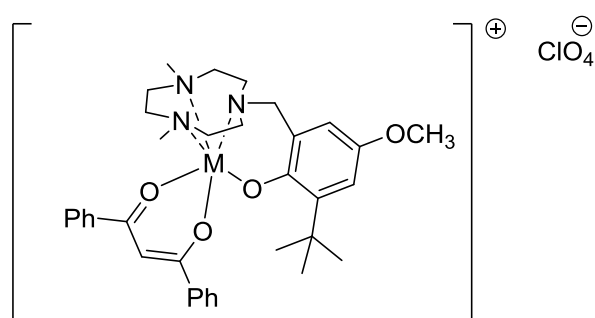
## Chapter 1 - An Introduction



$L = \mathbf{1.10}$   $R = R' = \text{CH}_3$   $X = \text{Cl}$   
 $L = \mathbf{1.11}$   $R = R' = \text{C}(\text{CH}_3)_3$   $X = \text{Cl}$   
 $L = \mathbf{1.12}$   $R = \text{CH}_3$ ,  $R' = \text{OCH}_3$   $X = \text{Cl}$   
 $L = \mathbf{1.13}$   $R = \text{C}(\text{CH}_3)_3$ ,  $R' = \text{SCH}_3$   $X = \text{Cl}$   
 $L = \mathbf{1.11}$   $R = R' = \text{C}(\text{CH}_3)_3$   $X = \text{O}_3\text{SCF}_3$   
 $L = \mathbf{1.11}$   $R = R' = \text{C}(\text{CH}_3)_3$   $X = \text{OBn}$   
 $L = \mathbf{1.11}$   $R = R' = \text{C}(\text{CH}_3)_3$   $X = \text{O}_2\text{CCH}_3$

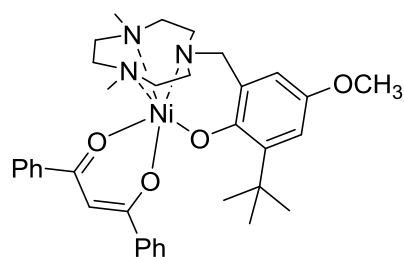


$L = \mathbf{1.10}$   $R = R' = \text{CH}_3$   $X = \text{Cl}$   
 $L = \mathbf{1.11}$   $R = R' = \text{C}(\text{CH}_3)_3$   $X = \text{Cl}$   
 $L = \mathbf{1.13}$   $R = \text{C}(\text{CH}_3)_3$ ,  $R' = \text{SCH}_3$   $X = \text{Cl}$

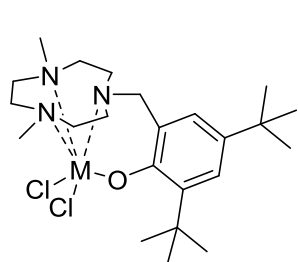


$L = \mathbf{1.14}$   $[\text{M}(\text{L})(\text{Ph}_2\text{acac})]\text{ClO}_4$

$\text{M} = \text{Co}^{\text{III}}$   
 $\text{M} = \text{Cr}^{\text{III}}$   
 $\text{M} = \text{Mn}^{\text{III}}$   
 $\text{M} = \text{Ga}^{\text{III}}$

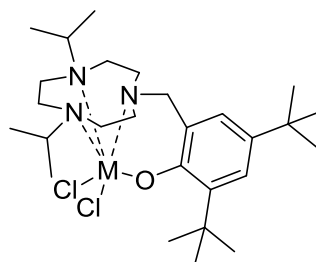


$L = \mathbf{1.14}$   $[\text{Ni}(\text{L})(\text{Ph}_2\text{acac})]$



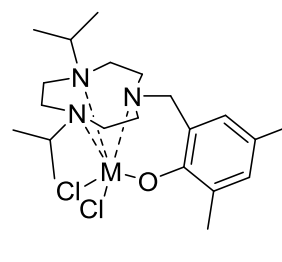
$L = \mathbf{1.15}$   $[\text{M}(\text{L})\text{Cl}_2]$

$\text{M} = \text{Al}^{\text{III}}$   
 $\text{M} = \text{Ga}^{\text{III}}$   
 $\text{M} = \text{In}^{\text{III}}$   
 $\text{M} = \text{Sc}^{\text{III}}$   
 $\text{M} = \text{Y}^{\text{III}}$   
 $\text{M} = \text{Ti}^{\text{III}}$   
 $\text{M} = \text{V}^{\text{III}}$   
 $\text{M} = \text{Ti}^{\text{III}}$



$L = \mathbf{1.11}$   $[\text{M}(\text{L})\text{Cl}_2]$

$\text{M} = \text{Ga}^{\text{III}}$   
 $\text{M} = \text{In}^{\text{III}}$   
 $\text{M} = \text{Sc}^{\text{III}}$   
 $\text{M} = \text{Y}^{\text{III}}$   
 $\text{M} = \text{Ti}^{\text{III}}$   
 $\text{M} = \text{V}^{\text{III}}$   
 $\text{M} = \text{Cr}^{\text{III}}$   
 $\text{M} = \text{Ti}^{\text{III}}$



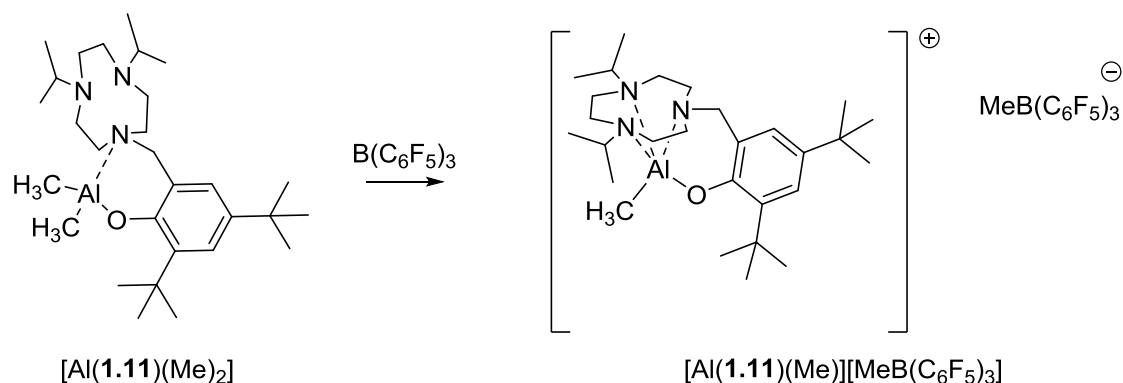
$L = \mathbf{1.10}$   $[\text{M}(\text{L})\text{Cl}_2]$

$\text{M} = \text{Ga}^{\text{III}}$   
 $\text{M} = \text{In}^{\text{III}}$   
 $\text{M} = \text{Sc}^{\text{III}}$   
 $\text{M} = \text{Ti}^{\text{III}}$

**Figure 8** Mono-substituted 1,4,7-triazacyclononane (TACN) complexes<sup>73–78</sup>



Mono-substituted 1,4,7-triazacyclononanes are interesting tetradentate ligands. The lower coordination number of these ligands compared to the tri-substituted analogues allows for reactivity at the remaining metal coordination sites. Different variations of phenoxide mono-pendant arm TACN ligands with both methyl and isopropyl groups on the non-donor-functionalised nitrogens of the TACN ring and with a variety of ortho and para substituents on the phenoxy ring were complexed to Cu<sup>I</sup>,<sup>79</sup> Cu<sup>II</sup>,<sup>73,74</sup> Zn<sup>II</sup>,<sup>74</sup> Cr<sup>III</sup>, Mn<sup>III</sup>, Co<sup>III</sup>, Ni<sup>II</sup> and Ga<sup>III</sup> (Figure 8).<sup>75</sup> The copper complexes were studied as models for the active site of galactose and glyoxal oxidases.<sup>73,74</sup> The ligands (3,5-dimethyl-2-hydroxybenzyl)-4,7-diisopropyl-TACN (**1.10**), (3,5-di-*tert*-butyl-2-hydroxybenzyl)-4,7-diisopropyl-TACN (**1.11**) and (3,5-di-*tert*-butyl-2-hydroxybenzyl)-4,7-dimethyl-TACN (**1.15**) were reacted with a series of group 3, 13 and early transition metals to give complexes of Al<sup>III</sup>, Ga<sup>III</sup>, In<sup>III</sup>, Tl<sup>III</sup>, Sc<sup>III</sup>,<sup>76</sup> Y<sup>III</sup>, Ti<sup>III</sup>,<sup>77</sup> V<sup>III</sup>, Cr<sup>III</sup>.<sup>78</sup>



**Scheme 12** Change in **1.11** ligand binding from  $\kappa^2$  to  $\kappa^4$  upon the abstraction of a methyl co-ligand.<sup>80</sup>

In the mono-pendant arm examples above, all of the available donors are bonded to the metal centre,<sup>73–78</sup> however Mountford *et al.* reported the formation of an aluminium complex with a mono phenoxy pendant arm TACN ligand bound to the metal centre in a  $\kappa^2$  arrangement through the phenoxide and one nitrogen of the TACN ring, rather than the conventional  $\kappa^4$  binding mode.<sup>80</sup> Reaction of AlMe<sub>3</sub> with **1.11** yielded an approximately tetrahedral complex containing the two methyl co-ligands and the pendant arm TACN ligand bonded in a  $\kappa^2$  manner, [Al(**1.11**)(Me)<sub>2</sub>]. Reaction of this complex with B(C<sub>6</sub>F<sub>5</sub>)<sub>3</sub> abstracted a methyl group and gave the cationic organoaluminum

compound  $[\text{Al}(\mathbf{1.11})(\text{Me})]^+$  (Scheme 12). Interestingly, following this transformation, the ligand now binds to the aluminium centre through all of its available donors in a  $\kappa^4$  manner. A variation of this ligand with a 2-hydroxy-2-methylethyl pendant arm in place of the phenoxy, shows similar interconversion of coordination modes in a bimetallic aluminium methyl complex.<sup>81</sup> An indium complex with **1.11** also shows the same variation from  $\kappa^2$  to  $\kappa^4$  upon formation of the cationic organoindium species.<sup>81</sup> Mountford and colleagues reported that these metal complexes were fluxional in solution. This hemilability, along with the ability to modify and tune the electronic and stereochemical properties of the pendant arm macrocycle, suggest that these compounds might be effective ligands in homogeneous catalysis. However, the reactivity of both the neutral and cationic forms of the compounds has so far been limited.<sup>80–82</sup>

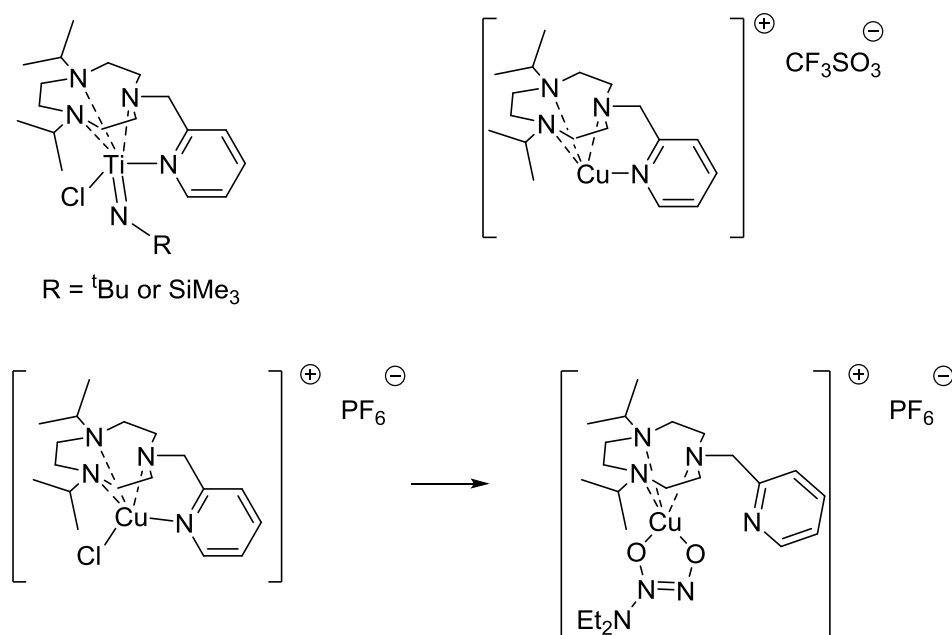


**Figure 9** Pyridyl pendant arm (**1.16**) macrocycle complexes<sup>77,83,84</sup>

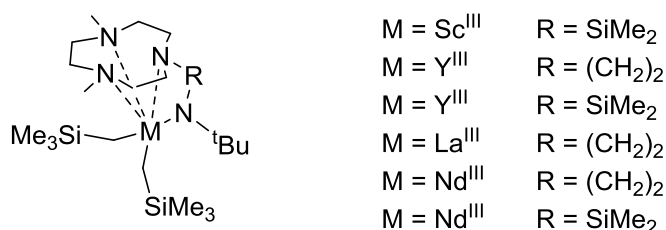


**Figure 10** Metal complexes of amide functionalised TACN ligands **1.17** (R = (CH<sub>2</sub>)<sub>2</sub>) and **1.18** (R = SiMe<sub>2</sub>)<sup>85–89</sup>

Other examples of mono-pendant arm macrocycles have also been explored as ligands. 1-(2-pyridylmethyl)-4,7-diisopropyl-TACN (**1.16**) (Figure 9) is a tetradentate neutral ligand and has been utilised to stabilise a Ti imido complex.<sup>77</sup> It has also been complexed to Cu<sup>I</sup><sup>83</sup> and Cu<sup>II</sup>.<sup>84</sup> The pyridyl group of the ligand showed hemilability in these compounds, but TACN ring remained bound to metal centre. Hessen and colleagues have studied an amido pendant arm TACN ligand with either an ethyl (L = **1.17**) or dimethylsilyl (L = **1.18**) bridge. Bisalkyl complexes with Sc<sup>III</sup>, Y<sup>III</sup>, La<sup>III</sup> and Nd<sup>III</sup> were synthesised (Figure 10). The cationic forms of the compounds were efficient catalysts in the polymerisation of ethylene. The reactivity of these compounds was affected by the choice of pendant arm linker with the ethyl giving more stability than the dimethylsilyl bridge.<sup>85–89</sup>

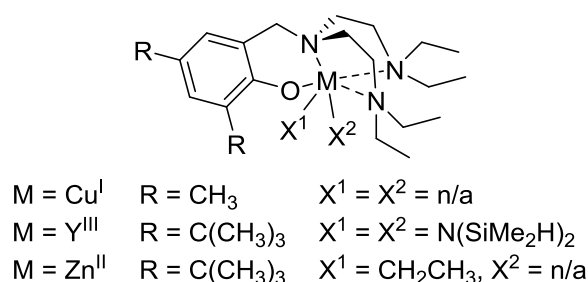


**Figure 11** Tripodal phenoxytriamine (**1.19**) metal complexes. When M = Cu and Zn the ligand binds  $\kappa^3$  with one diethylamino group unbound<sup>90–92</sup>

Complexes bearing the tripodal phenoxytriamine ligand are also of interest (Figure 11). These compounds have an “open” TACN structure and the same phenoxy pendant arm as the mono phenoxy substituted TACN ligands discussed earlier. Matyjaszewski reported the formation of a Cu<sup>I</sup> complex with 2,4-di-methyl-6-bis[2-(diethylamino)ethyl]aminomethylphenol (**1.19**). This complex was used as a catalyst for atom transfer radical polymerisation of *n*-

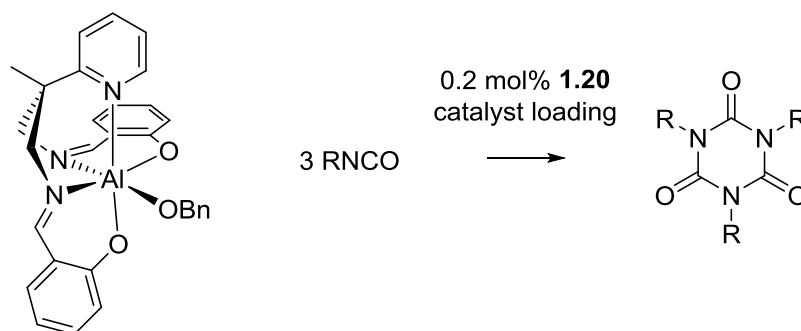
butyl acrylate.<sup>90</sup> Yeldon reported the formation of a chromium chloride complex with the same ligand. In this complex, the potentially tetradentate ligand bound to the metal centre in a  $\kappa^4$  manner, however when coordinated to zinc the same ligand bound in a  $\kappa^3$  manner.<sup>91</sup> A yttrium example was synthesised from  $[Y(N(SiMe_2H)_2)_3(THF)_2]$  in which the ligand was formally bound in a  $\kappa^3$  arrangement. However, the authors reported that the compound had complex and temperature dependant NMR spectra, indicative of a fluxional system in solution, most likely arising from rapid exchange of the diethylamino pendant arms. The complex proved to be an effective catalyst for the ROP of  $\epsilon$ -caprolactone and lactide achieving good activity at room temperature, high molecular weights, and good selectivity under optimised conditions.<sup>92</sup>

There have been some limited examples of complexes bearing macrocyclic ligands being utilised in catalysis.<sup>92</sup> There is great potential for further research in this area, the ability to tune the electronics and sterics of these ligands along with good compatibility with a variety of metals are very attractive features. The examples which show hemilabile binding to a metal centre are of particular interest, as a dynamic coordination sphere may allow for greater reactivity offering substrates more opportunity to access the metal centre. Hemilability has proved to be a highly advantageous feature for effective homogeneous catalysts used in a variety of transformations.<sup>93</sup>

### **1.6 Hemilabile ligands**

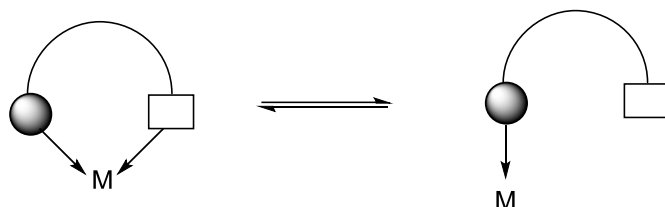
Previous work in the Ward group has shown that catalysts containing the hemilabile pyridyl-bis(phenoxyimine) (salpy) ligand were very effective for the ring-opening polymerisation (ROP) of lactide and  $\epsilon$ -caprolactone.  $[Al(Salpy)(OBn)]$  (**1.20**) was also extremely efficient in the trimerisation of isocyanates to isocyanurates (Scheme 13). Isocyanurates are useful compounds found in a wide variety of applications from building insulation to pesticides. The hemilability of the pyridine pendant arm in the salpy ligand has been shown to be crucial to the activity of these catalysts.<sup>94</sup>

Al(Salpy)(OBn) **1.20**

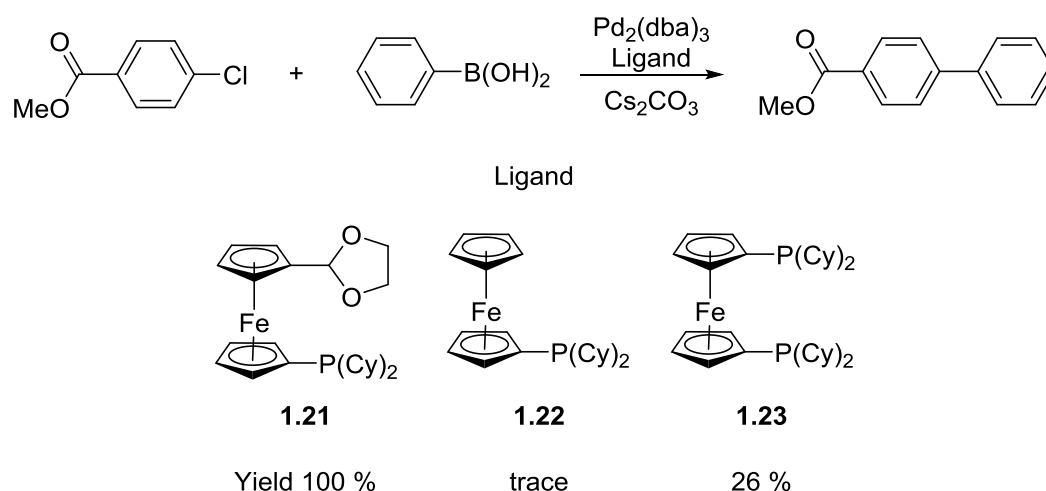


**Scheme 13** Cyclotrimerisation of isocyanates catalysed by [Al(Salpy)(OBn)] (**1.20**)<sup>94</sup>

There have been many examples of metal complexes containing hemilabile ligands which are effective catalysts for a wide variety of reactions. Hemilabile ligands contain two or more coordination sites and have a dynamic coordination sphere around a metal centre. One or more of the metal donors can associate and dissociate depending on the chemical environment of the complex. Dissociation of a ligand donor may open a coordination site enabling reactivity towards a substrate, but in a hemilabile ligand system this dissociation is reversible and the donor can potentially recoordinate to stabilise a metal centre following the reaction (Scheme 14). A flexible coordination sphere can enable the binding/release of co-ligands, stabilise variable metal oxidation states and adapt to different geometric constraints. Metal complexes containing hemilabile ligands have been active as catalysts for a number of reactions including hydroformylation, epoxidation, hydrogenation, carbonylation, polymerisation and cross-coupling reactions.<sup>93,95</sup>



**Scheme 14** Bonding modes of hemilabile ligand



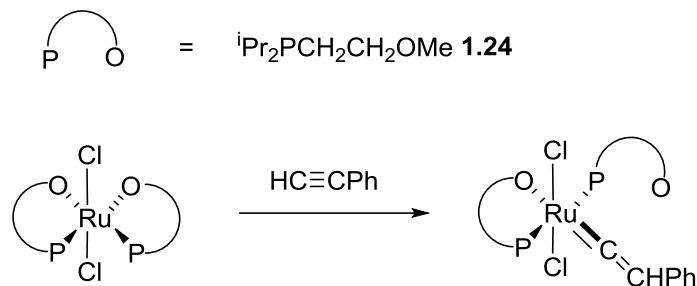
**Scheme 15** Effect of ligand on the Pd catalysed Suzuki Cross-Coupling<sup>96</sup>

In the Suzuki coupling of haloarenes and aryl boronic acids, a  $\text{Pd}(\text{PPh}_3)_4$  catalyst is commonly used. However, in order to undergo the oxidative addition of an aryl halide, which is the first step in the catalytic cycle, the catalyst must dissociate two of its strongly bound phosphine ligands. This dissociation forms the active  $\text{Pd}^0(\text{PPh}_3)_2$ , but these coordinatively unsaturated species are very unstable and decomposition can cause poor turnover numbers. Hemilabile ligands have been found to be very effective for the Suzuki coupling of haloarenes and aryl boronic acids. They have the ability to stabilise coordinatively unsaturated species and catalytic intermediates preventing decomposition, while maintaining the high reactivity. For example, in the coupling between 4-chlorobenzonitrile and phenyl boronic acid (Scheme 15), the flexible mixed phosphine–ether ligand (**1.21**) outperformed the monophosphine (**1.22**) and diphosphine (**1.23**) analogues (isolated yields 100%, trace and 26% respectively). The combination of a strongly coordinating phosphine group and a weaker ether donor was the most effective.<sup>96</sup>

The presence of a hemilabile ligand can enable reactivity between a metal complex and a substrate that would not normally occur. A ruthenium chloride complex containing a P–O ether phosphine ligand (**1.24**) will react with phenyl acetylene to yield a ruthenium vinylidene. In order for this to occur, an oxygen donor from the hemilabile ligand must dissociate from the metal centre to provide an open coordination site for reaction (Scheme 16). Ruthenium

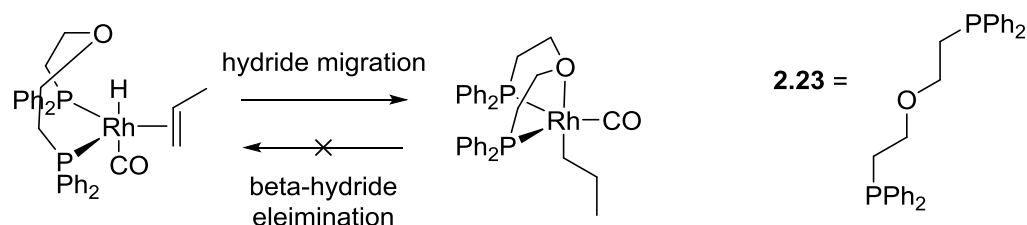
## Chapter 1 - An Introduction

complexes containing  $\text{P}^i\text{Pr}_3$  ligands instead of the hemilabile ligand did not perform this transformation.<sup>97</sup>



**Scheme 16** Isomerisation promoted by a hemilabile ligand<sup>97</sup>

A tridentate diphosphine ether (**1.25**) was an effective ligand for the rhodium-catalysed hydroformylation of alkenes. The catalyst was highly active and showed very little isomerisation (which leads to undesirable internal alkenes). The presence of the hemilabile ether group was reported to be influential as it hindered the beta-hydride elimination reaction, which is responsible for the isomerisation process; it does this by competing with the hydride for the coordination site, and thus disfavours the beta-hydride elimination (Scheme 17).<sup>95,98</sup>



**Scheme 17** Suppression of beta-hydride elimination<sup>95,98</sup>

Aluminium complexes with the pendant arm macrocycle ligand **1.15** (**L1**) were selected as potential catalysts for the synthesis of hydrolysable polyesters. Whilst the reactivity of such complexes has so far been limited, the hemilability reported for **1.11**,<sup>80</sup> lead us to be optimistic that  $[\text{Al}(\text{L1})\text{Cl}_2]$  (**1**) and  $[\text{Al}(\text{L1})(\text{O}^i\text{Pr})_2]$  (**2**) may be effective catalysts for the ROCOP of epoxides and cyclic anhydrides and the ROP of  $\epsilon$ -caprolactone; the outcome of these studies are the principal subject of this thesis.

**1.7 References for Chapter 1**

- 1 Editorial, *Nat. Commun.*, 2018, **9**, 2157.
- 2 R. J. Ouellette and J. D. Rawn, in *Principles of Organic Chemistry*, eds. R. J. Ouellette and J. D. Rawn, Elsevier, Boston, 2015, pp. 397–419.
- 3 J.-F. Lutz, J.-M. Lehn, E. W. Meijer and K. Matyjaszewski, *Nat. Rev. Mater.*, 2016, **1**, 1–14.
- 4 R. Geyer, J. R. Jambeck and K. L. Law, *Sci. Adv.*, 2017, **3**, e1700782.
- 5 A. Rudin and P. Choi, in *The Elements of Polymer Science & Engineering (Third Edition)*, eds. A. Rudin and P. Choi, Academic Press, Boston, 2013, pp. 1–62.
- 6 K. Balani, V. Verma, A. Agarwal and R. Narayan, in *Biosurfaces*, John Wiley & Sons, Ltd, 2015, pp. 329–344.
- 7 A. Rudin and P. Choi, in *The Elements of Polymer Science & Engineering (Third Edition)*, eds. A. Rudin and P. Choi, Academic Press, Boston, 2013, pp. 149–229.
- 8 M. Chanda and S. K. Roy, *Industrial Polymers, Specialty Polymers, and Their Applications*, CRC Press, 2008.
- 9 J. Stejny, *Polym. Bull.*, 1996, **36**, 617–621.
- 10 A. Shefer and M. Gottlieb, *Macromolecules*, 1992, **25**, 4036–4042.
- 11 A. Rudin and P. Choi, in *The Elements of Polymer Science & Engineering (Third Edition)*, eds. A. Rudin and P. Choi, Academic Press, Boston, 2013, pp. 89–148.
- 12 A. Rudin and P. Choi, in *The Elements of Polymer Science & Engineering (Third Edition)*, eds. A. Rudin and P. Choi, Academic Press, Boston, 2013, pp. 63–87.
- 13 A. Rudin and P. Choi, in *The Elements of Polymer Science & Engineering (Third Edition)*, eds. A. Rudin and P. Choi, Academic Press, Boston, 2013, pp. 305–339.
- 14 A. Rudin and P. Choi, in *The Elements of Polymer Science & Engineering (Third Edition)*, eds. A. Rudin and P. Choi, Academic Press, Boston, 2013, pp. 341–389.



## Chapter 1 - An Introduction

- 15 A. Rudin and P. Choi, in *The Elements of Polymer Science & Engineering (Third Edition)*, eds. A. Rudin and P. Choi, Academic Press, Boston, 2013, pp. 449–493.
- 16 A. Duda and A. Kowalski, in *Handbook of Ring-Opening Polymerization*, John Wiley & Sons, Ltd, 2009, pp. 1–51.
- 17 T. Endo, in *Handbook of Ring-Opening Polymerization*, John Wiley & Sons, Ltd, 2009, pp. 53–63.
- 18 W. Kuran, *Prog. Polym. Sci.*, 1998, **23**, 919–992.
- 19 A.-C. Albertsson, Ed., *Degradable Aliphatic Polyesters*, Springer-Verlag, Berlin Heidelberg, 2002.
- 20 A.-C. Albertsson, I. K. Varma and R. K. Srivastava, in *Handbook of Ring-Opening Polymerization*, John Wiley & Sons, Ltd, 2009, pp. 287–306.
- 21 O. Dechy-Cabaret, B. Martin-Vaca and D. Bourissou, in *Handbook of Ring-Opening Polymerization*, John Wiley & Sons, Ltd, 2009, pp. 255–286.
- 22 Ph. Dubois, N. Ropson, R. Jérôme and Ph. Teyssié, *Macromolecules*, 1996, **29**, 1965–1975.
- 23 A.-C. Albertsson and I. K. Varma, *Biomacromolecules*, 2003, **4**, 1466–1486.
- 24 P. J. A. I. Veld, E. M. Veler, P. V. D. Witte, J. Hamhuis, P. J. Dijkstra and J. Feijen, *J. Polym. Sci. Part Polym. Chem.*, 1997, **35**, 219–226.
- 25 M. P. Dreyfuss and P. Dreyfuss, *Polymer*, 1965, **6**, 93–95.
- 26 W.-F. Su, in *Principles of Polymer Design and Synthesis*, ed. W.-F. Su, Springer, Berlin, Heidelberg, 2013, pp. 267–299.
- 27 G. Odian, in *Principles of Polymerization*, John Wiley & Sons, Ltd, 2004, pp. 544–618.
- 28 F. S. Dainton and K. J. Ivin, *Q. Rev. Chem. Soc.*, 1958, **12**, 61–92.
- 29 M. J. Sanford, N. J. V. Zee and G. W. Coates, *Chem. Sci.*, 2017, **9**, 134–142.
- 30 J. Hopewell, R. Dvorak and E. Kosior, *Philos. Trans. R. Soc. B Biol. Sci.*, 2009, **364**, 2115–2126.
- 31 R. A. Gross and B. Kalra, *Science*, 2002, **297**, 803–807.
- 32 S. Lambert and M. Wagner, *Chem. Soc. Rev.*, 2017, **46**, 6855–6871.

## Chapter 1 - An Introduction

- 33 A. Schecter, *Dioxins and Health*, Springer Science & Business Media, 2013.
- 34 A. P. I. S. A. Dr. and L. A. Bosnea, *Food Rev. Int.*, 2001, **17**, 291–346.
- 35 J. Oehlmann, U. Schulte-Oehlmann, W. Kloas, O. Jagnytsch, I. Lutz, K. O. Kusk, L. Wollenberger, E. M. Santos, G. C. Paull, K. J. W. Van Look and C. R. Tyler, *Philos. Trans. R. Soc. B Biol. Sci.*, 2009, **364**, 2047–2062.
- 36 E. L. Teuten, J. M. Saquing, D. R. U. Knappe, M. A. Barlaz, S. Jonsson, A. Björn, S. J. Rowland, R. C. Thompson, T. S. Galloway, R. Yamashita, D. Ochi, Y. Watanuki, C. Moore, P. H. Viet, T. S. Tana, M. Prudente, R. Boonyatumanond, M. P. Zakaria, K. Akkhavong, Y. Ogata, H. Hirai, S. Iwasa, K. Mizukawa, Y. Hagino, A. Imamura, M. Saha and H. Takada, *Philos. Trans. R. Soc. B Biol. Sci.*, 2009, **364**, 2027–2045.
- 37 H. K. Webb, J. Arnott, R. J. Crawford and E. P. Ivanova, *Polymers*, 2013, **5**, 1–18.
- 38 M. M. Jones, *Mar. Pollut. Bull.*, 1995, **30**, 25–33.
- 39 S. E. Nelms, J. Barnett, A. Brownlow, N. J. Davison, R. Deaville, T. S. Galloway, P. K. Lindeque, D. Santillo and B. J. Godley, *Sci. Rep.*, 2019, **9**, 1–8.
- 40 C. Sonnenschein and A. M. Soto, *J. Steroid Biochem. Mol. Biol.*, 1998, **65**, 143–150.
- 41 P. G. Ryan, C. J. Moore, J. A. van Franeker and C. L. Moloney, *Philos. Trans. R. Soc. B Biol. Sci.*, 2009, **364**, 1999–2012.
- 42 G. L. Gregory, E. M. López-Vidal and A. Buchard, *Chem. Commun.*, 2017, **53**, 2198–2217.
- 43 G. X. De Hoe, M. T. Zumstein, B. J. Tiegs, J. P. Brutman, K. McNeill, M. Sander, G. W. Coates and M. A. Hillmyer, *J. Am. Chem. Soc.*, 2018, **140**, 963–973.
- 44 S. Paul, Y. Zhu, C. Romain, R. Brooks, P. K. Saini and C. K. Williams, *Chem. Commun.*, 2015, **51**, 6459–6479.
- 45 N. Spassky, M. Wisniewski, C. Pluta and A. L. Borgne, *Macromol. Chem. Phys.*, 1996, **197**, 2627–2637.
- 46 S. Inkinen, M. Hakkarainen, A.-C. Albertsson and A. Södergård, *Biomacromolecules*, 2011, **12**, 523–532.

## Chapter 1 - An Introduction

- 47 Y. Ikada, K. Jamshidi, H. Tsuji and S. H. Hyon, *Macromolecules*, 1987, **20**, 904–906.
- 48 H. Tsuji, S. H. Hyon and Y. Ikada, *Macromolecules*, 1991, **24**, 5651–5656.
- 49 N. Nomura, R. Ishii, Y. Yamamoto and T. Kondo, *Chem. – Eur. J.*, 2007, **13**, 4433–4451.
- 50 Z. Qu, R. Duan, X. Pang, B. Gao, X. Li, Z. Tang, X. Wang and X. Chen, *J. Polym. Sci. Part Polym. Chem.*, 2014, **52**, 1344–1352.
- 51 N. Nomura, R. Ishii, M. Akakura and K. Aoi, *J. Am. Chem. Soc.*, 2002, **124**, 5938–5939.
- 52 R. F. Storey and J. W. Sherman, *Macromolecules*, 2002, **35**, 1504–1512.
- 53 A. Arbaoui and C. Redshaw, *Polym. Chem.*, 2010, **1**, 801–826.
- 54 W. H. Carothers, *Chem. Rev.*, 1931, **8**, 353–426.
- 55 R. A. Gross, A. Kumar and B. Kalra, *Chem. Rev.*, 2001, **101**, 2097–2124.
- 56 Y. Shibasaki, H. Sanada, M. Yokoi, F. Sanda and T. Endo, *Macromolecules*, 2000, **33**, 4316–4320.
- 57 K. Ito and Y. Yamashita, *Macromolecules*, 1978, **11**, 68–72.
- 58 W. Yao, Y. Mu, A. Gao, W. Gao and L. Ye, *Dalton Trans.*, 2008, 3199–3206.
- 59 J. M. Longo, M. J. Sanford and G. W. Coates, *Chem. Rev.*, 2016, **116**, 15167–15197.
- 60 R. C. Jeske, A. M. DiCiccio and G. W. Coates, *J. Am. Chem. Soc.*, 2007, **129**, 11330–11331.
- 61 N. J. Van Zee and G. W. Coates, *Angew. Chem. Int. Ed Engl.*, 2015, **54**, 2665–2668.
- 62 P. V. Bernhardt and G. A. Lawrance, *Coord. Chem. Rev.*, 1990, **104**, 297–343.
- 63 H.-J. Buschmann, in *Stereochemical and Stereophysical Behaviour of Macrocycles*, ed. I. Bernal, Elsevier, Amsterdam, 1987, vol. 2, pp. 103–185.
- 64 I. A. Fallis, *Annu. Rep. Sect. Inorg. Chem.*, 2002, **98**, 321–368.

## Chapter 1 - An Introduction

- 65 C. J. Broan, J. P. L. Cox, A. S. Craig, R. Katakya, D. Parker, A. Harrison, A. M. Randall and G. Ferguson, *J. Chem. Soc. Perkin Trans. 2*, 1991, 87–99.
- 66 B. Adam, E. Bill, E. Bothe, B. Goerdts, G. Haselhorst, K. Hildenbrand, A. Sokolowski, S. Steenken, T. Weyhermüller and K. Wieghardt, *Chem. – Eur. J.*, 1997, **3**, 308–319.
- 67 U. Bossek, D. Hanke, K. Wieghardt and B. Nuber, *Polyhedron*, 1993, **12**, 1–5.
- 68 E. Cole, R. C. B. Copley, J. A. K. Howard, D. Parker, G. Ferguson, J. F. Gallagher, B. Kaitner, A. Harrison and L. Royle, *J. Chem. Soc. Dalton Trans.*, 1994, 1619–1629.
- 69 O. Schlager, K. Wieghardt and B. Nuber, *Inorg. Chem.*, 1995, **34**, 6456–6462.
- 70 O. Schlager, K. Wieghardt and B. Nuber, *Inorg. Chem.*, 1995, **34**, 6449–6455.
- 71 O. Schlager, K. Wieghardt, H. Grondéy, A. Rufinska and B. Nuber, *Inorg. Chem.*, 1995, **34**, 6440–6448.
- 72 I. A. Fallis, R. D. Farley, K. M. Abdul Malik, D. M. Murphy and H. J. Smith, *J. Chem. Soc. Dalton Trans.*, 2000, 3632–3639.
- 73 J. A. Halfen, V. G. Young and W. B. Tolman, *Angew. Chem. Int. Ed. Engl.*, 1996, **35**, 1687–1690.
- 74 J. A. Halfen, B. A. Jazdzewski, S. Mahapatra, L. M. Berreau, E. C. Wilkinson, L. Que and W. B. Tolman, *J. Am. Chem. Soc.*, 1997, **119**, 8217–8227.
- 75 J. Müller, A. Kikuchi, E. Bill, T. Weyhermüller, P. Hildebrandt, L. Ould-Moussa and K. Wieghardt, *Inorganica Chim. Acta*, 2000, **297**, 265–277.
- 76 M. E. G. Skinner, B. R. Tyrrell, B. D. Ward and P. Mountford, *J. Organomet. Chem.*, 2002, **647**, 145–150.
- 77 J. D. Gardner, D. A. Robson, L. H. Rees and P. Mountford, *Inorg. Chem.*, 2001, **40**, 820–824.
- 78 S. Y. Bylikin, D. A. Robson, N. A. H. Male, L. H. Rees, P. Mountford and M. Schröder, *J. Chem. Soc. Dalton Trans.*, 2001, 170–180.

## Chapter 1 - An Introduction

- 79 B. A. Jazdzewski, A. M. Reynolds, P. L. Holland, V. G. Young, S. Kaderli, A. D. Zuberbühler and W. B. Tolman, *JBIC J. Biol. Inorg. Chem.*, 2003, **8**, 381–393.
- 80 D. A. Robson, L. H. Rees, P. Mountford and M. Schröder, *Chem. Commun.*, 2000, 1269–1270.
- 81 D. A. Robson, S. Y. Bylikin, M. Cantuel, N. A. H. Male, L. H. Rees, P. Mountford and M. Schröder, *J. Chem. Soc. Dalton Trans.*, 2001, 157–169.
- 82 S. C. Lawrence, B. D. Ward, S. R. Dubberley, C. M. Kozak and P. Mountford, *Chem. Commun.*, 2003, 2880–2881.
- 83 J. A. Halfen, V. G. Young and W. B. Tolman, *J. Am. Chem. Soc.*, 1996, **118**, 10920–10921.
- 84 J. L. Schneider, J. A. Halfen, V. G. Young, V. G. Y. Jason A. Halfen and W. B. Tolman, *New J. Chem.*, 1998, **22**, 459–466.
- 85 S. Bambirra, D. van Leusen, C. G. J. Tazelaar, A. Meetsma and B. Hessen, *Organometallics*, 2007, **26**, 1014–1023.
- 86 S. Bambirra, A. Meetsma, B. Hessen and A. P. Bruins, *Organometallics*, 2006, **25**, 3486–3495.
- 87 C. G. J. Tazelaar, S. Bambirra, D. van Leusen, A. Meetsma, B. Hessen and J. H. Teuben, *Organometallics*, 2004, **23**, 936–939.
- 88 S. Bambirra, D. van Leusen, A. Meetsma, B. Hessen and J. H. Teuben, *Chem. Commun.*, 2001, 637–638.
- 89 W. A. Chomitz and J. Arnold, *Chem. – Eur. J.*, 2009, **15**, 2020–2030.
- 90 Y. Inoue and K. Matyjaszewski, *Macromolecules*, 2003, **36**, 7432–7438.
- 91 A. R. F. Cox, V. C. Gibson, E. L. Marshall, A. J. P. White and D. Yeldon, *Dalton Trans.*, 2006, 5014–5023.
- 92 I. Westmoreland and J. Arnold, *Dalton Trans.*, 2006, **0**, 4155–4163.
- 93 P. Braunstein and F. Naud, *Angew. Chem. Int. Ed.*, 2001, **40**, 680–699.
- 94 M. A. Bahili, E. C. Stokes, R. C. Amesbury, D. M. C. Ould, B. Christo, R. J. Horne, B. M. Kariuki, J. A. Stewart, R. L. Taylor, P. A. Williams, M. D. Jones, K. D. M. Harris and B. D. Ward, *Chem. Commun.*, 2019, **55**, 7679–7682.

## **Chapter 1 - An Introduction**

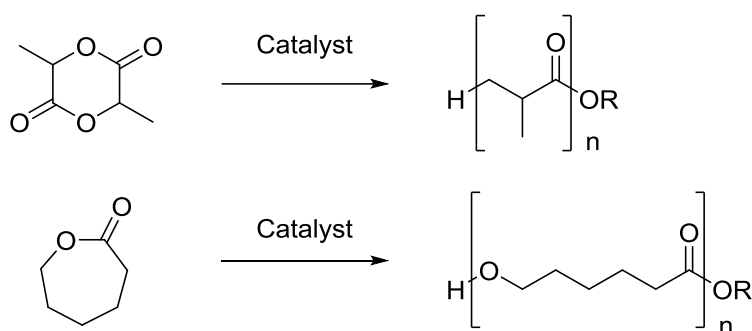
- 95 G. M. Adams and A. S. Weller, *Coord. Chem. Rev.*, 2018, **355**, 150–172.
- 96 Z. Weng, S. Teo and T. S. A. Hor, *Acc. Chem. Res.*, 2007, **40**, 676–684.
- 97 H. Werner, A. Stark, M. Schulz and J. Wolf, *Organometallics*, 1992, **11**, 1126–1130.
- 98 A. Buhling, P. C. J. Kamer, P. W. N. M. van Leeuwen, J. W. Elgersma, K. Goubitz and J. Fraanje, *Organometallics*, 1997, **16**, 3027–3037.

# Chapter 2

**Formation of polyesters via the ring-opening copolymerisation of epoxides and cyclic anhydrides**

## **2.1 Ring-opening copolymerisation (ROCOP) of epoxides and cyclic anhydrides**

There are a number of existing and well-established polymerisations that also yield biodegradable polyesters, such as the ring-opening polymerisations of lactides and caprolactones (Scheme 1). These reactions produce useful plastics and have both been commercialised, however a disadvantage of these materials is that it is very difficult to vary the properties of the polymers.<sup>1</sup> The most common methods for altering the properties of a polymer are by changing the polymer molecular weight, varying the identity of the monomers, post-polymerisation modification (PPM), and by using additives or blends of different polymers. The limited number of available monomers for the ROP of lactide and caprolactone means that the properties and therefore number of applications of these plastics is restricted.<sup>2</sup> The ability to carry out PPM is limited due to the lack of additional appropriate functional groups on the monomers.<sup>1,3-9</sup> There has been some success in producing new monomers with diverse structures however this is proving synthetically challenging. Using polymer blends and additives to improve the properties of polymers have their disadvantages. The reasons being they are no longer single component, meaning the plastic cannot be easily injection moulded, and also using polymer blends and additives makes the processing and recycling of the polymers more difficult.<sup>10</sup> Additives also have the issue of leaching out of the material over time and as many are toxic this is of great concern.<sup>11-13</sup>

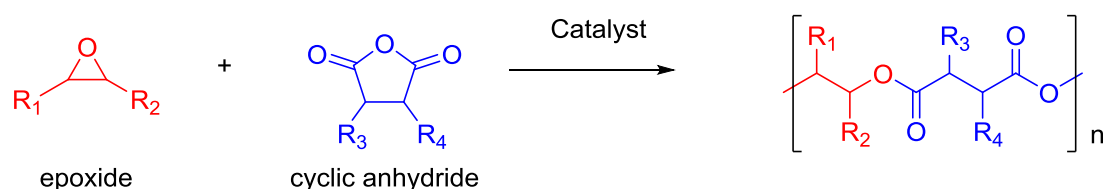


**Scheme 1** Ring-opening polymerisation of lactide (top) and  $\epsilon$ -caprolactone (bottom)



## Chapter 2 - Formation of polyesters via the ring-opening copolymerisation of epoxides and cyclic anhydrides

The ring-opening copolymerisation (ROCOP) of epoxides and cyclic anhydrides is an extremely versatile reaction yielding hydrolysable (biodegradable or compostable) polyesters (Scheme 2).<sup>14</sup> Coates and Van Zee showed the polyesters produced from this polymerisation could be reductively degraded to the alcohol forms of the monomers with  $\text{LiAlH}_4$ .<sup>15</sup> Hao *et al.* reported that this type of polymer will degrade in water and that these polyesters are attractive candidates for biomedical applications.<sup>14</sup> As well as being biodegradable, hydrolysable polymers can, in principle, be depolymerised and the monomers recovered for the re-synthesis of virgin polymers, paving the way for infinite use-reuse cycles that polymer reprocessing does not allow.<sup>16</sup>



**Scheme 2** ROCOP of epoxides and cyclic anhydrides

The ROCOP of epoxides and cyclic anhydrides is an addition polymerisation which has many advantages over step-growth condensation reactions.<sup>1</sup> This reaction has the potential to produce a wide range of plastics with a variety of properties. A major advantage of this copolymerisation over many of the other polymerisations yielding biodegradable plastics, is the ease at which the polymer micro-structure can be varied by changing the identity of the epoxide and cyclic anhydride monomers. The vast number of readily available epoxides and cyclic anhydrides means that there are thousands of different possible monomer combinations, each giving a unique set of physical and mechanical properties.<sup>17</sup>

The ability to vary the polymer microstructure in the ROCOP of epoxides and cyclic anhydrides should allow the production of a wide variety of plastics with varying properties, fostering the ability to tune the polymers to meet specific needs.<sup>17,18</sup> Monomers containing functional groups in addition to either the cyclic anhydride or epoxide are readily available and can be used in the polymerisation without any added complications. Examples of these

## Chapter 2 - Formation of polyesters via the ring-opening copolymerisation of epoxides and cyclic anhydrides

monomers are epichlorohydrin (ECH),<sup>19,20</sup> tetrahydrophthalic anhydride (CEA) and 4-vinylcyclohexene oxide (VCHO).<sup>20</sup> These all contain functional groups capable of undergoing further reactions to functionalise the polymer chain with additional chemical architecture or to cross-link the polymer chains. Both approaches have been used to alter and improve the properties of plastics.<sup>1</sup> The tunability resulting from the ease at which the monomers can be varied and the ability to carry out PPM should reduce the need to use polymer blends and additives.

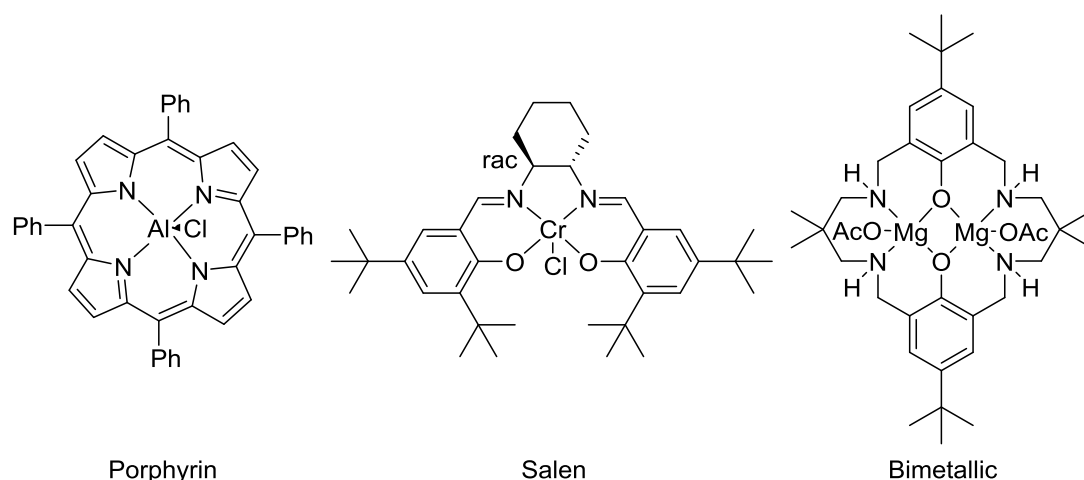


**Figure 1** Porphyrin, salen and bimetallic catalysts for the ring-opening copolymerisation of epoxides and cyclic anhydrides<sup>1</sup>

In 1985 Aida and Inoue reported the first well-controlled ROCOP of propylene oxide (PO) and phthalic anhydride (PhA) using an aluminium porphyrin catalyst.<sup>21</sup> Subsequently further examples of porphyrin catalysts based on aluminium,<sup>22,23</sup> chromium,<sup>22,24–26</sup> manganese,<sup>24,27</sup> iron<sup>27</sup> and cobalt<sup>22,24</sup> were explored. Over recent years, a great deal of work has been focused on developing new catalysts, many of which were based on metal salen and related systems.<sup>1</sup> A wide variety of ligands have been combined with aluminium,<sup>19,23,24,28–31</sup> chromium,<sup>15,20,23,24,28–30,32–36</sup> manganese,<sup>24,28,30,36,37</sup> iron,<sup>19,38</sup> zinc<sup>23</sup> and cobalt<sup>23,24,28–30,33,36,39–41</sup> for use as catalysts in the ROCOP of a range of different epoxides and cyclic anhydrides. Recently, a number of bimetallic catalysts have been synthesised and have exhibited activity in the ROCOP of epoxides and anhydrides.<sup>18,33,35,42–47</sup> The porphyrin catalyst used by Aida and Inoue, and representative examples of salen and bimetallic catalysts, are shown in Figure 1.

## Chapter 2 - Formation of polyesters via the ring-opening copolymerisation of epoxides and cyclic anhydrides

A wide variety of epoxides and cyclic anhydrides (Figure 2) have been utilised in this polymerisation which have yielded a diverse array of plastics with different chemical structures and physical properties. Commonly used epoxides are propylene oxide (PO),<sup>2,3,15,19,21,27,28,31,32,39,48</sup> cyclohexene oxide (CHO),<sup>2,19,20,25,27–29,32,35,37,38,42–53</sup> styrene oxide (SO)<sup>20,24,26,27,32,37,48,53</sup> and (ECH)<sup>3,20,23,27,35,53</sup>. Frequently used anhydrides are maleic anhydride (MA),<sup>2,3,22–24,27,32,34,35,37,46,47,50,51</sup> succinic anhydride (SA),<sup>2,3,22,25,27–29,32,34,35,39,54,55</sup> and phthalic anhydride (PhA).<sup>3,20–22,24,25,29,32,34,37,38,41–45,48,49</sup>

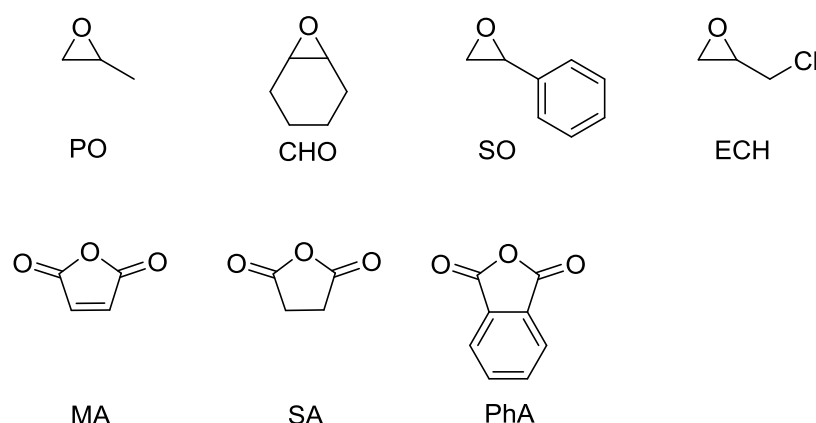


**Figure 2** Commonly used epoxides and anhydrides<sup>1</sup>

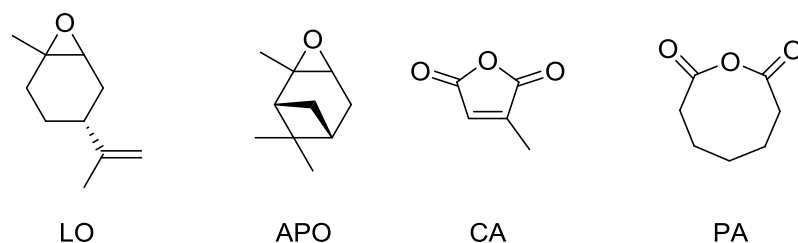


**Figure 3** Examples of bio-derived epoxides and anhydrides<sup>1</sup>

There are a number of bio-derived epoxides and cyclic anhydrides which have been used as monomers in the ROCOP reaction (Figure 3). Examples of such monomers are limonene oxide (LO),<sup>2,30,36</sup> α-pinene oxide (APO),<sup>28</sup> succinic anhydride (SA),<sup>2</sup> citraconic anhydride (CA)<sup>19</sup> and pimelic anhydride (PA).<sup>28</sup> Van Zee and Coates reported the copolymerisation of a series of tricyclic anhydrides formed from the Diels-Alder reaction of bio-derived MA and CA with a series of sustainable dienes;<sup>19</sup> Williams *et al.* showed how the commonly used monomer CHO can be synthesised from the renewably sourced 1,4-

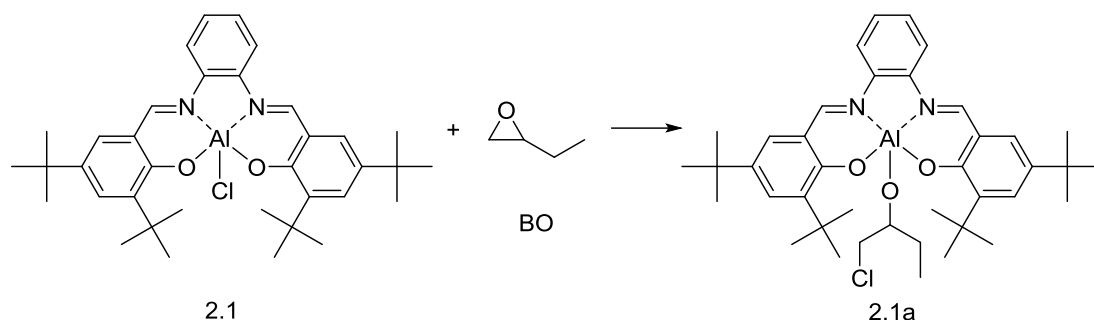
## **Chapter 2 - Formation of polyesters via the ring-opening copolymerisation of epoxides and cyclic anhydrides**

cyclohexadiene, and Lobo *et al.* showed how PhA (another common monomer for ROCOP reactions) can also be produced from biomass-derived starting materials,<sup>56</sup> thereby demonstrating that there is significant potential for bio-derived feedstocks.<sup>33</sup> These monomers have been utilised to form renewable or partially renewable polyesters which, in addition to being alternatives to fossil-fuel based polymers, have high bio-compatibility and degrade to biologically benign compounds.<sup>15,19</sup>

Many ROCOP catalysts are used in conjunction with nucleophilic co-catalysts such as halides (as iminium or ammonium salts), phosphines or 4-dimethylaminopyridine (DMAP). The most regularly used is bis(triphenylphosphoranylidene)ammonium chloride (PPNCl); this co-catalyst is reported to give the fastest rates of reaction compared to other nucleophilic reagents.<sup>29</sup> These co-catalysts have also been utilised to some extent on their own as organocatalysts.<sup>52,57</sup>

Co-catalysts can enhance the rate of the epoxide-anhydride ROCOP and prevent side reactions such as trans-esterification from occurring. They also improve the selectivity of the polymerisation, playing a key role in ensuring high levels of alternation between the two monomers in the polymer chain.<sup>29</sup> The selectivity of a polymer formed from the ROCOP of epoxides and cyclic anhydrides can be readily elucidated by studying its <sup>1</sup>H NMR spectrum. The sequential addition of an epoxide and cyclic anhydride to a polymer chain results in an ester linkage. An undesirable side reaction may however occur in which the addition of an epoxide is followed by another epoxide, resulting in an ether linkage; this decreases the degree of alternation in the polymer chain, and since ethers are not hydrolysed in the same manner as esters, ether linkages consequently decrease the bio-degradability of the polymers. The protons adjacent to ester and ether groups in a polymer chain have significantly different <sup>1</sup>H NMR chemical shifts, therefore the alternating selectivity of a polymer's microstructure can be calculated by a comparison of the integrals of the ester and ether signals in their <sup>1</sup>H NMR spectra.<sup>58</sup>

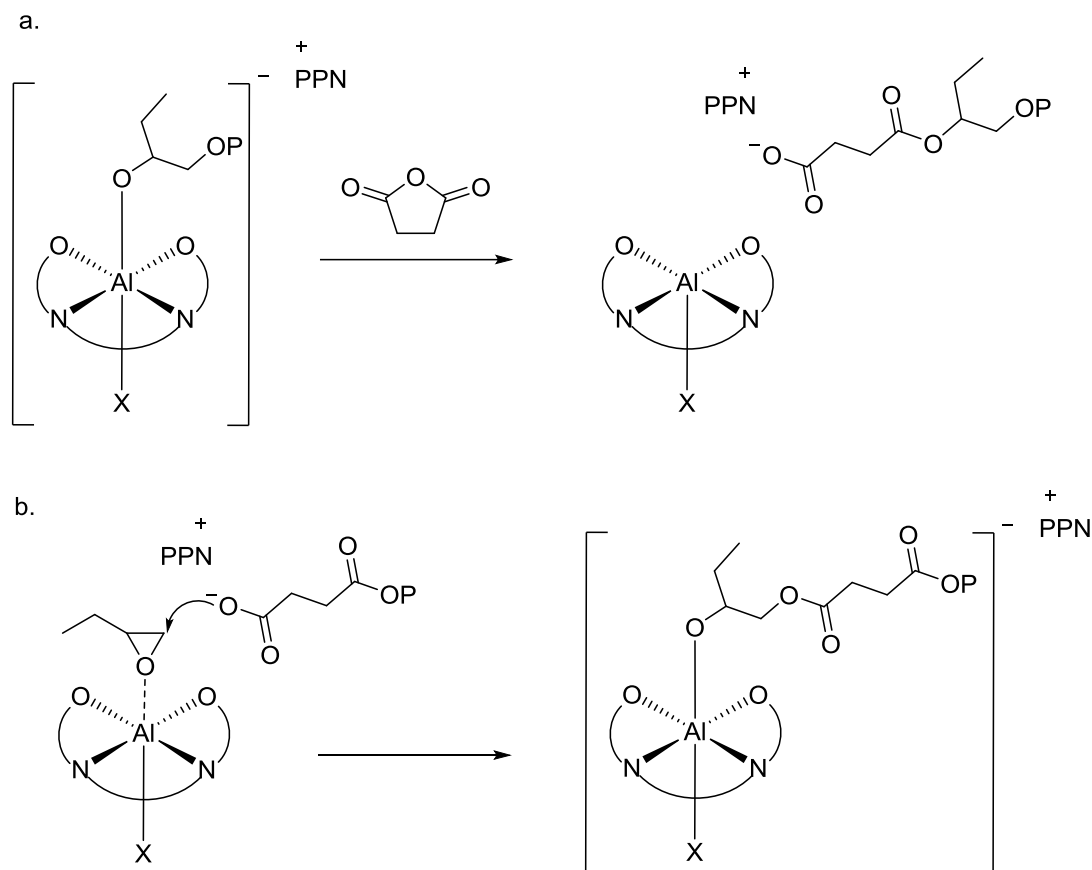
**Chapter 2 - Formation of polyesters via the ring-opening copolymerisation of epoxides and cyclic anhydrides**



**Scheme 3** [Al(Salph)Cl] (**2.1**) pre-catalyst used for ring-opening copolymerisation (ROCOP) mechanistic analyses. Initiation reaction of **2.1** and BO<sup>58</sup>

Over recent years, the mechanism of the ROCOP of epoxides and cyclic anhydrides has been studied in detail; in particular, the role of the nucleophilic co-catalyst in enhancing the rate and alternating selectivity of the ROCOP reaction was not fully understood until recently. The initiation step occurs by the coordination of an epoxide to the metal centre, and subsequent ring-opening by a nucleophile. As many ROCOP pre-catalysts bear chloride co-ligands and PPNCI is the most common co-catalyst, the initiation reaction most widely studied is where a chloride ion acts as the nucleophile. Coates *et al.* carried out a detailed mechanistic study of the ROCOP of epoxides and cyclic anhydrides (specifically carbic anhydride and butene oxide (BO) catalysed by [Al(salph)Cl] (**2.1**) (Scheme 3). The pre-catalyst **2.1** rapidly reacts with an epoxide to yield a metal alkoxide, [Al(salph)(OCH(Et)(CH<sub>2</sub>Cl))] (**2.1a**). A second epoxide can then coordinate to the metal centre allowing for the attack of another chloride ion<sup>22</sup> (from the PPNCI co-catalyst) yielding an anionic bis(alkoxide) complex [Al(salph){OCH(Et)(CH<sub>2</sub>Cl)}<sub>2</sub>]<sup>−</sup> (**2.1b**), with a PPN<sup>+</sup> cation.

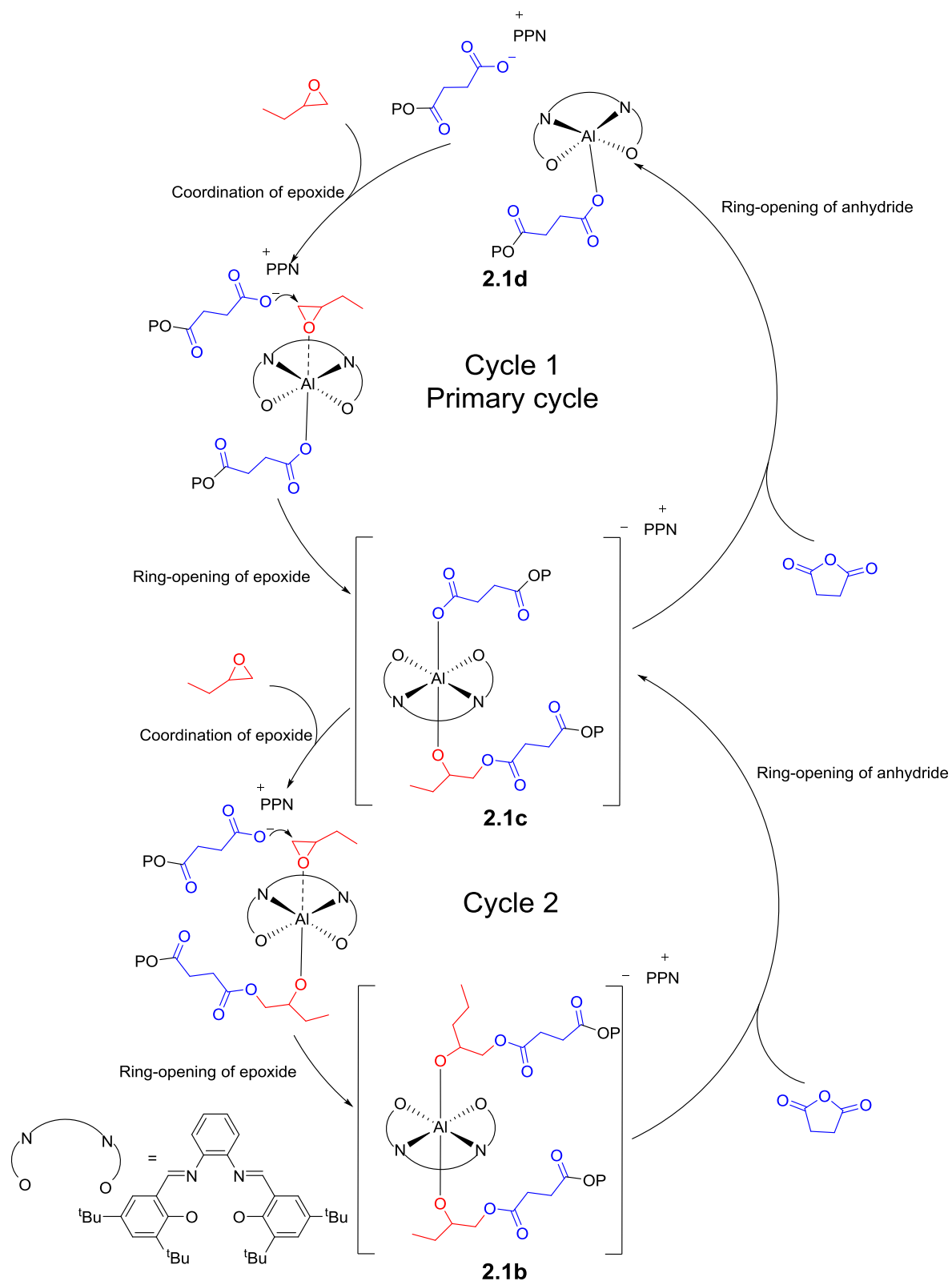
**Chapter 2 - Formation of polyesters via the ring-opening copolymerisation of epoxides and cyclic anhydrides**



**Scheme 4** Simplified propagation reactions of aluminium salen complex with BO and SA where X is either an alkoxide or carboxylate co-ligand and P is a growing polymer chain. a. Ring-opening of SA. b. Ring-opening of BO<sup>58</sup>

The propagation of the ROCOP reaction can be described by two steps (Scheme 4): a) the ring-opening of a cyclic anhydride by the metal-alkoxide species to afford a metal-carboxylate, where the carboxylate is the terminus of a polymer chain; b) the opening of an epoxide by a carboxylate-terminated polymer chain to afford a metal-alkoxide complex. These steps will occur sequentially for a highly selective ROCOP catalyst to add anhydrides and epoxides to the growing polymer chain. A catalytic cycle is shown in Scheme 5.

**Chapter 2 - Formation of polyesters via the ring-opening copolymerisation of epoxides and cyclic anhydrides**



**Scheme 5** Proposed mechanism for copolymerisation of BO and SA<sup>58</sup>

## **Chapter 2 - Formation of polyesters via the ring-opening copolymerisation of epoxides and cyclic anhydrides**

Given that the initiation process yields a bis(alkoxide) complex, the first step in the propagation involves **2.1b** ring-opening an anhydride molecule to yield a metal alkoxide/carboxylate (Scheme 5, **2.1c**). Species **2.1c** can react either with an epoxide to re-form the bis(alkoxide) (**2.1b**, Scheme 5, cycle 2) or with a second anhydride yielding a bis(carboxylate) (**2.1d**, Scheme 5, cycle 1). The reaction pathway is determined by the relative rate of ring-opening of the epoxide and anhydride. The ring-opening of an anhydride is much faster than that of an epoxide.<sup>32</sup> Coates *et al.* reported that the anhydride ring-opening in their system is approximately 50x faster than the epoxide ring-opening; in order for the rates of the ring-opening the epoxide and anhydride to be comparable, the reaction must be approximately 92% complete. It therefore stands to reason that **2.1c** is more likely to be transformed to the bis(carboxylate) species **2.1d** (which is the steady-state species in the catalytic cycle) rather than the bis(alkoxide) **2.1b**, thus making cycle 1 (Scheme 5) the dominant ROCOP pathway; cycle 2, involving the bis(alkoxide) **2.1b**, only becomes viable at low anhydride concentrations as the reaction nears completion.<sup>58</sup>

The ROCOP is first order with respect to the epoxide and the rate-limiting step for the reaction is the ring-opening of epoxide,<sup>32</sup> which occurs following the dissociation of a carboxylate-terminated polymer chain and subsequent coordination of an epoxide monomer to the metal centre. Reaction of an external carboxylate with the activated epoxide leads to ring-opening and the formation of an alkoxide-terminated polymer chain (Scheme 5, cycles 1 and 2). The presence of PPN<sup>+</sup> facilitates the dissociation of the carboxylate from the metal centre, and thereby fully explains the role of the co-catalyst in enhancing both the rate of reaction (through improved initiation ensuring more of the pre-catalyst enters the cycle) and selectivity (through involvement in the propagation).<sup>58</sup> Unlike the carboxylate, an alkoxide terminated polymer is very unlikely to decoordinate, therefore the reaction of an alkoxide with an epoxide must take place internally at a metal centre. This internal reaction would have a much higher activation energy than the external attack of a decoordinated carboxylate-terminated polymer and this kinetic control gives rise to high selectivity for the alternating ring-opening polymerisation of the epoxide and

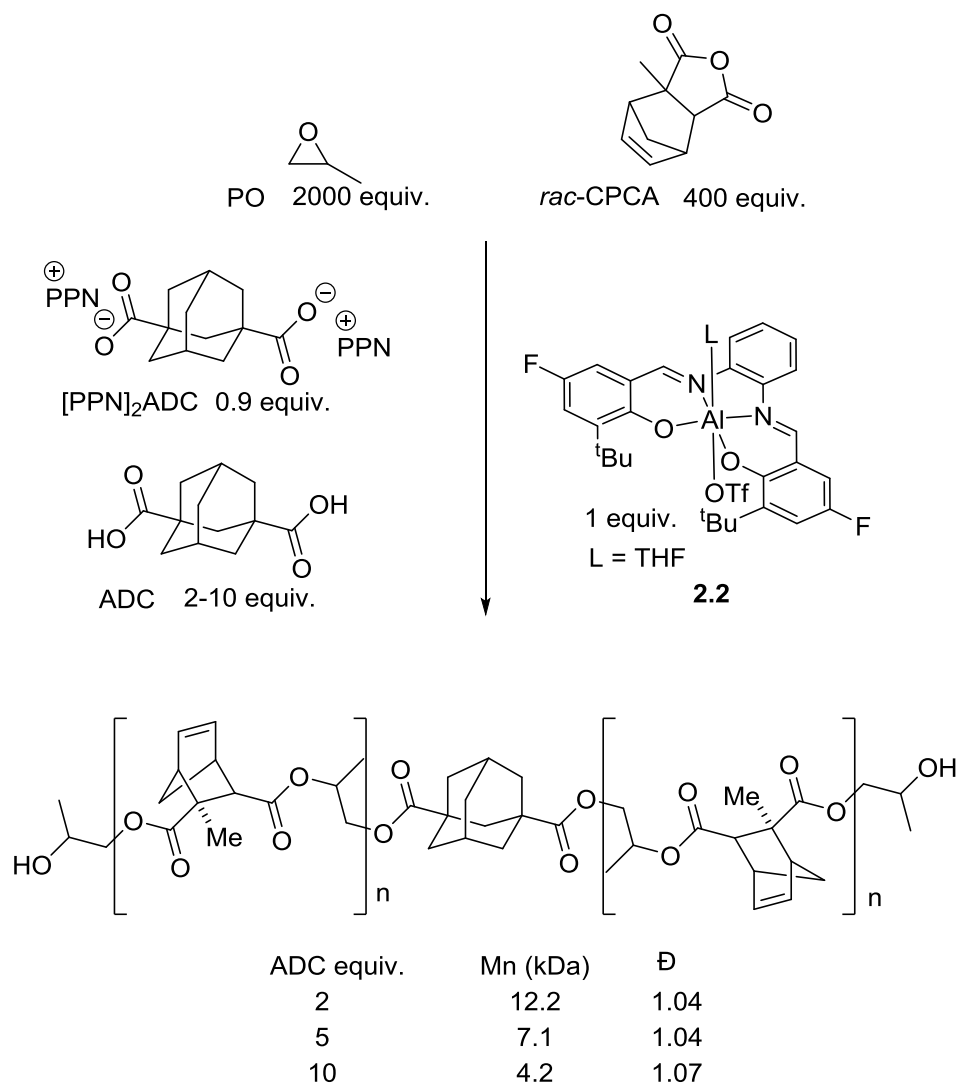


## **Chapter 2 - Formation of polyesters via the ring-opening copolymerisation of epoxides and cyclic anhydrides**

cyclic anhydride monomers. Darensbourg *et al.* reported that for cyclohexane anhydride (CHA), the rate of reaction with epoxide decreased in the order of PO > CHO ≥ SO.<sup>32</sup> The reaction of an alkoxide with an anhydride is rapid and takes place at the metal centre (Scheme 5, cycles 1 and 2).<sup>58</sup> The ring-opening of the anhydride occurs by the same mechanism as other cyclic esters such as lactones or lactide. Williams and colleagues exploited this commonality to produce block copolyesters combining the ROCOP of epoxides and cyclic anhydrides and the ROP of  $\epsilon$ -decalactone.<sup>43</sup>

The excellent work by Coates and colleagues<sup>58</sup> provides a good understanding of the ROCOP of epoxides and cyclic anhydrides catalysed by **2.1**. The mechanism will likely be applicable to other aluminium based homogeneous catalysts with planar  $\kappa^4$  ligands. However further research is required to establish whether different catalytic systems will work by this mechanism. For example, what effect will changing from an aluminium based catalyst to a non-labile metal such as Co<sup>III</sup> or Cr<sup>III</sup> have on a mechanism which is dependant on ligand dissociation? Another question is how the mechanism will be affected by non-planar ligand systems?

**Chapter 2 - Formation of polyesters via the ring-opening copolymerisation of epoxides and cyclic anhydrides**



**Scheme 6** Reversible deactivation anionic ring-opening copolymerisation (ROCOP)<sup>59</sup>

A recurring observation in the ROCOP of epoxides and cyclic anhydrides is bimodal molecular weight distributions in the resulting polymers. This causes large apparent dispersities ( $\bar{D}$ ) for polymers that would yield narrow  $\bar{D}$  had they been unimodal. The bimodality is a result of the presence of bifunctional initiators, in addition to the desired monofunctional initiators. The most common bifunctional impurity is a diacid, formed from the hydrolysis of the anhydride monomer. As both carboxylic acid groups can initiate polymerisation, the polymer chains formed have approximately twice the molecular weight of those formed by monofunctional initiators such as chloride. Coates and colleagues reported an effective route to unimodal

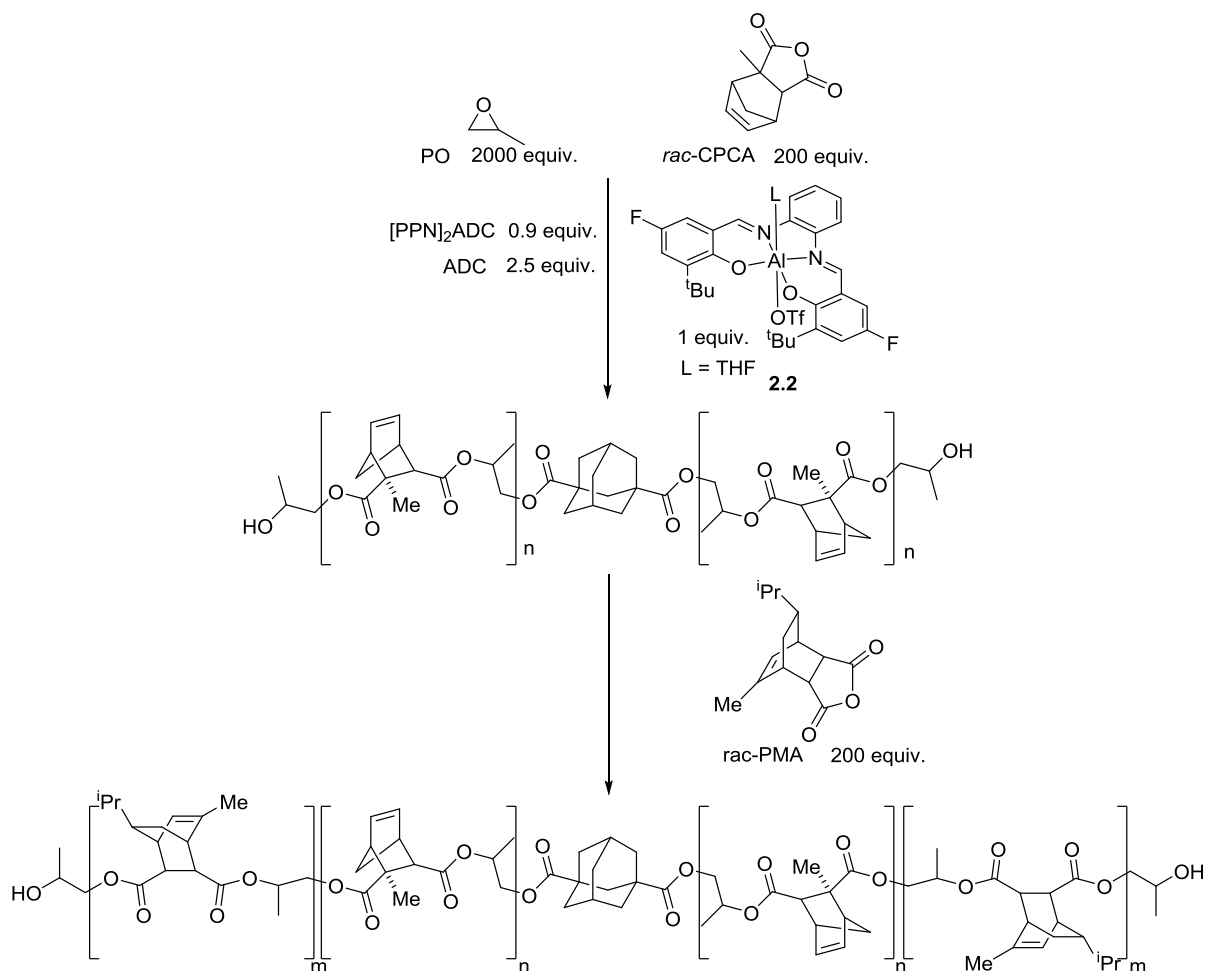
## **Chapter 2 - Formation of polyesters via the ring-opening copolymerisation of epoxides and cyclic anhydrides**

polymer distributions by purposely utilising bifunctional initiators in the absence of the usual monofunctional examples, therefore giving approximately the same molecular weight distribution as any polymer chains initiated by the diacid impurity. To achieve this, a non-initiating aluminium homogeneous catalyst was synthesised,  $[\text{Al}(\text{Salph})(\text{OTf})]$  (**2.2**). Complex **2.2** was similar to those previously reported by Coates (i.e. contained the same supporting ligand) except that it contained a triflate co-ligand as opposed to the commonly used chloride. The low nucleophilicity of the triflate ion means that it is not capable of ring-opening an epoxide monomer and initiating polymerisation. Since co-catalysts such as  $\text{PPNCl}$  contain chloride ions which initiate polymerisation, an alternative is required. The co-catalyst selected was the  $\text{PPN}$  salt of 1,3-adamantanedicarboxylic acid ( $[\text{PPN}]_2[\text{ADC}]$ ) which provides the  $\text{PPN}^+$  crucial in ROCOP propagation and is a bifunctional initiator. In this work, chain transfer agents (CTAs) were also used and allowed for the generation of multiple polymer chains per metal centre and greater control over molecular weight. Reversible proton transfer between the polymer chains in the system allow them to shuttle between an active and dormant state, maintaining the advantages of a living polymerisation. This catalytic system was utilised in the ROCOP reaction of propylene oxide and a citraconic anhydride (CA) based tricyclic anhydride (*rac*-CPCA, the cycloadduct of CA and cyclopentadiene) yielding polyesters with narrow  $\text{Đ}$  and controllable molecular weight (Scheme 6). Using this system Coates *et al.* copolymerised a series of different epoxides and cyclic anhydrides and formed a series of polyesters with very low  $\text{Đ} \leq 1.1$ .<sup>59</sup>

Having successfully synthesised unimodal polymers with low  $\text{Đ}$ , Coates and co-workers utilised their highly controllable system to produce multiblock copolymers. The ability to produce a multiblock copolymer is very desirable as it allows for even greater control and variation of polymer properties. The first polymer block was made up of PO and CPCA. Once this reaction was complete, a second MA based tricyclic anhydride (*rac*-PMA, the cycloadduct of MA and  $\alpha$ -phellandrene) was added, which reacted with the remaining PO (Scheme 7). The  $M_n$  and  $\text{Đ}$  of the first block and multiblock were 6,600  $\text{g mol}^{-1}$ ,  $\text{Đ} = 1.05$  and 13,800  $\text{g mol}^{-1}$ , 1.04 respectively. The increase in  $M_n$ ,

**Chapter 2 - Formation of polyesters via the ring-opening copolymerisation of epoxides and cyclic anhydrides**

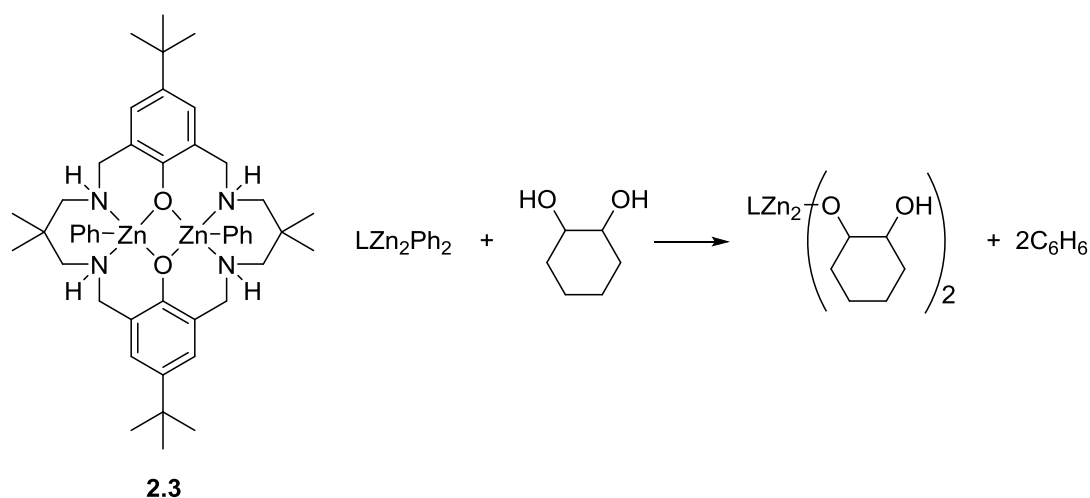
unimodality and low Đ indicated that the two blocks were joined and that the polymerisation remained selective and controlled.<sup>59</sup>



**Scheme 7** Formation of a multiblock copolymer from the ring-opening copolymerisation (ROCOP) reaction of PO with two cyclic anhydrides.<sup>59</sup>

## Chapter 2 - Formation of polyesters via the ring-opening copolymerisation of epoxides and cyclic anhydrides

Another method for producing unimodal polyesters was reported by Williams and colleagues, who utilised a bimetallic zinc catalyst (**2.3**) in conjunction with 1,2-cyclohexanediol. The zinc catalyst contained phenyl co-ligands which reacted *in situ* with the diol to give a zinc alkoxide and benzene (Scheme 8). The polymerisation was initiated by the bifunctional diol alone, giving unimodal molecular weight distributions and low Đ. Excess diol was added as a chain transfer agent in order to further control the molecular weight of the polymer synthesised.<sup>43</sup>



Bimetallic zinc phenyl catalyst

**Scheme 8** Bimetallic zinc phenyl catalyst and catalyst activation step<sup>43</sup>

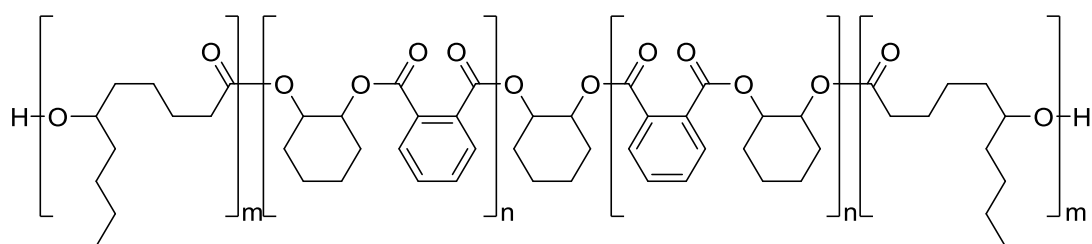


**Figure 4** Block polyester from the ring-opening copolymerisation (ROCOP) of PhA and CHO and the ring-opening polymerisation (ROP) of  $\epsilon$ -DL<sup>43</sup>

This highly controlled polymerisation can also be used for preparing multiblock copolymers (Figure 4). Williams *et al.* combined the ROCOP of epoxides and cyclic anhydrides and the ROP of lactones. The polyester formed had an ABA configuration, where the ROCOP polymer formed the first (central) block and the ROP formed blocks on either end; in this one-pot synthesis, the ROCOP reaction goes to completion (100% conversion of anhydride) before the ROP

## **Chapter 2 - Formation of polyesters via the ring-opening copolymerisation of epoxides and cyclic anhydrides**

of the lactone commences. This control is not simply a result of the ROCOP being the substantially faster reaction; surprisingly, despite the ROP of  $\epsilon$ -decalactone ( $\epsilon$ -DL) ( $\text{TOF} = 160 \text{ h}^{-1}$ ) being faster in isolation, it only proceeds following the completion of the ROCOP of PhA and CHO ( $\text{TOF} = 25 \text{ h}^{-1}$ ). The authors proposed that the faster rate of insertion of PhA into the zinc alkoxide intermediate (common in both catalytic cycles) was responsible. The subsequent ring-opening of the epoxide is slow, meaning the steady state species is the zinc carboxylate, a concurrent finding to Coates and colleagues.<sup>58</sup> As this carboxylate intermediate cannot react with the  $\epsilon$ -DL, the ROCOP reaction goes to completion before any lactone reacts. Block copolymers containing alternative monomers, 4-vinyl-1-cyclohexene oxide (VCHO), rac-lactide, and  $\delta$ -valerolactone were also synthesised.<sup>43</sup>

### **2.2 Synthesis and characterisation of $[\text{Al}(\text{L1})\text{Cl}_2]$ (1)**

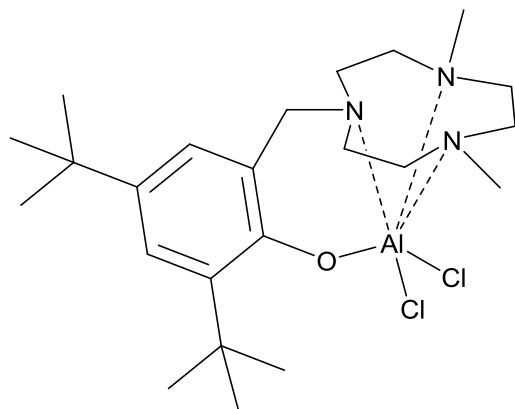
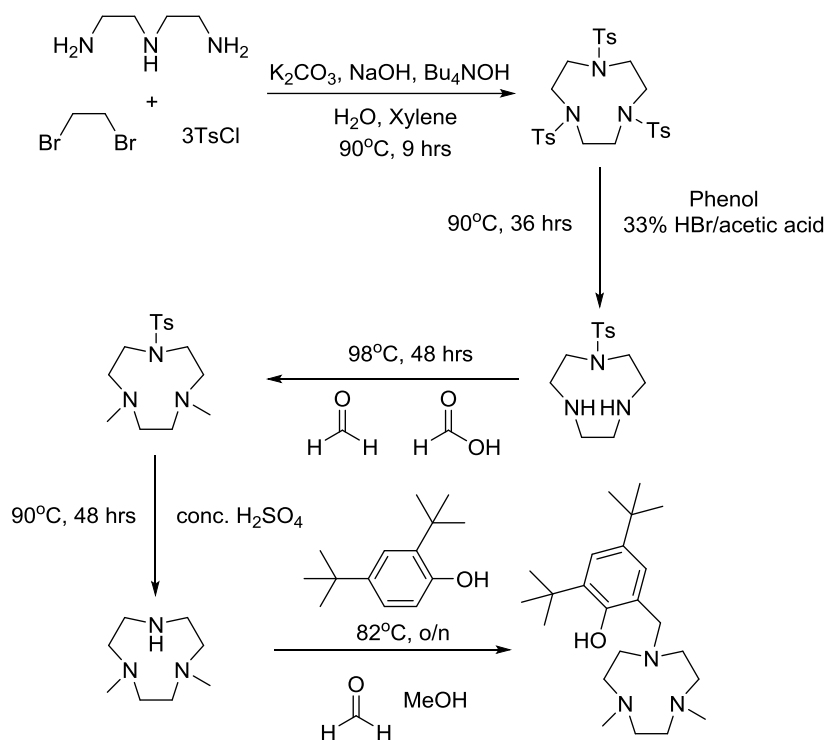


**Figure 5**  $[\text{Al}(\text{L1})\text{Cl}_2]$  (**1**)

A range of catalysts have been developed for the ROCOP of epoxides and cyclic anhydrides, these have been proven effective for the copolymerisation of a variety of monomers. The majority of the work in this area has been focussed on catalyst systems based on salen ligands, it is therefore of interest to explore the efficacy of catalysts with markedly different structures.<sup>1</sup>  $[\text{Al}(\text{L1})\text{Cl}_2]$  (**1**) (Figure 5) was selected, as complexes of this type have been reported to exhibit hemilabile ligand-metal binding,<sup>60</sup> which has been shown to be an advantageous property in other examples of homogeneous catalysis, but complexes of this type have not been previously employed as catalysts.<sup>61–66</sup>

**Chapter 2 - Formation of polyesters via the ring-opening copolymerisation of epoxides and cyclic anhydrides**

The pendant arm TACN proligand **HL1** was synthesised according to a literature method.<sup>67,68</sup> In a multistep procedure, summarised in Scheme 9, the 1,4-dimethyl-1,4,7-triazacyclononane (TACN) macrocycle was first prepared as described by Flassbeck and Wieghardt,<sup>67</sup> and a *tert*-butylphenoxy pendant arm was appended through a procedure reported by Mountford and colleagues.<sup>68</sup>



**Scheme 9** Synthesis of **HL1**<sup>67,68</sup>

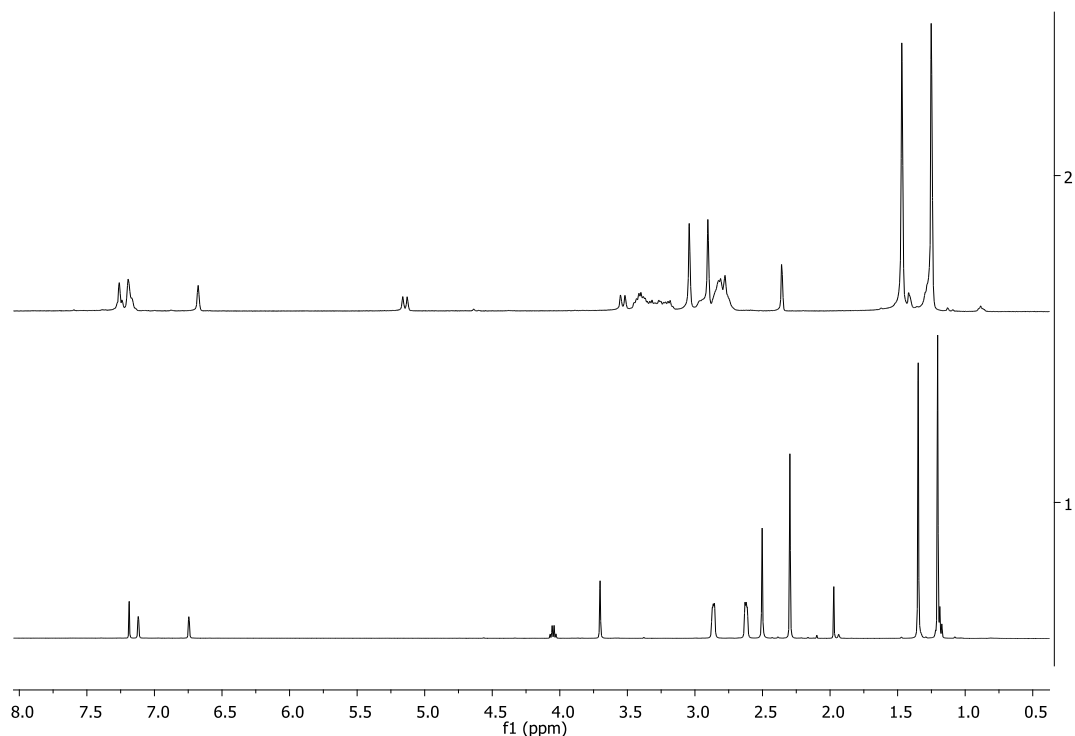


**Figure 6** Comparison of the <sup>1</sup>H NMR spectra (400 MHz, CDCl<sub>3</sub>) of [Al(L1)Cl<sub>2</sub>] (**1**, top) and (500 MHz, CDCl<sub>3</sub>) **HL1** (bottom)

Previously **1** was synthesised from the salt metathesis reaction of AlCl<sub>3</sub> with **KL1** (the potassium salt of HL1).<sup>68</sup> In this thesis, a more expedient route was found by reacting ethylaluminium dichloride directly with **HL1**. The reaction produced the desired complex and ethane as a by-product. The advantages of this route are that the extra step necessary to produce **KL1** is not required and as the side-product produced is a gas it is therefore easily removed from the reaction. The <sup>1</sup>H NMR spectra of **1** and **HL1** are shown in Figure 6. The significant difference between the <sup>1</sup>H NMR spectrum of **1** compared to that of **HL1** is good evidence for coordination to aluminium. There is a considerable change in chemical shift for one of the aromatic phenoxy protons from 6.82 ppm in the free ligand to 6.69 ppm in **1**; the close proximity of the aromatic proton to the metal centre explains this difference. The other aromatic proton does not show a significant difference in chemical shift between the free and coordinated ligand. Another considerable change in the <sup>1</sup>H NMR spectrum is in the chemical environment of the methylene bridge between the macrocycle and the phenoxy group. In the free ligand, the methylene proton signal appears



## Chapter 2 - Formation of polyesters via the ring-opening copolymerisation of epoxides and cyclic anhydrides

as a singlet with an integration of 2 H and a chemical shift of 3.77 ppm. This is due to the equivalency of both protons in the free ligand. However upon coordination, these protons are diastereotopic causing the appearance of two doublets with very different chemical shifts. Each doublet has an integration of 1 and chemical shifts of 5.15 and 3.54 ppm. Both signals have a large  $J$  value of 13.5 Hz resulting from the geminal coupling. When complexed to a metal centre in a  $\kappa^4$  manner the pendant arm of **L1** twists in order to achieve an octahedral coordination environment, this ligand arrangement makes the complex  $C_1$  symmetric. This lack of symmetry causes the methylene bridge protons and many other chemical environments to become inequivalent. Figure 7 shows the crystal structure of an analogous scandium complex containing the ligand **L1**, the low symmetry structure is exemplified by the fact that one NMe group is *trans* to the phenoxide and the other is *trans* to an alkoxide co-ligand.<sup>69</sup>

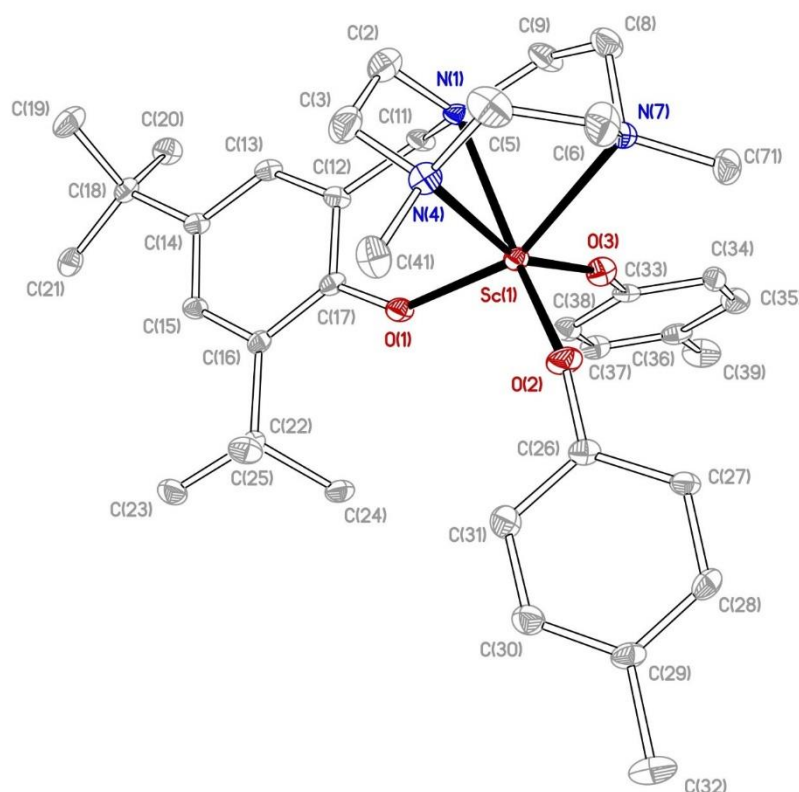


**Figure 7** Solid-state structure of [Sc(L1)(OTol)<sub>2</sub>]. H atoms and solvent removed for clarity<sup>69</sup>

## **Chapter 2** - Formation of polyesters via the ring-opening copolymerisation of epoxides and cyclic anhydrides

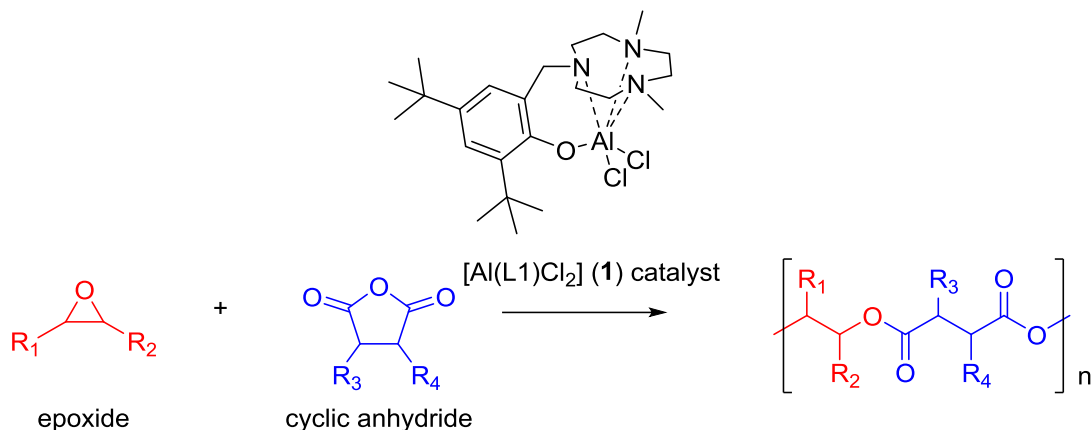
In the free ligand, the N-substituted methyl group protons of the TACN ring are equivalent and therefore appear as one signal (2.37 ppm) with an integration of 6 (each methyl group contributing 3). When the ligand is coordinated to the aluminium centre, the two methyl groups become inequivalent and appear as two separate signals with chemical shifts of 3.04 and 2.91 ppm. The downfield shift following complexation indicates that the nitrogen donors of the TACN ring may be involved in coordination to the aluminium centre, as expected. The six methylene groups of the TACN ring appear as three chemical environments in the free ligand  $^1\text{H}$  NMR spectrum. Coordination of the ligand causes these protons to become inequivalent and they appear as an overlapping multiplet in the  $^1\text{H}$  NMR spectrum of **1**. For the  $^t\text{Bu}$  protons, there is very little change between the coordinated and free ligand. The NMR spectra recorded for **1** concurs with the data reported for the complex by Mountford *et al.*<sup>68</sup>

Complex **1** is quite different to the pre-catalysts previously employed for the ROCOP of epoxides and cyclic anhydrides. The majority of the catalysts employed utilise supporting ligands based on the porphyrin,  $\beta$ -diiminate and most prominently salen ligand classes. The catalytic systems incorporating these ligands have been effective for the ROCOP reaction, however they are all similar in that the ligand is arranged in planar geometry around the metal centre, giving two active sites lying mutually *trans* to one another. **L1** invokes a markedly different coordination geometry to the aforementioned ligands with the macrocyclic TACN ring binding in a hemilabile face capping manner and the phenoxy pendant arm binding strongly to the aluminium. There are no previous reports of **L1** metal complexes acting as catalysts. Macrocyclic ligands of this type often form very stable and inert compounds, however the hypothesis of this thesis was that **1** has the potential to be an effective catalyst due to its hemilability.<sup>68</sup>

**2.3 Ring-opening copolymerisation (ROCOP) of epoxides and cyclic anhydrides catalysed by [Al(L1)Cl<sub>2</sub>] (1)**

**2.3.1 Choice of monomers**

[Al(L1)Cl<sub>2</sub>] (1) was explored as a catalyst for the alternating ring-opening copolymerisation (ROCOP) of epoxides and cyclic anhydrides to give biodegradable polyesters (Scheme 10).



**Scheme 10** Ring-opening copolymerisation (ROCOP) of epoxides and cyclic anhydrides catalysed by [Al(L1)Cl<sub>2</sub>] (1)

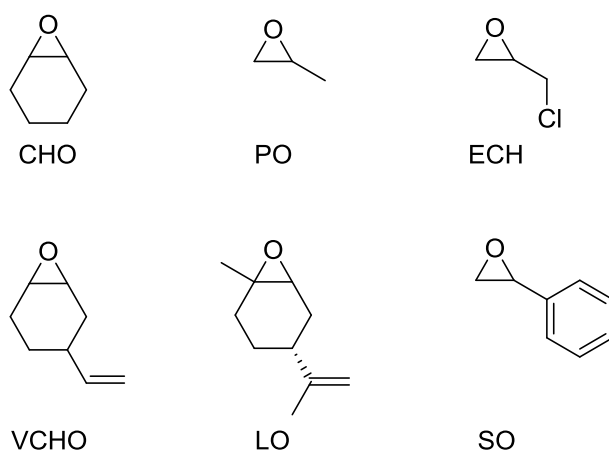


**Figure 8** Epoxides used in the ring-opening copolymerisation (ROCOP) reaction catalysed by [Al(L1)Cl<sub>2</sub>] (1)

The epoxides selected for this study are shown in Figure 8. Cyclohexene oxide (CHO) and propylene oxide (PO) have been used extensively in the ROCOP

**Chapter 2 - Formation of polyesters via the ring-opening copolymerisation of epoxides and cyclic anhydrides**

of epoxides and cyclic anhydrides. Their reactivity with a number of different anhydrides make them ideal candidates for use in our study with a new catalytic system. Previous reports in the literature enable comparison of **1** with existing catalysts.

Epichlorohydrin (ECH) and 4-vinyl-cyclohexene oxide (VCHO) have been selected because they will show similar reactivity to PO and CHO respectively, but they have the advantage of additional functional groups that are candidates for post-polymerisation modification (PPM). ECH contains reactive carbon–chlorine bonds, which have been exploited previously.<sup>70</sup> VCHO has been used before as a monomer in the ROCOP of epoxides and cyclic anhydrides. The copolymers produced contain pendant vinyl groups which readily undergo PPM.<sup>1</sup>

Limonene oxide (LO) is an attractive candidate for use in the ROCOP of epoxides and cyclic anhydrides because it is derived from renewable feedstocks. This enables the production of, depending on the anhydride, bioderived or partially bioderived copolymers. This monomer also contains additional functionality in the form of the alkene functional group. Styrene oxide (SO) was also selected as a monomer of interest. Copolymers with SO will have quite different polymer structures to those synthesised from the other monomers because of the phenyl group present in the polymer backbone.

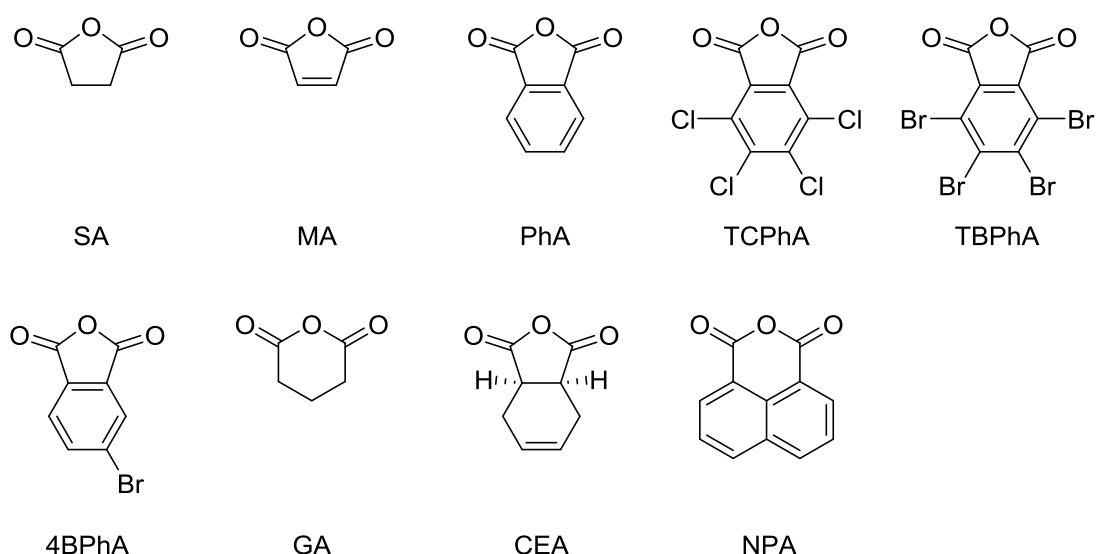


**Figure 9** Cyclic anhydrides used in the ring-opening copolymerisation (ROCOP) reaction catalysed by  $[\text{Al}(\text{L1})\text{Cl}_2]$  (**1**)

## **Chapter 2 - Formation of polyesters via the ring-opening copolymerisation of epoxides and cyclic anhydrides**

The cyclic anhydrides selected for this study are shown in Figure 9. Maleic anhydride (MA), succinic anhydride (SA) and glutaric anhydride (GA) are simple monocyclic anhydrides. SA and GA should yield polyesters with a more flexible backbone. GA is also of interest because it is a six membered cyclic anhydride as opposed to the more commonly used five membered rings. MA includes an internal alkene group which can be utilised for PPM reactions.<sup>71</sup>

Phthalic anhydride (PhA) is a very useful bicyclic anhydride. It is commonly used as a monomer for ROCOP with a variety of different epoxides. It produces less flexible polyesters than SA and GA because of the aromaticity in the polymer backbone. An attractive feature of utilising PhA is that the NMR spectra are simpler, this is because all of the aromatic protons of PhA have chemical shifts >7ppm in <sup>1</sup>H NMR spectra, meaning the rest of the spectrum contains only the epoxide-derived signals.

Tetrachlorophthalic anhydride (TCPPhA) and tetrabromophthalic anhydride (TBPhA) will most likely have similar reactivity to PhA, however these monomers have not received a great deal of interest in the literature. They are highly appealing monomers as the inclusion of halogens into the polymer chains should greatly affect properties such as glass-transition temperature and flame retardancy; these properties are of great importance and determine what applications a plastic is suitable for. 4-Bromophthalic anhydride (4BPhA) was selected because polymers containing this monomer would have the potential for PPM through reactions with the aryl-bromine bond.

cis-1,2,3,6-Tetrahydrophthalic anhydride (CEA) will also form polymers with the potential for PPM, due to the alkene functionality present in the monomer. It is also of interest because it has a similar structure to PhA without the aromaticity. Finally, 1,8-naphthalic anhydride (NPA) was also selected as a monomer. It has a similar 6-membered cyclic anhydride ring like GA but has the rigidity of the naphthalene ring.

### **2.3.2 Initial polymerisation studies**

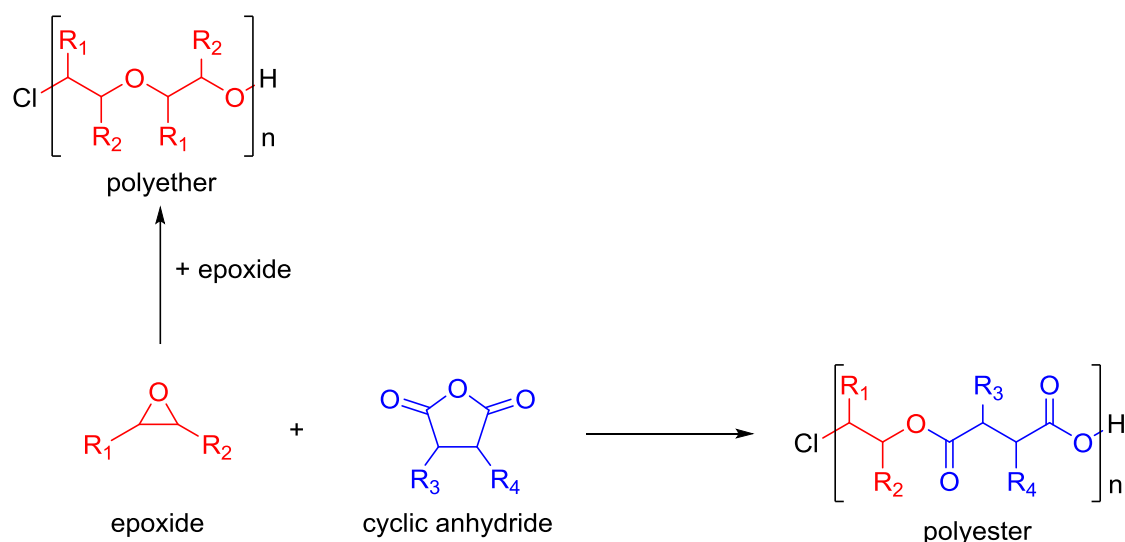
This project investigated the efficiency of [Al(L1)Cl<sub>2</sub>] (**1**) as a homogeneous catalyst for the ROCOP of epoxides and cyclic anhydrides. A major advantage

## **Chapter 2** - *Formation of polyesters via the ring-opening copolymerisation of epoxides and cyclic anhydrides*

of this reaction is the fact that it is a copolymerisation from two different sets of monomers with complementary functionality. There are a copious number of readily-available derivatives of both monomer classes, exhibiting a wide variety of chemical structures, allowing for the facile variation of polymer properties by altering the identities of the monomers used in the ROCOP reaction (Figures 1 and 2).<sup>1</sup> The potential tunability is extremely advantageous. Varying polymer properties is very difficult for many of the alternative and established routes to biodegradable polyesters. The aim of this project is to synthesise polyesters from a range of monomers and illustrate how selecting different monomers can affect the properties of the plastics produced, such as the glass-transition temperature and flame retardancy; the material properties of the polymers will be discussed in Chapter 3.

In the ROCOP of epoxides and cyclic anhydrides, the reaction conditions can have a significant impact on the polymer synthesised. An important challenge is to promote the alternating reaction of the epoxide and anhydride monomers producing a polymer with only polyester linkages. Another pathway is for an epoxide to react following another epoxide to form an ether linkage. Polyethers are useful plastics in their own right, however the resistance of the ether group towards hydrolysis renders them non-biodegradable. Preventing polyether formation and promoting the ester formation is crucial in the ROCOP of epoxides and cyclic anhydrides. Scheme 11 shows the possible reaction pathways.

**Chapter 2 - Formation of polyesters via the ring-opening copolymerisation of epoxides and cyclic anhydrides**



**Scheme 11** Polyester and polyether formation in ring-opening copolymerisation (ROCOP) of epoxides and cyclic anhydrides. H and Cl end groups.

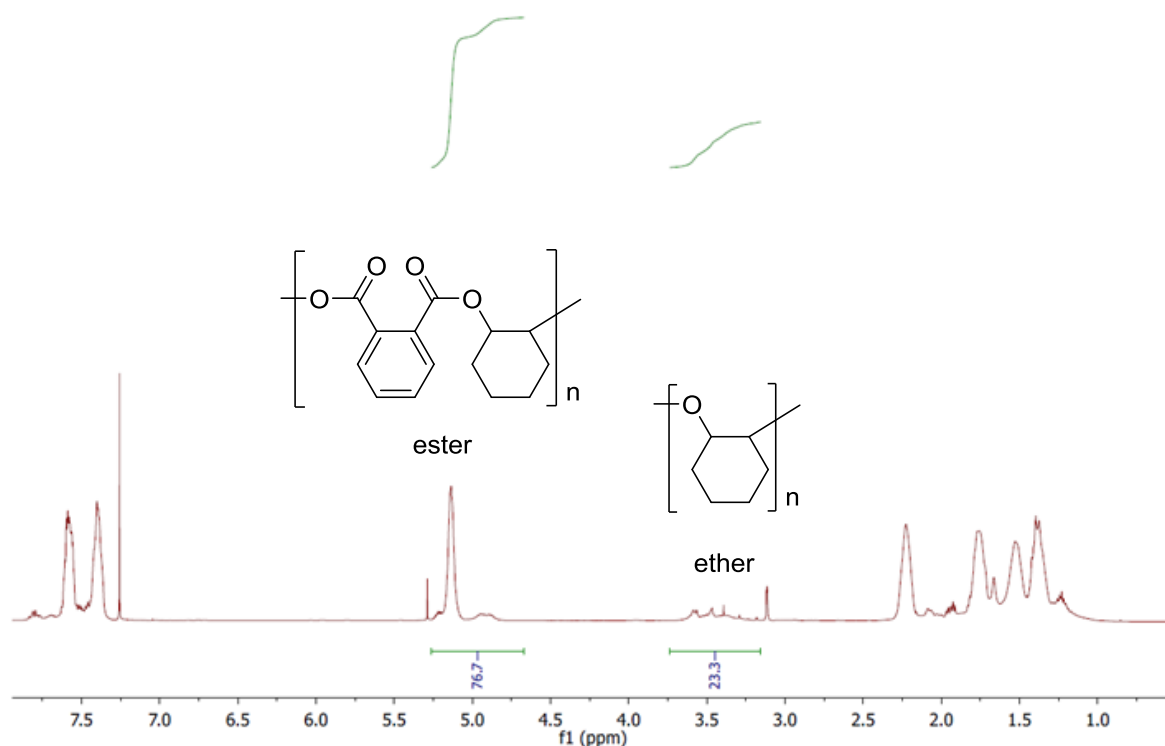


**Figure 10**  $^1\text{H}$  NMR (500 MHz,  $\text{CDCl}_3$ ) spectrum of CHO-PhA copolymer showing ester and ether regions

A polyester linkage can be distinguished from a polyether by  $^1\text{H}$  NMR spectroscopy. The selectivity of a ROCOP reaction is the percentage polyester (as opposed to polyether) in a given sample. This is calculated by the relative

## Chapter 2 - Formation of polyesters via the ring-opening copolymerisation of epoxides and cyclic anhydrides

integration of the ester signal compared to the ether ( $selectivity = \frac{100 \times ester\ integral}{ester\ integral + ether\ integral}$ ). For example, in ROCOP reactions with CHO the polymer exhibits a  $^1H$  NMR signal of approximately 5.25 ppm for an ester bond and 3.5 ppm for an ether (Figure 10).

In order to find the optimal conditions for the ROCOP of epoxides and anhydrides when catalysed by **1**, the monomers CHO and TPhA were selected. CHO has been used a great deal in the literature and has well-defined ester and ether regions. Considering selectivity is a key consideration, TPhA was chosen as it is  $^1H$  NMR silent so cannot obscure the ester and ether signals. The copolymerisation between CHO and TPhA was carried out in excess epoxide, stoichiometrically in toluene, and with and without a co-catalyst (Table 1). The selectivity of the polymers synthesised were obtained from their  $^1H$  NMR spectra, and their molecular weights and  $\bar{M}_w$  were measured by GPC.

**Table 1** Copolymerisation of CHO and TPhA under different reaction conditions

Entry	Solvent	Co-cat	Ratio	Yield (%) <sup>b</sup>	Selectivity (%) <sup>c</sup>	Mn <sup>d</sup>	$\bar{M}_w$ <sup>d</sup>
1 <sup>a</sup>	None	none	1000:200:1:0	57	3	-	-
2	Toluene <sup>e</sup>	none	200:200:1:0	99	65	<1250	-
3	Toluene <sup>e</sup>	PPNCI	200:200:1:1	99	99	9060	1.58
4	Toluene <sup>e</sup>	PPNCI	200:200:1:2	99	99	7350	1.33

6.4  $\mu$ mol  $[Al(L1)Cl_2]$  (**1**) catalyst. Ratio = [Epoxide]<sub>0</sub>: [Anhydride]<sub>0</sub>: [Catalyst]<sub>0</sub>: [Co-catalyst]<sub>0</sub>. Reactions heated at 80 °C for 2 hours. <sup>a</sup>Reaction time 5 hours. <sup>b</sup>Isolated yield. <sup>c</sup>Determined by comparison of ester and ether signals in  $^1H$  NMR spectra. <sup>d</sup>Determined by GPC calibrated using narrow Mn polystyrene (PS) standards, with units of  $g\ mol^{-1}$ . <sup>e</sup>0.5 ml of dry toluene added to reaction.

In entry 1, the reaction was carried out under solvent-free conditions with an excess of epoxide and without the presence of a co-catalyst. 1,000 molar equivalents of CHO, 200 equivalents of TPhA and 1 equivalent of **1** were combined and heated at 80 °C for 5 hours. The material isolated had an extremely low ester selectivity of 3%, indicating that the material is almost



## **Chapter 2** - Formation of polyesters via the ring-opening copolymerisation of epoxides and cyclic anhydrides

entirely polyether. This explains why the reaction became solid as the excess CHO, which was acting as a solvent, was consumed. As entry 1 is 97% polyether instead of polyester this material was not characterised by GPC.

Entry 1 showed that polyether formation was a major issue when the reaction was carried out in excess epoxide. Therefore the experiment was undertaken with stoichiometric epoxide and anhydride (200:200 equivalents), with 0.5 ml of dry toluene as a solvent (entry 2). This change in reaction conditions significantly increased the selectivity of the reaction from 3% in entry 1 to 65% in entry 2. This means that the dominant reaction is now the desired ROCOP of CHO and TPhA forming ester linkages, but polyether formation is still a significant side-reaction. The molecular weight was measured for entry 2, but was  $<1,250 \text{ g mol}^{-1}$  which is below the minimum detection limit of the GPC instrument. This suggests that the polymer from entry 2 is comprised of oligomers.

Many of the catalysts reported in the literature for the ROCOP of epoxides and cyclic anhydrides are employed in conjunction with a nucleophilic co-catalyst. Bis(triphenylphosphoranylidene)ammonium chloride (PPNCl, Figure 11) was selected and tested with **1** for the copolymerisation of CHO and TPhA. PPNCl has been shown to enable the external attack of a carboxylate intermediate on an epoxide, which is a crucial step in the ROCOP reaction.<sup>58</sup>

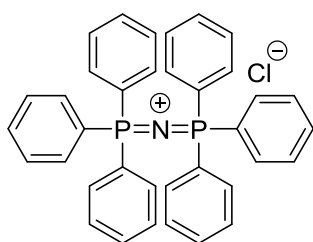


**Figure 11** Bis(triphenylphosphoranylidene)ammonium chloride (PPNCl)

### 2.3.3 Ring-opening copolymerisation (ROCOP) in solvent

In entries 3 and 4, 1 and 2 molar equivalents of PPNCI were used respectively. Both reactions were carried out with toluene as a solvent and were heated at 80 °C for 2 hours. The inclusion of PPNCI in entries 3 and 4 had a significant impact on the reaction. In both experiments, the polymers produced were perfectly selective towards polyester and were isolated in excellent yields. In both cases, GPC analysis of the polymers indicated good molecular weights with  $M_n = 9,060$  and  $7,350 \text{ g mol}^{-1}$  respectively. This shows that the inclusion of a co-catalyst has improved both the selectivity and molecular weight of the copolymers. There are slight differences between the polymers produced when 1 or 2 equivalents of PPNCI were used. In entry 3 when 1 equivalent of PPNCI was employed, a higher molecular weight and  $\bar{M}_w$  were found compared to entry 4 with 2 equivalents of co-catalyst. The lower  $\bar{M}_w$  in entry 4 suggests greater polymerisation control leading to a narrower distribution of polymer chain lengths. The decrease in molecular weight with the increase in co-catalyst is most likely a result of the additional chloride ions which can initiate polymer chains. The number of polymer chains is equal to the number of chlorides or initiators in the system. The molecular weight of the polymer sample may be tuned by varying the catalyst loading. Due to the greater control it was concluded that the reaction conditions in 4 with 2 equivalents of PPNCI are optimal. Previous work in the literature indicates that ROCOP with more than two molar equivalents does not improve reaction rates or  $\bar{M}_w$  and leads to a reduction in molecular weights.<sup>29</sup>

**Chapter 2** - Formation of polyesters via the ring-opening copolymerisation of epoxides and cyclic anhydrides

**Table 2** Ring-opening copolymerisation (ROCOP) of epoxides and cyclic anhydride carried out in solvent

Entry	Epoxide	Anhydride	Yield (%) <sup>a</sup>	Selectivity (%) <sup>b</sup>	Mn <sup>c</sup>	Đ <sup>c</sup>
5	CHO	PhA	80	99	11480	1.25
6	CHO	TCPPhA	74	93	15250	1.20
7	CHO	TBPhA	92	96	5100	2.02
8	ECH	PhA	86	95	5100	1.13
9	ECH	TCPPhA	90	95	9600	1.10
10	ECH	TBPhA	97	97	5900	1.33
11	PO	PhA	61	96	11200	1.18
12	PO	TCPPhA	98	96	11450	1.03
13	PO	TBPhA	89	98	8750	1.05
14 <sup>d</sup>	SO	TCPPhA	54	99	5290	1.25
15 <sup>d</sup>	SO	SA	84	97	3760	1.05

6.4  $\mu\text{mol}$   $[\text{Al}(\text{L1})\text{Cl}_2]$  (**1**) catalyst.  $[\text{Epoxide}]_0:[\text{Anhydride}]_0:[\text{Catalyst}]_0:[\text{PPNCl}]_0 = 400:400:1:2$ . 1 ml of dry toluene added to reaction. Reactions heated at 80 °C for 18 hours. <sup>a</sup>Isolated yield. <sup>b</sup>Determined by comparison of ester and ether signals in <sup>1</sup>H NMR. <sup>c</sup>Determined by GPC using triple detection, with units of  $\text{g mol}^{-1}$ . <sup>d</sup> $[\text{Epoxide}]_0:[\text{Anhydride}]_0:[\text{Catalyst}]_0:[\text{PPNCl}]_0 = 200:200:1:2$ . 0.5 ml of dry toluene added to reaction. Reaction heated at 100 °C for 2 hours.

In order to achieve higher molecular weight polymers, the epoxide:anhydride:catalyst:co-catalyst ratio was increased to 400:400:1:2. To maintain solubility, the amount of dry toluene added to the reaction was increased to 1 ml. All combinations of the epoxides CHO, PO and ECH and the anhydrides PhA, TCPPhA and TBPhA were tested for the ROCOP reaction. In addition, the monomers MA, SA and SO were also employed in the copolymerisation reaction. The polymers formed from these reactions were isolated and their selectivity towards ester linkages and molecular weight measured. The results of these copolymerisations are shown in Table 2.

The wide variety of monomers combined in this study show the efficacy of **1**. All of the polymers synthesised have high selectivities across all monomer

## **Chapter 2** - Formation of polyesters via the ring-opening copolymerisation of epoxides and cyclic anhydrides

combinations (93 – 99%) and they were all isolated in good to excellent yields. Both examples with SO produced polymers with relatively low molecular weights, SO–TCPhA (entry 14) and SO–SA (entry 15) had  $M_n$  of 5,290  $\text{gmol}^{-1}$  and 3,760  $\text{gmol}^{-1}$  respectively. The  $\bar{D}$  for entries 14 (1.25) and 15 (1.05) were low, indicating the polymerisation was well-controlled. Copolymerisation with MA was attempted however these reactions yielded dark brown insoluble solids which could not be characterised. Duchateau and colleagues suggested that cross-linking of the MA copolymer chains was occurring during the reaction and causing the formation of the insoluble solid.<sup>24</sup>

The copolymers from the nine possible monomer combinations of CHO, ECH, PO, PhA, TCPhA and TBPhA gave molecular weights within the range of  $M_n = 5,100 - 15,250 \text{ gmol}^{-1}$ . The polymers (entries 5 – 13) have good  $\bar{D}$  (1.03 – 1.33), apart from entry 7 (CHO–TBPhA) which has a higher  $\bar{D}$  of 2.02. This indicates that changing the monomer can significantly affect the properties of the polymers produced by the catalytic system. The copolymers with PO and the TCPhA polymers all had high molecular weights and narrow  $\bar{D}$ . However, other than these observations, there were no clear trends on the effect of specific monomers on polymer properties. Of the copolymers with CHO, entries 5 and 6 had high  $M_n$  of 11,480 and 15,250  $\text{gmol}^{-1}$  and good  $\bar{D}$  of 1.25 and 1.2, whereas CHO–TBPhA (entry 7) had considerably lower molecular weights and higher  $\bar{D}$  of 5,100  $\text{gmol}^{-1}$  and 2.02 respectively. ECH–TBPhA (entry 10) also had similarly low molecular weight ( $M_n = 5,900 \text{ gmol}^{-1}$ ) and relatively high  $\bar{D}$  (1.33), whereas PO–TBPhA (entry 13) has far better properties compared to entries 7 and 10 with higher  $M_n$  (8,750  $\text{gmol}^{-1}$ ) and excellent  $\bar{D}$  (1.05). This suggests that TBPhA alone isn't responsible for low molecular weight and high  $\bar{D}$ . ECH–PhA (entry 8) and ECH–TBPhA (entry 10) had lower  $M_n$  (5,100  $\text{gmol}^{-1}$  and 5,900  $\text{gmol}^{-1}$ ) whereas ECH–TCPhA (entry 9) has a higher  $M_n$  (9,600  $\text{gmol}^{-1}$ ). Copolymers of PhA with CHO (entry 5) and PO (entry 11) had high  $M_n$  but ECH–PhA (entry 8) had a far lower  $M_n$ .

The results in Table 2 indicate that **1** is an effective catalyst for the ROCOP of epoxides and cyclic anhydrides, and more importantly demonstrate unequivocally that ligand systems that do not support the often-used planar- $\kappa^4$  coordination motif can be effective catalysts for preparing epoxide-anhydride

## **Chapter 2 - Formation of polyesters via the ring-opening copolymerisation of epoxides and cyclic anhydrides**

copolymers. A variety of monomer combinations were explored and many of the copolymers synthesised had high molecular weights and low Đ. The polymer chains also had highly alternating (AB)<sub>n</sub> microstructures evidenced by the high selectivity to ester linkages.

One disadvantage of the method used to synthesise the polymers in Table 2 is the use of a solvent in the reaction. It has been shown in the literature that it is possible to carry out the ROCOP of epoxides and cyclic anhydrides under solvent-free conditions with an excess of epoxide.<sup>1</sup> In this method, the epoxide acts as a solvent as well as a reactant. One consideration when using an excess of epoxide is the increased likelihood of forming ether linkages, therefore forming polymers with lower ester selectivity and decreasing the degree of monomer alternation. Evidence of this is entry 1 (Table 1) where a polymer with only 3% selectivity was produced when the reaction was carried out in excess CHO. The inclusion of the PPNCI co-catalyst increased the ester selectivity and polymer molecular weight when the reactions were carried out with toluene as a solvent. It is therefore likely the co-catalyst will have a similar beneficial effect when the reaction is carried out solvent free, in bulk epoxide. The reaction time for the ROCOP of epoxides and cyclic anhydrides is of greater importance when the reaction is carried out in excess epoxide compared to when it is carried out in a solvent. Following the complete conversion of the anhydride, the remaining epoxide can continue to react forming polyether and decreasing the apparent selectivity, but in reality producing a block copolymer of the type (polyester)<sub>n</sub>–(polyether)<sub>m</sub>. In order to produce highly alternating copolymers, selecting the optimal reaction time is crucial so that the reaction is terminated as close to 100% anhydride conversion, but without going over-time.

### 2.3.4 Ring-opening copolymerisation (ROCOP) in bulk epoxide

There are many advantages to using solvent-free conditions for the ROCOP of epoxides and cyclic anhydrides. The reactions are more sustainable, reducing the number of chemicals required and eliminating the need for the solvent to be removed from the product (the excess epoxide can in principle be used in further ROCOP reactions).<sup>72,73</sup> Carrying out the reaction in excess epoxide substantially increases the rate of the ROCOP reaction. As the rate determining step of the reaction is the ring-opening of the epoxide, the rate equation can be approximated as  $\text{rate} = k[\text{epoxide}]$  and therefore the higher concentration of this monomer increases the rate of the reaction. In order to evaluate the efficacy of **1** as a catalyst for the solvent-free ROCOP of epoxides and cyclic anhydrides, experiments were carried out at a reactant ratio epoxide:anhydride:catalyst:co-catalyst = 2,000:400:1:2.

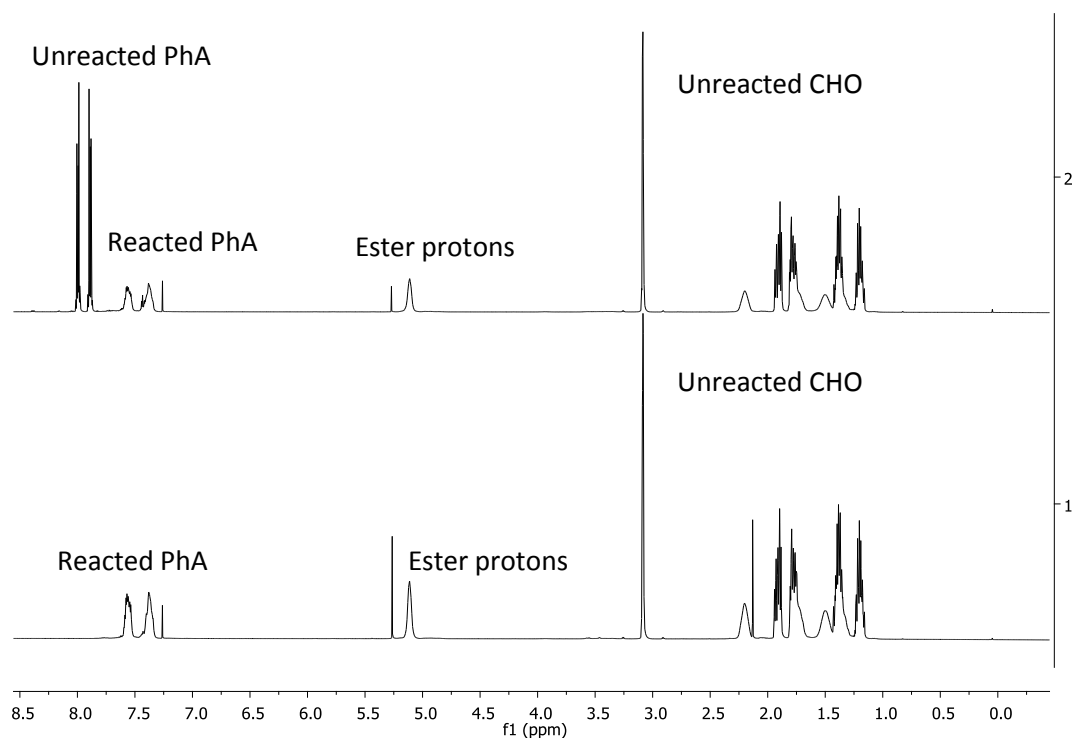


**Figure 12** Comparison of the crude <sup>1</sup>H NMR spectra (500 MHz, CDCl<sub>3</sub>) of CHO–PhA co-polymers at 50% (top, entry 16) and 100% (bottom, entry 17) conversion

In order to identify the optimal reaction time for the solvent free ROCOP, tests were carried out with different epoxides and PhA at various reaction times; the

## **Chapter 2 - Formation of polyesters via the ring-opening copolymerisation of epoxides and cyclic anhydrides**

polymerisation is complete when all of the anhydride is consumed. PhA was selected as the anhydride monomer because the comparison of unreacted PhA and reacted PhA in  $^1\text{H}$  NMR spectra is straightforward; the monomer and polymer signals are distinct, and not obscured by other proton environments making it possible to easily calculate conversion. Figure 12 shows the crude  $^1\text{H}$  NMR spectra for CHO–PhA at 50% and 100% conversion, in which the signals attributed to unreacted PhA at around 8 ppm and reacted PhA at approximately 7.5 ppm are indicated. Comparing the integrals of these signals gives the reaction conversion. Also present in the spectra is the ester signal at 5.1 ppm, the epoxide signal of unreacted CHO at 3.1 ppm and a mixture of signals associated with reacted and unreacted CHO between 1 – 2.5 ppm.

**Table 3** Solvent-free ROCOP of epoxides with PhA

Entry	Epoxide	Anhydride	Time (mins)	Conversion (%) <sup>a</sup>
16	CHO	PhA	60	50
17	CHO	PhA	120	100
18	ECH	PhA	30	49
19	ECH	PhA	60	100
20	PO	PhA	45	35
21	PO	PhA	120	100
22	VCHO	PhA	60	51
23	VCHO	PhA	120	100

6.4  $\mu\text{mol}$   $[\text{Al}(\text{L}1)\text{Cl}_2]$  (**1**) catalyst.  $[\text{Epoxide}]_0:[\text{Anhydride}]_0:[\text{Catalyst}]_0:[\text{PPNCl}]_0 = 2000:400:1:2$ . Reactions heated at 80 °C. <sup>a</sup>Conversion (%) calculated by comparison of the aromatic signals of reacted and unreacted PhA.

As the ring-opening of the epoxide monomer is the rate determining step, the optimal reaction time for a given epoxide with PhA can be applied to other cyclic anhydride monomers, so long as the epoxide is unchanged. The conversion of PhA with the epoxides CHO, ECH, PO and VCHO were measured at different reaction times to determine the time at which 100% conversion was achieved. The results are shown in Table 3.

Reactions with CHO, PO and VCHO all had similar rates of reaction. 100% conversion of PhA was achieved after 2 hours at 80 °C (entries 17, 21 and 23).

**Chapter 2** - *Formation of polyesters via the ring-opening copolymerisation of epoxides and cyclic anhydrides*

After 1 hour, 50% and 51% conversions were recorded for CHO–PhA (entry 16) and VCHO–PhA (entry 22) respectively. This is expected, as the only difference between these epoxides is the additional vinyl functional group in VCHO and this is far removed from the reactive epoxide functionality, so is unlikely to affect reactivity. After 45 minutes, a conversion of 35% was recorded for PO–PhA (entry 20), indicating that this polymerisation progresses at a similar rate to those with CHO and VCHO. The reaction of ECH and PhA was faster than the other examples and complete conversion was achieved after 1 hour under the same conditions (entry 19). After 30 minutes, 50% conversion was recorded for this reaction (entry 18). The ester selectivities of the polymers isolated at 100% conversion were all >95% (entries 17, 19, 21 and 23). This indicates that the polymer chains comprise of highly alternating monomer units and that no significant polyether had formed following the consumption of the anhydride monomer; performing the reaction under solvent-free conditions with excess epoxide had no overall detrimental effect on the polymer microstructure compared to when the reaction was performed in toluene.



**Chapter 2 - Formation of polyesters via the ring-opening copolymerisation of epoxides and cyclic anhydrides**

**Table 4** Solvent-free ROCOP of a variety of different epoxides and cyclic anhydrides

Entry	Epoxide	Anhydride	Time (hrs)	Yield (%) <sup>a</sup>	Selectivity (%) <sup>b</sup>	Mn <sup>c</sup> (gmol <sup>-1</sup> )	Đ <sup>c</sup>
24	CHO	PhA	2	78	99	14500	1.21
25	CHO	TCPhA	2	98	99	18660	1.58
26	CHO	TBPhA	2	90	95	10880	1.66
27	CHO	4BPhA	2	92	72	5520	1.31
28	CHO	CEA	2	84	86	<1250	-
29	ECH	PhA	1	64	99	3630	1.54
30	ECH	TCPhA	1	97	99	8890	1.44
31	ECH	TBPhA	1	84	96	14520	1.46
32	ECH	4BPhA	1	93	95	4800	1.13
33	ECH	CEA	1	64	99	4530	1.37
34	PO	PhA	2	66	99	17880	1.14
35	PO	TCPhA	2	90	95	7040	1.24
36	PO	TBPhA	2	97	97	10060	1.82
37	PO	4BPhA	2	93	81	4240	1.55
38	PO	CEA	2	91	99	2260	1.28
39	VCHO	PhA	2	71	99	13690	1.21
40	VCHO	TCPhA	2	90	99	17170	1.39
41	VCHO	TBPhA	2	96	99	22200	1.67
42	VCHO	4BPhA	2	90	77	4890	1.12
43	VCHO	CEA	2	94	99	2100	1.15
44 <sup>d</sup>	LO	TCPhA	2	71	99	3100	1.18
45 <sup>d</sup>	LO	PhA	2	81	99	2800	1.27

6.4 μmol [Al(L1)Cl<sub>2</sub>] (1) catalyst. [Epoxide]<sub>0</sub>: [Anhydride]<sub>0</sub>: [Catalyst]<sub>0</sub>: [PPNCl]<sub>0</sub> = 2000:400:1:2. Reactions heated at 80 °C. <sup>a</sup>Isolated yield. <sup>b</sup>Determined by comparison of ester and ether signals in <sup>1</sup>H NMR spectra. <sup>c</sup>Determined by GPC using triple detection. <sup>d</sup>[Epoxide]<sub>0</sub>: [Anhydride]<sub>0</sub>: [Catalyst]<sub>0</sub>: [PPNCl]<sub>0</sub> = 1000:200:1:1. Reaction heated at 150 °C.

## **Chapter 2** - Formation of polyesters via the ring-opening copolymerisation of epoxides and cyclic anhydrides

Using the optimal reaction times for CHO, ECH, PO and VCHO, solvent-free reactions of these epoxides with the cyclic anhydrides PhA, TCPPhA, TBPhA, 4BPhA and CEA were attempted. The results of these copolymerisations are shown in Table 4.

The results in Table 4 show that **1** is an effective catalyst for the solvent-free ROCOP of epoxides and cyclic anhydrides across a two-dimensional array of substrates. Compared to the same experiment carried out with a solvent, the reaction time is much improved requiring only 2 hours for the polymerisations with the epoxides CHO, PO and VCHO and 1 hour for reactions with ECH. All polyesters were isolated in good to excellent yields. The vast majority of experiments produced polymer chains comprised of highly alternating epoxide and anhydrides monomer units, illustrated by high selectivity to ester linkages  $\geq 95\%$ . Exceptions with lower selectivity are the copolymerisation of CHO with 4BPhA (entry 27) and CEA (entry 28) which yielded polymers with 72% and 86% respectively. The copolymers PO–4BPhA (entry 37) and VCHO–4BPhA (entry 42) have ester selectivity of 81% and 77% respectively. These results suggest reactions with 4BPhA tend to give polymers with higher ether content (i.e. lower selectivities); only ECH–4BPhA (entry 32) had a selectivity  $\geq 95\%$ .

The copolymers shown in Table 4 have a variety of molecular weights. The copolymerisations with CEA all gave low molecular weight polymers. CHO–CEA (entry 28) had a  $M_n$  of  $<1,250 \text{ g mol}^{-1}$ , while reactions with ECH, PO and VCHO gave polymers with  $M_n$  between  $2,100 - 4,530 \text{ g mol}^{-1}$ . Reactions with 4BPhA also gave low molecular weight products with  $M_n$  values between  $4,240 - 5,520 \text{ g mol}^{-1}$ . Polymers with PhA tended to give polymers with relatively high molecular weights, copolymerisation with CHO, PO and VCHO (entries 24, 34 and 39) yielded products with  $M_n$  between  $13,690 - 17,880 \text{ g mol}^{-1}$ . The ECH analogue produced a very different result with a very low  $M_n$  of  $3,630 \text{ g mol}^{-1}$ . TCPPhA copolymers exhibited moderate to good molecular weights, CHO–TCPPhA and VCHO–TCPPhA (entries 25 and 40) had  $M_n$  values of  $18,660$  and  $17,170 \text{ g mol}^{-1}$  respectively, whereas ECH–TCPPhA and PO–TCPPhA copolymers (entries 30 and 35) had slightly lower  $M_n$  of  $8,890$  and  $7,040 \text{ g mol}^{-1}$ . Copolymers of TBPhA all exhibited high molecular weights, with  $M_n > 10,000 \text{ g mol}^{-1}$ . CHO–TBPhA (entry 26),

## **Chapter 2 - Formation of polyesters via the ring-opening copolymerisation of epoxides and cyclic anhydrides**

ECH–TBPhA (entry 31) and PO–TBPhA (entry 36) had  $M_n$  between 10,060 – 14,520  $\text{g mol}^{-1}$ , while for VCHO–TBPhA (entry 41) an extremely high  $M_n$  of 22,200  $\text{g mol}^{-1}$  was recorded.

The  $\bar{D}$  of the copolymers produced in the solvent-free ROCOP of epoxides and cyclic anhydrides also varied greatly. The lowest  $\bar{D}$  and therefore greatest control over polymer chain length was found for the copolymers with the PhA monomer. The polymers produced from the reaction of PhA with CHO (entry 24), PO (entry 34) and VCHO (entry 39) all had  $\bar{D}$  values  $\leq 1.21$ . The exception to this was ECH–PhA (entry 29) which produced a higher  $\bar{D}$  value of 1.54. All examples had  $\bar{D} < 2$  indicating moderate to good control over the polymerisation. The TCPHA containing copolymers tended to give higher  $\bar{D}$  than those synthesised with PhA, only PO–TCPHA (entry 35) had a similar value (1.24). The copolymer VCHO–TCPHA (entry 40) exhibited a slightly higher  $\bar{D}$  of 1.39, while for CHO–TCPHA (entry 25) and ECH–TCPHA (entry 30)  $\bar{D}$  values of 1.58 and 1.44 were recorded respectively. Polyesters containing TBPhA gave relatively high  $\bar{D}$ , all examples (entries 26, 31, 36 and 41) had values between 1.46–1.82. Copolymers of 4BPhA gave a variety of  $\bar{D}$  values. ECH–4BPhA (entry 32) and VCHO–4BPhA (entry 42) gave low values of 1.13 and 1.12 respectively, conversely for CHO–4BPhA (entry 27) and PO–4BPhA (entry 37)  $\bar{D}$  values of 1.31 and 1.55 were recorded. Similarly the CEA copolymers (entries 33, 38 and 43) yielded a variety of  $\bar{D}$  values between 1.15 – 1.37.

The solvent free ROCOP of GA and NPA with various epoxides was attempted, however neither anhydride successfully yielded copolymer. Reactions with GA did produce a viscous oil, however GPC analysis indicated that the material formed was very low molecular weight oligomers with  $M_n < 1,250$ . NPA anhydride did not react with any of the epoxides under the conditions reported in this thesis. The solubility of NPA in all the epoxides tested seemed to be an issue, as very little, if any, dissolved during the reaction. Kleij and colleagues reported the formation of a copolymer from the reaction of CHO and NPA. The polymerisation required 30 hours to achieve a conversion of 41%. This report indicates that copolymerisation with NPA is

## **Chapter 2** - Formation of polyesters via the ring-opening copolymerisation of epoxides and cyclic anhydrides

possible, however **1** is clearly not an effective catalyst for polymerisation with this monomer.<sup>36</sup>

The ROCOP of LO with the anhydrides TCPhA and PhA was explored. LO is a very attractive monomer as it is derived from renewable chemical feedstocks. Any copolymers which are produced with LO are bioderived or partially bioderived. PhA can also be synthesised completely from biomass sources. Lobo and colleagues reported its synthesis from biomass derived furan and maleic anhydride.<sup>56</sup> The ROCOP reactions with LO were carried out under solvent-free reaction conditions that were slightly different to the previous reactions. A [Epoxide]<sub>0</sub>: [Anhydride]<sub>0</sub>: [Catalyst]<sub>0</sub>: [PPNCl]<sub>0</sub> reactant ratio of 1000:200:1:1 was employed and the reaction temperature was increased to 150 °C. The polymerisation of LO and TCPhA (entry 44) yielded a polymer with a relatively low  $M_n$  of 3,100 g mol<sup>-1</sup> with a low  $\bar{D}$  value of 1.18. LO–PhA (entry 46) produced a copolymer with similar properties recording a  $M_n$  of 2,800 g mol<sup>-1</sup> and a  $\bar{D}$  of 1.27.

The variety of molecular weights and  $\bar{D}$  reported for the polyesters in Table 4 may be caused by impurities in the monomers (Chapter 2.6) or the likelihood of transesterification reactions (Chapter 2.5).

**Chapter 2 - Formation of polyesters via the ring-opening copolymerisation of epoxides and cyclic anhydrides**

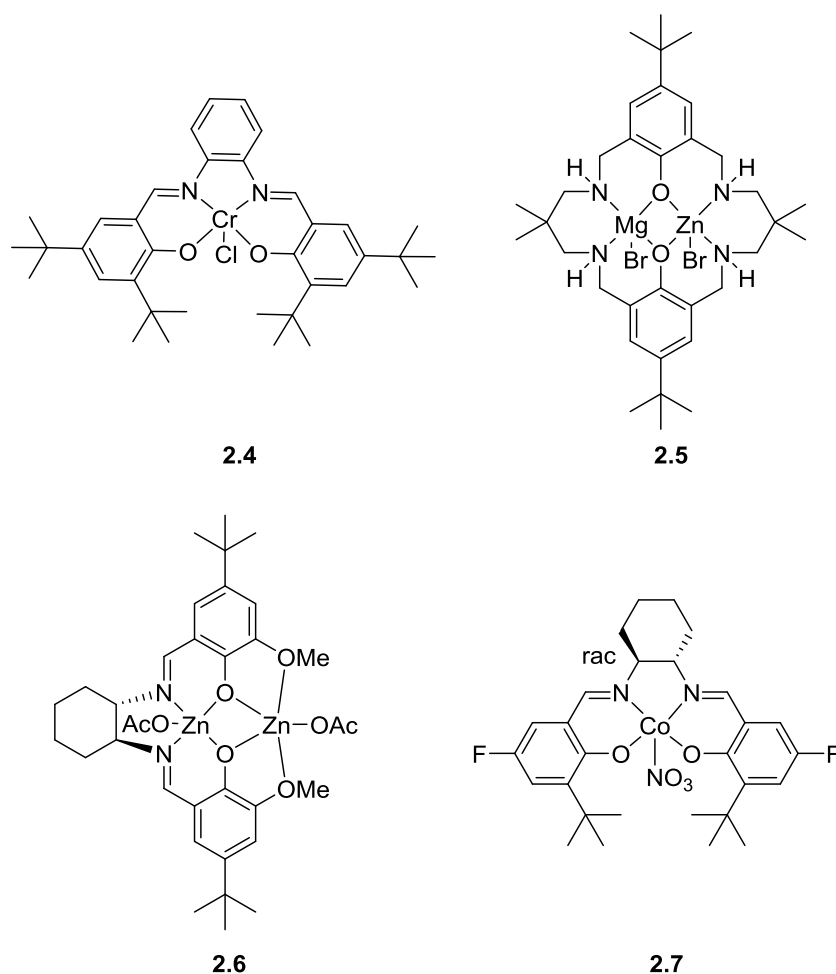


**Figure 13** Alternative catalysts for ROCOP of epoxides and cyclic anhydrides<sup>3,29,42</sup>

Comparison with other examples in the literature suggests that **1** is a relatively fast catalyst for the ROCOP of epoxides and anhydrides. To quantify the activity of a catalyst, the turnover number (TON) and turnover frequency (TOF) can be calculated. The TON is the number of moles of monomer reacted divided by the moles of catalyst. TOF is equal to the TON divided by reaction time (hours). For the copolymerisations with the epoxides CHO, PO and VCHO a TOF of 200 h<sup>-1</sup> was recorded using **1** at 80 °C. Reactions with ECH had TOFs of 400 h<sup>-1</sup> under the same conditions. For some catalysts in the literature TOF's have been calculated. For the ROCOP of CHO and PhA catalysed by [Cr(saloph)Cl] (**2.4**) (Figure 13) with 1 equivalent of PPNCl at 110 °C a TOF of 245 h<sup>-1</sup> was measured.<sup>29</sup> Williams and co-workers have reported the activity of a variety of bimetallic catalysts for the copolymerisation of CHO

## **Chapter 2 - Formation of polyesters via the ring-opening copolymerisation of epoxides and cyclic anhydrides**

and PhA at 100 °C.<sup>42</sup> The fastest were a mixed metal magnesium – zinc bimetallic catalyst (**2.5**) (Figure 13) and zinc acetate salen based bimetallic catalyst (**2.6**) (Figure 13) with TOF of 188<sup>49</sup> and 198<sup>44</sup> h<sup>-1</sup> respectively. Coates *et al.* reported the copolymerisation of both ECH and PO with PhA catalysed by [Co(III)(salcy)(NO<sub>3</sub>)] (**2.7**) (Figure 13) at 30 °C. For the reaction with ECH and PO, TOF values of 128 and 80 h<sup>-1</sup> were reported respectively.<sup>3</sup> Whilst the recorded TOF are relatively low, the fact these catalysts are active at such low temperatures is remarkable. The catalyst loading utilised in our copolymerisations with **1** were very low (0.25 mol%). In many catalytic systems for the ROCOP of epoxides and cyclic anhydrides, at low catalytic loadings only moderate or poor activity is exhibited. The excellent activity of **1** at very low loading is a significant advantage, as it reduces cost, minimises catalyst residue and allows access to high molecular weight polymers.<sup>74</sup> The catalytic loadings of the catalysts **2.4-7** are 0.4, 1, 1 and 0.25 mol% respectively.<sup>3,29,44,49</sup>

The polymerisation catalysed by **1** in this study and **2.7** in the work by Coates *et al.* were carried out at the same catalyst loading. In both systems the PO–PhA produced had good molecular weights, when catalysed by **1** the Mn of the copolymer was 17,880 gmol<sup>-1</sup>, which is slightly lower than that produced by **2.7** (19,100 gmol<sup>-1</sup>). However, based on the fact that in the reaction with **1**, the number of initiators was twice the number in the **2.7** system, the theoretical molecular weight is half. The control exhibited by both systems was excellent, recording Đ's of 1.14 and 1.16 for **1** and **2.7** respectively. The performance of **1** for the formation of ECH–PhA in bulk epoxide (entry 29) was worse than that of **2.7** in terms of molecular weight and control. When the ECH–PhA copolymer was synthesised in toluene the molecular weight and Đ improved (entry 8), however the molecular weight was still lower than the copolymer produced with **2.7**. The ECH–PhA synthesised in entry 8 had a Mn of 5,100 gmol<sup>-1</sup> and a Đ of 1.13 compared to 21,000 gmol<sup>-1</sup> and 1.13 for **2.7**.<sup>3</sup> In the synthesis of CHO–PhA by **1**, good control over the polymerisation was exhibited, the Đ (1.21) achieved was very similar to that reported for CHO–PhA, catalysed by **2.4** and **2.6**. The molecular weight of CHO–PhA generated with **1** (Mn = 14,500 gmol<sup>-1</sup>) was very similar to **2.4** (Mn = 15,000 gmol<sup>-1</sup>) and much greater than that produced by **2.6** (Mn = 5,300 gmol<sup>-1</sup>).

## **Chapter 2 - Formation of polyesters via the ring-opening copolymerisation of epoxides and cyclic anhydrides**

The effect of a solvent-free ROCOP reaction compared to one utilising toluene as a solvent can be further quantified by examining the copolymers produced from the reactions of the epoxides CHO, ECH and PO with the anhydrides PhA, TcPhA and TBPhA synthesised with **1** under the two sets of conditions. Higher molecular weights and lower polymer dispersities were achieved by using a solvent and equimolar quantities of monomer for the copolymers, ECH–PhA (entries 8, Table 2 and 29, Table 4), ECH–TcPhA (entries 9, Table 2 and 30, Table 4) and PO–TcPhA (entries 12, Table 2 and 35, Table 4). Conversely higher molecular weights and lower polymer dispersities were achieved without solvent and with excess epoxide for the copolymers CHO–PhA (entries 5, Table 2 and 24, Table 4), CHO–TBPhA (entries 7, Table 2 and 26, Table 4) and PO–PhA (entries 11, Table 2 and 34, Table 4). For the copolymers CHO–TcPhA (entries 6, Table 2 and 25, Table 4), ECH–TBPhA (entries 10, Table 2 and 31, Table 4) and PO–TBPhA (entries 13, Table 2 and 36, Table 4) higher molecular weights were achieved with excess epoxide whereas lower  $\bar{M}_n$  and greater polymerisation control was attained when the reactions were carried out with a solvent. This comparison indicates that for different monomer combinations, higher molecular weights and lower polydispersity indices can be achieved through different reaction conditions, and that there is not necessarily any obvious trend by which the optimum conditions can be predicted. Solvent free ROCOP reactions have the advantage of higher reaction rates compared to reactions with a solvent, however when considering polymer molecular weight and  $\bar{M}_n$ , neither solvent free nor reactions in toluene are most effective in all cases.

### **2.4 Mechanistic studies**

In order to gain a greater understanding of the mechanism of the ROCOP of epoxides and cyclic anhydrides catalysed by **1**, the initiation of the polymerisation was studied by *in situ* NMR experiments involving the stoichiometric reaction of **1** with ECH in the presence of 1 equivalent of PPNCl. Density functional theory (DFT) calculations were also carried out to probe the overall mechanism of polymerisation with **1**.

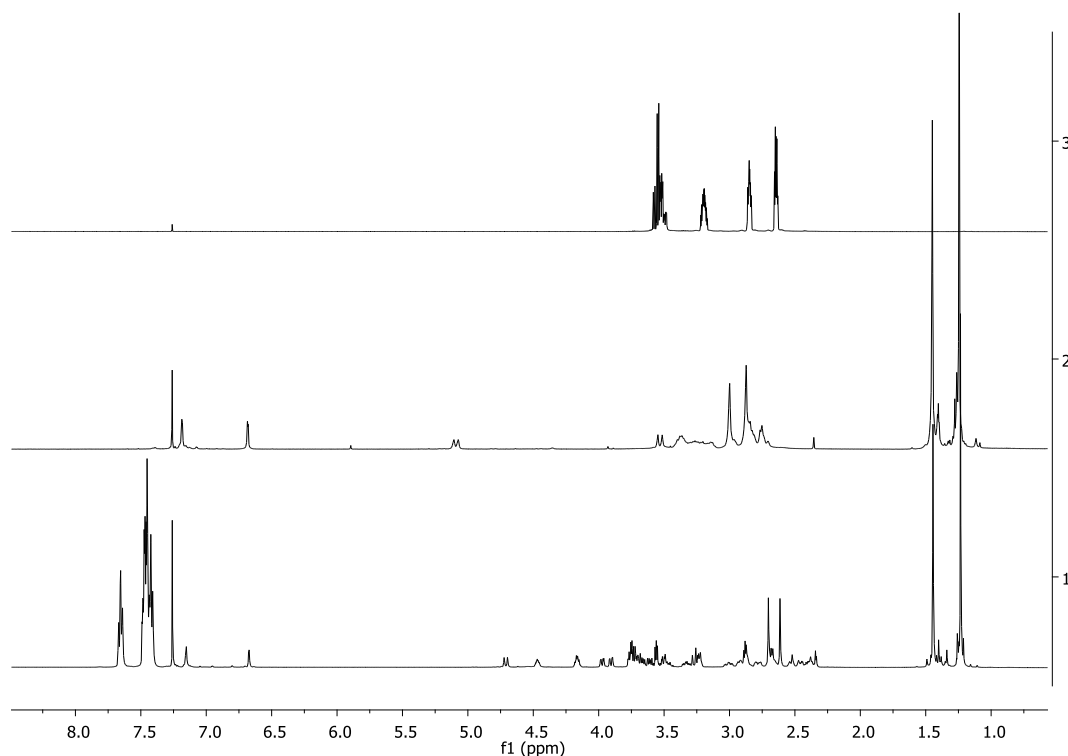


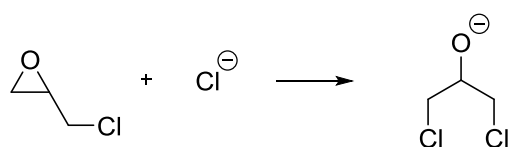
**Figure 14**  $^1\text{H}$  NMR (500 MHz,  $\text{CDCl}_3$ ) spectra of **1** (spectrum 1), NMRexp1 (spectrum 2) and (400 MHz,  $\text{CDCl}_3$ ) of ECH (spectrum 3).

In an NMR scale reaction, **1** was combined with 2 molar equivalents of ECH and 1 equivalent of PPNCl in  $\text{CDCl}_3$  (NMRexp1). After 24 hours, NMR spectra of the mixture were recorded (shown in appendix). Figure 14 shows the  $^1\text{H}$  NMR spectra of **1** before the reaction and following addition of ECH (NMRexp1). It is clear from the spectra that following addition of ECH, significant changes to **1** have arisen. A substantial change to the chemical shift of the methylene bridge between the phenoxy and TACN rings of **L1** has occurred; in **1** this chemical environment gave rise to two sets of doublets at 5.09 and 3.53 ppm, whereas in NMRexp1 these signals have shifted to 4.71 and 3.27 ppm. This considerable change is good evidence for a reaction taking place between **1** and ECH. In addition, a series of new resonances appeared in the  $^1\text{H}$  NMR spectrum of NMRexp1 between 2.25 – 5 ppm, none of which correspond to unreacted ECH. Analysis of the  $^1\text{H}$ ,  $^{13}\text{C}$  and DEPT-135 NMR spectra and the 2D COSY and HSQC NMR experiments indicate that the new signals are produced by alkoxides generated from the ring-opening of ECH. New multiplets at 4.47 and 4.17 ppm appear in the  $^1\text{H}$  NMR spectrum of

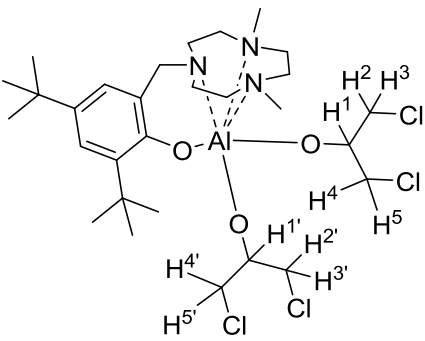


**Chapter 2 - Formation of polyesters via the ring-opening copolymerisation of epoxides and cyclic anhydrides**

NMRexp1. The integration of these peaks and the signals in the DEPT-135 indicates that these signals are CH groups. COSY suggests that each of these signals are related to a set of four other resonances. According to the DEPT-135 these signals are CH<sub>2</sub> groups. The two signals that appear to be doublets at 3.98 and 3.91 ppm are from protons on different carbons according to the HSQC spectrum and each integrate to approximately 1. Whilst both protons are on different carbons, both signals correlate to the multiplet at 4.47 ppm and two other signals at 3.70 and 3.65 ppm in the COSY experiment. The signal at 3.98 ppm correlates to the signal at 3.70 ppm, whilst the signals at 3.91 and 3.65 ppm correlate, suggesting each pair belong to protons which are bound to the same CH<sub>2</sub> carbon. The multiplet at 4.17 ppm correlates to signals at 3.74, 3.60, 3.49 and 3.23 ppm. Correlations between one pair of signals at 3.74 and 3.60 ppm and another at 3.49 and 3.23 ppm suggest that each pair relate to protons bound to the same carbon.



**Scheme 12** Ring-opening of ECH following nucleophilic attack of a chloride ion

	Nucleus	$\delta_H$ (ppm)
<b>1A</b>	H <sup>1</sup>	4.17
	H <sup>1'</sup>	4.47
	H <sup>2</sup>	3.74
	H <sup>2'</sup>	3.98
	H <sup>3</sup>	3.60
	H <sup>3'</sup>	3.70
	H <sup>4</sup>	3.49
	H <sup>4'</sup>	3.91
	H <sup>5</sup>	3.23
	H <sup>5'</sup>	3.65

**Figure 15** Proposed complex formed in NMRexp1

## Chapter 2 - Formation of polyesters via the ring-opening copolymerisation of epoxides and cyclic anhydrides

Coates *et al.* reported that in the initiation step of the ROCOP mechanism, the epoxide is ring-opened by nucleophilic attack of a chloride at the least substituted carbon of the epoxide and therefore in the case of ECH yielding the alkoxide shown in Scheme 12. Based on the NMR data gathered in NMRexp1, the result of the addition of ECH to **1** yielded a new complex **1A** (Figure 15) which contained two alkoxide units in which all protons are inequivalent giving rise to 10  $^1\text{H}$  NMR signals. In Figure 15 the proton environments  $\text{H}^1 - \text{H}^5$  and  $\text{H}^{1'} - \text{H}^{5'}$  are labelled and correspond to the following signals in the  $^1\text{H}$  NMR: 4.17, 3.74, 3.60, 3.49 and 3.23 ppm are assigned to  $\text{H}^1$ ,  $\text{H}^2$ ,  $\text{H}^3$ ,  $\text{H}^4$  and  $\text{H}^5$  respectively and 4.47, 3.98, 3.70, 3.91 and 3.65 ppm are assigned to  $\text{H}^{1'}$ ,  $\text{H}^{2'}$ ,  $\text{H}^{3'}$ ,  $\text{H}^{4'}$  and  $\text{H}^{5'}$  respectively.

In NMRexp2, 1 molar equivalent of ECH was added to **1** in the presence of PPNCI and the  $^1\text{H}$  NMR spectrum of the mixture after 24 hours is shown in Figure 16.

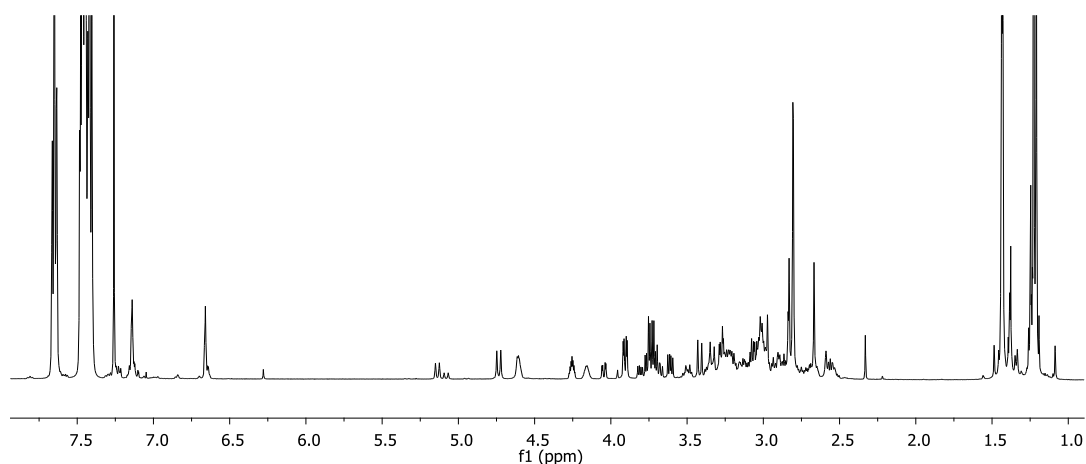


**Figure 16**  $^1\text{H}$  NMR spectrum (500 MHz,  $\text{CDCl}_3$ ) of NMRexp2

Differences between the  $^1\text{H}$  NMR spectra of NMRexp2 and that of **1** indicates that a reaction has occurred. However unlike in NMRexp1 where NMR data suggests that one major product had been formed, in NMRexp2 it seems that multiple aluminium complexes have been generated. Evidence of this can be found in the  $^1\text{H}$  (Figure 16),  $^{13}\text{C}$ , DEPT-135, COSY, and HSQC NMR measurements of NMRexp2 (shown in appendix). Three doublets at chemical shifts of 5.14, 5.08 and 4.74 ppm are visible in the  $^1\text{H}$  NMR spectrum of NMRexp2. These peaks are each a result of a single proton from the ligand

## Chapter 2 - Formation of polyesters via the ring-opening copolymerisation of epoxides and cyclic anhydrides

methylene bridges in three different aluminium complexes. A COSY experiment confirms that each doublet correlates to another at lower chemical shifts (the signals at 5.14, 5.08 and 4.74 ppm correlate to resonances at 3.33, 3.49 and 3.42 ppm respectively), while the signals at 3.49 and 3.33 ppm are obscured by other resonances, the doublet at 3.42 ppm is unobscured and has the same integration as the signal at 4.74 ppm. Further evidence that these signals in the  $^1\text{H}$  NMR spectrum are ligand methylene groups, can be seen in the HSQC which indicates that each set of doublets corresponds to a single carbon signal and 135-DEPT confirms that these are  $\text{CH}_2$  carbons. Whilst the doublet at 5.08 ppm matches well with a methylene signal in **1**, neither of the other sets of doublets match with those of **1A**.

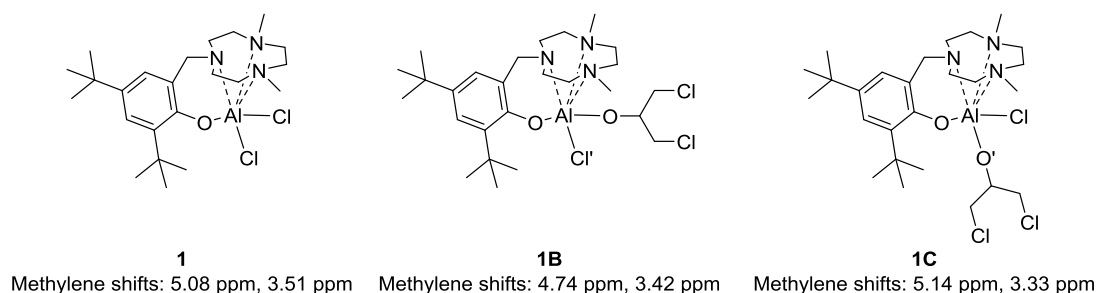


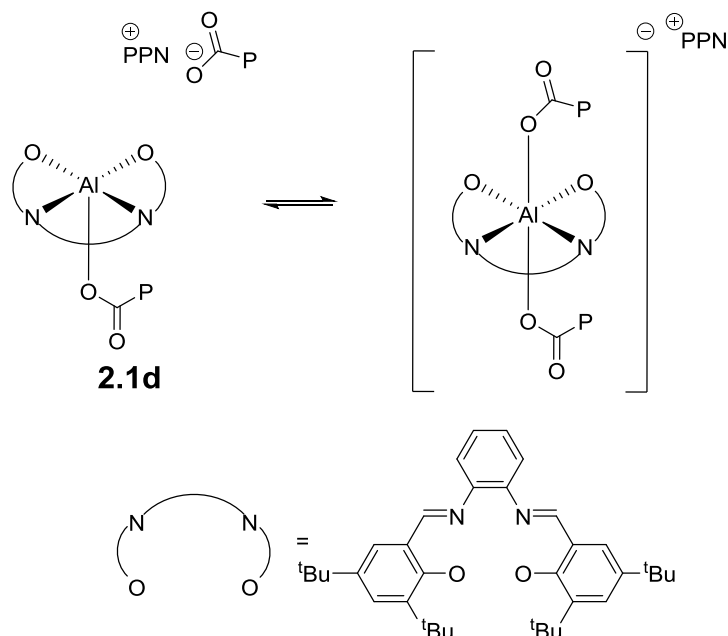
**Figure 17** Species generated in NMRexp2

Based on these observations, the species present in NMRexp2 include unreacted catalyst **1** and another two additional aluminium complexes. Considering only one equivalent of ECH was added in NMRexp2, the additional complexes evident in the  $^1\text{H}$  NMR spectrum can be tentatively assigned as the complex  $[\text{Al}(\text{L1})(\text{Cl})\{\text{OCH}(\text{CH}_2\text{Cl})_2\}]$  (**1B**) and  $[\text{Al}(\text{L1})(\text{Cl}')\{\text{OCH}(\text{CH}_2\text{Cl})_2\}]$  (**1C**), where **1B** and **1C** are diastereoisomers. The complexes **1**, **1B** and **1C** are shown in Figure 17 along with the chemical shifts of the methylene groups of each species.

The stoichiometric reactions NMRexp1 and NMRexp2 in which ECH was combined with **1** and  $\text{PPNCl}$ , suggest that nucleophilic attack of ECH by chloride gives rise to aluminium alkoxide complexes **1A-C**. This is good evidence for the involvement of **1** in the initiation step of the ROCOP mechanism and is consistent with the mechanism proposed by Coates *et al.*<sup>58</sup>

## Chapter 2 - Formation of polyesters via the ring-opening copolymerisation of epoxides and cyclic anhydrides

Reactions of 1 and 2 equivalents of ECH gave rise to stepwise conversion of **1** to species consistent with  $[\text{Al}(\text{L1})(\text{Cl})\{\text{OCH}(\text{CH}_2\text{Cl})_2\}]$  and  $[\text{Al}(\text{L1})\{\text{OCH}(\text{CH}_2\text{Cl})_2\}_2]$ .



**Scheme 13** Steady state species in the ring-opening copolymerisation (ROCOP) mechanism reported by Coates *et al.*<sup>58</sup>

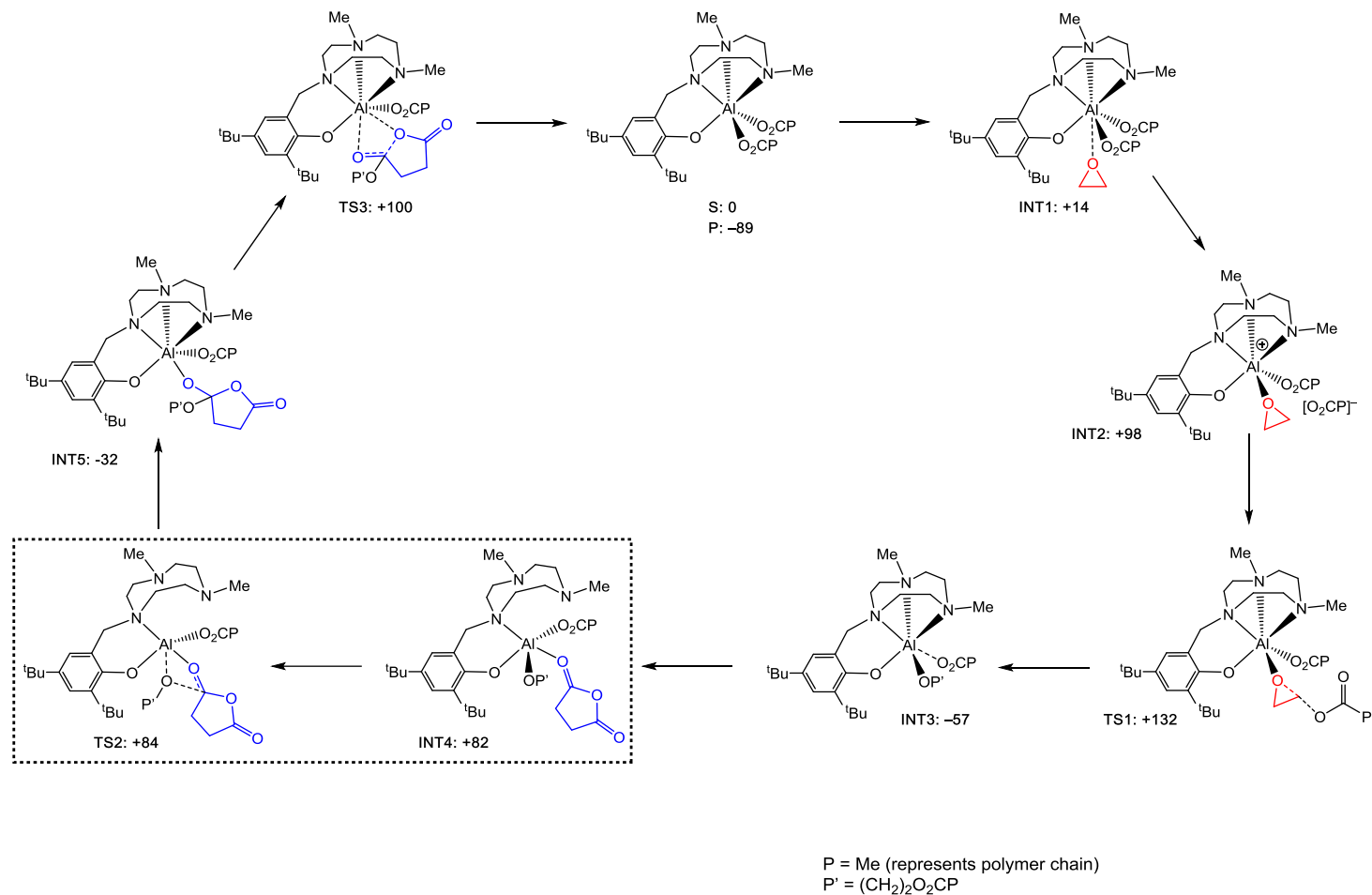
Whilst there are similarities between the initiation step for the ROCOP with **1** and that reported by Coates, when considering the overall mechanism there are a number of areas where catalysis with **1** will differ. The difficulties in applying the Coates mechanism to **1** arise due to the fact that a dianionic Salen-type ligand was the base of the proposed mechanism, which is very different from the monoanionic **L1**. A 5-coordinate aluminium complex is formed with the Salen ligand, which was converted to a 6-coordinate anionic resting state **2.1d** (Scheme 13). In order for the coordination and subsequent ring-opening of an epoxide monomer, one of the carboxylate-terminated polymer chains decoordinates (*affording a neutral complex* and a free anionic polymer chain). External attack of the decoordinated polymer chain causes ring-opening of the coordinated epoxide, yielding an alkoxide.<sup>58</sup> These transformations are entirely convincing for the 5-coordinate Salen-aluminium system. It is however unclear how the principles of this mechanism would apply to the ROCOP of epoxides and cyclic anhydrides catalysed by **1**, where

**Chapter 2** - Formation of polyesters via the ring-opening copolymerisation of epoxides and cyclic anhydrides

coordination of a seventh donor to the aluminium centre is unlikely due to its coordinative saturation, and moreover decoordination of a polymer chain from the implied 6-coordinate  $[\text{Al}(\text{L1})(\text{O}_2\text{CP})_2]$  ( $\text{O}_2\text{CP}$  = carboxylate-terminated polymer chain) would lead to a highly energetically disfavoured separated ion pair, *i.e.* a cationic complex and a free anionic polymer chain.

In order to elucidate the ROCOP mechanism with **1**, density functional calculations were undertaken by Dr. Benjamin Ward, to probe the copolymerisation of ethylene oxide and succinic anhydride catalysed by the model complex  $[\text{Al}(\text{L1})(\text{O}_2\text{CMe})_2]$ , with acetate ligands representing carboxylate-terminated polymer chains (Scheme 14).<sup>75</sup> Calculated structures are shown in the appendix.

## Chapter 2 - Formation of polyesters via the ring-opening copolymerisation of epoxides and cyclic anhydrides



**Scheme 14** Proposed catalytic cycle for the ring-opening copolymerisation (ROCOP) of epoxides and anhydrides by **1**; P = Me and represents the polymer chain, P' =  $(\text{CH}_2)_2\text{O}_2\text{CP}$ . Gibbs energies ( $G_{rel}$ ) in  $\text{kJ mol}^{-1}$  (298 K) calculated using M06-2X | cc-pDTZ/cc-pV(T+d)Z are shown alongside each label. Boxed section highlights the hemilability of the macrocyclic ligand.

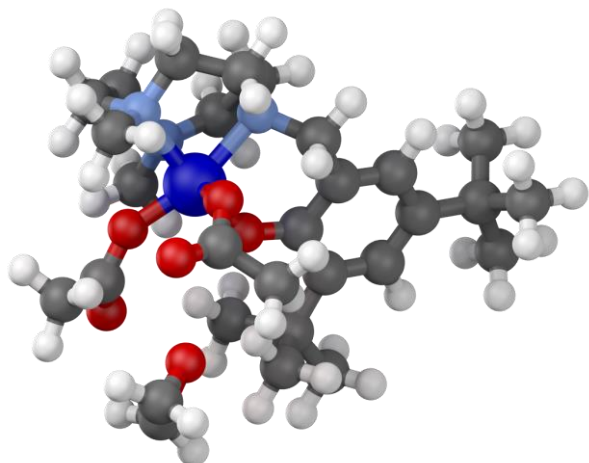


**Figure 18** Calculated structure of INT1 [M06-2X | cc-pVTZ/cc-pV(T+d)Z]

As expected, decooordination of an acetate yielding  $[\text{Al}(\text{L1})(\text{O}_2\text{CMe})]^+$  was highly endergonic with a  $G_{\text{rel}} = +266 \text{ kJ mol}^{-1}$ , which increased further to  $+281 \text{ kJ mol}^{-1}$  upon epoxide coordination; this pathway was therefore deemed non-viable. Instead, the epoxide engages in weak interactions with the aluminium centre (**INT1**, Figure 18). The aluminium–oxygen bond distance is  $4.14 \text{ \AA}$  which is marginally longer than the sum of the equilibrium van der Waals radii ( $\Sigma r_{\text{vdW}} = 4.11 \text{ \AA}$ ).<sup>76</sup> Although Bader’s quantum theory of atoms in molecules (QTAIM) indicated that there was no bond critical point (BCP) between these atoms,<sup>77</sup> the natural bonding orbital (NBO) analysis indicates a weak donor-acceptor interaction between the aluminium and the oxygen of the epoxide; this interaction is best described as approximately sp-p.<sup>78</sup> QTAIM analysis indicated a number of BCPs (with weak electron density maxima,  $\rho$ ) were identified between the epoxide and C–H groups on the ligand periphery, consistent with weak van der Waals type interactions being the principal forces holding the epoxide in its calculated position.

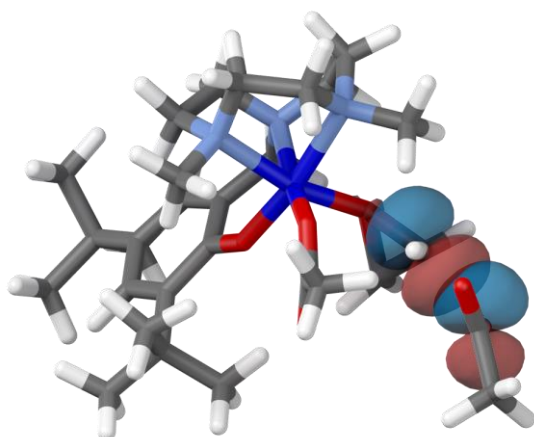


**Figure 19** Donor-acceptor interaction associated with the reaction coordinate for **TS1** [M06-2X | cc-pVTZ/cc-pV(T+d)Z]

Whilst the complete decooordination of an acetate ligand is unrealistic when the resulting cation and anion are treated as independent entities (*i.e.* infinite separation of cation and anion), a partially decoordinated carboxylate present in a close ion-pair structure is viable (**INT2**). The carboxylate is held in close proximity to the coordinated epoxide by various weak interactions with the ligand periphery. QTAIM analysis gives BCP's (with small  $\rho$  values) from the carboxylate ion to proximal CH bonds of the **L1** methyl groups, the coordinated acetate and the epoxide. These interactions place the carboxylate in an ideal position for subsequent nucleophilic attack on the epoxide monomer. NBO analyses suggest that the nucleophilic attack may be described as an oxygen p-based lone pair donating into an empty carbon-based p orbital (Figure 19). The transition state for the ring-opening of the coordinated epoxide by the carboxylate (**TS1**) is the highest point in the energy profile, which is consistent with other reports<sup>58</sup> and is only slightly higher in energy than **INT2**.

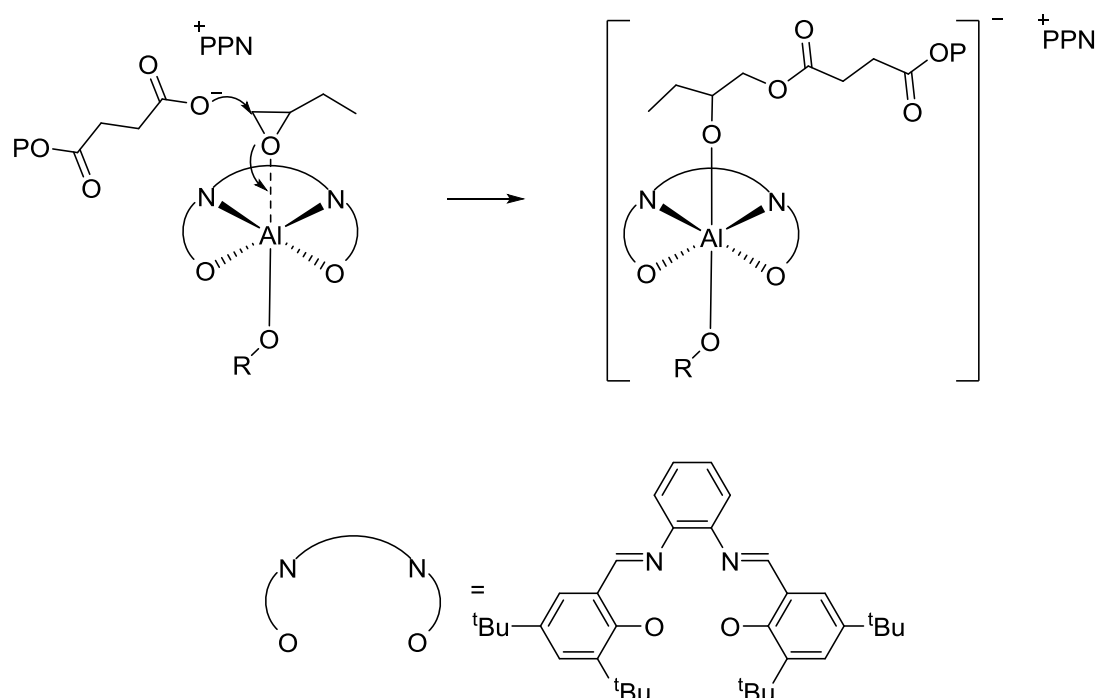
The ring-opening of the epoxide is followed by the coordination of the anhydride. The addition of an anhydride to the newly formed alkoxide proceeds in a comparable manner to the commonly accepted coordination-insertion mechanism for the ring-opening of cyclic esters, namely migratory insertion over a carbonyl followed by ring-opening at the ester C–O bond.<sup>79</sup> Decoordination of an alkoxide or carboxylate is infeasible, but pre-coordination of the anhydride (**INT4**) was found to be almost isoenergetic with the migratory insertion transition state (**TS2**). Structural examination of **INT4** and **TS2**



**Chapter 2 - Formation of polyesters via the ring-opening copolymerisation of epoxides and cyclic anhydrides**

indicate that the coordination of the TACN ring of **L1** to the aluminium centre is variable and labile. In **INT4**, two of the TACN nitrogen donors are decoordinated leading to a formally  $\kappa^2$ -**L1** ligand. The aluminium–nitrogen bond distance for the coordinated nitrogen is 2.11 Å, whereas the decoordinated nitrogens have bond distances of 3.04 Å and 3.49 Å. QTAIM analysis gives no BCP's between these nitrogens and the aluminium centre, although the bond distances are within the sum of the equilibrium van der Waals radii ( $\text{Al-N } \Sigma r_{\text{vdW}} = 4.19 \text{ Å}$ ).<sup>76</sup> NBO analysis indicates that there are weak interactions between these nitrogens and the aluminium, which take the form of s-s and s-p donor-accepter interactions. From these calculations we can conclude that while there are not formal bonds between the aluminium centre and two of the nitrogens of **L1**, weak interactions are still present. In **TS2**, the TACN ring is not fully bound to the aluminium centre during the insertion of the alkoxide over the anhydride carbonyl. At this stage, one of the ligand nitrogens is fully bonded to the aluminium, one is decoordinated and bonding of the final nitrogen is ambiguous ( $d_{\text{Al-N}} = 2.104 \text{ Å}$ ,  $2.628 \text{ Å}$ , and  $3.284 \text{ Å}$ ). QTAIM analysis indicates that a BCP is only present for the shortest Al–N ( $2.104 \text{ Å}$ ) bond. Based on these results, **L1** is bound to the aluminium centre in a  $\kappa^2$  coordination mode at **TS2**. Following the migratory insertion, **L1** resumes coordination of the aluminium metal in a  $\kappa^4$  manner and remains in this mode throughout the remainder of the catalytic cycle. Ring-opening of the anhydride tallies well with the established mechanism for the ROP of cyclic esters.<sup>58,79</sup>

**Chapter 2** - Formation of polyesters via the ring-opening copolymerisation of epoxides and cyclic anhydrides



**Scheme 15** Ring-opening of an epoxide by **2.1d**. P is a polymer chain and OR is an alkoxide or a carboxylate<sup>58</sup>

It is clear from the calculations that there are differences in the mechanism when the reaction is catalysed by **1** compared to the aluminium-Salen system employed by Coates.<sup>58</sup> Full decooordination of the carboxylate-terminated polymer to allow coordination of an epoxide monomer does not take place with **1**, instead a partially decoordinated carboxylate present in a close ion-pair structure is formed. This variation compared to the mechanism based on **2.1d** may be an advantage. **2.1d** and other metal-salen based catalysts exhibit poor activity at low catalyst loadings. In these systems, the ring-opening of a coordinated epoxide is achieved by external attack of a co-catalyst-associated carboxylate-terminated propagating chain (Scheme 15). Therefore dilution of the catalyst and co-catalyst at low loadings can inhibit this nucleophilic attack on the epoxide and therefore reduce the rate of reaction.<sup>74</sup>

**Chapter 2 - Formation of polyesters via the ring-opening copolymerisation of epoxides and cyclic anhydrides**

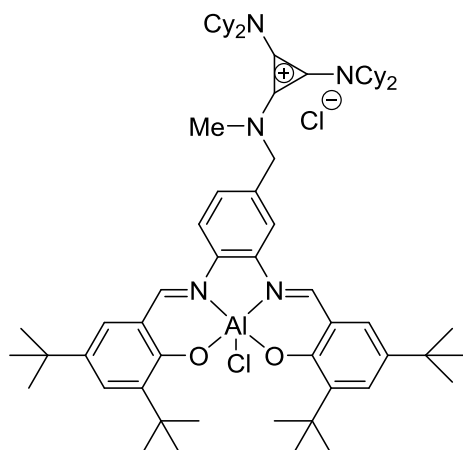


**Figure 20** Tethered metal salen/nucleophilic co-catalyst system (**2.8**)<sup>74</sup>

**Table 5** Synthesis of ECH–PhA catalysed by **1** at various catalyst loadings

Entry	Catalyst loading (mol%)	Reaction time (h)	TOF (h <sup>-1</sup> )
46 <sup>a</sup>	0.5	0.5	392
29 <sup>b</sup>	0.25	1	400
47 <sup>c</sup>	0.125	2	400

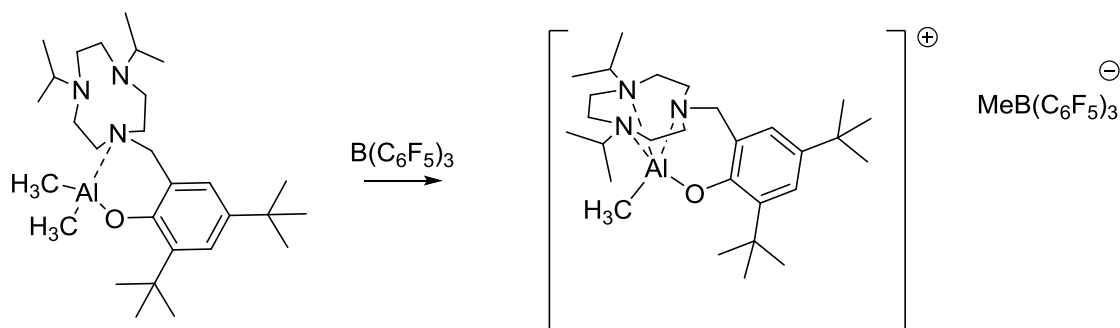
6.4  $\mu\text{mol}$   $[\text{Al}(\text{L}1)\text{Cl}_2]$  (**1**) catalyst. Reactions heated at 80 °C. ECH:PhA:1:PPNCl = <sup>a</sup>1000:200:1:2, <sup>b</sup>2000:400:1:2, <sup>c</sup>4000:800:1:2.

In order to mitigate this effect, Coates and colleagues developed bifunctional, tethered metal salen/nucleophilic co-catalyst systems. An example of such a catalyst (**2.8**) is shown in Figure 20. Unlike the separate catalyst/co-catalyst system where the activity declined with catalyst loading, the activity of **2.8** remained constant at loadings as low as 0.025 mol%.<sup>74</sup> Given that in the calculated mechanism for **1**, the carboxylate terminated polymer chain does not completely decoordinate from the complex, dilution should not influence the rate of epoxide ring-opening. The propagating carboxylate remains bound by weak interactions in an ideal position for the subsequent nucleophilic attack on the epoxide monomer. The ring-opening of the epoxide is the rate determining step for the ROCOP of epoxides and cyclic anhydrides. Preliminary tests indicate that the activity of **1** remains constant as the catalyst loading is decreased. The copolymerisation of ECH and PhA with **1** was undertaken at catalyst loadings of 0.5, 0.25 and 0.125 mol% and in all reactions a TOF of  $\approx 400 \text{ h}^{-1}$  was recorded (Table 5). The activity achieved by

**Chapter 2 - Formation of polyesters via the ring-opening copolymerisation of epoxides and cyclic anhydrides**

**1** is far higher than **2.8** for which a TOF of  $\approx 90 \text{ h}^{-1}$  was reported.<sup>74</sup> Further tests at a wider range of catalyst loadings should be carried out to confirm that the catalytic activity remains constant.

During the migratory insertion of the alkoxide to the anhydride carbonyl, **L1** exhibits hemilabile bonding to the aluminium centre. The complex exhibits a  $\kappa^4$  state prior to migratory insertion which changes to a  $\kappa^2$  binding mode at **INT4** and following migratory insertion (**INT5**) returns to  $\kappa^4$ . During this transformation the complex passes through a transition state in which the ligand bonding can be considered either  $\kappa^2$  or  $\kappa^3$  (**TS2**). Weak interactions between the decoordinated nitrogens and the aluminium centre were seen in the NBO analyses and indicate that while the nitrogens are not bound to the metal in a conventional manner, they could be considered to have weak donor-acceptor interactions. Decoordination of the TACN macrocycle is surprising, although is more understandable for closed shell main group metals such as aluminium, which have no ligand field stabilization effects. Similar hemilability has been reported in the literature, Mountford *et al.* identified hemilabile bonding in a very similar organometallic complex (Scheme 16).<sup>80</sup> It is perhaps an obvious question whether or not a more discrete  $\kappa^2$  binding mode could be involved in the catalytic cycle, *i.e.* where two of the nitrogens are completely removed from the aluminium centre as observed in  $[\text{Al}(\text{2.9})\text{Me}_2]$ . This possibility was considered and computed but the epoxide-opening transition state was found to be  $160 \text{ kJ mol}^{-1}$ , and so this pathway was not considered further.



**Scheme 16** Hemilabile  $[\text{Al}(\text{2.9})\text{Me}_2]$ <sup>80</sup>

Estimated  $\Delta G^\ddagger$  for the solvent free ROCOP of epoxides and anhydrides can be calculated from the approximate polymerisation half-life ( $t_{1/2}$ ). The observed

**Chapter 2 - Formation of polyesters via the ring-opening copolymerisation of epoxides and cyclic anhydrides**

rate constant ( $k_{\text{obs}}$ ) can be calculated from Equation 1. The rate constant ( $k$ ) can be calculated from Equation 2. The estimated  $\Delta G^\ddagger$  can be calculated from the Eyring equation (Equation 3).

$$t_{\frac{1}{2}} = \frac{\ln 2}{k_{\text{obs}}}$$

**Equation 1** Relation between half-life and observed rate constant

$$k = \frac{k_{\text{obs}}}{[Al]}$$

**Equation 2** Calculation of rate constant

$$k = \frac{k_b T}{h} e^{\frac{-\Delta G^\ddagger}{RT}}$$

**Equation 3** Eyring equation

For the bulk copolymerisation of CHO and PhA (Table 3, Entry 16) the approximate polymerisation half-life is 1 hour. The estimated  $\Delta G^\ddagger$  for this copolymerisation is 97 KJmol<sup>-1</sup>. This number is lower than the value calculated using DFT of 132 KJmol<sup>-1</sup>. It is well established that the free energies of bimolecular processes can be substantially overestimated. This arises from the entropy model used in quantum mechanical simulation software that overestimates the entropy reduction in such processes, since it relies on ideal gas phase volumes rather than solution volumes. This can be offset somewhat by scaling the entropy terms (and therefore the free energies) using the Sackur-Tetrode equation (as has been carried out in the calculations in this thesis). However one would still expect the free energy terms to be somewhat higher than those estimated experimentally.<sup>81</sup>

### **2.5 Detailed polymer analysis using MALDI-TOF mass spectrometry**

In order to gain further understanding of the structure of the polymers synthesised in the ROCOP of epoxides and cyclic anhydrides, a MALDI mass spectrum was recorded for ECH–PhA (entry 8) as a representative example. The spectrum was recorded at the National Mass Spectrometry Facility. The positive linear MALDI spectrum produced for ECH–PhA is shown in Figure 21.

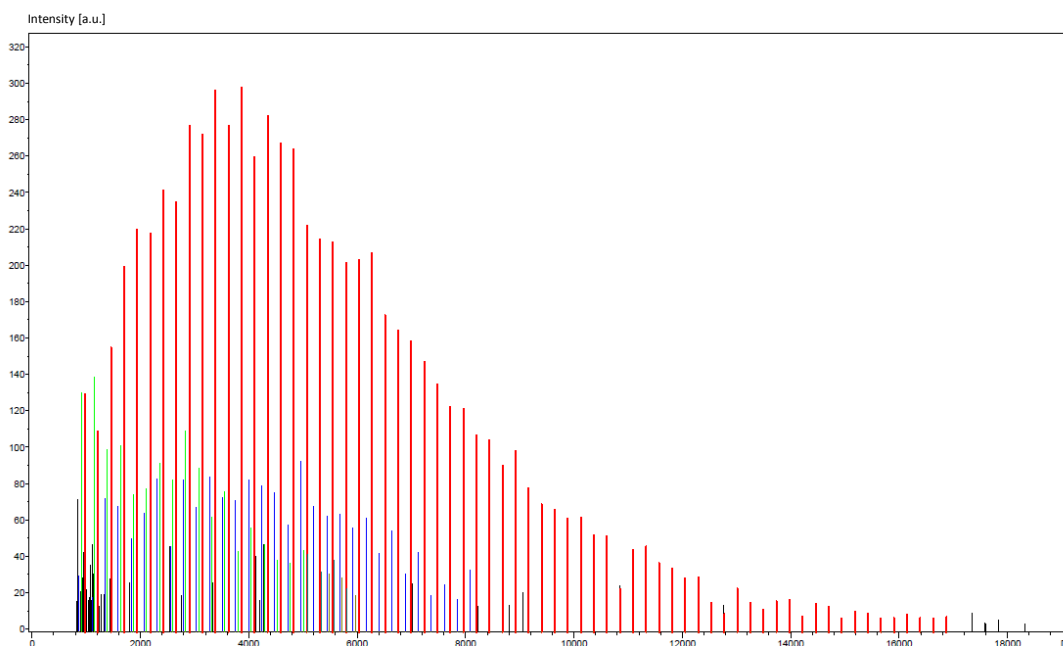


**Figure 21** Positive linear MALDI-TOF mass spectrum of ECH–PhA (entry 8)

The  $M_n$  and  $\bar{D}$  values for ECH–PHA were calculated from the linear MALDI spectrum using the Bruker Polytools software; values of  $5,370 \text{ g mol}^{-1}$  and 1.32 were found respectively, compared to the values obtained by GPC (entry 8, Table 2,  $5,100 \text{ g mol}^{-1}$ ,  $\bar{D} = 1.13$ ). The  $M_n$  calculated from the MALDI spectrum was very similar, whereas the  $\bar{D}$  measured by the two techniques did vary with a lower value obtained with GPC. The MALDI spectrum in Figure 21 is made up of multiple polymer series, differentiated by colour.

## Chapter 2 - Formation of polyesters via the ring-opening copolymerisation of epoxides and cyclic anhydrides

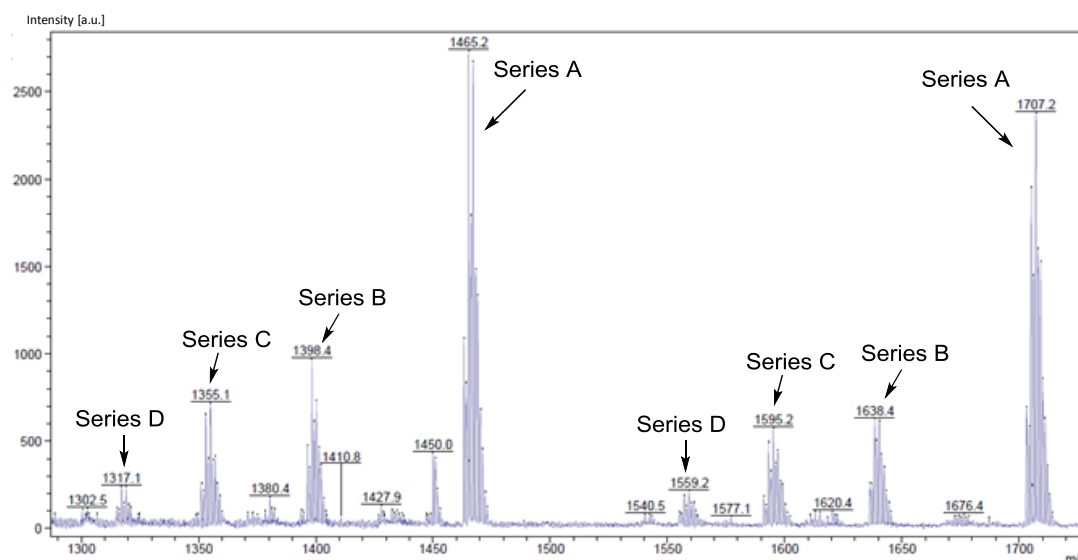


**Figure 22** Reflectron MALDI-TOF mass spectrum of ECH-PhA between 1300 – 1750 m/z

In order to understand the differences in the series, a higher resolution reflectron MALDI-TOF mass spectrum was recorded of ECH-PhA (entry **8**). Figure 22 shows a section of this spectrum between 1,300 – 1,750 m/z. This spectrum clearly shows the multiple polymer series. It also confirms that as expected, the difference between each peak in series is 240 m/z. 240 m/z is the mass of the copolymer repeat unit containing the ring-opened form of both monomers. As the insertion of the anhydride monomer in the ROCOP reaction is extremely rapid, it is unlikely that peaks showing mass differences in the MALDI spectrum resulting from the addition of individual monomers will be observed.<sup>58</sup> The peak m/z difference equal to the mass of the copolymer unit and the absence of polymer series containing excess epoxide proves that the polymer is comprised of alternating monomer units and has high ester selectivity as suggested by the <sup>1</sup>H NMR spectra.

In Figure 22, the four most prominent polymer series, A, B, C and D are shown. Figure 22 shows two peaks for each series, with the higher mass peak 240 m/z units greater than the respective lower mass peak for the series. The peak at 1,450 m/z in Figure 22 was not considered to be part of a polymer series, as it is not related to any other peak in the MALDI spectrum by either the mass of the polymer repeat unit or the mass of a single monomer unit. Other low

## **Chapter 2** - Formation of polyesters via the ring-opening copolymerisation of epoxides and cyclic anhydrides

intensity peaks in spectrum may be polymer series but were not investigated further.

Polymer series A corresponds to the sodiated polymer chain with equal numbers of ring-opened epoxide and anhydride,  $[(\text{Na})(\text{ECH})_n(\text{PhA})_n]^+$ . For example, the peak at 1,465.2 m/z is from a  $[(\text{Na})(\text{ECH})_6(\text{PhA})_6]^+$  species. Surprisingly, this polymer series has no end groups. The expected end groups would be the initiating Cl and a H atom (protonation of the terminating Al–O upon workup). One mechanism that would yield a species with what appears to be no end groups, would be the formation of large macrocyclic polymers. This is doubtful however, as the formation of these macrocycles becomes less likely with increasing molecular weight and this series includes polymers with molecular weights of nearly 20,000  $\text{gmol}^{-1}$ . What is more probable is that an elimination or “backbiting” reaction is taking place, which may be more complex than simply affording a cyclic polymer. This process leads to the loss of HCl which is far more likely to occur in ECH–PhA compared to most polymers because of the high chlorine content all along the chains instead of just the single chlorine that initiated the polymerisation.

Polymer series C corresponds to the sodiated polymer, with one additional epoxide monomer compared to anhydride, and with H and Cl end groups,  $[(\text{Na})(\text{H})(\text{ECH})_{n+1}(\text{PhA})_n(\text{Cl})]^+$ . For example, the peak at 1,355.1 m/z is from the species,  $[(\text{Na})(\text{H})(\text{ECH})_6(\text{PhA})_5(\text{Cl})]^+$ . In this example, the expected H and Cl end groups are present. The presence of  $n+1$  epoxide is due to the final catalytic cycle ending with the ring-opening of an epoxide monomer as opposed to an anhydride. This can be explained by the mechanism for the ROCOP of epoxides and cyclic anhydrides reported by Coates and colleagues, shown in Scheme 5.<sup>58</sup> Under normal conditions, the steady state species is the dicarboxylate intermediate, this is because the ring-opening of an anhydride is fast compared to that of an epoxide. If the polymerisation is halted at this point, a carboxylate polymer intermediate yields a polymer with equal monomers of epoxide and anhydride. Whenever an alkoxide species (where epoxide is  $n+1$ ) is formed in the catalytic cycle, it very quickly reacts making the overall alkoxide concentration very low. This means if the reaction is halted under steady state conditions the probability of observing a polymer



## Chapter 2 - Formation of polyesters via the ring-opening copolymerisation of epoxides and cyclic anhydrides

with  $n+1$  epoxides is small. However, when the concentration of anhydride decreases, the rate of anhydride ring-opening reaction becomes comparable to that of the epoxide. At this point, the relative concentration of the mixed alkoxide – carboxylate aluminium intermediate increases. At low anhydride concentration, cycle 2 in Scheme 5 becomes active giving rise to aluminium alkoxide species in which the polymers have  $n+1$  epoxides. If the reaction is halted when the polymer chain is in the form of an alkoxide, it will have one additional epoxide monomer compared to anhydride and in the case of ECH–PhA, a formula of  $[(\text{ECH})_{n+1}(\text{PhA})_n]$ .

Series D is the equivalent of series C but without the presence of the H and Cl end groups,  $[(\text{Na})(\text{ECH})_{n+1}(\text{PhA})_n]^+$ . The peaks at 1,317.1 and 1,559.2  $m/z$  present in the MALDI spectrum of ECH–PhA (entry 8) in Figure 22 correspond to polymers with formulas of  $[(\text{Na})(\text{ECH})_6(\text{PhA})_5]^+$  and  $[(\text{Na})(\text{ECH})_7(\text{PhA})_6]^+$  respectively. The same reasons for the lack of end groups and  $n+1$  epoxides that were given above also apply to this polymer series.

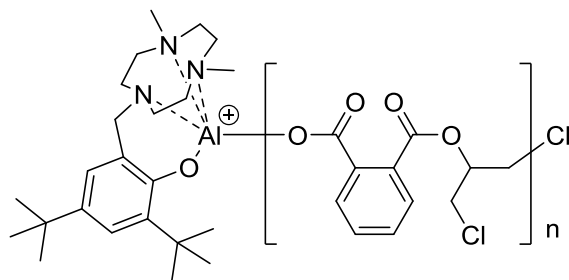


**Figure 23** ECH–PhA polymer series B observed in the MALDI-TOF mass spectrum

The source of polymer series B was surprising and very much unexpected. Series B equates to a polymer chain with equal numbers of ECH and PhA with a Cl from polymer initiation and the catalyst (AlL1) still attached to the other end,  $[\{\text{Al}(\text{L1})\}(\text{ECH})_n(\text{PhA})_n(\text{Cl})]^+$ , (Figure 23). The peaks at 1,398.4 and 1,638.4  $m/z$  in Figure 22 correspond to  $[\{\text{Al}(\text{L1})\}(\text{ECH})_4(\text{PhA})_4(\text{Cl})]^+$  and  $[\{\text{Al}(\text{L1})\}(\text{ECH})_5(\text{PhA})_5(\text{Cl})]^+$  respectively. It would be expected that the catalyst is removed from the polymers by way of a protonation reaction with methanol during the workup producing the H end group, which makes this result surprising. The catalyst 1 had always been treated as air/moisture sensitive

## Chapter 2 - Formation of polyesters via the ring-opening copolymerisation of epoxides and cyclic anhydrides

and it was thought that any catalytic intermediates would also degrade unless under inert conditions. MALDI-TOF mass spectrometry is a very energy-intensive technique where polymers are irradiated by a laser causing ablation and ionization, therefore it is remarkable that the catalyst remained attached to the polymer chain during this process and was detected. As is shown in Figure 22, series B containing the aluminium macrocycle catalyst is the second most intense signal, illustrating the stability of the species. Before the MALDI-TOF measurement was carried out, the polymer was stored as a solid in air for a number of months, in which time the catalyst remained attached to the polymer. All of these observations suggest that the catalyst **1** is much more stable than anticipated. As previously discussed, macrocyclic complexes are often very inert, a feature exploited for the design of nuclear medicines *etc.*<sup>68,82,83</sup> Given that the catalyst remained bound to the polymer chain throughout the harsh conditions it was subjected to, it was predicted that this catalyst may be effective for the ROCOP of epoxides and cyclic anhydrides in air.

**Table 6** ROCOP of CHO and PhA by [Al(L1)Cl<sub>2</sub>] (**1**)

Entry	Conditions	Selectivity (%) <sup>a</sup>	Mn (gmol <sup>-1</sup> ) <sup>b</sup>	Đ <sup>b</sup>
48	Inert	99	13700	1.08
49	Air	99	8550	1.13

6.4 μmol [Al(L1)Cl<sub>2</sub>] (**1**) catalyst. [CHO]<sub>0</sub>: [PhA]<sub>0</sub>: [Catalyst]<sub>0</sub>: [PPNCl]<sub>0</sub> = 2000:400:1:2. Reactions heated at 80 °C for 2 hours. Both reactions had >97 % conversion of PhA.

<sup>a</sup>Determined by comparison of ester and ether signals in <sup>1</sup>H NMR. <sup>b</sup>Determined by GPC using triple detection.

To test this theory, the ROCOP of CHO and PhA catalysed by **1** was undertaken using the same batches of reactants under inert conditions and in air. The experimental procedure for the inert atmosphere control experiment was the same as the standard ROCOP reaction with bulk epoxide. For the experiment in air, the catalyst and PPNCl were weighed directly into the reaction vial, the correct amounts of PhA and CHO were prepared separately, and all of the reactants were brought out of the glove box and open to air. All components were left to stand open in air for 5 minutes to allow for the inert

## Chapter 2 - Formation of polyesters via the ring-opening copolymerisation of epoxides and cyclic anhydrides

N<sub>2</sub> atmosphere to dissipate. The reactants were then combined in the reaction vial which was sealed in air and heated at 80 °C for 2 hours. CHO dried with CaH<sub>2</sub> and purified PhA were used in both reactions (prior to their exposure to air). The copolymerisation of unpurified monomers may be possible, but this was not explored because high concentrations of water and terephthalic acid impurity would significantly affect the M<sub>n</sub> and Đ of the polymer produced and would cloud the interpretation of catalyst performance. The polymer generated from the reaction in air along with the control experiment were isolated and the ester selectivity, molecular weight and Đ were measured. The results of these experiments are shown in Table 6.

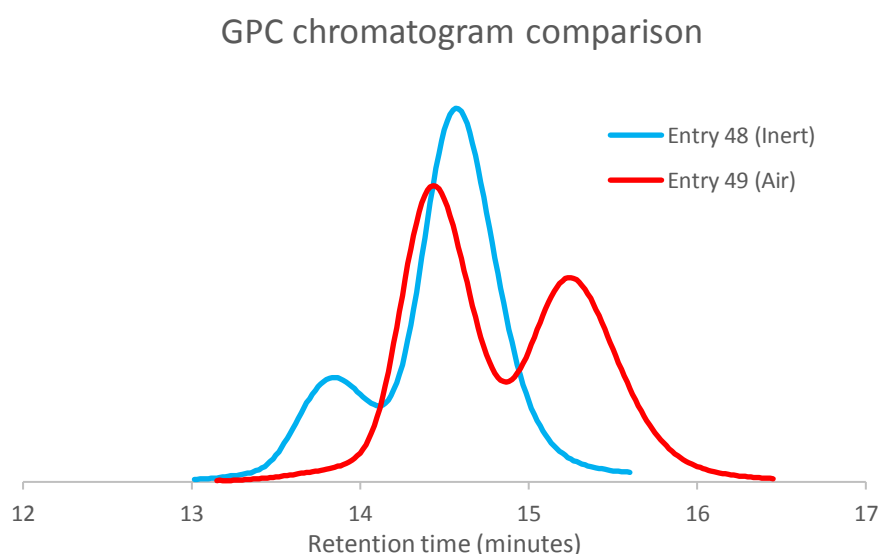


**Figure 24** Comparison of GPC chromatograms of reactions in air and under inert conditions

Entry 49 (Table 6) indicates that **1** is an effective catalyst for the ROCOP of CHO and PhA in air. The polymer produced had good molecular weight and excellent Đ. Like the control experiment (entry 48, Table 6), the copolymer produced had perfect ester selectivity indicating the polymer chain is comprised of alternating monomer units. The polymer synthesised in air (entry 49) has a lower molecular weight and a slightly higher Đ than the control. This is most likely a result of the presence of H<sub>2</sub>O when the reaction was undertaken in air. H<sub>2</sub>O can initiate polymerisation and can act as a chain transfer agent. A greater number of initiators and therefore polymer chains in

## **Chapter 2** - Formation of polyesters via the ring-opening copolymerisation of epoxides and cyclic anhydrides

the reaction causes the molecular weight of the sample to decrease. Although one other explanation that cannot be discounted is that despite using the same batches of reactants, human error when measuring out reactants could contribute to differences in molecular weight. Unlike  $\text{Cl}^-$ ,  $\text{H}_2\text{O}$  is a bifunctional initiator, which will produce polymer chains with approximately twice the  $M_n$  of those initiated by  $\text{Cl}^-$ , giving the overall sample a more bimodal distribution of polymer chain lengths resulting in a higher  $\bar{D}$ . This effect can be observed by comparison of the respective GPC traces of the copolymers synthesised in air and under inert conditions, shown in Figure 24. In a GPC with a size exclusion column, polymer chains with higher molecular weight pass through the column more quickly and are therefore detected earlier.

The GPC chromatogram of the control sample (entry 48) shows a small degree of bimodality. In addition to the main peak at approximately 14.5 minutes, there is a small peak at the shorter retention time ~13.7 minutes. The larger peak at higher retention time equates to smaller molecular weight polymers initiated by  $\text{Cl}^-$ . The smaller peak at lower retention time is a higher molecular weight peak caused by bifunctional initiators. The sources of these bifunctional initiators are either adventitious water or diacid impurities in the anhydride present despite purification of the monomers and the reaction being undertaken in an inert atmosphere.<sup>59</sup> The GPC chromatogram produced for the reaction carried out in air (entry 49) appears significantly different to the control experiment (entry 48). In entry 49 there is substantially more of the higher molecular weight polymer (lower retention time) compared to the lower molecular weight peak (higher retention time). As the reactants used in the two experiments are from the same batches and errors in weighing have no bearing on bimodality or  $\bar{D}$ , these differences must be a result of the reaction being carried out in air which means much higher  $\text{H}_2\text{O}$  levels. This increased  $\text{H}_2\text{O}$  level causes a substantial increase in the concentration of bifunctional initiators, increasing the relative size of the higher molecular weight peak in the GPC trace leading to a higher  $\bar{D}$ .

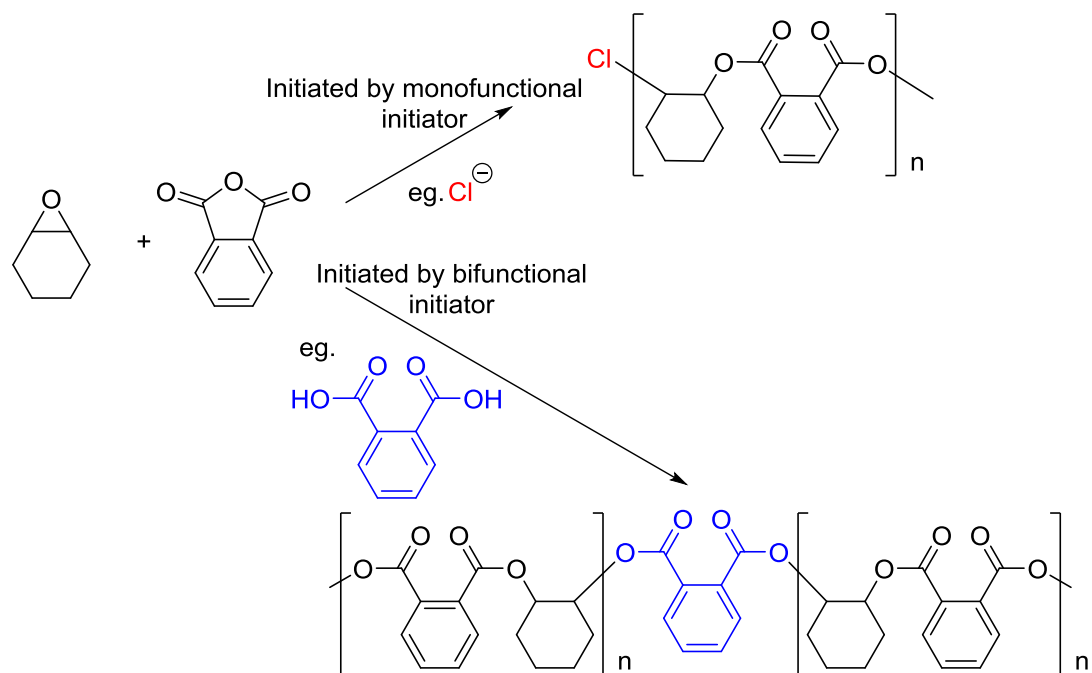
These results indicate that **1** is an effective catalyst for the ROCOP of epoxides and cyclic anhydrides even when carried out in air. The copolymerisation of CHO and PhA in air yielded polymers with good  $M_n$  and excellent  $\bar{D}$ .

## Chapter 2 - Formation of polyesters via the ring-opening copolymerisation of epoxides and cyclic anhydrides

Compared to a control experiment undertaken in an inert atmosphere, the  $M_n$  was lower and the  $\bar{D}$  was slightly higher most likely due to the presence of  $H_2O$  in the air. This work highlights in addition to the high TOF recorded, the stability and robustness of the **1** catalyst and is, to the best of our knowledge the first example of the ROCOP of epoxides and anhydrides successfully undertaken in air.

### 2.6 Reducing the bimodality of polymer molecular weight distributions

An issue with the ROCOP of epoxides and cyclic anhydrides is the formation of polymers with bimodal molecular weight distributions. This is caused by bifunctional polymerisation initiators in addition to the intended monofunctional initiators present in the catalytic system (Scheme 17). The most common sources of these bifunctional impurities is either adventitious water or diacid impurities in the anhydride.<sup>59</sup>



**Scheme 17** Ring-opening copolymerisation (ROCOP) of CHO and PhA initiated by both mono- and bifunctional initiators

There have been some successful reports in the literature of systems which yield unimodal polymer molecular weight distributions and therefore low  $\bar{D}$ . Williams and colleagues investigated the use of a zinc organometallic species in combination with a bifunctional diol additive. This system works through an

## **Chapter 2** - Formation of polyesters via the ring-opening copolymerisation of epoxides and cyclic anhydrides

*in situ* reaction of the zinc complex with the alcohol liberating the inert side product benzene. The polymerisation can therefore only be initiated by the bifunctional alkoxide groups.<sup>43</sup> Coates *et al.* employed a slightly different approach utilising an aluminium complex with non-initiating triflate co-ligands. This complex was used in conjunction with bifunctional co-catalyst and chain transfer agents. The authors explored a series of chain transfer agents and showed how these could be used to control polymer Mn.<sup>59</sup>

Utilising **1** as a catalyst in the ROCOP of epoxides and cyclic anhydrides effectively synthesised polyesters with good molecular weights and good to moderate Đ. It is clear from looking at a GPC trace that many of the polymers formed have bimodal or multimodal distributions which increase Đ. For example, the GPC trace of entry 24 synthesised from CHO and PhA is shown in Figure 25.

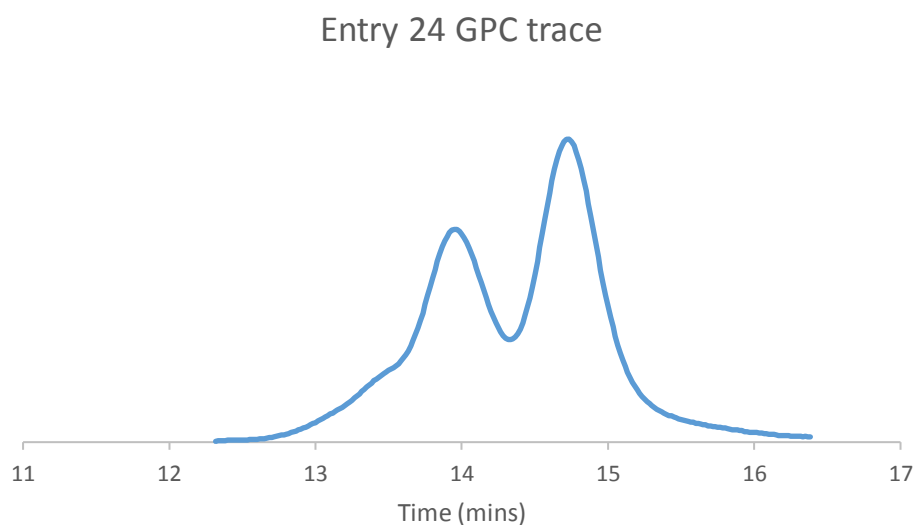


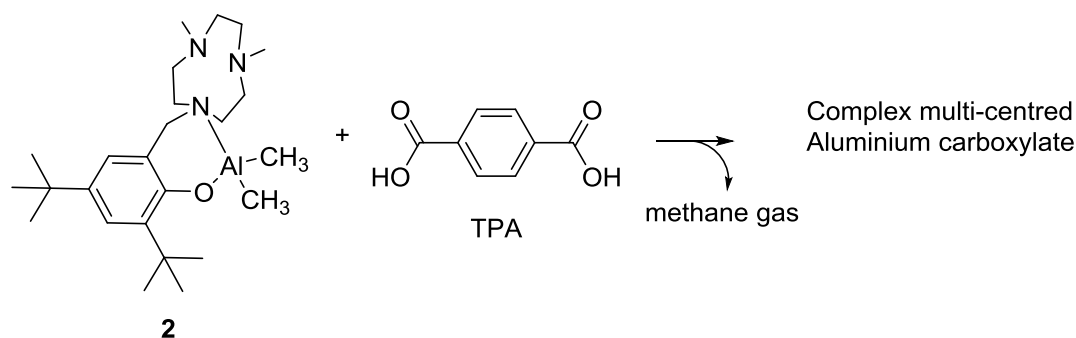
**Figure 25** GPC trace of entry 24

The GPC trace of entry 24 shows clearly a bimodal distribution. The lower intensity peak at higher molecular weight is a result of initiation by bifunctional impurities in the reaction and the higher intensity peak at lower molecular weight is the polymer initiated as intended by chloride. The higher molecular weight peak is approximately double the molecular weight of the smaller. This is because a polymer chain initiated by a bifunctional initiator grows from both

**Chapter 2 - Formation of polyesters via the ring-opening copolymerisation of epoxides and cyclic anhydrides**

ends at the same rate as a polymer chain initiated by a monofunctional initiator which only grows from one end.

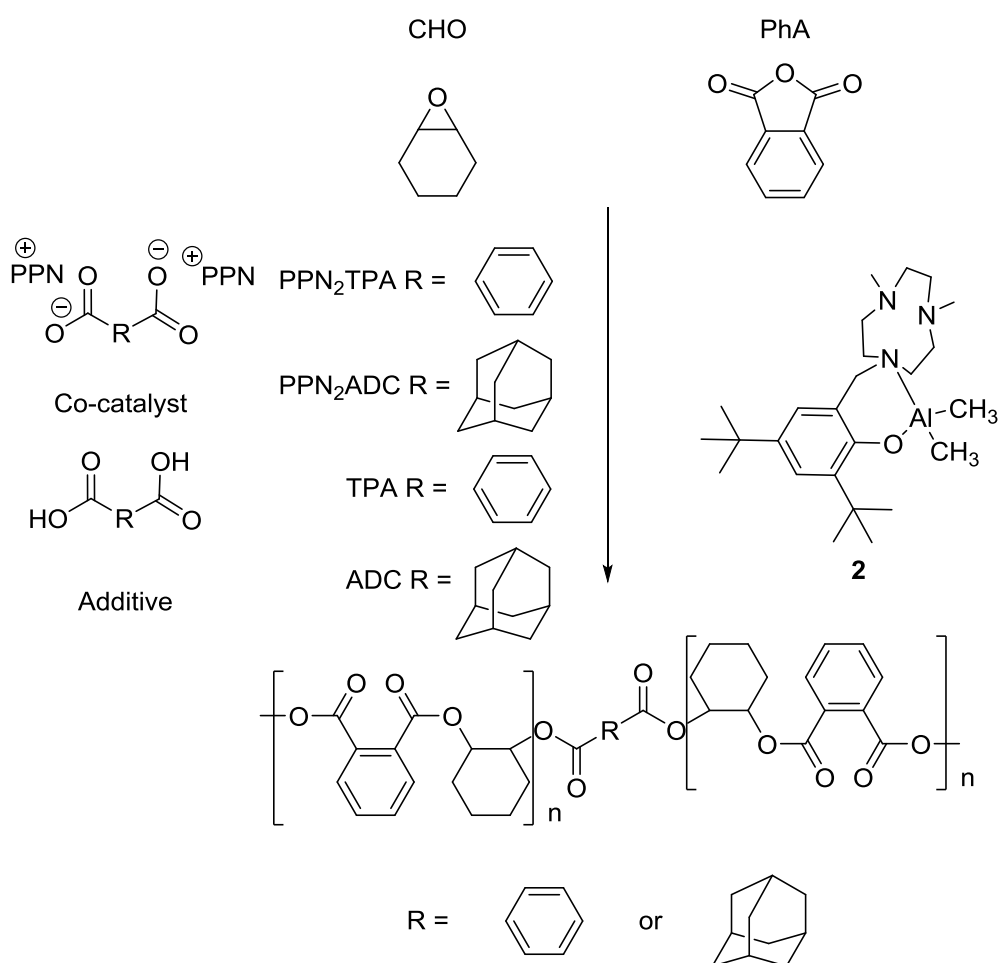
To achieve greater polymerisation control and lower the Đ, a catalytic system utilising bifunctional initiators was developed. When the catalyst **1** and PPNCI co-catalyst were employed, chloride ions initiated polymerisation. In order to replace the chloride initiators with bifunctional initiators, a new catalyst and co-catalyst are required. One possible option for the catalyst would be to synthesise a metal complex containing bifunctional co-ligands. However, it would be very difficult to synthesise and isolate such a compound due to the tendency to form ill-defined polymeric materials. Attempts were made to synthesise a non-initiating aluminium triflate catalyst of the form  $[\text{Al}(\text{L1})(\text{OTf})_2]$  but a well-defined species could not be isolated. Another approach would be to utilise a highly reactive aluminium organometallic complex used in conjunction with a bifunctional additive which will react *in situ*.  $[\text{Al}(\text{L1})(\text{Me})_2]$  (**2**) was selected as a catalyst and terephthalic acid (TPA) as an additive. These two compounds will react *in situ* to yield methane gas and a complex multi-centred aluminium carboxylate catalyst (Scheme 18). Conversion of the methyl co-ligands to methane gas prevents polymerisation initiation by the monofunctional methyl groups and means therefore that the ROCOP can only be initiated by the bifunctional dicarboxylate species.



**Scheme 18** *In situ* reaction of  $\text{Al}(\text{L1})(\text{Me})_2$  (**2**) and terephthalic acid (TPA)

**Chapter 2 - Formation of polyesters via the ring-opening copolymerisation of epoxides and cyclic anhydrides**

The ROCOP of epoxides and cyclic anhydrides catalysed by **1** required a PPNCI co-catalyst. This means that the **2** – TPA catalytic system will also require a nucleophilic co-catalyst. PPNCI is not however a viable candidate as it contains chloride which can initiate polymerisation leading to an overall bimodal polymer molecular weight distribution. The PPN salt of TPA (PPN<sub>2</sub>TPA) was synthesised as an appropriate co-catalyst, which provides the PPN<sup>+</sup> crucial for effective polymerisation and contains only a bifunctional initiator. PPN<sub>2</sub>TPA was synthesised by a literature method.<sup>59</sup> Scheme 19 shows the overall catalytic system.



**Scheme 19** Bifunctional catalytic system

The ROCOP of CHO and PhA catalysed by a bifunctional catalytic system was explored. The pre-catalyst **2** was used in conjunction with the co-catalyst PPN<sub>2</sub>TPA and additive TPA. 1 equivalent of each of the pre-catalyst, co-catalyst and additive were used. The polyester formed was isolated and the



## Chapter 2 - Formation of polyesters via the ring-opening copolymerisation of epoxides and cyclic anhydrides

molecular weight was measured by GPC in order to investigate the degree of bimodality in the polymer sample. The results for this experiment (48) and the results of a control sample synthesised with **1** and PPNCl (entry 24) are shown in Table 7. The CHO and PhA used in these polymerisations were from the same batch of reactants. Compared to the control (24), experiment 48 gave polymers with similar  $M_n$  and improved  $\bar{D}$ . There was a slight decrease in the  $M_n$  but the  $\bar{D}$  decreased from 1.21 to 1.13.

**Table 7** Bifunctional catalytic system

Exp	Catalyst	Co-cat	Equivs.	Additive	Equivs.	Toluene <sup>a</sup>	$M_n^b$	$\bar{D}^b$
24	<b>1</b>	PPNCl	2	-	-	-	14500	1.21
50	<b>2</b>	PPN <sub>2</sub> TPA	1	TPA	1	-	12240	1.13
51	<b>2</b>	PPN <sub>2</sub> TPA	1	TPA	1	0.1ml	14130	1.13

6.4  $\mu\text{mol}$  catalyst.  $[\text{CHO}]_0:[\text{PhA}]_0:[\text{Cat}]_0 = 2000:400:1$ . Heated for 2 hours at 80 °C. PhA conversion >99%. <sup>a</sup>Dry toluene added in glove box. <sup>b</sup>Determined by GPC using triple detection, with units of  $\text{gmol}^{-1}$ .

GPC chromatogram comparison

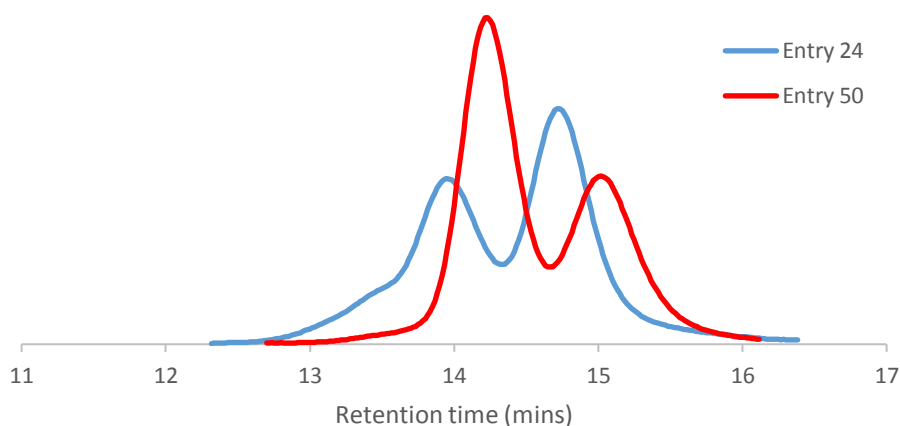


**Figure 26** Comparison of GPC traces of CHO–PhA

The effect of changing the catalytic system is clear by comparison of the GPC traces of polymers 50 and 24, shown in Figure 26. Entry 50 is still bimodal to some extent, however there are significant differences to entry 24. In entry 50 the higher molecular weight peak (lower retention time) is the larger peak unlike in entry 24 where it is the smaller. In entry 50, the higher molecular

## **Chapter 2 - Formation of polyesters via the ring-opening copolymerisation of epoxides and cyclic anhydrides**

weight peak is by far the biggest peak in the GPC trace whereas in entry 24, while the lower molecular weight peak is the larger of the two, they are much more similar in intensity. This indicates that in experiment 50 there was greater control over the polymerisation initiation which produced a more selective reaction leading to the lower  $\bar{M}_n$ . The presence of the lower molecular weight polymer fraction however suggests that the catalytic system employed did not completely remove all the monofunctional initiators.

One possible explanation for the presence of monofunctional initiators could be that the reaction of **2** with TPA yielding methane and an aluminium carboxylate was incomplete. This would mean methyl groups would still be present in the reaction and could initiate polymerisation. The protonation reaction must be substantially faster than the rate of polymer initiation to prevent methyl groups generating polymer chains. Polymers initiated by methyl groups would have molecular weights approximately half that of those initiated by the dicarboxylate initiators and would therefore account for the smaller peak in the GPC trace at lower molecular weight.

In order to address this potential issue, the polymerisation was repeated under the same conditions but an extra step was included to allow for the complete reaction of **2** and TPA (experiment 51). In the reaction vial the correct masses of **2** and TPA were added along with 0.1 ml dry toluene. This mixture was stirred for 5 minutes before the epoxide and cyclic anhydride were added. This should give more time for the reaction to finish before polymerisation takes place. Unfortunately this additional step did not have the desired effect. The  $\bar{M}_n$  in polymer 51 was the same (1.13) as in polymer 50. This indicates that the rate of the *in situ* reaction was not the issue causing the bimodality in entry 50.

In experiment 51, the combination of **2** and TPA in toluene produced a heterogeneous mixture. TPA was insoluble or only partially soluble in toluene which may explain the incomplete reaction of **2** and TPA as heterogeneous reactions are often far less facile than homogeneous.

The lack of solubility of TPA could be the reason for some degree of bimodality remaining in the polymer sample. One approach to address this problem is to add an excess of the TPA. The additional dicarboxylic acid would increase the

## Chapter 2 - Formation of polyesters via the ring-opening copolymerisation of epoxides and cyclic anhydrides

chance of a complete *in situ* reaction of the **2** complex. To investigate this approach further, experiments were carried out with 2 equivalents (entry 52) and 5 equivalents (entry 53) of TPA. The excess TPA which doesn't react with an aluminium methyl group will act as a chain-transfer agent (CTA) and also initiate polymer chains which will lower the overall molecular weight of the polymer sample. Coates *et al.* showed how CTA's can be used in the ROCOP of epoxides and cyclic anhydrides to control molecular weight.<sup>59</sup>

**Table 8** Effect of increasing molar equivalents of TPA

Exp	Catalyst	Co-cat	Equivs.	Additives	Equivs.	Mn <sup>b</sup>	Đ <sup>b</sup>
24	<b>1</b>	PPNCl	2	-	-	14500	1.21
50	<b>2</b>	PPN <sub>2</sub> TPA	1	TPA	1	12240	1.13
52 <sup>a</sup>	<b>2</b>	PPN <sub>2</sub> TPA	1	TPA	2	8950	1.11
53 <sup>a</sup>	<b>2</b>	PPN <sub>2</sub> TPA	1	TPA	5	8480	1.09

6.4 μmol catalyst. [CHO]<sub>0</sub>: [PhA]<sub>0</sub>: [Cat]<sub>0</sub> = 2000:400:1. Heated for 2 hours at 80 °C. PhA conversion >99%. <sup>a</sup>Heated for 2 hours 15 minutes. <sup>b</sup>Determined by GPC using triple detection, with units of gmol<sup>-1</sup>.

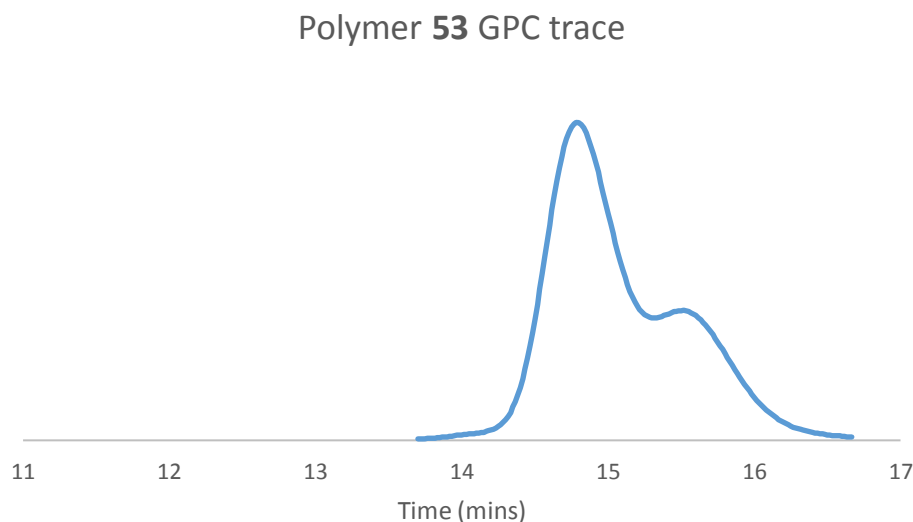


**Figure 27** GPC trace of CHO–PhA from entry 53

In both experiments 52 and 53 (Table 8), polymers of good Mn and Đ were produced. As expected, the Mn of the polymer produced decreased as the equivalents of TPA increased. Upon changing from 1 equivalent of TPA to 2 equivalents, there was a very slight decrease in Đ from 1.13 to 1.11. The Đ

## **Chapter 2** - Formation of polyesters via the ring-opening copolymerisation of epoxides and cyclic anhydrides

decreased again to 1.09 following the increase to 5 equivalents of TPA. Experiments 52 and 53 required slightly longer reaction times compared with entry 50, however complete conversion was still achieved after 2 hours 15 minutes. The  $\bar{D}$  achieved indicates that the polymerisation is extremely selective and well controlled. The GPC trace of polymer 53 is shown in Figure 27. This shows that the bimodality has decreased substantially compared to polymers 24 and 50 but that some still remains. This shows that even lower  $\bar{D}$  could be achieved.

If TPA solubility is a problem than selecting a more soluble alternative may be an option. 1,3-Adamantanedicarboxylic acid (ADC) was chosen, and the ROCOP of CHO and PhA was investigated with 1, 2 and 5 equivalents of this additive. The PPN salt of ADC (PPN<sub>2</sub>ADC) was synthesised through a literature procedure<sup>59</sup> and used as a co-catalyst in conjunction with **2** and the ADC additive. Utilising the more soluble ADC should lead to a faster reaction with **2** compared to TPA, because the mixture will be more homogeneous (Table 9).

**Table 9** Effect of increasing molar equivalents of ADC

Exp	Catalyst	Co-cat	Equivs.	Additives	Equivs.	Mn <sup>b</sup>	$\bar{D}^b$
24	<b>1</b>	PPNCl	2	-	-	14500	1.21
54 <sup>a</sup>	<b>2</b>	PPN <sub>2</sub> ADC	1	ADC	1	18540	1.08
55	<b>2</b>	PPN <sub>2</sub> ADC	1	ADC	2	14790	1.09
56	<b>2</b>	PPN <sub>2</sub> ADC	1	ADC	5	11410	1.16

6.4  $\mu$ mol catalyst. [CHO]<sub>0</sub>: [PhA]<sub>0</sub>: [Cat]<sub>0</sub> = 2000:400:1. Heated for 2 hours at 80 °C. PhA conversion >99%. <sup>a</sup>Heated for 2 hours 15 minutes. <sup>b</sup>Determined by GPC using triple detection, with units of gmol<sup>-1</sup>.

In experiment 54 with 1 equivalent of ADC, 2 hours 15 minutes was required for complete conversion of PhA. A  $\bar{D}$  of 1.08 was measured for this polymer sample. This value is lower than the  $\bar{D}$  measured for entry 50 in which 1 equivalent of TPA was used as the additive. Upon increasing the equivalents of ADC to 2 (entry 55) and 5 (entry 56)  $\bar{D}$  of 1.09 and 1.16 were measured respectively. This shows the trend of decreasing  $\bar{D}$  with increasing equivalents of additive seen with TPA, is not present when ADC is used as the additive. In

## **Chapter 2** - Formation of polyesters via the ring-opening copolymerisation of epoxides and cyclic anhydrides

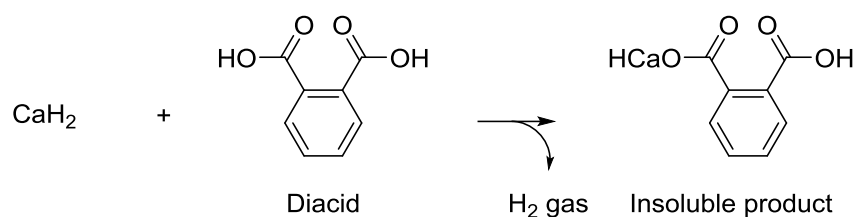
fact, the  $\bar{M}_n$  increased to 1.16 upon increasing to 5 equivalents of ADC. While using 1 equivalent of ADC produced the polymer with the lowest  $\bar{M}_n$ , it did not resolve the bimodal polymer molecular weight observation.

Polymer samples 54, 55 and 56 synthesised with ADC show how increasing the number of equivalents of additive decreases the molecular weight. As the number of equivalents of ADC increases from 1 to 2 to 5 the  $\bar{M}_n$  decreases from 18,540 to 14,790 to 11,410  $\text{g mol}^{-1}$ . This is evidence that ADC is acting as a CTA.

All of the polymers synthesised with ADC had a higher molecular weight than the equivalent reaction with TPA as an additive. The two respective sets of reactions were carried out with different batches of purified PhA. The difference in molecular weight between the respective sets of results show the effect of impurities in the cyclic anhydride. The lower  $\bar{M}_n$  recorded for polymers 50, 52, 53 compared to polymers 54, 55 and 56 is likely a result of a higher concentration of diacid impurity in the PhA starting material. As the diacid impurity acts as a polymerisation initiator, it has a significant impact on the reaction even when present only in catalytic amounts. Therefore, a small increase in impurity concentration can significantly decrease the  $\bar{M}_n$  of the polymer sample because of the generation of more polymer chains. Hošťálek and colleagues examined the effect of impurities on the copolymerisation of CHO and PhA and showed how in particular, the levels of phthalic acid can affect polymer  $\bar{M}_n$  and  $\bar{M}_w$ .<sup>57</sup>

In order to remove the diacid impurities in PhA, additional purification was explored. The normal approach to purify the anhydride was a hot filtration of a chloroform solution containing dissolved PhA. The chloroform was then removed by evaporation and the solid PhA obtained was sublimed by heating under vacuum. This purified anhydride was stored and handled in a nitrogen filled glove box.

**Chapter 2 - Formation of polyesters via the ring-opening copolymerisation of epoxides and cyclic anhydrides**



**Scheme 20** Reaction of diacid with CaH<sub>2</sub>

For the more rigorous removal of diacid impurities, a new approach utilising CaH<sub>2</sub> was explored. PhA was dissolved in dry DCM and under inert atmosphere was stirred overnight with CaH<sub>2</sub>. The DCM solution was isolated by filtration and the solvent removed under vacuum. The solid obtained was then sublimed and placed in the glove box. The rationale behind this procedure was that the CaH<sub>2</sub> would react with any diacid yielding an insoluble calcium salt and H<sub>2</sub> gas. This reaction is shown in Scheme 20. The impurity would then be separated from the soluble anhydride by filtration and subsequent sublimation. CaH<sub>2</sub> would also remove any water present in the system.

To evaluate the effectiveness of this additional purification with CaH<sub>2</sub>, the copolymerisation of CHO and PhA catalysed by **1** and PPNCl was carried out using the specially purified PhA (entry 57) and compared to the reaction with the standard PhA (entry 58). All other reactants were kept the same and were used from the same batch of chemicals. The Mn and Đ of the polymers produced were measured by GPC and the results are shown in Table 10.

**Table 10** ROCOP with purified PhA

Exp	PhA purification	Mn <sup>a</sup>	Đ <sup>a</sup>
57	With CaH <sub>2</sub>	14500	1.18
58	Without CaH <sub>2</sub>	13250	1.17

6.4 μmol catalyst. Catalyst is [Al(L1)Cl<sub>2</sub>] (**1**). [CHO]<sub>0</sub>: [PhA]<sub>0</sub>: [Cat]<sub>0</sub>: [PPNCl]<sub>0</sub> = 2000:400:1:2. Heated for 2 hours at 80 °C. PhA conversion >99%. <sup>a</sup>Determined by GPC using triple detection, with units of g mol<sup>-1</sup>.

The results in Table 10 indicate that the additional purification of the PhA with CaH<sub>2</sub> did not improve the polymerisation. If successful, the polymer Đ should have decreased as the bimodal nature of the polymer molecular weight is

**Chapter 2 - Formation of polyesters via the ring-opening copolymerisation of epoxides and cyclic anhydrides**

reduced. The GPC traces of the two reactions are almost identical indicating the extra purification had no effect.

**Table 11** Effect of co-catalyst on bimodality

Exp	Catalyst	Co-cat	Equivs.	Additives	Equivs.	Mn <sup>b</sup>	Đ <sup>b</sup>
50	2	PPN <sub>2</sub> TPA	1	TPA	1	12240	1.13
52 <sup>a</sup>	2	PPN <sub>2</sub> TPA	1	TPA	2	8950	1.11
59	2	PPN <sub>2</sub> TPA	2	TPA	2	8770	1.39
53 <sup>a</sup>	2	PPN <sub>2</sub> TPA	1	TPA	5	8480	1.09
60	2	PPN <sub>2</sub> TPA	2	TPA	5	8220	1.49
54 <sup>a</sup>	2	PPN <sub>2</sub> ADC	1	ADC	1	18540	1.08
55	2	PPN <sub>2</sub> ADC	1	ADC	2	14790	1.09
61	2	PPN <sub>2</sub> ADC	2	ADC	2	16240	1.35
56	2	PPN <sub>2</sub> ADC	1	ADC	5	11410	1.16
62	2	PPN <sub>2</sub> ADC	2	ADC	5	13370	1.35

6.4 μmol catalyst. [CHO]<sub>0</sub>: [PhA]<sub>0</sub>: [Cat]<sub>0</sub> = 2000:400:1. Heated for 2 hours at 80 °C. PhA conversion >99%. <sup>a</sup>Heated for 2 hours 15 minutes. <sup>b</sup>Determined by GPC using triple detection, with units of gmol<sup>-1</sup>.

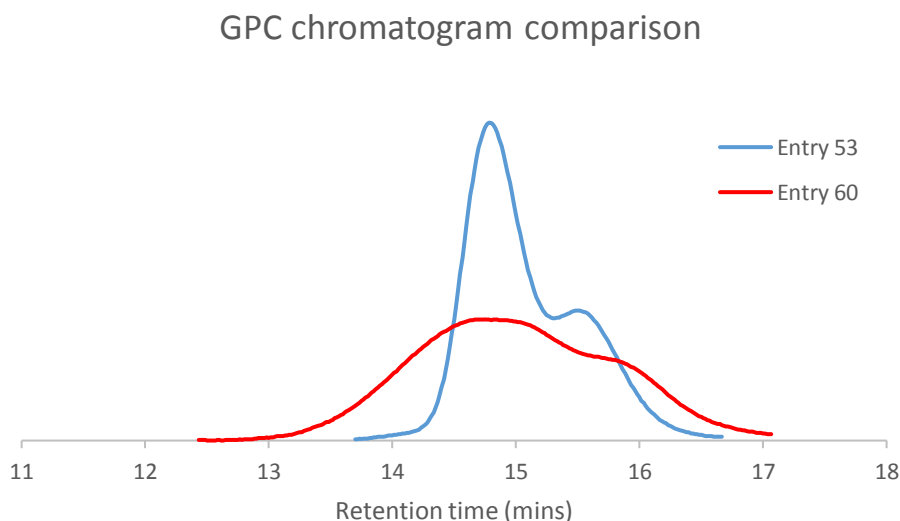


**Figure 28** Comparison of CHO–PhA GPC traces

The effect of increasing the molar equivalents of co-catalyst was also examined (Table 11). Varying the equivalents of PPN<sub>2</sub>TPA and PPN<sub>2</sub>ADC from 1 to 2 saw only minor changes in polymer Mn, however it had a significant

## **Chapter 2 - Formation of polyesters via the ring-opening copolymerisation of epoxides and cyclic anhydrides**

impact on the  $\bar{M}_n$  of the polyesters. In all cases, changing from 1 equivalent of co-catalyst to 2 saw a substantial increase in  $\bar{M}_n$ . This indicates a loss of selectivity and polymerisation control. The largest difference in  $\bar{M}_n$  was seen for polymers 60 and 53 where values of 1.49 and 1.09 were measured respectively. The difference in the GPC traces of the polymers is shown in Figure 28. It is clear that in experiment 60, the polymer has a much wider distribution of polymer chain lengths than 53. For this catalytic system employed in the copolymerisation of CHO and PhA, increasing the molar equivalents of co-catalyst significantly increases the polymer  $\bar{M}_n$  and has a detrimental effect on the reaction. The observation for these bifunctional co-catalysts is contrary to the results reported for many other co-catalysts including the commonly used PPNCl and DMAP where increasing the molar equivalents was not found to impact negatively on the polymerisation.<sup>29</sup>

### **2.7 Summary**

In this chapter, the ROCOP of epoxides and cyclic anhydrides catalysed by a homogeneous macrocycle catalyst was investigated. **1** is a mono pendant arm TACN aluminium complex where the ligand exhibits hemilabile metal binding. **1** proved to be an effective catalyst for the ROCOP of a series of different epoxides and cyclic anhydrides in both a solvent and under solvent free conditions. This is the first example of catalysis with this metal complex. **1** has a structure that is markedly different to the majority of the catalysts previously employed in this polymerisation and indicates that aluminium complexes with active sites arranged in a *cis* geometry can be effective catalysts. DFT calculations suggest that the hemilability in the catalyst is a crucial factor contributing towards its efficacy in the ROCOP reaction, but in a more subtle manifestation than expected. **1** proved to be an extremely robust catalyst which worked efficiently in air. This is, to the best of our knowledge, the first example of a catalyst for the ROCOP of epoxides and cyclic anhydrides which functioned successfully without the need for an inert atmosphere. A wide variety of copolymers were synthesised and many examples had good molecular weights and low  $\bar{M}_n$ . A new catalytic system utilising **2** and bifunctional initiator was developed to reduce bimodality and  $\bar{M}_n$ . This system successfully reduced the bimodality and a  $\bar{M}_n$  of 1.08 was achieved, indicating



## **Chapter 2 - Formation of polyesters via the ring-opening copolymerisation of epoxides and cyclic anhydrides**

the polymerisation was extremely well controlled. Further work investigating the glass-transition temperature, flame retardancy and potential for post-polymerisation modification will be discussed in the next chapters.

### **2.8 References for Chapter 2**

- 1 J. M. Longo, M. J. Sanford and G. W. Coates, *Chem. Rev.*, 2016, **116**, 15167–15197.
- 2 R. C. Jeske, A. M. DiCiccio and G. W. Coates, *J. Am. Chem. Soc.*, 2007, **129**, 11330–11331.
- 3 A. M. DiCiccio, J. M. Longo, G. G. Rodríguez-Calero and G. W. Coates, *J. Am. Chem. Soc.*, 2016, **138**, 7107–7113.
- 4 C. Detrembleur, M. Mazza, X. Lou, O. Halleux, Ph. Lecomte, D. Mecerreyes, J. L. Hedrick and R. Jérôme, *Macromolecules*, 2000, **33**, 7751–7760.
- 5 X. Lou, C. Detrembleur, Ph. Lecomte and R. Jérôme, *Macromolecules*, 2001, **34**, 5806–5811.
- 6 X. Lou, C. Detrembleur, P. Lecomte and R. Jérôme, *Macromol. Rapid Commun.*, 2002, **23**, 126–129.
- 7 X. Lou, C. Detrembleur, P. Lecomte and R. Jérôme, *J. Polym. Sci. Part Polym. Chem.*, 2002, **40**, 2286–2297.
- 8 S. Lenoir, R. Riva, X. Lou, Ch. Detrembleur, R. Jérôme and Ph. Lecomte, *Macromolecules*, 2004, **37**, 4055–4061.
- 9 R. Riva, S. Schmeits, F. Stoffelbach, C. Jérôme, R. Jérôme and P. Lecomte, *Chem. Commun.*, 2005, 5334–5336.
- 10 J. Hopewell, R. Dvorak and E. Kosior, *Philos. Trans. R. Soc. B Biol. Sci.*, 2009, **364**, 2115–2126.
- 11 Y. Wu, G. Z. Miller, J. Gearhart, K. Romanak, V. Lopez-Avila and M. Venier, *Environ. Sci. Technol. Lett.*, 2019, **6**, 14–20.
- 12 A. Marklund, B. Andersson and P. Haglund, *Chemosphere*, 2003, **53**, 1137–1146.
- 13 J. K. Fink, *Reactive Polymers Fundamentals and Applications: A Concise Guide to Industrial Polymers*, William Andrew, 2013.
- 14 L. Feng, Y. Liu, J. Hao, X. Li, C. Xiong and X. Deng, *Macromol. Chem. Phys.*, 2011, **212**, 2626–2632.

**Chapter 2 - Formation of polyesters via the ring-opening copolymerisation of epoxides and cyclic anhydrides**

- 15 N. J. Van Zee and G. W. Coates, *Angew. Chem. Int. Ed Engl.*, 2015, **54**, 2665–2668.
- 16 J. Payne, P. McKeown, M. F. Mahon, E. A. C. Emanuelsson and M. D. Jones, *Polym. Chem.*, 2020, **11**, 2381–2389.
- 17 S. Paul, Y. Zhu, C. Romain, R. Brooks, P. K. Saini and C. K. Williams, *Chem. Commun.*, 2015, **51**, 6459–6479.
- 18 J. Li, Y. Liu, W.-M. Ren and X.-B. Lu, *J. Am. Chem. Soc.*, 2016, **138**, 11493–11496.
- 19 M. J. Sanford, L. Peña Carrodegua, N. J. Van Zee, A. W. Kleij and G. W. Coates, *Macromolecules*, 2016, **49**, 6394–6400.
- 20 G. Si, L. Zhang, B. Han, Z. Duan, B. Li, J. Dong, X. Li and B. Liu, *Polym. Chem.*, 2015, **6**, 6372–6377.
- 21 T. Aida and S. Inoue, *J. Am. Chem. Soc.*, 1985, **107**, 1358–1364.
- 22 A. Bernard, C. Chatterjee and M. H. Chisholm, *Polymer*, 2013, **54**, 2639–2646.
- 23 A. M. DiCiccio and G. W. Coates, *J. Am. Chem. Soc.*, 2011, **133**, 10724–10727.
- 24 E. H. Nejad, A. Paoniasari, C. E. Koning and R. Duchateau, *Polym. Chem.*, 2012, **3**, 1308–1313.
- 25 S. Huijser, E. HosseiniNejad, R. Sablong, C. de Jong, C. E. Koning and R. Duchateau, *Macromolecules*, 2011, **44**, 1132–1139.
- 26 N. D. Harrold, Y. Li and M. H. Chisholm, *Macromolecules*, 2013, **46**, 692–698.
- 27 C. Robert, T. Ohkawara and K. Nozaki, *Chem. – Eur. J.*, 2014, **20**, 4789–4795.
- 28 C. Robert, F. de Montigny and C. M. Thomas, *Nat. Commun.*, 2011, **2**, 586.
- 29 E. Hosseini Nejad, C. G. W. van Melis, T. J. Vermeer, C. E. Koning and R. Duchateau, *Macromolecules*, 2012, **45**, 1770–1776.
- 30 E. H. Nejad, A. Paoniasari, C. G. W. van Melis, C. E. Koning and R. Duchateau, *Macromolecules*, 2013, **46**, 631–637.
- 31 N. J. Van Zee, M. J. Sanford and G. W. Coates, *J. Am. Chem. Soc.*, 2016, **138**, 2755–2761.

**Chapter 2 - Formation of polyesters via the ring-opening copolymerisation of epoxides and cyclic anhydrides**

- 32 D. J. Darensbourg, R. R. Poland and C. Escobedo, *Macromolecules*, 2012, **45**, 2242–2248.
- 33 M. Winkler, C. Romain, M. A. R. Meier and C. K. Williams, *Green Chem.*, 2014, **17**, 300–306.
- 34 U. Biermann, A. Sehlinger, M. A. R. Meier and J. O. Metzger, *Eur. J. Lipid Sci. Technol.*, 2016, **118**, 104–110.
- 35 J. Liu, Y.-Y. Bao, Y. Liu, W.-M. Ren and X.-B. Lu, *Polym. Chem.*, 2013, **4**, 1439–1444.
- 36 C. Martín, A. Pizzolante, E. C. Escudero-Adán and A. W. Kleij, *Eur. J. Inorg. Chem.*, **2018**, 1921–1927.
- 37 D.-F. Liu, L.-Q. Zhu, J. Wu, L.-Y. Wu and X.-Q. Lü, *RSC Adv.*, 2015, **5**, 3854–3859.
- 38 R. Mundil, Z. Hošťálek, I. Šeděnková and J. Merna, *Macromol. Res.*, 2015, **23**, 161–166.
- 39 J. M. Longo, A. M. DiCiccio and G. W. Coates, *J. Am. Chem. Soc.*, 2014, **136**, 15897–15900.
- 40 Z. Duan, X. Wang, Q. Gao, L. Zhang, B. Liu and I. Kim, *J. Polym. Sci. Part Polym. Chem.*, 2014, **52**, 789–795.
- 41 J. Y. Jeon, S. C. Eo, J. K. Varghese and B. Y. Lee, *Beilstein J. Org. Chem.*, 2014, **10**, 1787–1795.
- 42 P. K. Saini, C. Romain, Y. Zhu and C. K. Williams, *Polym. Chem.*, 2014, **5**, 6068–6075.
- 43 Y. Zhu, C. Romain and C. K. Williams, *J. Am. Chem. Soc.*, 2015, **137**, 12179–12182.
- 44 A. Thevenon, J. A. Garden, A. J. P. White and C. K. Williams, *Inorg. Chem.*, 2015, **54**, 11906–11915.
- 45 C.-Y. Yu, H.-J. Chuang and B.-T. Ko, *Catal. Sci. Technol.*, 2016, **6**, 1779–1791.
- 46 L. Zhu, D. Liu, L. Wu, W. Feng, X. Zhang, J. Wu, D. Fan, X. Lü, R. Lu and Q. Shi, *Inorg. Chem. Commun.*, 2013, **37**, 182–185.
- 47 D.-F. Liu, L.-Y. Wu, W.-X. Feng, X.-M. Zhang, J. Wu, L.-Q. Zhu, D.-D. Fan, X.-Q. Lü and Q. Shi, *J. Mol. Catal. Chem.*, 2014, **382**, 136–145.

**Chapter 2 - Formation of polyesters via the ring-opening copolymerisation of epoxides and cyclic anhydrides**

- 48 T. Aida, K. Sanuki and S. Inoue, *Macromolecules*, 1985, **18**, 1049–1055.
- 49 J. A. Garden, P. K. Saini and C. K. Williams, *J. Am. Chem. Soc.*, 2015, **137**, 15078–15081.
- 50 L. Wu, D. Fan, X. Lü and R. Lu, *Chin. J. Polym. Sci.*, 2014, **32**, 768–777.
- 51 D. Liu, Z. Zhang, X. Zhang and X. Lü, *Aust. J. Chem.*, 2016, **69**, 47–55.
- 52 B. Han, L. Zhang, B. Liu, X. Dong, I. Kim, Z. Duan and P. Theato, *Macromolecules*, 2015, **48**, 3431–3437.
- 53 R. Baumgartner, Z. Song, Y. Zhang and J. Cheng, *Polym. Chem.*, 2015, **6**, 3586–3590.
- 54 Y. Maeda, A. Nakayama, N. Kawasaki, K. Hayashi, S. Aiba and N. Yamamoto, *Polymer*, 1997, **38**, 4719–4725.
- 55 A. Takasu, T. Bando, Y. Morimoto, Y. Shibata and T. Hirabayashi, *Biomacromolecules*, 2005, **6**, 1707–1712.
- 56 E. Mahmoud, D. A. Watson and R. F. Lobo, *Green Chem.*, 2013, **16**, 167–175.
- 57 Z. Hošťálek, O. Trhlíková, Z. Walterová, T. Martinez, F. Peruch, H. Cramail and J. Merna, *Eur. Polym. J.*, 2017, **88**, 433–447.
- 58 M. E. Fieser, M. J. Sanford, L. A. Mitchell, C. R. Dunbar, M. Mandal, N. J. Van Zee, D. M. Urness, C. J. Cramer, G. W. Coates and W. B. Tolman, *J. Am. Chem. Soc.*, 2017, **139**, 15222–15231.
- 59 M. J. Sanford, N. J. V. Zee and G. W. Coates, *Chem. Sci.*, 2017, **9**, 134–142.
- 60 D. A. Robson, S. Y. Bylikin, M. Cantuel, N. A. H. Male, L. H. Rees, P. Mountford and M. Schröder, *J. Chem. Soc. Dalton Trans.*, 2001, 157–169.
- 61 M. A. Bahili, E. C. Stokes, R. C. Amesbury, D. M. C. Ould, B. Christo, R. J. Horne, B. M. Kariuki, J. A. Stewart, R. L. Taylor, P. A. Williams, M. D. Jones, K. D. M. Harris and B. D. Ward, *Chem. Commun.*, 2019, **55**, 7679–7682.
- 62 P. Braunstein and F. Naud, *Angew. Chem. Int. Ed.*, 2001, **40**, 680–699.

**Chapter 2 - Formation of polyesters via the ring-opening copolymerisation of epoxides and cyclic anhydrides**

- 63 G. M. Adams and A. S. Weller, *Coord. Chem. Rev.*, 2018, **355**, 150–172.
- 64 Z. Weng, S. Teo and T. S. A. Hor, *Acc. Chem. Res.*, 2007, **40**, 676–684.
- 65 H. Werner, A. Stark, M. Schulz and J. Wolf, *Organometallics*, 1992, **11**, 1126–1130.
- 66 A. Buhling, P. C. J. Kamer, P. W. N. M. van Leeuwen, J. W. Elgersma, K. Goubitz and J. Fraanje, *Organometallics*, 1997, **16**, 3027–3037.
- 67 C. Flassbeck and K. Wiegardt, *Z. Für Anorg. Allg. Chem.*, 1992, **608**, 60–68.
- 68 S. Y. Bylikin, D. A. Robson, N. A. H. Male, L. H. Rees, P. Mountford and M. Schröder, *J. Chem. Soc. Dalton Trans.*, 2001, 170–180.
- 69 M. E. G. Skinner, B. R. Tyrrell, B. D. Ward and P. Mountford, *J. Organomet. Chem.*, 2002, **647**, 145–150.
- 70 J. Zhang, H. Liu, H. Liu, J. Hu, S. Tan and T. Wu, *Polym. Bull.*, 2017, **74**, 625–639.
- 71 N. Yi, T. T. D. Chen, J. Unruangsri, Y. Zhu and C. K. Williams, *Chem. Sci.*, 2019, **10**, 9974–9980.
- 72 E. S. Beach, Z. Cui and P. T. Anastas, *Energy Environ. Sci.*, 2009, **2**, 1038.
- 73 P. T. Anastas and J. C. Warner, *Green Chemistry: Theory and Practice*, Oxford University Press, New York, 1998.
- 74 B. A. Abel, C. A. L. Lidston and G. W. Coates, *J. Am. Chem. Soc.*, 2019, **141**, 12760–12769.
- 75 M. J. Frisch, G. W. Trucks, H. B. Schlegel, G. E. Scuseria, M. A. Robb, J. R. Cheeseman, G. Scalmani, V. Barone, G. A. Petersson, H. Nakatsuji, X. Li, M. Caricato, A. V. Marenich, J. Bloino, B. G. Janesko, R. Gomperts, B. Mennucci, H. P. Hratchian, J. V. Ortiz, A. F. Izmaylov, J. L. Sonnenberg, Williams, F. Ding, F. Lipparini, F. Egidi, J. Goings, B. Peng, A. Petrone, T. Henderson, D. Ranasinghe, V. G. Zakrzewski, J. Gao, N. Rega, G. Zheng, W. Liang, M. Hada, M. Ehara, K. Toyota, R. Fukuda, J. Hasegawa, M. Ishida, T. Nakajima, Y. Honda, O. Kitao, H. Nakai, T. Vreven, K. Throssell, J. A. Montgomery Jr., J. E. Peralta, F. Ogliaro, M. J.

**Chapter 2 - Formation of polyesters via the ring-opening copolymerisation of epoxides and cyclic anhydrides**

- Bearpark, J. J. Heyd, E. N. Brothers, K. N. Kudin, V. N. Staroverov, T. A. Keith, R. Kobayashi, J. Normand, K. Raghavachari, A. P. Rendell, J. C. Burant, S. S. Iyengar, J. Tomasi, M. Cossi, J. M. Millam, M. Klene, C. Adamo, R. Cammi, J. W. Ochterski, R. L. Martin, K. Morokuma, O. Farkas, J. B. Foresman and D. J. Fox, *Gaussian 09 Rev. D.01*, Wallingford, CT, 2016.
- 76 S. S. Batsanov, *Inorg. Mater.*, 2001, **37**, 871–885.
- 77 T. A. Keith, *AIMAll*, TK Gristmill Software, Overland Park KS, USA, 2017.
- 78 E. D. Glendening, J. K. Badenhoop, A. E. Reed, J. E. Carpenter, J. E. Bohmann, C. M. Morales, C. R. Landis and F. Weinhold, *NBO 6.0*, Theoretical Chemistry Institute, University of Wisconsin, Madison, 2013.
- 79 A.-C. Albertsson, I. K. Varma and R. K. Srivastava, in *Handbook of Ring-Opening Polymerization*, John Wiley & Sons, Ltd, 2009, pp. 287–306.
- 80 D. A. Robson, L. H. Rees, P. Mountford and M. Schröder, *Chem. Commun.*, 2000, 1269–1270.
- 81 S.-J. Li and D.-C. Fang, *Phys. Chem. Chem. Phys.*, 2016, **18**, 30815–30823.
- 82 P. V. Bernhardt and G. A. Lawrance, *Coord. Chem. Rev.*, 1990, **104**, 297–343.
- 83 W. A. Chomitz and J. Arnold, *Chem. – Eur. J.*, 2009, **15**, 2020–2030.

# Chapter 3

## Thermal and flame retardant properties of the copolymers

**3.1 Flame retardancy and thermal properties of copolymers**

The ring-opening copolymerisation (ROCOP) of epoxides and cyclic anhydrides yields hydrolysable polyesters. Biodegradability or recyclability are extremely important properties which are receiving a great deal of attention in the media, this is driven by concerns over the persistence of conventional plastics in the environment where they take hundreds of years to degrade.<sup>1</sup> Their environmental persistence means that plastics are accumulating in the natural environment on both land and in the seas and oceans.<sup>2-6</sup> Plastics are also entering the food chains of animals, causing health issues.<sup>7</sup> As a result of these serious problems, there is significant motivation to replace existing, environmentally damaging plastics with sustainable, degradable alternatives. However for this to take place, new biodegradable/recyclable plastics must be developed which can display competitive properties to those existing plastics.<sup>8,9</sup>

Copolymers of epoxides and cyclic anhydrides have great potential as biodegradable polyesters with a diverse range of useful properties in addition to their innate hydrolysability.<sup>10</sup> The wide variety of potential epoxide and cyclic anhydride monomer combinations make it possible to introduce different properties to the polymers at the point of synthesis, and offer the potential to design or tune a plastic with a particular property or application in mind.<sup>11,12</sup> In order to explore the capability of the ROCOP reaction to produce plastics with specific, desirable characteristics, we attempted to introduce the important, desirable property of flame retardancy without the use of an additive. This was achieved by the introduction of flame retardant monomers in the copolymerisation procedure. In this preliminary study, the chlorine containing tetrachlorophthalic anhydride (TCPhA) and the bromine containing tetrabromophthalic anhydride (TBPhA) were selected as monomers for the copolymerisation. The thermal properties of these plastics were also explored. Variation of the epoxide and anhydride monomers is postulated to yield copolymers with a wide range of glass transition temperatures ( $T_g$ s). The ability to produce polymers with high or low glass transition temperatures would be very useful, increasing the number of potential applications.<sup>11</sup> For example polyimides are a group of plastics which exhibit excellent thermal



### **Chapter 3 - Thermal and flame retardant properties of the copolymers**

stabilities >500 °C and are utilised for a range of applications such as high temperature mechanical seals, electrical insulation and in the aerospace industry.<sup>13</sup> Plastics with extremely low glass transition temperatures are also extremely useful, these plastics are used at temperatures higher than their glass transition temperatures where they exhibit high flexibility and elasticity. Examples of this type of plastic are elastomers such as polybutadiene or polyisoprene.<sup>14</sup>

#### **3.2 Introduction to flame retardancy in plastics**

The flammability of polymers is an immensely important issue in the plastics industry. As most polymers utilised for consumer or industrial applications are derived from hydrocarbons, they are necessarily flammable.<sup>15</sup> When exposed to fire, these materials burn very quickly releasing large amounts of heat, which fuels the intensity of the fire, and a substantial amount of smoke, which can be deadly if inhaled.<sup>16</sup> Considering the extensive use of plastics in wide ranging applications such as in construction, home furnishings, packaging, electronic devices and in aviation *etc.*, their flammability is an important issue.<sup>17–19</sup> In 39 countries with populations totalling 2.5 billion, between 1993 and 2016 over 1 million people were killed in fires. In 2016 there were 3,390 fire deaths in the USA, 8,749 deaths in Russia and 367 in the UK. Per 100,000 people, the number of fire deaths in the USA, Russia and the UK were 1, 6 and 0.6 respectively. In the USA alone there were 1,342,000 fires in 2016; of these fires 35% were in building structures and 15% in vehicles.<sup>20</sup> According to the Aircraft Crashes Record Office, in the 1,662 aircraft accidents occurring from 2001 to 2010 in which 15,962 people lost their lives, improving the fire resistance of the plastic materials used would have reduced the severity of the incidents and number of fatalities.<sup>16</sup>

The mechanism by which plastics burn is as follows: If the temperature of a plastic reaches its pyrolysis temperature it starts to break down into flammable or non-flammable gases, liquid condensates and solid char. If the temperature is high enough, the flammable gases and any flammable liquid condensates combust, producing more heat. Any non-flammable material produced such as inert gases or char, inhibit the fire as they do not act as fuel and can form

### Chapter 3 - Thermal and flame retardant properties of the copolymers

a barrier preventing the fire from reaching more flammable material. For any combustion to take place three factors are required, fuel in the form of a flammable material, heat and oxygen.<sup>21</sup> The flammability properties of some commonly used plastics are shown in Table 1. For each plastic the ignition temperature, limiting oxygen index (LOI), total heat of combustion and the peak heat release rate are given.<sup>16</sup> The LOI of a material is the percentage atmospheric oxygen required to sustain a flame. Many of the plastics shown in Table 1 have a LOI lower than the percentage oxygen in air (21%) indicating they will readily burn under ambient conditions.

**Table 1** Flammability of some commonly used polymers

Polymer	Ignition temp °C	LOI (%)	Total heat of combustion (kJ/g) <sup>a</sup>	Peak heat release rate (kW/m <sup>2</sup> ) <sup>a</sup>
Polyethylene	370	18	37	1130
Polypropylene	330	18	44	1300
Nylon-6	430	25	30	1272
Poly(styrene)	319	18	28	407
Poly(acrylonitrile)	480	27	28	343
Epoxy resin	427	19	25	755
Unsaturated polyester	330	20	23	985

<sup>a</sup>Data measured at 50 flux. Data published by Das *et al.*<sup>16</sup>

Due to the dangers of using these highly flammable plastics, flame retardants are often added to materials. Flame retardants can inhibit a fire in a number of ways. Many flame retardants produce non-flammable gases or solid char as by-products of pyrolysis. The production of inert gases dilutes the concentration of oxygen (which is a crucial ingredient for fire) in the local atmosphere around a burning material and increases the concentration of non-flammable gases, thereby slowing the rate of burning. This method is known as vapour or gas phase flame retardancy. The formation of char on the surface of a burning plastic provides a protective layer between the fire and the potentially flammable material below. This char layer prevents the transfer of

### **Chapter 3 - Thermal and flame retardant properties of the copolymers**

heat making it more difficult to reach the ignition temperature and hinders the mass transfer between the gas phase and the condensed phase, preventing combustion. Flame retardants which behave in this way are said to operate via a condensed phase mechanism. Finally, a material can function as a flame retardant by acting as a heat sink. These chemicals decompose endothermically, reducing the energy in the fire and therefore preventing the temperature reaching the pyrolysis point of the flammable polymer. Table 2 shows typical types of flame retardants; it gives examples and details their mechanism of fire inhibition.<sup>16,22</sup>

**Table 2** Examples of common flame retardants<sup>16,22</sup>

Type of flame retardant	Examples of flame retardant	Working mechanism
Metal oxides	Magnesium hydroxide, aluminium hydroxide, alumina trihydrate, calcium carbonate	Heat sink
Boron based	Boric acid, borax, zinc borate, boron phosphate	Forms isolating layer
Halogen based	TCPPhA, TBPhA, PBDEs, PBB	Gas phase
Phosphorous based	THPC, Red Phosphorous, PBDPP, BDP, DOPO	Condensed phase

Halogen based flame retardants act in the gas phase and are extremely effective flame retardants. Examples of this class of flame retardants are tetrachlorophthalic anhydride (TCPPhA) or tetrabromophthalic anhydride (TBPhA). Halogenated flame retardants work by removing H<sup>•</sup> and OH<sup>•</sup> radicals from the flammable gases by reaction with Br or Cl, resulting in a slowdown in burning. However, the use of many of these compounds is being phased out due to environmental concerns. Polybrominated biphenyls (PBB) and polybrominated diphenyl ethers (PBDE) which have been used for a number applications, have had their use restricted or banned in a number of countries.<sup>16</sup>

### Chapter 3 - Thermal and flame retardant properties of the copolymers

As some of the brominated flame retardants were phased out, phosphorous-containing alternatives became more prevalent. These compounds made up 20% of all flame retardants used in Europe in 2006. Generally, phosphorus-containing flame retardants can be split into three categories, organophosphinate, organo-phosphonate and phosphate esters, these compounds mainly operate in the condensed phase. Examples of phosphorus-based flame retardants are red phosphorous, tetrakis(hydroxymethyl)phosphonium chloride (THPC), resorcinol bis(diphenyl phosphate) (PBDPP), bisphenol A bis(diphenyl phosphate) (BDP) and 9,10-dihydro-9-oxa-10-phosphaphenanthrene-10-oxide (DOPO) shown in Figure 1. When the phosphorous-containing flame retardants are heated, they react with one another to form a polymeric material which acts as a char layer, shielding the rest of the polymer from the oxygen required for combustion.<sup>23</sup> These compounds can also cause cross-linking of polymer chains at elevated temperatures, this process may occur following dehydration of the polymer structure or the phosphorous-based flame retardant, or else the decomposition product may acts as a cross-linker. In addition to condensed phase flame retardancy, some phosphorous-based flame retardants exhibit vapour phase flame retardancy where reactive  $H^{\bullet}$  and  $OH^{\bullet}$  species are removed inhibiting the flame.<sup>24</sup> Like many of the halogen-containing flame retardants, some organophosphorus alternatives exhibit similar toxicity and are therefore also an environmental concern.<sup>25</sup>

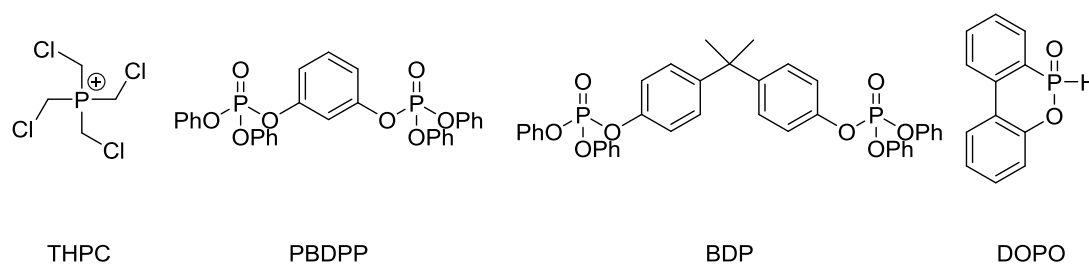


**Figure 1** Phosphorous based flame retardants<sup>23</sup>

Metal oxides can act as flame retardants and smoke suppressants. The production of smoke in a fire can be deadly as it contains poisonous gases such as carbon monoxide and reduces the concentration of  $O_2$  in the atmosphere which can cause death by asphyxiation. Copper, molybdenum and zinc oxides reduce the heat release rate and increase char formation in

### **Chapter 3 - Thermal and flame retardant properties of the copolymers**

poly(vinyl chloride) (PVC).<sup>26</sup> MgO and Fe<sub>2</sub>O<sub>3</sub> have been shown to increase the char formation and decreases heat release rates in polyurethanes.<sup>27</sup>

Boron containing compounds such boric acid, zinc borate and boron phosphate act as flame retardants and smoke suppressants for both halogen containing and halogen free polymers. Boron based flame retardants show synergistic effects when used in conjunction with halogen based flame retardants. They can catalyse cross-linking of polymer chains by dehydrohalogenation which increases char formation and decreases smoke formation. Boron containing flame retardants can also act as afterglow suppressants.<sup>28</sup>

A major issue with many of these flame retardants is that they are not covalently bound to the plastic materials they are added to. This means that over the lifetime of the material, flame retardant chemicals can leach out and accumulate in the environment.<sup>29–31</sup> This process may occur by the flame retardant simply leaching out of the polymer surface, or by volatilization or abrasion.<sup>32</sup> As some flame retardants are used in proportions as high as 30% by weight, leaching can lead to significant ecological damage.<sup>31,33</sup> New approaches are required which impart flame retardancy to plastics without posing risks to health and the environment. This does not mean that all flame retardants should be completely removed, fires are highly toxic regardless of whether materials contain flame retardants. The smoke produced by fires causes more deaths than the extreme temperatures produced. The main toxic component of smoke is carbon monoxide. Extremely toxic CO levels of 10 – 50,000 ppm have been found in smoke produced from fires. Eliminating or slowing the rate of burning is key to reducing fire deaths and the use of flame retardants is an effective measure to achieve this. For example, sofas without flame retardants posed a greater cancer risk due to polycyclic aromatic hydrocarbons than those with flame retardants as the fire resistant examples are involved in fewer and smaller fires.<sup>19</sup>

The toxicity of flame retardants must be addressed and new approaches to introduce fire resistance to materials are required. One approach that avoids the issue of flame retardant leaching, is to include flame retardant monomers

### Chapter 3 - Thermal and flame retardant properties of the copolymers

in the synthesis of a plastic. These monomers react and form part of the polymer chain and are therefore covalently bound within the polymer matrix and cannot leach out.<sup>22,34</sup>

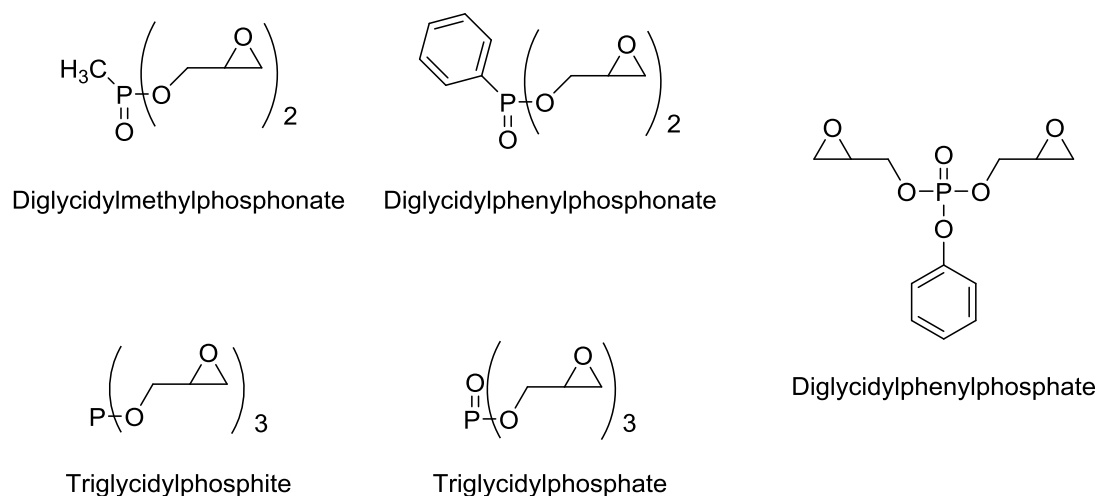


**Figure 2** Flame retardant organophosphorus epoxy monomers<sup>35</sup>

Hergenrother and colleagues reported the synthesis of additive-free, flame retardant epoxy resins, for use in the exterior structures of subsonic aviation aircraft. This was achieved by the introduction of organophosphorus epoxy monomers as shown in Figure 2. The inclusion of these monomers successfully improved the flame resistance of the epoxy resins by increasing the char formation during burning.<sup>35</sup>

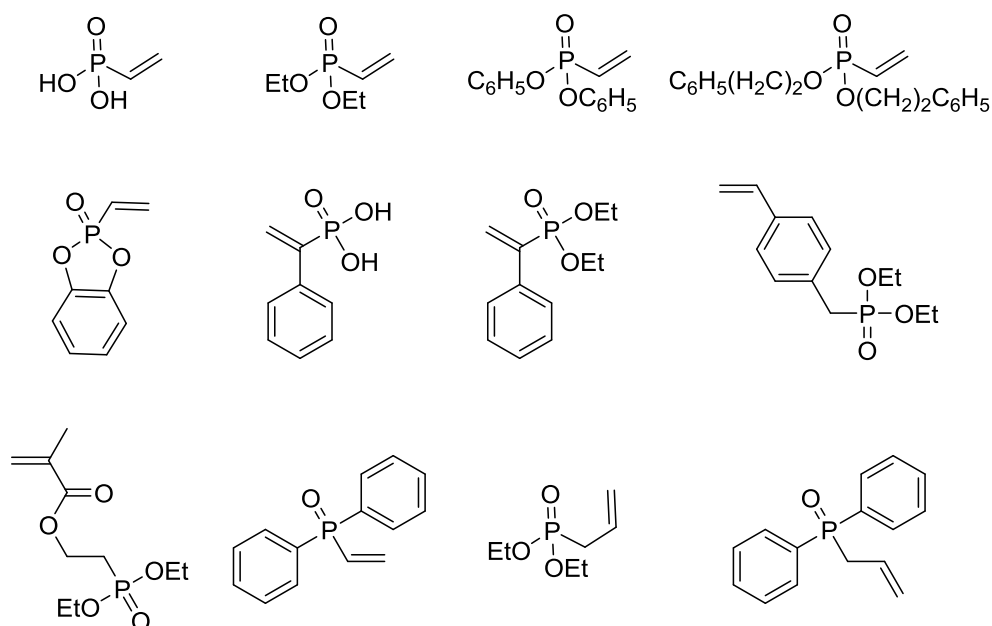


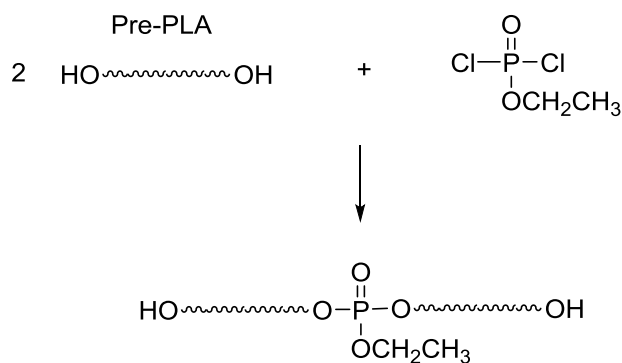
**Figure 3** Flame retardant vinyl phosphate monomers<sup>34</sup>

### Chapter 3 - Thermal and flame retardant properties of the copolymers

Copolymerisation of vinyl phosphates (Figure 3) with commonly used polymers such as polystyrene, poly(methyl methacrylate), poly(acrylonitrile) and poly(acrylamide) increased the flame retardancy of these plastics. The polymers are produced by a free-radical catalysed mechanism. Even with low proportions of phosphates, the improvement in flame retardancy is comparable to that achieved by additives which must be employed at higher concentrations.<sup>34</sup>

Polyphosphate esters can be formed from the condensation reaction of bisphenols and aryl or alkyl phosphorodichloridates. These polymers are flame retardant because of the high phosphorus content.<sup>36,37</sup> Poly(phosphoramidate esters) can be produced through a similar polycondensation mechanism.<sup>38–40</sup> Flame retardant poly(amide)s, poly(imide)s and poly(urethane)s can be generated by copolymerisation with a phosphorus containing comonomer or direct polymerisation of these flame retardant monomers leads to extremely fire resistant polymers.<sup>34</sup>

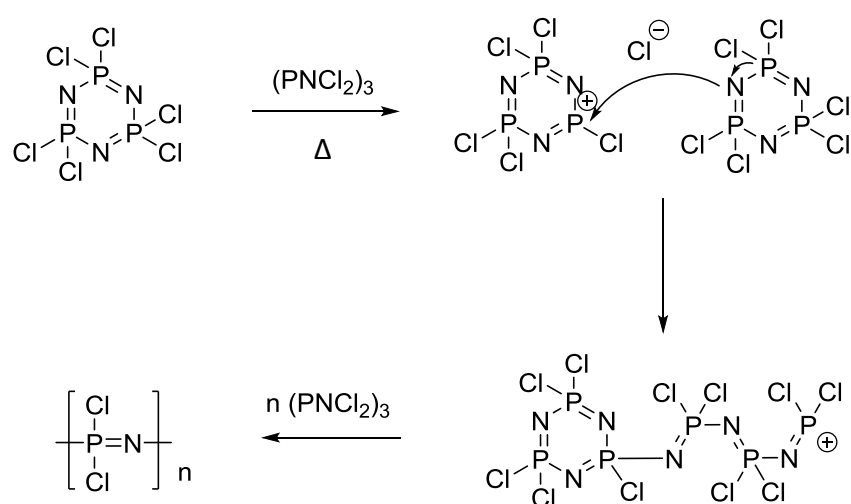
Wang *et al.* reported the synthesis of flame retardant poly(lactic acid) (PLA). PLA is a biodegradable polymer which can be synthesised from renewable feedstocks. This was achieved by pre-forming chains of PLA through a polycondensation reaction, these dihydroxyl terminated chains then reacted with ethyl phosphorodichloridate which linked chains together and introduced the flame retardant phosphorus into the polymer backbone. This reaction is illustrated in Scheme 1. The introduction of the phosphate chain linker reduced the peak heat release rate to 274 W/g from 480 W/g for commercial PLA.<sup>41</sup>



**Scheme 1** Preparation of flame retardant PLA<sup>41</sup>

### Chapter 3 - Thermal and flame retardant properties of the copolymers

In order to introduce flame retardancy into poly(ethylene-1,4-terephthalate) (PET) or poly(ethylene-2,6-naphthalate) (PEN), phosphorus containing monomers with carboxylic acid groups were included in the polymerisation reaction. These monomers undergo the same condensation reactions with the diols used in the formation of these plastics. The introduction of these monomers greatly improved the flame retardancy. However in some cases, this led to a reduction in the toughness of the plastic, demonstrating how changing the monomers can also affect the mechanical properties of the plastic as well as the fire resistance.<sup>34</sup>



**Scheme 2** Formation of poly(phosphazene)<sup>42,43</sup>

The ring-opening polymerisation of hexachlorocyclotriphosphazene yields inherently flame retardant polymers due to the very high levels of phosphorous in the materials. This mechanism can be employed to form the homopolymer, a poly(phosphazene), or can be combined with other monomers to produce copolymers with more varied properties.<sup>42,43</sup> The homopolymerisation requires high temperatures, typically 250 °C for several hours. These forcing conditions are needed to enable the cleavage of the Cl-P bonds, a crucial step in the ring-opening polymerisation mechanism (Scheme 2), however excessive heating can cause substantial cross-linking of polymer chains to occur. Post-polymerisation modification of the poly(phosphazene) by organic nucleophiles can produce a variety of poly(organo)phosphazenes with wide ranging properties.<sup>44</sup>



Silicon containing compounds have great potential as environmentally friendly alternatives to many conventional flame retardants. Only a small quantity of silicon is required to impart fire resistance into a plastic material. Silicon based flame retardants act both in the vapour phase by removing reactive radicals and in the solid phase by increasing char formation.<sup>34</sup>

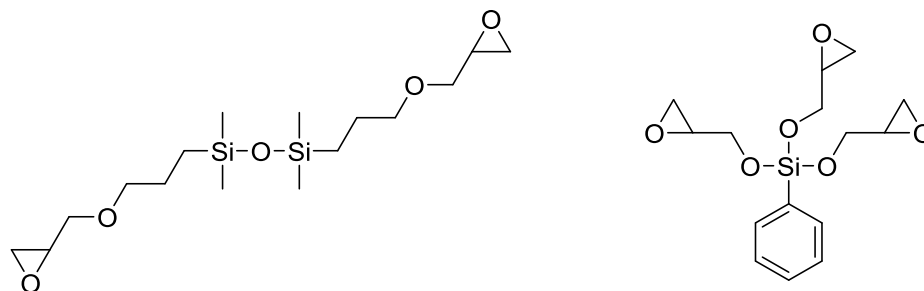
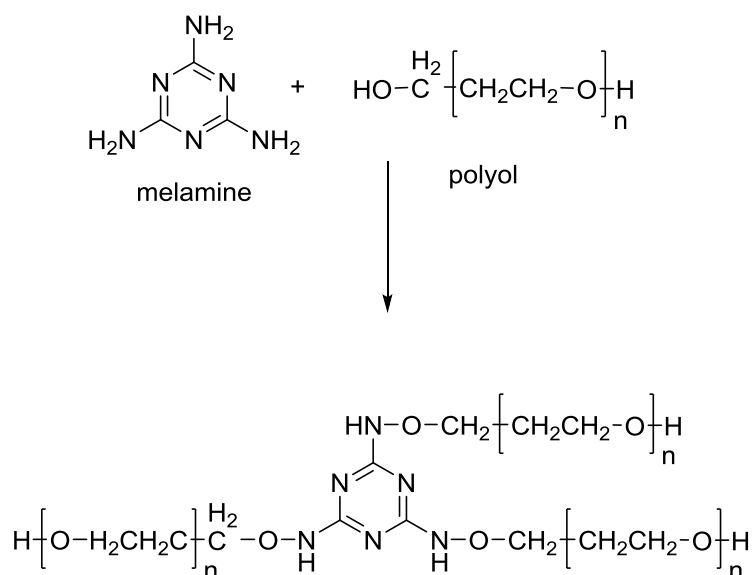


**Figure 4** Silicon containing epoxides<sup>45</sup>

The flame retardancy of diphenylmethane-4,4-diisocyanate (MDI) based elastomeric polyurethanes may be increased by the addition of siloxanes, functionalised with amine, epoxy and methacrylate moieties into the polymer matrix. Even at siloxane levels of 5%, a 70% reduction in the peak heat release rate (PHRR) (a key parameter defining flammability) was achieved.<sup>46</sup> Hydroxy- or amine-terminated siloxanes can be used to impart fire resistance into epoxy resins. Not only does this increase the flame retardancy of the material, in some cases it can improve other properties of the plastic such as dielectric strength and surface resistance.<sup>47</sup> Silicon containing epoxides can be used to produce flame retardant epoxy resin when they are either used alone in a homopolymerisation or in combination with a co-monomer such as a diamine (Figure 4).<sup>45</sup>

### Chapter 3 - Thermal and flame retardant properties of the copolymers



**Scheme 3** Reaction of melamine and polyol<sup>34</sup>

Nitrogen containing flame retardants are another class of environmentally friendly flame retardants with low toxicity. An additional advantage of using nitrogen containing compounds is that polymers incorporating them are still readily recyclable. A commonly used example of a nitrogen based flame retardant is melamine. It has been used in nylon, with acrylonitrile butadiene styrene and in rigid polyurethane foams to introduce fire resistance.<sup>34,48</sup> The reaction of melamine with an example polyol is shown in Scheme 3.

Oxazene can be used to form a variety of flame retardant polymers. This monomer can be homopolymerised to form flame resistant plastics or copolymerised with an epoxy resin to yield polymers with additional useful characteristics such as good mechanical and electrical properties and low density.<sup>34</sup>

Polyisocyanurates are commonly used plastics, they have innate flame retardant properties because of their high nitrogen content and cyclic structures. Copolymerisation of a diisocyanate and a polyol leads to heavily cross-linked polyurethane foams. These materials have excellent thermal insulation properties. An excess of isocyanate causes the formation of isocyanurate rings in a cyclotrimerisation reaction in the polymer matrix leading to improved properties such as thermal stability and rigidity.<sup>49</sup>

### **Chapter 3 - Thermal and flame retardant properties of the copolymers**

The introduction of a flame retardant monomer into a polymer chain is a very effective way to improve fire resistance. A major advantage of utilising flame retardant reactive monomers, which are covalently bound within the polymer matrix as opposed to more simple flame retardants which are just mixed into the material, is that the fire resistant monomer cannot leach out of the plastic. In a copolymerisation, the proportion of a flame retardant monomer included in the polymer can be varied to produce optimal properties. Flame retardancy may be achieved with only a small proportion of the fire resistant monomer.<sup>16</sup> A polymer chain containing flame retardant monomers may be used in isolation or can be mixed with other polymers in a plastic material that consists of a polymer blend. This can be a powerful approach which can combine advantageous properties from different polymers such as combining flame retardancy with good mechanical strength.

#### **3.3 Thermal properties of polyesters synthesised from the ring-opening copolymerisation (ROCOP) of epoxides and cyclic anhydrides**

A real advantage of plastics is that a wide variety of thermal properties can be attained. The chemical structure of the polymer, the molecular weight, the degree of cross-linking and how the polymer chains pack together, affects how plastic behaves at different temperatures. The glass-transition temperature ( $T_g$ ) determines whether the polymer is a hard and brittle material or a soft and flexible elastomer and the melt temperature ( $T_m$ ) indicates the point at which the polymer becomes a viscous liquid.<sup>50</sup> These characteristics influence which applications a plastic is suitable for. Depending on the requirements of a plastic, a variety of  $T_g$  values may be needed. A particular challenge for biodegradable polymers is attaining a  $T_g$  greater than 100 °C making them suitable for high temperature applications such as withstanding boiling water.<sup>11,12</sup> Additives may be added to improve the properties of biodegradable plastics however their introduction can prevent the degradation of these materials once they are discarded, therefore single component plastics capable of displaying specific properties are desirable.<sup>51</sup> An example of a polymer with a high glass transition temperature is polycarbonate with a  $T_g$  of 150 °C, whilst an example of a low glass transition temperature polymer is low density polyethylene which has a  $T_g$  of -120 °C.<sup>52</sup> If new flame retardant

### Chapter 3 - Thermal and flame retardant properties of the copolymers

polymers are to be effective for a wide range of applications, examples with a range of  $T_g$  values are required.

The ROCOP of epoxides and cyclic anhydrides yields thermoplastic polyesters. Thermoplastics can be either amorphous or crystalline materials. These two classifications of polymers show very different properties. Crystalline polymers are often more dense than amorphous polymers, as the polymer chains pack more efficiently in the material. The crystallinity introduces greater hardness, wear and corrosion resistance, less creep or time dependant behaviour, and increased resistance to cracking.<sup>11</sup>

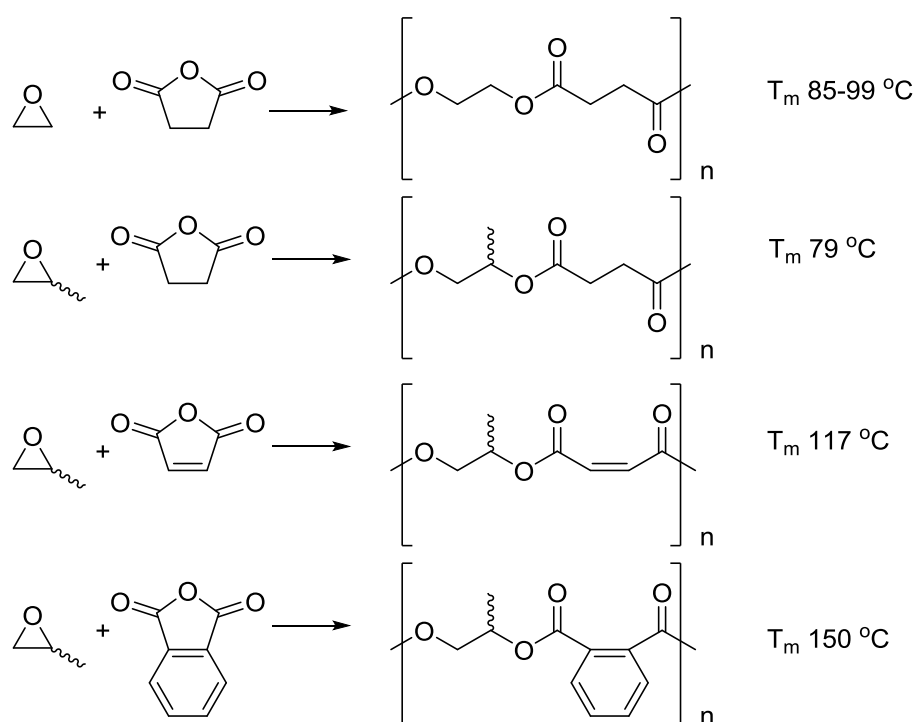


**Figure 5** Semi-crystalline polyesters from the ring-opening copolymerisation (ROCOP) of epoxides and cyclic anhydrides<sup>53-55</sup>

There are limited examples of semi-crystalline polyesters formed from the ROCOP of epoxides and cyclic anhydrides (Figure 5). Maeda *et al.* reported the formation of a semi-crystalline polymer from the reaction of ethylene oxide and succinic anhydride (SA) with a melting point ranging from 85 – 99 °C depending on the degree of anhydride incorporation in the polymer.<sup>53</sup> Coates also reported semi-crystalline, stereoregular isotactic polyesters from the copolymerisation of different isomers of propylene oxide (PO) with maleic anhydride (MA), SA and phthalic anhydride (PhA). In order for crystallinity to

### Chapter 3 - Thermal and flame retardant properties of the copolymers

return to these melted polymers, annealing for over seven days or precipitation with an anti-solvent is required.<sup>54,55</sup>

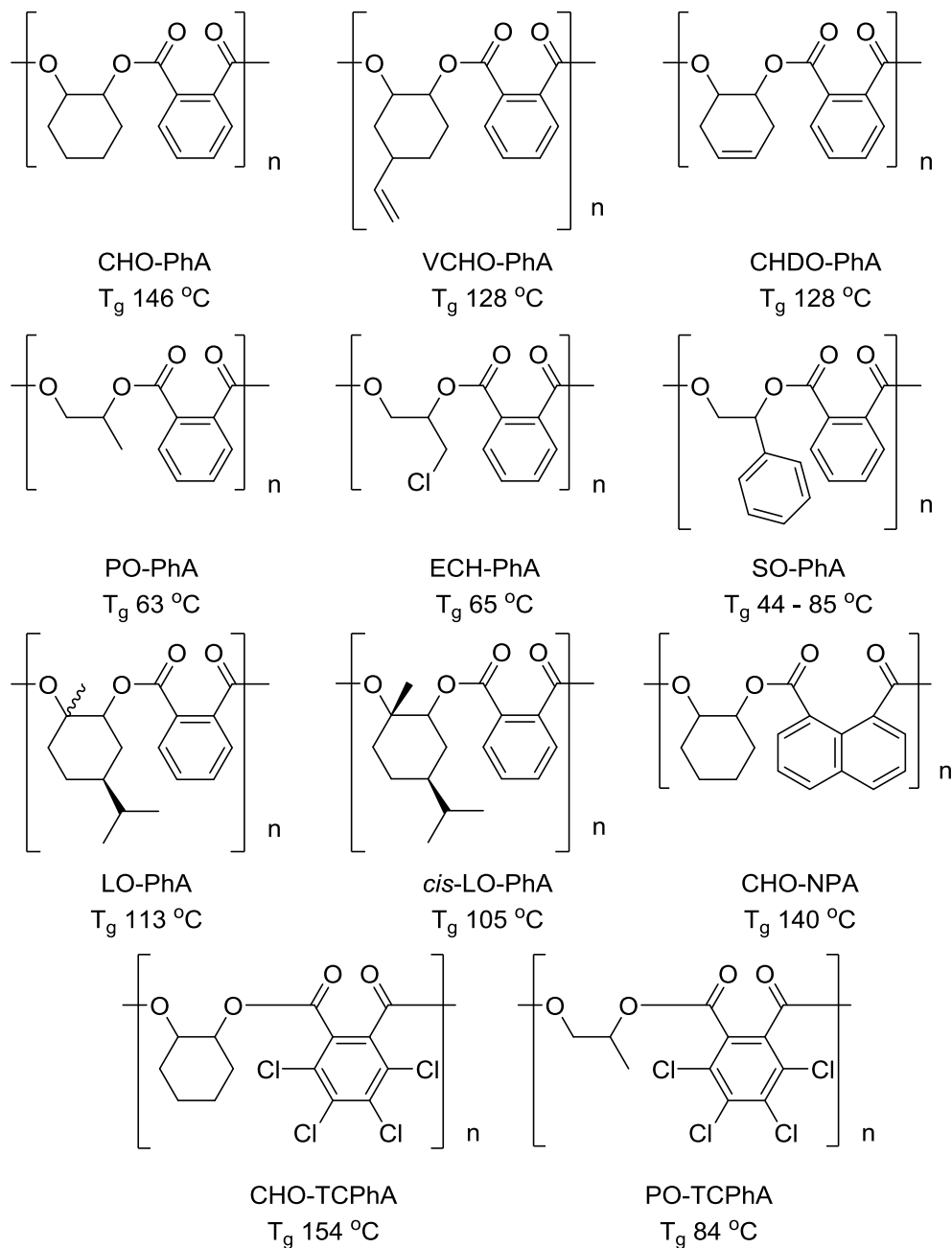


**Figure 6** Copolymers containing aromatic monomers<sup>56–59</sup>

There are far more examples of amorphous polyesters from the ROCOP of epoxides and cyclic anhydrides relative to crystalline examples, and the thermal properties of these polymers has been investigated more thoroughly. In an amorphous plastic the polymer chains are arranged in an irregular manner. These plastics are often softer and have a lower melting point. The temperature at which a polymer changes from a glassy material to a rubbery

### Chapter 3 - Thermal and flame retardant properties of the copolymers

state is the glass transition temperature ( $T_g$ ). Varying the identity of the epoxide and cyclic anhydride monomers can greatly influence the  $T_g$  of the copolymers. The use of monomers containing aromatic groups can produce polymers with higher  $T_g$ , (Figure 6).<sup>52</sup>

Aromaticity in the polymer backbone provides greater thermal stability.<sup>11</sup> PhA copolymerised with cyclohexene oxide (CHO), 4-vinylcyclohexene oxide (VCHO) and cyclohexadiene oxide (CHDO) yielded polyesters with  $T_g$  values of 146 °C, 128 °C and 128 °C respectively.<sup>56,57</sup> Copolymerisation of PhA with PO, (PO–PhA) and epichlorohydrin (ECH), (ECH–PhA) yielded polymers with  $T_g$  values of 63 and 65 °C respectively.<sup>58</sup> Nejad *et al.* showed how the  $T_g$  varied for a series of styrene oxide (SO) and PhA copolymers (SO–PhA).  $T_g$  values of 44 – 70 °C were reported for SO–PhA copolymers with  $M_n$  ranging from 3,600 – 7,100  $\text{gmol}^{-1}$ .<sup>59</sup> Hošťálek and colleagues reported a higher value of 85 °C for a SO–PhA copolymer with a  $M_n$  of 13,500  $\text{gmol}^{-1}$ .<sup>58</sup> These differing values for the SO–PhA copolymers show how  $T_g$  increases with molecular weight. The copolymerisation of limonene oxide (LO) with PhA produced a copolymer of relatively low molecular weight ( $M_n = 5,100 \text{ gmol}^{-1}$ ), but despite this, a relatively high  $T_g$  of 113 °C was measured. Higher  $T_g$  values may be achieved if a LO–PhA copolymer of greater molecular weight was synthesised. The *cis*-isomer of LO was also utilised in a copolymerisation with PhA. The copolymer generated had a very low molecular weight ( $M_n = 2000 \text{ gmol}^{-1}$ ) but still a relatively high  $T_g$  of 105 °C.<sup>58</sup>

Hošťálek and co-workers investigated the use of TCPhA as a monomer in the ROCOP of epoxides and cyclic anhydrides. The inclusion of the chlorine atoms in the polymer chain caused an increase in the  $T_g$  compared to copolymers with PhA.  $T_g$  values of 154 °C and 84 °C were recorded for CHO–TCPhA and PO–TCPhA respectively, these values are much higher than the PhA containing congeners.<sup>58</sup>

Higher  $T_g$  values can be achieved by utilising monomers with greater aromaticity. The larger ring system in naphthalic anhydride (NPA) gives rise to polymers with a more rigid backbone and improved thermal properties. A  $T_g$

### Chapter 3 - Thermal and flame retardant properties of the copolymers

of 140 °C was recorded for CHO–NPA. This copolymer had a  $T_g$ , 10 degrees higher than the PhA analogue.<sup>58</sup>

Restricting the rotational freedom in the backbone of polymer chains increases the  $T_g$  of a polymer. Decreasing the flexibility of polymer means that chains cannot readily move past one another. Evidence of this is the higher  $T_g$  values of CHO–PhA and VCHO–PhA (146 °C and 128 °C respectively) compared to PO–PhA and ECH–PhA (63 °C and 65 °C respectively).<sup>56–58</sup> The use of the bicyclic anhydrides CHO or VCHO prevents free rotation of the O–C–C–O bond in the polymer chain.

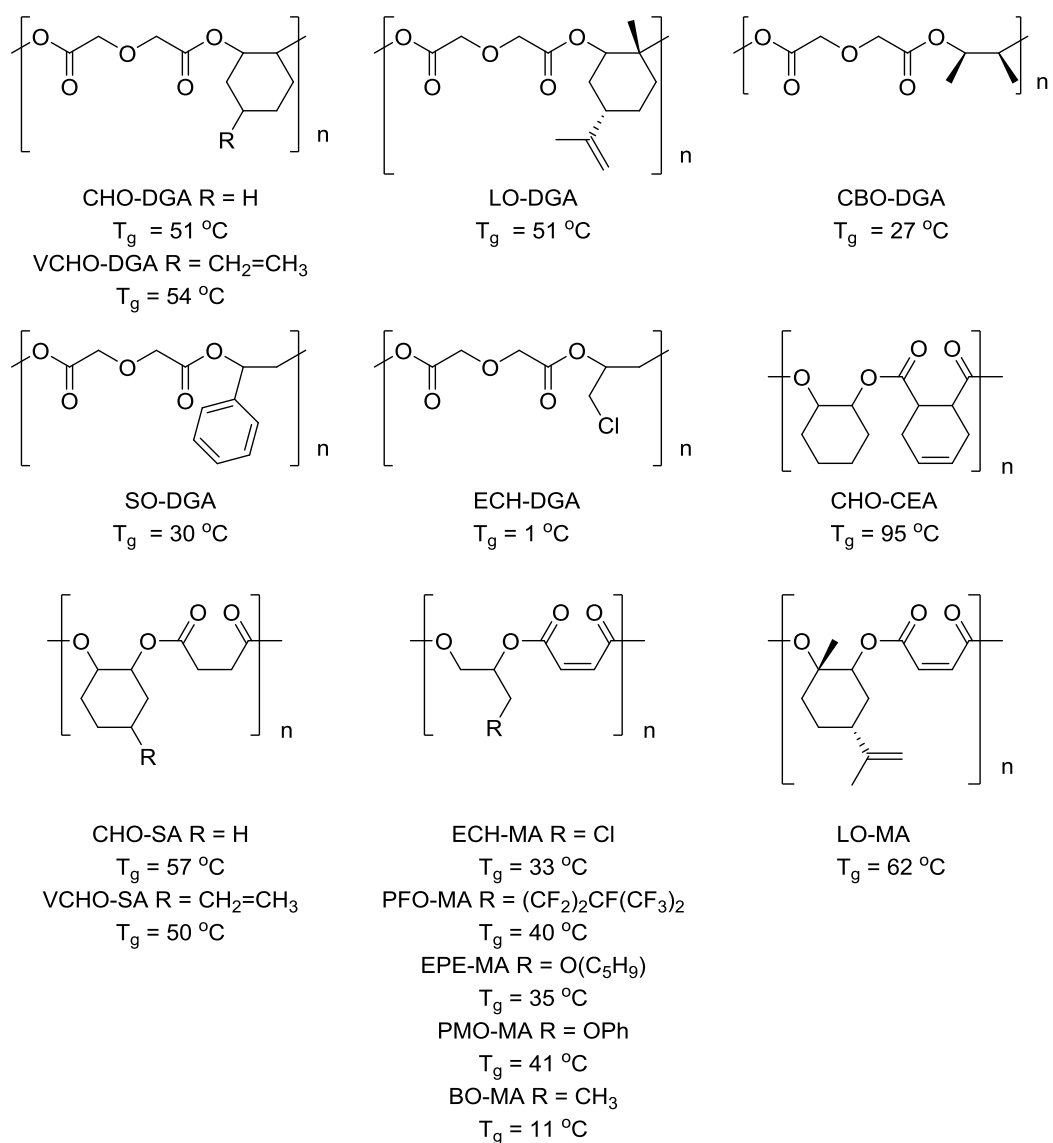


**Figure 7** Glass transition temperatures ( $T_g$ ) of aliphatic polyesters<sup>58,60–62</sup>

### **Chapter 3 - Thermal and flame retardant properties of the copolymers**

A number of other different monomer combinations have been explored which give aliphatic polyesters (Figure 7). The combination of succinic anhydride (SA) with CHO and VCHO produced polymers with  $T_g$  values of 57 °C and 50 °C respectively. This shows that the addition of the pendant vinyl group from VCHO causes a slight decrease in  $T_g$ , the same effect was observed for the PhA analogues (Figure 6). Diglycolic anhydride (DGA) formed copolymers with the epoxides, CHO, VCHO, LO, ECH, SO and *cis*-butene oxide (CBO). The  $T_g$ s of these polyesters ranged from 1 °C to 54 °C.<sup>58,60</sup> The copolymerisation of CHO and cyclohexene anhydride (CEA) produced a copolymer with a  $T_g$  of 95 °C.<sup>61</sup> Perfluoroisopentylpropylene oxide (PFO), epoxypropyl tetrahydropyranyl ether (EPE), (phenyloxymethyl)oxirane (PMO), 1-butene oxide (BO), LO and ECH were copolymerised with MA yielding polyesters with  $T_g$  values between 33 – 62 °C.<sup>60,62</sup> These aliphatic polyesters are shown in Figure 7.

A route to high  $T_g$  aliphatic polyesters is to use tricyclic monomers. Terpene-based anhydrides were used in conjunction with PO to produce copolymers with  $T_g$  values up to 109 °C. The tricyclic anhydrides were synthesised from MA through a Diels-Alder reaction with monoterpene dienes. As terpenes are an abundant and sustainable chemical feedstock, these copolymerisations formed partially renewable polyesters.<sup>63,64</sup> The reaction of the tricyclic monomer norbornene anhydride (NA) and CHO yielded polymers with  $T_g$  between 111 and 130 °C.<sup>65</sup>



### Chapter 3 - Thermal and flame retardant properties of the copolymers

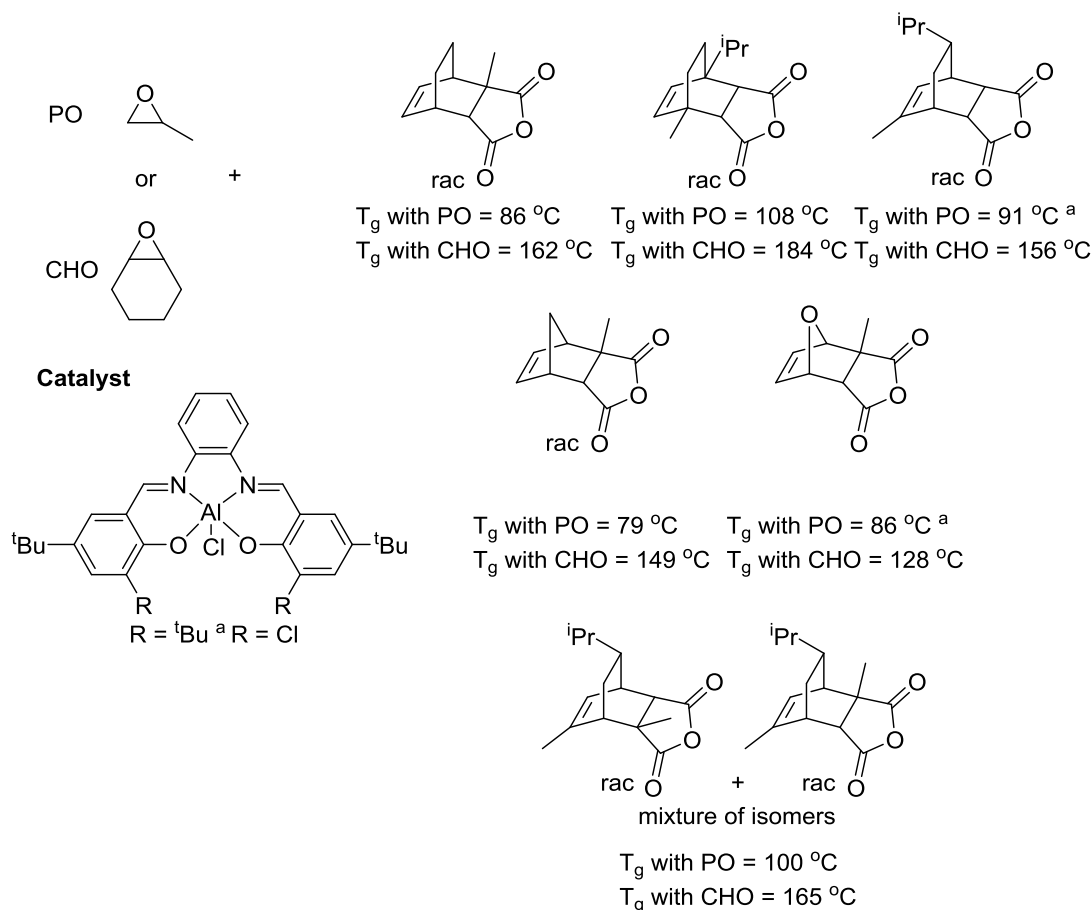


**Figure 8** Copolymers formed from the reaction of tricyclic anhydrides with CHO and PO<sup>66</sup>

Coates and co-workers undertook a detailed study utilising sustainably synthesised tricyclic anhydrides with the epoxides PO and CHO to produce high  $T_g$  aliphatic polyesters (Figure 8). Changing the identity of the epoxide monomer significantly affected the  $T_g$  of the plastics generated; copolymers with CHO gave much higher  $T_g$  values (124 °C – 184 °C) than those with PO (66 °C – 108 °C).<sup>66</sup>

### Chapter 3 - Thermal and flame retardant properties of the copolymers

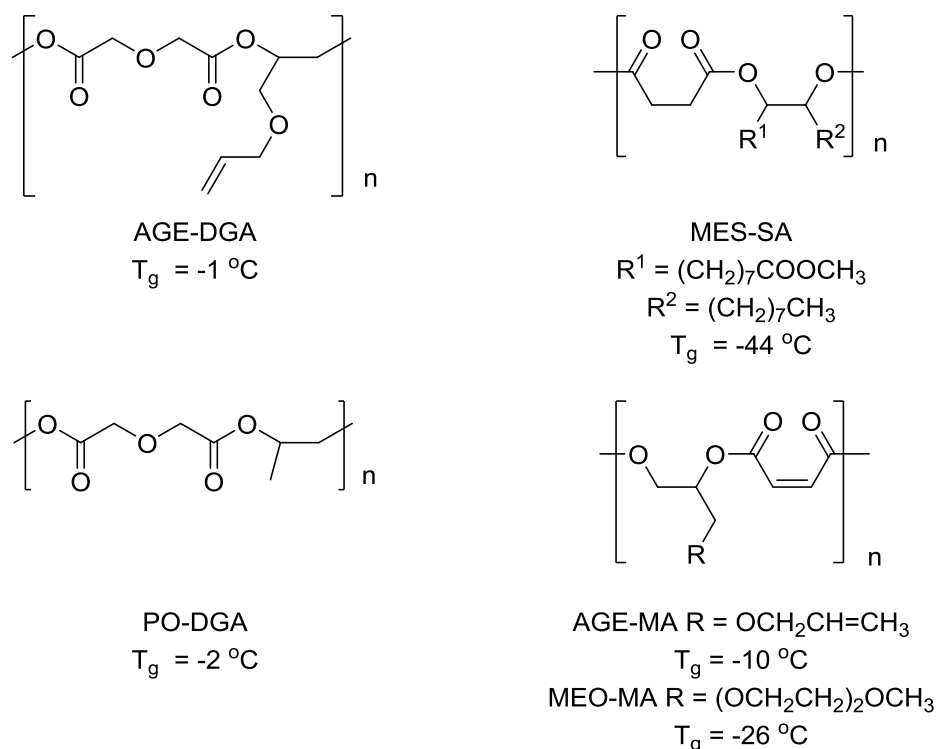


**Figure 9** Copolymers with low  $T_g$ s<sup>56,60,62,67</sup>

Plastics with low  $T_g$  values are also useful for some specific applications such as in elastomers.<sup>11</sup> Polymers with flexible backbones or long side chains tend to have lower  $T_g$ s (Figure 9). Lui *et al.* reported the copolymerisation of DGA and allyl glycidyl ether (AGE) yielding a polymer with a  $T_g$  of  $-1\text{ }^{\circ}\text{C}$ .<sup>56</sup> A  $T_g$  of  $-44\text{ }^{\circ}\text{C}$  was recorded for the copolymer synthesised from methyl-9,10-epoxystearate (MES) and SA copolymer.<sup>67</sup> The copolymerisation of PO and DGA yielded a polyester with a  $T_g$  of  $-2\text{ }^{\circ}\text{C}$ .<sup>60</sup> DiCiccio and Coates reported the synthesis of polymers with low  $T_g$  values by reacting MA with AGE and 2-[2-(2-methoxyethoxy)ethoxy]methyl oxirane (MEO). The reaction of MA with AGE gave a polymer with a  $T_g$  of  $-10\text{ }^{\circ}\text{C}$ , whilst with MEO the  $T_g$  of the copolymer formed was  $-26\text{ }^{\circ}\text{C}$ .<sup>62</sup> The low  $T_g$  polymers shown in Figure 9 have flexible backbones and long flexible side chains which prevent efficient packing of polymer chains reducing thermal stability.<sup>11</sup>

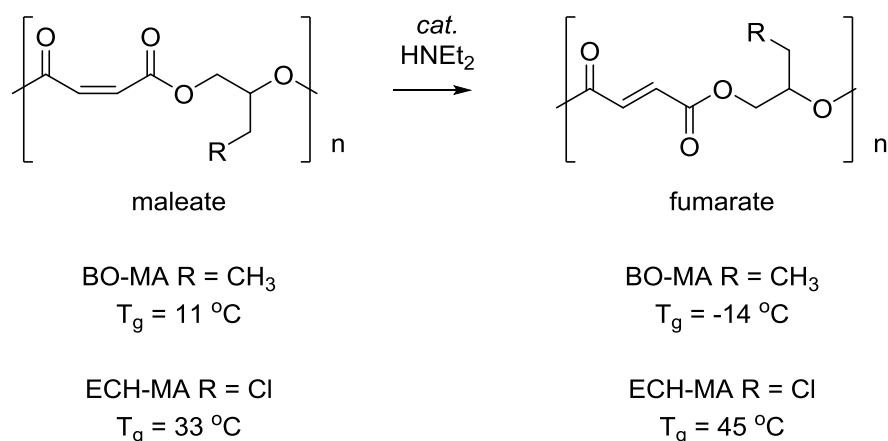


**Figure 10** The effect of isomerisation on the T<sub>g</sub> of MA containing copolymers<sup>62</sup>

The work by DiCiccio and Coates also showed how the properties of a polymer may be altered by isomerisation (Figure 10). A series of MA copolymers were synthesised and the effect on T<sub>g</sub> of changing between the cis/trans isomer of the double bond in the polymer backbone was explored. The isomerisation was catalysed by diethyl amine. Changing from the maleate (cis) to the fumarate (trans) isomer altered the T<sub>g</sub> of the polymers, however the effect varied for different examples. For most of the copolymers, the isomerisation caused an increase in T<sub>g</sub>. The polymers synthesised from ECH, PFO and PMO saw an elevation of 9 – 13 °C. For the examples with EPE and AGE, the increase was very small (1°C and 4 °C respectively). The most drastic change following isomerisation to the fumarate was observed for the BO copolymer, where the T<sub>g</sub> decreased from 11 °C to -14 °C. For the copolymer MEO–MA, a more modest decrease of 3 °C was observed. Figure 10 shows the isomerisation can have a considerably different effect upon two very similar polymers. The only difference between BO–MA and ECH–MA is a methyl group as opposed to a chlorine, yet the transformation caused a decrease of 25 °C for the BO example and an increase of 12 °C for the ECH copolymer.<sup>62</sup>

The copolymerisation of racemic PO and SA<sup>61</sup> gave a polymer with very different thermal properties compared to when enantiopure PO was used in the polymerisation.<sup>55</sup> Racemic PO gave a polyester with a very low T<sub>g</sub> value of -39 °C, whereas the isotactic polymer has a T<sub>g</sub> of -4 °C. These examples illustrate the effect polymer stereochemistry has on thermal properties.

### Chapter 3 - Thermal and flame retardant properties of the copolymers

Williams and colleagues showed how multiblock copolymers can be used to tune the thermal properties of polymers (Figure 11). Varying the relative amounts of the poly(cyclohexylene phthalate) (CHO–PhA) and poly(decylactone) (PDL) blocks, the  $T_g$  values could be varied from  $-58 - 97\text{ }^{\circ}\text{C}$ . The homopolymers of CHO – PhA and PDL had  $T_g$  values of  $97\text{ }^{\circ}\text{C}$  and  $-58\text{ }^{\circ}\text{C}$  respectively. A tri-block polymer containing 33% CHO–PhA had a  $T_g$  of  $-49\text{ }^{\circ}\text{C}$ , while an example with 81 % CHO–PhA had a  $T_g$  of  $55\text{ }^{\circ}\text{C}$ . When the relative proportions of each block were more even, quite different thermal properties were achieved. When the polymer contained 42% CHO–PhA two  $T_g$  values were observed ( $-49\text{ }^{\circ}\text{C}$  and  $57\text{ }^{\circ}\text{C}$ ). In order to prove that this outcome was the result of the generation of a tri-block copolymer, the  $T_g$  of a blend of the two homopolymers was also measured. The polymer blend showed identical  $T_g$  values to the homopolymers. The presence of two  $T_g$ s indicates that microphase separation of the polymer blocks has occurred.<sup>68</sup>

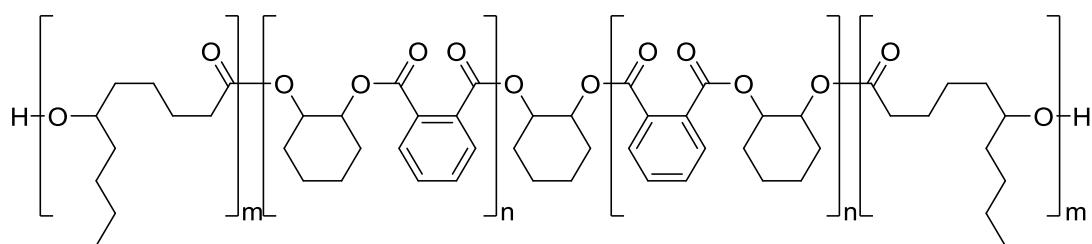
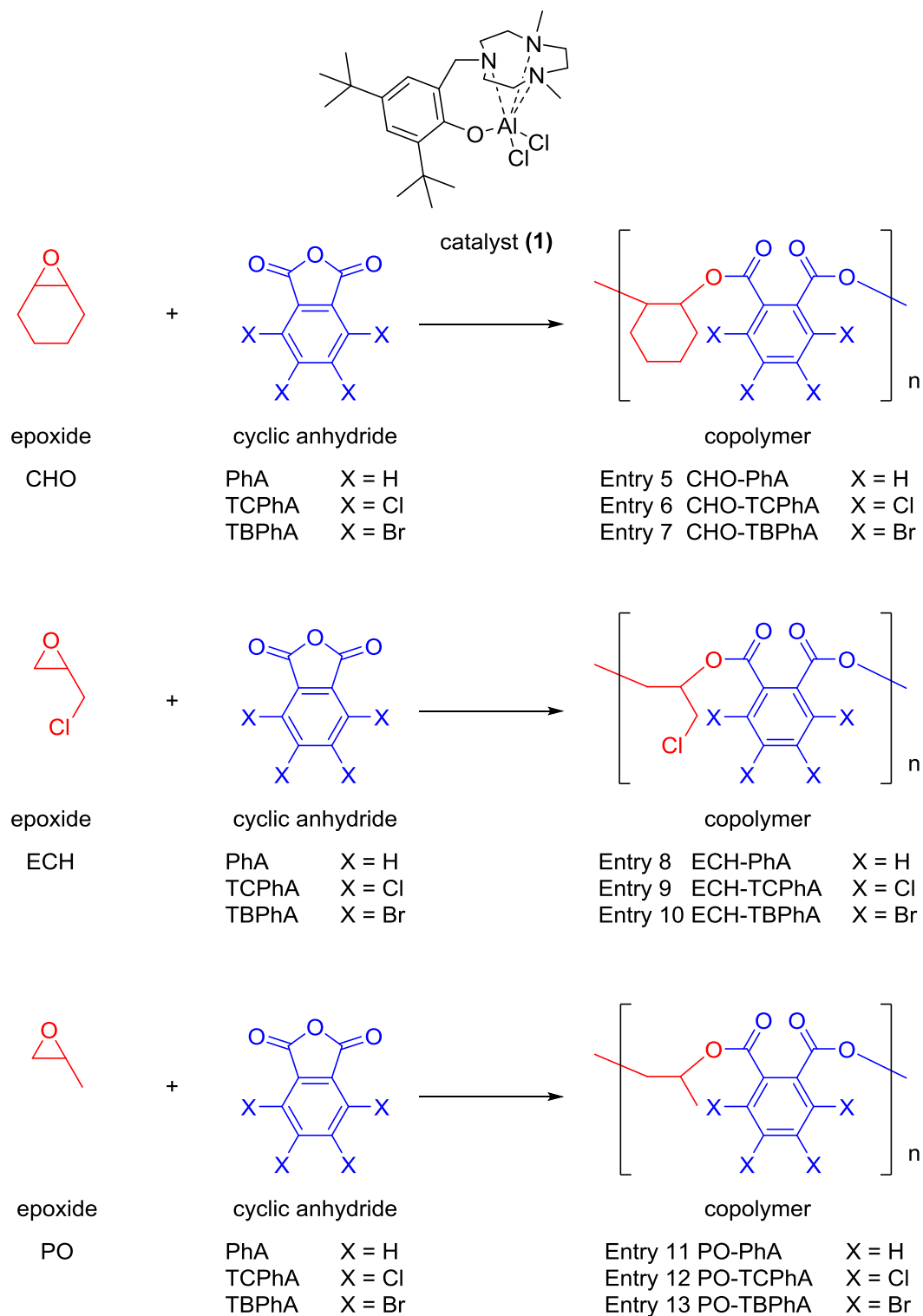


**Figure 11** Block polyester from the ring-opening copolymerisation (ROCOP) of PhA and CHO and the ring-opening polymerisation (ROP) of  $\epsilon$ -DL<sup>68</sup>

**3.4 Flame retardancy analysis of epoxide and anhydride copolymers**



**Scheme 4** ROCOP of PhA, TcPhA and TBPhA with CHO, ECH and PO

In order to introduce flame retardancy into the polyesters synthesised by the ROCOP reaction, the cyclic anhydrides TcPhA and TBPhA were selected as monomers and copolymerised with the epoxides CHO, ECH and PO. It was

### **Chapter 3 - Thermal and flame retardant properties of the copolymers**

reasoned that the high halogen content of TCPPhA and TBPhA would impart fire resistance to the polyesters. CHO, ECH and PO were also combined with PhA to provide flame retardant free analogues to act as control samples for comparison with the TCPPhA and TBPhA copolymers. These ROCOP reactions are summarised in Scheme 4.

The synthesis of the copolymers (entries 5 – 13 Table 2, Chapter 2.3.3) was catalysed by the novel homogeneous catalyst  $[Al(L1)Cl_2]$  (**1**), as described in Chapter 2. The polymerisations were carried out with toluene as a solvent, the full experimental procedure employed in the synthesis of these polyesters is detailed in the experimental (Chapter 7.2). The ester selectivity, the polymer molecular weights and the polymer dispersities ( $\bar{D}$ ) are shown in Table 2 (Chapter 2.3.3). The polymers produced all had very high ester selectivity indicating the polymer chains comprised of highly alternating monomer units. All of the polyesters were isolated in good to excellent yields. The  $M_n$  of the polymers ranged from moderate to good and all except entry 7 which has a higher  $\bar{D}$  value of 2.02, had low  $\bar{D}$  between 1.03 – 1.33.

A preliminary screening of the flame retardancy introduced by utilising the TCPPhA and TBPhA monomers was carried out by measuring the limiting oxygen indices (LOIs) of the plastics. This work was carried out in collaboration with Prof Baljinder Kandola and Chen Zhou from the University of Bolton. Raw data was recorded by Chen Zhou. For this study, the copolymers of PhA, TCPPhA and TBPhA with CHO were selected. CHO–PhA (entry 5) was chosen as a control sample as it does not contain the flame retardant halogen. The copolymers with CHO were expected to exhibit greater flammability than those synthesised from the other epoxides (ECH and PO), as the inclusion of CHO gives the greatest proportion of carbon and hydrogen atoms in the polymers, which act as fuel when a material burns.

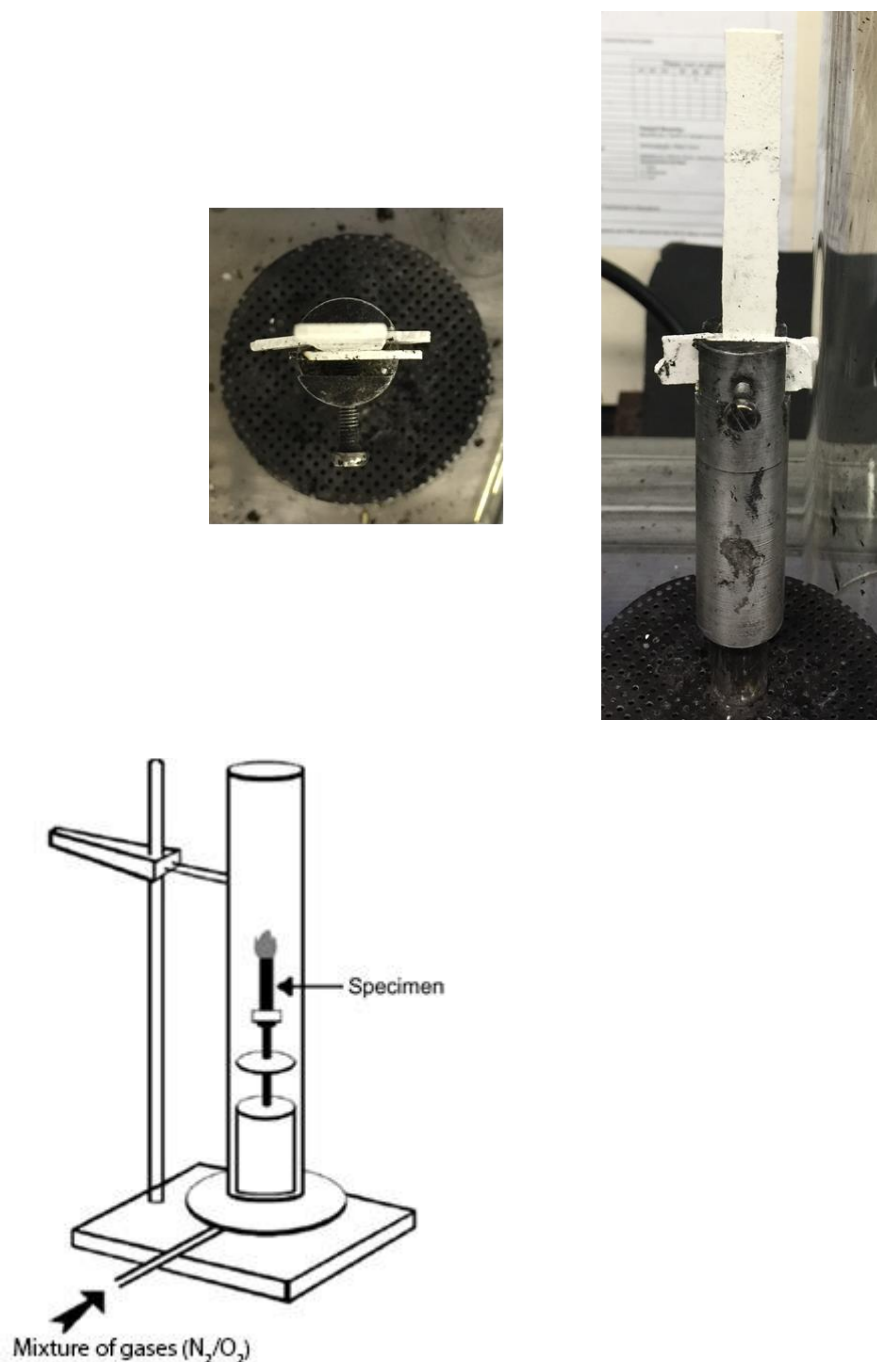


**Figure 12** Experimental setup for LOI measurements<sup>69</sup>

The LOI of a polymer is the percentage atmospheric oxygen required to sustain a flame. If oxygen levels greater than the atmospheric oxygen level in air (20.95% at sea level) are required to sustain a flame then the material is flame retardant. For the control sample CHO-PhA (entry 5), an LOI of 20.2% was recorded, which as expected indicates that the plastic will sustain a burn in air under normal conditions. The experimental details for the LOI measurements are given in the experimental, (Chapter 7.1). Figure 12 is an

### **Chapter 3 - Thermal and flame retardant properties of the copolymers**

image showing the experimental setup. The strips of copolymer (Chapter 7.14) were clamped vertically and the flame applied to the end of the strip to initiate burning. In order to prevent breakage of the brittle strips of plastic when clamped, extra small strips were placed at the base to increase the thickness at the clamping point. This extra material does not affect the LOI test as the flame does not come into contact with this section. The introduction of TCPhA and TBPhA (entries 6 and 7) saw an increase in the LOI compared to CHO-PhA, recording values of 21.4% and 53.9% respectively indicating that flame retardancy had been introduced.

The introduction of TCPhA saw only a modest increase in the LOI compared to CHO-PhA. An LOI greater than 20.95% confirms flame retardancy had been achieved but a higher value was expected. This result suggests only a limited degree of fire resistance had been introduced.

The introduction of TBPhA had a much greater effect on the LOI than the inclusion of TCPhA. The LOI value of 53.9% indicates that the material is highly flame retardant. At high oxygen levels, shining and flashing of the flame was observed as the material burned.

In certain circumstances, materials may be utilised in environments with higher O<sub>2</sub> levels such as in aircraft, submarines, spacecraft *etc.* For such applications flame retardant plastics are required which show high LOI. However in these circumstances the introduction of flame retardancy through the use of additives is problematic, as leaching of these chemicals into the enclosed environments may cause serious health problems,<sup>70</sup> therefore highly flame retardant, single component polymers would be highly suited for these applications.

While LOI testing is an effective screening technique providing an insight into a polymers flame retardancy it does not provide a rigorous assessment of fire properties. In the LOI testing carried out on entries 5 – 7, variation in the density of the polymer strips caused by differences in the degree of compression achieved when the polymers were pressed into sheets will affect fire performance. The methods used to process a polymer will effect flame



retardancy, for example different results would be recorded if a polymer was injection moulded or 3D printed.<sup>71</sup>

### 3.4.1 Pyrolysis combustion flow calorimetry (PCFC) analysis

Detailed combustion analysis on all of the nine copolymers (entries 5 – 13) was obtained by pyrolysis combustion flow calorimetry (PCFC). This work was carried out in collaboration with Prof Baljinder Kandola and Chen Zhou from the University of Bolton. Raw data was recorded by Chen Zhou. The method is a very useful technique for studying the flammability of plastics on a small (mg) scale. The characteristic data provided by PCFC is the peak of heat release rate (PHRR, W/g), heat release capacity (HRC, J/g.K), total heat release (THR, kJ/g) and temperature at peak release rate ( $T_{\max}$ , °C). The PCFC data for the copolymers (5 – 13) are shown in Table 3.

**Table 3** Pyrolysis combustion flow calorimetry (PCFC) data of copolymers

entry	Epoxide	anhydride	HRC (J/g.K)	THR (kJ/g)	$T_{\max}$ (°C)	$P_b$
5	CHO	PhA	616±12	25.0±0.8	354±0	0.975
6	CHO	TCPhA	408±18	16.0±0.2	335±0	0.0668
7	CHO	TBPhA	211±8	7.9±0.4	322±1	1.83x10 <sup>-4</sup>
8	ECH	PhA	403±21	16.7±1.1	348±2	0.0580
9	ECH	TCPhA	208±39	11.7±2.0	355±1	1.67x10 <sup>-4</sup>
10	ECH	TBPhA	128±11	6.9±0.4	342±2	1.48x10 <sup>-5</sup>
11	PO	PhA	548±36	24.7±1.8	361±1	0.833
12	PO	TCPhA	216±13	11.9±0.4	359±1	2.13x10 <sup>-4</sup>
13	PO	TBPhA	141±1	6.8±0.1	351±1	2.19x10 <sup>-5</sup>

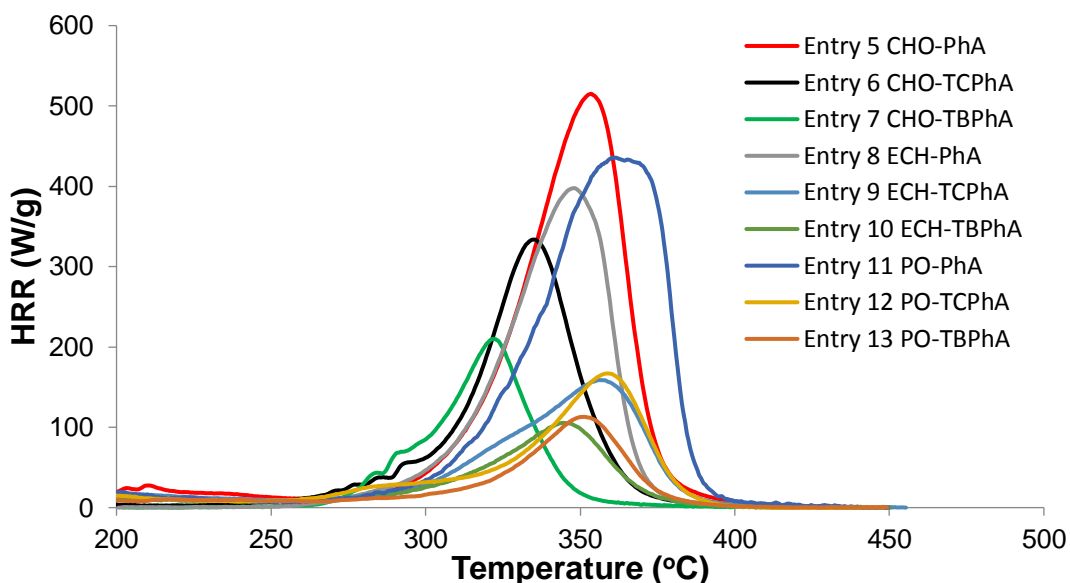


**Figure 13** Pyrolysis combustion flow calorimetry (PCFC) measurements of epoxide and anhydride copolymers showing heat release rate (HRR) versus temperature

The heat release capacity (HRC) of the copolymers is an extremely important factor in determining the flame retardancy of a material. The HRC is thought of as the intrinsic flammability parameter of a material because it is independent of heating rate. The HRC is equal to the PHRR / heating rate. In simple terms, the HRC is the amount of energy released by a substance as it burns. Figure 13 shows how the heat release rate (HRR, W/g) of the polymers varied with temperature. It also illustrates how the THR and  $T_{\max}$  vary for the different copolymers.

As expected, the HRC of the control samples 5 and 11 were relatively high due to the lack of flame retardant monomers and the high levels of carbon and hydrogen. CHO-PhA (entry 5) gave a HRC value of 616 J/g.K and a value of 548 J/g.K was recorded for PO-PhA (entry 11). The lower HRC for the copolymer with PO is most likely due to the lower proportion of carbon and hydrogen compared to the CHO analogue. For comparison the HRC of the commonly used plastic polyethylene is 1,676 J/g.K and the well-established biodegradable plastic poly(caprolactone) is 526 J/g.K. ECH-PhA (entry 8) shows a great deal more flame retardancy and lower HRC (403 J/g.K) than the other control samples. The only difference between the PO-PhA and

### Chapter 3 - Thermal and flame retardant properties of the copolymers

ECH–PhA copolymers is the additional chlorine from the ECH monomer. The presence of one chlorine in the polymer repeat unit caused a decrease in the HRC of 145 J/g.K. This is a clear indication of the flame retardancy imparted by a single chlorine. This trend of increasing HRC with epoxide of  $\text{ECH} < \text{PO} < \text{CHO}$  is also present for the TBPhA copolymers. For the copolymers of TCPPhA, the HRC's of the ECH and PO examples are equal within experimental error and the greatest HRC was recorded for the CHO copolymer. A plot of HRR against temperature for the three control samples containing PhA is shown in Figure 14.

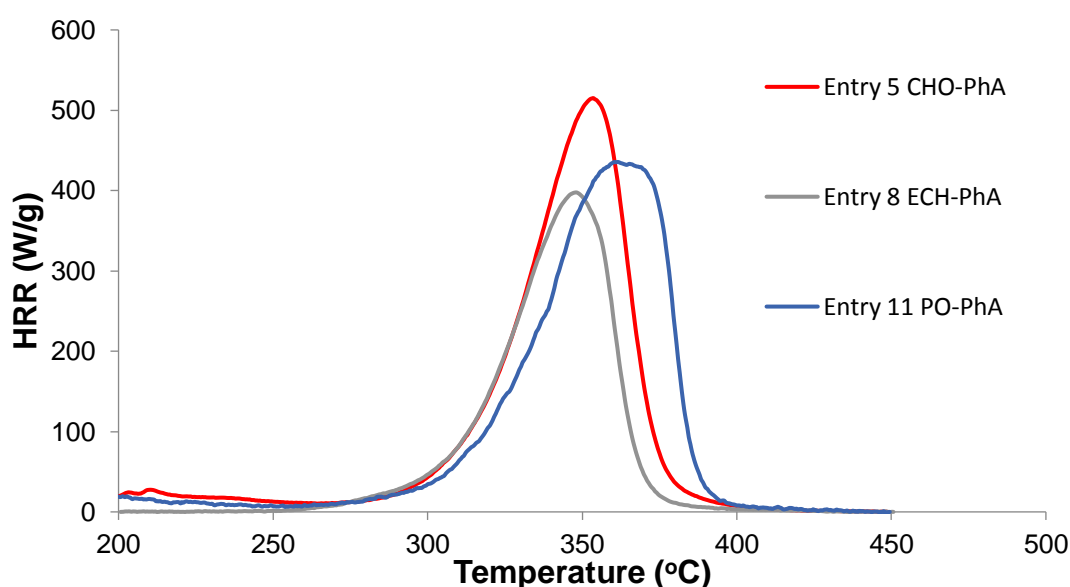


**Figure 14** Pyrolysis combustion flow calorimetry (PCFC) measurements of PhA copolymers showing heat release rate (HRR) versus temperature

The THR for the PhA copolymers shows a similar trend to HRC with CHO–PhA (entry 5) and PO–PhA (entry 11) recording high THR values (25.0 and 24.7 kJ/g respectively) and ECH–PhA (entry 8) exhibiting a significantly lower value (16.7 kJ/g). This result again highlights the effect of the ECH chlorine increasing flame retardancy.

PO–PhA (entry 11) has the highest  $T_{\text{max}}$  of the copolymers containing PhA. The value for this example is 361 °C compared to 354 °C and 348 °C for CHO–PhA (entry 5) and ECH–PhA (entry 8) respectively. A higher  $T_{\text{max}}$  is an advantageous property that contributes towards the fire retardancy of a

material, with a higher value indicating greater resistance to thermal degradation or pyrolysis.

The TCPPhA copolymers all showed significantly lower HRC values and greater flame retardancy than their PhA analogues. CHO–TCPPhA, ECH–TCPPhA and PO–TCPPhA (entries 6, 9 and 12) have HRC values of 408, 208 and 216 J/g.K respectively. The reduction in the HRC upon changing from PhA to TCPPhA was 208 J/g.K for the CHO copolymer, 195 J/g.K for ECH and 332 J/g.K for PO. The PO copolymers showed the greatest reduction following the substitution to TCPPhA. As expected the HRC values correlate to the chlorine content, as the HRC decreases from CHO–TCPPhA to PO–TCPPhA and to ECH–TCPPhA, the % wt. chlorine increases from 37% to 41% to 47%. A plot of HRR against temperature for the samples containing TCPPhA is shown in Figure 15.

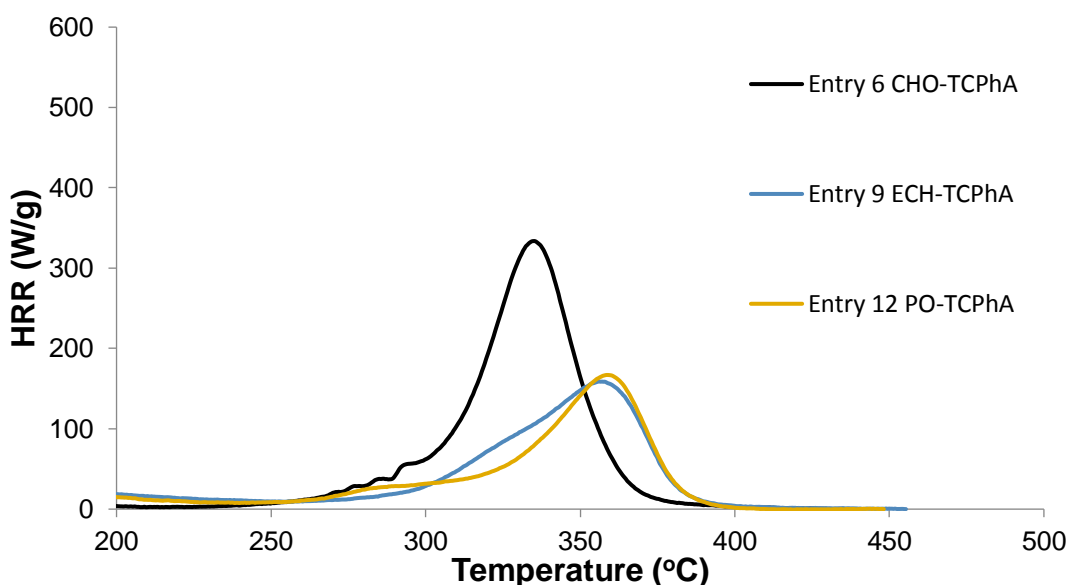


**Figure 15** Pyrolysis combustion flow calorimetry (PCFC) measurements of TCPPhA copolymers showing heat release rate (HRR) versus temperature

The THR of all the copolymers with TCPPhA decreased compared to the PhA analogues. The values measured for CHO–TCPPhA, ECH–TCPPhA and PO–TCPPhA (entries 6, 9 and 12) were 16.0, 11.7 and 11.9 kJ/g respectively. The THR of CHO–TCPPhA was significantly greater than the ECH and PO containing examples, showing a different trend to PhA containing copolymers.

### Chapter 3 - Thermal and flame retardant properties of the copolymers

A similar trend to the THR is present for the  $T_{\max}$  values of the TcPhA copolymers. The  $T_{\max}$  for CHO–TcPhA (entry 5) is 335 °C, much lower than the values recorded for ECH–TcPhA and PO–TcPhA (entry 9, 355 °C and entry 12, 359 °C respectively). In the PhA copolymers, the example with the lowest  $T_{\max}$  was ECH–PhA, whereas for the TcPhA polymers CHO–TcPhA has by far the lowest  $T_{\max}$ .

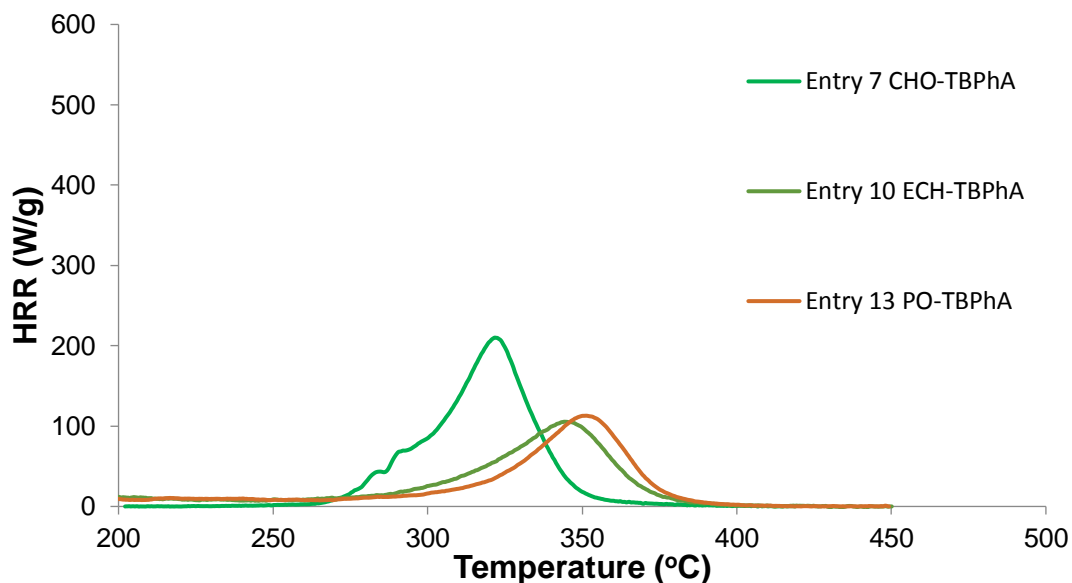


**Figure 16** Pyrolysis combustion flow calorimetry (PCFC) measurements of TBPhA copolymers showing heat release rate (HRR) versus temperature

The copolymers containing TBPhA all showed improved flame retardancy and low HRC values. For each of the epoxides used in the experiments, the lowest HRC was achieved for the copolymer containing TBPhA. For CHO–TBPhA (entry 7), ECH–TBPhA (entry 10), PO–TBPhA (entry 13) HRC values of 211, 128 and 141 J/g.K respectively were recorded. In all cases, there was a significant improvement in flame retardancy for the TBPhA compared to TcPhA examples. A plot of HRR against temperature for the samples containing TBPhA is shown in Figure 16. Changing the anhydride from TcPhA to TBPhA in the CHO copolymers saw a reduction in the HRC by 197 J/g.K. For the ECH copolymers, the HRC decreased by 80 J/g.K and for PO copolymers the reduction was 75 J/g.K. The lowest HRC value was found for the ECH copolymer with the HRC increasing for PO–TBPhA and again for CHO–TBPhA. This does not correlate with the %wt. bromine where

### Chapter 3 - Thermal and flame retardant properties of the copolymers

PO-TBPhA < ECH-TBPhA  $\approx$  CHO-TBPhA. Looking only at %wt. bromine doesn't take into account of the additional chlorine present in ECH and when this is included in the increase in %wt. halogen, this does correlate to the trend of decreasing HRC where ECH-TBPhA < PO-TBPhA < CHO-TBPhA.

The THR decreased further when the epoxides were copolymerised with TBPhA. As with the TCPhA, CHO-TBPhA had a higher THR than the ECH and PO analogues, which have THR values that are the same within experimental error. For CHO-TBPhA (entry 7), ECH-TBPhA (entry 10) and PO-TBPhA (entry 13), THR values of 7.9, 6.9 and 6.8 kJ/g were recorded respectively.

As with the TCPhA copolymers, CHO-TBPhA has the lowest  $T_{\max}$  value. CHO-TBPhA (entry 7) has a  $T_{\max}$  of 322 °C as opposed to ECH-TBPhA (entry 10) and PO-TBPhA (entry 13) which have the higher  $T_{\max}$  values of 342 °C and 351 °C respectively. In the examples with the halogenated monomers TCPhA and TBPhA, copolymerisation with CHO caused a significant decrease in the  $T_{\max}$  compared to ECH and PO, indicating a decrease in thermal stability.

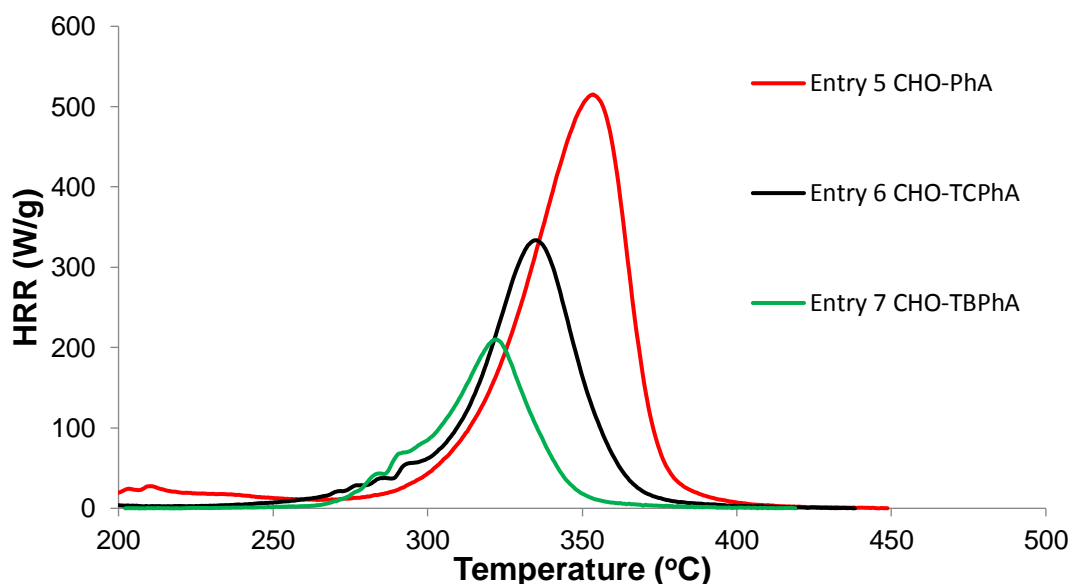


**Figure 17** Pyrolysis combustion flow calorimetry (PCFC) measurements of CHO copolymers showing heat release rate (HRR) versus temperature

In summary, for the copolymers of CHO, ECH and PO a trend of decreasing HRC and THR is observed when the anhydride is changed, with

### **Chapter 3 - Thermal and flame retardant properties of the copolymers**

PhA > TCPPhA > TBPhA. This trend is illustrated in Figure 17 which shows the copolymers of CHO as a representative example. The decrease in HRC and THR indicates an increase in flame retardancy with the most fire resistance observed for the TBPhA copolymers of each epoxide.

The  $T_{\max}$  values for all but one of the polymers decreased as the anhydride was changed from PhA to TCPPhA to TBPhA for each epoxide. This trend is illustrated in Figure 17 showing the CHO copolymers. The example which does not fit this trend is ECH–PhA which has a lower  $T_{\max}$  than ECH–TCPPhA. The results indicate that the inclusion of halogens into the copolymer reduces the  $T_{\max}$ . The inclusion of bromine causes a greater decrease than the introduction of chlorine. This effect is highlighted in the PhA copolymers where the ECH containing sample (which is the only sample with a halogen), has the lowest  $T_{\max}$ , whereas for all of the high halogen content polyesters the copolymer with CHO has the lowest  $T_{\max}$ .

The PCFC results indicate that the inclusion of halogens in the copolymer through the use of TCPPhA and TBPhA monomers significantly increases the flame retardancy of the plastics. Evidence of this is the reduction in the HRC and the THR. ECH–TBPhA and PO–TBPhA had extremely low HRC <150 J/g.K. The disadvantage of utilising the TCPPhA and TBPhA monomers is that the increase in fire resistance was accompanied by a decrease in the  $T_{\max}$  indicating the polymers start to degrade at lower temperatures. However this reduction in  $T_{\max}$  was relatively small, the largest difference in  $T_{\max}$  between a halogenated copolymer compared to the equivalent control sample was 32 °C. It is therefore reasonable to conclude that the significant increase in flame retardancy outweighs the slight decrease in the  $T_{\max}$ .

Every copolymer synthesised in this study has a lower HRC than polyethylene (1676 J/g.K) and all of the copolymers other than the control samples CHO–PhA and PO–PhA have lower HRC and therefore greater flame retardancy than poly(caprolactone) (526 J/g.K). In order for the probability of fire spreading in a material to be approximately zero, the HRC must be <400 J/g.K.<sup>72</sup> The PCFC results indicate that entries 7, 9, 10, 12 and 13 meet the criteria and are therefore extremely flame retardant. Many of the copolymers

### Chapter 3 - Thermal and flame retardant properties of the copolymers

synthesised in this study outperform the flame retardancy introduced into the biodegradable polyester PLA by Wang and colleagues.<sup>41</sup>

$$P_b = \frac{\exp[-15 + \frac{HRC}{33}]}{1 + \exp[-15 + \frac{HRC}{33}]}$$

**Equation 1** Equation relating  $P_b$  and HRC<sup>72</sup>

Using an equation published by Cogen *et al.* shown in Equation 1,<sup>72</sup> the HRC of the copolymers can be related to the decimal probability of a fire spreading in a material ( $P_b$ ). The equation was derived by plotting the probability of flame spread against HRC and mapping the results into a mathematical equation. The  $P_b$  of the copolymers is shown in Table 3. These probabilities are more relatable and understandable than the HRC values alone. CHO–PhA (entry 5) and PO–PhA (entry 11) both have very high  $P_b$ , 0.975 and 0.833 respectively. The other control sample ECH–PhA (entry 8) had a significantly lower  $P_b$  (0.058) showing the flame retarding effect of one chlorine atom in the polymer repeat unit. All of the TCPhA copolymers have low  $P_b$ 's, but the CHO example has a value substantially higher (entry 6, 0.0668) than the ECH and PO analogues (entry 9,  $1.67 \times 10^{-4}$  and entry 12,  $2.13 \times 10^{-4}$  respectively). This indicates how the greater proportion of carbon and hydrogen in the CHO copolymer increases flammability. The  $P_b$  values decrease even further when TBPhA was included in the copolymers. For each epoxide, the lowest  $P_b$  and therefore greatest flame retardancy was found for the TBPhA copolymers. The ECH and PO copolymers had extremely low  $P_b$ 's (entry 10,  $1.48 \times 10^{-5}$  and entry 13,  $2.19 \times 10^{-5}$  respectively) and the CHO example (entry 7) had a slightly higher value of  $1.83 \times 10^{-4}$ . The extremely low probabilities of fire propagation achieved in this study clearly show the excellent flame retardant potential of these copolymers.



**3.4.2 Thermogravimetric analysis (TGA) of the copolymers****Table 4** Thermogravimetric analysis (TGA) analysis of the copolymers

Entry	Sample	Air Atmosphere				
		T <sub>5%</sub> (°C)	T <sub>10%</sub> (°C)	T <sub>50%</sub> (°C)	Residue at 400 °C (%)	Residue at 650 °C (%)
5	CHO–PhA	227	309	343	2.2	0.4
6	CHO–TCPhA	241	274	324	4.3	0.5
7	CHO–TBPhA	301	310	327	5	0.3
8	ECH–PhA	289	309	341	4.4	0.1
9	ECH–TCPhA	205	266	341	9.2	0.5
10	ECH–TBPhA	279	299	335	14.4	0
11	PO–PhA	198	286	351	2.5	0
12	PO–TCPhA	178	236	344	13.5	0.5
13	PO–TBPhA	278	298	334	14.6	0.2
Entry	Sample	N <sub>2</sub> Atmosphere				
		T <sub>5%</sub> (°C)	T <sub>10%</sub> (°C)	T <sub>50%</sub> (°C)	Residue at 400 °C (%)	Residue at 650 °C (%)
5	CHO–PhA	269	312	342	1.2	0.6
6	CHO–TCPhA	240	275	325	4.1	1.2
7	CHO–TBPhA	311	317	332	4.4	0.1
8	ECH–PhA	277	300	337	5.4	3.3
9	ECH–TCPhA	202	262	338	10.2	5.5
10	ECH–TBPhA	279	297	332	14.4	6.4
11	PO–PhA	200	291	354	2.1	1
12	PO–TCPhA	185	245	344	14.7	8.5
13	PO–TBPhA	276	303	345	19.2	8.8

Thermogravimetric analysis (TGA) of the polymers indicate how they degrade with temperature and therefore how they behave in a fire. The TGA of polymer samples 5 – 13 were recorded in both air and nitrogen atmospheres (Table 4). The results in air indicate how the materials will behave under oxidising

conditions. The TGA experiments carried out in nitrogen evaluates thermal decomposition under inert conditions.

The temperature of the main decomposition step is the most important factor as this step corresponds to the largest mass loss from the sample and therefore the greatest amount of volatiles produced. This is characterised by the temperature at 50% mass loss ( $T_{50\%}$ ) (Table 4). All samples had very similar  $T_{50\%}$  values ranging from 324 – 351 °C in air. Interestingly, the examples with PhA gave the highest  $T_{50\%}$  values indicating that the introduction of the flame-retardant monomers TCPPhA and TBPhA slightly decreases the stability of the polymers at high temperatures. The most thermally stable polymer with the highest  $T_{50\%}$  was PO–PhA (entry 11) and least stable was CHO–TBPhA (entry 7). These results correlate well with the PCFC results, the  $T_{\max}$  for the copolymers ranged from 322 – 361 °C and a similar decrease was observed for the TCPPhA and TBPhA compared to the PhA copolymers.

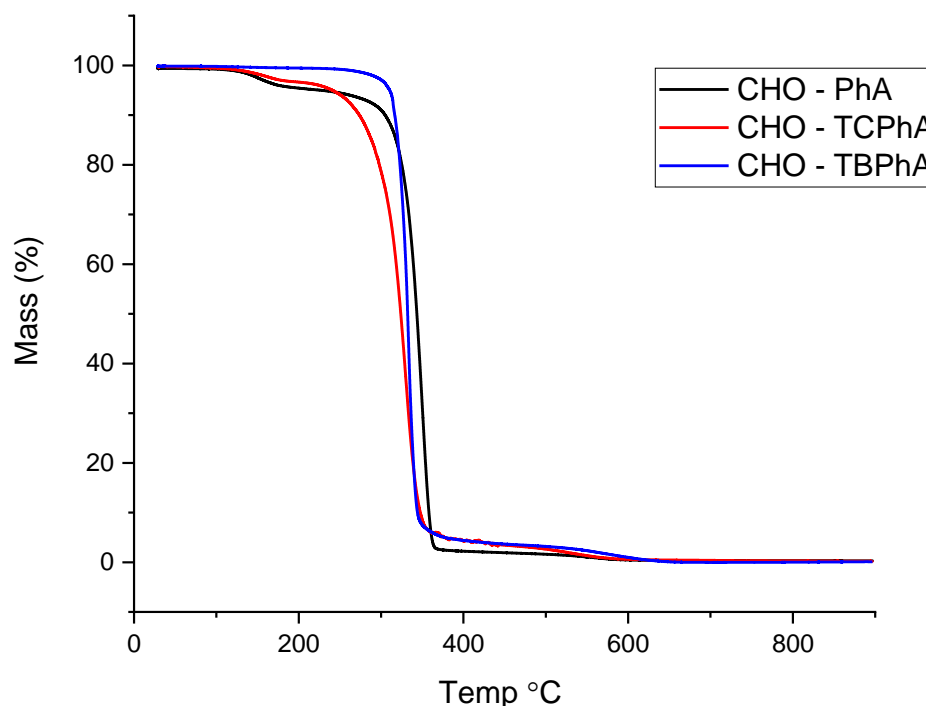


**Figure 18** Thermogravimetric analysis (TGA) graphs of copolymers synthesised from CHO and the anhydrides PhA, TCPPhA and TBPhA in air

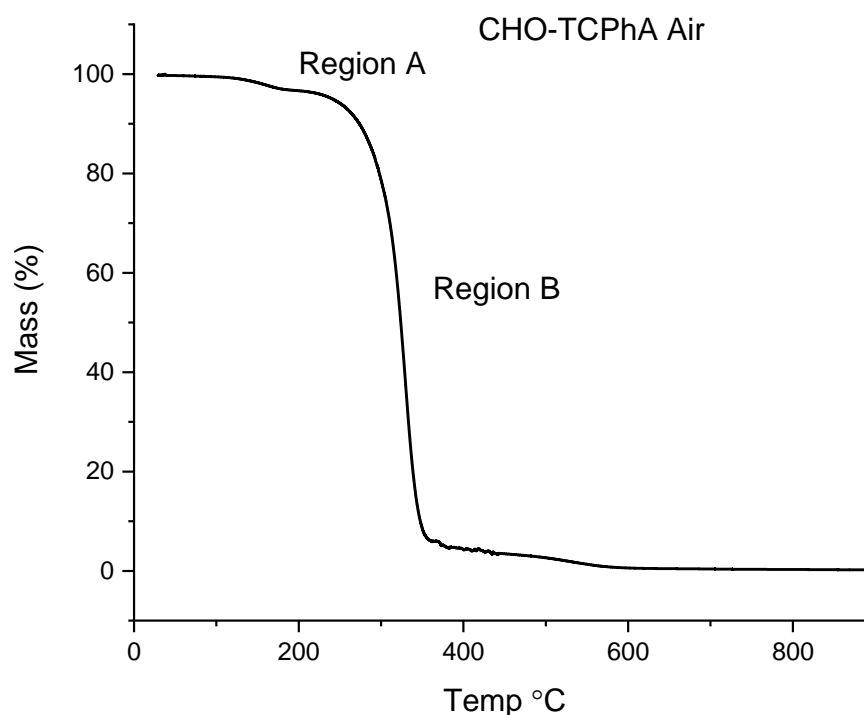


**Figure 19** Thermogravimetric analysis (TGA) of CHO–TCPPhA (entry 6) carried out in air. Region A relates to the initial mass loss at ~35 minutes. Region B relates to the main mass loss ~52 minutes

As can be seen from the TGA graphs, the decomposition of all the polymers is dominated by one main mass loss. In addition to this decomposition, some examples, CHO–PhA, CHO–TCPPhA, ECH–TCPPhA, PO–PhA and PO–TCPPhA (entries 5, 6, 9, 11 and 12) have an initial lower temperature mass loss. The TGA graphs of the CHO copolymers, carried out in air are shown as a representative example in Figure 18. In Figure 18, CHO–TCPPhA and CHO–PhA show an earlier initial mass loss at approximately 150 °C, whereas CHO–TBPhA shows negligible mass loss until temperatures >300 °C. In order to examine whether this early, lower temperature mass loss is polymer degradation, mass spectrometry (MS) was carried out on the gases produced during the TGA run. This allows identification of gaseous species generated during the experiment. The TGA for CHO–TCPPhA in air is shown in Figure 19, the initial mass loss at approximately 35 minutes and the main mass

loss at approximately 52 minutes which correspond to temperatures of 150 °C and 352 °C and are labelled region A and region B respectively.

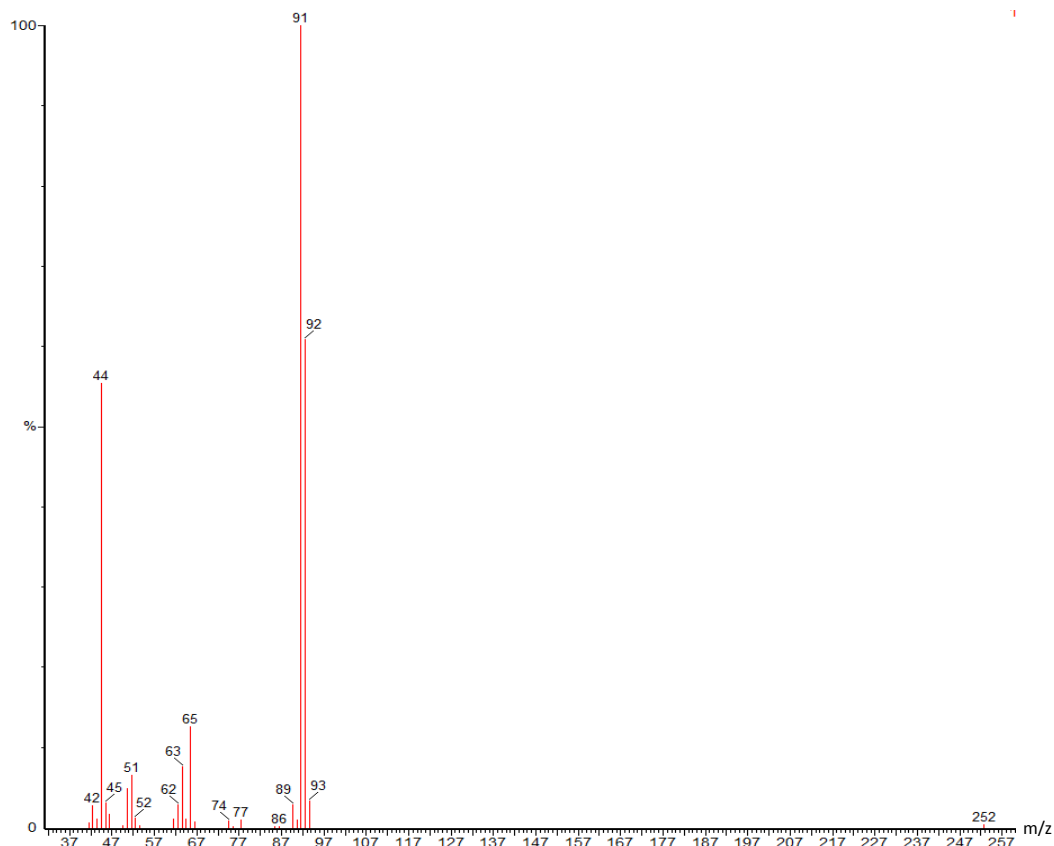


**Figure 20** EI-Mass spectrum of volatiles produced from the thermogravimetric analysis (TGA) of CHO–TcPhA carried out in air at 35 minutes corresponding to a temperature of 150 °C (Region A)

The mass spectrum at 35.5 minutes (Figure 20) was examined in order to gain some understanding of the cause of the initial mass loss in the TGA (Region A, Figure 19). The spectrum shows that the dominant species emitted by CHO–TcPhA (entry 6), when heated to approximately 150 °C in the TGA, is toluene. Toluene has an m/z of 92, which is clearly evident in the spectrum along with a peak at 91 which corresponds to toluene following the loss of a hydrogen. In the synthesis of the copolymers, the reaction between the epoxide and the anhydride was carried out with toluene as a solvent. Considerable effort was undertaken to dry the polymers and remove all solvents, including heating under vacuum, however this result indicates that solvent removal was not completely successful. Polymers are well known to absorb solvent in a process known as swelling. Solvent molecules can become

### **Chapter 3 - Thermal and flame retardant properties of the copolymers**

trapped in the pores of a polymer matrix or bound to polymers by non-covalent interactions.<sup>73</sup> As the only major peaks in the MS are associated with toluene and CO<sub>2</sub> ( $m/z = 44$ ), this indicates that the polymer has not been degraded at this temperature in the TGA experiment and that the initial mass loss is related to the evaporation of residual toluene.

T<sub>5%</sub> (the temperature corresponding to 5% mass loss)<sup>74,75</sup> is often considered the onset temperature for the decomposition of a substance, however the presence of the toluene in many of the copolymers makes this value artificially low. Therefore, comparing the T<sub>10%</sub> of the copolymers will give a more accurate comparison of the onset temperature of decomposition.

For the copolymers (entries 5 – 13), the T<sub>10%</sub> values varied from 236 – 310 °C in air. The copolymers containing TCPhA seemed to have lower T<sub>10%</sub> than the other copolymers. CHO–TCPhA (entry 6), ECH–TCPhA (entry 9) and PO–TCPhA (entry 12) have T<sub>10%</sub> of 274 °C, 266 °C and 236 °C respectively. Excluding these TCPhA examples, the rest of the copolymers have T<sub>10%</sub> in the range of 286 – 310 °C in air. These results suggest that TCPhA reduces the onset temperature of decomposition compared to the other anhydrides studied.

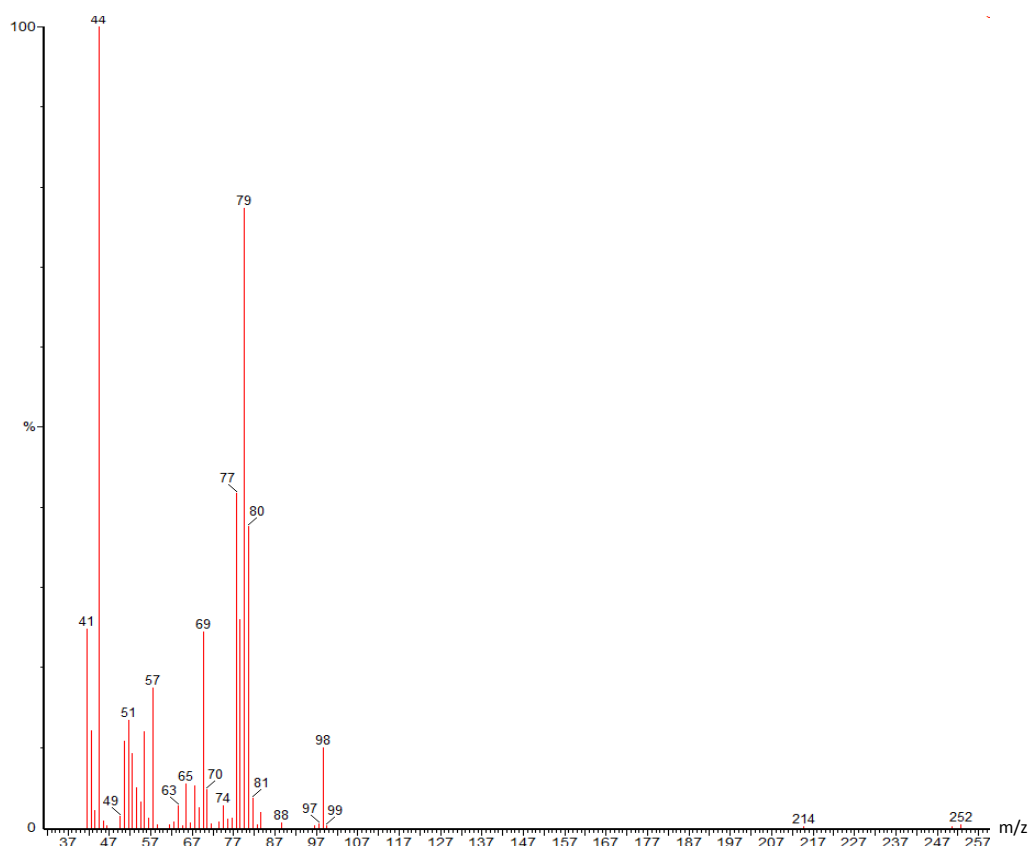


**Figure 21** EI-Mass spectrum of volatiles produced from the thermogravimetric analysis (TGA) of CHO–TCPhA carried out in air at 52 minutes corresponding to a temperature of 352 °C (Region B)

Region B (Figure 19) equates to the main mass loss in the TGA and therefore the majority of volatiles produced. The mass spectrum at 52 minutes, which equates to a temperature of approximately 352 °C was analysed. The mass spectrum at 52.5 minutes is shown in Figure 21. As the accurate mass was not measured, it is not possible to make exact assignment of peaks, but it does allow for tentative assignments which may be informative. The first thing to note in this spectrum, is the absence of toluene at  $m/z$  92. This suggests that this principal mass loss is a result of polymer degradation and not solvent evolution. The largest peak in the spectrum is at 79, this value is lower than the mass of either monomer used in the synthesis of the CHO–TCPhA copolymer indicating that this peak relates to a breakdown product. Another important peak in the spectrum is the peak at 98, this can be assigned to CHO. This peak is present in the MS of both of the experiments in air and  $N_2$  atmospheres carried out on CHO–TCPhA. This could be evidence for

### **Chapter 3 - Thermal and flame retardant properties of the copolymers**

depolymerisation. A small peak at 286 m/z is also visible in the MS spectrum recorded at 58.5 minutes, in addition to the peaks at 79 and 98. This peak at 286 m/z corresponds to the mass of TCPhA. The presence of both monomers in the mass spectrum is good evidence for depolymerisation occurring in addition to other degradation processes.

An important parameter for flame retardant materials, is the residual mass or char that remains at temperatures above the main decomposition step. Char-forming tendency of a polymer is an indication of flame retardancy, as the greater the char formed the less combustible volatile gases are produced. Char can also form a protective layer between a fire and the combustible material below. To evaluate the degree of char-formation, the percentage residual mass was recorded at 400 °C and 650 °C in both air and nitrogen atmospheres, shown in Table 4. The percentage residual mass at 400 °C represents char formation immediately following the main decomposition and the percentage residual mass at 650 °C represents the amount of char remaining at the end of the test.

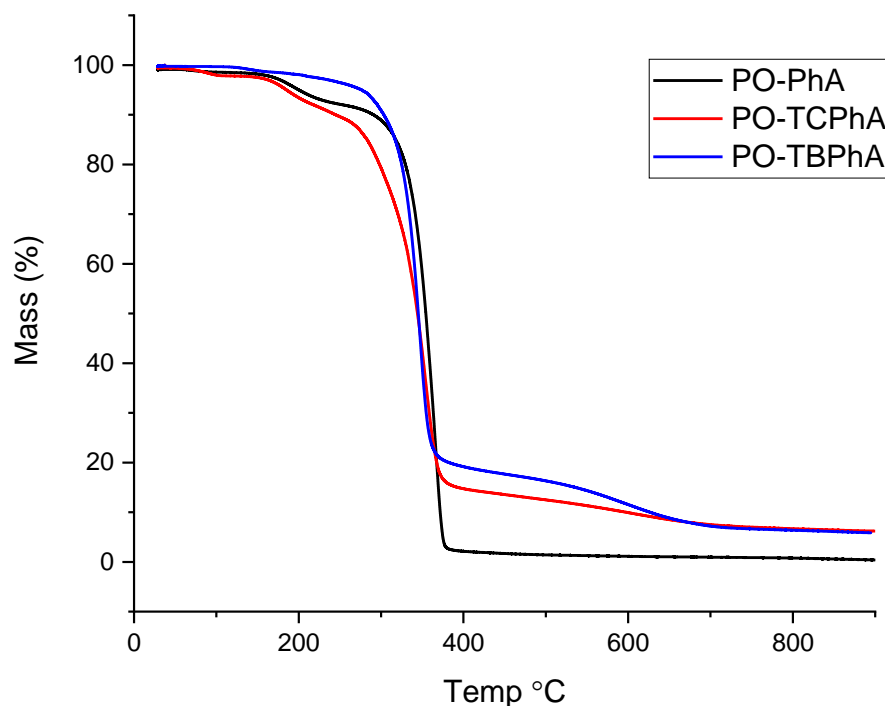


**Figure 22** Thermogravimetric analysis (TGA) graphs of PO containing copolymers in nitrogen atmosphere

CHO-PhA and PO-PhA (entries 5 and 11) have no significant char residue at the end of the test, even in nitrogen atmosphere, indicating that the polymer chains in these samples degrade through primarily chain scission or chain stripping. This mechanism may produce volatile, flammable degradation products. Halogen containing flame retardants are well known for acting in vapour phase by removing very reactive  $H^{\bullet}$  and  $OH^{\bullet}$  radicals through free-radical quenching mechanisms. They are not known to act in the condensed phase by promoting char formation.<sup>34</sup> Polymers synthesised from CHO with either TCPPhA (entry 6) or TBPhA (entry 7) showed a slight increase in residue at 400 °C in both air and  $N_2$  compared to CHO-PhA, however by 650 °C this mass had burned away. In all other examples, the introduction of halogens significantly increased char formation at 400 °C in both air and  $N_2$  and at 650 °C in  $N_2$ . This indicates that oxidation reactions (possible in an atmosphere of air) are required to completely decompose this char. The presence of TCPPhA and TBPhA in both the ECH and PO copolymers, caused substantial



### **Chapter 3 - Thermal and flame retardant properties of the copolymers**

char formation at 400 °C in both air and N<sub>2</sub> atmospheres and at 650 °C in nitrogen significant amounts of char remained. The copolymer with the greatest percentage of residual mass at 400 °C and 650 °C is PO–TBPhA (entry 13) with 19.2% and 8.8% recorded for the experiment in N<sub>2</sub>. For each epoxide, the amount of char increased following the substitution of PhA with TCPhA in the copolymers and increased further for the TBPhA samples. As a representative example, Figure 22 shows the TGA curves for the PO copolymers, which illustrates clearly how the char yield varies with anhydride.

The effect of halogens on char formation is highlighted by ECH–PhA (entry 8) which has only one halogen in the polymer repeat unit. ECH–PhA is identical to PO–PhA (entry 11) apart from the single halogen, however ECH–PhA has residual mass of 5.4% at 400 °C and 3.3% at 650 °C in N<sub>2</sub>, whereas PO–PhA has residual mass of 2.1% and 1% respectively. These results indicate that the presence of halogens *do* increase char formation and that these materials act in the condensed phase. One possible explanation for the formation of char in the halogenated copolymers with PO and ECH, is that at elevated temperatures, the polymer chains are cross-linking by dehydrohalogenation. Zinc borates are effective flame retardant additives and show a synergistic flame retardant effect when combined with chlorine- and bromine-containing materials. The dehydrohalogenation is catalysed by zinc species from the zinc borate additive, while the epoxide and anhydride copolymers synthesised in this study do not contain zinc, they may well contain significant levels of aluminium from the catalyst (**1**) used in their production. MALDI analysis of ECH–TCPhA (entry 9, Chapter 2.6) clearly indicated that **1** remained attached to the polymer chains following polymer workup. The residual aluminium may act in the same way as the zinc in the borate additive.<sup>28</sup>

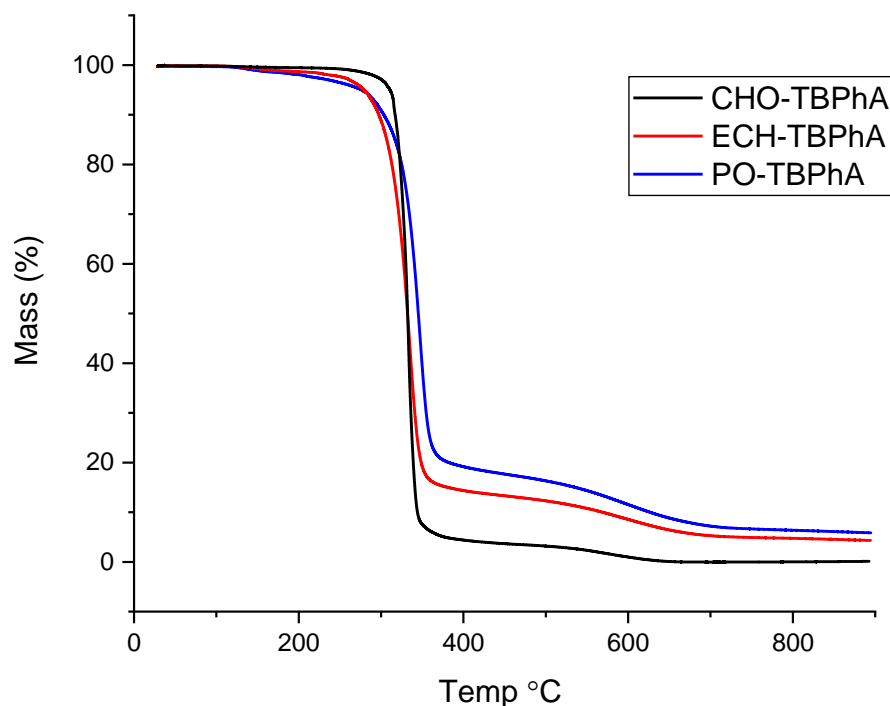


**Figure 23** Thermogravimetric analysis (TGA) graphs of TBPhA copolymers in N<sub>2</sub> atmosphere

The choice of epoxide also affects the char formation. For each anhydride, the residual mass at 400 °C was lowest for the CHO copolymer, increased for the ECH analogue and was highest for the PO example. Figure 23 shows the trend for increasing residual mass at 400 °C in N<sub>2</sub> where CHO < ECH < PO.

The TGA results indicate that the presence of halogens increases the flame retardancy of the polymers where they act in both the vapour phase and the condensed phase. The combination of a high T<sub>10%</sub> and high char formation would yield more effective flame retardant materials. These results also correlate with the results of the PCFC experiments showing the superior performance of the halogen containing copolymers.

### **3.5 Thermal properties of the copolymers**

While additive free flame retardancy has been introduced via the anhydride, variation of the monomers in the copolymerisation will also affect the thermal properties of the polymers. The thermal properties of a polymer can vary

### Chapter 3 - Thermal and flame retardant properties of the copolymers

greatly and can determine what applications a plastic is suitable for. Polyesters with a wide range of glass transition temperatures ( $T_g$ ), in addition to the excellent flame retardancy and hydrolysability, would be extremely useful to the world beyond academia.

The  $T_g$  of the flame retardant hydrolysable polymers formed from the ROCOP of epoxides and cyclic anhydrides was measured by dynamic mechanical analysis (DMA). Nine polyesters synthesised from the copolymerisation of the epoxides CHO, ECH and PO and the anhydrides PhA, TCPhA and TBPhA (entries 5 – 13) catalysed by **1** are shown in Table 5. The polymers had  $M_n$  values between 5,100 and 11,480  $\text{g mol}^{-1}$  and  $\bar{D}$  of 1.03 – 2.02.

**Table 5** Ring-opening copolymerisation (ROCOP) of epoxides and cyclic anhydride carried out in solvent

Entry	Epoxide	Anhydride	$M_n^a$	$\bar{D}^a$	$T_g^b$
5	CHO	PhA	11480	1.25	104±4
6	CHO	TCPhA	15250	1.20	166±5
7	CHO	TBPhA	5100	2.02	233±2
8	ECH	PhA	5100	1.13	68±1
9	ECH	TCPhA	9600	1.10	62±5
10	ECH	TBPhA	5900	1.33	124±6
11	PO	PhA	11200	1.18	39±1
12	PO	TCPhA	11450	1.03	34±5
13	PO	TBPhA	8750	1.05	104±6

6.4  $\mu\text{mol}$   $[\text{Al}(\text{L1})\text{Cl}_2]$  (**1**) catalyst. 1 equivalent = 6.4  $\mu\text{mol}$ .  $[\text{Epoxide}]_0:[\text{Anhydride}]_0:[\text{Catalyst}]_0:[\text{PPNCl}]_0 = 400:400:1:2$ . 1 ml of dry toluene added to reaction. Reactions heated at 80 °C for 18 hours. <sup>a</sup>Determined by GPC using triple detection, with units of  $\text{g mol}^{-1}$ . <sup>b</sup>Measured by DMA with units of °C.

The  $T_g$ s of the polymers were determined by dynamic mechanical analysis (DMA). More often, the  $T_g$  of polyesters is measured by differential scanning calorimetry (DSC). Measurement of the halogenated polyesters synthesised in this study by DSC was not possible because of the potential for the generation of halogenated decomposition products, therefore DMA was

### **Chapter 3 - Thermal and flame retardant properties of the copolymers**

utilised instead. The ratio of the loss modulus to the storage modulus is  $\tan \delta$ . The  $T_g$  is the temperature at the maxima of  $\tan \delta$ . This work was carried out in collaboration with Dr Mark Eaton and Kyriaki Gkaliou from Cardiff University. Raw data was recorded by Kyriaki Gkaliou.

The results in Table 5 show that the flame retardant polymers have  $T_g$  values encompassing a very wide temperature range, 34 °C to 233 °C. The considerable span of temperatures recorded indicate that these fire resistant plastics would be viable for applications requiring either low or high  $T_g$ . For the copolymer CHO–TBPhA (entry 7) a  $T_g$  of 233 °C was measured. This value is the highest reported for a polyester synthesised by the ROCOP of epoxides and cyclic anhydrides to date. The copolymer CHO–TBPhA (entry 7) also has a relatively low molecular weight which suggests that an even higher  $T_g$  may be attained for a larger molecular weight polymer. This result is significant as it shows the plastic is robust even at elevated temperatures. This viability at high temperatures combined with the excellent flame retardancy are extremely advantageous properties and show that hydrolysable plastics are feasible alternatives to current materials used for important applications, such as mechanical components and other heat-sensitive devices, where robustness under elevated temperatures and excellent flame-retardant credentials are crucial to success.

For the polymers synthesised from CHO (entries 5, 6 and 7), considerably higher  $T_g$ s were measured compared to the polyesters generated from ECH (entries 8 – 10) and PO (entries 11 – 13). For example, CHO–PhA (entry 5) has a  $T_g$  of 104 °C whereas ECH–PhA and PO–PhA (entries 8 and 11) had  $T_g$  values of 68 °C and 39 °C respectively. The higher  $T_g$  for the CHO copolymers is most likely a result of the cyclohexyl group in the polymer chain. This prevents the free rotation of the C–C bond derived from the epoxide in the polymer backbone, therefore yielding more rigid polymers and consequently higher  $T_g$ s.<sup>64</sup> The ECH and PO copolymers are much more flexible than the CHO examples and therefore have lower  $T_g$ s. These polymers do not have the constraint caused by the cyclohexyl ring in the backbone and therefore rotation around the C–C bond derived from the epoxide will readily occur. These results correlate well with the work of Coates *et al.* who observed higher  $T_g$ s

### Chapter 3 - Thermal and flame retardant properties of the copolymers

for polyesters with CHO than for the equivalent copolymers where PO was utilised as the epoxide monomer.<sup>66</sup>

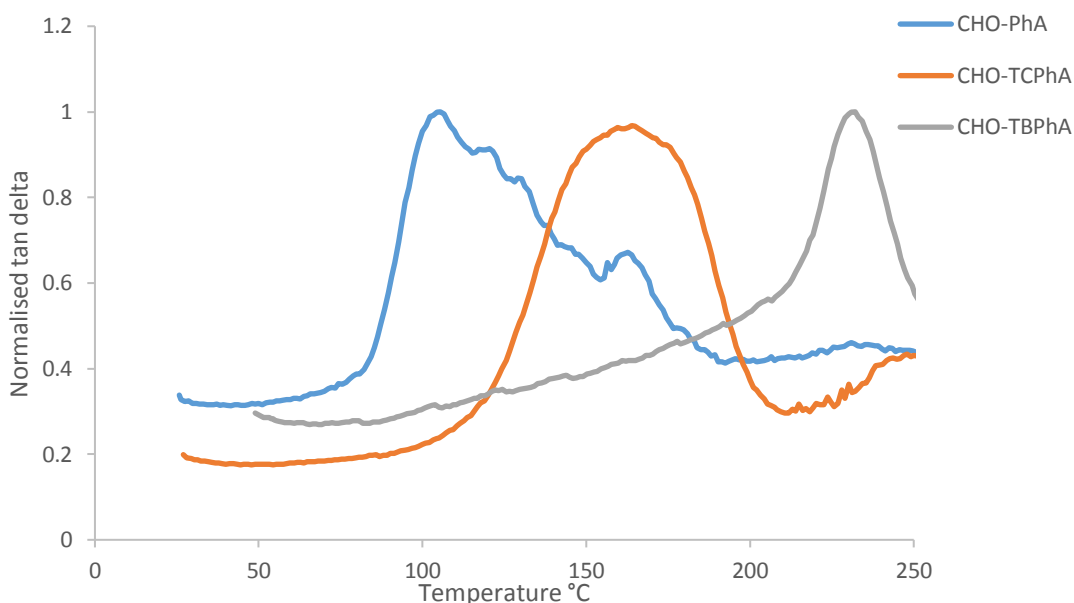


**Figure 24** Tan delta curves of CHO copolymers measured by dynamic mechanical analysis (DMA). The  $T_g$  value corresponds to the peak maximum

For the copolymers of CHO, a range of  $T_g$ s between 104 °C and 233 °C were recorded. Changing the identity of the anhydride monomer had a considerable effect on the CHO copolymers, where  $T_g$  increased for PhA < TCPPhA < TBPhA (Figure 24). Compared to the PhA (entry 5) copolymer, the  $T_g$  increased by 62 °C on changing to TCPPhA (entry 6). The  $T_g$  increased further by 67 °C when TBPhA was utilised in the ROCOP reaction with CHO (entry 7). The higher  $T_g$  values for the TCPPhA and TBPhA copolymers is most likely a result of hindered translational, vibrational and rotational motion of the polymer chains caused by the heavier halogens.<sup>76</sup>

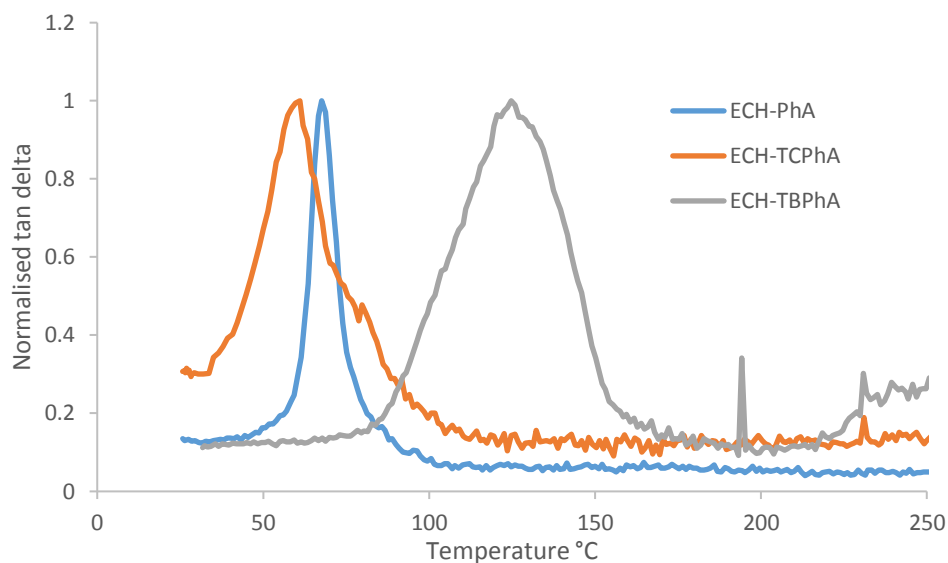


**Figure 25** Tan delta curves of ECH copolymers measured by dynamic mechanical analysis (DMA). The  $T_g$  value corresponds to the peak maximum. Like the copolymers of CHO, the polyester with the highest  $T_g$  of those synthesised from ECH was ECH-TBPhA (entry 10). ECH-TBPhA had a  $T_g$  of 124 °C, this is considerably higher than the values of 68 °C and 62 °C recorded for the PhA and TCPHA analogues (entries 8 and 9) respectively (Figure 25). Unlike the CHO copolymers, the polyesters synthesised from ECH did not show the same trend of increasing  $T_g$  for PhA < TCPHA < TBPhA. The copolymers ECH-PhA and ECH-TCPHA had very similar  $T_g$ s, with the TCPHA example recording a slightly lower value. While the use of TBPhA increased the  $T_g$  of the copolymer, the introduction of chlorine did not cause the same increase in the  $T_g$  that was observed in the CHO examples.

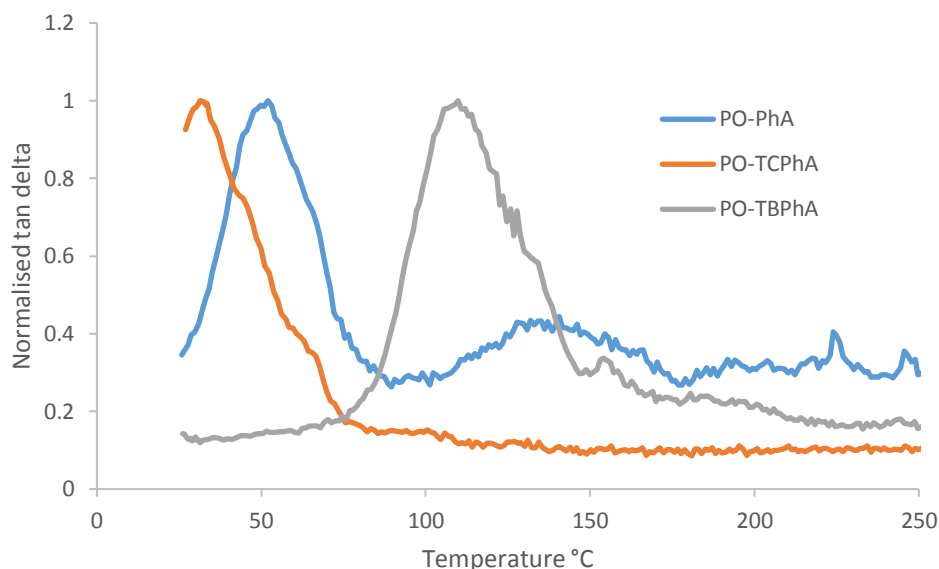


**Figure 26** Tan delta curves of PO copolymers measured by dynamic mechanical analysis (DMA). The  $T_g$  value corresponds to the peak maximum. For the copolymers of each anhydride, the lowest  $T_g$  value was measured for the example with PO. As was the case of the polymers synthesised from both CHO and ECH, the PO copolymer with the highest  $T_g$  was the TBPhA example ( $T_g = 104\text{ }^{\circ}\text{C}$ ). Like the ECH examples, the PO copolymers with PhA and TCPHA had similar  $T_g$  values ( $39\text{ }^{\circ}\text{C}$  and  $34\text{ }^{\circ}\text{C}$  respectively) which were significantly lower than the bromine containing congener. The comparable thermal properties of the copolymers of PO and ECH are most likely due to their similar polymer structures. The only difference between PO and ECH is a  $\text{CH}_3$  group as opposed to  $\text{CH}_2\text{Cl}$ . The tan delta curves of the PO copolymers are shown in Figure 26.

$T_g$  values have previously been reported for the copolymers, CHO-PhA, ECH-PhA, PO-PhA, CHO-TCPHA and PO-TCPHA. Most show comparable  $T_g$  values to those measured in this study by DMA. The exception to this is PO-TCPHA which recorded a far lower  $T_g$  when measured by DMA compared to the value reported by Hošťálek *et al.*<sup>58</sup> Hošťálek and colleagues recorded a  $T_g$  of  $84\text{ }^{\circ}\text{C}$  for PO-TCPHA by DSC whereas a lower value of  $34\text{ }^{\circ}\text{C}$  (entry 12) was measured by DMA. This disparity cannot be a result of differences in molecular weight, as  $T_g$  increases with polymer chain length and the PO-TCPHA copolymer synthesised in this study has a larger molecular weight.

### **Chapter 3 - Thermal and flame retardant properties of the copolymers**

The reason for this discrepancy is not clear, CHO–TCPhA was also synthesised and tested by Hošťálek *et al.* and a similar  $T_g$  value (154 °C) was reported to the value found in this study (entry 6, 166 °C).

#### **3.6 Summary**

In conclusion, additive free, flame retardant hydrolysable polyesters have been synthesised by the ROCOP of epoxides and cyclic anhydrides. Excellent fire resistance was achieved by the inclusion of TCPhA and TBPhA monomers. The most flame retardant polymer generated was ECH–TBPhA which had a HRC of 128 J/g.K. This corresponds to a decimal probability for a fire propagating in this material of  $1.48 \times 10^{-5}$ . For each of the epoxides used to produce copolymers, the examples with TBPhA produced the most flame retardant plastics. The TGA of the polyesters showed that their decomposition was dominated by one major mass loss. The TGA results suggest that copolymers with TBPhA are the most flame retardant. The higher  $T_{10\%}$  combined with greater char formation leads to higher fire resistance. The formation of char by these polymers is unexpected as halogen containing flame retardants are known to act in the vapour phase and not in the condensed phase. The evidence of char formation along with the conventional vapour phase retardancy is most likely the cause of the excellent flame retardancy of the TBPhA copolymers. The flame retardant polymers produced had an extremely wide range of  $T_g$ s (34 °C – 233 °C). The ability to achieve such wide ranging  $T_g$  values for the flame retardant polymers is very exciting and illustrates the potential of the ROCOP reaction to readily produce hydrolysable plastics with a wide variety of useful properties. The copolymer CHO–TBPhA had a  $T_g$  of 233 °C, which is the highest recorded value for a polyester synthesised by the ROCOP of epoxides and cyclic anhydrides. This shows that hydrolysable polymers may be produced with high  $T_g$ s making them suitable for use in applications that require good stability at high temperatures.



**3.7 References for Chapter 3**

- 1 M. Meier, *Green Chem.*, 2014, **16**, 1672–1672.
- 2 M. Cole, P. Lindeque, C. Halsband and T. S. Galloway, *Mar. Pollut. Bull.*, 2011, **62**, 2588–2597.
- 3 J. Hopewell, R. Dvorak and E. Kosior, *Philos. Trans. R. Soc. B Biol. Sci.*, 2009, **364**, 2115–2126.
- 4 M. Bergmann, S. Mützel, S. Primpke, M. B. Tekman, J. Trachsel and G. Gerdt, *Sci. Adv.*, 2019, **5**, eaax1157.
- 5 R. Geyer, J. R. Jambeck and K. L. Law, *Sci. Adv.*, 2017, **3**, e1700782.
- 6 H. Ritchie and M. Roser, *Our World In Data*, 2019, Published online at *OurWorldInData.org*.
- 7 A. J. Jamieson, L. S. R. Brooks, W. D. K. Reid, S. B. Piertney, B. E. Narayanaswamy and T. D. Linley, *R. Soc. Open Sci.*, **6**, 180667.
- 8 D. K. Schneiderman and M. A. Hillmyer, *Macromolecules*, 2017, **50**, 3733–3749.
- 9 Editorial, *Nat. Commun.*, 2018, **9**, 2157.
- 10 L. Feng, Y. Liu, J. Hao, X. Li, C. Xiong and X. Deng, *Macromol. Chem. Phys.*, 2011, **212**, 2626–2632.
- 11 J. M. Longo, M. J. Sanford and G. W. Coates, *Chem. Rev.*, 2016, **116**, 15167–15197.
- 12 S. Paul, Y. Zhu, C. Romain, R. Brooks, P. K. Saini and C. K. Williams, *Chem. Commun.*, 2015, **51**, 6459–6479.
- 13 L. W. McKeen, in *Film Properties of Plastics and Elastomers (Fourth Edition)*, ed. L. W. McKeen, William Andrew Publishing, 2017, pp. 147–185.
- 14 L. W. McKeen, in *Film Properties of Plastics and Elastomers (Fourth Edition)*, ed. L. W. McKeen, William Andrew Publishing, 2017, pp. 419–448.
- 15 G. Pál and H. Macskásy, in *Studies in Polymer Science*, eds. G. Pál and H. Macskásy, Elsevier, 1991, vol. 6, pp. V–VI.
- 16 M. Bar, R. Alagirusamy and A. Das, *Fibers Polym.*, 2015, **16**, 705–717.
- 17 V. Babrauskas and M. Simonson, *Fire Mater.*, 2007, **31**, 83–96.

### **Chapter 3 - Thermal and flame retardant properties of the copolymers**

- 18 J. Valiulis, *Fire Eng. Mag.*, 2015, 24.
- 19 G. L. Nelson, A. B. Morgan and C. A. Wilkie, in *Fire and Polymers VI: New Advances in Flame Retardant Chemistry and Science*, American Chemical Society, 2012, vol. 1118, pp. 1–13.
- 20 N. N. Brushlinsky, M. Ahrens, S. V. Sokolov and P. Wagner, *CTIF*, 2018, 23.
- 21 G. Pál and H. Macskásy, Eds., in *Studies in Polymer Science*, Elsevier, 1991, vol. 6, pp. 32–93.
- 22 G. Pál and H. Macskásy, Eds., in *Studies in Polymer Science*, Elsevier, 1991, vol. 6, pp. 337–414.
- 23 I. van der Veen and J. de Boer, *Chemosphere*, 2012, **88**, 1119–1153.
- 24 B. Scharrel, *Materials*, 2010, **3(10)**, 4710–4745.
- 25 C. Hirsch, B. Striegl, S. Mathes, C. Adlhart, M. Edelmann, E. Bono, S. Gaan, K. A. Salmeia, L. Hoelting, A. Krebs, J. Nyffeler, R. Pape, A. Bürkle, M. Leist, P. Wick and S. Schildknecht, *Arch. Toxicol.*, 2017, **91**, 407–425.
- 26 A. Rodolfo and L. H. I. Mei, *J. Appl. Polym. Sci.*, 2010, **118**, 2613–2623.
- 27 M. Lin, B. Li, Q. Li, S. Li and S. Zhang, *J. Appl. Polym. Sci.*, 2011, **121**, 1951–1960.
- 28 K. K. Shen, in *Polymer Green Flame Retardants*, eds. C. D. Papaspyrides and P. Kiliaris, Elsevier, Amsterdam, 2014, pp. 367–388.
- 29 Y.-J. Kim, M. Osako and S. Sakai, *Chemosphere*, 2006, **65**, 506–513.
- 30 Y. Wu, G. Z. Miller, J. Gearhart, K. Romanak, V. Lopez-Avila and M. Venier, *Environ. Sci. Technol. Lett.*, 2019, **6**, 14–20.
- 31 E. L. Teuten, J. M. Saquing, D. R. U. Knappe, M. A. Barlaz, S. Jonsson, A. Björn, S. J. Rowland, R. C. Thompson, T. S. Galloway, R. Yamashita, D. Ochi, Y. Watanuki, C. Moore, P. H. Viet, T. S. Tana, M. Prudente, R. Boonyatumanond, M. P. Zakaria, K. Akkhavong, Y. Ogata, H. Hirai, S. Iwasa, K. Mizukawa, Y. Hagino, A. Imamura, M. Saha and H. Takada, *Philos. Trans. R. Soc. B Biol. Sci.*, 2009, **364**, 2027–2045.
- 32 A. Marklund, B. Andersson and P. Haglund, *Chemosphere*, 2003, **53**, 1137–1146.
- 33 H. Guo, X. Zheng, S. Ru, X. Luo and B. Mai, *J. Environ. Sci.*, 2019, **85**, 200–207.

### **Chapter 3 - Thermal and flame retardant properties of the copolymers**

- 34 S.-Y. Lu and I. Hamerton, *Prog. Polym. Sci.*, 2002, **27**, 1661–1712.
- 35 P. M. Hergenrother, C. M. Thompson, J. G. Smith, J. W. Connell, J. A. Hinkley, R. E. Lyon and R. Moulton, *Polymer*, 2005, **46**, 5012–5024.
- 36 K. S. Annakutty and K. Kishore, *Polymer*, 1988, **29**, 756–761.
- 37 K. Kishore, K. S. Annakutty and I. M. Mallick, *Polymer*, 1988, **29**, 762–764.
- 38 P. Kannan and K. Kishore, *Eur. Polym. J.*, 1991, **27**, 1017–1021.
- 39 P. Kannan, Gangadhara and K. Kishore, *Polymer*, 1991, **32**, 1909–1913.
- 40 P. Kannan and K. Kishore, *Eur. Polym. J.*, 1991, **27**, 1017–1021.
- 41 D.-Y. Wang, Y.-P. Song, L. Lin, X.-L. Wang and Y.-Z. Wang, *Polymer*, 2011, **52**, 233–238.
- 42 Ph. Potin and R. De Jaeger, *Eur. Polym. J.*, 1991, **27**, 341–348.
- 43 C. W. Allen, *Coord. Chem. Rev.*, 1994, **130**, 137–173.
- 44 S. Rothmund and I. Teasdale, *Chem. Soc. Rev.*, 2016, **45**, 5200–5215.
- 45 W. J. Wang, L. H. Perng, G. H. Hsiue and F. C. Chang, *Polymer*, 2000, **41**, 6113–6122.
- 46 M. Iji and S. Serizawa, *NEC Res. Dev.*, 1998, **39**, 82–87.
- 47 M. Alagar, T. V. T. Velan, A. A. Kumar and V. Mohan, *Mater. Manuf. Process.*, 1999, **14**, 67–83.
- 48 C. Sivriev and L. Žabski, *Eur. Polym. J.*, 1994, **30**, 509–514.
- 49 P. Furtwengler and L. Avérous, *Polym. Chem.*, 2018, **9**, 4258–4287.
- 50 A. Rudin and P. Choi, in *The Elements of Polymer Science & Engineering (Third Edition)*, eds. A. Rudin and P. Choi, Academic Press, Boston, 2013, pp. 149–229.
- 51 S. Lambert and M. Wagner, *Chem. Soc. Rev.*, 2017, **46**, 6855–6871.
- 52 K. Balani, V. Verma, A. Agarwal and R. Narayan, in *Biosurfaces*, John Wiley & Sons, Ltd, 2015, pp. 329–344.
- 53 Y. Maeda, A. Nakayama, N. Kawasaki, K. Hayashi, S. Aiba and N. Yamamoto, *Polymer*, 1997, **38**, 4719–4725.
- 54 A. M. DiCiccio, J. M. Longo, G. G. Rodríguez-Calero and G. W. Coates, *J. Am. Chem. Soc.*, 2016, **138**, 7107–7113.

### Chapter 3 - Thermal and flame retardant properties of the copolymers

- 55 J. M. Longo, A. M. DiCiccio and G. W. Coates, *J. Am. Chem. Soc.*, 2014, **136**, 15897–15900.
- 56 G. Si, L. Zhang, B. Han, Z. Duan, B. Li, J. Dong, X. Li and B. Liu, *Polym. Chem.*, 2015, **6**, 6372–6377.
- 57 M. Winkler, C. Romain, M. A. R. Meier and C. K. Williams, *Green Chem.*, 2014, **17**, 300–306.
- 58 Z. Hošťálek, O. Trhlíková, Z. Walterová, T. Martinez, F. Peruch, H. Cramail and J. Merna, *Eur. Polym. J.*, 2017, **88**, 433–447.
- 59 E. H. Nejad, A. Paoniasari, C. E. Koning and R. Duchateau, *Polym. Chem.*, 2012, **3**, 1308–1313.
- 60 R. C. Jeske, A. M. DiCiccio and G. W. Coates, *J. Am. Chem. Soc.*, 2007, **129**, 11330–11331.
- 61 D. J. Darensbourg, R. R. Poland and C. Escobedo, *Macromolecules*, 2012, **45**, 2242–2248.
- 62 A. M. DiCiccio and G. W. Coates, *J. Am. Chem. Soc.*, 2011, **133**, 10724–10727.
- 63 K. A. D. Swift, *Top. Catal.*, 2004, **27**, 143–155.
- 64 N. J. Van Zee and G. W. Coates, *Angew. Chem. Int. Ed Engl.*, 2015, **54**, 2665–2668.
- 65 B. Han, L. Zhang, B. Liu, X. Dong, I. Kim, Z. Duan and P. Theato, *Macromolecules*, 2015, **48**, 3431–3437.
- 66 M. J. Sanford, L. Peña Carrodegua, N. J. Van Zee, A. W. Kleij and G. W. Coates, *Macromolecules*, 2016, **49**, 6394–6400.
- 67 U. Biermann, A. Sehlinger, M. A. R. Meier and J. O. Metzger, *Eur. J. Lipid Sci. Technol.*, 2016, **118**, 104–110.
- 68 Y. Zhu, C. Romain and C. K. Williams, *J. Am. Chem. Soc.*, 2015, **137**, 12179–12182.
- 69 M. Atagür, S. Demiroğlu and M. Ö. Seydibeyoğlu, in *Polyurethane Polymers*, eds. S. Thomas, J. Datta, J. T. Haponiuk and A. Reghunadhan, Elsevier, Amsterdam, 2017, pp. 499–524.
- 70 A. Christiansson, L. Hovander, I. Athanassiadis, K. Jakobsson and Å. Bergman, *Chemosphere*, 2008, **73**, 1654–1660.
- 71 P. Patel, T. R. Hull, A. A. Stec and R. E. Lyon, *Polym. Adv. Technol.*, 2011, **22**, 1100–1107.

### **Chapter 3 - Thermal and flame retardant properties of the copolymers**

- 72 J. M. Cogen, T. S. Lin and R. E. Lyon, *Fire Mater.*, 2009, **33**, 33–50.
- 73 C.-J. Hong, Y.-J. Kwark and T.-H. Han, *Fibers Polym.*, 2010, **11**, 851–855.
- 74 O. Zavgorodnya, J. L. Shamshina, M. Mittenthal, P. D. McCrary, G. P. Rachiero, H. M. Titi and R. D. Rogers, *New J. Chem.*, 2017, **41**, 1499–1508.
- 75 J. H. Kim, W. Lee, T. Kim, H.-G. Kim, B. Seo, C.-S. Lim and I. W. Cheong, *Appl. Sci.*, 2018, **8**, 1587.
- 76 H. Kageyama, K. Itano, W. Ishikawa and Y. Shirota, *J. Mater. Chem.*, 1996, **6**, 675–676.

# **Chapter 4**

## **Post-polymerisation modification of copolymers**

## **4.1 Introduction**

### **4.1.1 Post-polymerisation modification of polymers**

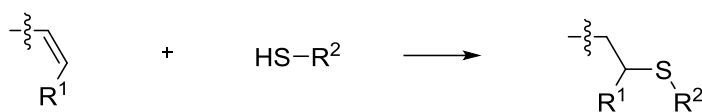
Post-polymerisation modification (PPM) is a powerful tool to vary the properties of a polymer. In this approach, the polymer chains are pre-formed and subsequently undergo a chemical transformation which alters the nature of the plastic. Hermann Staudinger, a pioneer of polymer science, termed PPM as the “transformation of a polymer into a derivative of equivalent molecular weight.” PPM reactions can be classified as those which add or remove chemical architecture, introduce new functional groups or cross-link polymer chains together producing an interlinked polymer network. These reactions can take place all along a polymer chain or on the polymer end groups.<sup>1</sup>

Many polymerisations are intolerant to the presence of common functional groups, this limits the range and variety of polymers that can be produced. PPM can be utilised to introduce these useful functionalities to preformed polymers which can extend the range of possible properties and therefore increase the number of potential applications.<sup>2</sup>

Control of functional polymer end groups is very useful, chain end PPM is an effective route to cross-link polymer chains and to produce complex block copolymers or dendritic structures.<sup>3,4</sup> Polymers with one reactive functional end group can be used as bioconjugates,<sup>5</sup> precursors for diblock copolymers<sup>6</sup> or for producing polymer brushes.<sup>7</sup> Polymers with identical functional groups at both chain ends may be utilised as cross-linkers or precursors for multiblock copolymers.<sup>8,9</sup>

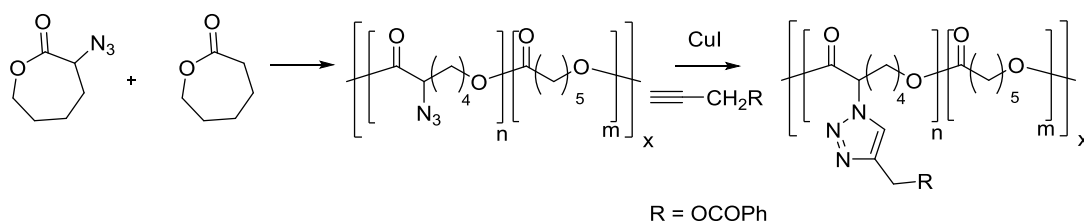
PPM can be used to transform functional groups that are present in the polymer repeat unit and therefore throughout the entire polymer chain. These functionalities can be found in the polymer backbone or on side groups pendant to the main chain. From the early 20<sup>th</sup> century, scientists have been using PPM to modify the properties of synthetic plastics. In 1948, Serniuk and colleagues reported the modification of butadiene polymers with aliphatic thiols utilising thiol-ene click chemistry.<sup>10</sup>

### 4.1.2 Post-polymerisation modification (PPM) reactions



**Scheme 1** Thiol-ene click reaction

Thiol-ene click chemistry has been used extensively for PPM.<sup>1,11–17</sup> In this modification, a thioether is formed from the anti-Markovnikov addition reaction of a thiol and alkene (Scheme 1). The transformation can be catalysed either by a radical initiator or photochemically. While both approaches are effective, milder conditions and shorter reaction times are required for the photochemically mediated processes.<sup>11</sup> A wide variety of polymers containing alkenes have been successfully combined with many structurally diverse thiols.<sup>1</sup> The thiol-ene reaction is an example of click chemistry, where a reaction is high yielding, has a large thermodynamic driving force, simple reaction conditions, regio- and stereospecific and has high atom economy.<sup>18</sup> In addition to the thiol-ene click reaction first used by Serniuk *et al.* there has been a wide variety of chemical reactions utilised for PPM. Campos and co-workers showed that the thiol-ene addition reaction was compatible with another example of click chemistry, the copper catalysed, 1,3 dipolar cycloaddition reaction of azides and alkynes (CuAAC).<sup>11</sup>



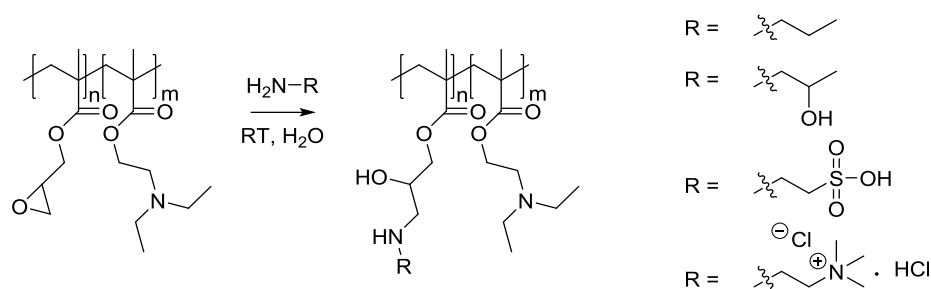
**Scheme 2** CuAAC post-polymerisation modification (PPM) of propargyl benzoate with an azide containing poly(caprolactone)<sup>19</sup>

The regioselective CuAAC transformation is catalysed by  $\text{Cu}^{\text{I}}$  and can be carried out under mild conditions in both aqueous and organic solvents. Following the development of polymerisations which are capable of tolerating monomers containing either the azide or alkyne functionalities, there was a rapid growth in the popularity CuAAC PPM.<sup>1,20</sup> This reaction has been utilised

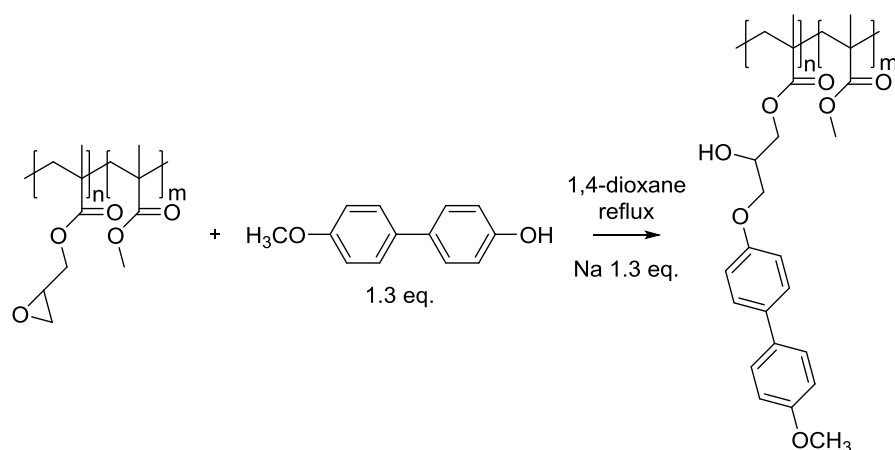


## Chapter 4 - Post-polymerisation modification of copolymers

for an extensive range of polymers with a diverse library of azide and alkyne substrates including biological molecules.<sup>21,22</sup> An example of a CuAAC PPM is the reaction of propargyl benzoate with an azide containing poly(caprolactone) (Scheme 2).<sup>19</sup> One consideration when using the CuAAC PPM is that removal of the copper catalyst is sometimes difficult due to the metal forming a complex with the triazole ring.<sup>1</sup>



**Scheme 3** Post-polymerisation modification (PPM) of epoxy containing copolymer with primary amines<sup>23</sup>

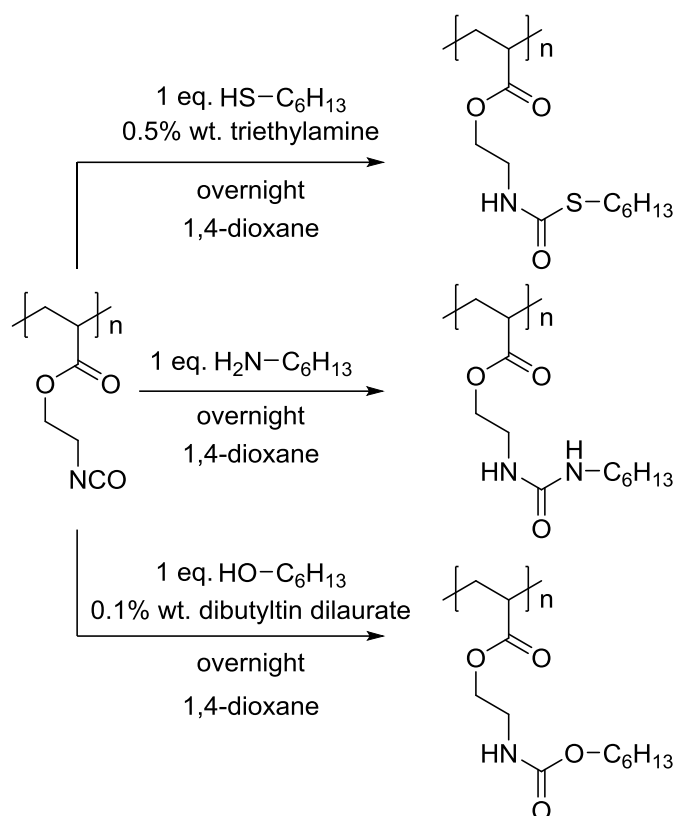


**Scheme 4** Post-polymerisation modification (PPM) of epoxy containing copolymer with 4-hydroxy-4'-methoxybiphenyl<sup>24</sup>

Polymers containing pendant epoxide groups are excellent candidates for PPM. Monomers containing epoxides can be effectively polymerised using free radical mediated polymerisations whilst avoiding side reactions, thereby leaving the epoxide intact.<sup>25</sup> Amines, alcohols and carboxylic acids are commonly used substrates in the PPM of epoxide-containing polymers.<sup>1</sup> Barbey and Klok reported the reaction of epoxy containing polymer brushes with primary amines.<sup>23</sup> The polymer brushes were generated by surface-initiated atom transfer radical polymerisation and were comprised of a

#### **Chapter 4 - Post-polymerisation modification of copolymers**

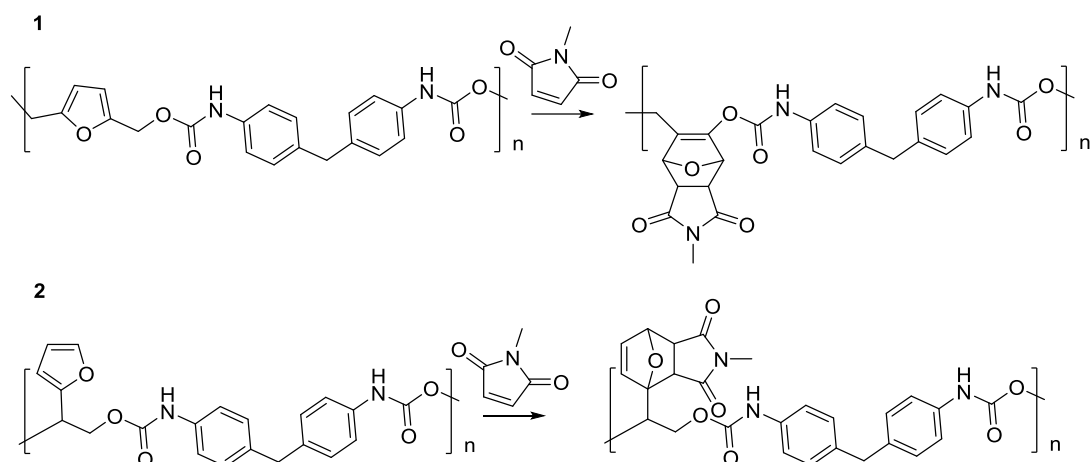
copolymer of poly(glycidyl methacrylate) and poly(2-(diethylamino)ethyl methacrylate). The primary amines reacted with the pendant epoxy group of the glycidyl methacrylate, this PPM was catalysed by the pendant tertiary amine group of diethylamino ethyl methacrylate. Using this approach, a series of primary amines were reacted with the epoxy containing copolymer at room temperature in water over 48 hours (Scheme 3). Navarro-Rodriguez and colleagues reported the PPM of poly(glycidyl methacrylate) and a poly(glycidyl methacrylate)-co-poly(methyl methacrylate) copolymer with 4-hydroxy-4'-methoxybiphenyl (Scheme 4). These reactions were carried out in 1,4-dioxane at reflux for 16 hours. In the PPM of the glycidyl methacrylate homopolymer 75% of the epoxy groups reacted, whereas in the copolymer complete conversion of epoxy groups was reported. It was reasoned that this disparity in reactivity was a result of the greater steric hindrance in the homopolymer, owing to the close proximity of the epoxy containing side chains. In the copolymer, the steric hindrance is reduced because of the increased distance between the glycidyl methacrylate monomer units due to the inclusion of the methyl methacrylate.<sup>24</sup>



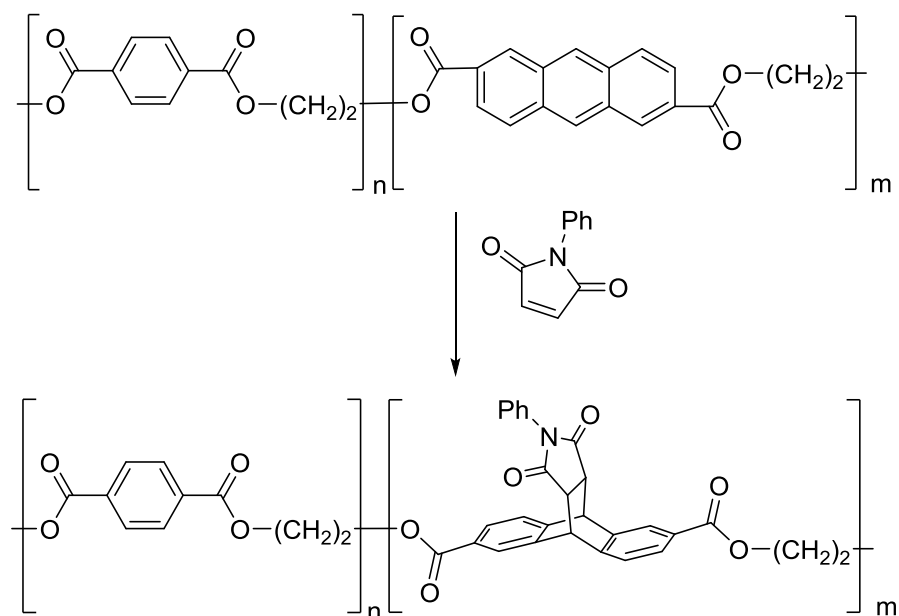
**Scheme 5** Post-polymerisation modification (PPM) of isocyanate containing polymer with hexanol, hexylamine and 1-hexanethiol<sup>26</sup>

Polymers bearing pendant isocyanate groups will readily undergo PPM with amines, alcohols and thiols forming urea, urethane and thiourea derivatives respectively.<sup>1,27</sup> Polymers of isocyanate-containing monomers can be produced using controlled radical polymerisation.<sup>28</sup> Flores and colleagues reported the PPM of a 2-(acryloyloxy)ethylisocyanate homopolymer with hexylamine, hexanol and 1-hexanethiol (Scheme 5). The reactions of amines and thiols with isocyanate groups occur rapidly but can be accelerated further by the presence of a catalytic amount of base, such as triethylamine. The equivalent reaction with alcohols is much slower but with the addition of dibutyltin dilaurate, quantitative conversion can be achieved.<sup>26</sup>

## Chapter 4 - Post-polymerisation modification of copolymers



**Scheme 6** Diels-Alder post-polymerisation modification (PPM) of *N*-methylmaleimide with polyurethane polymers containing furan groups in either the polymer backbone (1) or as a side chain (2)<sup>29</sup>

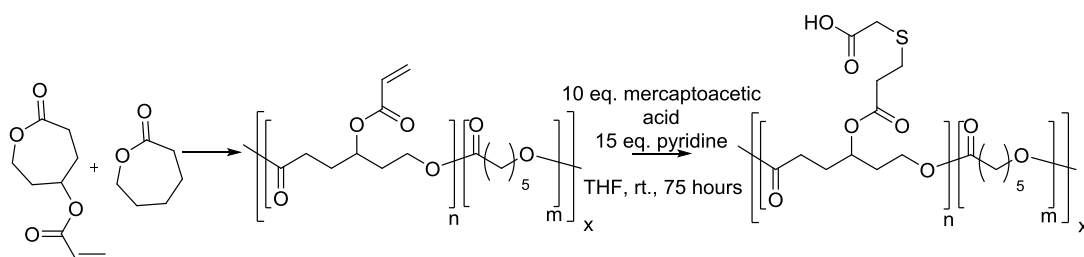


**Scheme 7** Post-polymerisation modification (PPM) of anthracene containing polymer<sup>30</sup>

The Diels-Alder cycloaddition of a diene and an alkene is a well-established chemical transformation that is considered an example of click chemistry.<sup>18</sup> It has good functional group tolerance, mild reaction conditions and is high yielding.<sup>1</sup> Dienes may be incorporated into a polymer by the polymerisation of monomers containing groups such as furan or anthracene moieties.<sup>31,32</sup> For example, Laita *et al.* reported a Diels-Alder PPM of a poly(urethane) with furan groups present either on a side chain or in the polymer backbone.<sup>29</sup> PPM via

## Chapter 4 - Post-polymerisation modification of copolymers

reaction of the furan with N-methylmaleimide proceeded to completion when the furan was located on a side-chain of the polymer, whereas conversion was limited to ~60% when the furan was incorporated into the polymer backbone; the difference in reactivity was attributed to the greater steric hindrance around the more highly substituted diene when a part of the polymer backbone (Scheme 6).<sup>29</sup> Jones and colleagues investigated the Diels-Alder PPM of an anthracene containing polymer, poly(ethylene terephthalate-co-2,6-anthracenedicarboxylate) with *N*-phenylmaleimide. The cycloaddition of the anthracene units in the polymer backbone and the maleimide had a conversion of 94% when the reaction was heated at 125 °C for 12 hours (Scheme 7).<sup>30</sup> Polymers containing maleimide functional groups can be prepared by polymerisation of masked maleimide monomers such as furan-maleimide cycloadducts.<sup>31,33</sup>

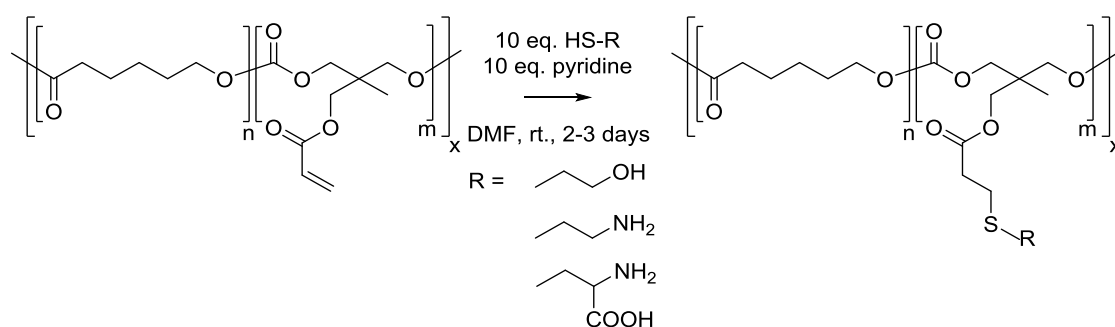


**Scheme 8** Michael addition of mercaptoacetic acid and poly( $\gamma$ -acryloyloxy- $\epsilon$ -caprolactone-co- $\epsilon$ -caprolactone)<sup>34</sup>

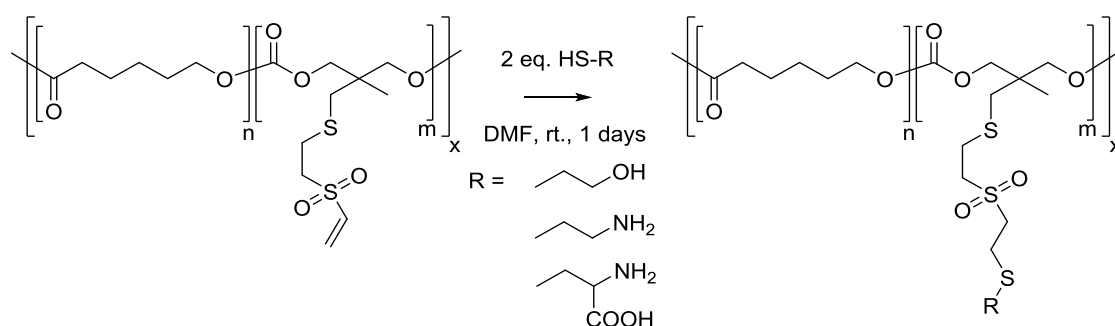
Michael-type addition reactions are a powerful tool for the functionalisation of polymers bearing Michael acceptors such as acrylates, maleimides or vinyl sulfones.<sup>1</sup> The PPM reaction of these polymers with thiols is highly efficient, selective, and can be undertaken in aqueous solutions.<sup>35</sup> Polymers containing acrylate groups can be produced by ring-opening polymerisations. Rieger and colleagues reported the Michael addition of mercaptoacetic acid and a random copolymer of  $\gamma$ -acryloyloxy- $\epsilon$ -caprolactone<sup>36</sup> and  $\epsilon$ -caprolactone.<sup>34</sup> 70% conversion was recorded after 75 hours at room temperature with pyridine as the catalyst (Scheme 8). Chen *et al.* synthesised copolymers of acryloyl carbonate with either  $\epsilon$ -caprolactone or rac-lactide. Functionalisation of these acrylate containing polymers was achieved by the Michael addition of 2-mercaptoethanol, 2-mercaptoethylamine hydrochloride and L-cysteine

## Chapter 4 - Post-polymerisation modification of copolymers

(Scheme 9).<sup>37</sup> Copolymers containing vinyl sulfone functional groups were synthesised by the ring-opening polymerisation of vinyl sulfone carbonate with either trimethylene carbonate,  $\epsilon$ -caprolactone or rac-lactide. The Michael addition reaction between a range of thiols including 2-mercaptoethanol, 2-mercaptoethylamine hydrochloride and L-cysteine and the vinyl sulfone containing copolymers achieved quantitative conversions after one day at room temperature in DMF.<sup>38</sup> Scheme 10 shows the PPM of the  $\epsilon$ -caprolactone and vinyl sulfone carbonate copolymer.



**Scheme 9** Michael addition of thiols and poly(acryloyl carbonate-co- $\epsilon$ -caprolactone)<sup>37</sup>

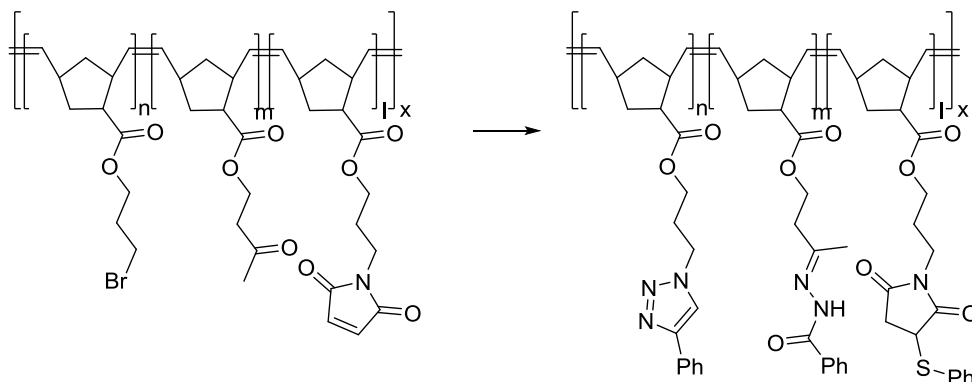


**Scheme 10** Michael addition of thiols and poly(vinyl sulfone carbonate-co- $\epsilon$ -caprolactone)<sup>38</sup>

Weck *et al.* produced a terpolymer amenable to PPM by a Michael addition reaction with thiophenol.<sup>39</sup> This polymer bearing maleimide groups was synthesised by ring-opening metathesis of functionalised norbornenes. The Michael addition of the thiol and the pendant maleimide groups was achieved at room temperature when 2 equivalents of thiol was used. In addition to the maleimide groups, this terpolymer also contained functional groups capable of undergoing PPM by CuAAC and hydrozone formation. All three of these

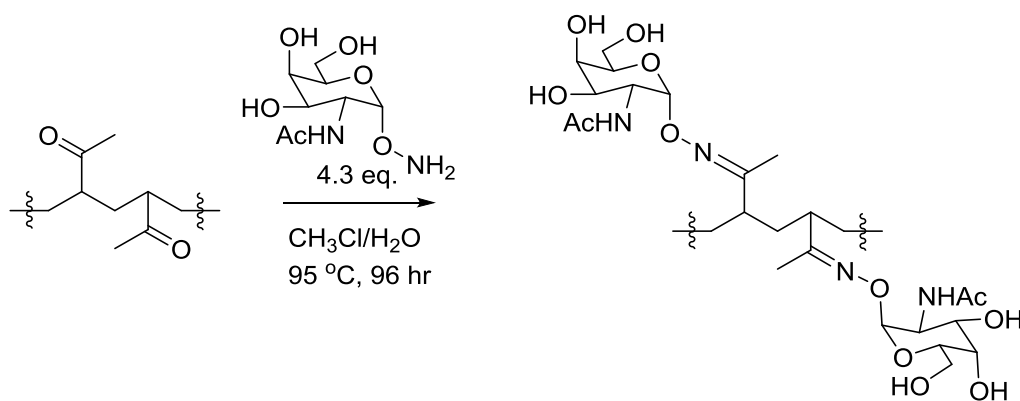
## Chapter 4 - Post-polymerisation modification of copolymers

modifications can be selectively achieved in a one pot reaction indicating the orthogonal nature of PPM's (Scheme 11).<sup>39,40</sup>



**Scheme 11** Orthogonal post-polymerisation modification (PPM) of multifunctional terpolymer<sup>39</sup>

Polymers containing ketone and aldehyde functional groups are excellent candidates for PPM.<sup>1</sup> These functionalities will readily react with amines, hydrazines and alkoxyamines yielding imines,<sup>41</sup> hydrazones,<sup>40</sup> and oximes<sup>42</sup> respectively. An example of this PPM reaction, is the reaction of amino-functionalised sugars with a methyl vinyl ketone derived polymer (Scheme 12).<sup>42</sup> Imines are relatively reactive bonds which are susceptible to hydrolysis however they can be converted to stable amines by reducing agents such as sodium borohydride.<sup>41</sup>

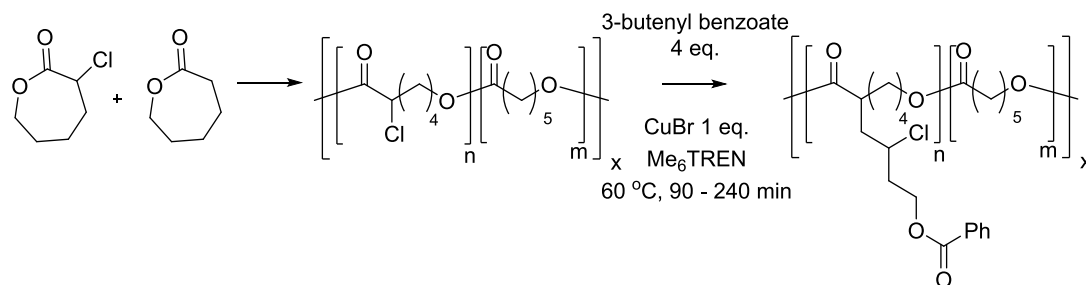


**Scheme 12** Post-polymerisation modification (PPM) of methyl vinyl ketone derived polymer with an amino-functionalised sugar<sup>42</sup>

The PPM reaction between alkyl halides and alkenes is known as atom-transfer radical addition (ATRA).<sup>43</sup> This reaction is catalysed by transition metal complexes and is tolerant to a variety of other functional groups such as

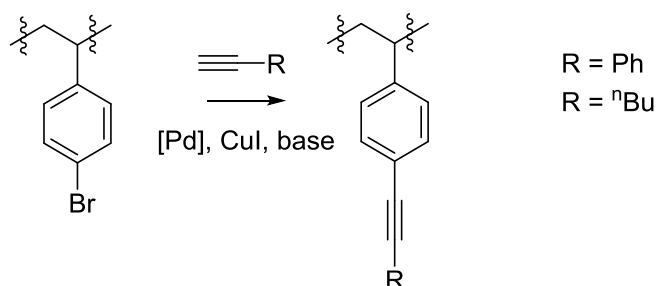
## Chapter 4 - Post-polymerisation modification of copolymers

alcohols, esters, epoxides and carboxylic acids.<sup>1</sup> Scheme 13 shows the ATRA reaction of a copolymer formed from  $\epsilon$ -caprolactone and  $\alpha$ -chloro- $\epsilon$ -caprolactone with 3-butenyl benzoate.<sup>44</sup>



**Scheme 13** Atom-transfer radical addition (ATRA) post-polymerisation modification (PPM) of  $\alpha$ -chloro- $\epsilon$ -caprolactone containing polyester<sup>44</sup>

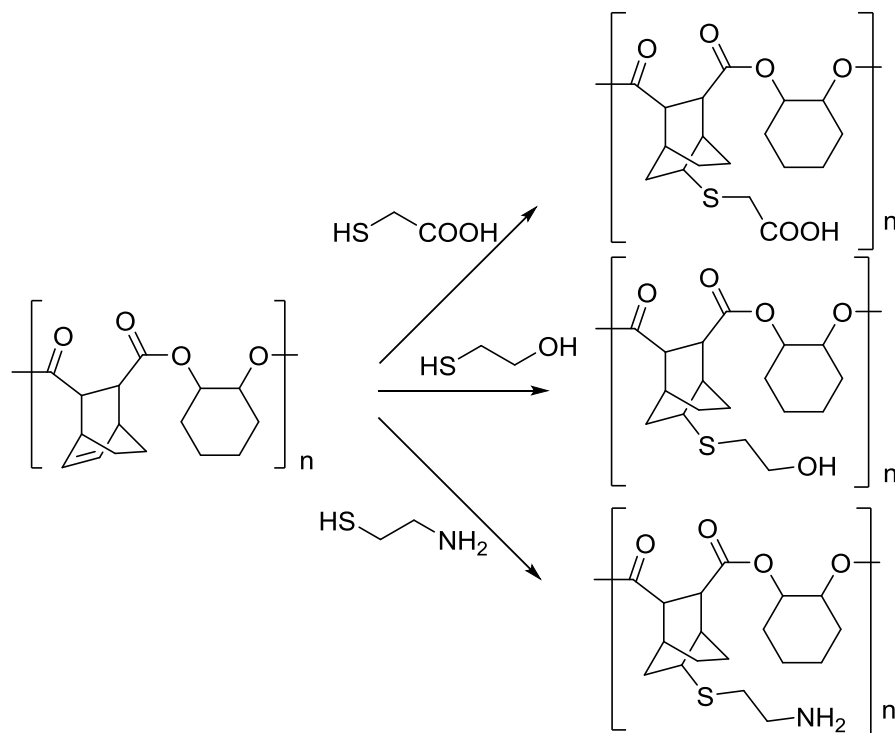
Palladium cross-coupling reactions have been utilised for PPM, these extremely effective reactions have very high functional group tolerance and form stable C-C bonds under mild conditions.<sup>45</sup> Whilst a wide variety of palladium-catalysed coupling reactions have been used extensively throughout organic chemistry, in the PPM of polymers, the Sonogashira coupling of organo halide groups with alkynes has been utilised most often.<sup>1</sup> Sessions *et al.* reported the palladium catalysed coupling reaction of poly(4-bromostyrene) with phenylacetylene or 1-hexyne at room temperature (Scheme 14).<sup>46</sup>



**Scheme 14** Palladium catalysed coupling reaction of poly(4-bromostyrene) with phenylacetylene or 1-hexyne<sup>46</sup>

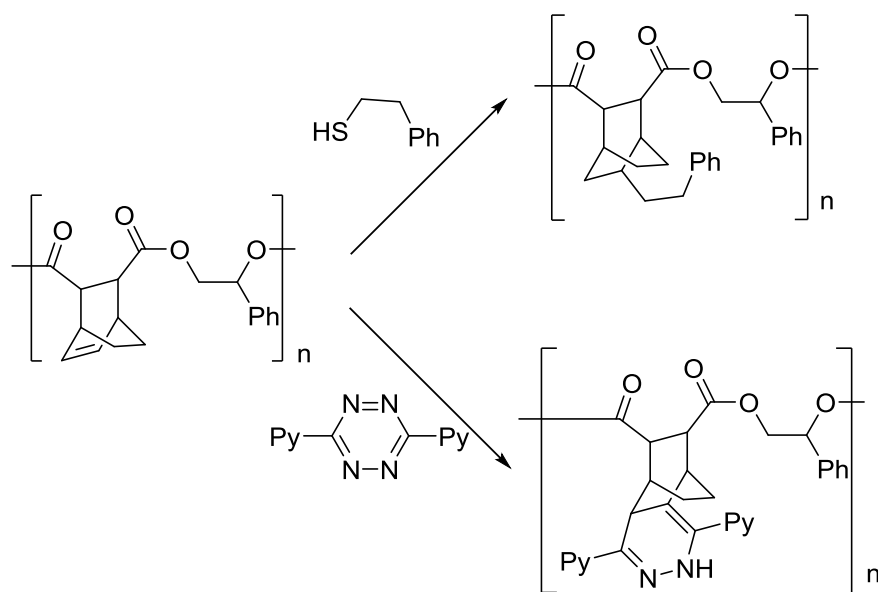


**4.1.2.1 Modification of copolymers synthesised from the ring-opening copolymerisation (ROCOP) of epoxides and cyclic anhydrides**

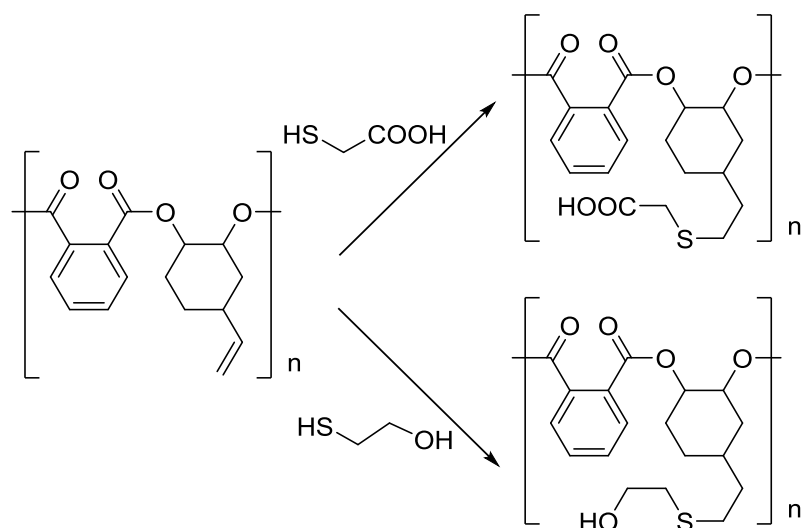


**Scheme 15** Thiol-ene click reaction of cyclohexene oxide and norbornene copolymers with thiols<sup>12</sup>

Post-polymerisation modification (PPM) has the potential to further tune the properties of the copolymers produced in the ring-opening copolymerisation (ROCOP) of epoxides and cyclic anhydrides. Liu *et al.* reported the synthesis of cyclohexene oxide (CHO) copolymers with cis-2,3-(exo, exo) or trans-2,3-(exo, endo) norbornene anhydride. The radical-initiated thiol-ene click reaction was utilised to modify the polymer chains by appending mercaptoacetic acid, mercaptoethanol and cysteamine, introducing a carboxylic acid, an alcohol and an amine group respectively (Scheme 15). The thiol-ene click reaction was initiated by azobis(isobutyronitrile) (AIBN) and proceeds via an anti-Markovnikov pathway. The PPM was successful and effectively varied the properties of the polymer, for example addition of mercaptoacetic acid to the polyester transformed the solubility, enabling the polymer to dissolve in ethanol following PPM whereas previously it was insoluble.<sup>12</sup>



**Scheme 16** Thiol-ene and azide click post-polymerisation modification (PPM) on styrene oxide and norbornene copolymers<sup>13</sup>



**Scheme 17** Thiol-ene click post-polymerisation modification (PPM) of 4-vinyl-cyclohexene oxide (VCHO) and phthalic anhydride (PhA)<sup>14</sup>

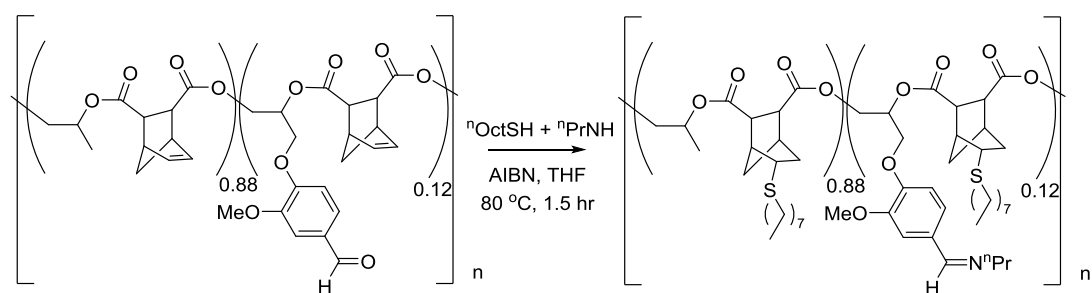
Norbornene anhydride (NA) was also copolymerised with styrene oxide (SO) and these polymers were functionalised by the photo-induced thiol-ene click and the tetrazine click reactions (Scheme 16). The addition of 2-phenylethanethiol, initiated by UV light exposure caused the  $T_g$  of the polymer to decrease from 87 °C to 68 °C illustrating again how PPM can be used to alter the properties of a copolymer. 3,6-Di-2-pyridyl-1,2,4,5-tetrazine reacted with the SO-NA copolymer resulting in a substantial change in the

## Chapter 4 - Post-polymerisation modification of copolymers

thermal properties. The introduction of the rigid aromatic azine caused the  $T_g$  to increase from 87 °C to 183 °C. Cheng and co-workers also showed how the polymer can be crosslinked by ring-opening metathesis polymerisation of the alkene in NA monomer catalysed by Grubbs' 3<sup>rd</sup> generation catalyst.<sup>13</sup> Another ROCOP monomer with a functionalisable double bond is 4-vinylcyclohexene oxide (VCHO). Liu and Li copolymerised this epoxide with phthalic anhydride (PhA) and performed the thiol-ene PPM to functionalise the polymer with mercaptoacetic acid and mercaptoethanol (Scheme 17).<sup>14</sup>

The ability to orthogonally functionalise copolymers provides the opportunity to control and tune polymer properties to an even greater extent. Properties such as thermal and mechanical behaviour, hydrophilicity, degradation kinetics and structural organisation may be controlled. This technology has the potential for application in targeted cell transfection, tissue engineering, antimicrobials and information storage.<sup>17,47</sup>

Coates *et al.* reported the orthogonal PPM of a polyester synthesised from the ROCOP of NA and an epoxide containing a pendant aldehyde. The alkene functionality was reacted with 1-octanethiol in a thiol-ene click reaction producing a thiol ether. The aldehyde moiety was reacted with *n*-propylamine yielding the corresponding imine. These two PPMs were carried out in tandem, in a one-pot reaction resulting in an orthogonally functionalised polyester (Scheme 18).<sup>16</sup>

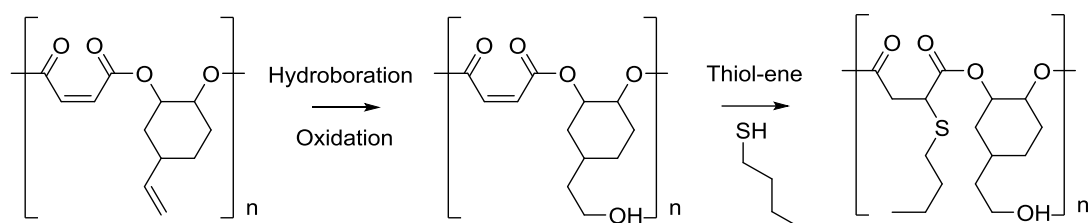


**Scheme 18** Orthogonal, one pot post-polymerisation modification (PPM)<sup>16</sup>

Williams and colleagues also reported orthogonal PPM of polyesters formed from the ROCOP of alkene containing epoxides and cyclic anhydrides. The epoxides used in the study contained pendant primary alkenes and the anhydrides contained secondary alkenes. The difference in the reactivity of

## Chapter 4 - Post-polymerisation modification of copolymers

primary and secondary alkenes in hydroboration reactions was utilised to selectively modify the primary vinyl group. Subsequent oxidation produced hydroxyl-appended polymers. The remaining secondary alkene groups were functionalised by UV-initiated, thiol-ene click reactions and a variety of thiols containing primary and tertiary amines and carboxylic acid groups were utilised. Scheme 19 shows a representative example of a VCHO–maleic anhydride copolymer functionalised by hydroboration oxidation and the thiol-ene click reaction with 1-butanethiol.<sup>17</sup>



**Scheme 19** Orthogonal post-polymerisation modification (PPM) of copolymer<sup>17</sup>

### 4.1.3 Introduction to the crosslinking of polymers

The crosslinking of thermoplastics is an effective approach to alter polymer properties. This process often improves the mechanical properties of a polymer such as the resistance to thermal degradation, and improves resistance to cracking, creep and cold flow. The degree of crosslinking greatly affects the extent to which polymer properties are modified.<sup>48</sup>

A lightly crosslinked material may be rigid or rubbery depending on temperature. Covalent bonds linking polymer chains together restricts mobility and increases the resistance to deformation. Lightly crosslinked materials retain many of the features of thermoplastics, as the polymer chains are still flexible between the crosslinks. These materials are often described as elastomers, of which a well-known example is vulcanised rubber.<sup>49</sup>

As the degree of crosslinking increases, the flexibility of the plastic decreases as polymer chain mobility is restricted until the glass transition temperature ( $T_g$ ) of the material exceeds the decomposition temperature. Polymers with high levels of crosslinking adopt hard, rigid properties like those of thermoset plastics. An example of such a material is a cured epoxy resin.<sup>50</sup>

#### **Chapter 4 - Post-polymerisation modification of copolymers**

In a crystalline polymer such as polyethylene, the material becomes more amorphous as the degree of crosslinking increases. This is due to the crosslinks preventing the polymer adopting the ordered crystalline structure. The effect of this change is a decrease in the melting point and the density of the polymer.<sup>51</sup>

Crosslinking has been used extensively in polyolefin chemistry to enhance their mechanical properties. The most commonly used methods for crosslinking these polymers are radiation crosslinking, crosslinking with organic peroxides and crosslinking with silane grafting agents.<sup>52</sup>

Crosslinking may be achieved through irradiation of polymer chains with X-rays or  $\gamma$ -rays. The high energy radiation causes covalent bond cleavage and allows for the generation of new bonds leading to the crosslinking of different polymer chains. Irradiation promotes the excitation or ionisation of molecules and the formation of highly reactive free radical species which will readily react with one another.<sup>53</sup>

For many polyolefins, such as polyethylene, low levels of irradiation results in an increase in flexibility and transparency as the plastic changes from crystalline to amorphous. Continued exposure to radiation causes the material to become harder and more brittle as the degree of crosslinking increases.<sup>51</sup> Other properties which are affected are tensile strength, yield strength, stiffness, solubility, elongation at break and crack resistance.<sup>54</sup> The degree of variation depends on the dose of radiation. When a polymer is irradiated degradation may occur, therefore when this approach is utilised for crosslinking, the dose of radiation must be carefully selected.<sup>51</sup>

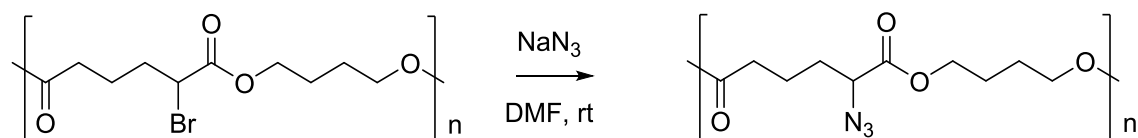
Crosslinking of polymers may be achieved by treatment with organic peroxides, this approach has been utilised for polymers such as polyethylene, polypropylene and polyvinylchloride.<sup>51</sup> The organic peroxides act as a source of free radicals which generate polymer centred radicals by hydrogen abstraction. Reaction of free radicals on adjacent polymer chains leads to crosslinking.<sup>55</sup> The advantage of this type of crosslinking is that organic peroxides are stable until heated to their decomposition temperature, meaning that the polymer and peroxide can be mixed, shaped and then heated to cause

## Chapter 4 - Post-polymerisation modification of copolymers

crosslinking. The major challenge with peroxide mediated crosslinking is the same as for radiative in that polymer degradation may occur.<sup>51</sup>

Crosslinking can be achieved by utilising silane crosslinking agents.<sup>51</sup> Initially a silane is grafted onto a polymer chain through radical chemistry. A polymer chain centred radical is generated by organic peroxide initiators, the free radical then reacts with an alkoxy silane. Hydrolysis of the silane alkoxy group then takes place and finally condensation of silanol groups on adjacent polymer chains achieves crosslinking.<sup>56</sup>

One advantage of silane crosslinking is the ability to tune the properties of the crosslinked plastic by varying the identity of the alkoxy silane reagent.<sup>51</sup> Silane crosslinking may be carried out in a two-step procedure, firstly, a silane is grafted onto a polyolefin, after which the polymer may be pelletized and stored, when required the material is subsequently crosslinked. This highly efficient process was developed in 1968 by Midland Silicones Company.<sup>57</sup> Alternatively, crosslinking can be achieved in a single step extrusion where all components are simultaneously mixed together in a procedure known as the Monosil process.<sup>51</sup>



**Scheme 20** Formation of azide containing polyester with the potential for crosslinking<sup>58</sup>

Crosslinking of polyesters is also possible, but requires different techniques compared to polyolefins, as intensive processes such as irradiation with X-rays or  $\gamma$ -rays leads to polymer degradation.<sup>51</sup> Shibata and colleagues reported the formation of an azide containing polyester which could be crosslinked through irradiation with UV light. The pendant azide functionalities were introduced to the copolymer of 2-bromoadipic acid and 1,4-butanediol by the reaction of the bromo groups with  $\text{NaN}_3$  (Scheme 20).<sup>58</sup> Olson *et al.* reported the formation of amorphous, degradable elastomers by crosslinking a *trans*- $\beta$ -hydromuconic acid – ethylene glycol copolymer. The polymer chains were crosslinked using benzoyl peroxide as a free radical initiator. Crosslinking

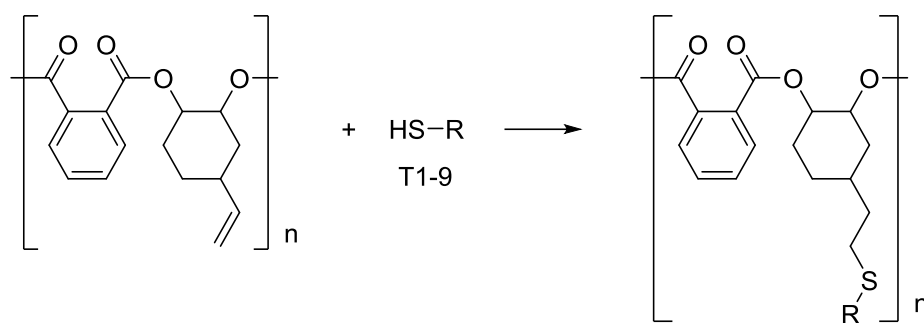
led to an increase in  $T_g$  of 15 °C. The properties of the elastomer were affected by the degree of crosslinking, which was controlled by the initiator concentration, reaction time and temperature. The length of the ethylene glycol section also affected properties with  $T_g$  decreasing as the length of the ethylene glycol increased. In addition to  $T_g$ , Young's modulus, ultimate stress and ultimate extension were modified by crosslinking.<sup>59</sup> Polyesters containing alkene groups in the polymer backbone can also be crosslinked by UV-irradiation.<sup>60</sup> Another approach to crosslink polyesters is to react the carbonyl groups of the polymer with biaminoxy compounds. This reaction leads to a polymer matrix linked by pH sensitive ketoxime ether linkages.<sup>61</sup>

### **4.2 Post-polymerisation modification of vinyl-containing copolymers using thiol-ene click chemistry**

As discussed in Section 4.1, post-polymerisation modification (PPM) is an effective method for varying the properties of polymers. A wide variety of properties can be altered such as glass transition temperature ( $T_g$ ), solubility or hydrophilicity. Crosslinking of polymer chains can also be introduced through PPM. Many of the polyesters produced by the ROCOP of epoxides and cyclic anhydrides contain functional groups that are candidates for PPM.<sup>15</sup> Examples of such copolymers are those synthesised in Chapter 2 containing vinylcyclohexene oxide (VCHO), epichlorohydrin (ECH) or 4-bromophthalic anhydride (4BPhA) monomers.

The copolymer from the ROCOP of VCHO and PhA was selected as a candidate for PPM due to the high molecular weight and low dispersity ( $\bar{D}$ ) of the polymer; non-functionalised copolymer samples were prepared using the phenoxide-appended 1,4,7-triazacyclononane aluminium catalyst (**1**) described in Chapter 2. The PPM selected for investigation was the radical-initiated thiol-ene click reaction in which thiols readily react with alkene functional groups to give a thioether in an atom economic process. There are a very wide range of structurally diverse thiols which have the potential to introduce a variety of different chemical architectures and functional groups to the polymer chain.<sup>62</sup> This will undoubtedly have an influence on the properties of the modified polymers.<sup>17</sup>

## Chapter 4 - Post-polymerisation modification of copolymers



**Scheme 21** Thiol-ene click reaction of a thiol with VCHO containing copolymer

A range of thiols were selected for the PPM reaction with VCHO–PhA copolymer (Scheme 21). Thiols with a variety of functional groups and distinctly different chemical architecture were chosen in order to elucidate any trends relating to the structure of the thiol and its subsequent effect on polymer properties following PPM.

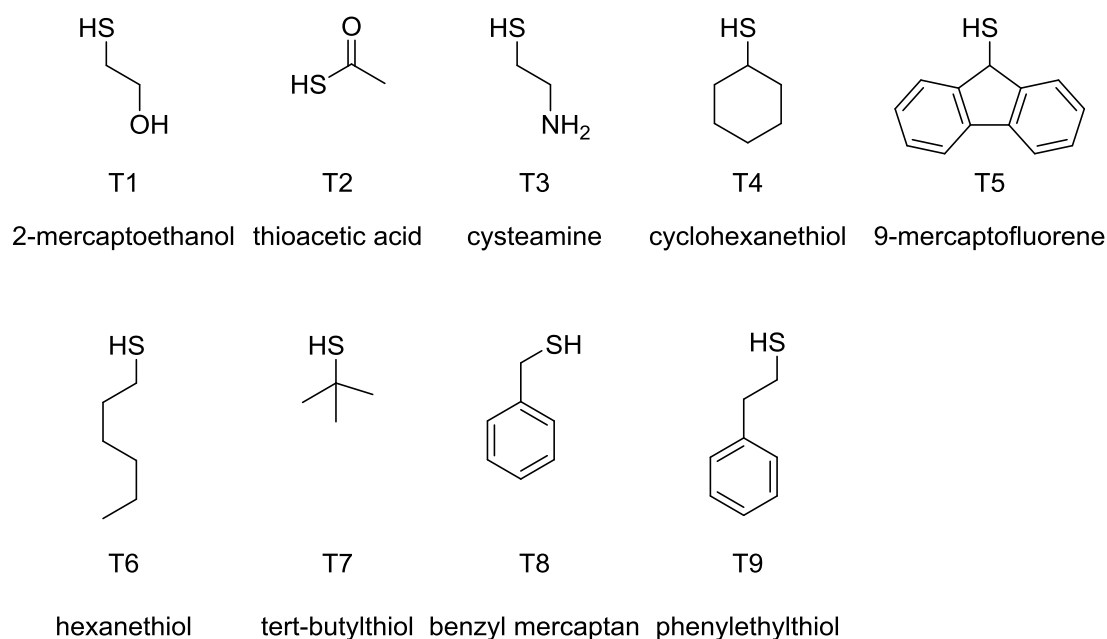


**Figure 1** Thiols used in PPM reactions

The selected thiols (T1 – 9) are shown in Figure 1. To illustrate the effect of the PPM on the mechanical properties of the copolymer, the  $T_g$  of the modified copolymers were measured, and any differences to the parent copolymer recorded.

The conditions used for the thiol-ene click reactions are quite forcing, in order to ensure complete conversion of the polymer vinyl groups. Uniform modifier incorporation is critical if any trends about the effect of different thiols on  $T_g$



are to be examined with any meaning; differing degrees of PPM conversion would make it very hard to make comparisons as even for the same thiol, a sample with a low degree of conversion may well give a very different  $T_g$  to one with high conversion. Previous work in this area by Liu and Li illustrates this issue, in the thiol-ene click reaction of a VCHO–PhA copolymer with 2-mercaptoethanol (T1), a conversion of only 65% was reported.<sup>14</sup> In this study, different thiols could lead to discrepancies in thiol uptake either by variations in reaction rate or by experimental error, therefore all PPM reactions were performed such that *all* of the vinyl groups were populated by the modifier, as a means of ensuring consistency between samples. Detailed reaction conditions are provided in the experimental (Chapter 7.4), however the key points are a fivefold excess of thiol to polymer, 66 mol% AIBN, heated at 80 °C in dry THF overnight.

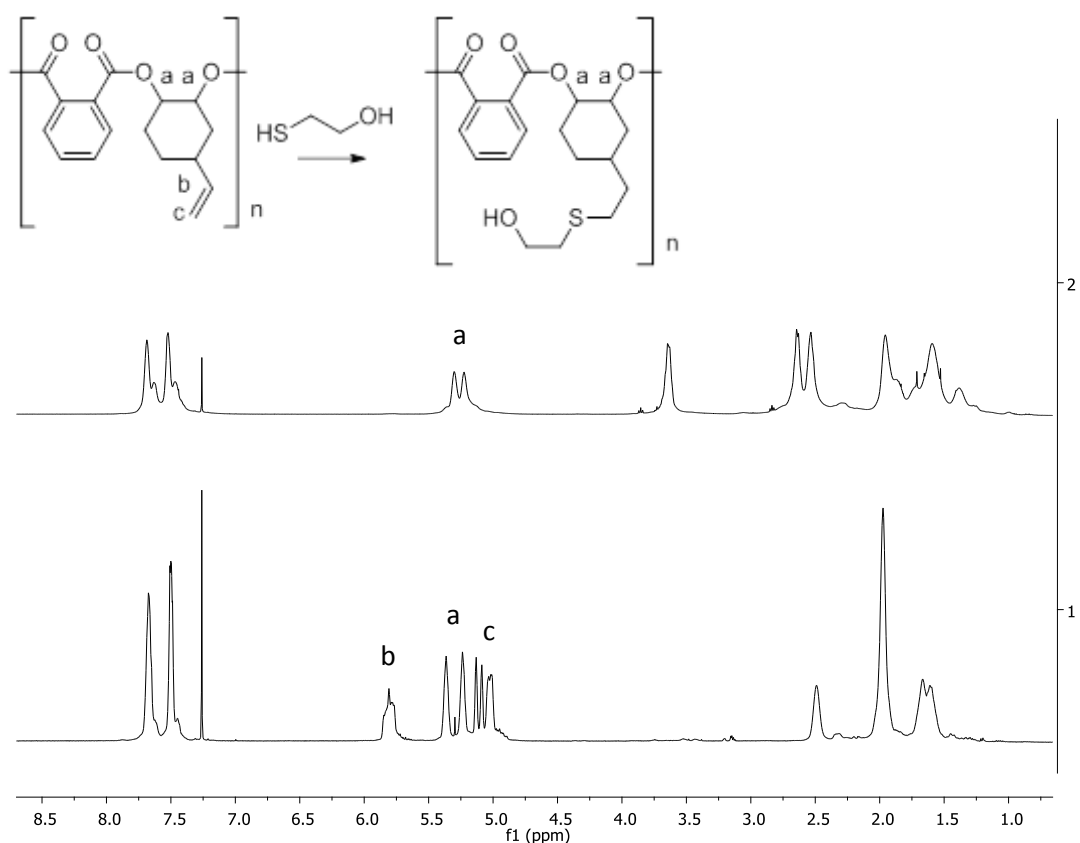


**Figure 2** <sup>1</sup>H NMR spectra (400 MHz, CDCl<sub>3</sub>) of VCHO–PhA (Spectrum 1, bottom) and (400 MHz, CDCl<sub>3</sub>) VCHO–PhA–T1 (Spectrum 2, top).

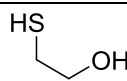
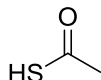
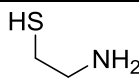
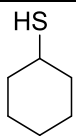
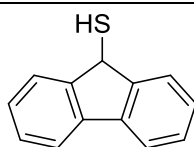
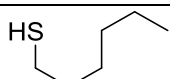
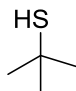
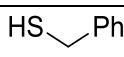
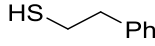
The conversion of the thiol-ene click PPM reaction with the VCHO–PhA copolymer was quantified using <sup>1</sup>H NMR spectroscopy. The

## Chapter 4 - Post-polymerisation modification of copolymers

integration of the vinyl group signals at 5 – 6 ppm, relative to the aromatic signals associated with the phenyl ring of phthalic anhydride at 7.5 – 7.8 ppm (which are left unaffected by the PPM reaction) were used to calculate the conversion (Figure 2).

The series of thiols T1 – 9 were tested for the thiol-ene click PPM reactions with the copolymer VCHO–PhA. The results are shown the Table 1.

**Table 1** PPM reactions of thiols T1 – 9 with VCHO–PhA

Thiol	Thiol structure	Conversion % <sup>a</sup>	Yield % <sup>b</sup>
T1		100	54
T2		0	0
T3		0	0
T4		100	61
T5		0	0
T6		100	55
T7		100	81
T8		0	0
T9		100	42

<sup>a</sup>Conversion calculated from <sup>1</sup>H NMR spectra. <sup>b</sup>Isolated yield.

The thiols probed in this study did not exhibit uniform reactivities in the PPM of VCHO–PhA copolymer. T1, T4, T6, T7 and T9 all successfully reacted with the copolymer and the modified polymer was isolated in moderate to good yields with the expected (and targeted) quantitative thiol uptake. Conversely, T2, T3, T5 and T8 showed no reactivity under the conditions employed, with

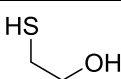
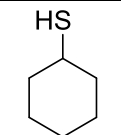
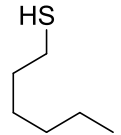
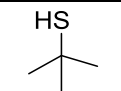
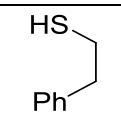
only non-functionalised copolymer being detected by  $^1\text{H}$  NMR spectroscopy. It is surprising that only quantitative or zero conversions were achieved based on crude  $^1\text{H}$  NMR measurements (i.e. there were no PPM reactions with mid-range thiol uptakes). That the successful reactions universally proceeded to 100% conversion is unsurprising, since forcing reaction conditions were invoked to achieve this outcome. The long reaction time and substantial excess of thiol meant that any small differences in reactivity of the thiols did not result in any observable differences to the molecular transformation of the copolymers. It is more surprising that some thiols failed to undergo PPM reactions even under such forcing conditions as those employed in this study.

In an attempt to rationalise the observed reactivities, it is possible to make some tentative conclusions based on the performances of the different thiols. Firstly, the steric hindrance around the thiol group doesn't seem to play a significant role, as the more sterically demanding T7 was found to react with the copolymer, as did the straight alkyl chain thiol T6. Conversely, close proximity of an aromatic group to the thiol functionality does seem to inhibit reactivity. This is illustrated by T8 and T9, where the thiol and the phenyl ring are separated by methylene and ethylene groups respectively; T9 successfully reacted with the VCHO–PhA copolymer whereas T8 did not, indicating the longer alkyl chain between the two functional groups in the thiol is important for reactivity. This may also explain why T5 showed no reactivity. The reason for this observation is unclear, since in no case are the thiol groups directly bonded to an aromatic system; if this were so then one could postulate radical deactivation in the aromatic ring, but that argument seems unlikely in the thiols used in this study. There is evidence in the literature of successful thiol-ene click reactions with T2, T3, and T8. Goessl and colleagues utilised the AIBN mediated thiol-ene click reaction to combine allyl ether terminated poly(ethylene glycol) and T2.<sup>63</sup> Han *et al.* successfully undertook the AIBN initiated thiol-ene click PPM of the copolymer formed from CHO and norbornene anhydride with T3.<sup>12</sup> Schlaad and colleagues reported the AIBN initiated thiol-ene reaction of T8 with 1,2-polybutadienes.<sup>64</sup> Additionally Benny *et al.*<sup>65</sup> and Kokotos *et al.*<sup>66</sup> reported the photoinitiated thiol-ene click reactions with T8. It is entirely possible that other extraneous factors are involved to

## Chapter 4 - Post-polymerisation modification of copolymers

affect the observed reactivity. The radical-initiated thiol-ene click reaction is air and moisture sensitive, therefore the presence of adventitious H<sub>2</sub>O or O<sub>2</sub> may be a reason for failed reactions, however identical experimental procedure was employed for every PPM experiment in order to remove the presence of air and moisture. Some reactants are quite unstable, such as AIBN or the thiols, which may degrade or undergo side reactions such as disulphide formation; a greater spectrum of substrates would need to be probed before any concrete conclusions drawn in relation to structure-activity relationships.<sup>62</sup>

**Table 2** Properties of VCHO–PhA copolymer before and after PPM by thiol addition

Entry	Thiol	Before PPM		After PPM			
		Mn <sup>a</sup> (gmol <sup>-1</sup> )	Đ <sup>a</sup>	Mn <sup>a</sup> (gmol <sup>-1</sup> )	Theoretical Mn increase (%)	Đ <sup>a</sup>	T <sub>g</sub> °C <sup>b</sup>
VCHO–PhA	-	12120	1.126	-	-	-	113±7
VCHO–PhA– T1		12120	1.126	25650	27	1.216	126±2
VCHO–PhA– T4		11750	1.151	19130	40	1.169	116±7
VCHO–PhA– T6		12030	1.137	21770	41	1.166	57±2
VCHO–PhA– T7		12030	1.137	14740	31	1.176	124±2
VCHO–PhA– T9		19530	1.161	30160	48	1.143	109±1

<sup>a</sup>Determined by GPC using triple detection. <sup>b</sup>Determined by DMA.

$$Mn \text{ percentage increase} = \frac{[(Mn \text{ after}) - (Mn \text{ before})]}{(Mn \text{ before})} \times 100$$

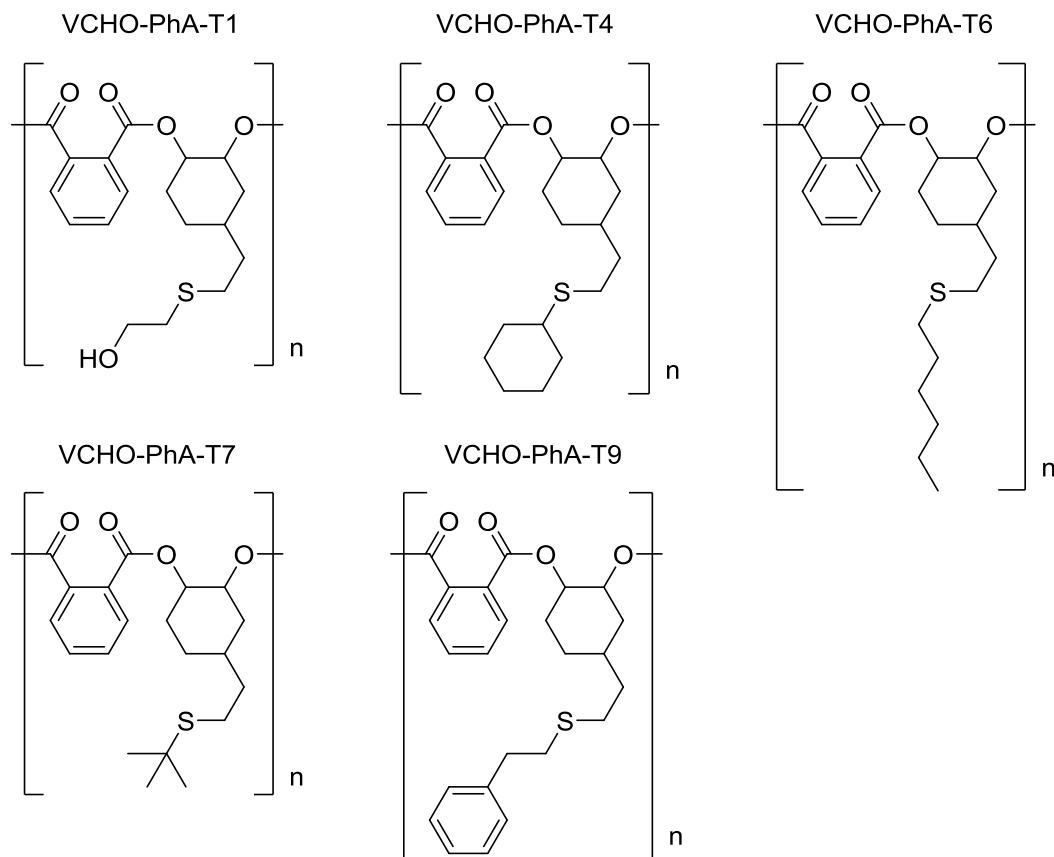
**Equation 1** Percentage increase of Mn

Table 2 shows how the polymer properties changed following the thiol-ene click PPM reactions. The number average molecular weight (Mn) and Đ of the polymer are shown before and after reaction with each thiol. The T<sub>g</sub> of the polymers is also reported and illustrates the effect on polymer mechanical properties following introduction of different sidechains along the polymer backbone.

Following the PPM reactions of VCHO–PhA with T1, T4, T6, T7 and T9, the molecular weight of the polymer increased in all cases. An increase is to be expected following the appendage of the thiols along the polymer chains. The increase in Mn varied from 7,380 – 13,530 g mol<sup>-1</sup> for all the thiols apart from T7 where a smaller increase of 2,710 g mol<sup>-1</sup> was observed. The increase in Mn can be quantified by the percentage increase calculated by Equation 1. PPM with T1 led to an increase in Mn of 112%, this is much higher than the theoretical percentage increase of 27% (assuming 100% conversion of vinyl groups). The percentage increase in Mn following the thiol-ene click reaction with T6 was far higher than what would be theoretically expected with values of 81% and 41% calculated for the percentage increase and theoretical percentage increase respectively. PPM with T4 and T9 gave rise to percentage increases in Mn (63% and 54% respectively) that were closer to the calculated theoretical increases (40% and 48% respectively). The larger than expected increase in Mn indicates that the introduction of branching has caused expansion of the dissolved polymer coil. Only for the PPM with T7 was the percentage increase in Mn (23%) lower than the calculated theoretical percentage increase (31%). Molecular weight determination of branched polymers by GPC often exhibits high levels of inaccuracy even when multiple detectors are employed.<sup>67</sup>

Gratifyingly following the PPM reactions and increase in Mn, the Đ remained low (1.14 – 1.22) indicating a controlled reaction in which the polymer backbone is unaffected; for example side-reactions involving chain scission

are expected to increase the dispersity since the chains would be split at random, thus increasing the range of molecular weights in the sample.



**Figure 3** Polymer repeat units following PPM reactions with thiols

These results indicate that the PPM reactions successfully attached thiols with a variety of chemical structures along the polymer chain. Figure 3 shows the polymer repeat unit following the thiol-ene click reactions with T1, T4, T6, T7 and T9. VCHO-PhA-T1 yielded a polymer with new hydroxyl functional groups along the chain. This new functionality is very useful as it opens the possibility of further reactions utilising the alcohol groups. It will also greatly influence the solubility, hydrophilicity and pH of the polymer. VCHO-PhA-T4 introduced pendant cyclohexyl groups to the copolymer. In VCHO-PhA-T6 a <sup>n</sup>hexyl group was added. VCHO-PhA-T7 introduced sterically demanding *tert*-butyl groups and VCHO-PhA-T9 saw the introduction of an aromatic phenyl group. These now chemically distinct polymers should have quite different polymer properties, despite being derived from a common base-polymer. The  $T_g$  values of these polymers were measured by Dynamic materials analysis

#### **Chapter 4 - Post-polymerisation modification of copolymers**

(DMA) and the results are shown in Table 2. This work was carried out in collaboration with Dr Mark Eaton and Kyriaki Gkaliou from Cardiff University. Raw data was recorded by Kyriaki Gkaliou. The  $T_g$  of VCHO–PhA is also given for comparison.  $T_g$  values for each sample before functionalisation were not obtained, but are not expected to be significantly different than the non-functionalised sample in VCHO–PhA, given the relatively large uncertainty of the  $T_g$  values of 7 °C. VCHO–PhA–T4 and VCHO–PhA–T9 had very similar  $T_g$  values (113 °C and 109 °C respectively) to the unmodified copolymer indicating the addition of pendant cyclohexyl and phenyl groups to VCHO–PhA had limited effect with regards to  $T_g$ . The addition of the  $n$ hexyl groups in VCHO–PhA–T6 had a significant effect on the  $T_g$ , changing from 113 °C to 57 °C. Long flexible alkyl chains are known to decrease the glass transition temperature of polymers<sup>15</sup> and so this result is perhaps unsurprising, but does showcase how the glass transition temperature can be modified in a targeted manner by judicious choice of modifier. The introduction of the *tert*-butyl groups in VCHO–PhA–T7 caused the  $T_g$  to increase to 124 °C. VCHO–PhA–T1 saw an increase in the  $T_g$  from 113 °C to 126 °C following appendage of hydroxyl groups to the polymer chain. The introduction of bulky and polar substituents is known to increase the  $T_g$  of a polymer; sterically demanding groups or functionalities which exhibit strong intermolecular forces of attraction such as hydrogen bonding, hinder the translational and rotational motion of polymer chains.<sup>49</sup>

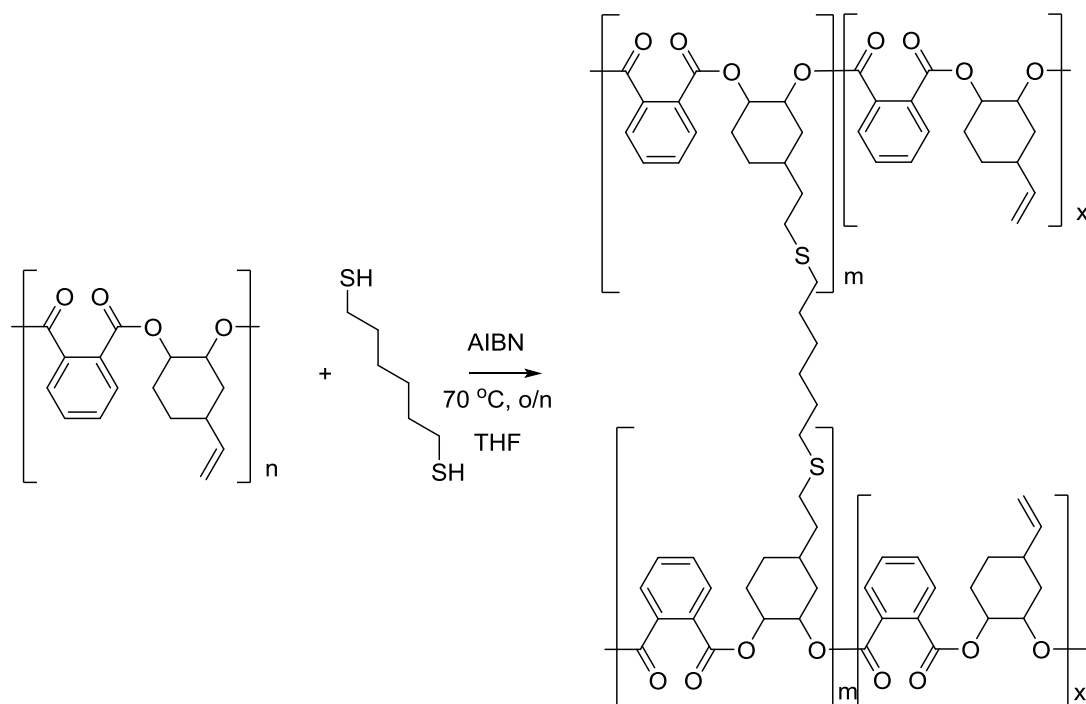
These results indicate that PPM through a thiol-ene click reaction can successfully vary polymer properties. This is illustrated by changes in polymer glass transition temperature ( $T_g$ ). This approach can therefore be used to fine tune polymer properties. The effect of the addition of T1, T7 and T6 on the  $T_g$  of the VCHO–PhA copolymer can be rationalised based on established knowledge of the effect of polymer structure on its properties. However to understand the full structure-property relationship, further PPM and analysis of VCHO–PhA with different thiols is required, and this may be the subject of further work in this field.

Whilst  $T_g$  has been used to demonstrate property tuning, there are other properties that can be probed such as solubility, hydrophilicity etc. There is

scope here to make polymers with a much greater spectrum of properties and this will be the subject of further research, which will follow on from this study.

### **4.3 Crosslinking of copolymers with dithiols**

Employing dithiols in the thiol-ene click reaction with the vinyl-containing polyester VCHO–PhA has the potential to introduce crosslinking into the polymer matrix. Crosslinking has been used extensively to modify the properties of polyolefins<sup>54</sup> and to a more limited extent polyesters.<sup>51</sup> Crosslinking can improve the mechanical properties of a plastic increasing characteristics such as glass transition temperature ( $T_g$ ), resistance to cracking and thermal degradation.<sup>68</sup>



**Scheme 22** VCHO–PhA crosslinked with 1,6-hexanedithiol

Many of the chemically/energy intensive techniques commonly employed to achieve crosslinking in polyolefins are not suitable for polyesters, as they cause polymer degradation.<sup>51</sup> The thiol-ene click reaction is a promising alternative approach to achieve crosslinking. To investigate this pathway, 1,6-hexanedithiol was selected as a crosslinking agent for the epoxide–anhydride copolymer VCHO–PhA, with the intention of the two thiol



groups bonding to different polymer chains to effect crosslinking. In this investigation the thiol-ene click reaction was catalysed by the free-radical initiator AIBN (Scheme 22). 1,6-Hexanedithiol is a good candidate for the crosslinking agent as the monofunctional 1-hexanethiol, utilised in the prior investigation into PPM (Chapter 4.2), successfully reacted with VCHO–PhA (VCHO–PhA–T6) yielding complete conversion of the polymer vinyl groups. It is important to achieve complete conversion in the crosslinking reaction to avoid appendage of the crosslinking agent to a polymer chain through one thiol group and not the other, and thereby producing a functionalised polymer with a pendant thiol and consequently not attaining the desired crosslinking. Similar reaction conditions to those used in the PPM of VCHO–PhA were employed for the crosslinking, however instead of an excess of thiol, the amount of 1,6-hexanedithiol was carefully controlled so as to control the degree of crosslinking in the final polymer.

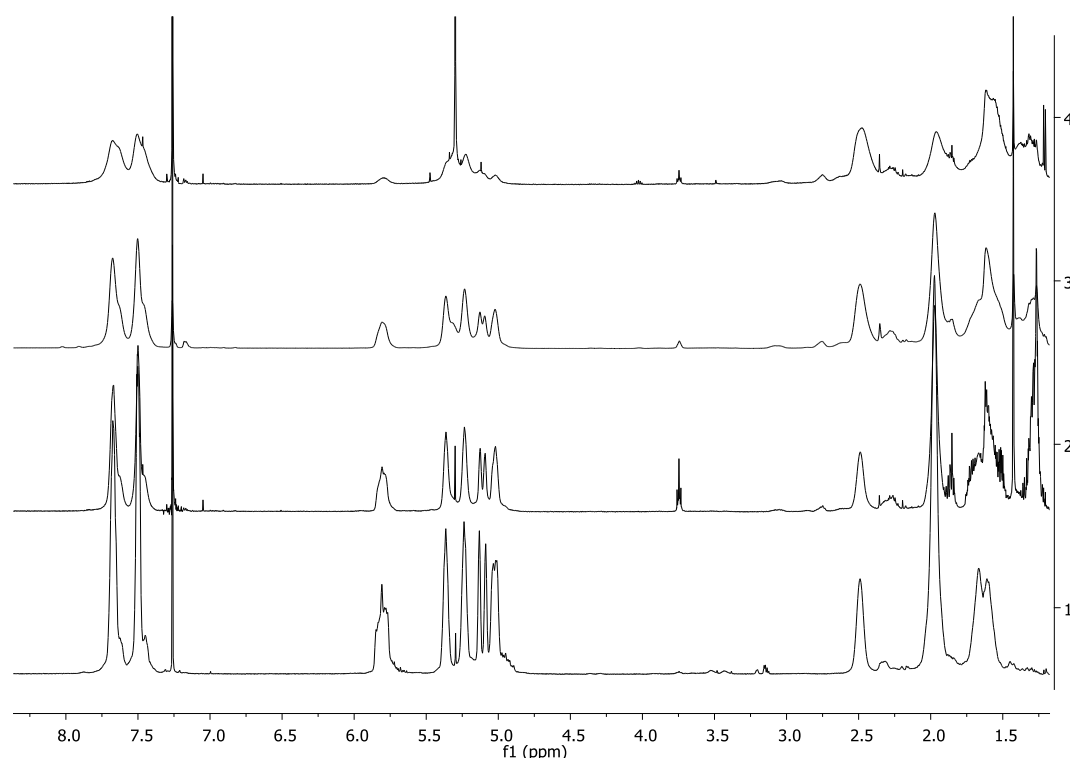


**Figure 4**  $^1\text{H}$  NMR spectra (400 MHz,  $\text{CDCl}_3$ ) of VCHO–PhA (1.), (500 MHz,  $\text{CDCl}_3$ ) VCHO–PhA–x10 (2.), VCHO–PhA–x20 (3.) and VCHO–PhA–x40 (4.)

To investigate how effectively the degree of crosslinking can be controlled, 10 mol%, 20 mol% and 40 mol% of 1,6-hexanedithiol was combined with

## Chapter 4 - Post-polymerisation modification of copolymers

VCHO–PhA and the degree of crosslinking achieved after 16 hours at 70 °C was determined by  $^1\text{H}$  NMR spectroscopy. The  $^1\text{H}$  NMR spectra of the starting polymer VCHO–PhA and the crosslinked polymers VCHO–PhA–x10, VCHO–PhA–x20 and VCHO–PhA–x40 which were formed following the addition of 10 mol%, 20 mol% and 40 mol% respectively are shown in Figure 4. As the degree of crosslinking increases, the signals in the spectra become broader. Increasing the crosslinking decreased the solubility of the polymer and this led to spectra with lower intensity. Despite this, the degree of crosslinking could still be ascertained for all reactions. In VCHO–PhA–x40, the resulting crosslinked polymer swelled when added to chloroform, this phenomenon is commonly observed in crosslinked polymers.<sup>69</sup>

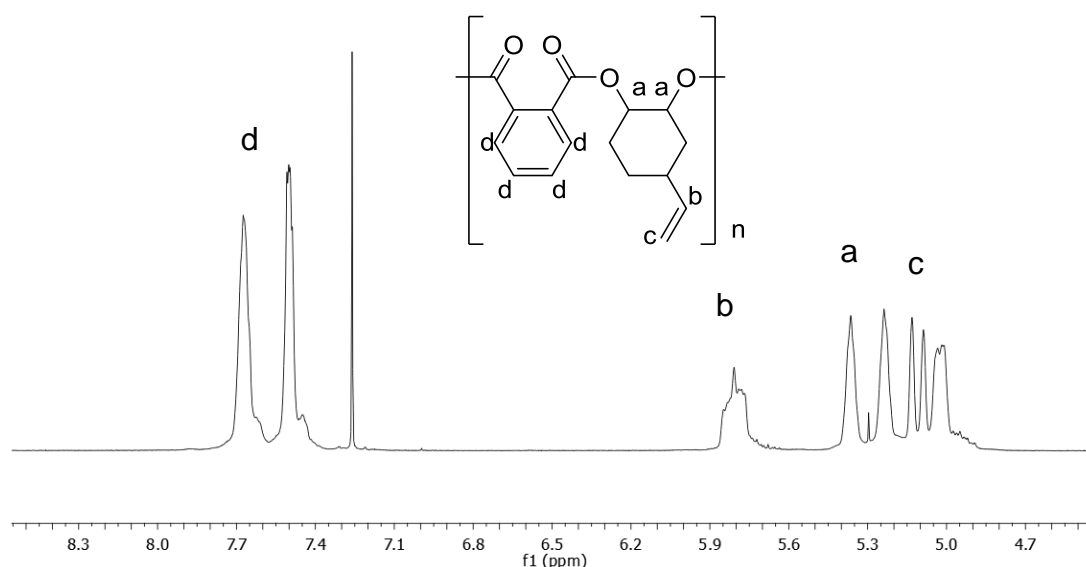


**Figure 5**  $^1\text{H}$  NMR (400 MHz,  $\text{CDCl}_3$ ) of VCHO–PhA

A section of the  $^1\text{H}$  NMR spectrum (4.5 – 8.5 ppm) of the non-functionalised copolymer VCHO–PhA is shown in Figure 5. In Figure 5, the signals in the spectrum are assigned to specific environments in the polymer repeat unit. The protons alpha to the ester bonds in the polymer backbone (a) are assigned to the resonances with chemical shifts of 5.24 and 5.36 ppm. The ( $-\text{CH}=\text{CH}_2$ ) proton of the vinyl group (b) corresponds to the signal at a chemical shift of 5.81 ppm. The ( $-\text{CH}=\text{CH}_2$ ) protons of the pendant vinyl group (c) gives rise to the multiplet at 5.08 ppm. The protons of the aromatic ring (d) correspond to the chemical shifts between 7.4 – 7.8 ppm.

## Chapter 4 - Post-polymerisation modification of copolymers

The product of the thiol-ene click reaction between the vinyl group of VCHO–PhA and 1,6-hexanedithiol is a thioether.<sup>62</sup> This transformation will cause the disappearance of the vinyl signals (b and c) in the <sup>1</sup>H NMR spectrum, with the concomitant appearance of new signals at <3 ppm associated with the thioether.

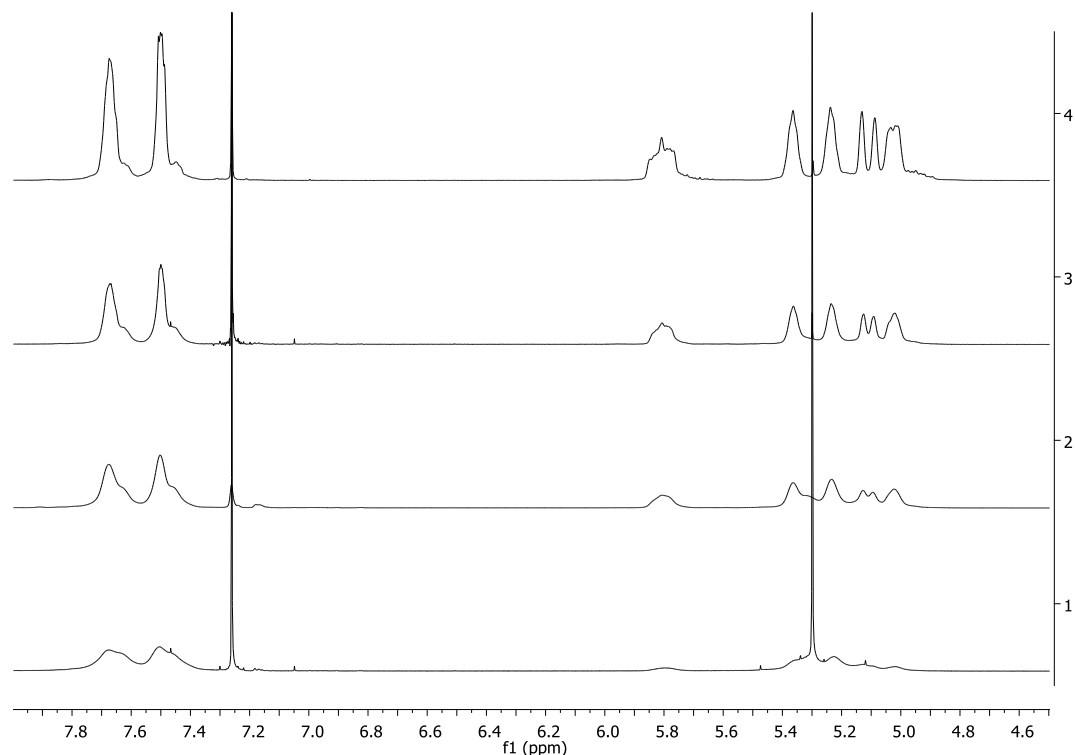


**Figure 6** <sup>1</sup>H NMR (400 MHz, CDCl<sub>3</sub>) spectra between 4.5 – 8 ppm of VCHO–PhA (4.), (500 MHz, CDCl<sub>3</sub>) VCHO–PhA–x10 (3.), VCHO–PhA–x20 (2.) and VCHO–PhA–x40 (1.)

**Table 3** The conversion of the vinyl group in the VCHO–PhA copolymer after crosslinking reaction.

Entry	1,6-hexanedithiol mol%	Conversion of vinyl group	
		Theoretical (%)	Actual (%) <sup>a</sup>
VCHO–PhA–x10	10	20	19
VCHO–PhA–x20	20	40	43
VCHO–PhA–x40	40	80	78

<sup>a</sup>Conversion calculated from <sup>1</sup>H NMR spectra

Conversion of the thiol-ene reaction can therefore be calculated as the relative decrease in integration of the vinyl group signals compared to those of an unaffected proton environment. In this study, the conversion, and therefore the

#### Chapter 4 - Post-polymerisation modification of copolymers

degree of crosslinking, was determined by comparing the relative intensity of the ( $-\text{CH}=\text{CH}_2$ ) (b) signals to those of the aromatic protons (d). In the starting copolymer VCHO–PhA, the relative integrations of b:d is 1.01:4. Following addition of 10, 20 and 40 mol% of 1,6-hexanedithiol, the ratio changed to 0.82:4, 0.58:4 and 0.23:4, equating to conversions of 19%, 43% and 78% respectively, (Figure 6). As shown in Table 3, the conversions determined by  $^1\text{H}$  NMR spectroscopy correspond well to the theoretical conversions based on the amount of 1,6-hexanedithiol used in each reaction. The slight variations are most likely caused by small differences between the intended quantity of a reactant and the actual quantity used. These results show that the degree of crosslinking introduced to VCHO–PhA by the thiol-ene click reaction with 1,6-hexanedithiol can be selectively controlled and the varied from a low level of crosslinking (19%) to a high level (78%).

Crosslinking of VCHO–PhA led to a significant decrease in the solubility of the polymer. This is a common effect of crosslinking.<sup>51</sup> The lack of solubility of VCHO–PhA–x10, VCHO–PhA–x20 and VCHO–PhA–x40 in THF meant that it was not possible to investigate the change in molecular weight of the polymer following crosslinking using GPC.

**Table 4** The  $T_g$  values of the crosslinked polymers VCHO–PhA–x20 and VCHO–PhA–x40 and the original copolymer VCHO–PhA.

Entry	Degree of crosslinking (%) <sup>a</sup>	$T_g$ (°C) <sup>b</sup>
VCHO–PhA	0	113±7
VCHO–PhA–x20	43	131±6
VCHO–PhA–x40	78	157±6

<sup>a</sup>Degree of crosslinking calculated from  $^1\text{H}$  NMR spectra. <sup>b</sup>Determined by DMA

The crosslinked polyesters VCHO–PhA–x20 and VCHO–PhA–x40, which have degrees of crosslinking of 43% and 78% respectively were analysed by DMA. This work was carried out in collaboration with Dr Mark Eaton and Kyriaki Gkaliou from Cardiff University. Raw data was recorded by Kyriaki Gkaliou. This investigation will measure the effect of crosslinking on the  $T_g$  of the polyesters. The  $T_g$  values of VCHO–PhA–x20 and VCHO–PhA–x40 and the starting copolymer VCHO–PhA are shown in Table 4. The  $T_g$  would be

## **Chapter 4 - Post-polymerisation modification of copolymers**

expected to increase as a result of crosslinking and the degree of crosslinking should influence the extent of the increase.<sup>50</sup>

The glass transition temperature of VCHO–PhA increased substantially after crosslinking. The  $T_g$  increased from 113 °C for the non-crosslinked polymer, to 131 °C for the 43% crosslinked polymer. The  $T_g$  increased further for the 78% crosslinked polymer for which a value of 157 °C was measured. This increase in  $T_g$  with the degree of crosslinking is a result of the decreasing translational freedom of polymer chains as they become more crosslinked. As it becomes more difficult for polymer chains to move past one another the  $T_g$  increases.<sup>70</sup> Considering the reaction with the monofunctional 1-hexanethiol (VCHO–PhA–T6) led to a significant *decrease* in  $T_g$  (57 °C) the fact the reactions with 1,6-hexanedithiol caused an increase in  $T_g$  is good evidence that crosslinking was achieved.

### **4.4 Summary**

In conclusion, the properties of copolymers synthesised via the ROCOP of cyclic anhydrides and epoxides were fine-tuned through post-polymerisation modification (PPM). In this study, the vinyl containing polyester VCHO–PhA was modified by reaction with a diverse range of thiols and crosslinked by the bifunctional 1,6-hexanedithiol. These transformations were achieved via AIBN initiated thiol-ene click chemistry.

In the PPM of VCHO–PhA, the thiols 2-mercaptoethanol, cyclohexanethiol, 1-hexanethiol, *tert*-butylthiol and phenylethylthiol were successfully appended and complete conversion of the polymer vinyl groups was achieved. As expected, the molecular weight of the polymer increased following PPM and gratifyingly the polymer Đ remained low (1.14-1.22), indicating that the PPM had not caused polymer degradation. The influence on mechanical properties was investigated by observing how PPM affected the  $T_g$  of the polymer. Reaction with cyclohexanethiol and phenylethylthiol led to only small changes in the  $T_g$  of the copolymer. The addition of the long alkyl group of 1-hexanethiol caused a significant decrease in  $T_g$  from 113 °C to 57 °C, while appendage of bulky *tert*-butyl groups and polar hydroxyl functionalities increased the  $T_g$  of the copolymer to 126 °C and 124 °C respectively.

## **Chapter 4 - Post-polymerisation modification of copolymers**

The copolymer VCHO–PhA could also be crosslinked by the thiol-ene addition of 1,6-hexanedithiol. The degree of crosslinking could be controlled by the quantity of 1,6-hexanedithiol added to the polymer. Addition of 10 mol%, 20 mol% and 40 mol% produced polymers with degrees of crosslinking of 19%, 43% and 78% respectively. The effect of crosslinking on the physical properties of the copolymer was investigated by measuring the change in the glass transition temperature ( $T_g$ ) of the polymer at different degrees of crosslinking. The  $T_g$  of VCHO–PhA increased from 113 °C to 131 °C when the polymer was 43% crosslinked, the  $T_g$  increased further to 157 °C when the polymer was 78% crosslinked. This work shows the degree of crosslinking and consequently the  $T_g$  of the copolymer can be controlled, and therefore tailored for specific applications.

In the future, the effect of PPM and crosslinking on other polymer properties such as hydrophilicity, solubility, polymer self-assembly, toughness and fracture resistance could be studied. The degree to which properties can be tuned by these approaches should be investigated by reacting different thiols with a variety of different epoxide–anhydride copolymers. The observed swelling of the crosslinked VCHO–PhA in presence of chloroform, highlights the potential of these copolymers as absorbent materials. Whilst not the focus of this project, it would be interesting to employ hydrophilic crosslinkers to make a water-absorbent polymer that would biodegrade, for example in disposable babies' nappies. Finally, PPM may be an effective approach to introduce useful properties to these hydrolysable polyesters such as flame retardancy or biological activity. These future investigations have been unlocked as a result of this study.

### **4.5 References for Chapter 4**

- 1 K. A. Günay, P. Theato and H.-A. Klok, *J. Polym. Sci. Part Polym. Chem.*, 2013, **51**, 1–28.
- 2 M. A. Gauthier, M. I. Gibson and H.-A. Klok, *Angew. Chem. Int. Ed.*, 2009, **48**, 48–58.
- 3 V. Percec, C. Grigoras and H.-J. Kim, *J. Polym. Sci. Part Polym. Chem.*, 2004, **42**, 505–513.

#### Chapter 4 - Post-polymerisation modification of copolymers

- 4 B. M. Rosen, G. Lligadas, C. Hahn and V. Percec, *J. Polym. Sci. Part Polym. Chem.*, 2009, **47**, 3940–3948.
- 5 M. Bathfield, F. D’Agosto, R. Spitz, M.-T. Charreyre and T. Delair, *J. Am. Chem. Soc.*, 2006, **128**, 2546–2547.
- 6 M. Li, P. De, S. R. Gondi and B. S. Sumerlin, *J. Polym. Sci. Part Polym. Chem.*, 2008, **46**, 5093–5100.
- 7 P. J. Roth and P. Theato, *Chem. Mater.*, 2008, **20**, 1614–1621.
- 8 P. J. Roth, K. T. Wiss, R. Zentel and P. Theato, *Macromolecules*, 2008, **41**, 8513–8519.
- 9 P. J. Roth, D. Kessler, R. Zentel and P. Theato, *J. Polym. Sci. Part Polym. Chem.*, 2009, **47**, 3118–3130.
- 10 G. E. Serniuk, F. W. Banes and M. W. Swaney, *J. Am. Chem. Soc.*, 1948, **70**, 1804–1808.
- 11 L. M. Campos, K. L. Killops, R. Sakai, J. M. J. Paulusse, D. Damiron, E. Drockenmuller, B. W. Messmore and C. J. Hawker, *Macromolecules*, 2008, **41**, 7063–7070.
- 12 B. Han, L. Zhang, B. Liu, X. Dong, I. Kim, Z. Duan and P. Theato, *Macromolecules*, 2015, **48**, 3431–3437.
- 13 R. Baumgartner, Z. Song, Y. Zhang and J. Cheng, *Polym. Chem.*, 2015, **6**, 3586–3590.
- 14 G. Si, L. Zhang, B. Han, Z. Duan, B. Li, J. Dong, X. Li and B. Liu, *Polym. Chem.*, 2015, **6**, 6372–6377.
- 15 J. M. Longo, M. J. Sanford and G. W. Coates, *Chem. Rev.*, 2016, **116**, 15167–15197.
- 16 M. J. Sanford, N. J. V. Zee and G. W. Coates, *Chem. Sci.*, 2017, **9**, 134–142.
- 17 N. Yi, T. T. D. Chen, J. Unruangsri, Y. Zhu and C. K. Williams, *Chem. Sci.*, 2019, **10**, 9974–9980.
- 18 H. C. Kolb, M. G. Finn and K. B. Sharpless, *Angew. Chem. Int. Ed.*, 2001, **40**, 2004–2021.
- 19 R. Riva, S. Schmeits, F. Stoffelbach, C. Jérôme, R. Jérôme and P. Lecomte, *Chem. Commun.*, 2005, 5334–5336.
- 20 V. Castro, H. Rodríguez and F. Albericio, *ACS Comb. Sci.*, 2016, **18**, 1–14.

#### **Chapter 4 - Post-polymerisation modification of copolymers**

- 21 K. Horisawa, *Front. Physiol.*, 2014, **5**, 457.
- 22 A. Salic and T. J. Mitchison, *Proc. Natl. Acad. Sci.*, 2008, **105**, 2415–2420.
- 23 R. Barbey and H.-A. Klok, *Langmuir*, 2010, **26**, 18219–18230.
- 24 D. Navarro-Rodriguez, F. J. Rodriguez-Gonzalez, J. Romero-Garcia, E. J. Jimenez-Regalado and D. Guillon, *Eur. Polym. J.*, 1998, **34**, 1039–1045.
- 25 S. Li, D. Cohen-Karni, E. Kallick, H. Edington and S. Averick, *Polymer*, 2016, **99**, 59–62.
- 26 J. D. Flores, J. Shin, C. E. Hoyle and C. L. McCormick, *Polym. Chem.*, 2010, **1**, 213–220.
- 27 J. Moraes, T. Maschmeyer and S. Perrier, *J. Polym. Sci. Part Polym. Chem.*, 2011, **49**, 2771–2782.
- 28 G. Moad, *Polym. Chem.*, 2016, **8**, 177–219.
- 29 H. Laita, S. Boufi and A. Gandini, *Eur. Polym. J.*, 1997, **33**, 1203–1211.
- 30 J. R. Jones, C. L. Liotta, D. M. Collard and D. A. Schiraldi, *Macromolecules*, 1999, **32**, 5786–5792.
- 31 I. Kosif, E.-J. Park, R. Sanyal and A. Sanyal, *Macromolecules*, 2010, **43**, 4140–4148.
- 32 T.-D. Kim, J. Luo, Y. Tian, J.-W. Ka, N. M. Tucker, M. Haller, J.-W. Kang and A. K.-Y. Jen, *Macromolecules*, 2006, **39**, 1676–1680.
- 33 T. Dispinar, R. Sanyal and A. Sanyal, *J. Polym. Sci. Part Polym. Chem.*, 2007, **45**, 4545–4551.
- 34 J. Rieger, K. V. Butsele, P. Lecomte, C. Detrembleur, R. Jérôme and C. Jérôme, *Chem. Commun.*, 2005, 274–276.
- 35 M. Friedman, J. F. Cavins and J. S. Wall, *J. Am. Chem. Soc.*, 1965, **87**, 3672–3682.
- 36 D. Mecerreyes, J. Humes, R. D. Miller, J. L. Hedrick, C. Detrembleur, P. Lecomte, R. Jérôme and J. S. Roman, *Macromol. Rapid Commun.*, 2000, **21**, 779–784.
- 37 W. Chen, H. Yang, R. Wang, R. Cheng, F. Meng, W. Wei and Z. Zhong, *Macromolecules*, 2010, **43**, 201–207.



#### **Chapter 4 - Post-polymerisation modification of copolymers**

- 38 R. Wang, W. Chen, F. Meng, R. Cheng, C. Deng, J. Feijen and Z. Zhong, *Macromolecules*, 2011, **44**, 6009–6016.
- 39 S. K. Yang and M. Weck, *Soft Matter*, 2009, **5**, 582–585.
- 40 S. K. Yang and M. Weck, *Macromolecules*, 2008, **41**, 346–351.
- 41 G. W. Gribble, *Chem. Soc. Rev.*, 1998, **27**, 395–404.
- 42 D. Rabuka, R. Parthasarathy, G. S. Lee, X. Chen, J. T. Groves and C. R. Bertozzi, *J. Am. Chem. Soc.*, 2007, **129**, 5462–5471.
- 43 R. Riva, J. Rieger, R. Jérôme and P. Lecomte, *J. Polym. Sci. Part Polym. Chem.*, 2006, **44**, 6015–6024.
- 44 S. Lenoir, R. Riva, X. Lou, Ch. Detrembleur, R. Jérôme and Ph. Lecomte, *Macromolecules*, 2004, **37**, 4055–4061.
- 45 P. Devendar, R.-Y. Qu, W.-M. Kang, B. He and G.-F. Yang, *J. Agric. Food Chem.*, 2018, **66**, 8914–8934.
- 46 L. B. Sessions, B. R. Cohen and R. B. Grubbs, *Macromolecules*, 2007, **40**, 1926–1933.
- 47 J.-F. Lutz, J.-M. Lehn, E. W. Meijer and K. Matyjaszewski, *Nat. Rev. Mater.*, 2016, **1**, 1–14.
- 48 B. Tonpheng, J. Yu and O. Andersson, *Phys. Chem. Chem. Phys.*, 2011, **13**, 15047–15054.
- 49 A. Rudin and P. Choi, in *The Elements of Polymer Science & Engineering (Third Edition)*, eds. A. Rudin and P. Choi, Academic Press, Boston, 2013, pp. 149–229.
- 50 J. A. Brydson, in *Plastics Materials (Seventh Edition)*, ed. J. A. Brydson, Butterworth-Heinemann, Oxford, 1999, pp. 43–58.
- 51 R. Patterson, A. Kandelbauer, U. Müller and H. Lammer, in *Handbook of Thermoset Plastics (Third Edition)*, eds. H. Dodiuk and S. H. Goodman, William Andrew Publishing, Boston, 2014, pp. 697–737.
- 52 M. Lazár, R. Rado and J. Rychlý, in *Polymer Physics*, Springer, Berlin, Heidelberg, 1990, pp. 149–197.
- 53 S. Rouif, *Nucl. Instrum. Methods Phys. Res. Sect. B Beam Interact. Mater. At.*, 2005, **236**, 68–72.
- 54 E. Oral, A. S. Malhi and O. K. Muratoglu, *Biomaterials*, 2006, **27**, 917–925.

#### **Chapter 4 - Post-polymerisation modification of copolymers**

- 55 S. Suyama, H. Ishigaki, Y. Watanabe and T. Nakamura, *Polym. J.*, 1995, **27**, 371–375.
- 56 M. Bengtsson and K. Oksman, *Compos. Part Appl. Sci. Manuf.*, 2006, **37**, 752–765.
- 57 United States, US3646155A, 1972.
- 58 Y. Shibata, H. Tanaka, A. Takasu and Y. Hayashi, *Polym. J.*, 2011, **43**, 272–278.
- 59 D. A. Olson, S. E. A. Gratton, J. M. DeSimone and V. V. Sheares, *J. Am. Chem. Soc.*, 2006, **128**, 13625–13633.
- 60 J. Du, Y. Fang and Y. Zheng, *Polymer*, 2007, **48**, 5541–5547.
- 61 B. A. V. Horn and K. L. Wooley, *Soft Matter*, 2007, **3**, 1032–1040.
- 62 C. E. Hoyle and C. N. Bowman, *Angew. Chem. Int. Ed.*, 2010, **49**, 1540–1573.
- 63 A. Goessl, N. Tirelli and J. A. Hubbell, *J. Biomater. Sci. Polym. Ed.*, 2004, **15**, 895–904.
- 64 J. Justynska, Z. Hordyjewicz and H. Schlaad, *Polymer*, 2005, **46**, 12057–12064.
- 65 T. R. Hayes, P. A. Lyon, E. Silva-Lopez, B. Twamley and P. D. Benny, *Inorg. Chem.*, 2013, **52**, 3259–3267.
- 66 D. Limnios and C. G. Kokotos, *Adv. Synth. Catal.*, 2017, **359**, 323–328.
- 67 M. Gaborieau and P. Castignolles, *Anal. Bioanal. Chem.*, 2011, **399**, 1413–1423.
- 68 J. Stejny, *Polym. Bull.*, 1996, **36**, 617–621.
- 69 S. Nandi and H. H. Winter, *Macromolecules*, 2005, **38**, 4447–4455.
- 70 C. G. Robertson and Wang, *Macromolecules*, 2004, **37**, 4266–4270.

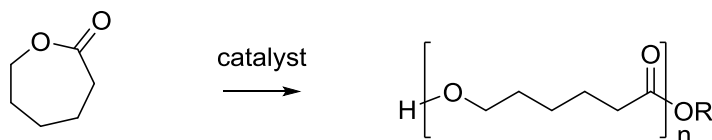
# Chapter 5

## Ring-opening polymerisation of $\epsilon$ -caprolactone

### 5.1 Introduction

#### 5.1.1 Poly( $\epsilon$ -caprolactone)

The ring-opening polymerisation (ROP) of  $\epsilon$ -caprolactone ( $\epsilon$ -CL) is an efficient route to biodegradable polyesters (Scheme 1). In addition to good hydrolysability, polycaprolactone (PCL) has good biocompatibility and mechanical properties. PCL will degrade over several months or several years depending on the conditions, the degree of crystallinity and molecular weight of the polyester. Various microbes found in nature will readily degrade PCL completely.<sup>1</sup> During the degradation, the amorphous region of the polymer is broken down first. PCL is a semicrystalline polymer which can possess a degree of crystallinity up to 69%.<sup>2</sup> The polymer is degraded through cleavage of ester bonds, this happens mainly by chain end scission at high temperatures or by random chain scission at lower temperatures.<sup>3</sup> The decomposition of PCL is autocatalysed by the carboxylic acid products of decomposition. The polymer breakdown can be accelerated by the presence of enzymes;<sup>4</sup> while PCL may be enzymatically degraded in nature, these enzymes are not present in the human body and therefore the polyester degradation *in vivo* is extremely slow.<sup>5,6</sup>



**Scheme 1** Ring-opening polymerisation (ROP) of  $\epsilon$ -caprolactone ( $\epsilon$ -CL)

The chains formed from the polymerisation of  $\epsilon$ -CL are relatively flexible compared to other commonly used biodegradable polyesters such as poly(lactic acid) (PLA). This means that PCL has a comparatively low melting point ( $T_m$ ) of between 58 – 65 °C and glass transition temperature ( $T_g$ ) of between -65 and -60 °C.<sup>2,6</sup> Another noteworthy characteristic of PCL is its exceptionally high ductility and elongation at breakage.<sup>6</sup> Thanks to its low melting point, PCL is easily processed by conventional melting techniques.<sup>7</sup> PCL is highly hydrophobic, this is the primary reason that PCL has longer degradation times than, for example, PLA. In addition to high solubility in a range of organic solvents, another useful feature of PCL is its miscibility with

## **Chapter 5 - Ring-opening polymerisation of $\epsilon$ -caprolactone**

other polymers such as poly(vinyl chloride), poly(styrene-acrylonitrile), poly(acrylonitrile butadiene styrene), poly(bisphenol-A), polycarbonates and nitrocellulose.<sup>2</sup> The formation of copolymers of PCL with other polymers is an effective approach to modify its properties, for example copolymerisation with PLA shortens degradation times.<sup>8</sup>

PCL is utilised as a biodegradable, nontoxic plastic for many varied applications such as bottles and films in food and drink packaging, and as biodegradable bags. It is also used as a surface coating for thermoplastic polyurethanes<sup>9</sup> and as adhesives.<sup>10</sup> PCL has many important applications in the biomedical sector. The low degradation rates *in vivo* and high biocompatibility of PCL makes it an effective material for the production of medical products such as sutures, wound dressings, scaffolds in tissue engineering and orthopaedic splints.<sup>11</sup> These characteristics combined with high permeability to small drug molecules make PCL a promising candidate for drug delivery systems.<sup>12</sup> PCL has been used to deliver drugs, antigens, antibodies, ribozymes, nerve growth factor, heparin, steroids, hormones and vitamins; PCL has been particularly effective in the delivery of contraceptives<sup>5</sup> and cancer drugs.<sup>13</sup>

$\epsilon$ -CL is most commonly synthesised by the Bayer Villiger oxidation of cyclohexanone. As cyclohexanone is derived from fossil fuel sources, the PCL produced cannot be classified as a bioplastic, however this biodegradable polyester still has the potential to play an important role as an alternative to non-degradable plastics.<sup>14</sup> The disadvantage of being fossil fuel based may be offset if PCL is recycled by depolymerisation, recovered monomers may be reused achieving a circular economy.<sup>15</sup> In addition to the Bayer Villiger oxidation,  $\epsilon$ -CL can also be synthesised from cyclohexanol using microorganisms; cyclohexanol is first converted to cyclohexanone using cyclohexanol dehydrogenase and this is then converted to  $\epsilon$ -CL by cyclohexanone monooxygenase.<sup>2</sup>

PCL can be synthesised by a polycondensation mechanism, however due to issues of low molecular weight and high polymer dispersities ( $\bar{D}$ ), this approach is not commonly employed. Braud *et al.* synthesised PCL oligomers

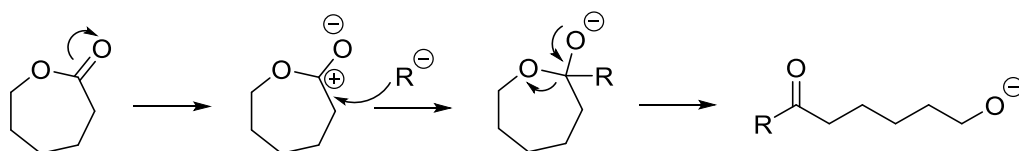
## Chapter 5 - Ring-opening polymerisation of $\epsilon$ -caprolactone

via the polycondensation of 6-hydroxyhexanoic acid. In order to increase conversion, the reaction was performed under vacuum to remove water and shift the equilibrium to towards PCL formation. The reaction was carried out for 6 hours over which time the temperature was gradually increased from 80 °C to 150 °C.

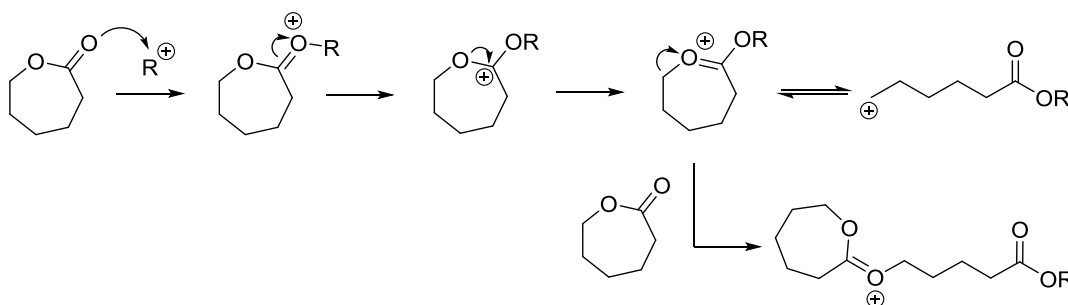
The preferred route to PCL is the ring-opening polymerisation (ROP) of  $\epsilon$ -CL. The ROP can proceed via a cationic, anionic, monomer-activated, coordination insertion or enzymatic mechanism.<sup>2</sup>

### 5.1.2 Ring-opening polymerisation (ROP) mechanisms for the formation of polycaprolactone (PCL) from $\epsilon$ -caprolactone ( $\epsilon$ -CL)

PCL is formed from  $\epsilon$ -CL via an anionic mechanism when the carbonyl carbon of the monomer is attacked by an anionic nucleophile, causing the ring-opening at the acyl-oxygen bond. The product of the ring-opening is an alkoxide, which propagates the formation of the polymer by attacking further monomer units.<sup>16</sup> Scheme 2 illustrates the initiation step for an anionic ROP of  $\epsilon$ -CL. The major issue with this route is the occurrence of high levels of transesterification or “back-biting” which limits the molecular weight of the PCL produced.<sup>2</sup>



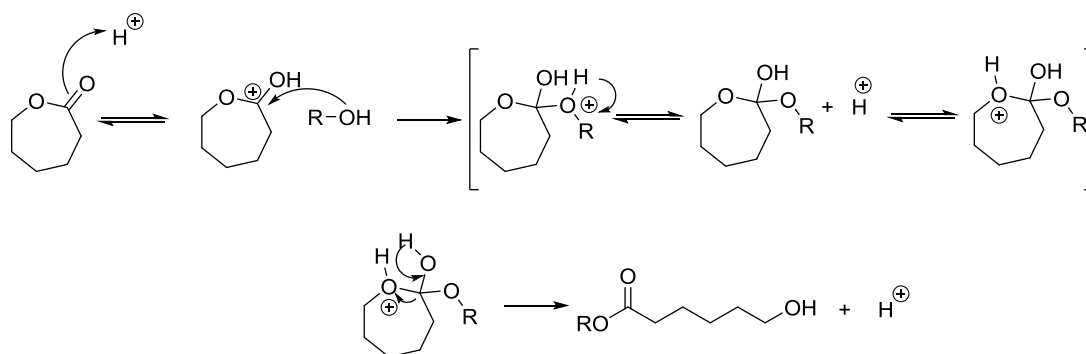
**Scheme 2** Anionic ring-opening polymerisation (ROP) of  $\epsilon$ -caprolactone ( $\epsilon$ -CL)<sup>2</sup>



**Scheme 3** Cationic ring-opening polymerisation (ROP) of  $\epsilon$ -caprolactone ( $\epsilon$ -CL)<sup>2</sup>

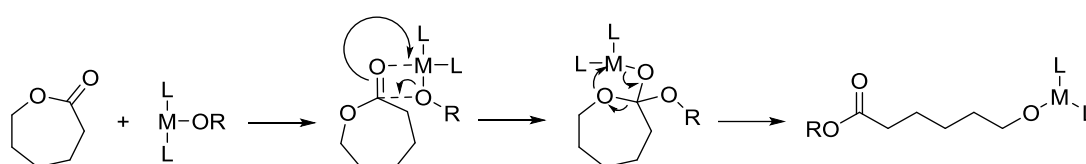
## Chapter 5 - Ring-opening polymerisation of $\epsilon$ -caprolactone

In the cationic ROP of  $\epsilon$ -CL, a cationic initiator is attacked by the carbonyl oxygen of the monomer. Following this reaction, the lactone ring contains a positive charge. The monomer can then spontaneously undergo ring-opening, alternatively attack of another  $\epsilon$ -CL can facilitate this rearrangement (Scheme 3).<sup>2</sup>



**Scheme 4** Activated monomer ring-opening polymerisation (ROP) of  $\epsilon$ -caprolactone ( $\epsilon$ -CL)<sup>17,18</sup>

ROP of  $\epsilon$ -CL via an anionic mechanism relies on the nucleophilic attack of an ionic initiator or a propagating chain end on a monomer; in the activated monomer mechanism, the monomer is first converted to a cationic species which is subsequently attacked by a hydroxyl polymer chain end (Scheme 4).<sup>17,18</sup> Kim *et al.* reported the polymerisation of  $\epsilon$ -CL and methoxy poly(ethylene glycol) catalysed by  $HCl.Et_2O$  producing a diblock copolymer.<sup>19</sup>



**Scheme 5** Coordination-insertion ring-opening polymerisation (ROP) of  $\epsilon$ -caprolactone ( $\epsilon$ -CL)<sup>2</sup>

A coordination-insertion mechanism (Scheme 5) is the most common mechanism employed to produce PCL from  $\epsilon$ -CL. It has many similarities to the anionic mechanism, but the monomer is activated by coordination to a metal centre. During the reaction, the metal centre is attached to the growing polymer chain through an alkoxide bond. The first step in the mechanism is the coordination of  $\epsilon$ -CL to the catalyst metal centre. This is followed by

## Chapter 5 - Ring-opening polymerisation of $\epsilon$ -caprolactone

insertion of a metal alkoxide co-ligand into the carbonyl group by nucleophilic addition. The  $\epsilon$ -CL ring is then opened by acyl-oxygen bond cleavage forming a metal alkoxide. Propagation can occur following coordination of another monomer unit and subsequent insertion of the alkoxide terminated polymer chain into the carbonyl group of  $\epsilon$ -CL. Hydrolysis of the metal hydroxide bond terminates the polymerisation yielding a polymer with a hydroxyl end group. The identity of the other end of the polymer chain depends on the initiator utilised in the polymerisation, for example if aluminium isopropoxide was used the polymer would be capped with an isopropyl ester.<sup>20,21</sup>

### 5.1.3 Catalysts for the ring-opening polymerisation (ROP) of $\epsilon$ -caprolactone ( $\epsilon$ -CL)

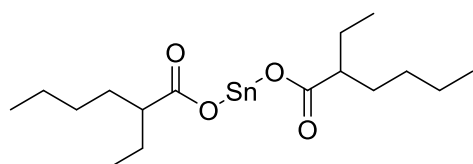
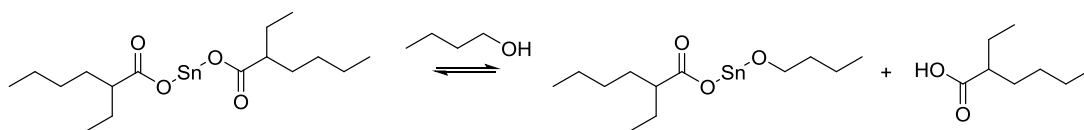


**Figure 1** Tin(II) octanoate ( $\text{Sn}(\text{Oct})_2$ )



**Scheme 6** Reaction of  $\text{Sn}(\text{Oct})_2$  with alcohol to yield the active species for the ring-opening polymerisation (ROP) of  $\epsilon$ -caprolactone ( $\epsilon$ -CL)<sup>23,24</sup>

The primary challenge in  $\epsilon$ -CL polymerisation is the production of polyester with controllable molecular weight and low Đ. The most commonly used metal complex utilised as a catalyst for the ROP of  $\epsilon$ -CL is tin(II) octanoate,  $\text{Sn}(\text{Oct})_2$  (Figure 1). The tin catalyst is employed in conjunction with an initiator, normally an alcohol. The main advantages of a tin(II) octanoate catalytic system is its commercial availability, the ease of handling and its solubility in most organic solvents. The main disadvantage of this system is that it requires high temperatures to achieve high monomer conversion and this leads to greater inter- and intramolecular transesterification and thus a higher Đ.<sup>22</sup> Kowalski and colleagues proved that the ROP of  $\epsilon$ -CL with tin(II) octanoate and an alcohol was a living polymerisation. Their work showed that prior to the



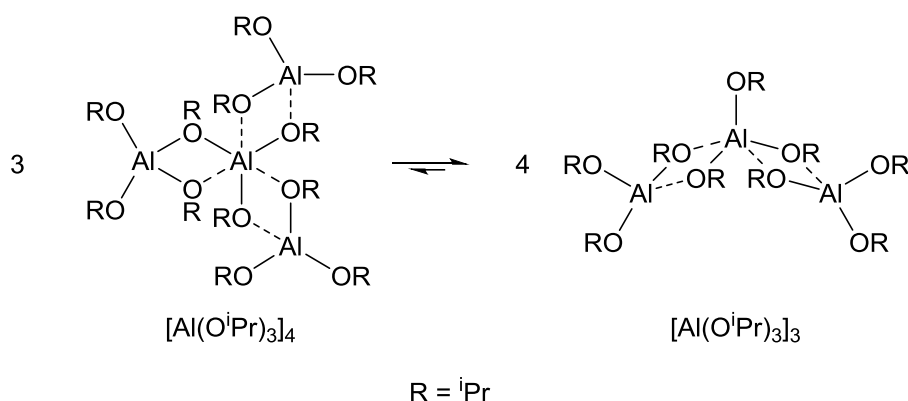
## Chapter 5 - Ring-opening polymerisation of $\epsilon$ -caprolactone

polymerisation, the catalytically active species is produced by the reaction of the alcohol with the tin complex (Scheme 6). This reaction exists in an equilibrium and the greater the ratio of alcohol:tin, the greater the number of active species present in the reaction. If an excess of alcohol is added to the reaction, it acts as a chain transfer agent as well as an initiator. Addition of carboxylic acids deactivates the catalyst and reduces the rate of polymerisation. If  $\text{Sn}(\text{Oct})_2$  is employed without a nucleophilic initiator (such as an alcohol) then hydroxyl-containing impurities present in very small amounts may initiate the reaction, however in these circumstances the reaction is uncontrolled.<sup>23,24</sup>

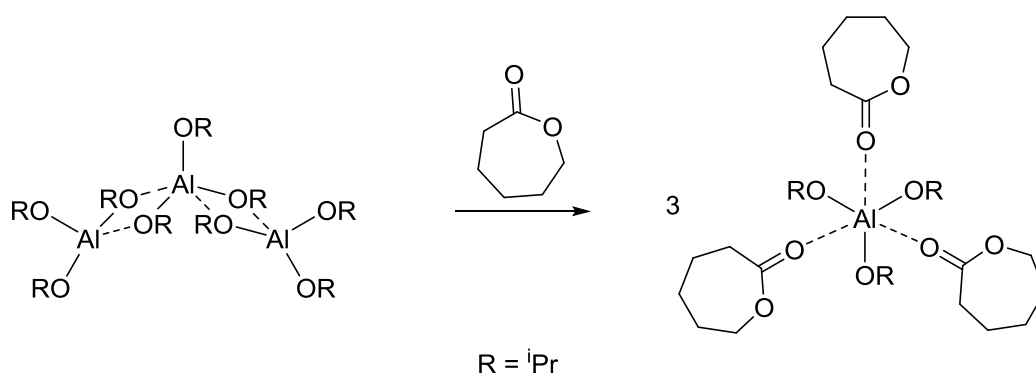
Aluminium-based catalysts have been used extensively for the ROP of  $\epsilon$ -CL.<sup>25</sup> While many have lower reactivity than catalytic systems based on other metals they offer excellent control over the polymerisation.<sup>2</sup>

Evidence of the control possible with catalyst systems based upon aluminium is illustrated by the work of Wang and Kunioka, who compared different metal triflates as catalysts for the ROP of  $\epsilon$ -CL carried out at 60 °C in air without stirring. Aluminium(III) triflate was the best-performing catalyst producing PCL with a number average molecular weight ( $M_n$ ) of 18,400  $\text{g mol}^{-1}$  and a  $\bar{D}$  of 1.94. Copper(II) triflate also produced PCL but presented inferior control as the polymer produced had lower  $M_n$  and higher  $\bar{D}$  (16,400  $\text{g mol}^{-1}$  and 1.97 respectively). Of the other metal triflates tested, lanthanum(III) and samarium(III) triflates only produced oligomers, and sodium, magnesium and ytterbium(III) triflates did not catalyse the polymerisation.<sup>26</sup> Duda *et al.* investigated a range of alkyl aluminium alkoxides and found that only the alkoxide and not alkyl groups will initiate polymerisation; faster rates of reaction were recorded for bulkier alkyl groups.<sup>27</sup>

## Chapter 5 - Ring-opening polymerisation of $\epsilon$ -caprolactone



**Scheme 7** Equilibrium between the trimer  $[Al(O^iPr)_3]_3$  and tetramer  $[Al(O^iPr)_3]_4$  of aluminium isopropoxide<sup>28</sup>



**Scheme 8** Dissociation of the trimer  $[Al(O^iPr)_3]_3$  in  $\epsilon$ -caprolactone ( $\epsilon$ -CL)<sup>2,29,30</sup>

Aluminium isopropoxide is a commonly used catalyst for the ROP of  $\epsilon$ -CL. The rate of reaction is slower than other catalysts such as  $Sn(Oct)_2$ , but offers greater control of the reaction which translates into lower  $\bar{D}$ . Aluminium isopropoxide doesn't exist as a monometallic complex, instead the molecules form trimers or tetramers in order to greater satisfy the coordination sphere of the aluminium metal centre. The trimer  $[Al(O^iPr)_3]_3$  and the tetramer  $[Al(O^iPr)_3]_4$  exist in an equilibrium which lies towards the tetramer (Scheme 7). These multi-centred aluminium complexes have different reactivities for the ROP of  $\epsilon$ -CL, with  $[Al(O^iPr)_3]_3$  being more reactive and exhibiting greater control over the reaction. Distillation of aluminium isopropoxide gives almost entirely the trimer, which converts to the tetramer over time.<sup>28</sup> When  $[Al(O^iPr)_3]_3$  dissolves in  $\epsilon$ -CL, the trimer structure dissociates into a monomeric structure stabilised by coordination of  $\epsilon$ -CL monomers (Scheme 8). This monomeric complex is the active species for the ROP of  $\epsilon$ -CL.<sup>2,29,30</sup> Amgoune and colleagues

## Chapter 5 - Ring-opening polymerisation of $\epsilon$ -caprolactone

reported that the ROP of  $\epsilon$ -CL catalysed by aluminium isopropoxide for 1 hour at room temperature in toluene produced PCL with a  $M_n$  of 41,800  $\text{gmol}^{-1}$  and a  $\bar{D}$  of 1.66. The reaction was carried out with a catalyst:monomer ratio of 1:500 and a monomer conversion of 90% achieved. The authors did not report that they had purified the aluminium isopropoxide so we must assume that the catalyst consisted of trimers and tetramers.<sup>31</sup> Duda *et al.* studied the ROP of  $\epsilon$ -CL with the pure trimer  $[\text{Al}(\text{O}^i\text{Pr})_3]_3$  and saw 100% conversion of  $\epsilon$ -CL after 0.2 hours at 20 °C in toluene. The catalyst:monomer ratio was 1:333 and the PCL produced had a  $M_n$  of 12,200  $\text{gmol}^{-1}$  and a  $\bar{D}$  of 1.10.<sup>32</sup> The difference in reactivity and control in these two examples shows the benefits of using the pure trimer as opposed to the mixture of aluminium isopropoxide species. However the purification of the catalyst adds additional complexity and expense to the process which makes this often unfeasible in an industrial setting. The ROP of  $\epsilon$ -CL with aluminium isopropoxide is more controlled at lower temperatures (0 – 25 °C) as opposed to higher ( $\sim$ 100 °C).<sup>33</sup>

Catalytic systems based on methyl aluminium diphenolate complexes proved to be effective for the ROP of  $\epsilon$ -CL, offering control over molecular weight and  $\bar{D}$ . In order to form a catalytically active species, the metal catalyst must react with the isopropanol initiator. If this reaction does not take place then polymerisation will not occur. The complexes studied are shown in Figure 2 and are comprised of phenolate ligands with phenyl groups in the *ortho* position (**5.1a**), *tert*-butyl groups in the *ortho* and a methyl group in the *para* (**5.1b**) or *tert*-butyl groups in the *para* (**5.1c**). When the reactions were carried out at room temperature with a monomer:catalyst: $i\text{PrOH}$  ratio of 50:0.3:1 PCL samples with  $M_n$  of 6,300 – 6,800  $\text{gmol}^{-1}$  and  $\bar{D}$  of 1.19 – 1.27 were produced. **5.1a** gave the lowest  $\bar{D}$  and therefore had the greatest control in the polymerisation while **5.1c** had the highest rate of reaction.<sup>34</sup>

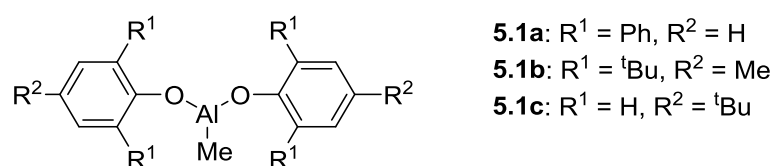


**Figure 2** Methyl aluminium diphenolate pre-catalysts for the ring-opening polymerisation (ROP) of  $\epsilon$ -caprolactone ( $\epsilon$ -CL)<sup>34</sup>

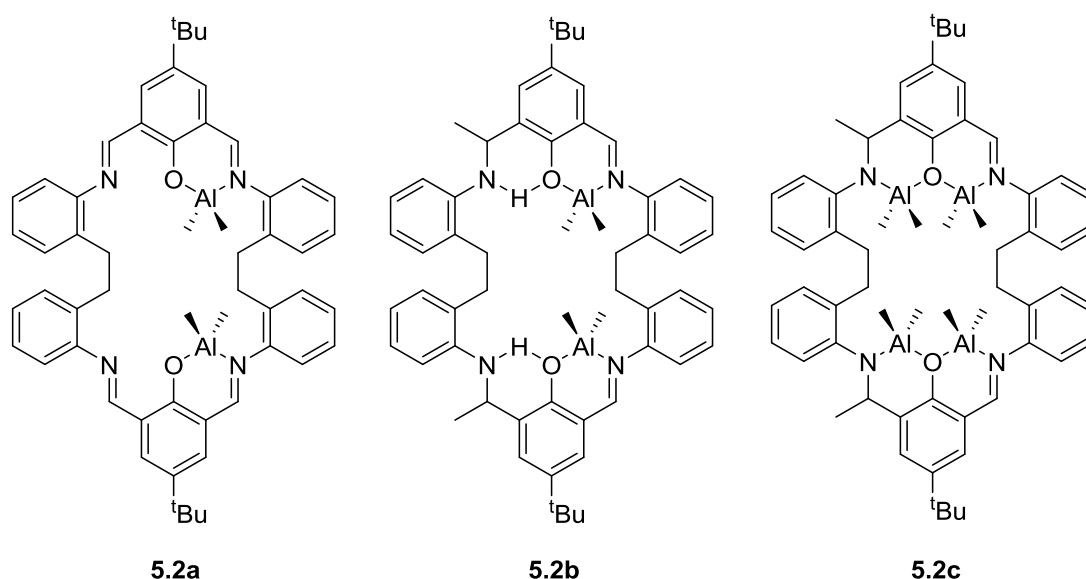


**Figure 3** Multinuclear alkylaluminium macrocyclic Schiff base precatalysts for the ring-opening polymerisation (ROP) of  $\epsilon$ -caprolactone ( $\epsilon$ -CL)<sup>35</sup>

Arbaoui and colleagues reported the activity of multinuclear alkylaluminium macrocyclic Schiff base complexes in the ROP of  $\epsilon$ -CL. Complexes **5.2a**, **5.2b** and **5.2c** shown in Figure 3. The active catalytic species were produced from the reaction of these complexes with benzyl alcohol. The polymerisations were carried out with a 500:0.5:1 ratio of monomer:complex:alcohol and were heated at 25 °C in toluene. The complex which produced the highest reaction rate was **5.2b**, polymerising 99% of the  $\epsilon$ -CL in 12 hours and yielding PCL with a  $M_n$  of 49,500  $\text{g mol}^{-1}$  and a  $\bar{D}$  of 1.7. Polymerisations with **5.2a** and **5.2c** were slower taking 72 hours and 24 hours to give conversions >98% but both produced PCL with lower  $\bar{D}$  (1.6 and 1.5 respectively).<sup>35</sup>

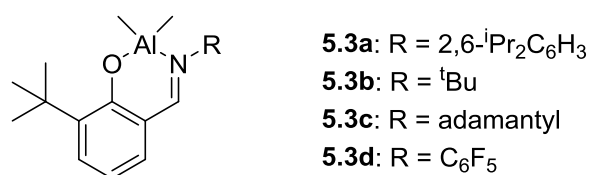


**Figure 4** Dimethylaluminium salicylaldimines used in the ring-opening polymerisation (ROP) of  $\epsilon$ -caprolactone ( $\epsilon$ -CL)<sup>36</sup>

A range of salicylaldimines with different substituents on the imino group were tested as precatalysts for the ROP of  $\epsilon$ -CL. Ligands with 2,6- $i$ Pr<sub>2</sub>C<sub>6</sub>H<sub>3</sub> (**5.3a**),  $t$ Bu (**5.3b**), adamantyl (**5.3c**) and C<sub>6</sub>F<sub>5</sub> (**5.3d**) groups were complexed to aluminium (Figure 4). Moderate to high molecular weights and good to

moderate control was achieved using these catalytic systems. The rate of reaction varied with identity of the substituent on the imino group in the order  $\text{C}_6\text{F}_5$  (**5.3d**)  $\gg$  2,6- $\text{iPr}_2\text{C}_6\text{H}_3$  (**5.3a**)  $\gg$   $\text{tBu}$  (**5.3b**)  $>$  adamantyl (**5.3c**). The catalyst-initiator **5.3d**- $n$ -butylalcohol polymerised 99% of 250 equivalents of  $\epsilon$ -CL after 30 minutes. It is clear from this work that the identity of the substituent plays an important role in determining the efficiency of the catalyst. Based on the examples in this study by Iwasa and colleagues, aromatic and electron withdrawing substituents give rise to more active catalysts.<sup>36</sup>

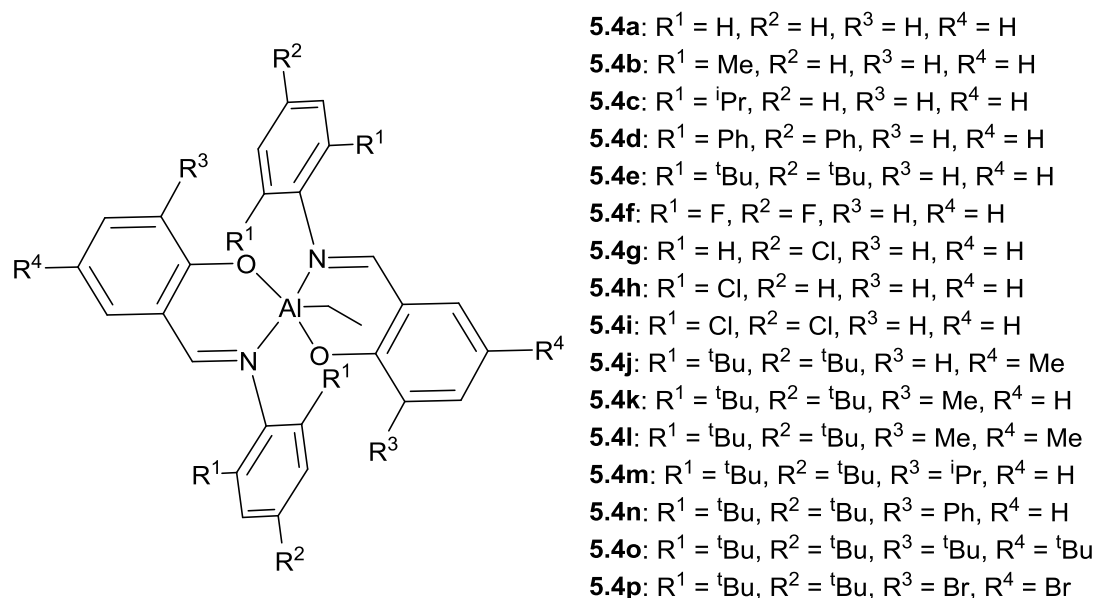


**Figure 5** Ethylaluminium disalicylaldimines used in the ring-opening polymerisation (ROP) of  $\epsilon$ -caprolactone ( $\epsilon$ -CL)<sup>37</sup>

Alkylaluminium complexes with two salicylaldimine ligands have also been studied as precatalysts for the ROP of  $\epsilon$ -CL. The complexes tested (**5.4a-p**) are shown in Figure 5. The substituents of the aniline group greatly affected the rate of reaction, this effect is exemplified by the disparity in rate between the unsubstituted **5.4a** and the *tert*-butyl substituted **5.4e** for which the monomer conversions reported were 31% after 24 hours and 86% after 1 hour respectively. Increasing the steric demand of the substituents of the aniline group increased the activity of the catalyst. Evidence of this can be seen in **5.4a-c** where changing  $\text{R}^1$  from a H, to a Me group and to an  $\text{iPr}$  group increased conversion of  $\epsilon$ -CL after 24 hours from 31% to 80% and 97% respectively. Substitution of the salicylidene moiety also affected reactivity as

## Chapter 5 - Ring-opening polymerisation of $\epsilon$ -caprolactone

illustrated by the difference in reactivity of the unsubstituted salicylidene **5.4e** and the methyl substituted analogue **5.4f** (giving conversions of 86% after 1 hour and 96% after 10 minutes respectively). **5.4f** combined with benzyl alcohol yielded PCL with an  $M_n$  of 29,800  $\text{g mol}^{-1}$  and a  $\bar{D}$  of 1.1 after 10 minutes at 25 °C.<sup>37</sup>

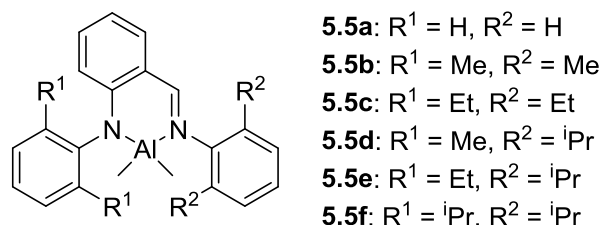


**Figure 6** Dimethylaluminium anilido-imine complexes used in the ring-opening polymerisation (ROP) of  $\epsilon$ -caprolactone ( $\epsilon$ -CL)<sup>38</sup>

Yao *et al.* studied similar complexes for the ROP of  $\epsilon$ -CL, but the anilido-imine ligands utilised in this study contained only nitrogen donors. The complexes synthesised are shown in Figure 6. The effect on the polymerisation of the substitution of various alkyl groups on the aniline rings was explored. The precatalyst **5.5a** (containing the unsubstituted ligand) was tested in the ROP of  $\epsilon$ -CL and proved to be highly efficient and offered excellent control. At a monomer:precatalyst ratio of 200:1, a conversion of 95.6% was recorded after only 4.5 minutes at 70 °C in toluene. The PCL produced had a  $M_n$  of 23,600  $\text{g mol}^{-1}$  and a  $\bar{D}$  of 1.14. When the catalyst loading was reduced by half, a conversion of 92.6% was recorded after 14 minutes. As expected, the polymer synthesised had a higher  $M_n$  (46,800  $\text{g mol}^{-1}$ ) but the control of the reaction decreased ( $\bar{D} = 1.56$ ). The substitution of the aniline rings (**5.5b-f**) did not improve the rate of reaction, but the polymerisation remained efficient with conversions >90% achieved in less than 5 minutes. Control over the polymerisation decreased slightly for **5.5b-f** compared to the unsubstituted ligand (**5.5a**) but still remained less than 1.3.<sup>38</sup>

A series of alkoxy aluminium porphyrin complexes were tested as catalyst for the ROP of  $\epsilon$ -CL. The identity of the polymer end groups of PCL were varied by selecting different alcohol additives. The alcohols acted as initiators for the polymerisation and as chain transfer agents. Increasing the molar equivalents

of alcohol additive reduced the molecular weight of the PCL produced. These catalytic systems had very slow rates of reaction and required between 220 hours and 24 days to achieve complete conversion. The polymer produced did have a narrow molecular weight distribution.<sup>39</sup>

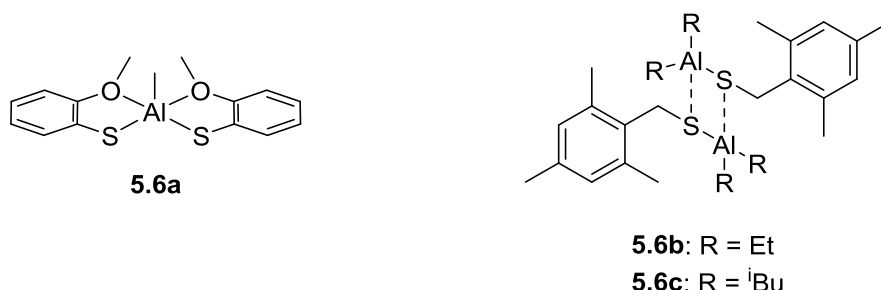


**Figure 7** Aluminium thiolate catalysts for the ring-opening polymerisation (ROP) of  $\epsilon$ -caprolactone ( $\epsilon$ -CL)<sup>40</sup>

Huang and colleagues investigated the use of aluminium thiolate catalysts, shown in Figure 7. Polymerisation in this system was initiated by insertion of a thiol ligand into the carbonyl group of  $\epsilon$ -CL and this yields PCL with a thioether end group. Methylaluminium bis(2-methoxybenzenethiolate) (**5.6a**) proved to be an effective catalyst for the ROP of  $\epsilon$ -CL. 93% conversion of monomer was achieved after 2 hours at 25 °C when 200 molar equivalents of  $\epsilon$ -CL was combined with 1 equivalent of catalyst. PCL of good molecular weight ( $M_n$  of 45,300  $\text{gmol}^{-1}$ ) and excellent molecular weight distribution ( $\mathcal{D}$  of 1.19) was produced. Thiolate complexes with 2,4,6-methylbenzenethiolate ligands were also studied as catalysts. The product of the reaction of 2,4,6-methylbenzylmercaptan and an aluminium alkyl precursor yielded dimeric, bimetallic species (**5.6b** and **5.6c**) (Figure 7). Under identical conditions to **5.6a**, tetraethyl-bisaluminium bis(2,4,6-methylbenzenethiolate) (**5.6b**) required 5 hours to achieve complete conversion of  $\epsilon$ -CL to PCL. The PCL produced by **5.6b** had much higher molecular weight ( $M_n = 117,200 \text{ gmol}^{-1}$ ) compared to the polymer generated by **5.6a**, this indicates that the polymerisation initiation in **5.6b** was slow or incomplete. The catalytic performance of tetra<sup>i</sup>butyl-bisaluminium bis(2,4,6-methylbenzenethiolate) (**5.6c**) illustrated the effect of alkyl groups on reactivity. The <sup>i</sup>butyl analogue (**5.6c**) was a significantly slower catalyst requiring 20 hours to convert 60 molar

## Chapter 5 - Ring-opening polymerisation of $\epsilon$ -caprolactone

equivalents of  $\epsilon$ -CL to PCL. Both **5.6b** and **5.6c** exhibited moderate control of the polymerisation with  $\bar{D}$ 's of 1.37 and 1.21 respectively.<sup>40</sup>

Group 2 metal complexes have been used extensively as catalysts for the ROP of  $\epsilon$ -CL. They often show very high activity and have low toxicity. Magnesium and calcium based catalysts are by far the most studied of the Group 2 metals and a variety of ligands have been used in different catalytic systems.<sup>2</sup>

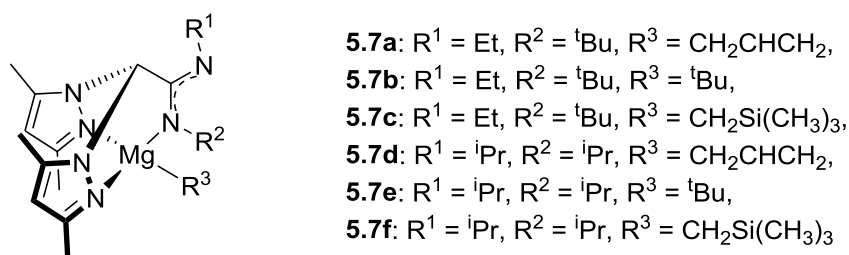


**Figure 8** Alkyl heteroscorpionate magnesium catalysts for the ring-opening polymerisation (ROP) of  $\epsilon$ -caprolactone ( $\epsilon$ -CL)<sup>41</sup>

Sánchez-Barba and colleagues investigated alkyl heteroscorpionate magnesium catalysts for the ROP of  $\epsilon$ -CL (Figure 8). These complexes produced PCL of moderate to high molecular weight, proved to be highly active and offered good to moderate control of molecular weight distribution. The polymerisation catalysed by **5.7a-f** was initiated by an alkyl group. The identity of the alkyl co-ligand most affected the activity of the catalyst. When the alkyl group was  $\text{CH}_2\text{SiMe}_3$ , the ROP of 500 molar equivalents of  $\epsilon$ -CL took one minute or less. The groups on the amidine backbone also affect activity to a lesser extent with the most active complex (**5.7f**) containing *iso*-propyl groups. **5.7f** took only 10 seconds to polymerise 500 molar equivalents at 20 °C. The polyester synthesised had a  $M_n$  of 59,000  $\text{gmol}^{-1}$  and a  $\bar{D}$  of 1.45. Increasing the amount of monomer by a factor of 10 yielded PCL with a  $M_n$  of 160,000  $\text{gmol}^{-1}$  and a  $\bar{D}$  of 1.42. **5.7a** had lower activity than **5.7f** but offered greater control yielding PCL with a  $\bar{D}$  of 1.16.<sup>41</sup>



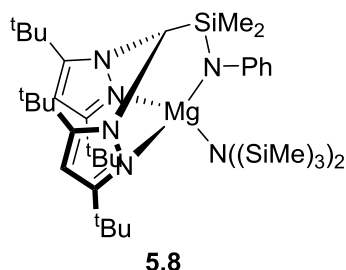


**Figure 9** Magnesium heteroscorpionate for the ring-opening polymerisation (ROP) of  $\epsilon$ -caprolactone ( $\epsilon$ -CL)<sup>42</sup>

Mountford and co-workers synthesised the magnesium heteroscorpionate complex **5.8** shown in Figure 9. **5.8** was tested as a catalyst for the ROP of  $\epsilon$ -CL. The reaction of 100 molar equivalents of monomer at 23 °C in THF for 30 minutes generated PCL with a percentage yield of 81%, a  $M_n$  of 66,620  $\text{gmol}^{-1}$  and a  $\bar{D}$  of 1.67. **5.8** is a highly active catalyst but does not exhibit a high level of control over the reaction. The distribution of molecular weight was wider if the polymerisation is carried out in toluene as opposed to THF. When toluene was the solvent, the PCL produced had a  $\bar{D}$  of 2.79. This increase in  $\bar{D}$  is most likely due to the occurrence of intra- or intermolecular transesterification reactions. These reactions require a vacant coordination site for the “backbiting” to proceed. In the THF reactions, coordination of solvent to the metal centre reduces the availability of the vacant site and therefore transesterification is reduced.<sup>42</sup>

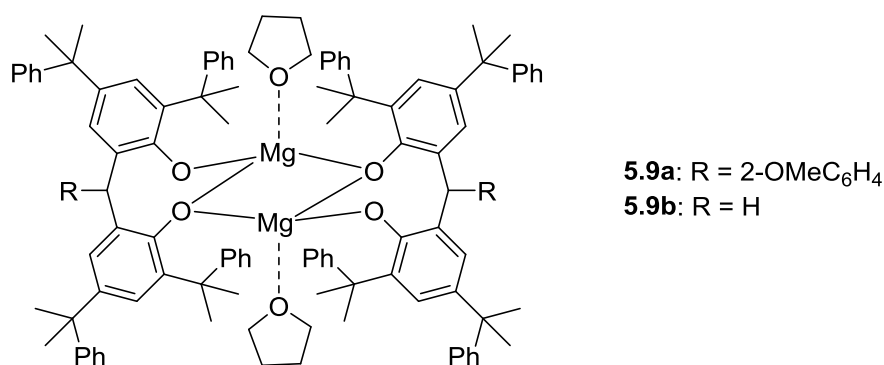
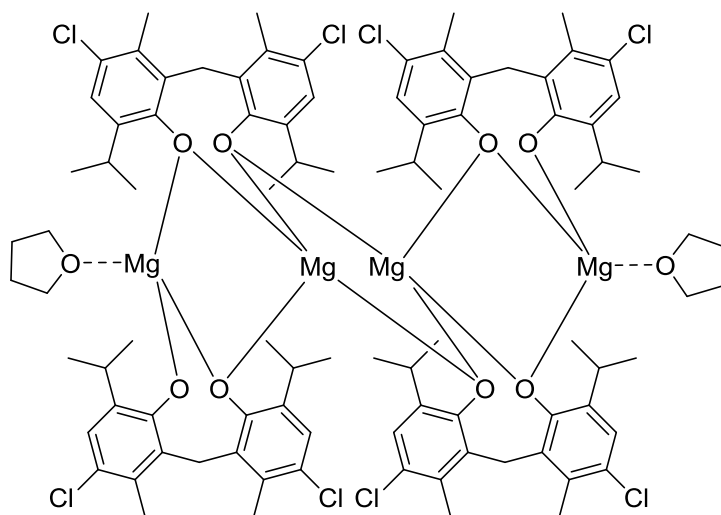


**Figure 10** Bimetallic magnesium complexes for the ring-opening polymerisation (ROP) of  $\epsilon$ -caprolactone ( $\epsilon$ -CL)<sup>43</sup>

## Chapter 5 - Ring-opening polymerisation of $\epsilon$ -caprolactone

Yu *et al.* synthesised bimetallic magnesium complexes ligated by sterically demanding bidentate phenoxide compounds (**5.9a** and **5.9b**) (Figure 10). **5.9a** was the more active catalyst polymerising 100 equivalents of  $\epsilon$ -CL in 2 hours at 25 °C yielding PCL with a  $M_n$  of 9,300  $\text{gmol}^{-1}$  and a  $\bar{D}$  of 1.06. **5.9b** proved to be a slower catalyst requiring 3 hours at 70 °C to polymerise 100 equivalents of monomer and did not provide the same high level of control over the reaction as **5.9a** producing PCL with a higher  $\bar{D}$  of 1.24.<sup>43</sup>

A multi-centred aryloxy complex based on the ligand 2,2'-methylenebis(4-chloro-6-isopropyl-3-methylphenol) (**5.10**) (Figure 11) was synthesised and tested in combination with benzyl alcohol as a catalyst for the ROP of  $\epsilon$ -CL. This system offered good activity and control yielding PCL with a  $M_n$  of 13,800  $\text{gmol}^{-1}$  and a  $\bar{D}$  of 1.11 from the polymerisation of 200 equivalents of  $\epsilon$ -CL at 56 °C for 3 hours. A linear relationship between the molecular weight and the ratio of monomer:initiator was found suggesting the presence of a living polymerisation.<sup>44</sup>



**5.10**

**Figure 11** Multi-centred aryloxy magnesium complex for the ring-opening polymerisation (ROP) of  $\epsilon$ -caprolactone ( $\epsilon$ -CL)<sup>44</sup>

## Chapter 5 - Ring-opening polymerisation of $\epsilon$ -caprolactone

Like magnesium, calcium is non-toxic and does not tend to form highly coloured compounds, therefore it is an attractive metal for use in catalysts for the ROP of  $\epsilon$ -CL. Calcium complexes are often highly active catalysts for this polymerisation.<sup>2</sup>

Simple calcium compounds such as calcium methoxide and calcium bistrimethylsilylamide bistetrahydrofuran  $[(\text{Ca}(\text{N}(\text{SiMe}_3)_2)_2\text{THF}_2)]$  are active catalysts for the ROP of  $\epsilon$ -CL. The bulk polymerisation of  $\epsilon$ -CL by commercial calcium methoxide (monomer:catalyst ratio of 100:1) at 120 °C required only 10 minutes of heating to completely convert the monomer to PCL with a  $M_n$  of 22,200  $\text{gmol}^{-1}$  and a  $\bar{D}$  of 1.25.<sup>45</sup>  $[(\text{Ca}(\text{N}(\text{SiMe}_3)_2)_2\text{THF}_2)]$  proved to be an effective catalyst for the polymerisation when used in conjunction with an alcohol initiator. When isopropanol is utilised as the initiator, the reaction of 100 equivalents of  $\epsilon$ -CL took only 6 minutes at room temperature. The PCL generated had a  $M_n$  of 6,200  $\text{gmol}^{-1}$  and a  $\bar{D}$  of 1.24. When methanol was utilised as the initiator under identical reaction conditions, the rate of reaction remained the same and the PCL produced had a  $M_n$  of 9,000  $\text{gmol}^{-1}$  and a  $\bar{D}$  of 1.29. The importance of including an alcohol initiator is illustrated by the fact that when  $[(\text{Ca}(\text{N}(\text{SiMe}_3)_2)_2\text{THF}_2)]$  alone is used to catalyse the reaction the molecular weight distribution of the polymer produced is far larger, as evidenced by the  $\bar{D}$  of 2.39.<sup>46</sup>

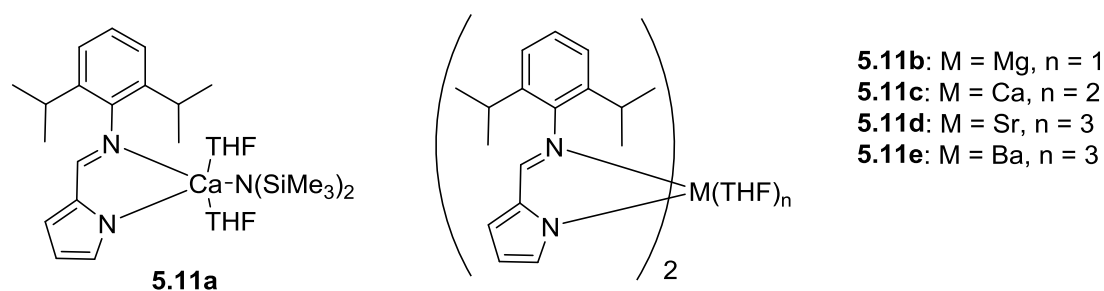


**Figure 12** Group 2 metal N-aryliminopyrrolyl catalysts for the ring-opening polymerisation (ROP) of  $\epsilon$ -caprolactone ( $\epsilon$ -CL)<sup>47</sup>

Panda and co-workers synthesised group 2 metal complexes based on an N-aryliminopyrrolyl ligand (**5.11a-e**) (Figure 12) and explored their efficiencies as catalysts for the ROP of  $\epsilon$ -CL. **5.11a** comprises of a calcium metal centre ligated by one N-aryliminopyrrolyl ligand and a bistrimethylsilylamide co-ligand. This complex was an extremely active catalyst for the synthesis of PCL.

## Chapter 5 - Ring-opening polymerisation of $\epsilon$ -caprolactone

Near complete conversion of  $\epsilon$ -CL was achieved after only 3 minutes at room temperature in toluene. The polymer produced had a  $M_n$  of 18,000  $\text{g mol}^{-1}$  and a  $\bar{D}$  of 1.8. The high  $\bar{D}$  indicates that while the catalyst is very active it does not have good control over the polymerisation. The activity of the homoleptic N-aryliminopyrrolyl complexes (**5.11b-e**) varied depending on the identity of the metal centre. When  $M = \text{Mg}$  and  $\text{Ca}$  (**5.11b** and **5.11c** respectively) only a small amount of PCL was produced, whereas when  $M = \text{Sr}$  and  $\text{Ba}$  (**5.11d** and **5.11e** respectively) a conversion  $\geq 97\%$  was recorded under the same conditions. The PCL produced by the reactions with **5.11d** and **5.11e** had very high molecular weight  $\geq 100,000 \text{ g mol}^{-1}$  indicating inefficient initiation of the polymerisation.<sup>47</sup>

Catalysts based on the rare earth elements have received a great deal of attention as many are non-toxic and show good activity and control for the ROP of  $\epsilon$ -CL.<sup>2</sup> Nomura and colleagues compared a wide range of rare earth metal triflates as catalysts for the ROP of  $\epsilon$ -CL. The reactions were carried out at 25 °C, with a catalyst loading of 2 mol% and 1 molar equivalent of benzyl alcohol. Of the reactions which achieved 100% completion, the PCL had a  $M_n$  between 1,700 and 3,500  $\text{g mol}^{-1}$  and a  $\bar{D}$  that ranged from 1.13 – 1.30. The rate of reaction of the metal triflates varied in the order  $\text{Sc} > \text{La} > \text{Ce} > \text{Yb} > \text{Lu} > \text{Eu} > \text{Y} > \text{Gd} \approx \text{Nd}$  requiring reaction times between 2 and 120 hours. The major advantage of rare earth triflates is that they can tolerate the presence of water in a reaction, reducing the need for rigorously dry reactants.<sup>48</sup>

Further examples of rare earth metal catalysts for the ROP of  $\epsilon$ -CL can be found in the recent review by Lyubov, Tolpygin and Trifonov.<sup>49</sup> Details of catalytic systems based on transition metals can be found in the review by Labet and Thielemans.<sup>2</sup> Enzymatic polymerisation of  $\epsilon$ -CL has been studied and the lipase from *Candida Antarctica* has proved particularly effective.<sup>50-52</sup> Finally the ROP of  $\epsilon$ -CL may be catalysed by metal-free organocatalysts.<sup>53,54</sup>

In the literature there have been many examples of catalysts for the ROP of  $\epsilon$ -CL which are based on aluminium complexes, a high proportion of these utilise iminophenolate ligands. Catalytic systems based on macrocyclic

aluminium complexes are much rarer. This is surprising given the highly tunable nature and good compatibility of these ligands with aluminium. It is therefore of interest to explore the efficacy of aluminium catalysts containing the pendant arm triazacyclononane (TACN) ligand in the ROP of  $\epsilon$ -CL.

### **5.2 Synthesis and characterisation of $[\text{Al}(\text{L1})(\text{O}^i\text{Pr})_2] \text{ (3)}$**

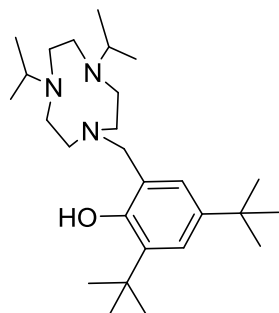
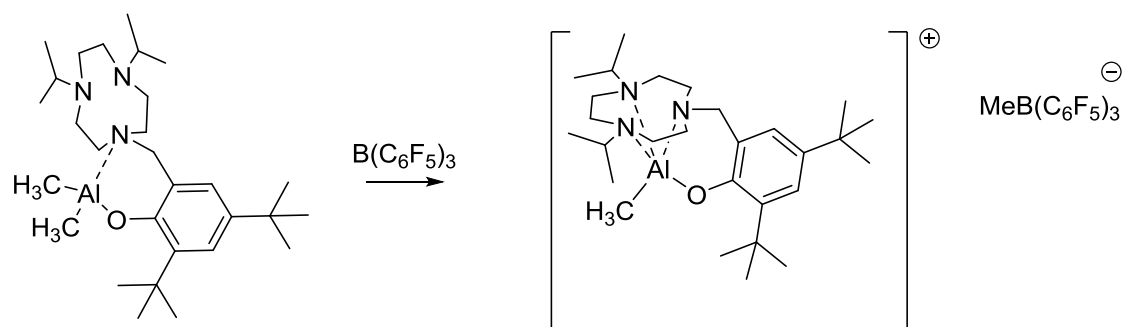


**Figure 13** 1,4-Diisopropyl-1,4,7-triazacyclononane ligand (**5.12**)

The pendant-arm TACN proligand (**5.12**) (Figure 13) will readily form a coordination complex with a variety of metals. Mountford *et al.* reported that the methyl aluminium complex with a 1,4-diisopropyl-1,4,7-triazacyclononane ligand  $[\text{Al}(\text{5.12})(\text{Me})_2]$  exhibits fluxional behaviour. The macrocyclic TACN ligand in **5.12** shows hemilabile bonding to the aluminium metal centre (Scheme 9).<sup>55</sup> Hemilability has proven to be an advantageous property for a range of homogeneous catalysts utilised for a variety of reactions.<sup>56–61</sup>



**Scheme 9** Hemilabile  $[\text{Al}(\text{5.12})(\text{Me})_2]$ <sup>55</sup>

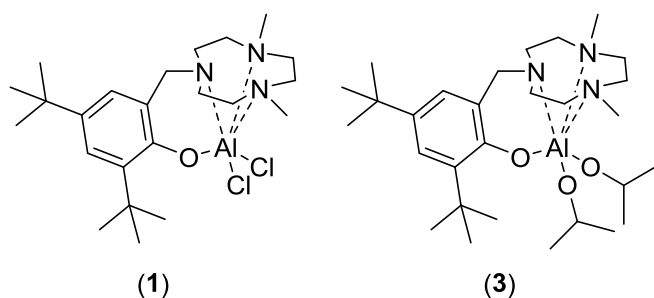


**Figure 14**  $[\text{Al}(\text{L1})\text{Cl}_2]$  (**1**) and  $[\text{Al}(\text{L1})(\text{OiPr})_2]$  (**3**)

The macrocyclic aluminium complex  $[\text{Al}(\text{L1})\text{Cl}_2]$  (**1**) (Figure 14) proved to be an effective and versatile catalyst for ring-opening copolymerisation (ROCOP) of cyclic anhydrides and epoxides (Chapter 2), converting 400 equivalents of epoxide and anhydride into polyester after 1 – 2 hours at 80 °C. **1** exhibited good control over the polymerisation achieving  $\bar{D}$  as low as 1.08.

Following the success of **1** as a catalyst for the ROCOP of epoxides and cyclic anhydrides, the efficacy of this type of catalyst for the ROP of  $\epsilon$ -CL was investigated. The coordination-insertion mechanisms of the copolymerisation of epoxides and anhydrides and the ROP of  $\epsilon$ -CL have many similarities, in the propagation of both polymerisations, insertion of an alkoxide into the carbonyl group of a monomer by nucleophilic addition and ring-opening are both key steps in propagation of each reaction.<sup>62</sup>

The aluminium isopropoxide complex  $[\text{Al}(\text{L1})(\text{OiPr})_2]$  (**3**) (Figure 14) was formed from the reaction of 1,4-dimethyl-1,4,7-triazacyclononane (**HL1**) and  $\text{AlMe}_3$  in toluene which was stirred overnight. Subsequently isopropanol was added to the reaction and following stirring overnight, (**3**) was obtained by removal of the solvent under vacuum.

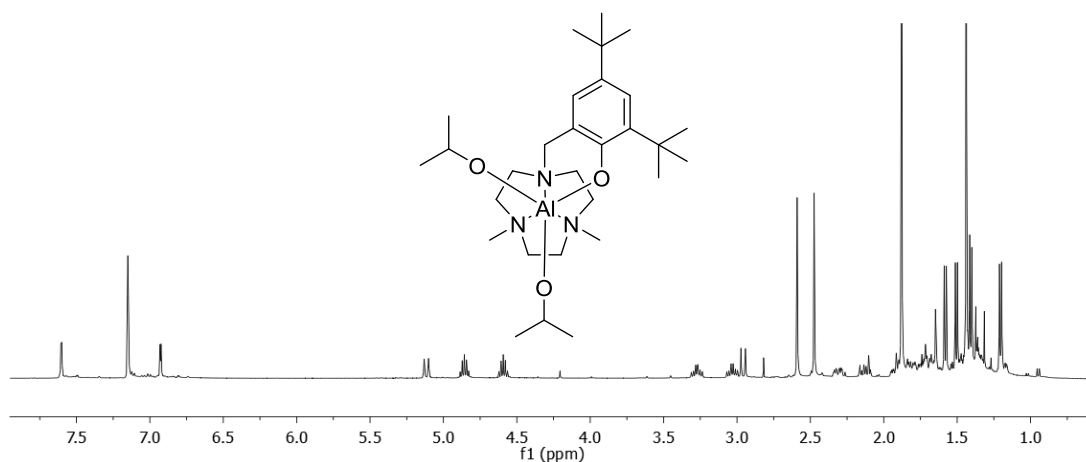


**Figure 15**  $^1\text{H}$  NMR spectrum (500 MHz,  $\text{CDCl}_3$ ) of  $[\text{Al}(\text{L1})(\text{OiPr})_2]$  (**3**)

The  $^1\text{H}$  NMR spectrum of **3** is shown in Figure 15. The two protons of the phenyl ring produce signals at 7.61 and 6.93 ppm. The protons of the methylene bridge are inequivalent when the ligand is coordinated to the metal centre and therefore appear as two doublets in the  $^1\text{H}$  NMR spectrum, one at 5.13 ppm and the other at 2.97 ppm. The methyl groups bound to the nitrogens of the TACN ring give rise to doublets at 2.60 and 2.49 ppm and the protons of the ligand *tert*-butyl groups produce singlets at 1.89 and 1.45 ppm. Good evidence for the formation of the alkoxide complex is the presence of signals attributed to the protons of isopropoxide co-ligands. The protons of the two isopropoxide groups are inequivalent [**A**( $\text{OCH}(\text{CH}_3)_2$ ) and (**B**( $\text{OCH}(\text{CH}_3)_2$ )] and additionally, the two methyl groups on the same isopropoxide co-ligand are also inequivalent. Two distinctive septets are present in the spectrum at 4.86 ppm [**A**( $\text{OCH}(\text{CH}_3)_2$ )] and 4.60 ppm [**B**( $\text{OCH}(\text{CH}_3)_2$ )]. The methyl groups of [**A**( $\text{OCH}(\text{CH}_3)_2$ )] appear as two doublets at 1.59 and 1.51 ppm, while the doublets at 1.42 and 1.21 ppm are produced by the resonances from the methyl groups of [**B**( $\text{OCH}(\text{CH}_3)_2$ )].

### **5.3 ROP of $\epsilon$ -CL catalysed by $[\text{Al}(\text{L1})(\text{OiPr})_2]$ (**3**) and $[\text{Al}(\text{L1})(\text{Me})_2]$ (**2**)**

Given that **1** proved to be an effective catalyst for the ROCOP of epoxides and cyclic anhydrides, it stands to reason that the alkoxide analogue **3** will be effective for the mechanistically similar ROP of  $\epsilon$ -CL.

## Chapter 5 - Ring-opening polymerisation of $\epsilon$ -caprolactone

**3** was combined with either 100 or 400 molar equivalents of  $\epsilon$ -CL in 3 ml of toluene and heated at 80 °C. After the desired reaction time, a crude  $^1\text{H}$  NMR spectrum was recorded to determine conversion of  $\epsilon$ -CL to PCL and the polymer was isolated by precipitation induced by the addition of methanol. The polymer was analysed by GPC to determine the molecular weight and  $\bar{D}$ . The results are shown in Table 1 (entries 63 – 65). Expected molecular weights are calculated by Equation 1.

$$\begin{aligned} &\text{Expected molecular weight} \\ &= [(Mr \text{ of CL}) \times (\text{moles of CL: moles of initiator}) \\ &\quad + (Mr \text{ of end groups})] \times \frac{\text{conversion}}{100} \end{aligned}$$

**Equation 1** Expected molecular weight calculation

**Table 1** Ring-opening polymerisation (ROP) of  $\epsilon$ -caprolactone ( $\epsilon$ -CL)

Entry	Cat	Ratio $\epsilon$ -CL:Al:BnOH	Time (hours)	Conv (%)	Actual Mn	Expected Mn	$\bar{D}$
63	<b>3</b>	400:1:0	24	94	20880	21520	1.15
64	<b>3</b>	100:1:0	24	99	13200	5710	1.29
65	<b>3</b>	100:1:0	6	72	11240	4150	1.28
66 <sup>a</sup>	<b>2</b>	400:1:1	24	83	23780	37980	1.12
67 <sup>a</sup>	<b>2</b>	100:1:1	6	88	11520	10140	1.25
68	<b>2</b>	400:1:0	24	41	21230	9370	1.14
69	<b>2</b>	100:1:0	6	67	22650	3830	1.13

Reactions stirred at 500 rpm in 3ml toluene. 1 equivalent of catalyst = 0.015 mmol. Reactions prepared under an inert atmosphere in a glove box. Mn corrected. <sup>a</sup>1 molar equivalent of BnOH was added to the catalyst in the form of a 1 wt% BnOH solution in dry toluene.

A conversion of 94% was achieved when 400 molar equivalents of  $\epsilon$ -CL was heated for 24 hours with **3** (entry 63). The PCL produced had a Mn of 20,880  $\text{gmol}^{-1}$  and a  $\bar{D}$  of 1.15. When the catalyst loading was increased so that the monomer:**3** ratio was 100:1, near complete conversion (99%) was achieved after 24 hours (entry 64). As expected, the Mn of the PCL decreased



compared to entry 1 to 13,200  $\text{gmol}^{-1}$ . When the reaction time was reduced to 6 hours, the conversion of monomer to polymer decreased to 72% and the molecular weight dropped slightly (entry 65). The molecular weight measured in entry 63 was close to the expected molecular weight calculated from the ratio of monomer to catalyst and assuming that each molecule of catalyst gives two polymer chains due to the presence of two isopropoxide co-ligands per aluminium. For entries 64 and 65 the measured molecular weight was much higher than the expected molecular weight, indicating slow polymerisation initiation. This is surprising as the only difference in these experiments is the presence of 100 molar equivalents of  $\epsilon$ -CL compared to 400 in entry 63. The higher concentration of  $\epsilon$ -CL in entry 63 may increase the rate of initiation as the initiation rate is proportional to monomer concentration. Another explanation could be that the higher concentration of  $\epsilon$ -CL in entry 63 helps to solubilise the catalyst complex therefore increasing the efficiency of polymer initiation. The catalyst may solubilise as it reacts with the monomer and as this rate of reaction is proportional to the monomer concentration, the greater the monomer concentration the faster the dissolution of the catalyst. Faster catalyst dissolution would lead to a more efficient initiation.<sup>2</sup>

It has previously been reported in the literature that the addition of one equivalent of alcohol per aluminium metal centre produced the optimal catalyst for the ROP of  $\epsilon$ -CL.<sup>63</sup> To ascertain whether this phenomenon applied to the aluminium catalysts formed from the **HL1** ligand, the ROP of  $\epsilon$ -CL was undertaken in the presence of the aluminium methyl complex  $[\text{Al}(\text{L1})(\text{Me})_2]$  (**2**) and 1 equivalent of BnOH (Table 1, entries 66 and 67). **2** is an intermediate formed in the synthesis of **3**, generated from the reaction of **HL1** and  $\text{AlMe}_3$ . **2** was isolated after stirring the ligand and  $\text{AlMe}_3$  overnight and by subsequently removing the toluene solvent under vacuum. In entries 66 and 67, addition of 1 equivalent of BnOH to **2** led to an *in situ* protonolysis reaction. In entry 66, where the  $\epsilon$ -CL:**2**:BnOH ratio was 400:1:1, a conversion of 83% was recorded after 24 hours. The PCL produced had a  $M_n$  of 23,780  $\text{gmol}^{-1}$  and a  $\bar{D}$  of 1.12. When the molar equivalents of monomer was reduced to 100, a conversion of 88% was recorded after 6 hours and the PCL generated had a  $M_n$  of 11,520  $\text{gmol}^{-1}$  and a  $\bar{D}$  of 1.25 (entry 67). For entries 66 and 67, the expected

molecular weight is calculated assuming that one polymer chain is generated per aluminium centre. The measured molecular weight in entry 67 showed good agreement to the expected molecular weight, whereas in entry 66 the measured molecular weight was significantly lower than the expected value. A potential explanation for this is the occurrence of backbiting at longer reaction times. Greater control of the polymerisation was achieved when **2** was used with 1 molar equivalent of BnOH, compared to when **3** was used as the catalyst under the same reaction conditions.

The  $^1\text{H}$  NMR spectra of **2** are extremely broad and could not be accurately assigned. The complex containing the isopropyl congener of **L1** (**5.12**) was characterised by Mountford *et al.* and the reported NMR data are comparable to **2**, however unlike for **5.12**, VT NMR experiments ( $-80\text{ }^\circ\text{C}$ ) did not cause the signals in **2** to decoalesce. The structural assignment of **2** is further supported by the observation that reaction with isopropyl alcohol and benzyl alcohol gave the corresponding alkoxide complexes **3** and **4** (Figure 16). **4** was synthesised from the reaction of **2** with 2.2 molar equivalents of benzyl alcohol and the resulting aluminium alkoxide complex was fully characterised. Formation of **4** is good evidence that the *in situ* protonation reaction of **2** with 1 molar equivalent of BnOH will take place (entries 66 and 67).

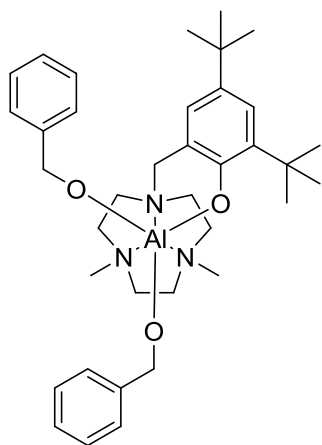


**Figure 16**  $[\text{Al}(\text{L1})(\text{OBn})_2]$  (**4**)

When **2** was used as a catalyst for the ROP of  $\epsilon$ -CL in the absence of an alcohol initiator, PCL was still produced (Table 1, entries 68 and 69). However the rate of reaction decreased and the molecular weight of the polymer was

far higher than what would be expected. The expected molecular weights for entries 68 and 69 are calculated assuming that each aluminium centre generates two polymer chains. The higher than expected molecular weight could be a result of slow initiation by methyl groups.

The catalytic systems tested utilising **2** and **3** proved to be active for the ROP of  $\epsilon$ -CL. Compared to other systems reported in the literature, the activity measured for **2** and **3** was moderate.<sup>2</sup> Good reaction control was exhibited by the catalysts, all of which produced PCL with  $\bar{D}$ 's <1.3. The catalytic system which imparted the greatest degree of control was the combination of **2** with 1 molar equivalent of BnOH initiator (entry 66), yielding PCL with a  $\bar{D}$  of 1.12. This observation correlates to previous observations in the literature which report that a initiator to aluminium ratio 1:1 gives an optimal catalytic system.<sup>63</sup>

#### **5.4 Mechanistic investigation**

The ROP mechanism of  $\epsilon$ -CL with **3** was probed using density functional calculations undertaken by Dr. Benjamin Ward.<sup>64</sup> For computational simplicity the model complex,  $[\text{Al}(\text{L}1)(\text{OMe})_2]$  (**5<sub>qm</sub>**) was employed in the calculations in place of **3**. All calculations employed the M06-2X functional, which is particularly suited to main group systems; the cc-pVTZ basis set was used for all elements except for aluminium, for which we used cc-pV(T+d)Z; this basis set gives a better description of the d-polarisation functions for 3p elements. Calculated structures are shown in the appendix.

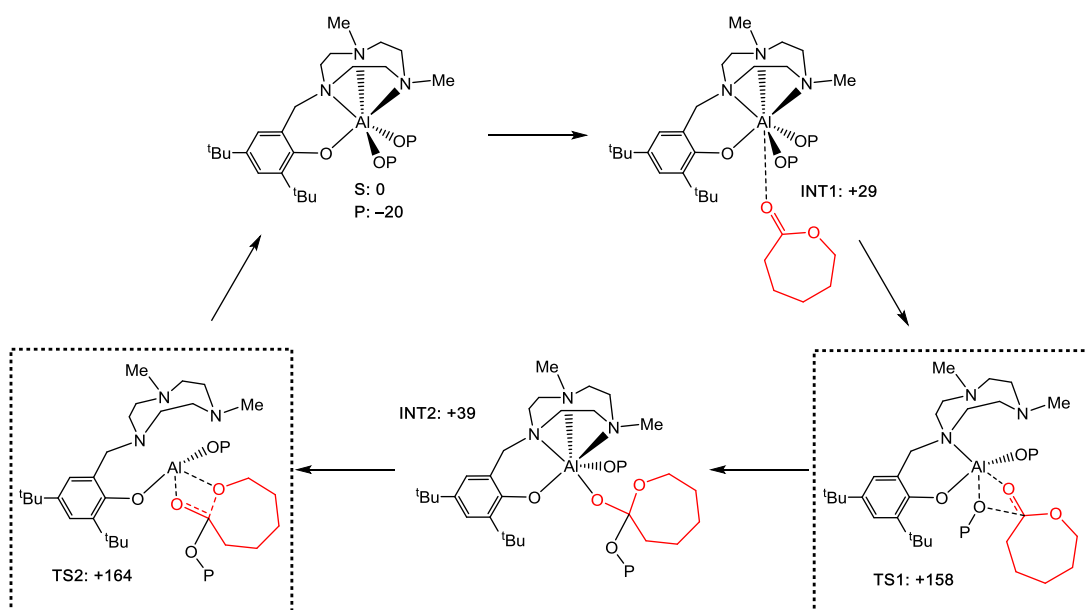
Using atomic coordinates from X-ray crystallographic analyses as suitable starting points,<sup>55</sup> the  $\kappa^4$  and  $\kappa^2$  structures of **2**, **3** and **5<sub>qm</sub>** were optimised. For both **3** and **5<sub>qm</sub>**, the  $\kappa^4$  structure is the most stable as would be expected on the basis of the macrocycle effect. The differences in energy between the  $\kappa^4$  and  $\kappa^2$  structures is relatively small,  $\Delta G = 34.3 \text{ kJ mol}^{-1}$  and  $\Delta G = 45.4 \text{ kJ mol}^{-1}$  for **3** and **5<sub>qm</sub>** respectively. The slightly lower  $\kappa^4$ - $\kappa^2$  energy difference for **3** compared to **5<sub>qm</sub>** is most likely a result of the greater steric demands of an isopropyl group relative to a methyl. In contrast to the alkoxide complexes **3** and **5<sub>qm</sub>**, the most stable calculated structure for the organometallic species **2** was  $\kappa^2$ , where  $\Delta G = 9.4 \text{ kJ mol}^{-1}$ . The very small difference in energy between the two structures indicate that both isomers may be observable

experimentally with the  $\kappa^2$  isomer as the major component, consistent with reports by Mountford *et al.*<sup>55,65</sup> Given the relatively small energy differences between the  $\kappa^4$  and  $\kappa^2$  isomers and given that **1** exhibited hemilability in the ROCOP of epoxides and cyclic anhydrides, it is likely that hemilabile transformations will occur during the ROP of  $\epsilon$ -CL. The mechanism based on both  $\kappa^4$  and  $\kappa^2$  species was probed.

Since the pre-catalyst complex **3** is six coordinate in its most stable form, and therefore could be considered to be coordinatively saturated, we first examined whether the ROP could proceed *via* the decoordination of an alkoxide ligand affording a cationic complex  $[\text{Al}(\text{L1})(\text{O}^i\text{Pr})]^+$ . This was calculated for the model complex **5<sub>qm</sub>**, for which formation of  $[\text{Al}(\text{L1})(\text{OMe})]^+$  lies at  $\Delta G = +448.1$  kJ mol<sup>-1</sup>. When coordination of  $\epsilon$ -CL to the cationic complex was included in the calculation  $[[\text{Al}(\text{L1})(\text{OMe})(\epsilon\text{-CL})]^+]$ , the  $\Delta G = +383.7$  kJ mol<sup>-1</sup>. The high  $\Delta G$  values recorded, indicate that decooordination of an alkoxide co-ligand is not a viable reaction pathway and therefore it was not probed further.

A viable structure with pre-coordination of  $\epsilon$ -CL to **5<sub>qm</sub>** forming a direct Al-O=C bond could not be identified, this is perhaps unsurprising as **5<sub>qm</sub>** is already six coordinate and monomer coordination would lead to a seven coordinate species. However, calculations suggest that there is a viable stationary point where a  $\epsilon$ -CL molecule associates with the catalyst complex in a weak donor-acceptor interaction (**INT1**). Examination of this structure using Natural Bonding Orbital (NBO) analysis indicates only a very weak O...Al interaction;<sup>66</sup> Bader's quantum theory of atoms in molecules (QTAIM) calculations indicate a number of bond critical points (BCPs),<sup>67</sup> with small associated electron density maxima ( $\rho$ ) between proximal C-H groups from the *tert*-butyl moiety of **L1**, and the coordinated OMe ligands. From this we infer that this structure corresponds to the  $\epsilon$ -CL held in place by weak van der Waals forces.

## Chapter 5 - Ring-opening polymerisation of $\epsilon$ -caprolactone



**Scheme 10** Calculated mechanism for the polymerisation of  $\epsilon$ -caprolactone ( $\epsilon$ -CL) by  $[\text{Al}(\text{L1})(\text{OMe})_2]$  (**5<sub>qm</sub>**). Relative free energies ( $G_{\text{rel}}$ , kJ mol<sup>-1</sup>) (298 K) are given beside each structure. Structures contained within dashed boxes contain one or more “non-bonding” nitrogen donors [M06-2X | cc-pV(T+d)Z/cc-PVTZ]

The calculations lead us to propose the reaction pathway shown in Scheme 10 for the ROP of  $\epsilon$ -CL catalysed by **5<sub>qm</sub>**, which is based upon the well-established coordination-insertion mechanism that is common in the polymerisation of cyclic esters.<sup>20,21</sup>

For the polymerisation of  $\epsilon$ -CL to occur experimentally, substantial heating was required, it is therefore expected that the calculated activation energies for the reaction are high; the migratory insertion over the carbonyl **TS1** and ring-opening **TS2** transition states lie at  $G_{\text{rel}} = +158$  and  $+164$  kJ mol<sup>-1</sup>, respectively.

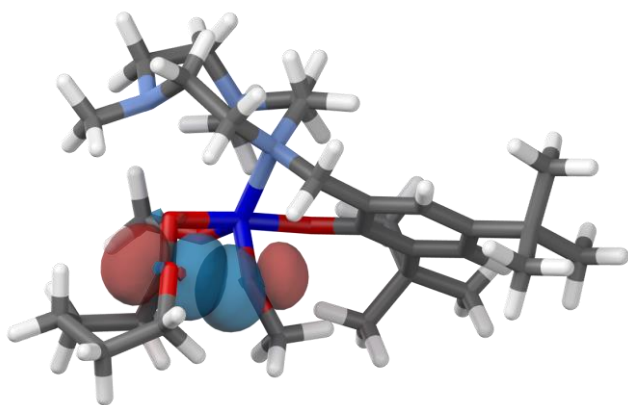


**Figure 17** Calculated structure of **TS1**, showing the donor-acceptor interactions associated with the forming O=C...OMe bond obtained from NBO analysis [M06-2X | cc-pV(T+d)Z/cc-PVTZ].

Figure 17 shows the calculated structure of **TS1** and indicates the donor-acceptor interactions associated with the migratory insertion of the alkoxide to the carbonyl of  $\epsilon$ -CL. The NBO second order perturbation analysis indicates that **TS1** can be described as a  $sp^3$  oxygen lone pair donating into a vacant p orbital of the carbonyl carbon.

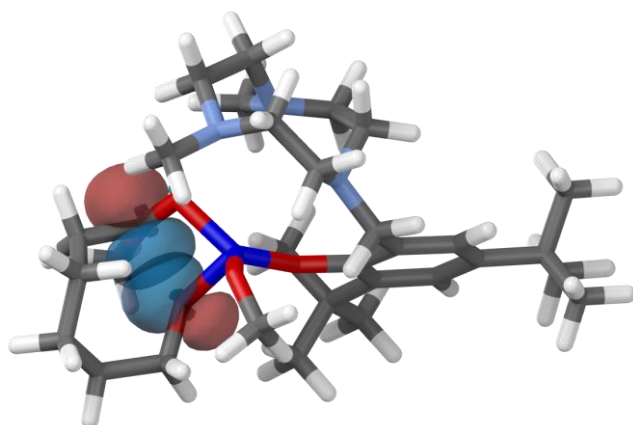


**Figure 18** Calculated structure of **TS2**, showing the donor-acceptor interactions associated with the breaking C–O bond, obtained from NBO analysis [M06-2X | cc-pV(T+d)Z/cc-PVTZ]

Following the migratory insertion, the next step in the mechanism is the ring-opening of the monomer, **TS2**. The ring-opening is defined as the breaking of the ring C–O bond and the simultaneous migration of the aluminium metal centre to the ring-oxygen, yielding an alkoxide ligand. NBO second order perturbation analysis indicates that the C–O bond breaks to give an empty

carbon based p orbital and a full oxygen  $sp^3$  orbital as depicted in Figure 18, formation of the new O–Al bond can be described as donation from an oxygen based  $sp^2$  hybrid into a vacant Al-based s orbital.

Considering  $[Al(L1)(Cl)_2]$  (**1**) exhibited hemilability when utilised as a catalyst for the ROCOP of epoxides and cyclic anhydrides (Chapter 2.4), it was of interest to determine whether hemilabile bonding was present during the ROP of  $\epsilon$ -CL with **5<sub>qm</sub>**. In the ROCOP reaction, calculations indicated that the ligand **L1** exhibited hemilabile bonding to the aluminium metal centre during the migratory insertion of an alkoxide into the carbonyl of an anhydride monomer. Prior to this transformation **L1** is bound in a  $\kappa^4$  manner, but after precoordination of an anhydride monomer, **L1** is bound in a  $\kappa^2$  arrangement where two of the triazacyclononane (TACN) nitrogens are decoordinated. During the transition state for the migratory insertion **L1** continues to bind in a  $\kappa^2$  manner ( $d_{Al-N} = 2.104 \text{ \AA}$ ,  $2.628 \text{ \AA}$ , and  $3.284 \text{ \AA}$ ). Following the migratory insertion, the bonding of **L1** to the aluminium centre returns to the  $\kappa^4$  binding mode. As **5<sub>qm</sub>** contains the same macrocyclic ligand and considering the many similarities between the ROP and ROCOP mechanisms,<sup>68</sup> the results of the DFT calculations for the ROP of  $\epsilon$ -CL catalysed by **4<sub>qm</sub>** was examined for evidence of similar hemilability.

Examination of the calculated structures at **TS1** and **TS2** showed that the complexes had some extremely long Al–N bond lengths:  $2.13 \text{ \AA}$ ,  $3.45 \text{ \AA}$  and  $3.12 \text{ \AA}$  in **TS1**, and  $3.04 \text{ \AA}$ ,  $3.34 \text{ \AA}$  and  $3.51 \text{ \AA}$  in **TS2**. Whilst all of these bond distances lie within the sum of the van der Waals radii ( $\Sigma r_{vdW}(Al-N) = 4.19 \text{ \AA}$ ),<sup>69</sup> it is clear that in **TS1** two, and in **TS2** all three, of the Al–N bonds are elongated to an extent that one would not normally consider to be within regular bonding distance. We therefore probed these structures using QTAIM calculations and NBO analyses.

QTAIM analysis of **TS1** indicated the presence of only one BCP, which was between the Al and N with the shortest bond distance ( $2.13 \text{ \AA}$ ). NBO second order perturbation analysis indicates the presence of donor-acceptor (D–A) interactions between the nitrogens of **L1** and the aluminium centre. The D–A interaction for the “bonded” nitrogen ( $2.13 \text{ \AA}$ ) is characterised as  $sp^4-s$  with an

associated energy of 138.9 kJ. The “non-bonding” nitrogens in **TS1** (3.45 Å and 3.12 Å) showed similar  $sp^6$ -s interactions, but these were of far lower energy (21.3 and 6.7 kJ).

QTAIM analysis of **TS2** indicated that there were no BCPs between the nitrogens of the TACN ring and the aluminium metal centre. NBO second order perturbation analysis indicate similar D–A interactions between the TACN nitrogens and the aluminium which were all of relatively low energy (26.8, 10.0 and 10.9 kJ).

These calculations suggest that elongation of 2 or 3 N–Al bonds occurs in **TS1** or **TS2** respectively, to such an extent that they cannot be considered bonds. This occurs to accommodate the transformation of  $\epsilon$ -CL at the aluminium metal centre. Despite the substantial elongation, an element of weak interaction remains as indicated by the NBO second order perturbation analysis, and the TACN ring remains pre-organised for re-coordination when required. All other calculated structures in the catalytic cycle exhibited  $\kappa^4$  bonding and showed BCP's between the aluminium and all nitrogens in the QTAIM analyses.

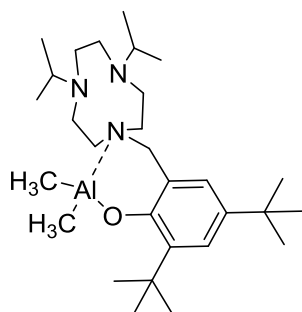


**Figure 19**  $[Al(\kappa^2\text{-}5.12)(Me)_2]$

The hemilability of **L1** when complexed to aluminium was first described by Mountford and colleagues, who reported and crystallographically verified the structure of  $[Al(\kappa^2\text{-}5.12)(Me)_2]$  (Figure 19).<sup>55</sup> **5.12** is an identical ligand to **L1**, apart from the presence of isopropyl groups bound to the non-donor-functionalised nitrogens of the TACN ring in the former, as opposed to methyl groups in the latter. To determine whether the active species in the ROP of  $\epsilon$ -CL had **L1** bound in a  $\kappa^2$  manner, the mechanism was calculated with  $[Al(\kappa^2\text{-}L1)(OMe)_2]$ . Whilst an unusual structural motif, the  $\kappa^2$  mechanism might be expected to be more likely on the basis of a lower coordination number of



## Chapter 5 - Ring-opening polymerisation of $\epsilon$ -caprolactone

Al in the transition state structures, particularly when one considers that the  $\kappa^4$  mechanism is so sterically demanding that the macrocycle is forced to partially de-coordinate to accommodate the transformations. However the transition state for the ring-opening of the monomer was found to lie at a much higher energy compared to the equivalent transition state (**TS2**) in the mechanism calculated for **5<sub>qm</sub>**,  $G_{\text{rel}} = +210 \text{ kJ mol}^{-1}$  cf.  $+164 \text{ kJ mol}^{-1}$ . The lower activation energy calculated for the more sterically demanding species is counter intuitive and therefore further investigation was required to understand the underlying cause. As the greatest energy difference between the two mechanisms was measured at the ring-opening transition state (**TS2**), this transformation was the focus of further examination. Calculation of the atomic charges at **TS2** for both mechanisms unearthed a substantial discrepancy, a higher positive charge on aluminium for the  $\kappa^4$  congener ( $+0.367$ ) was calculated, which was 32% higher than for the  $\kappa^2$  example ( $+0.277$ ). A higher positive charge may indicate greater electrophilicity at the metal centre in **TS2**. This may be rationalised by the fact that in the  $\kappa^2$  example, **L1** is bound to the Al through the oxygen and one nitrogen donor, whereas in the hemilabile “ $\kappa^4$ ” congener, **L1** is only bound to aluminium through the oxygen donor and is therefore in reality only  $\kappa^1$  at **TS2**, meaning it has a lower coordination number and greater electrophilicity. The  $G_{\text{rel}}$  at the transition state for the migratory insertion **TS1**, for both the “ $\kappa^4$ ” and “ $\kappa^2$ ” mechanisms were very similar in energy ( $+158$  and  $+155 \text{ kJ mol}^{-1}$  respectively) unlike the significant difference measured at **TS2**. The similarity in energy at **TS1** may be explained by the partial decoordination of the TACN ring in the “ $\kappa^4$ ” example, meaning the bonding of **L1** to the aluminium in both mechanisms may be described as  $\kappa^2$  and the only difference between the species at **TS1** is the presence of some weak interactions between the decoordinated nitrogens and aluminium in the “ $\kappa^4$ ” congener.

$$t_{\frac{1}{2}} = \frac{\ln 2}{k_{\text{obs}}}$$

**Equation 2** Relation between half-life and observed rate constant

$$k = \frac{k_{obs}}{[Al]}$$

**Equation 3** Calculation of rate constant

$$k = \frac{k_b T}{h} e^{\frac{-\Delta G^\ddagger}{RT}}$$

**Equation 4** Eyring equation

Estimated  $\Delta G^\ddagger$  can be calculated from the approximate polymerisation half-life ( $t_{1/2}$ ) for the ROP of  $\epsilon$ -CL. The  $t_{1/2}$  for the polymerisation of 100 equivalents of  $\epsilon$ -CL catalysed by **3** was 4.2 hr. The observed rate constant can be calculated from Equation 2 and the rate constant can subsequently be calculated from Equation 3.  $\Delta G^\ddagger$  can then be calculated from the rate constant using the Eyring equation (Equation 4). For the ROP of  $\epsilon$ -CL catalysed by **3** an approximate  $\Delta G^\ddagger$  of 101 KJmol<sup>-1</sup> was calculated. This number is lower than the  $\Delta G^\ddagger$  164 KJmol<sup>-1</sup> calculated by DFT. As was described in Chapter 2.4, it is well established that free energies are overestimated by DFT simulations. This is a result of the overestimation of the entropy reduction in the reaction. The overestimation can be somewhat offset by scaling the entropy terms using the Sackur-Tetrode equation (as has been carried out in the calculations in this thesis), however the free energy terms remain somewhat higher than those estimated experimentally.<sup>70</sup>

## **5.5 Summary**

In conclusion, aluminium complexes bearing the pendant arm TACN ligand **L1** proved to be active catalysts for the ROP of  $\epsilon$ -CL. The complex containing two isopropoxide co-ligands showed moderate activity and good to moderate control when utilised as a catalyst. The control of the polymerisation was improved when a catalytic system comprising of the organometallic species **2** and 1 molar equivalent of BnOH additive was utilised.

The mechanism of the ROP of  $\epsilon$ -CL with the model species **5<sub>qm</sub>** was investigated using DFT calculations. Of particular interest was the capacity for hemilabile binding between the TACN ring of **L1** and the aluminium centre in the complex. For both **3** and **5<sub>qm</sub>**, the structures with **L1** bound in a  $\kappa^4$  manner

were most stable, but the calculations indicate that the analogues with  $\kappa^2$  binding mode are low enough in energy to be considered accessible.

DFT calculations for the ROP of  $\epsilon$ -CL catalysed by  $[\text{Al}(\kappa^4\text{-L1})(\text{OMe})_2]$  indicated the point of highest energy in the mechanism was the transition state for the ring-opening of the monomer **TS2** ( $G_{\text{rel}} = +183.7 \text{ kJ mol}^{-1}$ ). The mechanism with  $[\text{Al}(\kappa^2\text{-L1})(\text{OMe})_2]$  was investigated, however **TS2** was found to lie at a much higher energy compared to the  $\kappa^4$  congener. The calculated mechanism for  $[\text{Al}(\kappa^4\text{-L1})(\text{OMe})_2]$  suggests that hemilability plays an important role in the polymerisation. At **TS1** and **TS2** the macrocyclic ligand **L1** binds to the aluminium centre in a  $\kappa^2$  and a  $\kappa^1$  manner respectively, temporarily reducing the coordination number and steric demand at the metal, allowing reactions involving the monomer to take place at the metal centre. QTAIM analysis suggests that at **TS1**, **L1** is bound to aluminium *via* the oxygen and one of the TACN ring nitrogens and at **TS2**, the ligand coordinates to the metal through the oxygen only. NBO second perturbation analyses indicate that the “decoordinated” nitrogens at both transition states, while not part of formal N–Al bonds, exhibit weak interactions to the metal centre meaning the ligand is held in close proximity and is pre-organised to recoordinate. Following the completion of the alkoxide insertion into the carbonyl and the ring-opening of the monomer, **L1** returns to the  $\kappa^4$  binding mode for the rest of the cycle. These calculations suggest that hemilability plays an important role in enabling the efficient catalysis of the ROP of  $\epsilon$ -CL with aluminium complexes bearing the pendent-arm TACN ligand **L1**.

**5.6 References for Chapter 5**

- 1 R. A. Gross and B. Kalra, *Science*, 2002, **297**, 803–807.
- 2 M. Labet and W. Thielemans, *Chem. Soc. Rev.*, 2009, **38**, 3484–3504.
- 3 L. G. Donaruma, *J. Polym. Sci. Part Polym. Chem.*, 1991, **29**, 1365–1365.
- 4 W. J. Cook, J. A. Cameron, J. P. Bell and S. J. Huang, *J. Polym. Sci. Polym. Lett. Ed.*, 1981, **19**, 159–165.
- 5 C. M. Buchanan, D. Dorschel, R. M. Gardner, R. J. Komarek, A. J. Matosky, A. W. White and M. D. Wood, *J. Environ. Polym. Degrad.*, 1996, **4**, 179–195.
- 6 X. Zhang, X. Peng and S. W. Zhang, in *Science and Principles of Biodegradable and Bioresorbable Medical Polymers*, ed. X. Zhang, Woodhead Publishing, 2017, pp. 217–254.
- 7 R. E. Cameron and A. Kamvari-Moghaddam, in *Durability and Reliability of Medical Polymers*, eds. M. Jenkins and A. Stamboulis, Woodhead Publishing, 2012, pp. 96–118.
- 8 B. Saad and U. W. Suter, in *Encyclopedia of Materials: Science and Technology*, eds. K. H. J. Buschow, R. W. Cahn, M. C. Flemings, B. Ilshner, E. J. Kramer, S. Mahajan and P. Veyssi re, Elsevier, Oxford, 2001, pp. 551–555.
- 9 T. Diki , W. Ming, P. Th ne, R. Benthem and G. With, *J. Polym. Sci. Part Polym. Chem.*, 2007, **46**, 218–227.
- 10 S. Roisman, A. L. Dotan and D. Y. Lewitus, *Polym. Adv. Technol.*, 2020, **31**, 3194–3201.
- 11 E. Malikmammadov, T. E. Tanir, A. Kiziltay, V. Hasirci and N. Hasirci, *J. Biomater. Sci. Polym. Ed.*, 2018, **29**, 863–893.
- 12 E. Rudnik, in *Plastic Films in Food Packaging*, ed. S. Ebnesajjad, William Andrew Publishing, Oxford, 2013, pp. 217–248.
- 13 S. M. Espinoza, H. I. Patil, E. S. M. Martinez, R. C. Pimentel and P. P. Ige, *Int. J. Polym. Mater. Polym. Biomater.*, 2020, **69**, 85–126.
- 14 S. Lambert and M. Wagner, *Chem. Soc. Rev.*, 2017, **46**, 6855–6871.

## Chapter 5 - Ring-opening polymerisation of $\epsilon$ -caprolactone

- 15 J. Payne, P. McKeown and M. D. Jones, *Polym. Degrad. Stab.*, 2019, **165**, 170–181.
- 16 K. M. Stridsberg, M. Ryner and A.-C. Albertsson, in *Degradable Aliphatic Polyesters*, Springer, Berlin, Heidelberg, 2002, pp. 41–65.
- 17 T. Endo, in *Handbook of Ring-Opening Polymerization*, John Wiley & Sons, Ltd, 2009, pp. 53–63.
- 18 P. Lewinski, J. Pretula, K. Kaluzynski, S. Kaźmierski and S. Penczek, *J. Catal.*, 2019, **371**, 305–312.
- 19 M. S. Kim, K. S. Seo, G. Khang and H. B. Lee, *Macromol. Rapid Commun.*, 2005, **26**, 643–648.
- 20 H. R. Kricheldorf, M. Berl and N. Scharnagl, *Macromolecules*, 1988, **21**, 286–293.
- 21 P. Dubois, C. Jacobs, R. Jerome and P. Teyssie, *Macromolecules*, 1991, **24**, 2266–2270.
- 22 M. Möller, R. Kånge and J. L. Hedrick, *J. Polym. Sci. Part Polym. Chem.*, 2000, **38**, 2067–2074.
- 23 A. Kowalski, A. Duda and S. Penczek, *Macromol. Rapid Commun.*, 1998, **19**, 567–572.
- 24 A. Duda, S. Penczek, A. Kowalski and J. Libiszowski, *Macromol. Symp.*, 2000, **153**, 41–53.
- 25 X. Yu, C. Zhang and Z. Wang, *ChemistrySelect*, 2020, **5**, 426–429.
- 26 Y. Wang and M. Kunioka, *Macromol. Symp.*, 2005, **224**, 193–206.
- 27 A. Duda, Z. Florjanczyk, A. Hofman, S. Slomkowski and S. Penczek, *Macromolecules*, 1990, **23**, 1640–1646.
- 28 N. Ropson, P. Dubois, R. Jerome and P. Teyssie, *Macromolecules*, 1993, **26**, 6378–6385.
- 29 N. Ropson, Ph. Dubois, R. Jerome and Ph. Teyssie, *Macromolecules*, 1995, **28**, 7589–7598.
- 30 N. Ropson, Ph. Dubois, R. Jerome and Ph. Teyssie, *Macromolecules*, 1994, **27**, 5950–5956.
- 31 A. Amgoune, L. Lavanant, C. M. Thomas, Y. Chi, R. Welter, S. Dagorne and J.-F. Carpentier, *Organometallics*, 2005, **24**, 6279–6282.
- 32 A. Duda, S. Penczek, P. Dubois, D. Mecerreyes and R. Jérôme, *Macromol. Chem. Phys.*, 1996, **197**, 1273–1283.

## Chapter 5 - Ring-opening polymerisation of $\epsilon$ -caprolactone

- 33 C. Jacobs, P. Dubois, R. Jerome and P. Teyssie, *Macromolecules*, 1991, **24**, 3027–3034.
- 34 M. Akatsuka, T. Aida and S. Inoue, *Macromolecules*, 1995, **28**, 1320–1322.
- 35 A. Arbaoui, C. Redshaw and D. L. Hughes, *Chem. Commun.*, 2008, 4717–4719.
- 36 N. Iwasa, J. Liu and K. Nomura, *Catal. Commun.*, 2008, **9**, 1148–1152.
- 37 N. Nomura, T. Aoyama, R. Ishii and T. Kondo, *Macromolecules*, 2005, **38**, 5363–5366.
- 38 W. Yao, Y. Mu, A. Gao, Q. Su, Y. Liu and Y. Zhang, *Polymer*, 2008, **49**, 2486–2491.
- 39 M. Endo, T. Aida and S. Inoue, *Macromolecules*, 1987, **20**, 2982–2988.
- 40 C.-H. Huang, F.-C. Wang, B.-T. Ko, T.-L. Yu and C.-C. Lin, *Macromolecules*, 2001, **34**, 356–361.
- 41 L. F. Sánchez-Barba, A. Garcés, M. Fajardo, C. Alonso-Moreno, J. Fernández-Baeza, A. Otero, A. Antiñolo, J. Tejeda, A. Lara-Sánchez and M. I. López-Solera, *Organometallics*, 2007, **26**, 6403–6411.
- 42 M. L. Barros, M. G. Cushion, A. D. Schwarz, Z. R. Turner and P. Mountford, *Dalton Trans.*, 2019, **48**, 4124–4138.
- 43 T.-L. Yu, C.-C. Wu, C.-C. Chen, B.-H. Huang, J. Wu and C.-C. Lin, *Polymer*, 2005, **46**, 5909–5917.
- 44 M.-L. Shueh, Y.-S. Wang, B.-H. Huang, C.-Y. Kuo and C.-C. Lin, *Macromolecules*, 2004, **37**, 5155–5162.
- 45 Z. Zhong, M. J. K. Ankoné, P. J. Dijkstra, C. Birg, M. Westerhausen and J. Feijen, *Polym. Bull.*, 2001, **46**, 51–57.
- 46 Z. Zhong, P. J. Dijkstra, C. Birg, M. Westerhausen and J. Feijen, *Macromolecules*, 2001, **34**, 3863–3868.
- 47 T. K. Panda, K. Yamamoto, K. Yamamoto, H. Kaneko, Y. Yang, H. Tsurugi and K. Mashima, *Organometallics*, 2012, **31**, 2268–2274.
- 48 N. Nomura, A. Taira, A. Nakase, T. Tomioka and M. Okada, *Tetrahedron*, 2007, **63**, 8478–8484.

## Chapter 5 - Ring-opening polymerisation of $\epsilon$ -caprolactone

- 49 D. M. Lyubov, A. O. Tolpygin and A. A. Trifonov, *Coord. Chem. Rev.*, 2019, **392**, 83–145.
- 50 M. Castano, J. Zheng, J. E. Puskas and M. L. Becker, *Polym. Chem.*, 2014, **5**, 1891–1896.
- 51 A. Kumar and R. A. Gross, *Biomacromolecules*, 2000, **1**, 133–138.
- 52 M. Bankova, A. Kumar, G. Impallomeni, A. Ballistreri and R. A. Gross, *Macromolecules*, 2002, **35**, 6858–6866.
- 53 N. E. Kamber, W. Jeong, R. M. Waymouth, R. C. Pratt, B. G. G. Lohmeijer and J. L. Hedrick, *Chem. Rev.*, 2007, **107**, 5813–5840.
- 54 M. K. Kiesewetter, E. J. Shin, J. L. Hedrick and R. M. Waymouth, *Macromolecules*, 2010, **43**, 2093–2107.
- 55 D. A. Robson, L. H. Rees, P. Mountford and M. Schröder, *Chem. Commun.*, 2000, 1269–1270.
- 56 M. A. Bahili, E. C. Stokes, R. C. Amesbury, D. M. C. Ould, B. Christo, R. J. Horne, B. M. Kariuki, J. A. Stewart, R. L. Taylor, P. A. Williams, M. D. Jones, K. D. M. Harris and B. D. Ward, *Chem. Commun.*, 2019, **55**, 7679–7682.
- 57 P. Braunstein and F. Naud, *Angew. Chem. Int. Ed.*, 2001, **40**, 680–699.
- 58 G. M. Adams and A. S. Weller, *Coord. Chem. Rev.*, 2018, **355**, 150–172.
- 59 Z. Weng, S. Teo and T. S. A. Hor, *Acc. Chem. Res.*, 2007, **40**, 676–684.
- 60 H. Werner, A. Stark, M. Schulz and J. Wolf, *Organometallics*, 1992, **11**, 1126–1130.
- 61 A. Buhling, P. C. J. Kamer, P. W. N. M. van Leeuwen, J. W. Elgersma, K. Goubitz and J. Fraanje, *Organometallics*, 1997, **16**, 3027–3037.
- 62 A.-C. Albertsson, I. K. Varma and R. K. Srivastava, in *Handbook of Ring-Opening Polymerization*, John Wiley & Sons, Ltd, 2009, pp. 287–306.
- 63 X. Wang, K.-Q. Zhao, Y. Al-Khafaji, S. Mo, T. J. Prior, M. R. J. Elsegood and C. Redshaw, *Eur. J. Inorg. Chem.*, 2017, **2017**, 1951–1965.
- 64 M. J. Frisch, G. W. Trucks, H. B. Schlegel, G. E. Scuseria, M. A. Robb, J. R. Cheeseman, G. Scalmani, V. Barone, G. A. Petersson, H.

## Chapter 5 - Ring-opening polymerisation of $\epsilon$ -caprolactone

- Nakatsuji, X. Li, M. Caricato, A. V. Marenich, J. Bloino, B. G. Janesko, R. Gomperts, B. Mennucci, H. P. Hratchian, J. V. Ortiz, A. F. Izmaylov, J. L. Sonnenberg, Williams, F. Ding, F. Lipparini, F. Egidi, J. Goings, B. Peng, A. Petrone, T. Henderson, D. Ranasinghe, V. G. Zakrzewski, J. Gao, N. Rega, G. Zheng, W. Liang, M. Hada, M. Ehara, K. Toyota, R. Fukuda, J. Hasegawa, M. Ishida, T. Nakajima, Y. Honda, O. Kitao, H. Nakai, T. Vreven, K. Throssell, J. A. Montgomery Jr., J. E. Peralta, F. Ogliaro, M. J. Bearpark, J. J. Heyd, E. N. Brothers, K. N. Kudin, V. N. Staroverov, T. A. Keith, R. Kobayashi, J. Normand, K. Raghavachari, A. P. Rendell, J. C. Burant, S. S. Iyengar, J. Tomasi, M. Cossi, J. M. Millam, M. Klene, C. Adamo, R. Cammi, J. W. Ochterski, R. L. Martin, K. Morokuma, O. Farkas, J. B. Foresman and D. J. Fox, *Gaussian 09 Rev. D.01*, Wallingford, CT, 2016.
- 65 D. A. Robson, S. Y. Bylikin, M. Cantuel, N. A. H. Male, L. H. Rees, P. Mountford and M. Schröder, *J. Chem. Soc. Dalton Trans.*, 2001, 157–169.
- 66 E. D. Glendening, J. K. Badenhoop, A. E. Reed, J. E. Carpenter, J. E. Bohmann, C. M. Morales, C. R. Landis and F. Weinhold, *NBO 6.0*, Theoretical Chemistry Institute, University of Wisconsin, Madison, 2013.
- 67 T. A. Keith, *AIMAll*, TK Gristmill Software, Overland Park KS, USA, 2017.
- 68 Y. Zhu, C. Romain and C. K. Williams, *J. Am. Chem. Soc.*, 2015, **137**, 12179–12182.
- 69 S. S. Batsanov, *Inorg. Mater.*, 2001, **37**, 871–885.
- 70 S.-J. Li and D.-C. Fang, *Phys. Chem. Chem. Phys.*, 2016, **18**, 30815–30823.



# Chapter 6

## Overall summary and conclusion

**6.1 Overall summary and conclusion**

Aluminium phenoxy-triazacyclononane complexes were identified as potential homogeneous catalysts for the ring-opening copolymerisation (ROCOP) of epoxides and cyclic anhydrides, and the ring-opening polymerisation (ROP) of  $\epsilon$ -caprolactone ( $\epsilon$ -CL). This type of complex was selected because of the hemilability exhibited between the triazacyclononane (TACN) ring and aluminium centre.<sup>1–3</sup> The pro-ligand employed in this thesis was the 2,4-di-*tert*-butylphenol pendant arm 1,4-dimethyl-1,4,7-TACN (**HL1**). Reaction of **HL1** with ethylaluminium dichloride yielded the complex [Al(L1)Cl<sub>2</sub>] (**1**). Reaction of **HL1** with trimethylaluminium yielded the complex [Al(L1)Me<sub>2</sub>] (**2**) and the subsequent reaction with isopropanol yielded [Al(L1)(O<sup>*i*</sup>Pr)<sub>2</sub>] (**3**).

Complex **1** proved to be a highly effective catalyst for the ROCOP of epoxides and cyclic anhydrides. A wide range of monomers were copolymerised in both solvent and solvent-free conditions. Many of the polyesters produced had good molecular weights and low dispersities ( $\bar{D}$ ).

An epichlorohydrin–phthalic anhydride (ECH–PhA) copolymer was analysed by MALDI-TOF mass spectrometry, which uncovered the presence of polymer series where the catalyst (AlL1) was still attached to the polymer chain despite workup in protic solvents and exposure to air/moisture. This was highly unexpected as **1** was understood to be an air and moisture sensitive complex. This discovery indicated that **1** was potentially more stable in air than previously thought and as a result the ROCOP catalysed by **1** was undertaken in air rather than under inert conditions. Gratifyingly, **1** proved to be an effective catalyst for the copolymerisation of cyclohexene oxide (CHO) and phthalic anhydride (PhA) in air, yielding copolymer of good molecular weight and low  $\bar{D}$  (1.13). This is, to the best of our knowledge, the first example of a catalyst for the ROCOP of epoxides and cyclic anhydrides which functioned successfully without the need for an inert atmosphere.

Efforts were undertaken to further improve the  $\bar{D}$  of the copolymers synthesised, by reducing the bimodality of the polymer molecular weight distributions. The most common causes of a bimodal molecular weight distribution in a ROCOP reaction are diacid impurities in the cyclic anhydride,

## Chapter 6 - Overall summary and conclusion

and adventitious water that can initiate polymerisation.<sup>4</sup> To compensate for the presence of these impurities the catalytic system was modified. Instead of using **1** and bis(triphenylphosphine)iminium chloride (PPNCl), which are both a source of monofunctional chloride initiators, a new system yielding only bifunctional initiators was developed comprising of **2**, terephthalic acid (TPA) or 1,3-adamantanedicarboxylic acid (ADC) and their respective PPN salts. In this system an *in situ* protonation reaction occurs between the methyl co-ligands of **2** and the diacid (either TPA or ADC) yielding methane and most probably a complex multi-centred aluminium carboxylate. **2** with 1 equivalent of ADC and PPN<sub>2</sub>ADC yielded a CHO–PhA copolymer with a Đ of 1.08. This is a substantial improvement compared to the ROCOP catalysed by **3**. However examination of the GPC trace indicated that some degree of bimodality remained and therefore not all monofunctional initiators were removed.

A wide range of polymer properties are accessible via the ROCOP of epoxides and cyclic anhydrides.<sup>4</sup> In order to illustrate this, and the ease at which polymer characteristics can be varied, polyesters with the very important attribute of flame retardancy were synthesised. Nine copolymers from PhA, tetrachlorophthalic anhydride (TCPhA), tetrabromophthalic anhydride (TBPhA), CHO, ECH and propylene oxide (PO) were generated via the ROCOP catalysed by **1** and tested by Pyrolysis Combustion Flow Calorimetry (PCFC) and thermogravimetry (TGA). The copolymers derived from TCPhA and TBPhA exhibited excellent flame retardancy. The most flame retardant polymer generated was ECH–TBPhA which had a HRC of 128 J/g.K. For each of the epoxides used to produce copolymers, the examples with TBPhA produced the most flame retardant materials. These copolymers unexpectedly formed char on decomposition indicating that they exhibit both vapour phase and condensed phase flame retardancy which is unusual for halogen containing materials.<sup>5</sup>

The glass transition temperature ( $T_g$ ) of the nine copolymers was determined by Dynamic Mechanical Analyses (DMA). The polyesters showed an extremely wide range of  $T_g$ s (34 °C – 233 °C) illustrating the tunability of the ROCOP of epoxides and cyclic anhydrides. The  $T_g$  of CHO–TBPhA was

## **Chapter 6 - Overall summary and conclusion**

measured to be 233 °C which is, to the best of our knowledge, the highest reported  $T_g$  for a polymer formed from the ROCOP of epoxides and cyclic anhydrides. The ability to achieve such wide variety of  $T_g$  values for additive-free, flame retardant polymers is very exciting and illustrates the potential this copolymerisation to readily produce hydrolysable polyesters with a wide range of useful properties pertinent to real-world applications.

The properties of polymers can be varied by post-polymerisation modification.<sup>6</sup> Copolymers of 4-vinyl-cyclohexene oxide (VCHO) and PhA from the ROCOP catalysed by **1**, were modified by thiol-ene click reactions. A wide range of structurally diverse thiols were appended to the VCHO–PhA and the effect on  $T_g$  was investigated. Reaction with 1-hexanethiol and 2-mercaptoethanol caused the most significant changes in  $T_g$ , yielding polymers with values of 57 and 126 °C compared to 113 °C for the unmodified VCHO–PhA. Using the same process, crosslinking of VCHO–PhA was achieved by reaction with 1,6-hexanedithiol. The degree of crosslinking could be selectively controlled by varying the amount of 1,6-hexanedithiol used in the reaction. The degree of crosslinking had a substantial effect on the  $T_g$  of the copolymer which increased as the degree of crosslinking increased. Addition of 40 mol% 1,6-hexanedithiol to VCHO–PhA resulted in a 78% crosslinked polymer and the  $T_g$  increased from 113 °C for the unmodified copolymer, to 157 °C after crosslinking. PPM is an extremely effective method for varying polymer properties; there are many examples of epoxides and cyclic anhydrides ROCOP monomers which contain additional functional groups that may undergo PPM.<sup>4</sup> The work in this thesis exploring the thiol-ene click reaction illustrates this point. There is a whole host of alternative reactions that can be used for PPM and these may be the subject of future work in the field.<sup>6</sup>

The ROP of  $\epsilon$ -CL has many similarities to the ROCOP of epoxides and cyclic anhydrides.<sup>7</sup> **3** is the alkoxide congener of **1** and proved to effectively catalyse the ROP of  $\epsilon$ -CL. **3** showed moderate activity and good to moderate control. As had been reported in the literature, control was improved when organometallic congener **2** and BnOH were employed in a 1:1 ratio.<sup>8</sup>

## **Chapter 6 - Overall summary and conclusion**

The mechanisms of the ROCOP of epoxides and cyclic anhydrides and the ROP of  $\epsilon$ -CL catalysed by the aluminium phenoxy pendant arm macrocycle complexes **1** and **3** were investigated by density functional theory (DFT) calculations. These investigations highlighted how the hemilability of the aluminium catalysts plays an important role in the polymerisations contributing to the efficacy of the catalysts. In each mechanistic cycle the macrocycle ligand binds to the aluminium centre in a  $\kappa^4$  binding mode however when required, the TACN ring of the ligand can reduce its coordination number to allow for reaction at the metal centre. In both mechanisms, during the migratory insertion of the alkoxide into the carbonyl of the respective monomers, the ligand binds to aluminium in a  $\kappa^2$  binding mode. Additionally in the transition state for the ring-opening of the  $\epsilon$ -CL monomer, the ligand adopts a  $\kappa^1$  coordination mode. Bader's quantum theory of atoms in molecules (QTAIM) and natural bonding orbital (NBO) analyses indicate that the "decoordinated" nitrogens at the transition states, while not part of formal N–Al bonds, exhibit weak interactions to the metal centre meaning the ligand is held in close proximity and is pre-organised to re-coordinate.

In conclusion the work described in this thesis illustrates the potential to produce hydrolysable polyesters via the ROCOP of epoxides and cyclic anhydrides with a wide range of useful properties. The important attribute of flame retardancy was introduced without the need for additives. By varying the monomers used in the copolymerisation, polyesters with a wide range of  $T_g$ s were generated (34 °C – 233 °C), indicating how the hydrolysable polymers produced in this reaction may be suitable for a wide range of applications. The phenoxy pendant arm macrocycle ligand (**HL1**) is significantly different to many of the ligands previously used in the literature.<sup>4</sup> The efficacy of **1** as a ROCOP catalyst suggests other similar species such as metallocenes, constrained geometry complexes or other cis-dichloride complexes may also be effective. Other complexes which exhibit hemilability may also be promising candidates as catalysts for the ROCOP. Like **1**, these prospective catalysts may also show the same, highly desirable ability to catalyse the ROCOP of epoxides and cyclic anhydrides in air.

**6.2 References for Chapter 6**

- 1 S. Y. Bylikin, D. A. Robson, N. A. H. Male, L. H. Rees, P. Mountford and M. Schröder, *J. Chem. Soc. Dalton Trans.*, 2001, 170–180.
- 2 D. A. Robson, L. H. Rees, P. Mountford and M. Schröder, *Chem. Commun.*, 2000, 1269–1270.
- 3 D. A. Robson, S. Y. Bylikin, M. Cantuel, N. A. H. Male, L. H. Rees, P. Mountford and M. Schröder, *J. Chem. Soc. Dalton Trans.*, 2001, 157–169.
- 4 J. M. Longo, M. J. Sanford and G. W. Coates, *Chem. Rev.*, 2016, **116**, 15167–15197.
- 5 M. Bar, R. Alagirusamy and A. Das, *Fibers Polym.*, 2015, **16**, 705–717.
- 6 K. A. Günay, P. Theato and H.-A. Klok, *J. Polym. Sci. Part Polym. Chem.*, 2013, **51**, 1–28.
- 7 Y. Zhu, C. Romain and C. K. Williams, *J. Am. Chem. Soc.*, 2015, **137**, 12179–12182.
- 8 X. Wang, K.-Q. Zhao, Y. Al-Khafaji, S. Mo, T. J. Prior, M. R. J. Elsegood and C. Redshaw, *Eur. J. Inorg. Chem.*, 2017, **2017**, 1951–1965.

# **Chapter 7**

## **Experimental**

### **7.1 General methods and instrumentation**

All manipulations involving metal complexes and sample preparation for polymerisation studies were carried out using standard Schlenk line or glove-box techniques under an atmosphere of argon or of dinitrogen unless otherwise stated. Solvents were predried over activated 4 Å molecular sieves and were refluxed over potassium (tetrahydrofuran and benzene) or sodium wire / benzophenone (diethyl ether) under a dinitrogen atmosphere and collected by distillation. Other solvents were dried by passing through a column of activated alumina incorporated in an MBraun SPS800 solvent purification system (toluene, pentane and hexanes). Solvents (other than dichloromethane and THF) were stored over potassium mirrors. Deuterated solvents were dried over potassium ( $C_6D_6$ ) or calcium hydride ( $CDCl_3$ ), distilled under reduced pressure and stored under dinitrogen in Teflon valve ampoules.

$\epsilon$ -Caprolactone and all epoxides were dried by stirring over fresh calcium hydride for 48 hours and then distilled under reduced pressure. All anhydrides used in copolymerization were dissolved in  $CHCl_3$  and filtered while hot. The solvent was removed under vacuum and the solid purified by sublimation under reduced pressure. All other reagents were purchased from commercial suppliers and used as received, unless stated explicitly in the experimental text.

$^1H$  and  $^{13}C\{^1H\}$  spectra were recorded on Avance III HD 400 or Ascend 500 spectrometers.  $^1H$  and  $^{13}C$  assignments were confirmed with the use of two dimensional  $^1H\text{-}^1H$  and  $^{13}C\text{-}^1H$  NMR experiments.  $^1H$  and  $^{13}C$  spectra were referenced internally to residual protio-solvent ( $^1H$ ) or solvent ( $^{13}C$ ) resonances and are reported relative to tetramethylsilane ( $\delta = 0$  ppm). Chemical shifts are quoted in  $\delta$  (ppm) and coupling constants in Hertz. Mass spectra were recorded by the EPSRC National Mass Spectrometry Service.

Gel Permeation Chromatography data were obtained at the Cardiff Catalysis Institute, Cardiff University using ACQUITY Advanced Polymer Chromatography System or were measured on an Agilent 1260 Infinity II GPC system at the University of Bath.



## **Chapter 7 - Experimental**

The thermal decomposition was investigated with thermogravimetry (TGA) using a Perkin-Elmer TGA-FTIR-GCMS instrument incorporating Pyris 1 TGA, Frontier FTIR, Clarus 580 GC, and Clarus SQ8S MS components. All measurements were performed under air or nitrogen with a heating rate of 10 °C/min from room temperature to 900 °C. The temperature at 5%, 10% and 50% mass loss and the mass at 400 °C and 650 °C was measured.

Glass-transition temperatures ( $T_g$ ) were obtained from Dynamic Mechanical Analyses (DMA), carried out using a PerkinElmer DMA8000 [maxima of  $\tan(\delta_E)$ ,  $\tan(\delta_E)$  = ratio of loss modulus versus storage modulus]. It was used in a single cantilever mode at a fixed frequency (1 Hz) and deformation amplitude (0.05 mm). The samples were loaded in stainless steel material pocket in an average weight of 4-7 mg with a heating rate of 5 °C min<sup>-1</sup> between 20-300 °C. The material pocket allows the testing of non-self-supporting materials, a powder in this case. Whilst the magnitude of the storage modulus observed is dominated by the stainless-steel pocket the material transitions can still be clearly and accurately identified. At least three measurements were performed for all samples and an average was taken.

A pyrolysis combustion flow calorimeter (PCFC), Fire Testing Technology Ltd., UK, was used for flammability assessment of different samples. The heating rate was 1 °C/s to 750 °C in the pyrolysis zone. The pyrolysis was conducted under nitrogen. Following pyrolysis combustion takes place. The combustion temperature was set at 900 °C. The flow was a mixture of O<sub>2</sub>/N<sub>2</sub> 20/80 ml min<sup>-1</sup> and the sample weight was 3±0.5 mg. The results presented are averages of three experiments.

Limiting oxygen index (LOI) tests were undertaken in a manner similar to use for plastic sticks based on BS 4589-2:1999 standard. To effectively secure the plastic strips the thickness at the base was increased, this however does not affect the LOI test as the flame does not come into contact with this section.

### **7.2 Ring-opening copolymerisation (ROCOP) with solvent**

In a dinitrogen-filled glove box, **1**, PPNCl and cyclic anhydride were placed in an oven-dried screw-cap vial equipped with a magnetic stirrer bar. Epoxide and dry toluene (0.5 or 1 ml) were added, and the vial sealed and removed

## **Chapter 7 - Experimental**

from the glove box. The vial was placed in an aluminium heating block pre-heated to the appropriate temperature; the temperature was controlled by a thermocouple inserted into a “blank” reaction vial containing 2 ml of paraffin oil. The vial was stirred at 500 rpm at the required temperature for the required amount of time. The reaction mixture was diluted in 1 ml dichloromethane and precipitated with 100 ml of methanol or hexanes in air. The solvent was decanted and the solid dried under vacuum. Redissolving in DCM and precipitation was repeated as necessary to remove impurities.

### **7.3 Ring-opening copolymerisation (ROCOP) in bulk epoxide**

In a dinitrogen-filled glove box, **1**, PPNCI and cyclic anhydride were placed in an oven-dried screw-cap vial equipped with a magnetic stirrer bar. Epoxide was added, and the vial sealed and removed from the glove box. The vial was placed in an aluminium heating block pre-heated to the appropriate temperature; the temperature was controlled by a thermocouple inserted into a “blank” reaction vial containing 2 ml of paraffin oil. The vial was stirred at 500 rpm at the required temperature for the required amount of time. The reaction mixture was diluted in 1 ml dichloromethane and precipitated with 100 ml of methanol or hexanes in air. The solvent was decanted and the solid dried under vacuum. Redissolving in DCM and precipitation was repeated as necessary to remove impurities.

### **7.4 Post-polymerisation modification (PPM) of VCHO–PhA**

The copolymer VCHO–PhA (0.367 mmol or 1.044 mmol, 1 equiv.) and AIBN (66 mol%) were transferred to an oven dried Schlenk or a J Young flask with a stirrer bar and placed under an inert atmosphere. 5 ml of dry THF was added and the solids dissolved. Thiol (5 equiv.) was added to the solution which was stirred overnight at 70 °C. Subsequently the reaction was opened to air and the polymer was isolated by precipitation induced by the addition of 100 ml of methanol, hexanes or water. The solvent was decanted and the solid dried under vacuum. Precipitation was repeated as necessary to remove impurities.

### **7.5 Cross-linking of VCHO–PhA**

The copolymer VCHO–PhA (0.367 mmol, 1 equiv.) and AIBN (66 mol%) were transferred to an oven dried Schlenk or a J Young flask with a stirrer bar and placed under an inert atmosphere. 5 ml of dry THF was added and the solids dissolved. Hexanedithiol (10, 20 or 40 mol%) was added to the which was stirred overnight at 70 °C. Subsequently the reaction was opened to air and the polymer was isolated by precipitation induced by the addition of 100 ml of methanol or hexanes. The solvent was decanted and the solid dried under vacuum. Precipitation was repeated as necessary to remove impurities.

### **7.6 Ring-opening polymerisation (ROP) of $\epsilon$ -caprolactone ( $\epsilon$ -CL)**

In a dinitrogen-filled glove box **2** or **3** (0.015 mmol, 1 equiv.) was placed in an oven-dried screw-cap vial equipped with a magnetic stirrer bar. If BnOH is required it was added to the catalyst as a 1 wt% solution in dry toluene (0.16 ml) and stirred for 5 minutes. Dry toluene (3 ml) and  $\epsilon$ -CL (6 or 1.5 mmol) were added, and the vial sealed and removed from the glove box. The vial was placed in an aluminium heating block pre-heated to the appropriate temperature; the temperature was controlled by a thermocouple inserted into a “blank” reaction vial containing 2 ml of paraffin oil. The vial was stirred at 500 rpm at 80 °C for the required amount of time. The reaction mixture was precipitated with 100 ml of methanol. The solvent was decanted and the solid dried under vacuum. Precipitation was repeated as necessary to remove impurities.

### **7.7 Density functional calculations**

Calculations were performed using the Gaussian 09 software package.<sup>1</sup> Geometry optimizations were performed without symmetry constraints, using the M06-2X functional,<sup>2</sup> employing the cc-pV(T+d)Z for the aluminium, and cc-pVTZ on all other centres.<sup>3,4</sup> The nature of the optimized structures (minimum vs. saddle point) was determined by calculating the vibrational frequencies; transition state structures exhibited a single imaginary frequency which corresponded to the expected reaction coordinate. Entropy was scaled using the Sackur-Tetrode equation invoked via the GoodVibes program.<sup>5</sup> NBO

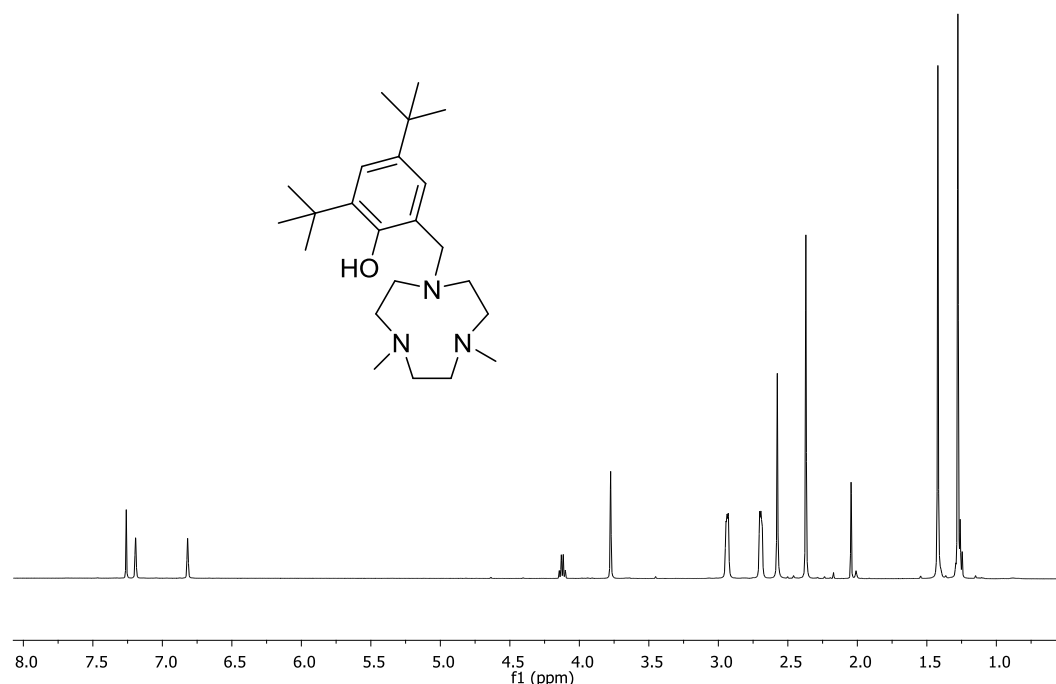
## Chapter 7 - Experimental

calculations were performed using NBO 6.0 invoked via the Gaussian 09 interface.<sup>6</sup> QTAIM calculations were performed using the AIMAll package.<sup>7</sup>

### 7.8 L1 pro-ligand synthesis

The pro-ligand **HL1** was synthesised according to a previously published method. The characterising data is consistent with the previous report.<sup>8,9</sup> An example <sup>1</sup>H NMR spectrum is provided for reference.

<sup>1</sup>H NMR spectrum (500 MHz, CDCl<sub>3</sub>) of the pro-ligand **HL1**



### 7.9 Synthesis of [Al(L1)Cl<sub>2</sub>] (**1**)

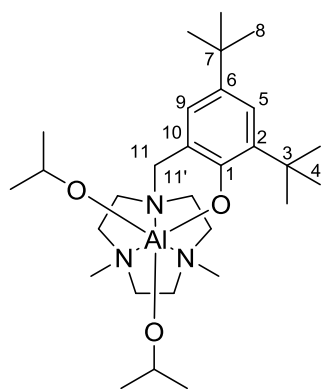
[Al(L1)Cl<sub>2</sub>] (**1**) was synthesised by a modified literature procedure as described below. Characterising data were consistent with the previous report.<sup>9</sup>

A solution of ligand **HL1** (223 mg, 5.937x10<sup>-4</sup> mol) in toluene (10 ml) was added to a solution of Al(Et)Cl<sub>2</sub> (0.33 ml, 1.8 M in toluene). A light brown solution formed upon addition. On stirring an off white suspension formed. After stirring overnight at room temperature a white precipitate formed. The solid was filtered from the solution and was washed with pentane (3 x 5 ml). The white solid was subsequently dried under vacuum. <sup>1</sup>H NMR, 400 MHz, CDCl<sub>3</sub>, 298 K, ppm): δ<sub>H</sub> 7.18 (1H, C<sub>6</sub>H<sub>2</sub>Bu<sup>t</sup>), 6.68 (1H, C<sub>6</sub>H<sub>2</sub>Bu<sup>t</sup>), 5.15 (d, J =

## Chapter 7 - Experimental

13.5, 1H, CH<sub>2</sub>Ar), 3.54 (d, J = 13.5, 1H, CH<sub>2</sub>Ar), 3.47–3.14 (m, 6H, NCH<sub>2</sub>CH<sub>2</sub>N), 3.04 (s, 3H, NMe), 2.91 (s, 3H, NMe), 2.88-2.69 (m, 6H, NCH<sub>2</sub>CH<sub>2</sub>N), 1.47 (s, 9H, CMe<sub>3</sub>), 1.25 (s, 9H, CMe<sub>3</sub>). <sup>13</sup>C {<sup>1</sup>H} NMR, 100 MHz, CDCl<sub>3</sub>, 298 K, ppm): δ<sub>C</sub> 156.955 (2-C<sub>6</sub>H<sub>2</sub>-Bu<sup>t</sup>), 138.830 and 137.281 (1-C<sub>6</sub>H<sub>2</sub>) and (3-C<sub>6</sub>H<sub>2</sub>), 123.498 and 123.195 (4-C<sub>6</sub>H<sub>2</sub>) and (6-C<sub>6</sub>H<sub>2</sub>), 118.763 (5-C<sub>6</sub>H<sub>2</sub>), 66.126 (NCH<sub>2</sub>Ar), 54.756, 54.359, 53.675, 53.275, 53.037 and 51.114 (NCH<sub>2</sub>CH<sub>2</sub>N), 50.626 and 50.123 (NMe), 35.286 and 34.063 (2 x CMe<sub>3</sub>), 31.933 and 30.507 (2 x CMe<sub>3</sub>). HR-MS (EI) for [Al(L1)(Cl<sub>2</sub>)<sup>+</sup>]: found (Calc. for C<sub>23</sub>H<sub>40</sub>N<sub>3</sub>OCl<sub>2</sub>) 471.2352 (471.2358). Anal. found (calc. for C<sub>23</sub>H<sub>40</sub>AlCl<sub>2</sub>N<sub>3</sub>O): C, 58.18 (58.47); H, 8.81 (8.53); N, 9.02 (8.89)

### 7.10 Synthesis of [Al(L1)(O<sup>i</sup>Pr)<sub>2</sub>] (**3**)

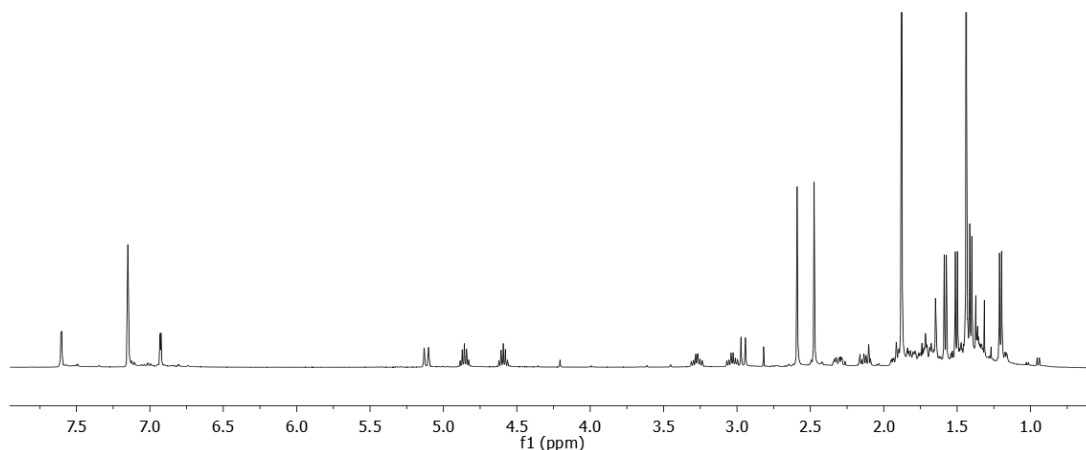


A solution of **HL1** (0.276 g, 7.344x10<sup>-4</sup> mol) in toluene (10 ml) was added slowly to a solution of Al(Me)<sub>3</sub> (0.37 ml, 2 M in toluene). The resulting solution was stirred overnight at room temperature, yielding a solution of **2**. To this solution iPrOH (11.25 ml, 1% in toluene) was added and the resulting colourless solution was stirred overnight. The solvent was subsequently removed under vacuum yielding a white solid **3** (0.263 g, 69%). <sup>1</sup>H NMR, 400 MHz, C<sub>6</sub>D<sub>6</sub>, 298 K, ppm): δ<sub>H</sub> 7.612 (d, J = 2.60, 1H, H<sup>5</sup>), 6.935 (d, J = 2.55, 1H, H<sup>9</sup>), 5.127 (d, J = 12.10, 1H, H<sup>11</sup>), 4.865 (sept, J = 5.82, 1H, OCH(CH<sub>3</sub>)<sub>2</sub>), 4.600 (sept, J = 5.82, 1H, OCH'(CH<sub>3</sub>)<sub>2</sub>), 3.283 (m, 1H, NCH<sub>2</sub>CH<sub>2</sub>N), 3.043 (app. td, app. <sup>2</sup>J = 11.72, app. <sup>3</sup>J = 5.57, 1H, NCH<sub>2</sub>CH<sub>2</sub>N), 2.967 (d, <sup>2</sup>J = 12.15, 1H, H<sup>11'</sup>), 2.600 (s, 3H, NCH<sub>3</sub>), 2.485 (s, 3H, NCH<sub>3</sub>), 2.325 (qd, <sup>2</sup>J = 14.34, <sup>3</sup>J = 5.93, <sup>3</sup>J = 2.29, 1H, NCH<sub>2</sub>CH<sub>2</sub>N), 2.18 – 1.15 (m, 10H, NCH<sub>2</sub>CH<sub>2</sub>N), 1.887 (s, 9H, CMe<sub>3</sub>), 1.589 (d, <sup>3</sup>J = 5.80, 3H, OCH(CH<sub>3</sub>)<sub>2</sub>), 1.513 (d, <sup>3</sup>J = 5.80, 3H, OCH(CH<sub>3</sub>)<sub>2</sub>), 1.446 (s, 9H, CMe<sub>3</sub>), 1.416 (d, <sup>3</sup>J = 6.00, 3H, OCH(CH<sub>3</sub>)<sub>2</sub>), 1.213

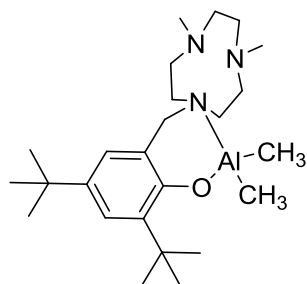
## Chapter 7 - Experimental

(d,  $^3J = 5.85$ , 3H,  $\text{OCH}(\text{CH}_3)_2$ ).  $^{13}\text{C}\{^1\text{H}\}$  NMR, 100 MHz,  $\text{C}_6\text{D}_6$ , 298 K, ppm):  $\delta_{\text{C}}$  160.838 ( $\text{C}^1$ ), 137.692 ( $\text{C}-\text{CMe}_3$ ), 135.449 ( $\text{C}-\text{CMe}_3$ ), 124.054 ( $\text{C}^9$ ), 123.814 ( $\text{C}^5$ ), 121.308 ( $\text{C}^{10}$ ), 66.084 ( $\text{C}^{11}$ ), 63.147 ( $\text{OCH}(\text{CH}_3)_2$ ), 63.051 ( $\text{OCH}(\text{CH}_3)_2$ ), 55.110 ( $\text{NCH}_2\text{CH}_2\text{N}$ ), 54.293 ( $\text{NCH}_2\text{CH}_2\text{N}$ ), 54.175 ( $\text{NCH}_2\text{CH}_2\text{N}$ ), 52.322 ( $\text{NCH}_2\text{CH}_2\text{N}$ ), 51.016 ( $\text{NCH}_2\text{CH}_2\text{N}$ ), 49.463 (N-Me), 49.346 (N-Me), 49.030 ( $\text{NCH}_2\text{CH}_2\text{N}$ ), 35.827 ( $\text{CMe}_3$ ), 34.167 ( $\text{CMe}_3$ ), 32.313 ( $\text{CMe}_3$ ), 31.092 ( $\text{CMe}_3$ ), 29.526 ( $\text{OCH}(\text{CH}_3)_2$ ), 29.350 ( $\text{OCH}(\text{CH}_3)_2$ ), 29.254 ( $\text{OCH}(\text{CH}_3)_2$ ), 28.438 ( $\text{OCH}(\text{CH}_3)_2$ ). HR-MS (EI) for  $[\text{Al}(\text{L1})(\text{O}^i\text{Pr})]^+$ : found (Calc. for  $\text{C}_{29}\text{H}_{54}\text{N}_3\text{O}_3\text{Al}$ ) 519.3983 (519.3975). As satisfactory elemental analysis could not be obtained, the  $^1\text{H}$  NMR spectrum is included to as indication of purity.

### $^1\text{H}$ NMR spectrum (500 MHz, $\text{C}_6\text{D}_6$ ) of **3**



### 7.11 Synthesis of $[\text{Al}(\text{L1})(\text{Me})_2]$ (**2**)

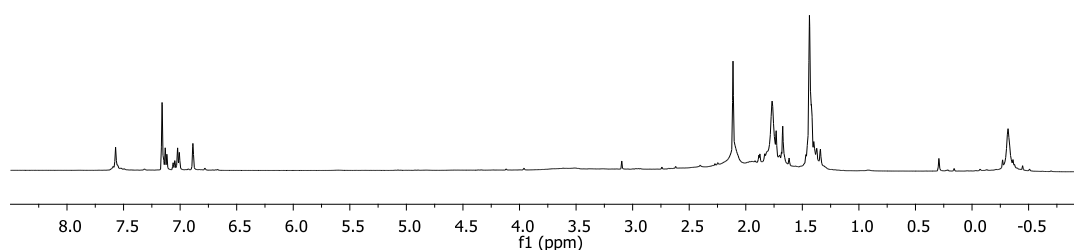


**2** was isolated as a white solid from the above procedure by removing the solvent under vacuum following stirring of the solution of **HL1** and  $\text{AlMe}_3$  in toluene overnight at room temperature. The NMR spectra of **2** were extremely broad and could not be accurately characterised. The  $^1\text{H}$  NMR is shown below. VT NMR did not provide spectra with well-defined signals. Satisfactory

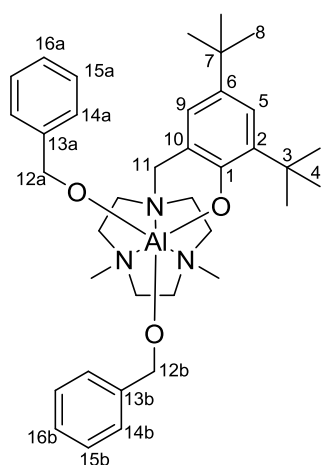
## Chapter 7 - Experimental

elemental analysis could not be obtained. The isopropyl congener was reported by Mountford *et al.*<sup>10</sup> The structural assignment is supported by the observation that reaction with isopropyl alcohol and benzyl alcohol gave the corresponding alkoxide complexes **3** and **4**.

### <sup>1</sup>H NMR spectrum (500 MHz, C<sub>6</sub>D<sub>6</sub>) of **2**



### 7.12 Synthesis of [Al(L1)(OBn)<sub>2</sub>] (**4**)



**2** (0.3g, 6.95x10<sup>-4</sup> mol) was dissolved in toluene (10 ml). To this pale yellow solution BnOH (2.2eq, 0.16 ml) was added which caused effervescence. The solution was stirred overnight, during this time a precipitate started to form. The solvent was subsequently removed under vacuum yielding an off white solid. This was washed with pentane yielding **4** (0.334, 78%). <sup>1</sup>H NMR, 500 MHz, CDCl<sub>3</sub>, 298 K, ppm): δ<sub>H</sub> 7.443 (d, J = 7.10, 2H, H<sup>13a</sup>), 7.279 (m, 4H, H<sup>15a</sup> and H<sup>14b</sup>), 7.218 (d, J = 2.63, 1H, H<sup>5</sup>), 7.184 (t, J = 7.48, 2H, H<sup>15b</sup>), 7.148 (t, J = 7.17, 1H, H<sup>16a</sup>), 7.074 (t, J = 7.48, 1H, H<sup>16b</sup>), 6.676 (d, J = 2.73, 1H, H<sup>9</sup>),

## Chapter 7 - Experimental

5.233 (d,  $J = 14.04$ , 1H,  $H^{12a}$ ), 5.171 (d,  $J = 14.04$ , 1H,  $H^{12a}$ ), 5.010 (d,  $J = 14.34$ , 1H,  $H^{12b}$ ), 4.851 (d,  $J = 12.53$ , 1H,  $H^{11}$ ), 4.741 (d,  $J = 14.34$ , 1H,  $H^{12b}$ ), 3.641 (m, 1H,  $NCH_2CH_2N$ ), 3.487 (m, 1H,  $NCH_2CH_2N$ ), 3.270 (d,  $J = 12.53$ , 1H,  $H^{11}$ ), 2.939 (m, 2H,  $NCH_2CH_2N$ ), 2.870 (s, 3H,  $NCH_3$ ), 2.798 (m, 4H  $NCH_2CH_2N$ ), 2.723 (s, 3H,  $NCH_3$ ), 2.650 (m, 1H,  $NCH_2CH_2N$ ), 2.543 (m, 1H,  $NCH_2CH_2N$ ), 2.436 (m, 2H,  $NCH_2CH_2N$ ), 2.308 (m, 1H,  $NCH_2CH_2N$ ), 1.541 (s, 9H,  $H^8$ ), 1.272 (s, 9H,  $H^4$ ).  $^{13}C\{^1H\}$  NMR, 125 MHz,  $CDCl_3$ , 298 K, ppm):  $\delta_C$  159.888 ( $C^1$ ), 149.343 ( $C^{13a}$ ), 149.176 ( $C^{13b}$ ), 137.142 ( $C^6$ ), 135.428 ( $C^2$ ), 127.731 ( $C^{15a}$ ), 127.584 ( $C^{15b}$ ), 126.382 ( $C^{14a}$ ), 126.299 ( $C^{14b}$ ), 125.082 ( $C^{16a}$ ), 124.935 ( $C^{16b}$ ), 124.097 ( $C^9$ ), 123.331 ( $C^5$ ), 120.609 ( $C^{10}$ ), 67.211 ( $C^{12a}$ ), 66.519 ( $C^{12b}$ ), 65.365 ( $C^{11}$ ), 55.147 ( $NCH_2CH_2$ ), 54.336  $2 \times (NCH_2CH_2)$ , 53.083 ( $NCH_2CH_2$ ), 51.970 ( $NCH_2CH_2$ ), 49.907 ( $NCH_2CH_2$ ), 49.176 ( $NCH_3$ ), 49.097 ( $NCH_3$ ), 35.458 ( $C^7$ ), 33.983 ( $C^3$ ), 32.011 ( $C^4$ ), 30.630 ( $C^8$ ). MS (ASAP (SOLID)):  $m/z$  (%) = 418.3  $[Al(L1)OH]^+$  (100), 376.3  $[HL1+H]^+$  (35), 616.4  $[Al(L1)(OBn)_2+H]^+$  (30) 508.3  $[Al(L1)OBn]^+$  (3). HR-MS (ASAP (SOLID)) for  $[Al(L1)(OBn)_2+H]^+$ : found (Calc. for  $C_{37}H_{55}N_3O_3Al$ ) 616.4061 (616.4059). Anal. found (Calc. for  $C_{37}H_{55}N_3O_3Al$ ) C 72.06 (72.16), H 9.01 (8.84), N 6.68 (6.82).

### 7.13 Synthesis of $PPN_2ADC$ and $PPN_2TPA$

$PPN_2ADC$  was synthesised according to a literature method.<sup>11</sup>

$PPN_2TCA$  was synthesised according to a modified a literature method.<sup>11</sup> Terephthalic acid (5g, 0.0301 mol) and NaOH (2.408g, 0.0602 mol) were combined in 50 ml of distilled water and stirred at 22 °C. After 1 hr the solvent was removed by rotary evaporation and the residue redissolved in the minimum amount of water and ethanol (200 ml). The white solid precipitated from this solution was collected, washed with diethyl ether and dried under vacuum.  $PPNCl$  (4.098g, 7.139 mmol) was dissolved in 100 ml of distilled water at 40 °C. 500 mg of the isolated white solid was dissolved in 10 ml distilled water and added slowly to the solution of  $PPNCl$  leading to precipitation of a white solid. The mixture was stirred at 40 °C for 1 hour and subsequently the precipitate was collected by filtration. The  $PPN_2TPA$  was washed with 125 ml of distilled water and 150 ml diethyl ether and dried under vacuum for 2 hours (1.625 g, 55%).  $^1H$  NMR, 500 MHz,  $DMSO-d_6$ , 298 K,



## Chapter 7 - Experimental

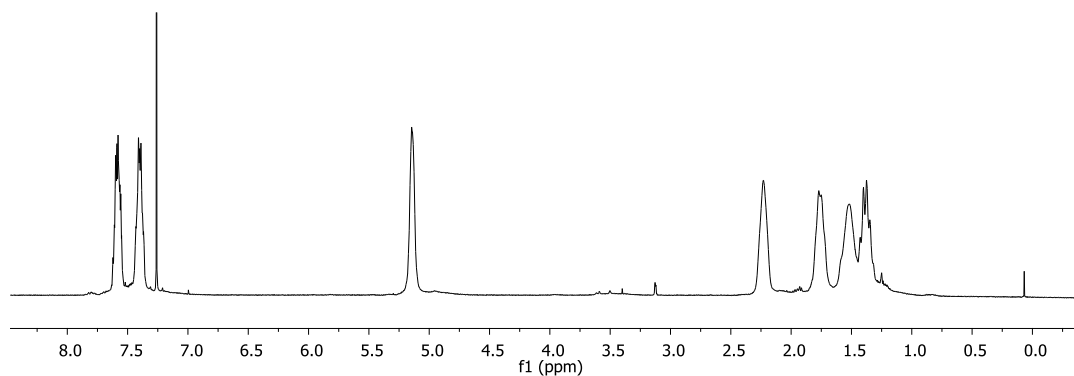
ppm):  $\delta_{\text{H}}$  7.71 (m, 12H) 7.56 (m, 52H).  $^{13}\text{C}\{^1\text{H}\}$  NMR, 125 MHz, DMSO- $\text{d}_6$ , 298 K, ppm):  $\delta_{\text{C}}$  168.53, 141.66, 133.68, 131.97, 129.53, 127.54, 127.34, 126.28.  $^{31}\text{P}$  NMR, 162 MHz, DMSO- $\text{d}_6$   $\delta_{\text{P}}$  20.76.

### **7.14 Preparation of polymer plates for flame-retardant testing**

The co-polymerisation reaction was performed under comparable conditions to those for standard-scale reactions, except for using 64  $\mu\text{mol}$  of catalyst and 25.6 mmol of anhydride and epoxide and 10 ml dry toluene. The reactions were performed in 28 ml screw cap vials. NMR spectra indicated that the microstructures of the co-polymers were not affected by the scale up procedure. The polymer powders were pressed into 100  $\times$  100  $\times$  2 mm plates using an aluminium template incorporating a movable piston. The press assembly was placed in a thermal hydraulic press and heated to 100  $^{\circ}\text{C}$  under 100 bar pressure for 20 min. The flammability testing was assessed by limiting oxygen index test in accordance with ISO 4589 using a Fire Testing Technology (FTT) instrument.

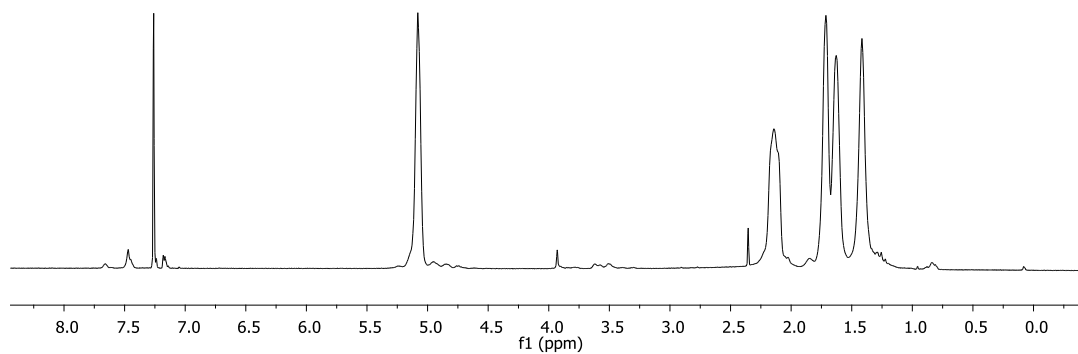
### **7.15 Representative $^1\text{H}$ NMR spectra of polymers**

**$^1\text{H}$  NMR spectrum (400 MHz,  $\text{CDCl}_3$ ) of CHO-PhA**

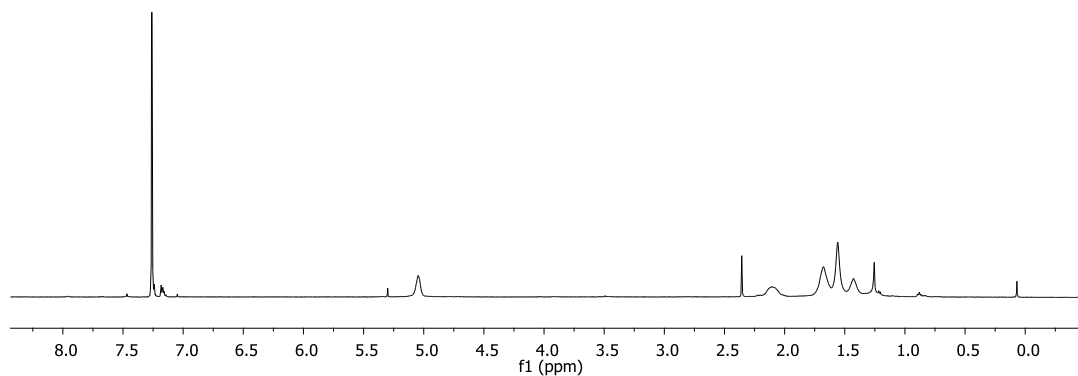


## Chapter 7 - Experimental

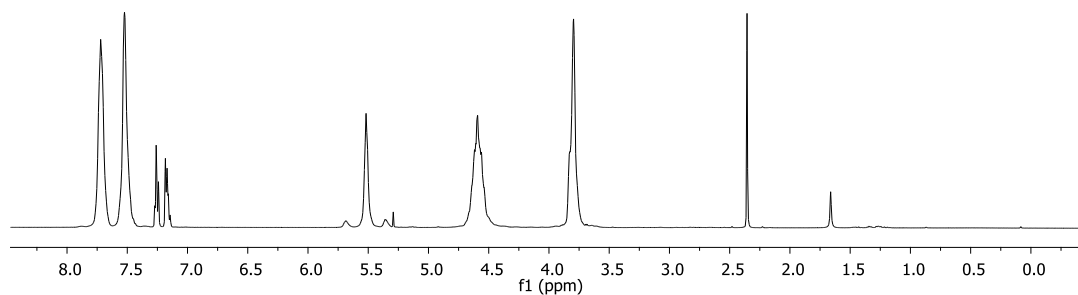
### $^1\text{H}$ NMR spectrum (500 MHz, $\text{CDCl}_3$ ) of CHO-TCPPhA



### $^1\text{H}$ NMR spectrum (500 MHz, $\text{CDCl}_3$ ) of CHO-TBPhA

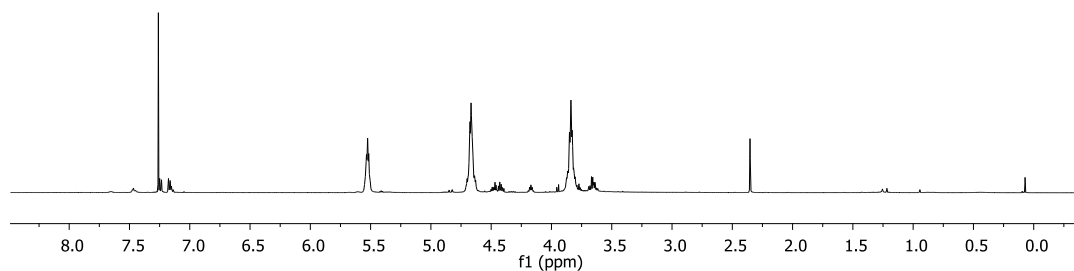


### $^1\text{H}$ NMR spectrum (500 MHz, $\text{CDCl}_3$ ) of ECH-PhA

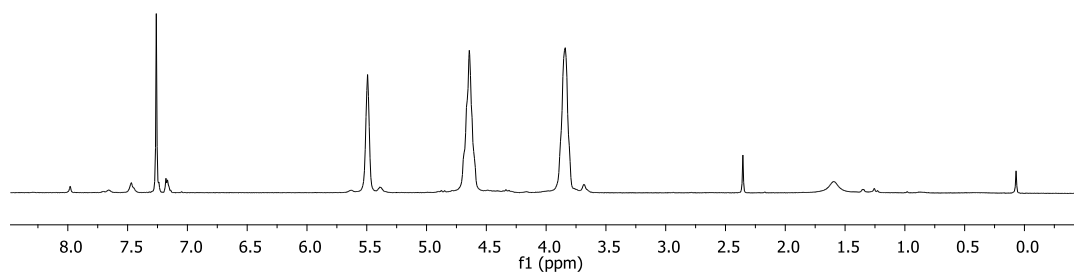


## Chapter 7 - Experimental

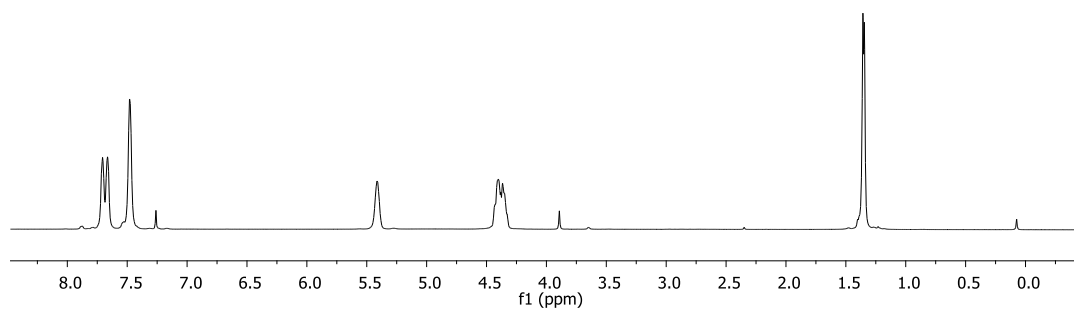
### $^1\text{H}$ NMR spectrum (500 MHz, $\text{CDCl}_3$ ) of ECH-TCPPhA



### $^1\text{H}$ NMR spectrum (500 MHz, $\text{CDCl}_3$ ) of ECH-TBPhA

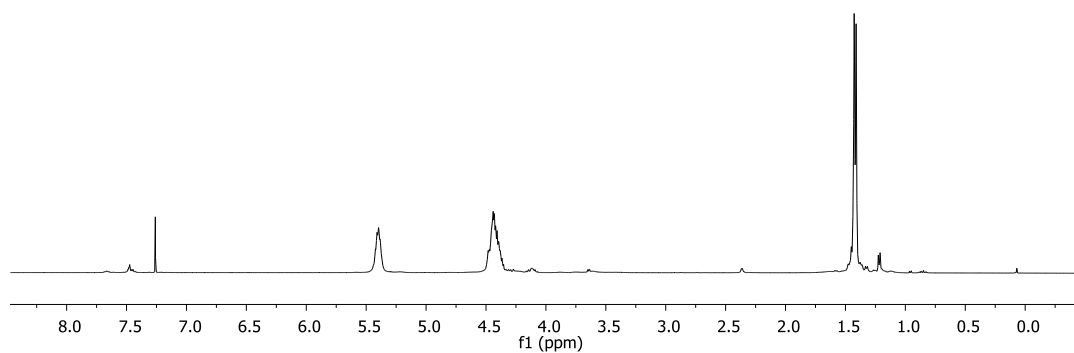


### $^1\text{H}$ NMR spectrum (500 MHz, $\text{CDCl}_3$ ) of PO-PhA

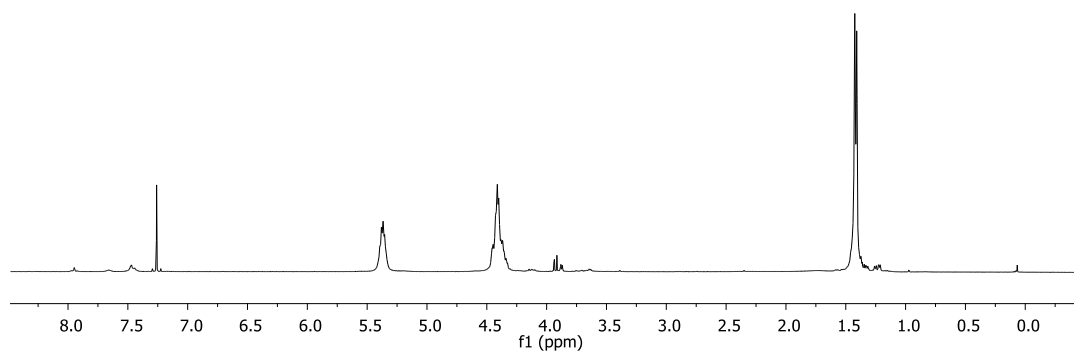


## Chapter 7 - Experimental

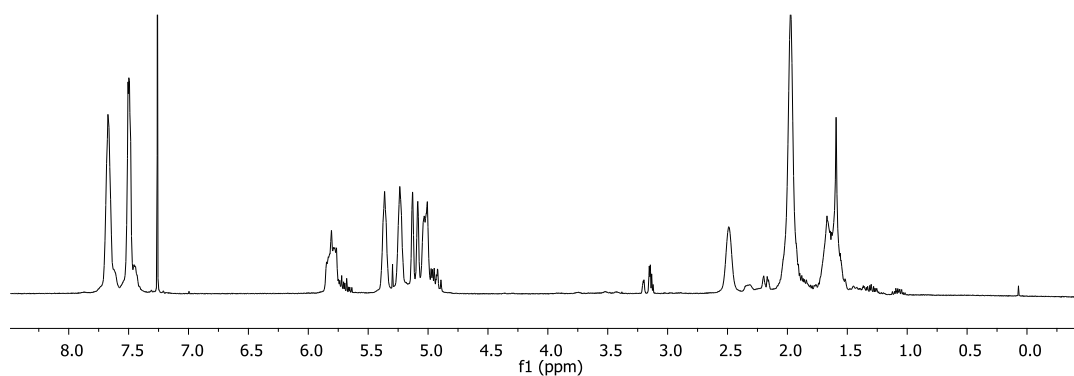
### $^1\text{H}$ NMR spectrum (400 MHz, $\text{CDCl}_3$ ) of PO-TCPPhA



### $^1\text{H}$ NMR spectrum (400 MHz, $\text{CDCl}_3$ ) of PO-TBPhA

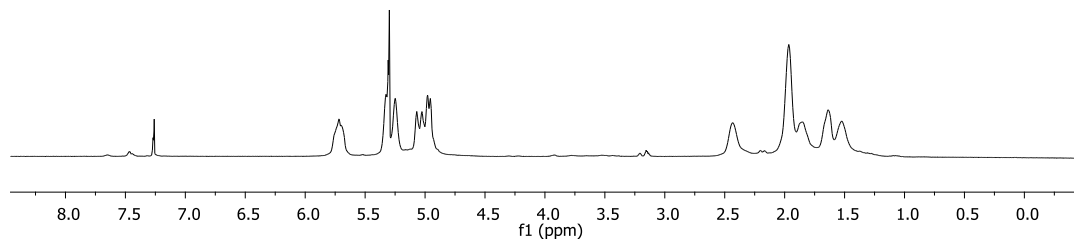


### $^1\text{H}$ NMR spectrum (400 MHz, $\text{CDCl}_3$ ) of VCHO-PhA

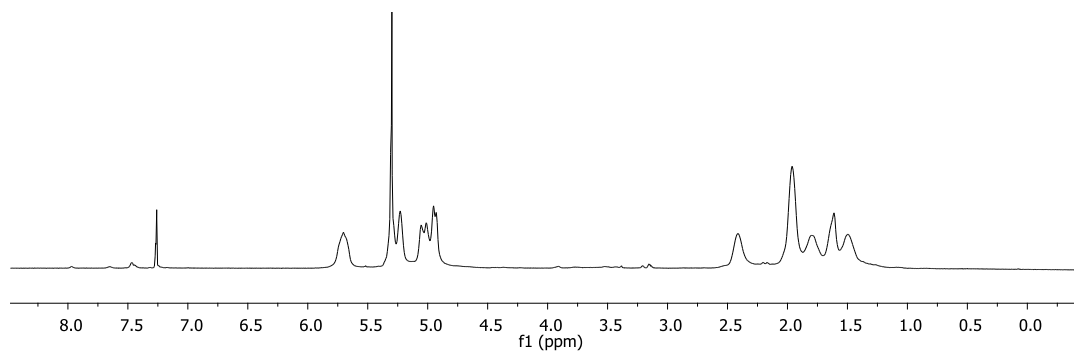


## Chapter 7 - Experimental

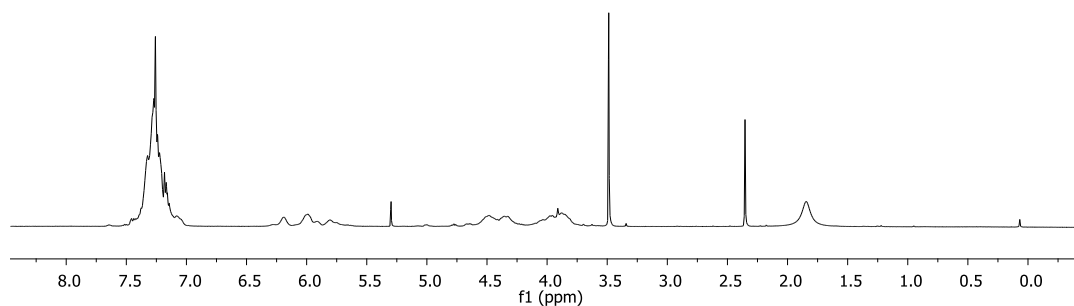
### $^1\text{H}$ NMR spectrum (400 MHz, $\text{CDCl}_3$ ) of VCHO–TCPPhA



### $^1\text{H}$ NMR spectrum (400 MHz, $\text{CDCl}_3$ ) of VCHO–TBPhA

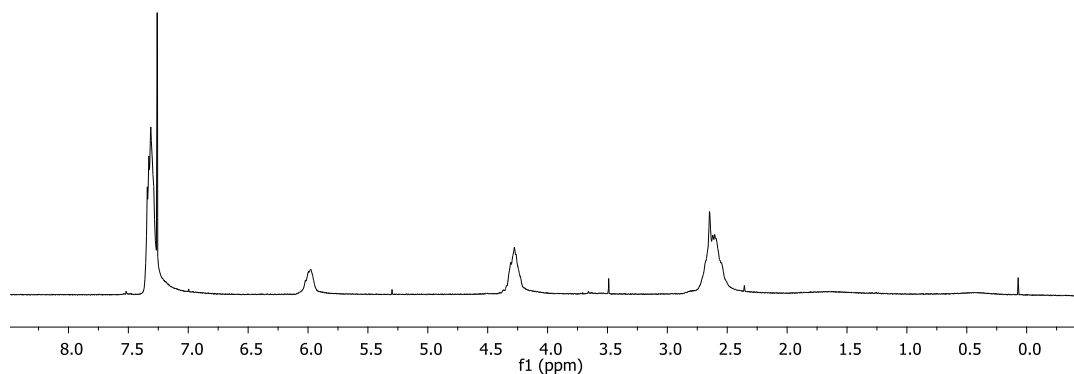


### $^1\text{H}$ NMR spectrum (500 MHz, $\text{CDCl}_3$ ) of SO–TCPPhA

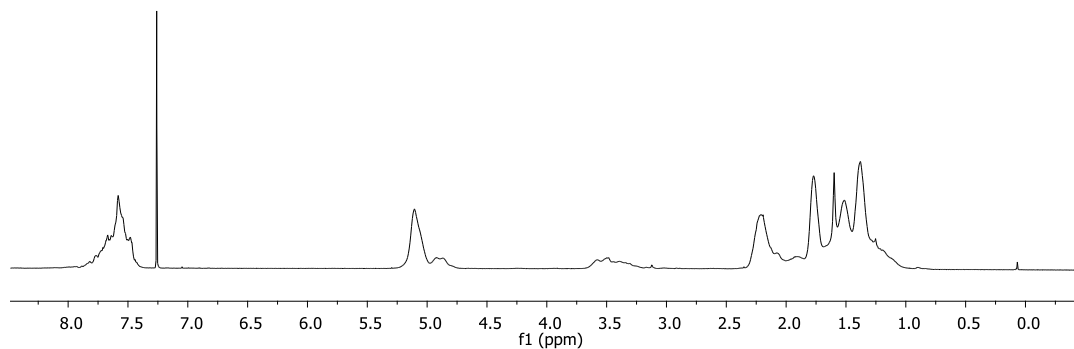


## Chapter 7 - Experimental

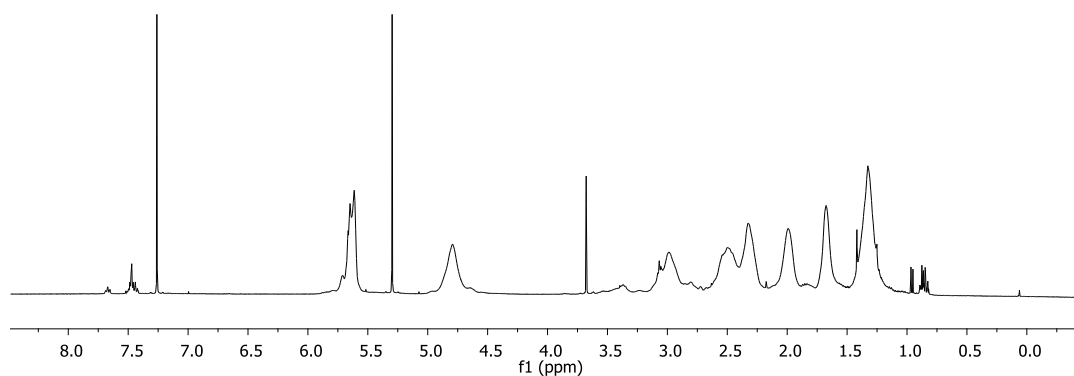
### $^1\text{H}$ NMR spectrum (400 MHz, $\text{CDCl}_3$ ) of SO-SA



### $^1\text{H}$ NMR spectrum (500 MHz, $\text{CDCl}_3$ ) of CHO-4BPhA

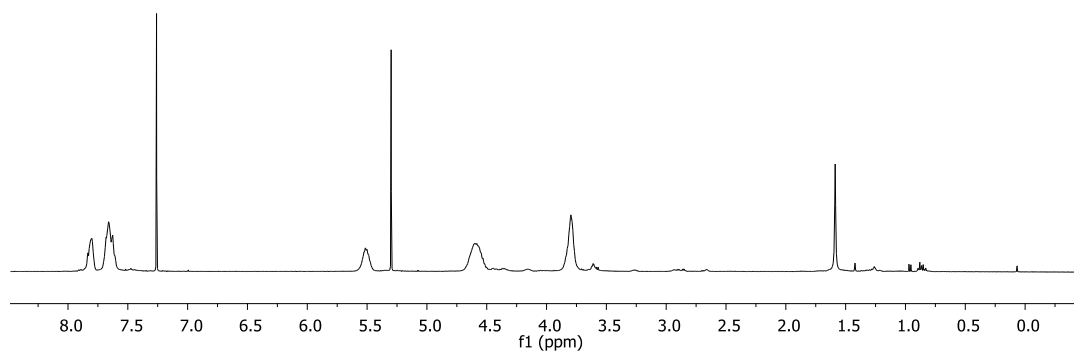


### $^1\text{H}$ NMR spectrum (400 MHz, $\text{CDCl}_3$ ) of CHO-CEA

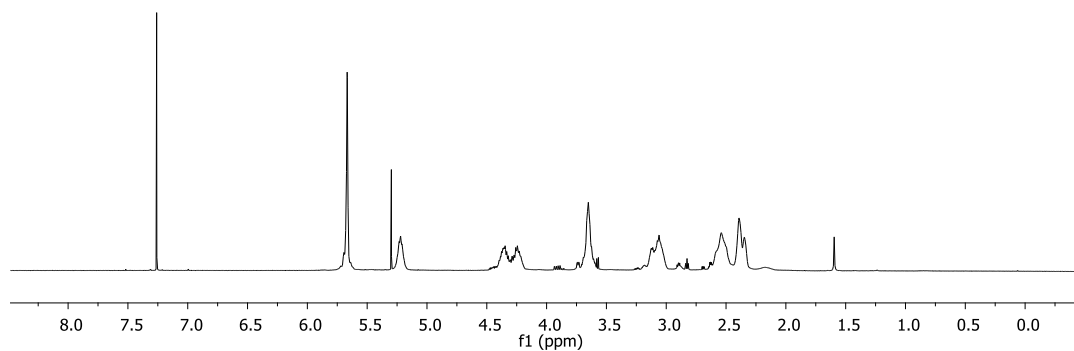


## Chapter 7 - Experimental

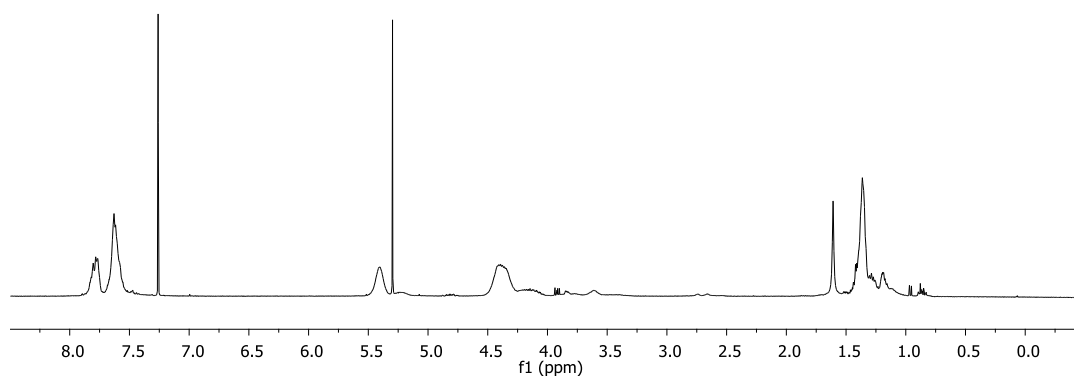
### $^1\text{H}$ NMR spectrum (400 MHz, $\text{CDCl}_3$ ) of ECH-4BPhA



### $^1\text{H}$ NMR spectrum (400 MHz, $\text{CDCl}_3$ ) of ECH-CEA

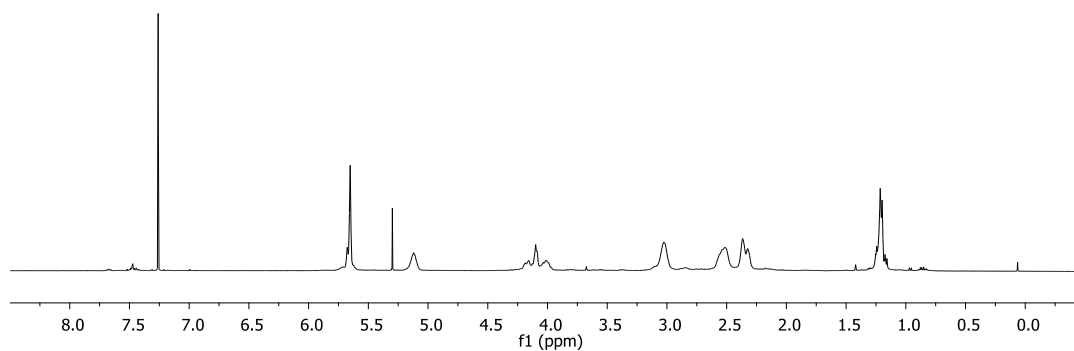


### $^1\text{H}$ NMR spectrum (400 MHz, $\text{CDCl}_3$ ) of PO-4BPhA

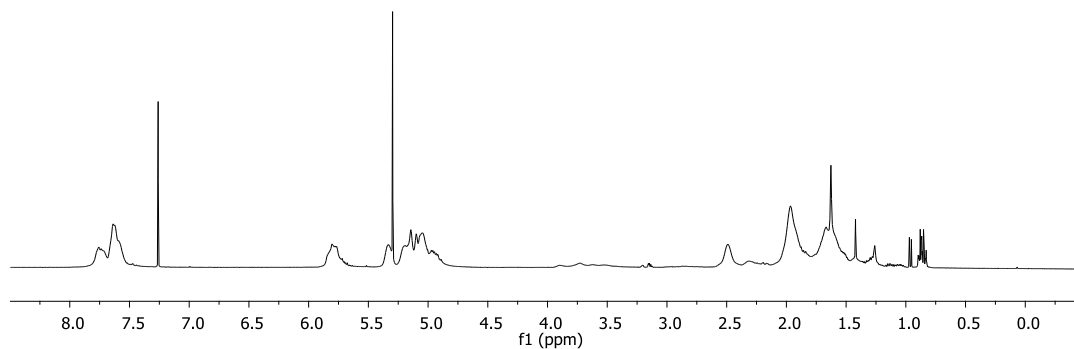


## Chapter 7 - Experimental

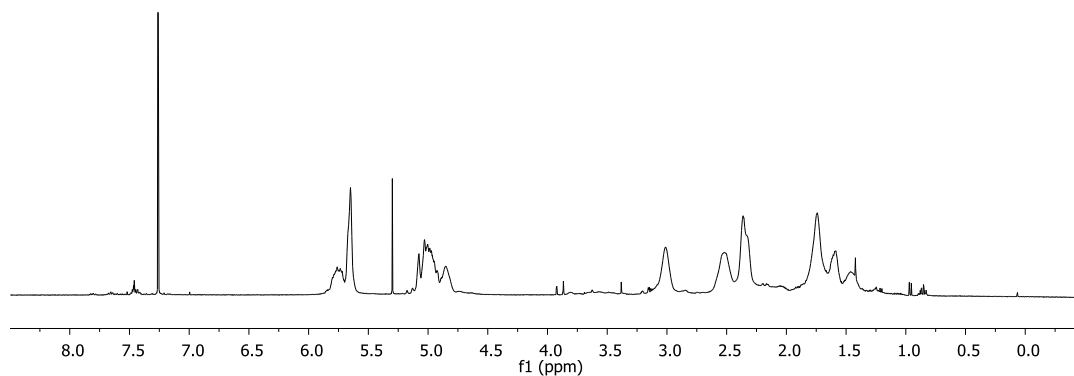
### $^1\text{H}$ NMR spectrum (400 MHz, $\text{CDCl}_3$ ) of PO-CEA



### $^1\text{H}$ NMR spectrum (400 MHz, $\text{CDCl}_3$ ) of VCHO-4BPhA



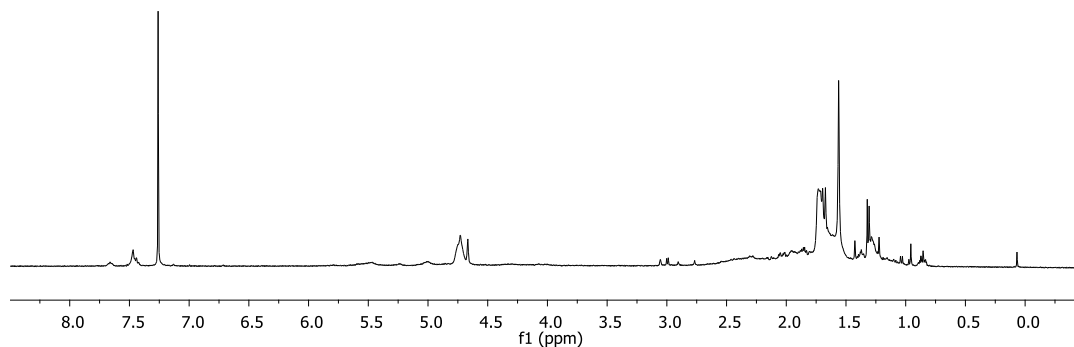
### $^1\text{H}$ NMR spectrum (400 MHz, $\text{CDCl}_3$ ) of VCHO-CEA



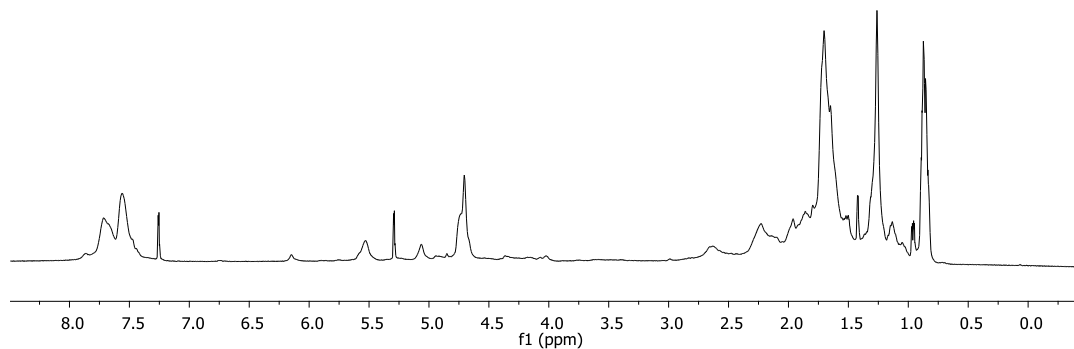


## Chapter 7 - Experimental

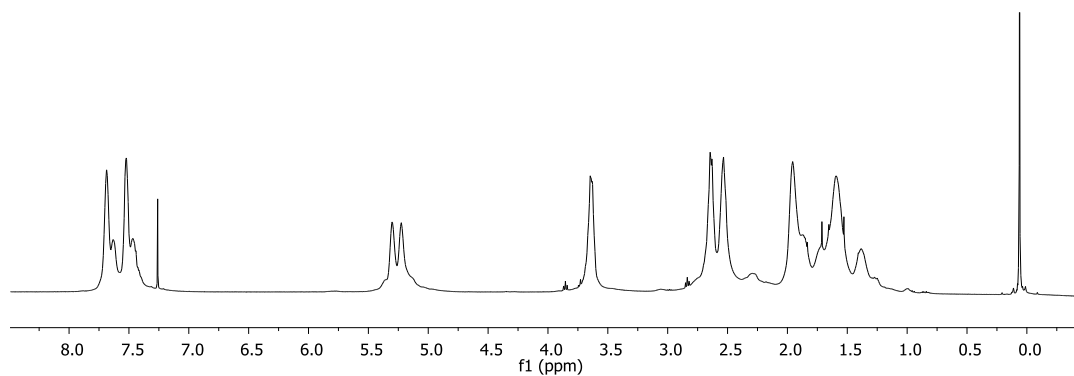
### $^1\text{H}$ NMR spectrum (400 MHz, $\text{CDCl}_3$ ) of LO-TCPPhA



### $^1\text{H}$ NMR spectrum (400 MHz, $\text{CDCl}_3$ ) of LO-PhA

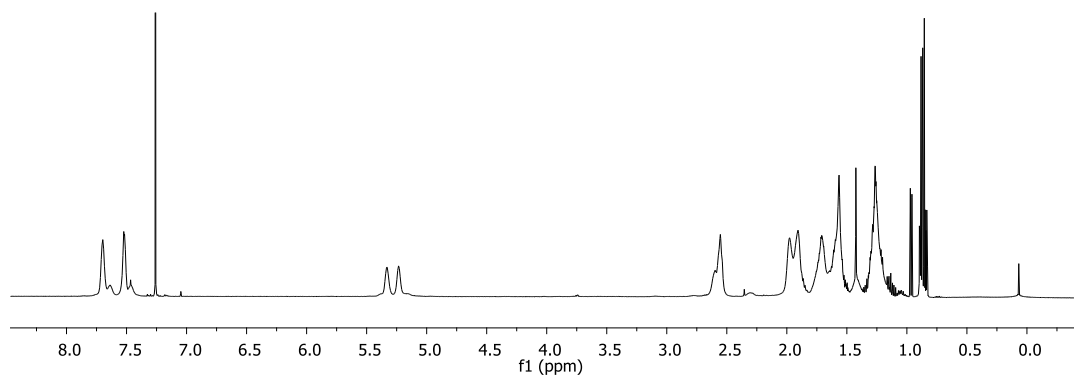


### $^1\text{H}$ NMR spectrum (400 MHz, $\text{CDCl}_3$ ) of VCHO-PhA-T1

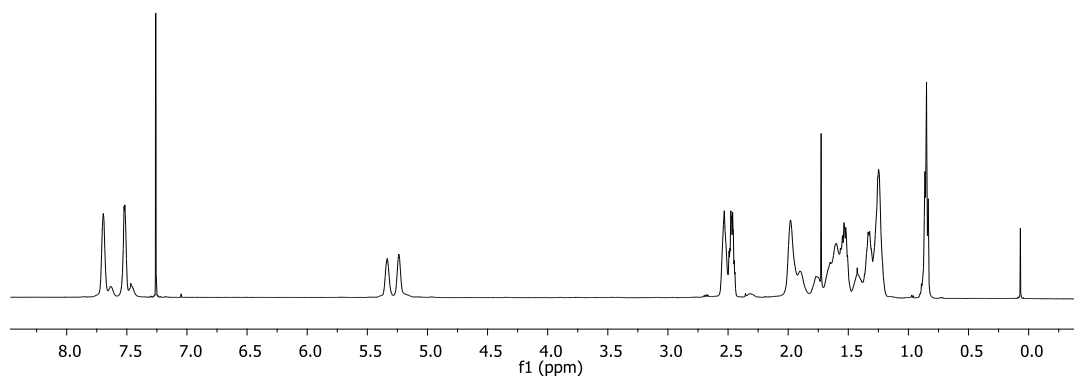


## Chapter 7 - Experimental

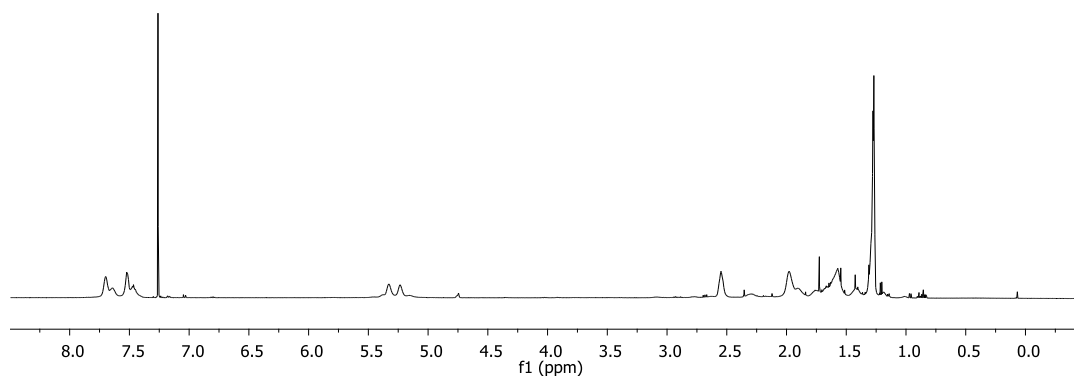
**$^1\text{H}$  NMR spectrum (500 MHz,  $\text{CDCl}_3$ ) of VCHO-PhA-T4**



**$^1\text{H}$  NMR spectrum (500 MHz,  $\text{CDCl}_3$ ) of VCHO-PhA-T6**

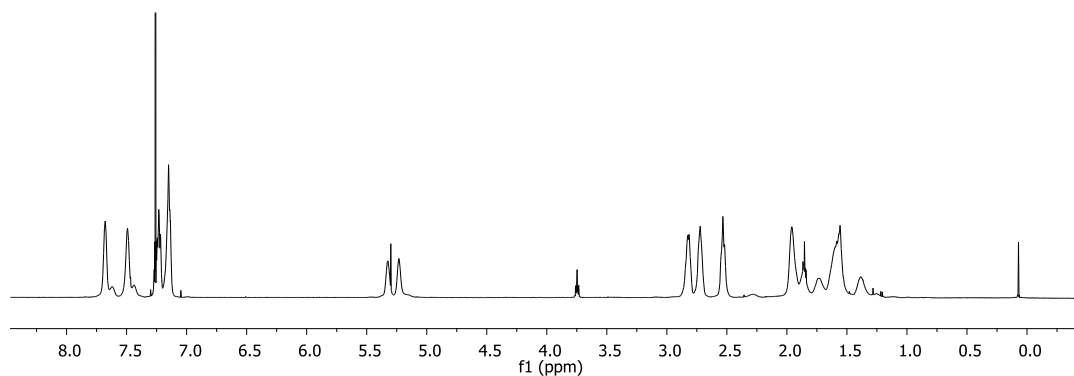


**$^1\text{H}$  NMR spectrum (500 MHz,  $\text{CDCl}_3$ ) of VCHO-PhA-T7**

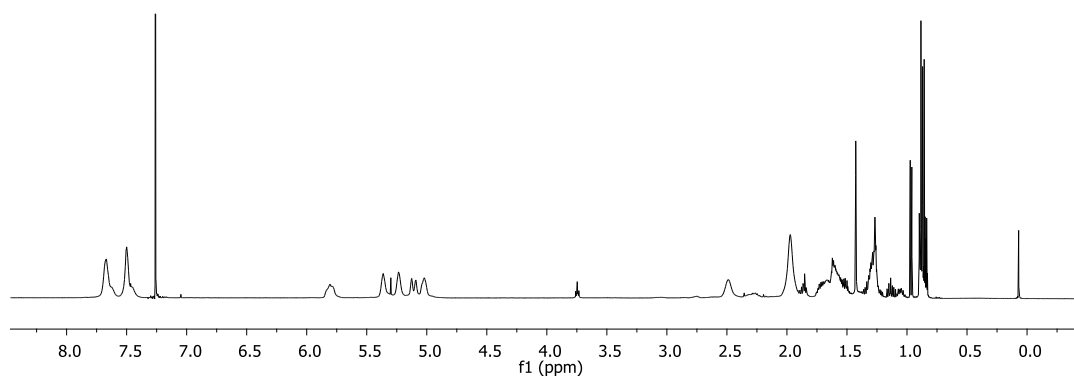


## Chapter 7 - Experimental

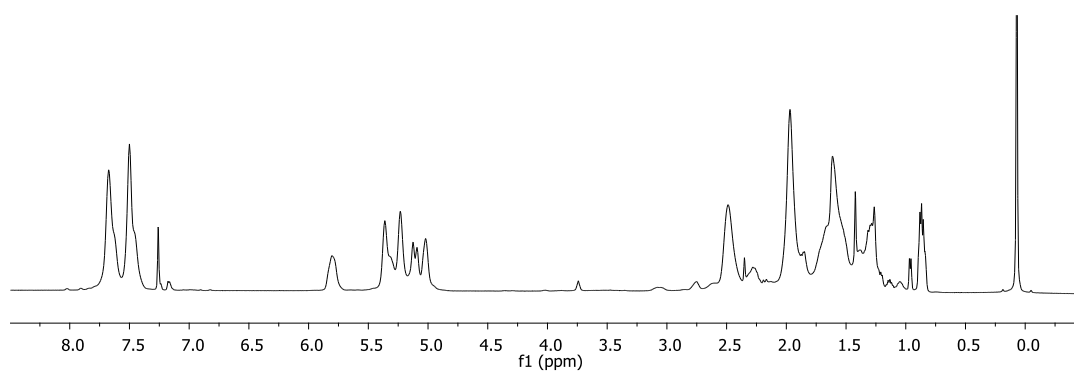
**$^1\text{H}$  NMR spectrum (500 MHz,  $\text{CDCl}_3$ ) of VCHO-PhA-T9**



**$^1\text{H}$  NMR spectrum (500 MHz,  $\text{CDCl}_3$ ) of VCHO-PhA-x10**

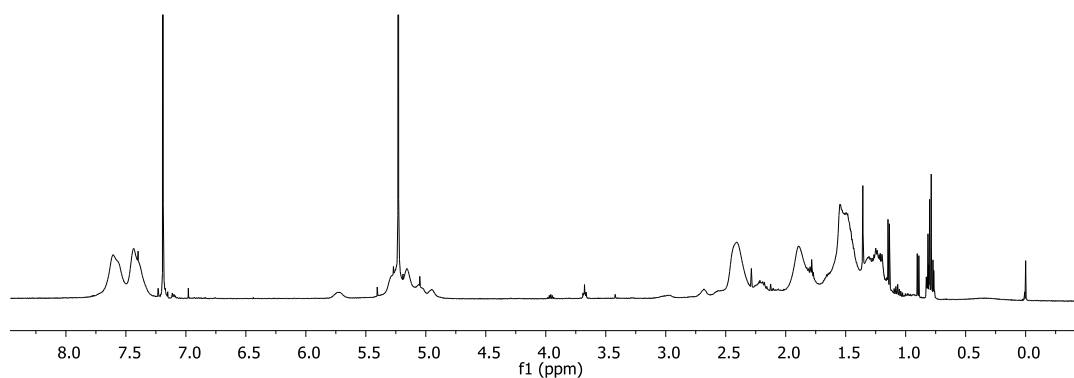


**$^1\text{H}$  NMR spectrum (500 MHz,  $\text{CDCl}_3$ ) of VCHO-PhA-x20**

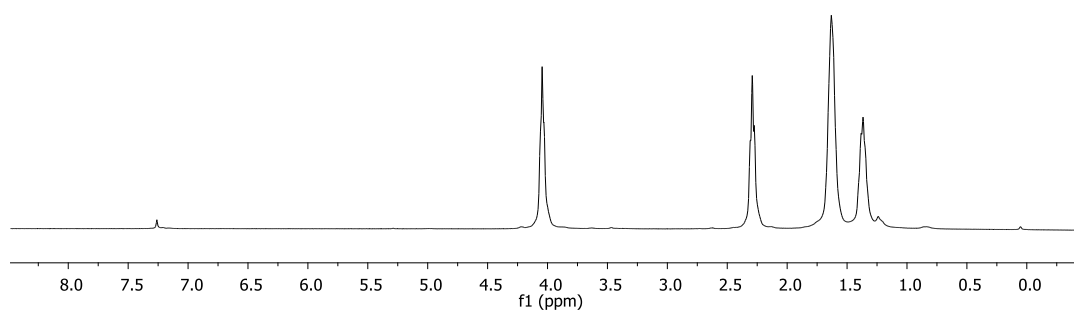


## Chapter 7 - Experimental

### $^1\text{H}$ NMR spectrum (500 MHz, $\text{CDCl}_3$ ) of VCHO-PhA-x40



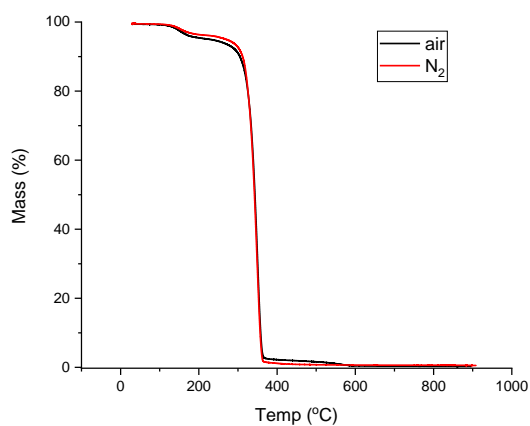
### $^1\text{H}$ NMR spectrum (400 MHz, $\text{CDCl}_3$ ) of polycaprolactone (PCL)



## 7.16 TGA curves of copolymers

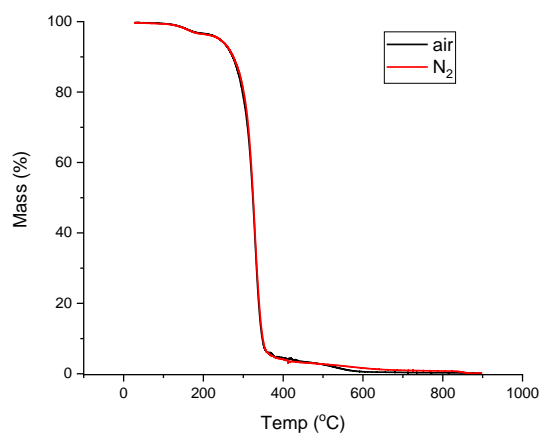
See 7.1 for procedure and data interpretation

### Entry 5 CHO-PhA

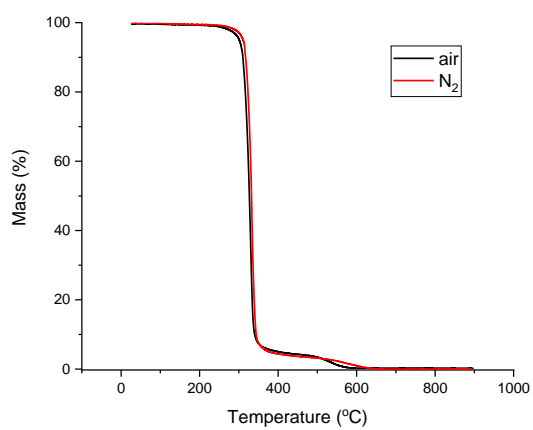


## Chapter 7 - Experimental

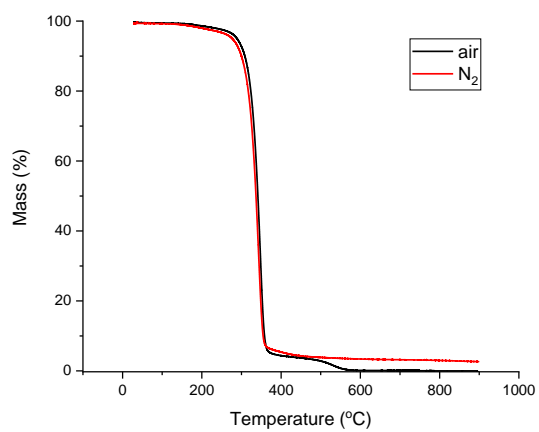
### Entry 6 CHO–TCPPhA



### Entry 7 CHO–TBPhA

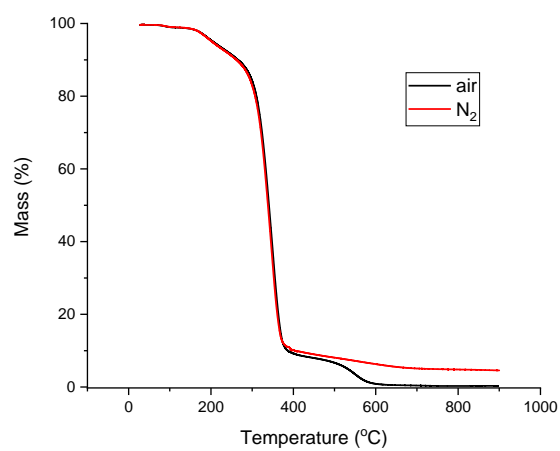


### Entry 8 ECH–PhA

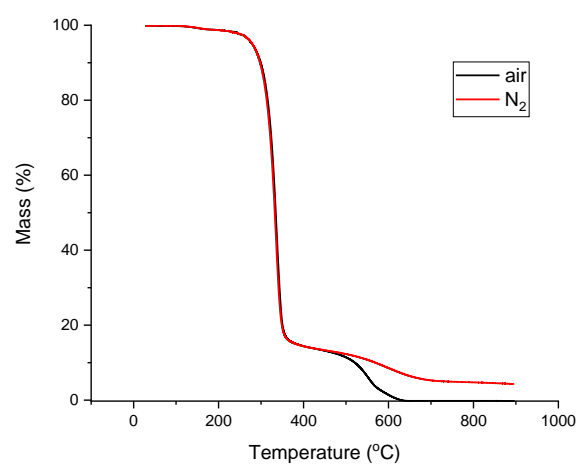


## Chapter 7 - Experimental

### Entry 9 ECH-TCPPhA

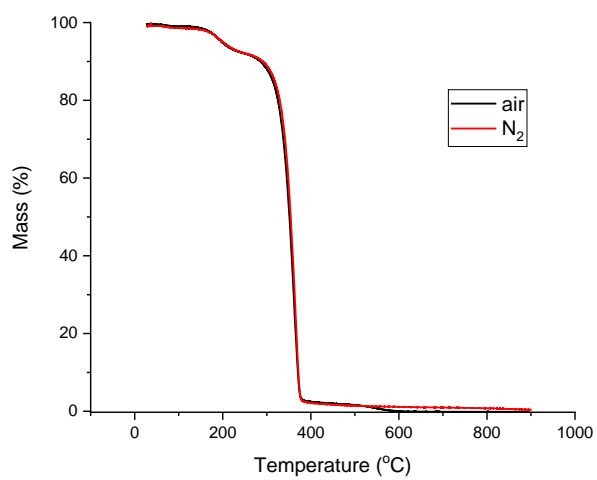


### Entry 10 ECH-TBPhA

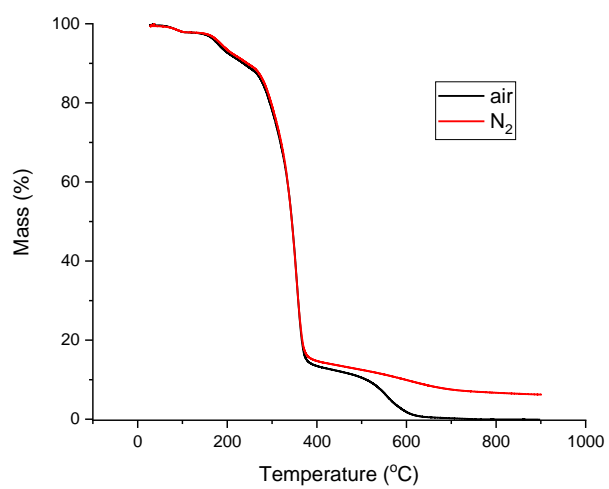


## Chapter 7 - Experimental

### Entry 11 PO-PhA

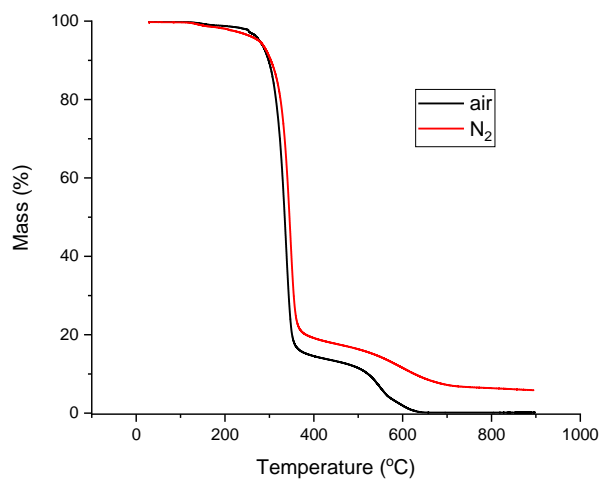


### Entry 12 PO-TCPPhA



## Chapter 7 - Experimental

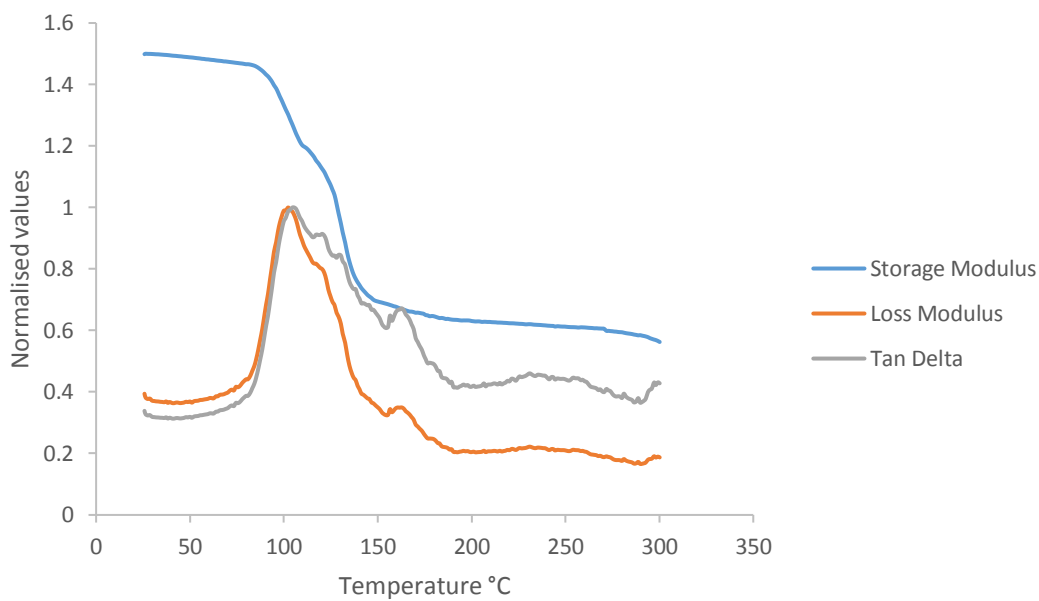
### Entry 13 PO-TBPhA



### 7.17 DMA curves for copolymers

See 7.1 for procedure and data interpretation

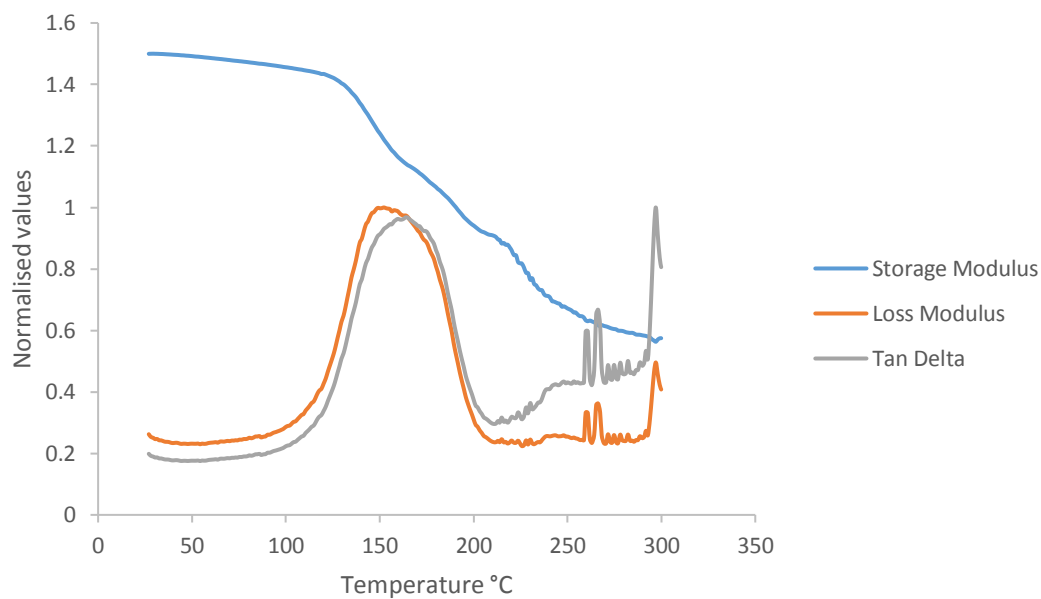
### Entry 5 CHO-PhA



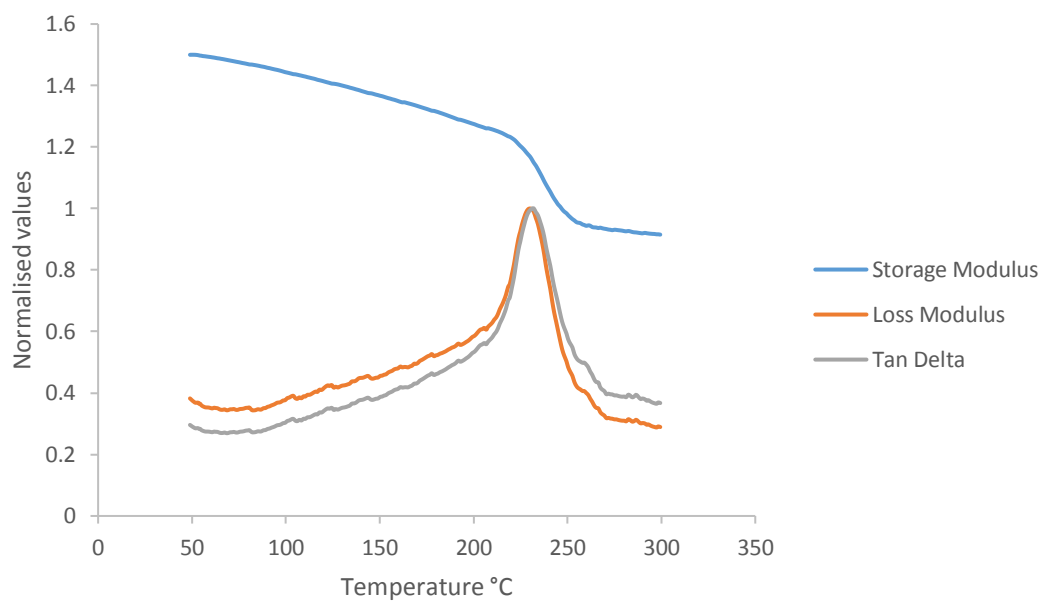


## Chapter 7 - Experimental

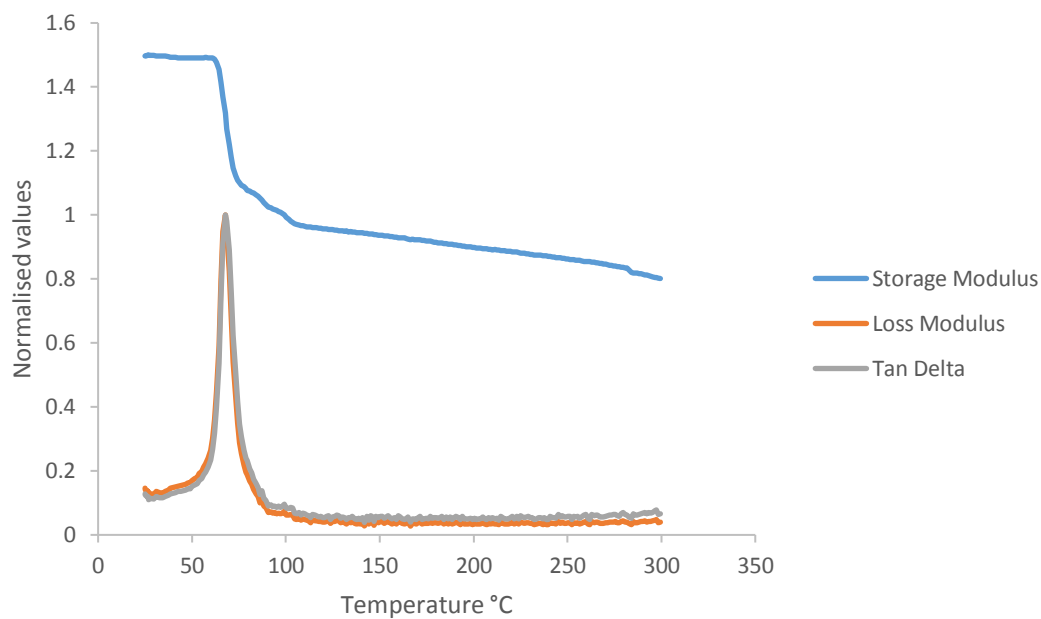
### Entry 6 CHO–TCPPhA



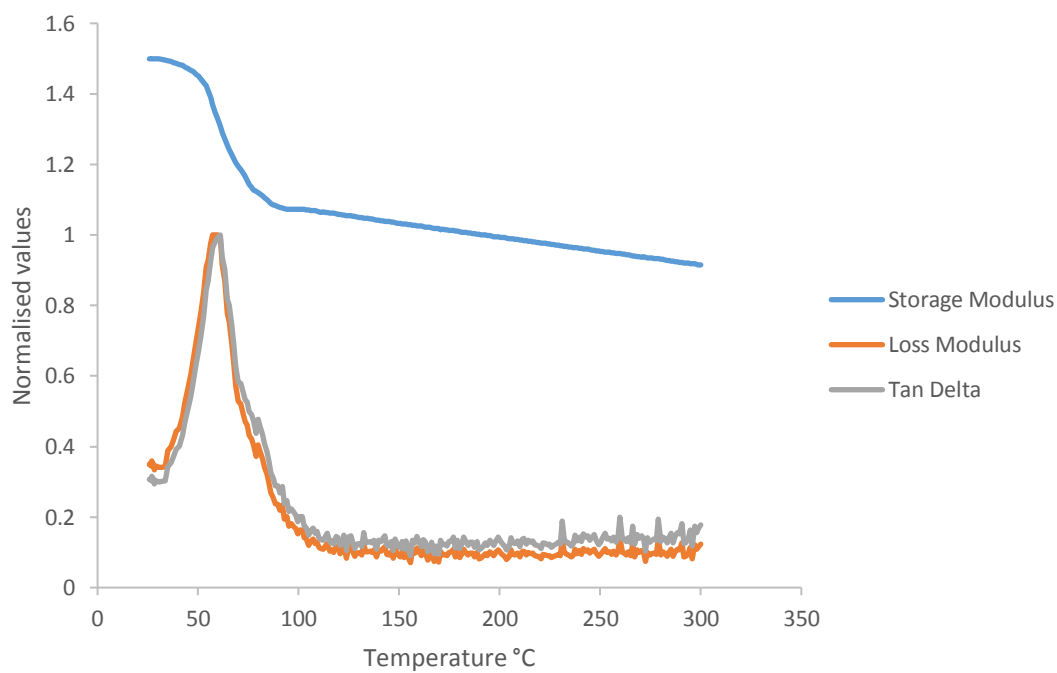
### Entry 7 CHO–TBPhA



**Entry 8 ECH-PhA**

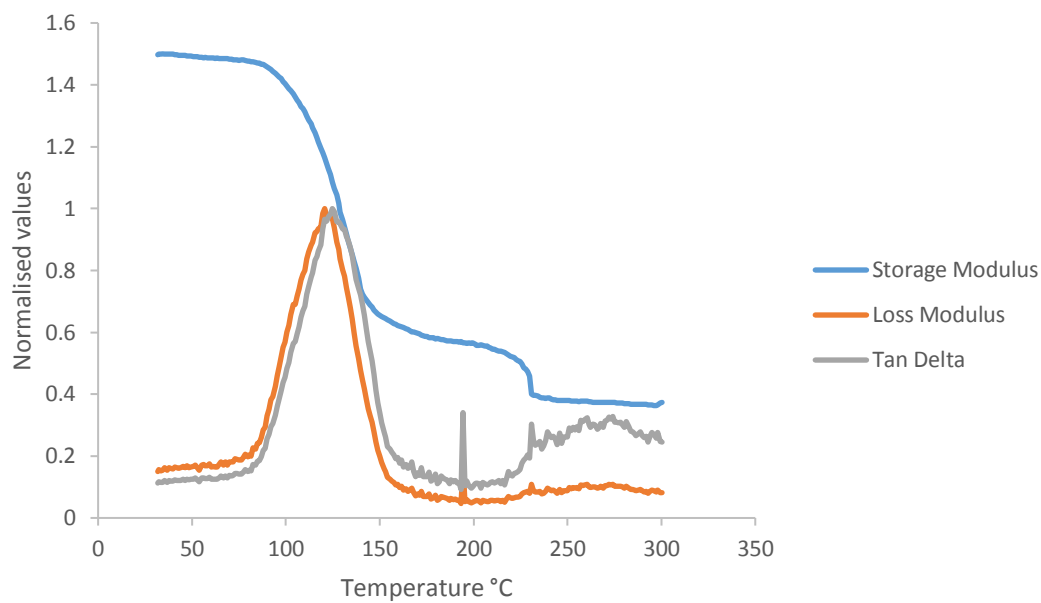


**Entry 9 ECH-TCPPhA**

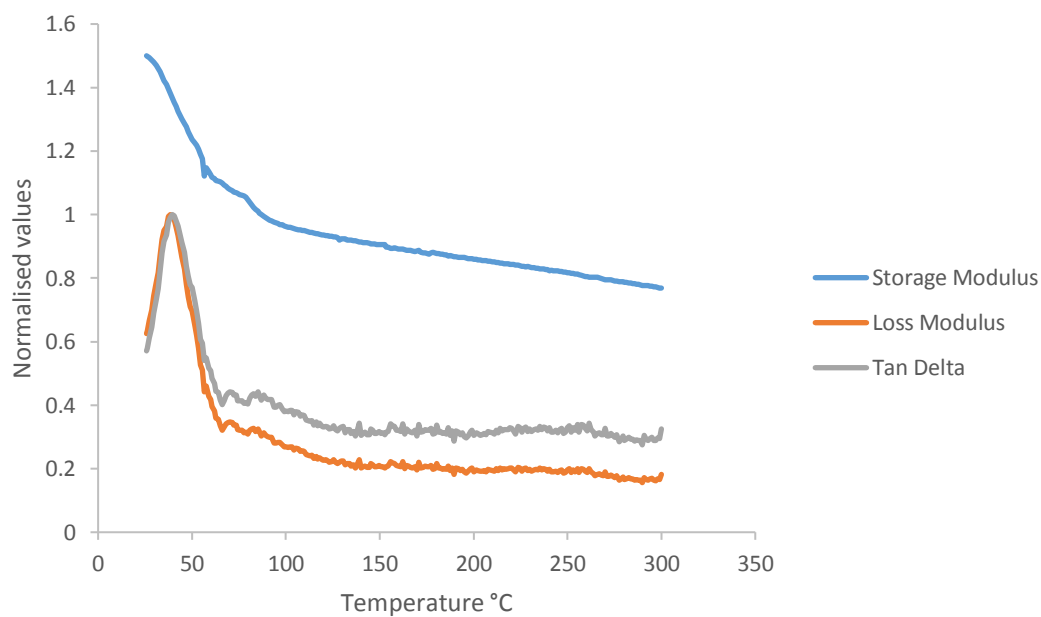


## Chapter 7 - Experimental

### Entry 10 ECH-TBPhA

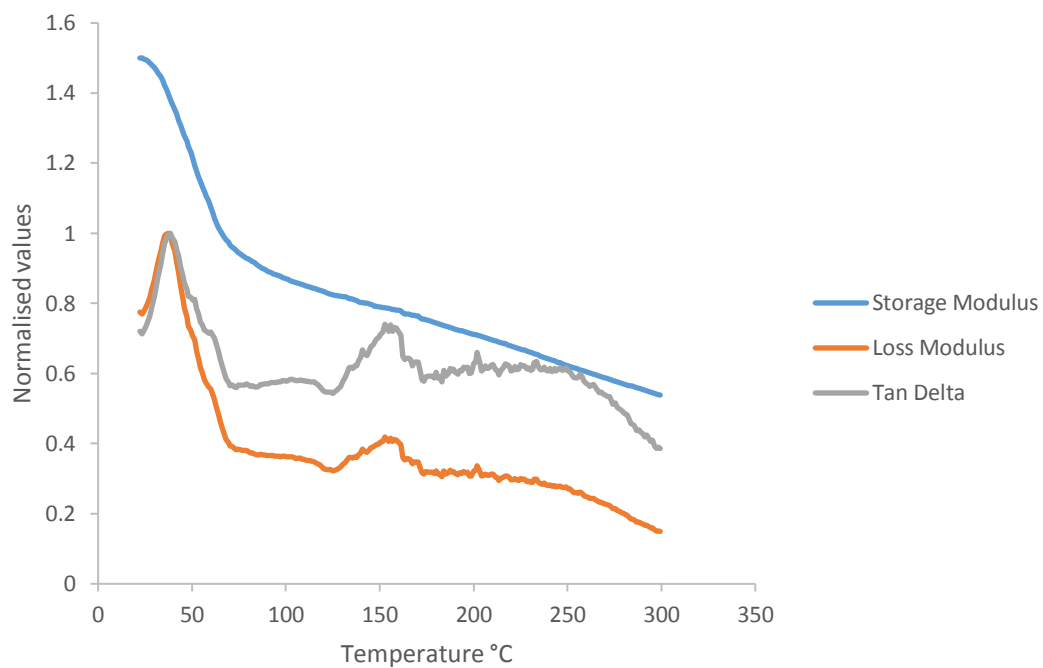


### Entry 11 PO-PhA

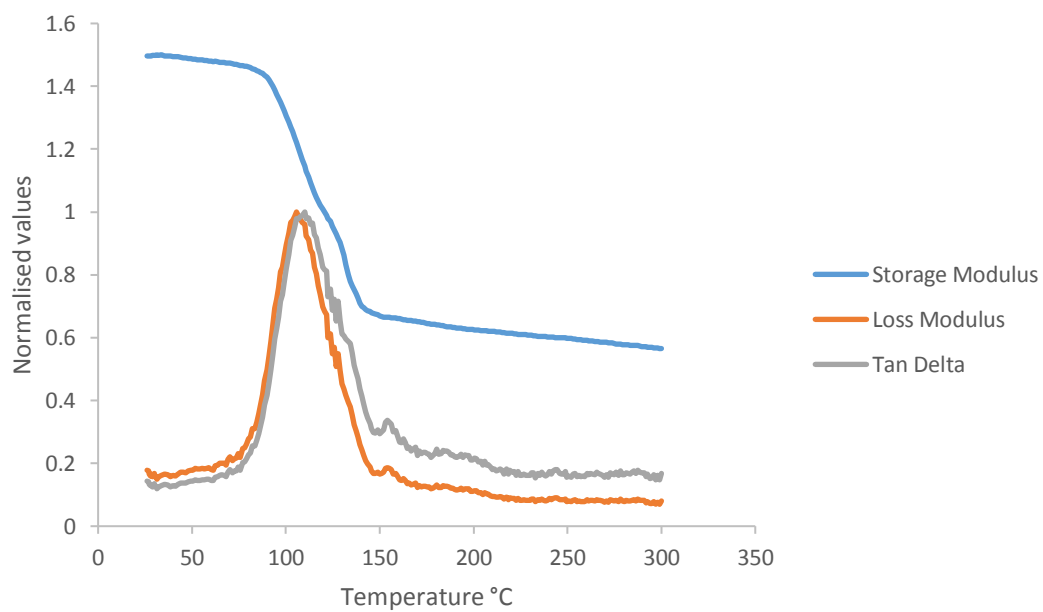


## Chapter 7 - Experimental

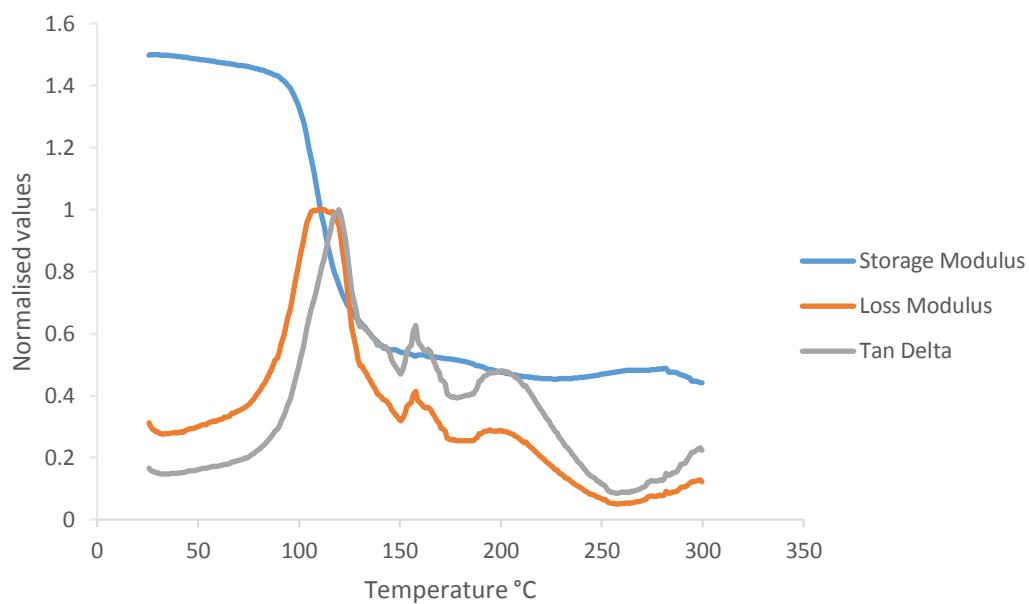
### Entry 12 PO-TCPPhA



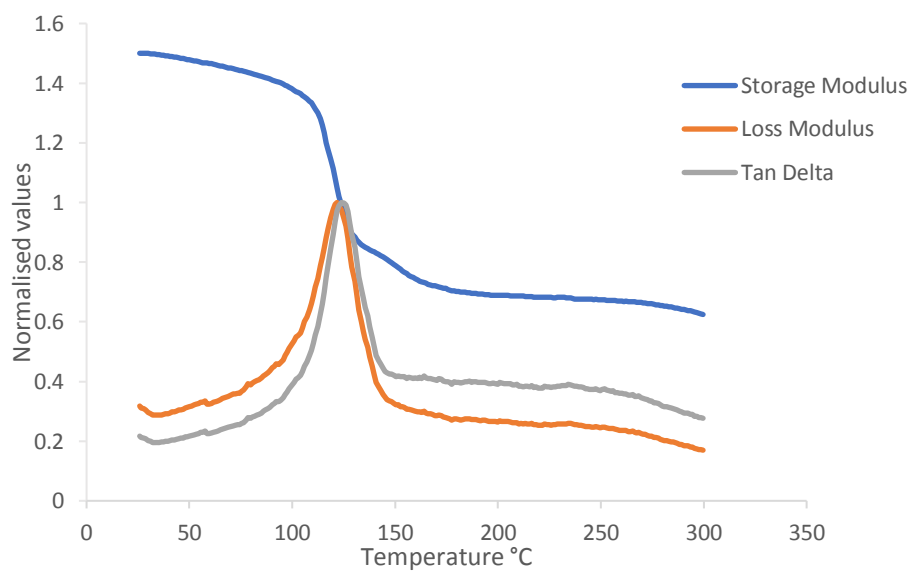
### Entry 13 PO-TBPhA



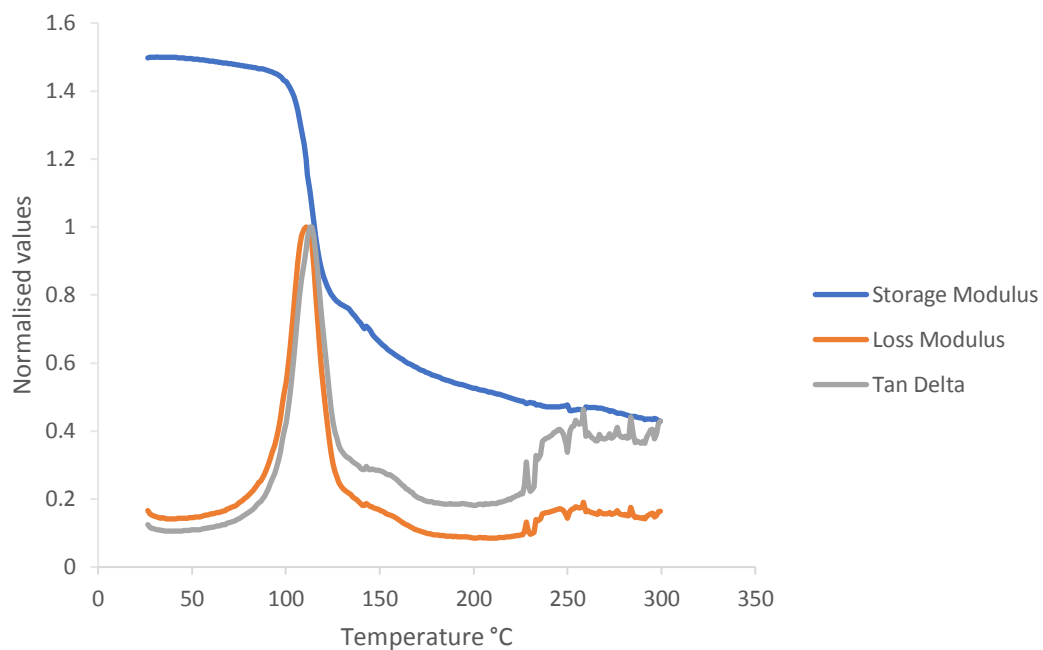
**VCHO-PhA**



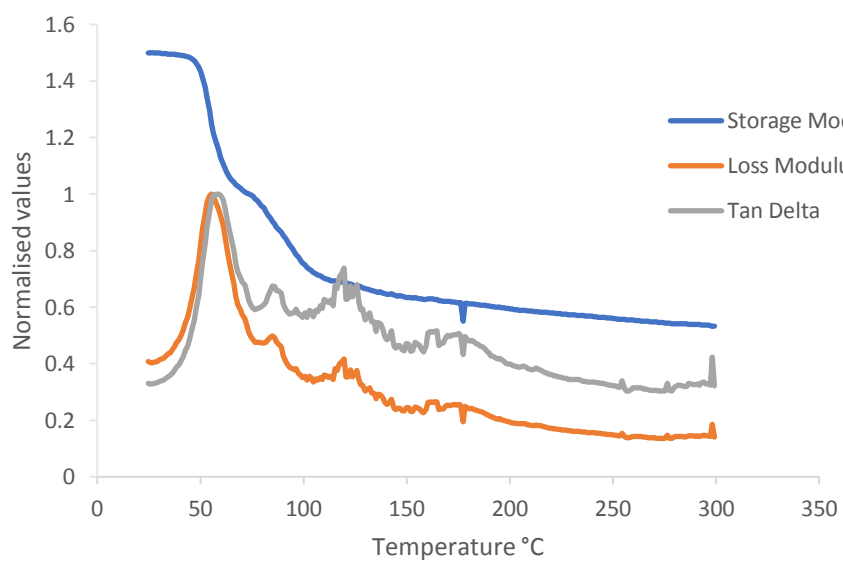
**VCHO-PhA-T1**



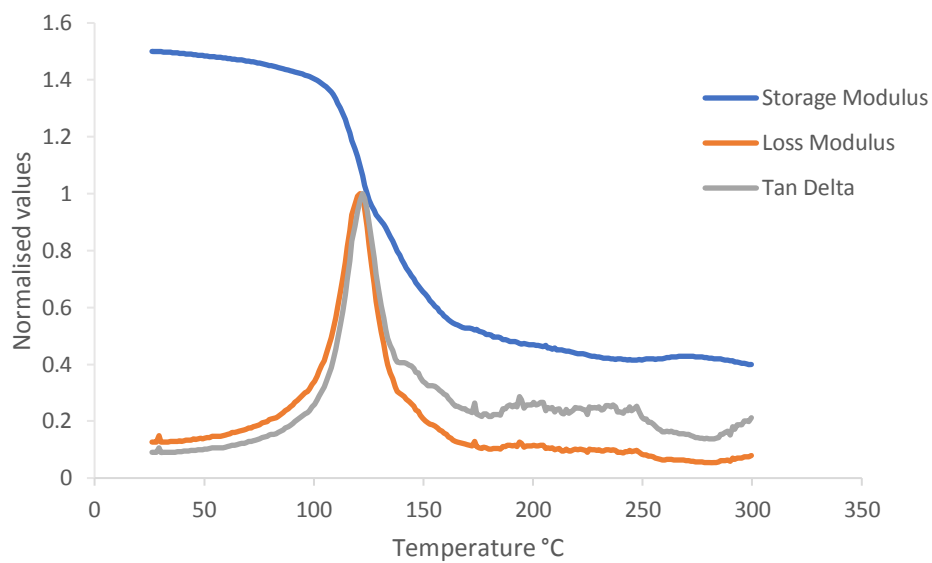
**VCHO-PhA-T4**



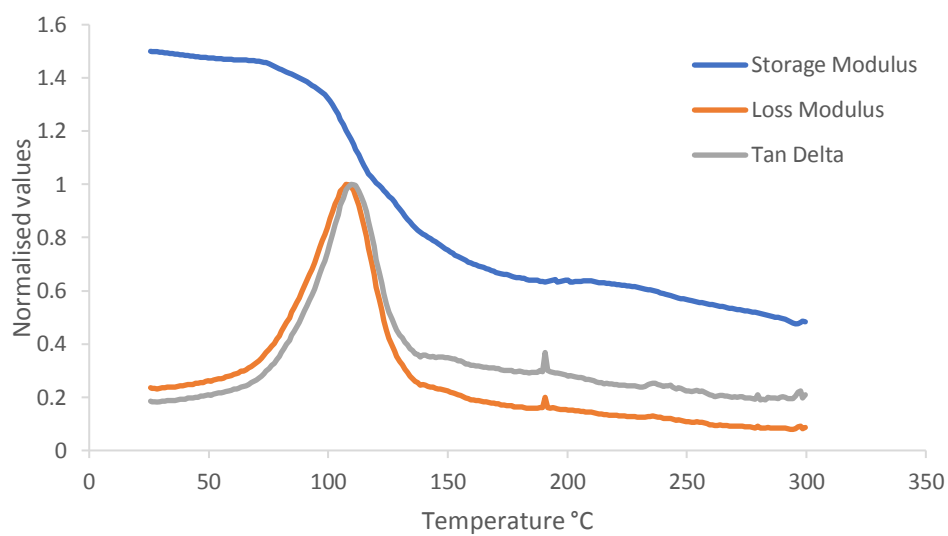
**VCHO-PhA-T6**



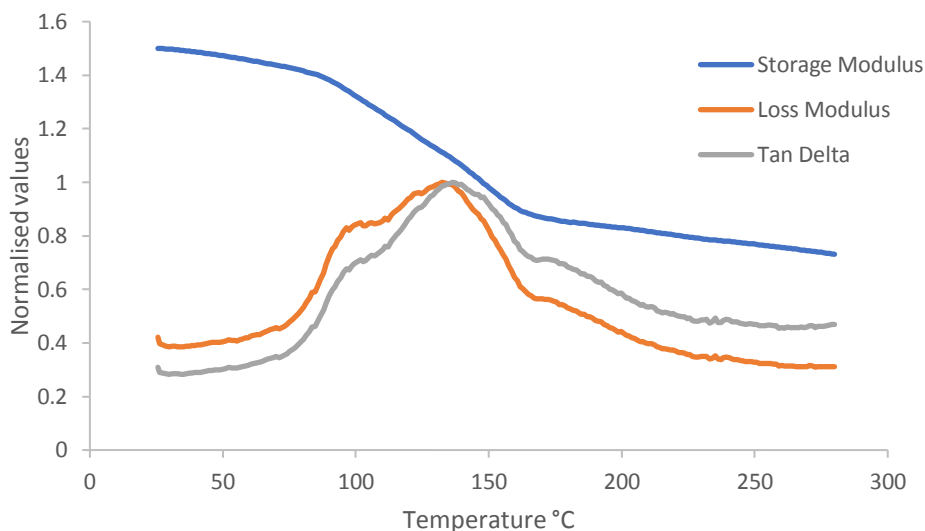
**VCHO-PhA-T7**



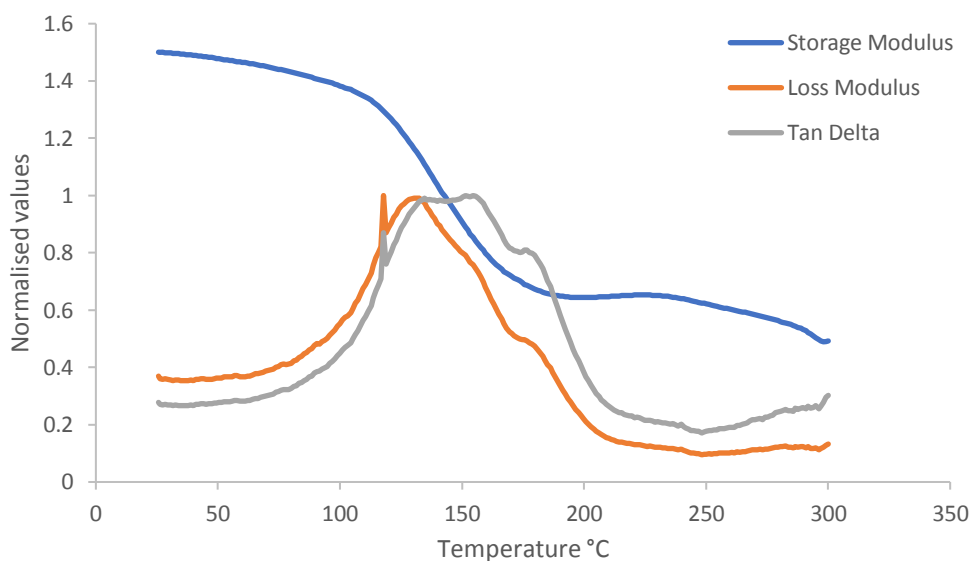
**VCHO-PhA-T9**



**VCHO-PhA-x20**



**VCHO-PhA-x40**



**7.18 References for Chapter 7**

- 1 M. J. Frisch, G. W. Trucks, H. B. Schlegel, G. E. Scuseria, M. A. Robb, J. R. Cheeseman, G. Scalmani, V. Barone, G. A. Petersson, H. Nakatsuji, X. Li, M. Caricato, A. V. Marenich, J. Bloino, B. G. Janesko, R. Gomperts, B. Mennucci, H. P. Hratchian, J. V. Ortiz, A. F. Izmaylov, J. L. Sonnenberg, Williams, F. Ding, F. Lipparini, F. Egidi, J. Goings, B. Peng, A. Petrone, T. Henderson, D. Ranasinghe, V. G. Zakrzewski, J. Gao, N.



## Chapter 7 - Experimental

- Rega, G. Zheng, W. Liang, M. Hada, M. Ehara, K. Toyota, R. Fukuda, J. Hasegawa, M. Ishida, T. Nakajima, Y. Honda, O. Kitao, H. Nakai, T. Vreven, K. Throssell, J. A. Montgomery Jr., J. E. Peralta, F. Ogliaro, M. J. Bearpark, J. J. Heyd, E. N. Brothers, K. N. Kudin, V. N. Staroverov, T. A. Keith, R. Kobayashi, J. Normand, K. Raghavachari, A. P. Rendell, J. C. Burant, S. S. Iyengar, J. Tomasi, M. Cossi, J. M. Millam, M. Klene, C. Adamo, R. Cammi, J. W. Ochterski, R. L. Martin, K. Morokuma, O. Farkas, J. B. Foresman and D. J. Fox, *Gaussian 09 Rev. D.01*, Wallingford, CT, 2016.
- 2 Y. Zhao and D. G. Truhlar, *Theor. Chem. Acc.*, 2008, **120**, 215–241.
- 3 T. H. Dunning, *J. Chem. Phys.*, 1989, **90**, 1007–1023.
- 4 T. H. Dunning, K. A. Peterson and A. K. Wilson, *J. Chem. Phys.*, 2001, **114**, 9244–9253.
- 5 G. Luchini, J. Alegre-Requena, IFunes, J. Rodríguez-Guerra, J. Chen and R. Paton, *GoodVibes v3.0.0*, 2019.
- 6 E. D. Glendening, J. K. Badenhoop, A. E. Reed, J. E. Carpenter, J. E. Bohmann, C. M. Morales, C. R. Landis and F. Weinhold, *NBO 6.0*, Theoretical Chemistry Institute, University of Wisconsin, Madison, 2013.
- 7 T. A. Keith, *AIMAll*, TK Gristmill Software, Overland Park KS, USA, 2017.
- 8 C. Flassbeck and K. Wieghardt, *Z. Für Anorg. Allg. Chem.*, 1992, **608**, 60–68.
- 9 S. Y. Bylikin, D. A. Robson, N. A. H. Male, L. H. Rees, P. Mountford and M. Schröder, *J. Chem. Soc. Dalton Trans.*, 2001, 170–180.
- 10 D. A. Robson, S. Y. Bylikin, M. Cantuel, N. A. H. Male, L. H. Rees, P. Mountford and M. Schröder, *J. Chem. Soc. Dalton Trans.*, 2001, 157–169.
- 11 M. J. Sanford, N. J. V. Zee and G. W. Coates, *Chem. Sci.*, 2017, **9**, 134–142.

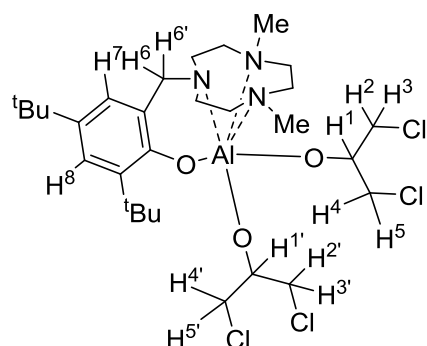
# Appendix

## Appendix

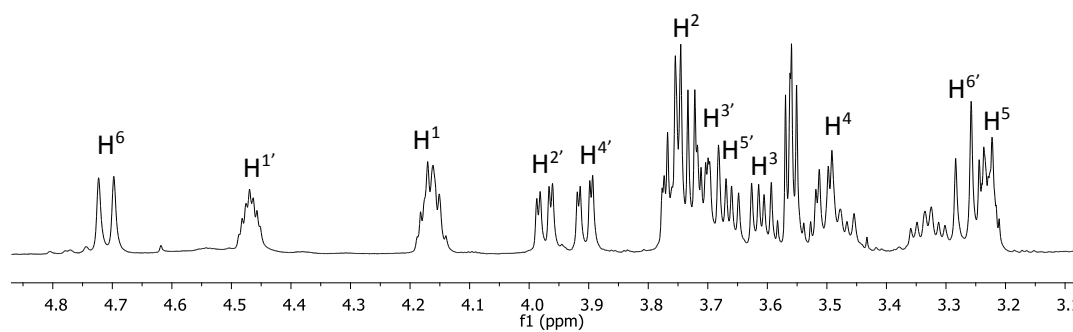
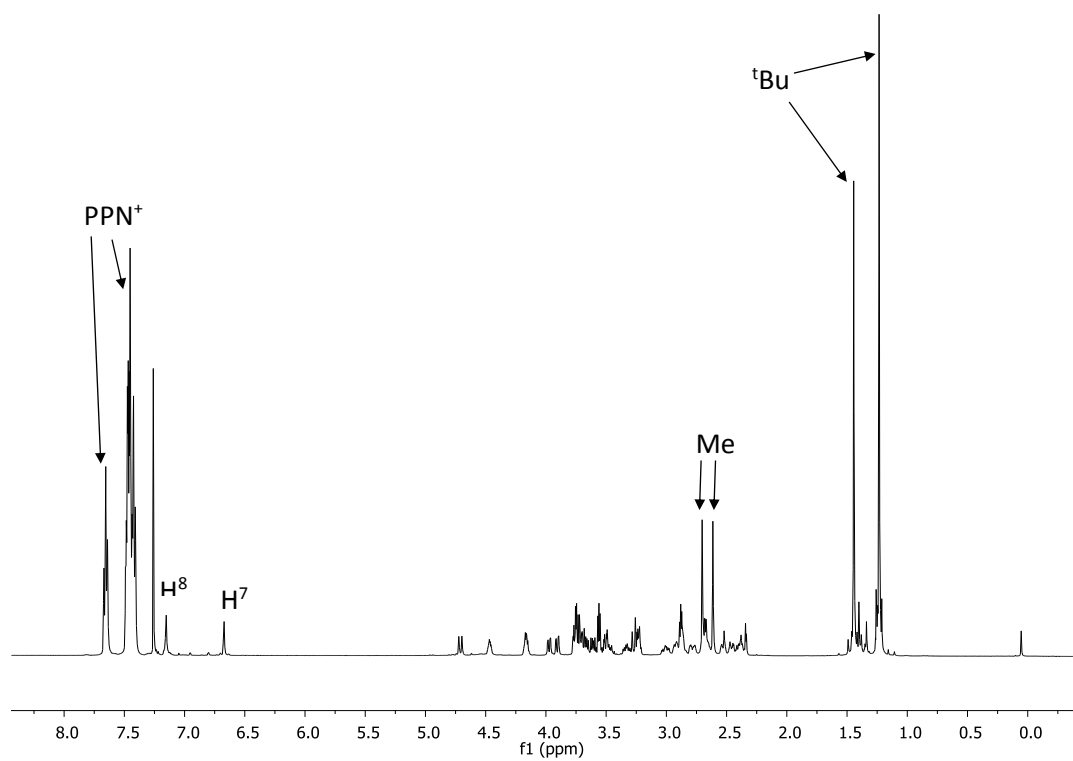
### Appendix

#### NMRexp1 spectra

#### $^1\text{H}$ NMR

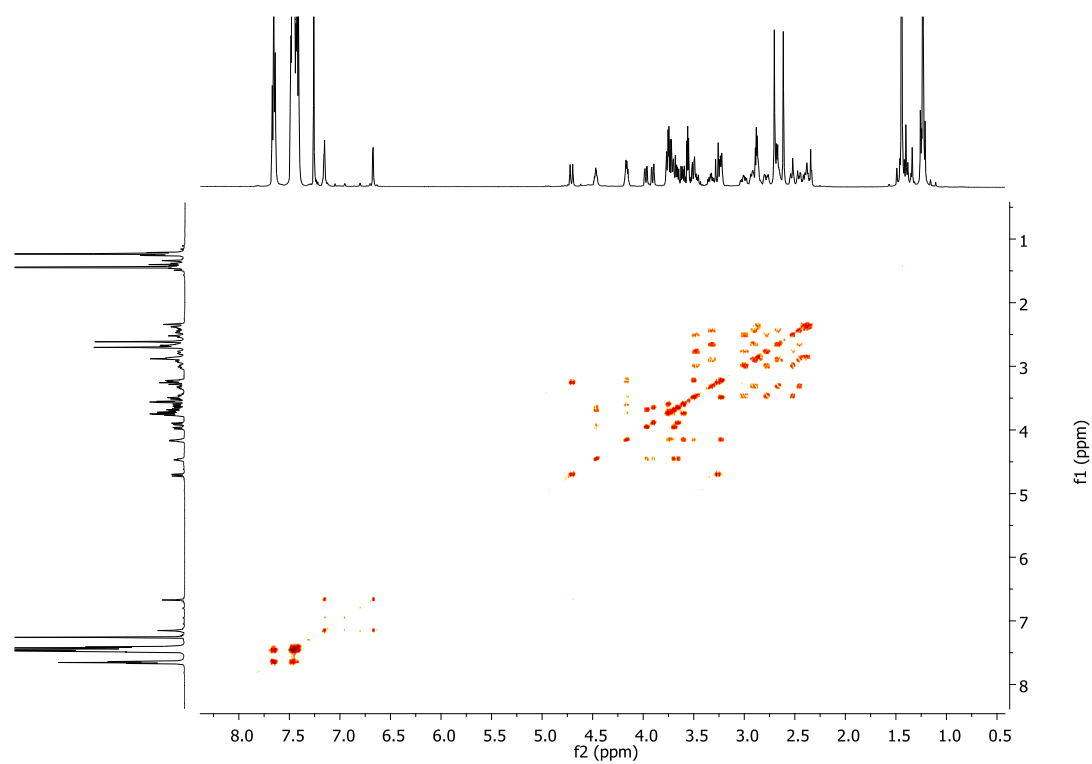


1A

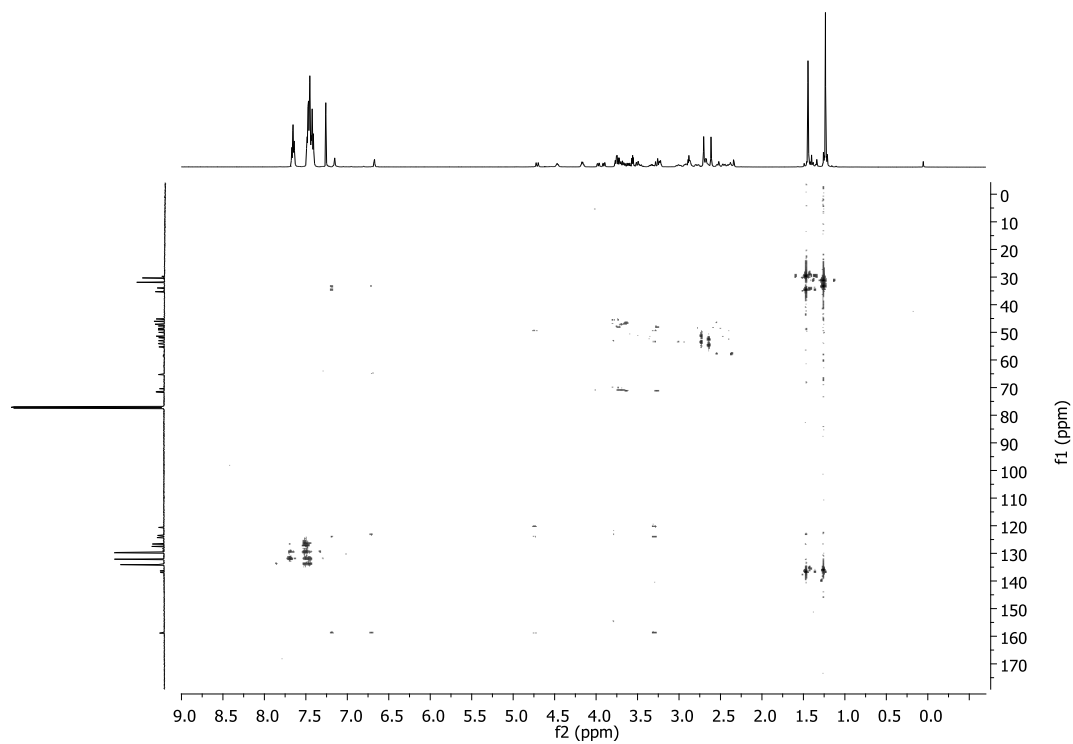


## Appendix

### COSY

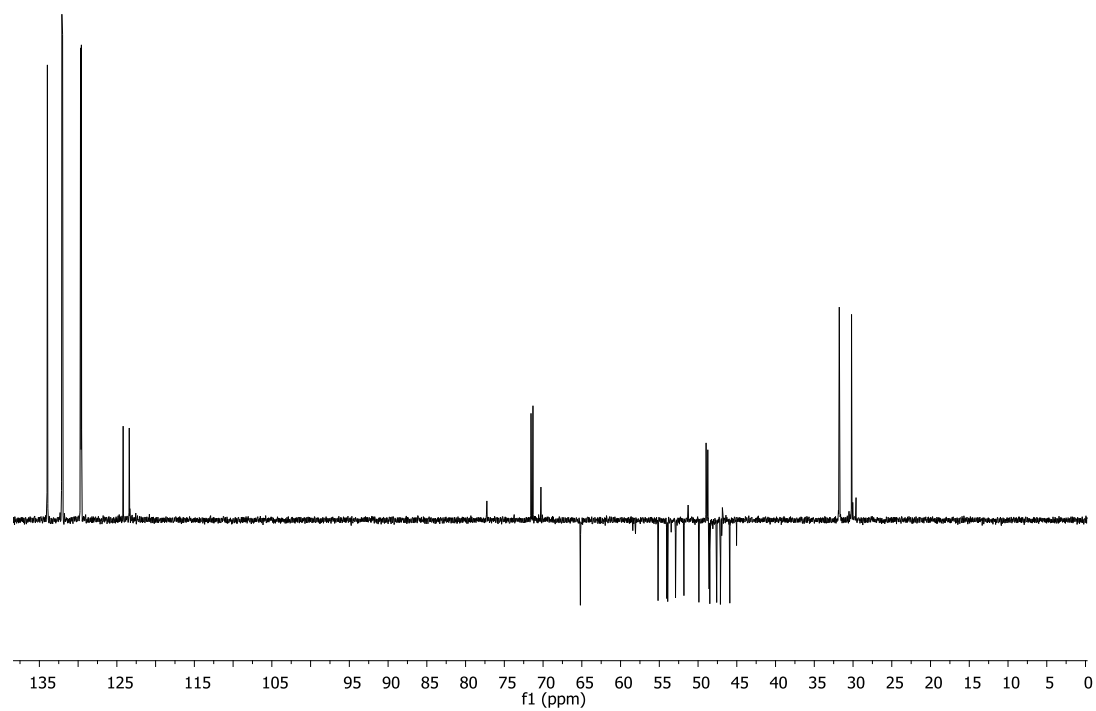


### HMBC

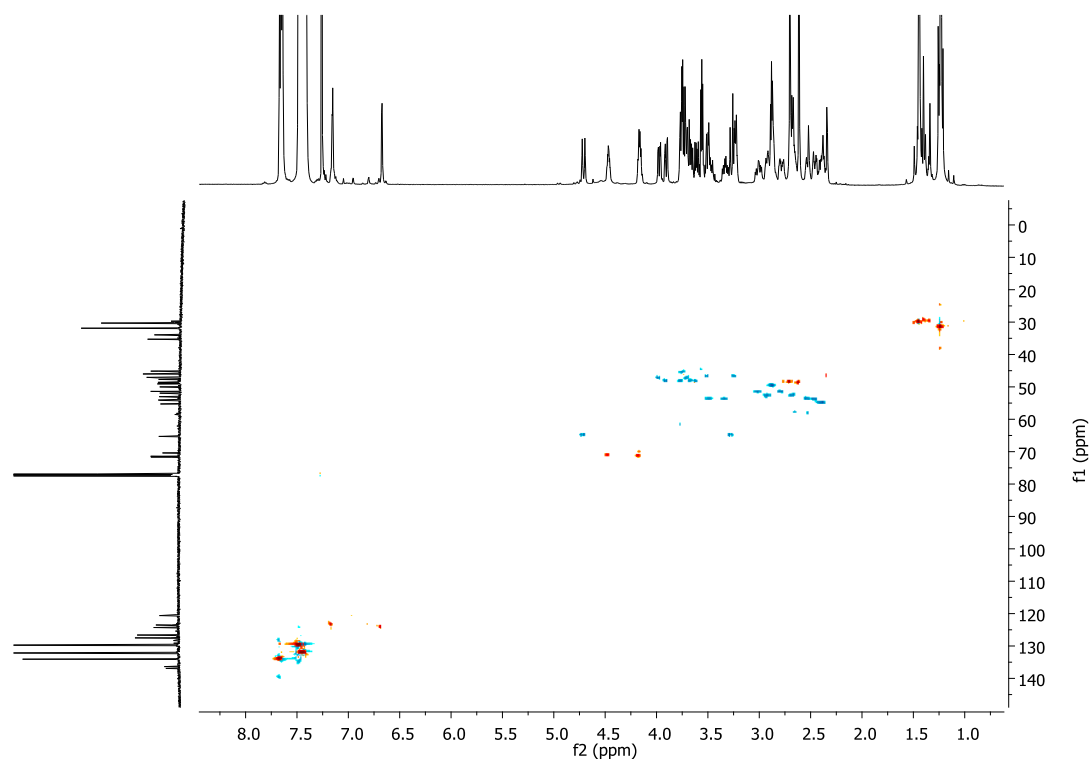


## Appendix

### DEPT-135

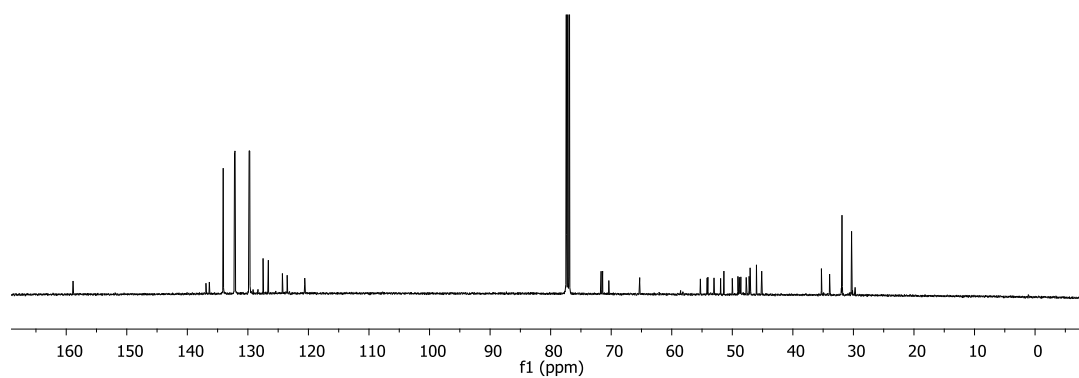


### HSQC



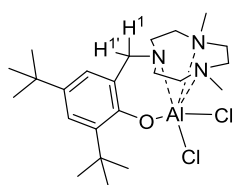
## Appendix

### $^{13}\text{C}$ NMR

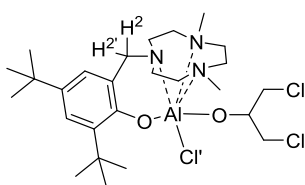


### NMRexp2 spectra

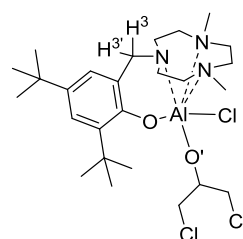
#### $^1\text{H}$ NMR



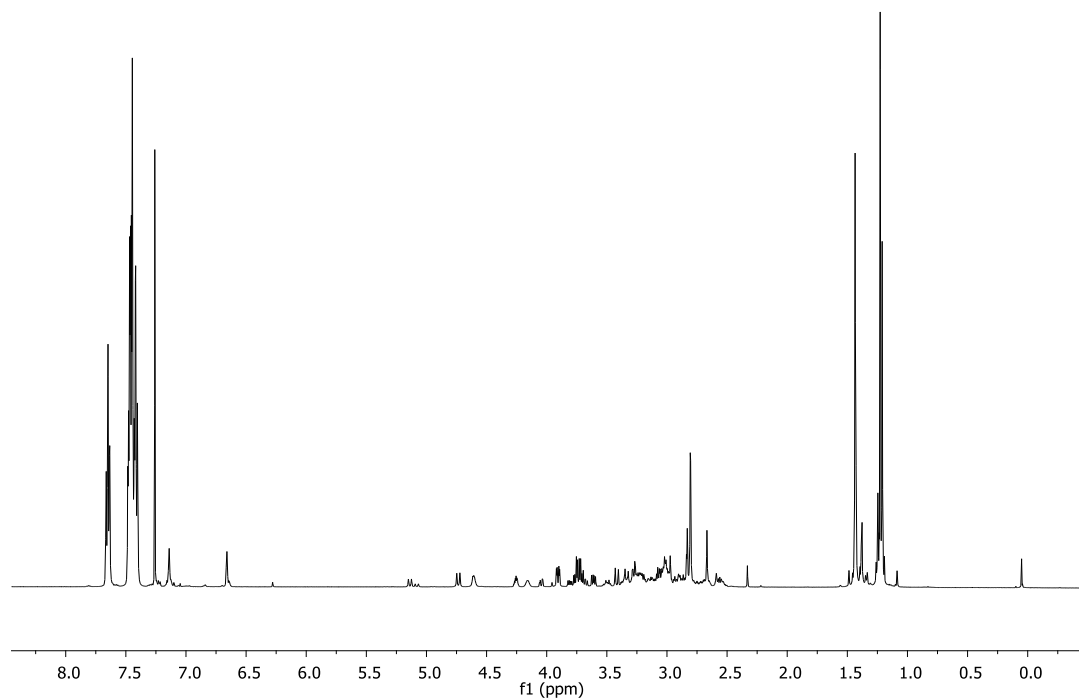
**1**



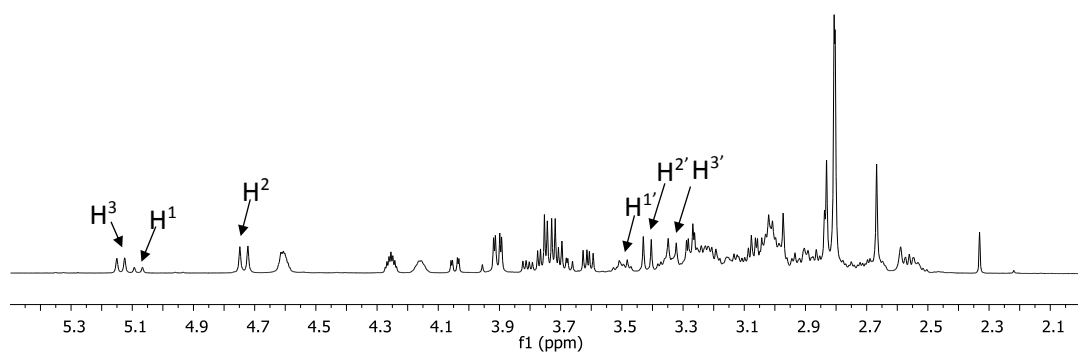
**1B**



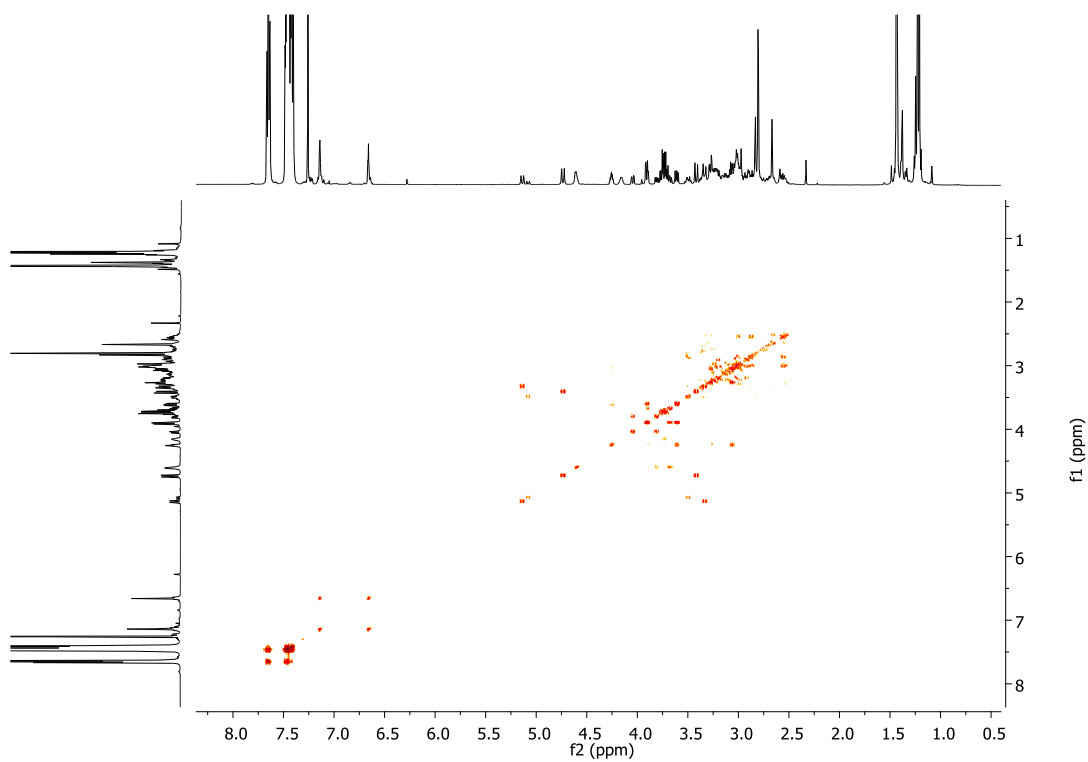
**1C**



## Appendix

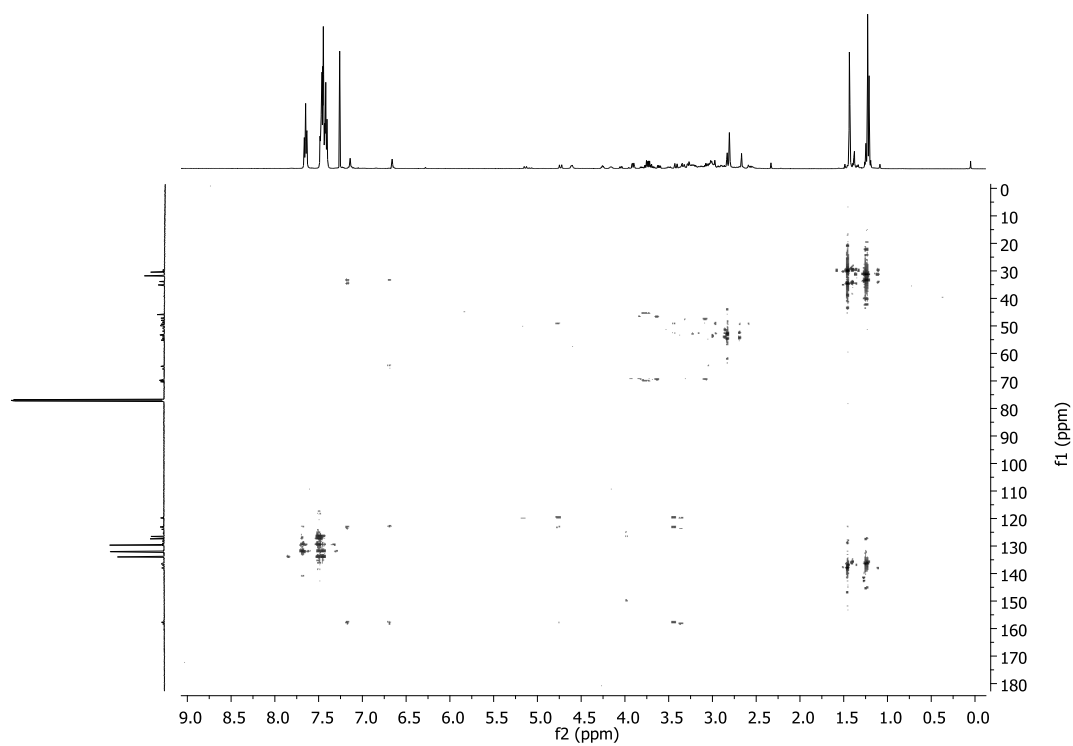


## COSY

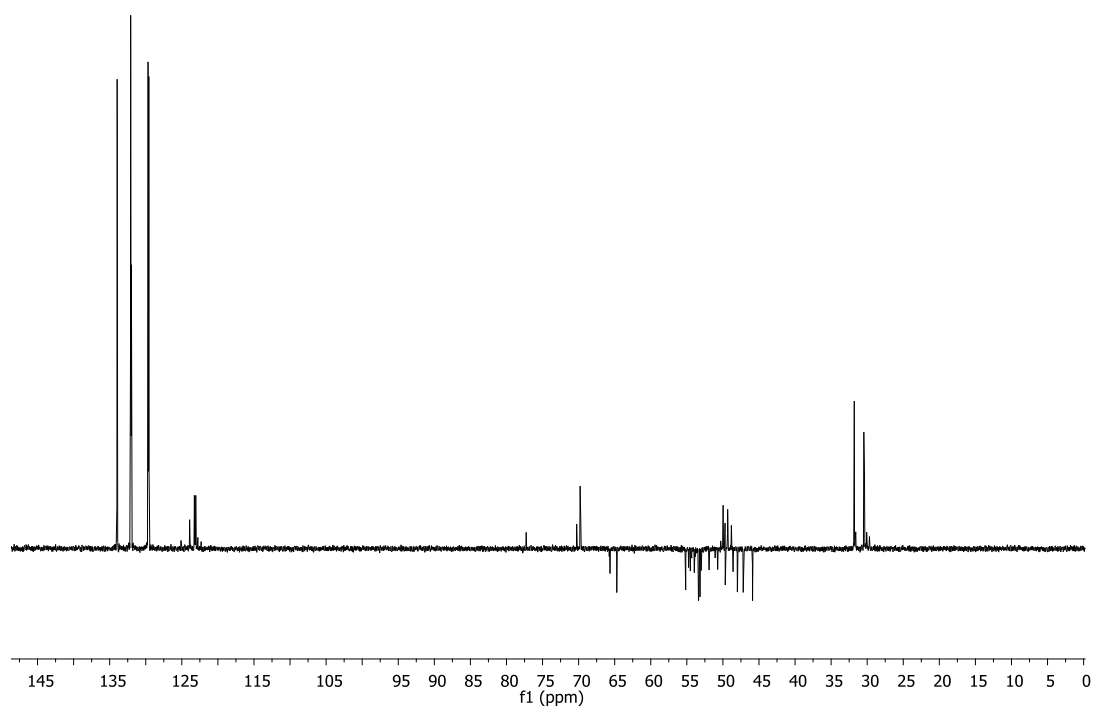


## Appendix

### HMBC



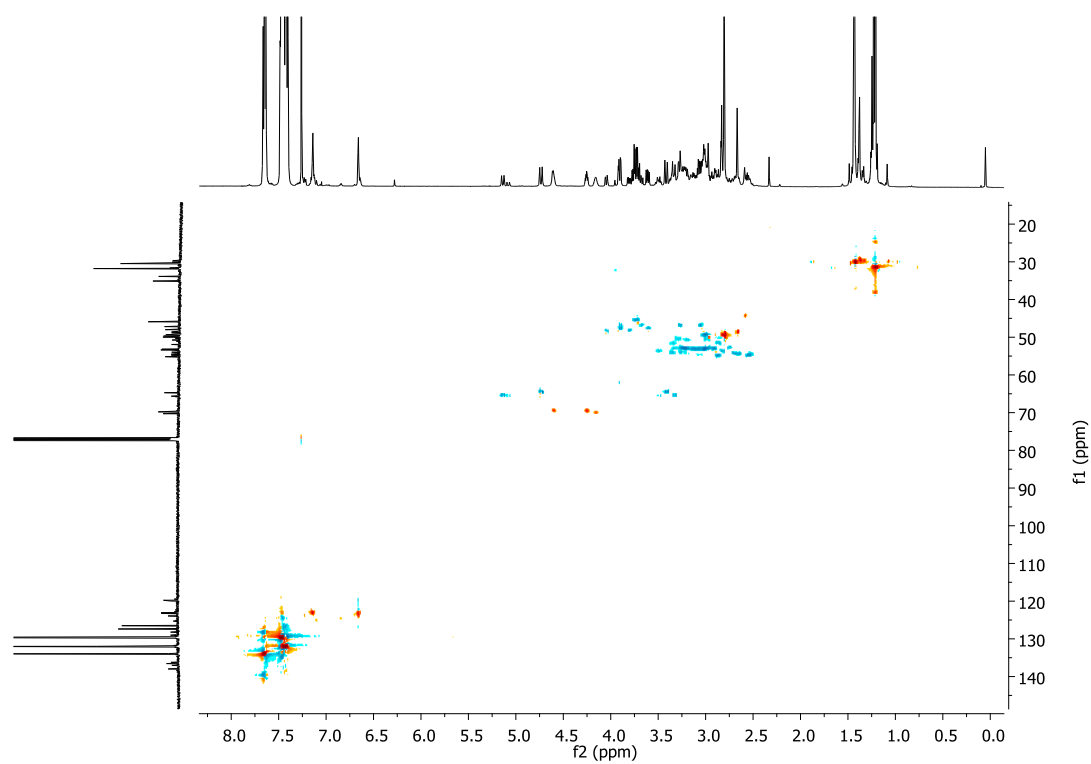
### DEPT-135



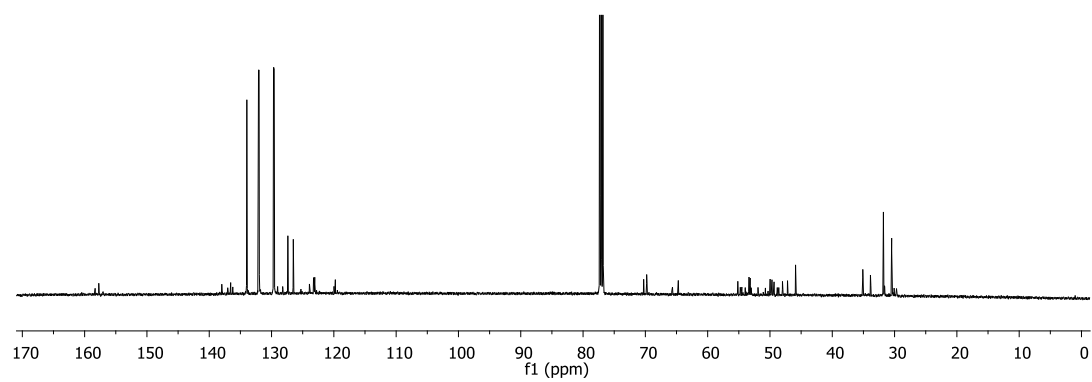


## Appendix

### HSQC



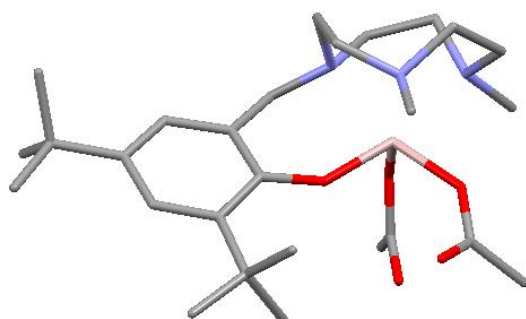
### $^{13}\text{C}$ NMR



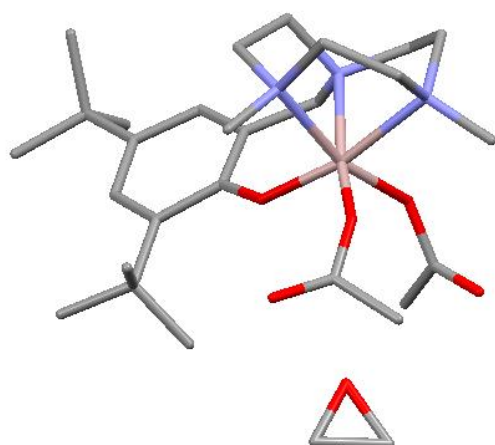
## Appendix

### DFT Mechanism ROCOP Calculated structures

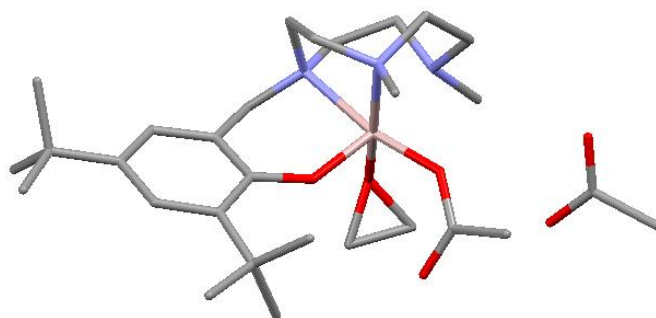
S



INT1

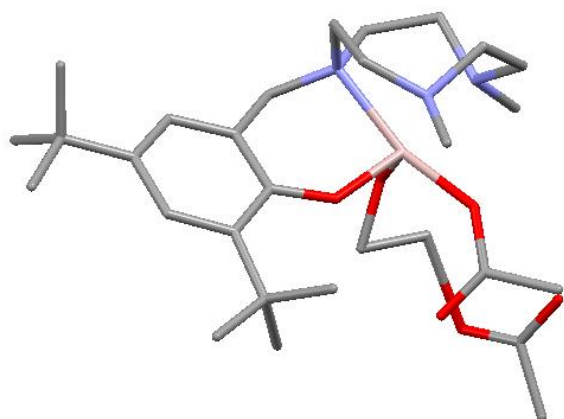


INT2

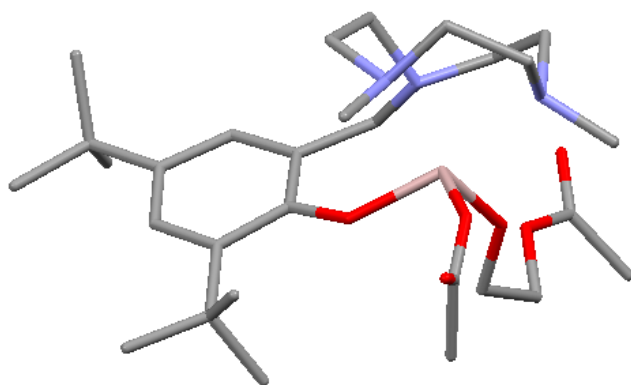


## Appendix

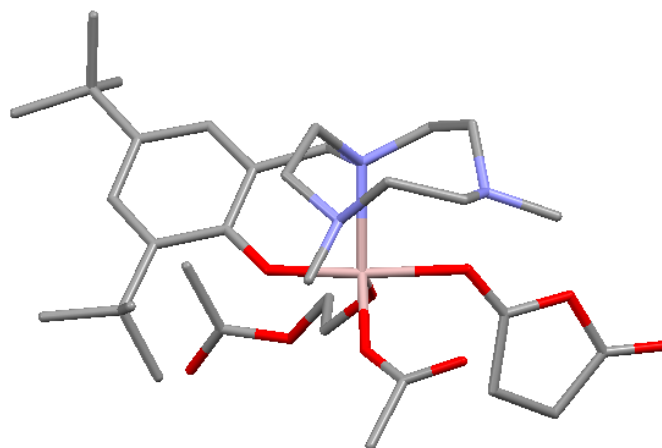
TS1



INT3

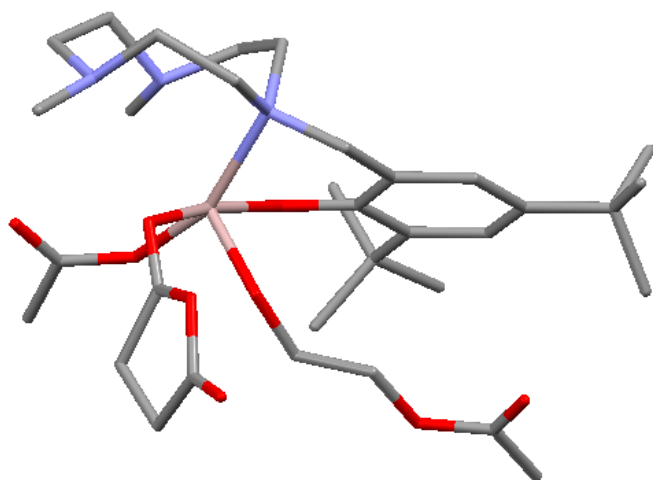


INT4

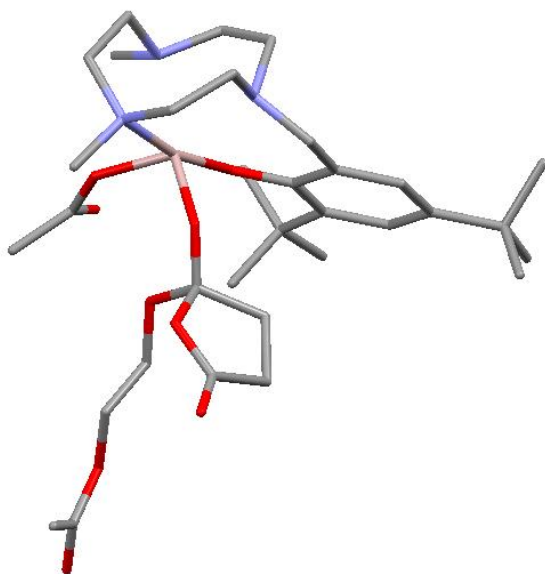


## Appendix

TS2

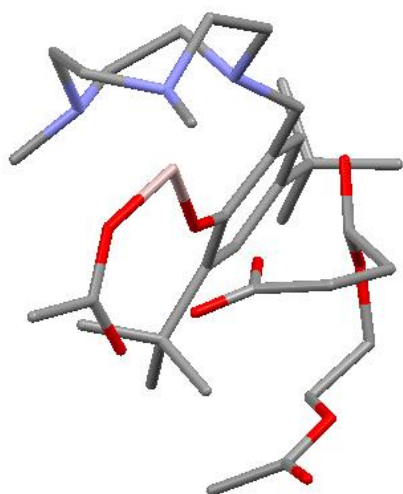


INT5



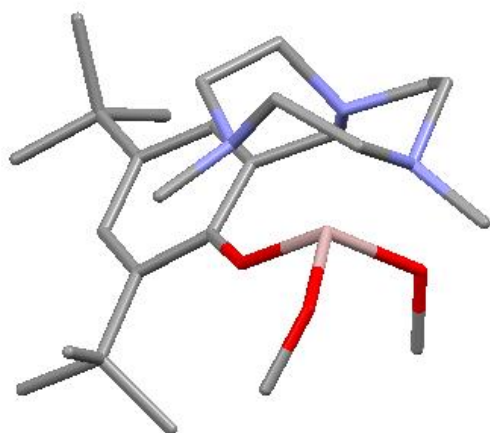
## Appendix

TS3



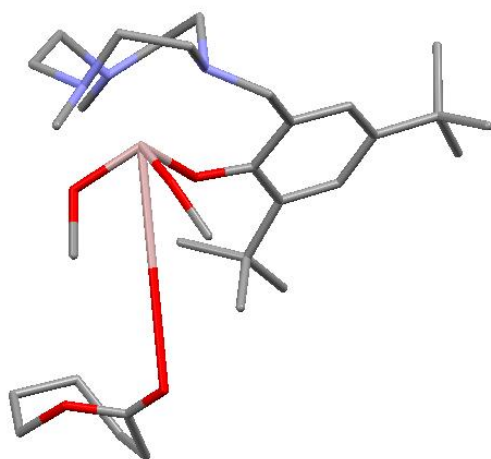
DFT Mechanism ROP Calculated structures

S

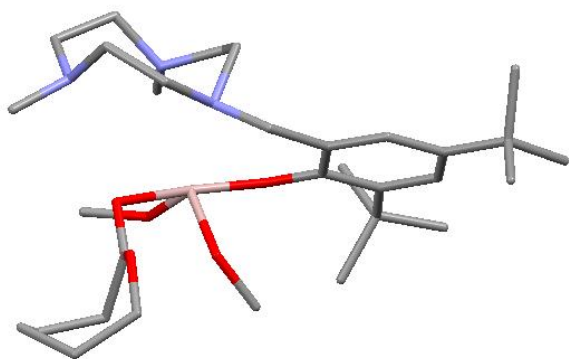


## Appendix

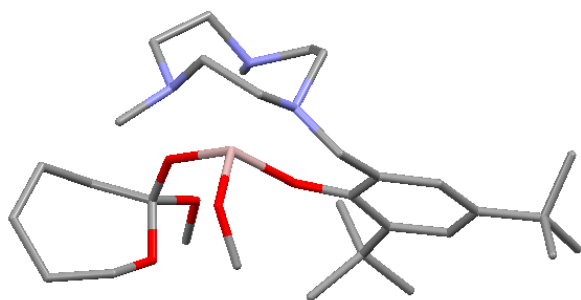
INT1



TS1



INT2



## Appendix

### TS2

